

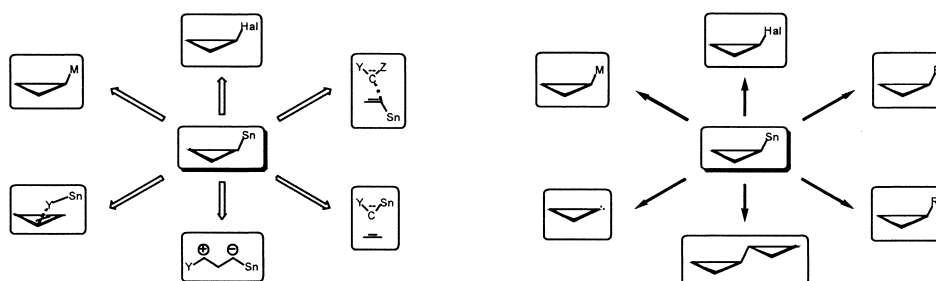
Contents

REPORT

Cyclopropylstannanes: synthesis and applications

Marina Rubina and Vladimir Gevorgyan*

pp 3129–3159

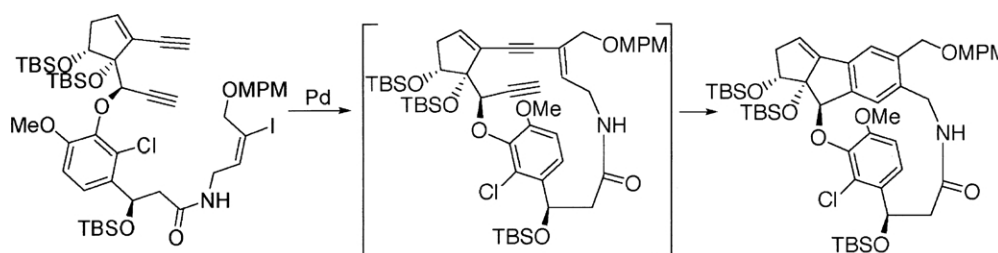


ARTICLES

Convergent approach to the maduropeptin chromophore: aryl ether formation of (R)-3-aryl-3-hydroxypropanamide and cyclization of macrolactam

Nobuki Kato, Satoshi Shimamura, Safraz Khan, Fumiyo Takeda, Yoko Kikai and Masahiro Hiramama*

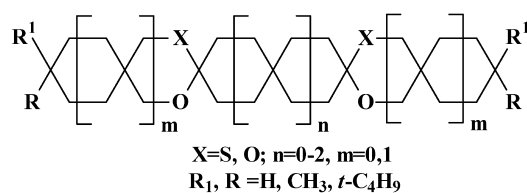
pp 3161–3172



Pentaspiranes and hexaspiranes with 1,3-dioxane or 1,3-oxathiane rings: synthesis and stereochemistry

Anamaria Terec, Ion Grosu,* Eric Condamine, Livain Breau, Gérard Plé, Yvan Ramondenc, Fernande D. Rochon, Valérie Peulon-Agasse and Dorina Opris

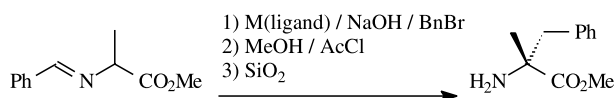
pp 3173–3189



Influence of the metal and chiral diamine on metal(II)salen catalysed, asymmetric synthesis of α -methyl α -amino acids

pp 3191–3204

Yuri N. Belokon, Jose Fuentes, Michael North* and Jonathan W. Steed

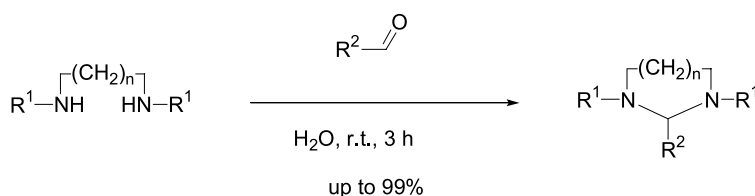


The influence of the metal and ligand on catalytic activity is investigated. For optimum results, M needs to be a first row transition metal capable forming square-planar complexes. A variety of salen type ligands were investigated and best results were obtained when substituents within the ethylene diamine part of the structure were present in *gauche* conformations.

Preparation of aminated in water

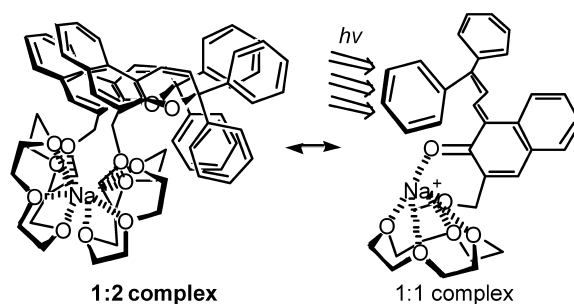
pp 3205–3210

Václav Jurčík and René Wilhelm*


Oxymethylcrowned chromene: photoswitchable stoichiometry of metal ion complex and ion-responsive photochromism

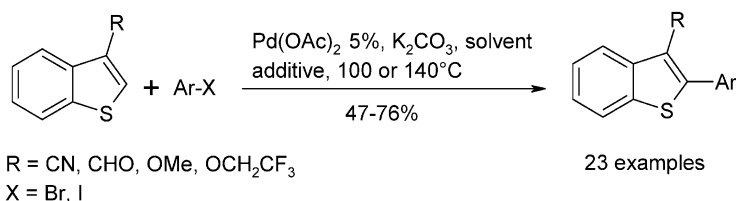
pp 3211–3220

Saleh A. Ahmed, Mutsuo Tanaka,* Hisanori Ando, Hitoshi Iwamoto and Keiichi Kimura*


An efficient phosphine-free palladium coupling for the synthesis of new 2-arylbenzo[*b*]thiophenes

pp 3221–3230

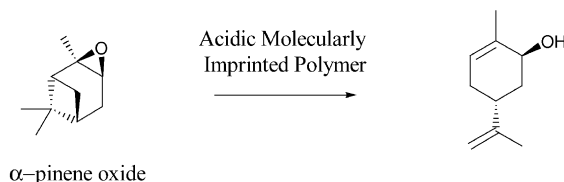
Jérémie Fournier Dit Chabert, Lionel Joucla, Emilie David and Marc Lemaire*



A study of some molecularly imprinted polymers as protic catalysts for the isomerisation of α -pinene oxide to *trans*-carveol

pp 3231–3241

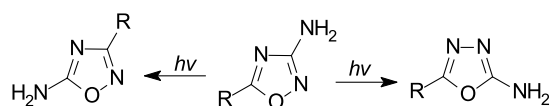
William B. Motherwell,* Matilda J. Bingham, Julien Pothier and Yvan Six



Theoretical study of photoinduced ring-isomerization in the 1,2,4-oxadiazole series

pp 3243–3249

Silvestre Buscemi, Maurizio D'Auria,* Andrea Pace, Ivana Pibiri and Nicolò Vivona



Self-assembly of β -turn forming synthetic tripeptides into supramolecular β -sheets and amyloid-like fibrils in the solid state

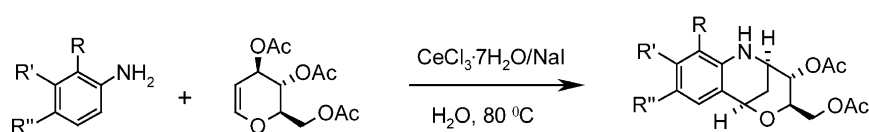
pp 3251–3259

Samir Kumar Maji, Debasish Haldar, Michael G. B. Drew, Arijit Banerjee, Apurba Kumar Das and Arindam Banerjee*

CeCl₃·H₂O/NaI-Promoted stereoselective synthesis of 2,4-disubstituted chiral tetrahydroquinolines

pp 3261–3266

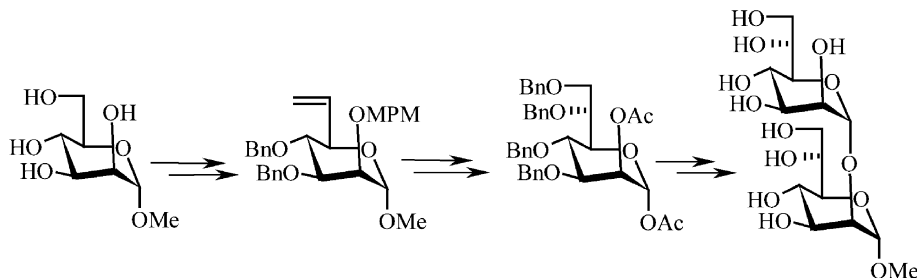
Jhillu S. Yadav,* B. V. S. Reddy, M. Srinivas and B. Padmavani



Synthesis of terminal disaccharide unit of *Klebsiella pneumoniae* ssp. R20

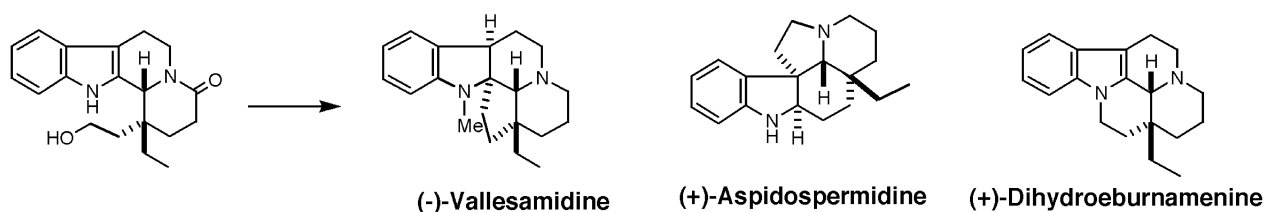
pp 3267–3271

Mukund K. Gurjar* and Arindam Talukdar

**Total syntheses of (–)-vallesamidine and related *Aspidosperma* and *Hunteria* type indole alkaloids from the common intermediate**

pp 3273–3282

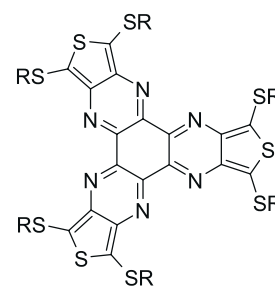
Hideo Tanino, Kazuhisa Fukuishi, Mina Ushiyama and Kunisuke Okada*

**Hexaazatriisothianaphthenes: new electron-transport mesogens?**

pp 3283–3291

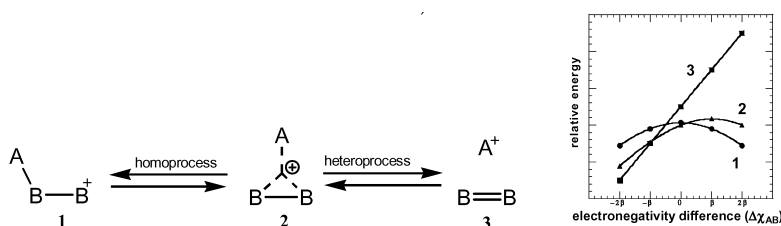
Matthias Lehmann, Vincent Lemaure, Jérôme Cornil, Jean-Luc Brédas, Simon Goddard, Ilaria Grizzi and Yves Geerts*

Hexaazatriisothianaphthenes substituted with six alkylsulfanyl chains have been synthesised and their thermotropic, photophysical and oxidation–reduction properties characterised. Their synthesis has been motivated by the results of quantum-chemical calculations that point to efficient transport properties for these new electron-deficient molecules.

**The influence of electronegativity on triangular three-centre two-electron bonds: the relative stability of carbon ions, π -complex chemistry and the $-2h\beta$ effect**

pp 3293–3309

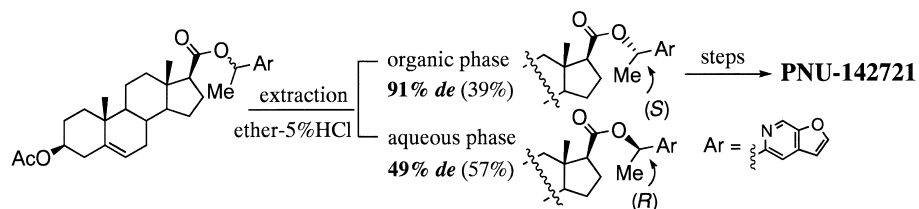
Christopher A. Ramsden*



**A novel separation technique of diastereomeric esters of pyridylethanols by extraction:
formal total synthesis of PNU-142721, HIV-1 reverse transcriptase inhibitor**

pp 3311–3317

Masato Matsugi, Kinuyo Itoh, Masatomo Nojima, Yuri Hagimoto and Yasuyuki Kita*



OTHER CONTENTS

Contributors to this issue
Instructions to contributors

p I
pp III–VI

*Corresponding author



Full text of this journal is available, on-line from **ScienceDirect**. Visit www.sciencedirect.com for more information.

CONTENTS
direct

This journal is part of **ContentsDirect**, the *free* alerting service which sends tables of contents by e-mail for Elsevier books and journals. You can register for **ContentsDirect** online at: <http://contentsdirect.elsevier.com>

Indexed/Abstracted in: AGRICOLA, Beilstein, BIOSIS Previews, CAB Abstracts, Chemical Abstracts, Chemical Engineering and Biotechnology Abstracts, Current Biotechnology Abstracts, Current Contents: Life Sciences, Current Contents: Physical, Chemical and Earth Sciences, Current Contents Search, Derwent Drug File, Ei Compendex, EMBASE/Excerpta Medica, Medline, PASCAL, Research Alert, Science Citation Index, SciSearch



ELSEVIER

ISSN 0040-4020



Tetrahedron report number 675

Cyclopropylstannanes: synthesis and applications

Marina Rubina and Vladimir Gevorgyan*

Department of Chemistry, University of Illinois at Chicago, 845 West Taylor Street, Chicago, IL 60607-7061, USA

Received 29 November 2003

Contents

1. Introduction	3129
2. Synthesis	3130
2.1. From cyclopropyl-containing precursors	3130
2.1.1. Direct deprotonation of cyclopropane	3130
2.1.2. Halogen–metal–tin exchange at halocyclopropanes	3131
2.2. 1,3-Cyclization reactions	3134
2.3. Addition of carbenes and carbenoids to olefins	3135
2.3.1. Addition of dihalocarbenes to vinylstannanes	3135
2.3.2. Simmons–Smith reaction	3135
2.3.3. Rh-Catalyzed addition of carbenoid species	3137
2.3.4. Addition of tin-containing carbenes to olefins	3137
2.4. Addition of tin-containing entities across the double bond of cyclopropenes and methylenecyclopropanes	3138
2.4.1. Addition of tin hydrides to cyclopropenes	3138
2.4.2. Addition of ditin and silicon–tin species to cyclopropenes	3139
2.4.3. Addition of tin–metal species to methylenecyclopropanes	3139
2.5. Miscellaneous	3139
2.5.1. Kulinkovich reaction	3139
2.5.2. Substitution at cyclopropyl ring with tin nucleophiles	3140
2.6. Cyclopropenylstannanes (synthesis and applications)	3140
3. Applications	3142
3.1. Transformations with preservation of the cyclopropyl ring	3142
3.1.1. Reactions involving tin–lithium exchange	3142
3.1.2. Tin–halogen exchange reactions	3148
3.1.3. Cross-coupling reactions	3150
3.1.4. Miscellaneous	3151
3.2. Reactions involving opening of the cyclopropyl ring	3153
3.2.1. Ring opening reactions involving ionic intermediates	3153
3.2.2. Radical-initiated ring opening	3155
3.2.3. Ring opening via α -elimination	3155
4. Conclusion	3156

1. Introduction

Cyclopropylstannanes are very versatile building blocks for

Keywords: Cyclopropylstannanes; Cyclopropenylstannanes; Synthesis; Applications; Transmetalation; Metal–halogen exchange; Cross-coupling; Hydrostannation.

* Corresponding author. Tel.: +1-312-355-3579; fax: +1-312-355-0836; e-mail address: vlad@uic.edu

synthetic organic chemistry (vide infra) and thus substantial attention has been paid by the synthetic community to development of efficient and selective methods for preparation of these useful synthons. Surprisingly, synthetic applications of cyclopropylstannanes have never been reviewed. The present review, although not comprehensive, highlights, in our judgment, the most important work on synthesis and chemistry of cyclopropylstannanes. Section 1 describes practical synthetic methods towards

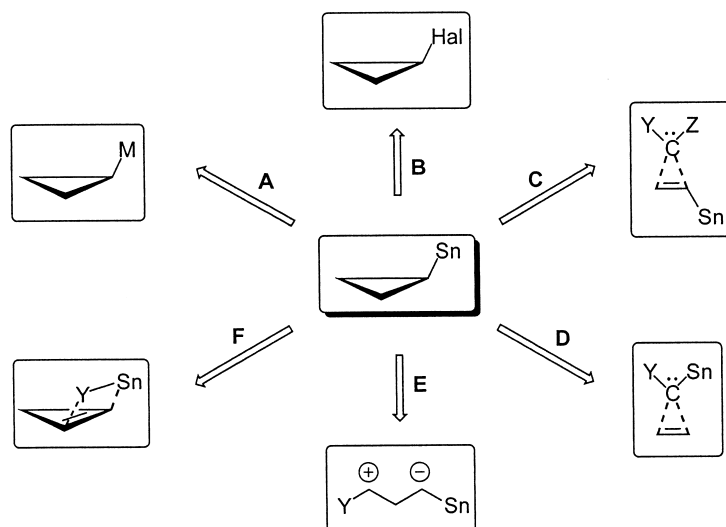


Figure 1.

cyclopropylstannanes, the most important of which are summarized in Figure 1. They involve reactions of cyclopropylmetals (Li, Mg) with tin electrophiles (A); displacement of cyclopropyl halides with stannyl lithium reagents (B); addition of carbenoid species to vinylstannanes (C); addition of stannylcarbenoids to alkenes (D); 1,3-cyclization reactions (E); and addition of tin entities across the double bond of cyclopropenes (F).

Section 2 illustrates applications of cyclopropylstannanes in organic synthesis (Fig. 2). This includes tin–metal exchange reactions (G); tin–halogen exchange reactions (H); direct electrophilic destannylation (I); transition metal-catalyzed cross-coupling reactions (J); oxidative homocoupling reactions (K); and α -elimination of 1-halocyclopropylstannanes (L).

In addition, preparation and synthetic applications of related compounds, cyclopropenylstannanes, are also discussed (Section 2.6). Finally, miscellaneous synthetic schemes are summarized at the end of each chapter.

2. Synthesis

2.1. From cyclopropyl-containing precursors

2.1.1. Direct deprotonation of cyclopropane. Direct deprotonation of unsubstituted cyclopropane has not been documented, which can be attributed to its rather low C–H acidity ($pK_a \sim 46$).¹ However, introduction of electron-withdrawing groups increases acidity of the geminal C–H and thereby allows for deprotonation with strong bases. Thus, sulfoxide **1** was successfully deprotonated with LDA in tetrahydrofuran followed by trapping with a tin electrophile to produce **3** in 78% yield (Scheme 1).²

Analogously, α -stannylsulfone **6** was prepared in 58% yield by deprotonation of **4** with *n*-butyllithium followed by reaction with tributyltin chloride (Scheme 2).^{3,4}

Optically active **9** was prepared from the corresponding carbamate **7** via deprotonation with *sec*-butyllithium followed by addition of trimethyltin chloride, in 43%

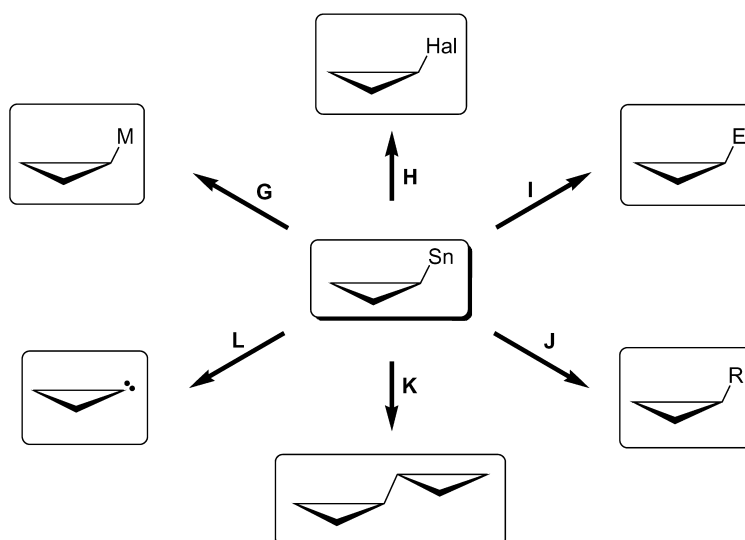
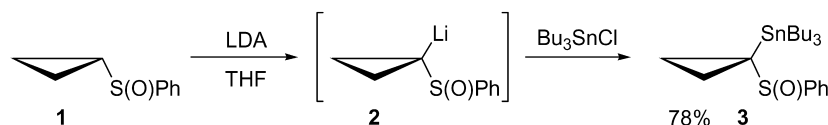
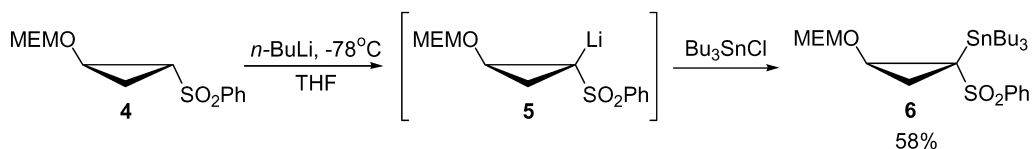


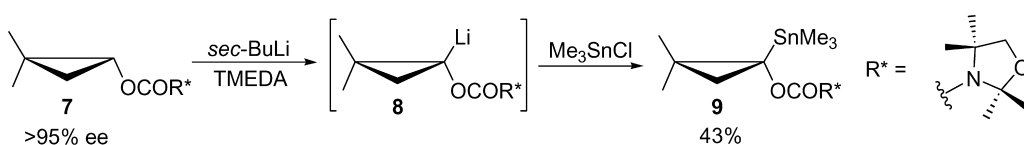
Figure 2.



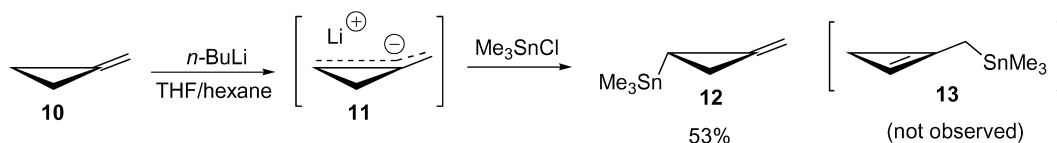
Scheme 1.



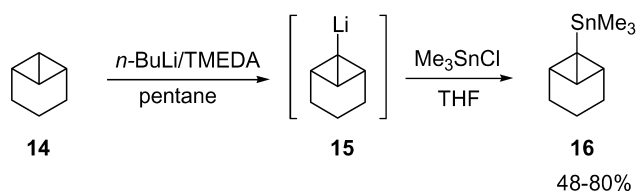
Scheme 2.



Scheme 3.



Scheme 4.



Scheme 5.

yield (Scheme 3).⁵ Cyclopropyllithium anion, which is configurationally stable at $-78\text{ }^{\circ}\text{C}$, gives rise to cyclopropylstannane with complete preservation of configuration at C-1.⁵

Methylenecyclopropane **10** represents another example of a cyclopropane with rather acidic protons (Scheme 4).⁶ Deprotonation of **10** with *n*-BuLi generates 1,2-dimethanoallylic anion **11**, which is quenched with trimethyltin chloride at the more hindered site to afford methylenecyclopropane **12**, thereby avoiding formation of the rather more strained cyclopropene species **13**, which would form through alternative quenching at the less hindered *exo*-methylene terminus.

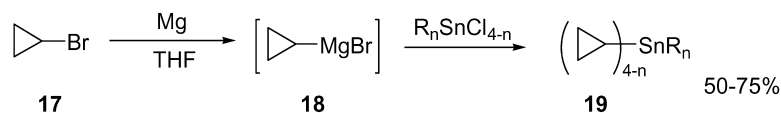
Compound **16** was synthesized by taking advantage of the high acidity of a bridgehead proton in the very strained

bicyclobutane **14**. Metalation of the latter with *n*-butyllithium followed by addition of Me_3SnCl afforded **16** in moderate to good yields (Scheme 5).^{7,8}

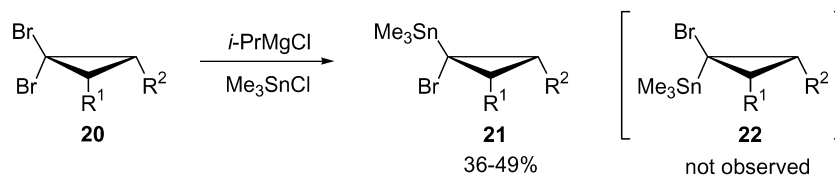
It is worth mentioning that, despite a few successful examples of direct deprotonation of cyclopropanes, the synthetic utility of this method is limited to substrates with enhanced C–H acidity.

2.1.2. Halogen–metal–tin exchange at halocyclopropanes. Cyclopropylstannanes via halogen–magnesium exchange. Efficient selective synthesis of cyclopropylstannanes via halogen–magnesium exchange was first demonstrated in the early 60s. This procedure allowed for synthesis of a number of cyclopropylstannanes in good yields from readily available bromide **17** (Scheme 6).⁹

Highly stereoselective monostannation of *gem*-dibromocyclopropanes was achieved via halogen to magnesium exchange with a Grignard reagent (Scheme 7).^{10,11} The reaction proceeds with perfect steric control from the least hindered face. Subsequent treatment of the resulting cyclopropylmagnesium species with trimethyltin chloride at $-70\text{ }^{\circ}\text{C}$ produces only cyclopropylstannane **21** with the trimethyltin group *anti*- to the present substituent in the ring. Although the yields are moderate, this approach can serve as



Scheme 6.



Scheme 7.

a complementary method to one involving lithium reagents, which allows for preparation of *syn*-isomers **22** (see below).

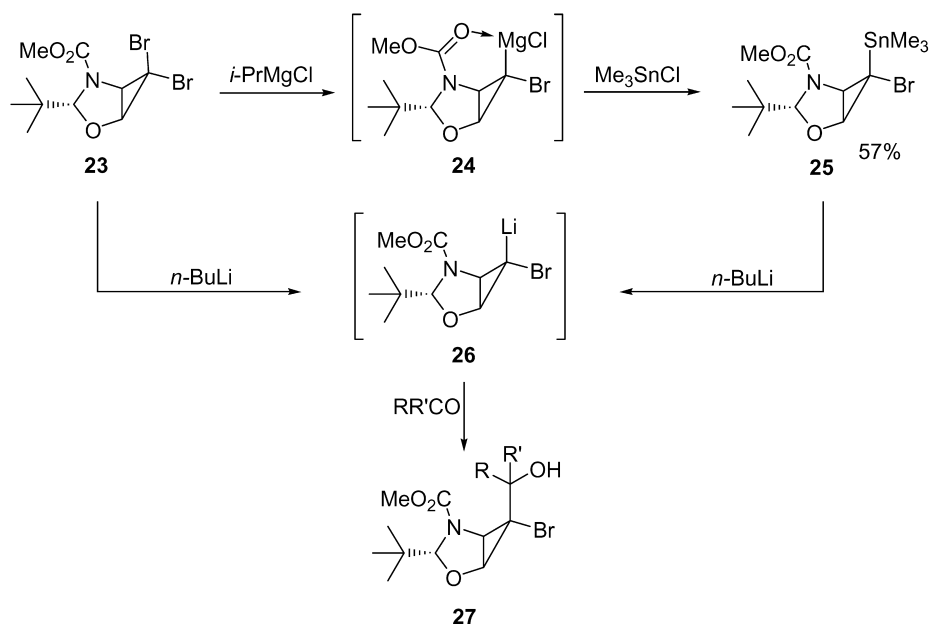
Seebach discovered directed monometalation of *gem*-dibromocyclopropane with isopropylmagnesium chloride in the oxazolidine series (Scheme 8).¹² The *syn*-magnesium carbanion was stabilized by the carbamate moiety in **24** providing a high degree of stereocontrol. Transmetalation of **24** with trimethyltin chloride afforded stannylated product **25** in 57% yield. Configuration of **25** was unambiguously confirmed by its conversion into lithium derivative **26** followed by trapping with an electrophile. The resulting product **27** had the same configuration as the compound obtained directly from **23** using organolithium reagent (Scheme 8).

Knochel found an analogous directing effect of an ester group in the dibromo-cyclopropylcarboxylate series (Scheme 9).¹³ Remarkably, it was shown that at low temperatures bulky isopropylmagnesium chloride did not compromise the stability of an ester group. Interestingly, the

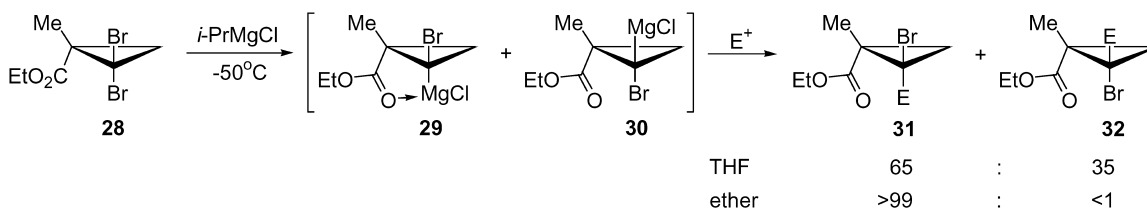
chelating effect of an ester group depended strongly upon the solvent used. Thus, treatment of dibromide **28** with the Grignard reagent in THF produced a mixture of isomeric cyclopropylmagnesium chlorides **29** and **30** in a 65:35 ratio as determined by the distribution of **29** and **30** with electrophiles. In contrast, analogous reaction performed in diethyl ether displayed perfect chelation control and proceeded in a highly diastereoselective fashion producing *cis*-magnesium species **29** exclusively. The latter can be selectively trapped by a number of electrophiles (Scheme 9).¹³

Knochel has also demonstrated that 2-iodocyclopropane-carboxylate **33** when treated with *i*-PrMgCl affords *cis*-**34**, which exhibited remarkable stability as a result of the chelating effect of the ester group (Scheme 10). Cyclopropylmagnesium chloride **34** reacted directly with a series of electrophiles, including Me_3SnCl , to form **35** in good yields.¹³

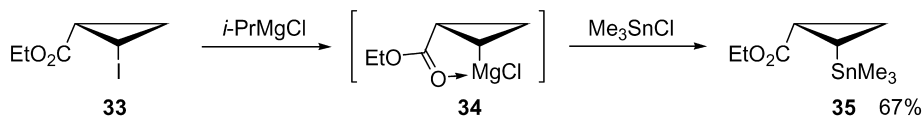
Cyclopropylstannanes via halogen to lithium exchange.



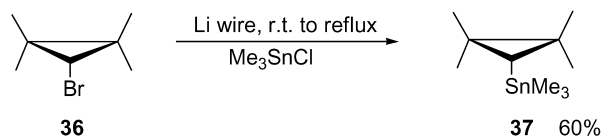
Scheme 8.



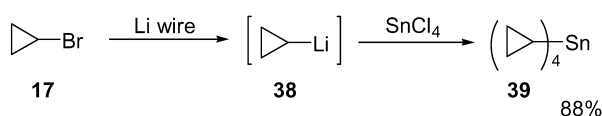
Scheme 9.



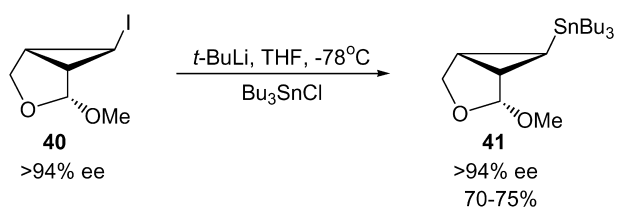
Scheme 10.



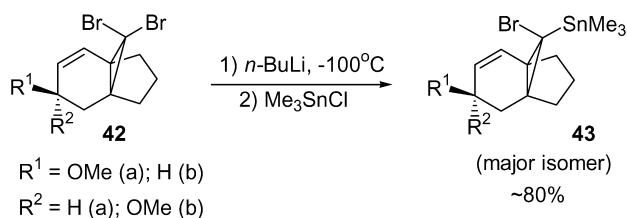
Scheme 11.



Scheme 12.



Scheme 13.



Scheme 14.

Halogen–lithium–tin exchange can be effected using lithium metal or a variety of alkyllithium reagents. The intermediate cyclopropyllithium species display higher stability when the reaction is carried out in diethyl ether, even at elevated temperatures, which allows for good yields of corresponding products. Thus, readily available cyclopropyl bromide **36** undergoes smooth tin–lithium exchange when reacted with lithium wire or lithium dispersion in diethyl ether (Scheme 11).¹⁴ The half-life of the resulting tetramethylcyclopropyllithium in ether at room temperature was determined to be 38 h. Corresponding stannylated

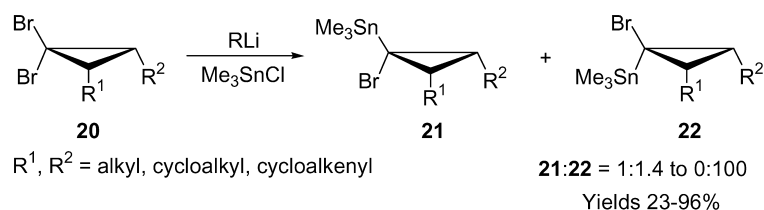
product **37** was isolated in good yield after addition of trimethyltin chloride (Scheme 11).

Likewise, tetracyclopropyltin **39** was prepared in very good yield by treatment of **17** with Li wire at 0 °C followed by reaction with SnCl_4 (Scheme 12).¹⁵

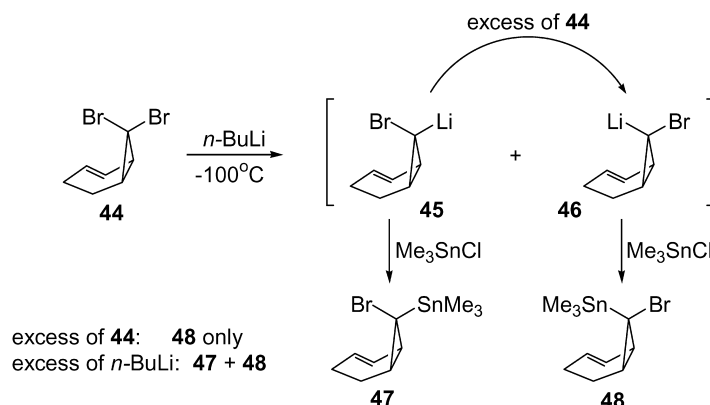
Halogen–lithium exchange with organolithium reagents is a much milder method as the reactions rapidly proceed at temperatures as low as -100°C . This method allows for easy access to configurationally defined lithiated cyclopropanes, which can stereoselectively be functionalized with variety of electrophiles. Thus, optically active iodocyclopropane **40**, obtained from allylic diazoacetate using Doyle's protocol,¹⁶ readily underwent consecutive iodine to lithium exchange and trapping with tin electrophile to provide **41** in good yield (Scheme 13).¹⁷ Possible epimerization due to the chelating effect of methoxy substituent was not observed in this case, as detected by NMR analyses of the crude reaction mixtures. This indicates that the intermediate cyclopropyl anion retained its configuration under the above-mentioned reaction conditions (Scheme 13).

A number of reports document the reaction of *gem*-dibromocyclopropanes with *n*-butyllithium followed by trapping with trimethyltin chloride (Schemes 14 and 15). In contrast to the analogous reaction with Grignard reagents, formation of *syn*-trimethylstannylcyclopropane **22** was observed predominantly or exclusively depending on the amount of *n*-BuLi used. Although the reasons for this are not completely understood, perfect facial selectivity was observed only when no excess of *n*-BuLi was present in the reaction;^{11,18,19} otherwise, mixtures of *syn*- and *anti*-products were obtained.^{20–23}

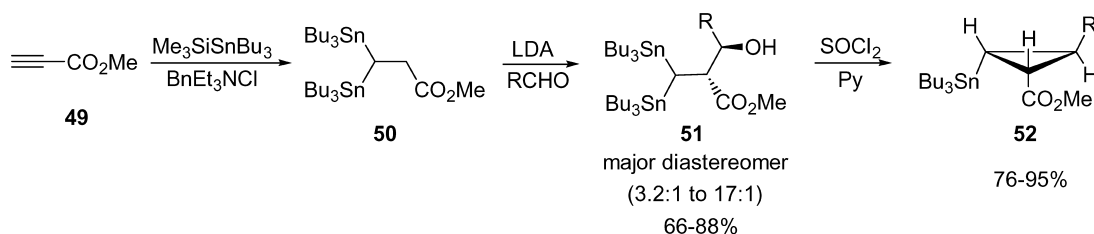
Thus, Warner demonstrated that when excess dibromide **44** was treated with *n*-BuLi, the initially formed carbanion **45** rapidly transformed into the isomeric **46**, which upon quenching with Me_3SnCl produced stannane **48** as the sole product. However, treatment of **44** with excess *n*-BuLi (1.3 equiv.) resulted in incomplete conversion of **45** into **46** and both cyclopropylstannanes **47** and **48** were formed (Scheme 16). Based on the above observations it was concluded that transformation **45** to **46** is a thermodynamically driven process.²⁴



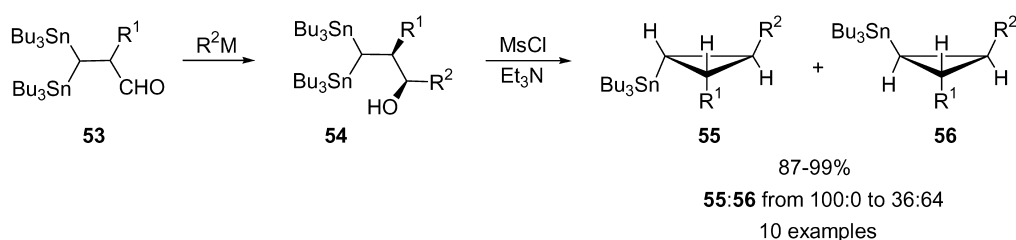
Scheme 15.



Scheme 16.



Scheme 17.



Scheme 18.

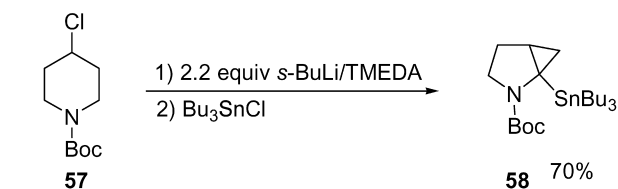
2.2. 1,3-Cyclization reactions

Functionalized cyclopropylstannanes are also accessible via 1,3-cyclization reactions of open chain precursors. This reaction requires substrates possessing both anion-stabilizing and good leaving groups, separated by a chain of three carbon atoms. Two different modes of 1,3-cyclization have been employed for synthesis of cyclopropylstannanes: (a) incorporation of the tin moiety into open-chain precursor, and (b) trapping of cyclopropylmetal species, obtained via 1,3-cyclization, with a tin electrophile.

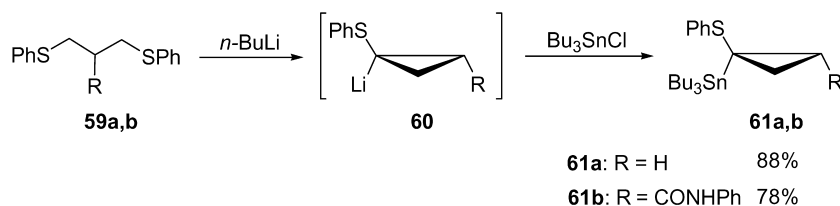
Mori has developed an efficient method for synthesis of bis(tributylstannyl)propionate **50**, an attractive versatile synthon, via sequential silastannylation–desilylation of methyl propiolate **49** (Scheme 17).²⁵ Propionate **50** obtained by this method has been effectively employed for the construction of a series of 1,2,3-trisubstituted cyclopropyl derivatives.²⁶ Thus, the α -anion, generated from **50** by treatment with LDA, underwent a diastereoselective cross-aldol reaction with an aldehyde to form **51**. Treatment of the major diastereomer of **51** with SOCl_2 in the presence of pyridine triggered a destannylation cyclization to produce cyclopropylstannane **52** as single isomer in good to very high yields (Scheme 17).

Alternatively, bis(tributylstannyl)propionate **50** can be converted into aldehyde **53** via alkylation followed by subsequent reduction with DIBAL-H.²⁷ Aldehyde **53** upon treatment with organometallic reagents gives alcohol **54**, which under mesylation conditions undergoes destannylation 1,3-cyclization to form isomeric cyclopropanes **55** and **56** in very high yields. In most cases **55** was formed as a major diastereomer (Scheme 18).²⁷

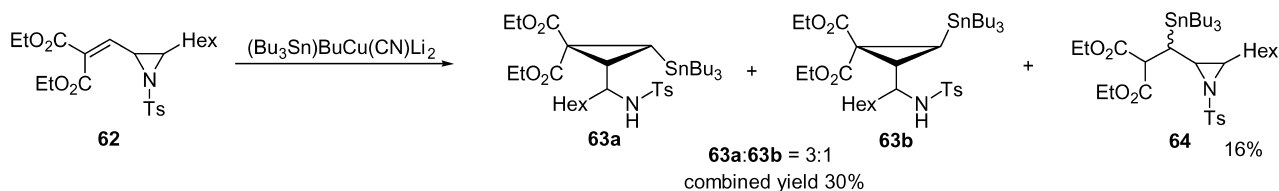
A lithiation–intramolecular cyclization reaction of *N*-Boc-4-chloropiperidine **57** with excess *s*-BuLi was reported by Beak.²⁸ The first equivalent of *s*-BuLi causes intramolecular nucleophilic substitution leading to bicyclic pyrrolidine, from which selective deprotonation by second equivalent of base followed by trapping with Bu_3SnCl affords **58** in good yield (Scheme 19).²⁸



Scheme 19.



Scheme 20.



Scheme 21.

Treatment of bis(phenylthio)propane **59a** with 2 equiv. of *n*-BuLi followed by the addition of Bu_3SnCl afforded α -stannyl cyclopropyl sulfide **61a** (Scheme 20, R=H, 88%).²⁹ Similarly, trisubstituted **61b** was obtained through cyclization of **59b** in 78% yield.³⁰ This easy and straightforward approach was only applied to the synthesis of geminally thio-substituted cyclopropylstannanes (Scheme 20).

The Michael-addition initiated ring closure (MIRC) reaction is a powerful approach for construction of highly substituted cyclopropane derivatives;³¹ however, when applied to synthesis of cyclopropylstannanes, suffers from poor yields and low facial selectivity. Thus, vinylaziridine **62** was treated with a stannylcuprate reagent affording diastereomeric cyclopropylstannanes **63a,b** in a mixture with non-cyclized Michael addition product **64** (Scheme 21).³²

2.3. Addition of carbenes and carbenoids to olefins

Addition of carbenes to olefins is arguably one of the most powerful methods for the construction of the three-membered ring. This methodology has been applied to the synthesis of cyclopropylstannanes using two different strategies. The first approach involves [2+1] cycloaddition of vinylstannanes and carbenoid species (tin resides at C2 unit). The second utilizes the analogous addition of tin-containing carbenes to olefins (tin resides at C1 unit).

2.3.1. Addition of dihalocarbenes to vinylstannanes.

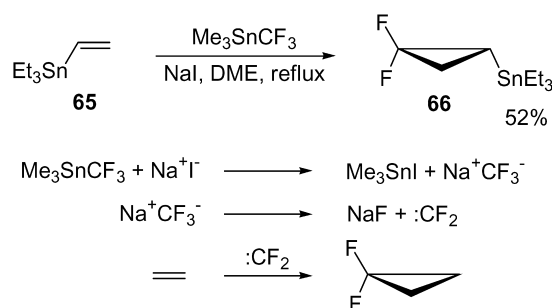
Generally, synthesis of cyclopropylstannanes via addition of dihalocarbenes to vinyltin derivatives cannot be considered as a reliable method, as it often provides low to moderate yields. There were only few reports documenting rather efficient conversion of unsubstituted vinyltin compounds into dihalocyclopropylstannanes. The success in these cases was achieved by applying very mild conditions (non-basic, non-nucleophilic, and non-Lewis-acidic) for generation of carbene species. The dihalocarbenes react smoothly with vinylstannanes **65** and **67**, producing reasonable yields of difluoro- and dichloro-cyclopropylstannanes **66** and **68**, respectively (Schemes 22 and 23).^{33,34}

Normally, standard Zn-assisted procedures for addition of

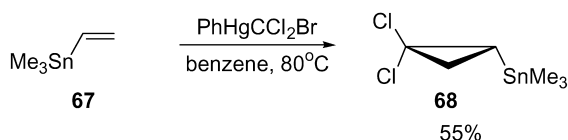
carbenoids to alkenes are not successful when applied to vinylstannanes which do not possess a directing group. These rather sensitive substrates were shown to undergo very sluggish cyclopropanation providing poor yields of corresponding cyclopropanes. The main reason for such inefficiency is zinc halide, generated in situ in this reaction. It causes redistribution of alkyl groups at the tin moiety between the starting vinyltrialkyltin and a product, leading to complicated mixtures of tetraalkylstannanes.^{9,35}

2.3.2. Simmons–Smith reaction. In contrast to moderately efficient additions of carbenoid species to vinyltin derivatives which do not possess directing/activating groups (see above), allylic alcohols possessing tin substituents undergo smooth Simmons–Smith cyclopropanation³⁶ in both stoichiometric and catalytic fashion.

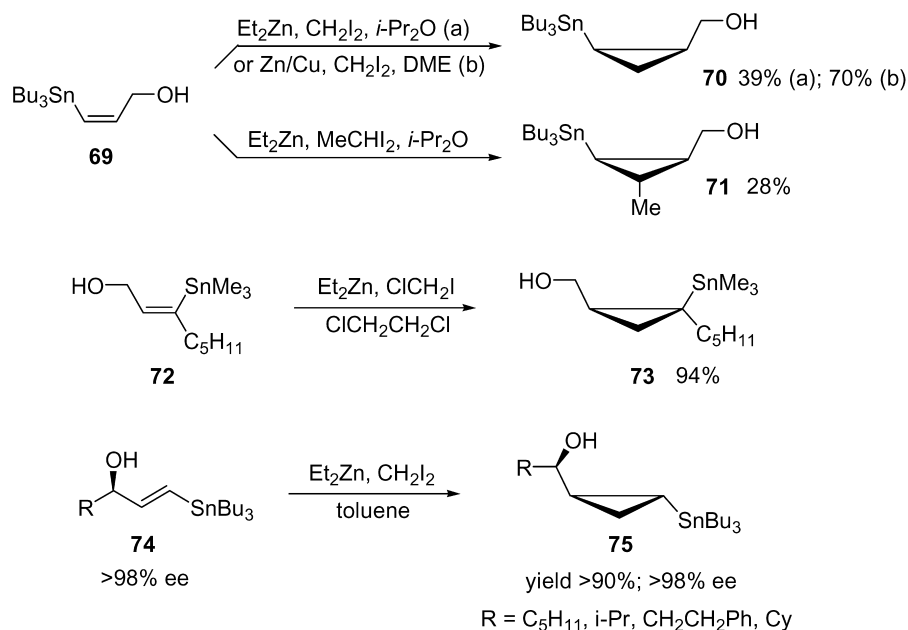
A series of di- and trisubstituted tin-containing cyclopropylcarbinols **70**, **71**, and **73** have been synthesized employing different variations of ‘traditional’ Et_2Zn –dihalomethane combinations (Scheme 24).^{37–41} Optically active cyclopropylstannane **75** has been efficiently



Scheme 22.



Scheme 23.



Scheme 24.

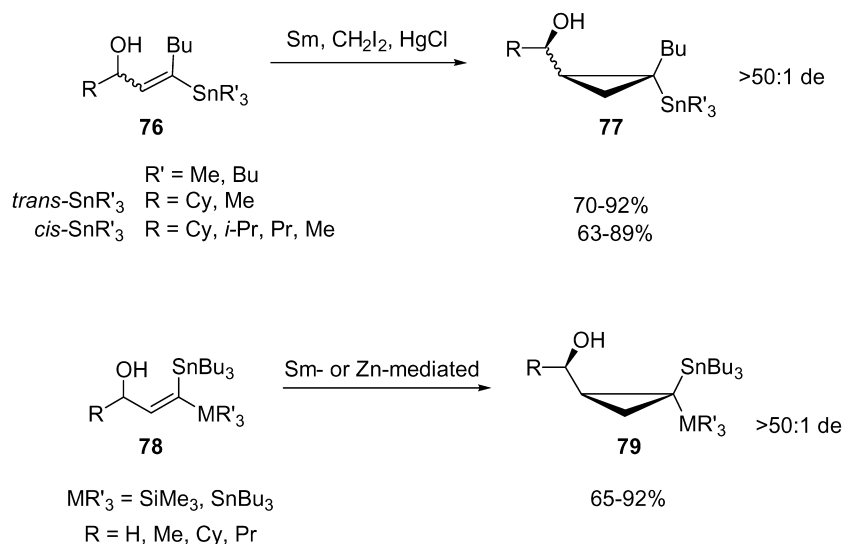
synthesized via highly diastereoselective cyclopropanation of chiral allylic alcohol **74** (Scheme 24).³⁷

Cyclopropanation involving Sm carbenoids have been extensively studied by Lautens.^{42–48} Usually generated from Sm/Hg amalgam or samarium iodide and dihalomethane, these carbenoids are often a more efficient alternative to the reactions with Zn reagents.³⁶ Somewhat disadvantageous is that Sm-promoted cyclopropanation often requires a large excess of Sm reagent to achieve high conversions, and yields can be non-reproducible with different Sm batches. A practical alternative to the Hg activator was found to be TMSCl, which sometimes improves stereoselectivity of the reaction and makes it less sensitive to the Sm source (Scheme 25).

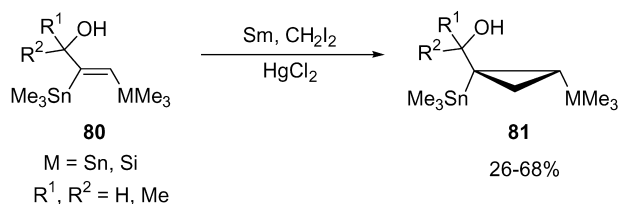
It was demonstrated that olefins bearing silicon and/or tin substituents undergo highly diastereoselective cyclo-

propanation in the presence of Sm. High selectivity in this reaction was observed for *Z*- di- or trisubstituted olefins, whereas disubstituted *E*-alkenes provided moderate selectivity. For a few substrates, a comparison with other cyclopropanating procedures was made.⁴⁴ While secondary allylic alcohol **78** ($\text{MR}'_3=\text{SiMe}_3$) bearing a cyclohexyl substituent reacted smoothly in the presence of Sm metal, the reaction with Zn/Cu couple resulted in predominant destannylation, and SmI_2 produced no reaction at all. In contrast, primary allylic alcohol **78** ($\text{MR}'_3=\text{SiMe}_3, \text{R}=\text{H}$) reacted smoothly in the presence of samarium iodide. This indicates that SmI_2 -mediated cyclopropanation is much more sensitive to steric effects than when metallic Sm is used. Attempted dichlorocyclopropanation of this substrate using chloroform and NaOH produced the corresponding allyl chloride only.

Although the Sm method has been shown to be very efficient



Scheme 25.

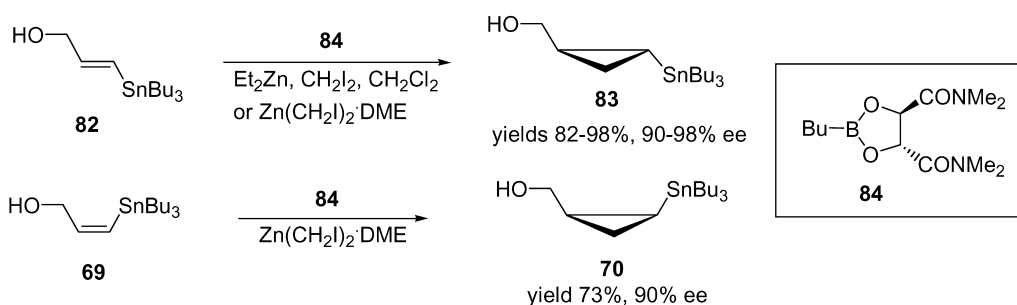


Scheme 26.

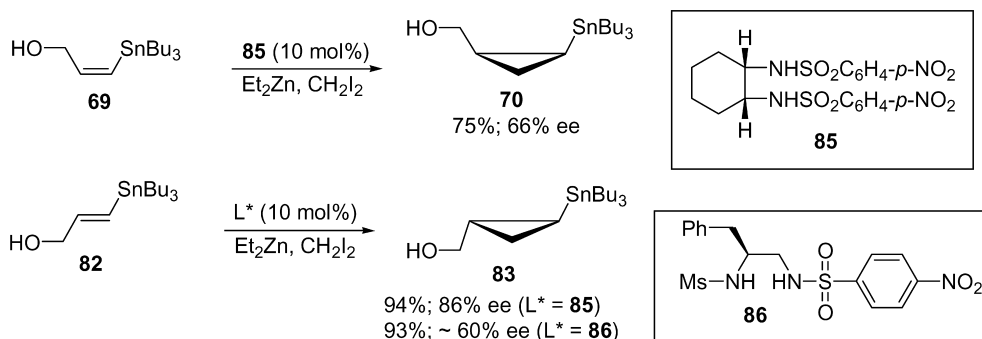
for 1,1-disubstituted alkenyl stannanes, it was only partially applicable to the 1,2-disubstituted substrates, as shown by Mitchell.⁴⁹ Even though primary alcohols **80** give acceptable yields of the products, this method fails when steric demands in the starting olefin increase. Secondary alcohols produced the corresponding products in very low yields, whereas tertiary analogs did not react at all (Scheme 26).

Asymmetric cyclopropanation reaction using stoichiometric amount of chiral dioxaborolane, discovered by Charette,³¹ was effectively applied to the synthesis of tin-containing cyclopropylmethanols.^{50–54} Both *trans*- and *cis*-alkenylstannanes were employed with similar efficiency, producing *trans*- (**83**) and *cis*-cyclopropylstannylmethanols (**70**), respectively, in high yields and enantiomeric excess (Scheme 27).

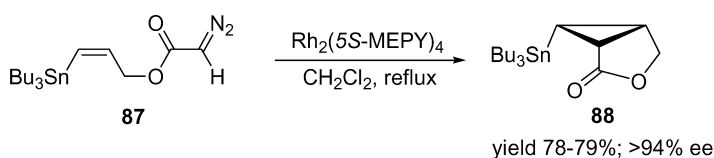
Catalytic enantioselective cyclopropanation of allylic



Scheme 27.



Scheme 28.



Scheme 29.

alcohols developed by Kobayashi was also extended to the synthesis of optically active cyclopropylstannanes. As in the case with other substituents, reaction with *trans*-alkene **82** produced **83** with higher enantiomeric excess (86%), compared to the analogous reaction with *cis*-isomer **69**, which afforded the corresponding cyclopropylstannane **70** with moderate ees only (66%, Scheme 28).⁵⁵ Disulfonamide ligand **86** reported by Imai displayed poorer enantiomeric induction in the reaction with *trans*-alkene **82** (~60% ee) (Scheme 28).⁵⁶

2.3.3. Rh-Catalyzed addition of carbenoid species.

Asymmetric intramolecular cyclopropanation of olefins via the Rh-catalyzed decomposition of diazoesters represents a very powerful approach to optically active cyclopropanes.⁵⁷ Excellent functional group compatibility and mild reaction conditions resulted in extensive application of this method in organic synthesis. Doyle demonstrated that using this methodology, chiral cyclopropylstannanes **88** can be obtained in good yield and very high degrees of enantioselectivity (Scheme 29).^{16,58}

2.3.4. Addition of tin-containing carbenes to olefins.

It should be mentioned that synthesis of cyclopropylstannanes via addition of tin-containing carbenes and carbenoids to olefins has proved less efficient compared to the methods described above, involving addition to vinyltins. Additional

α -carbanion stabilization by stannyl group allowed for preparation of rather stable tin-containing carbenoid species **90**, which was obtained in high yields from bis(diazoacetate) **89** and when reacted with isobutene under photolytic conditions gave cyclopropyltin derivative **91** in moderate yield (Scheme 30).⁵⁹

Insertion of metalated carbenes into olefins was further investigated on series of differently substituted alkenes.⁶⁰ Generally, trimethylstannyl diazoacetate **92** provided rather poor yields of the corresponding cyclopropylstannanes **94** except for the case with isobutene (70%, Scheme 31).

Poor yields were also obtained in the reaction of trimethylstannylcarbene **96** generated by treatment of chloromethyltrimethyltin **95** with LiTMP in cyclohexene-ether solution; norcarane **97** was isolated in 21% yield from a complex mixture of unidentified products (Scheme 32).⁶¹

α -Phosphinosubstituted cyclopropylstannane **99** was

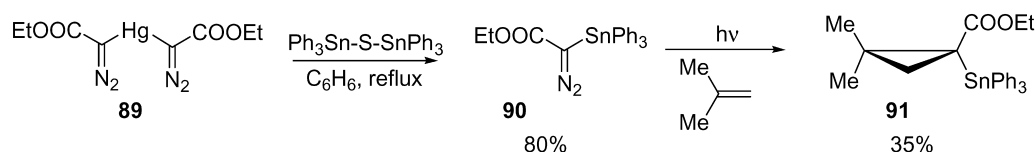
obtained in 55% yield as a mixture of diastereomers in the reaction of stannyl-containing carbenoids with acrylates (Scheme 33).⁶²

2.4. Addition of tin-containing entities across the double bond of cyclopropenes and methylenecyclopropanes

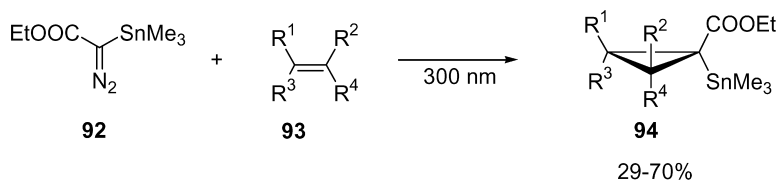
Addition of tin-containing species to the double bond of cyclopropenes and methylenecyclopropanes represents another very attractive and powerful approach to cyclopropylstannanes. Significant strain energy in unsaturated three-membered rings versus parent cyclopropanes is the reason for the high affinity of their double bonds towards various addition reactions.^{63,64} This methodology has been realized in the synthesis of series of cyclopropylstannanes via radical-initiated or transition metal-catalyzed addition of tin hydrides and tin-metal species to the unsaturated precursors.

2.4.1. Addition of tin hydrides to cyclopropenes.

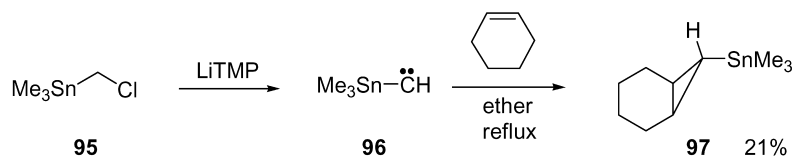
Nakamura demonstrated that radical-initiated *trans*-addition



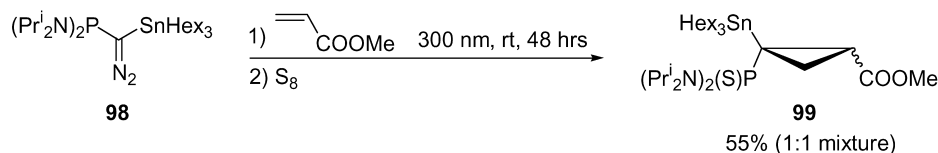
Scheme 30.



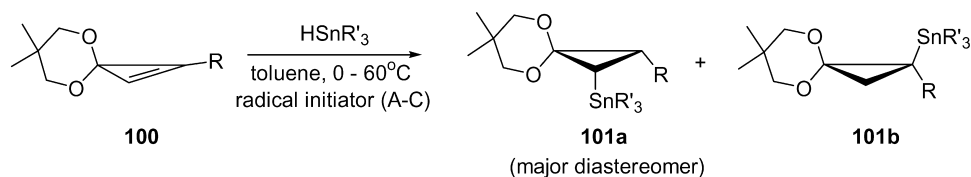
Scheme 31.



Scheme 32.



Scheme 33.



R = H, Me, 1-cyclohexanol, Ph, 1-hexenyl, SiMe₃

R' = Ph, Bu (one example)

Radical initiator A: AIBN, B: Bu₃B or Et₃B, C: ultrasound

Yields 64-100%

10 examples

Scheme 34.

of tin hydrides (mostly triphenyltin hydride) across the double bond of cyclopropenone acetals proceeds smoothly to afford a variety of stannylcyclopropanone acetals in high yields (Scheme 34).^{65,66} It was shown that the β -addition product, cyclopropylstannane **101a**, always formed as a major regioisomer and the regioselectivity depended on the size of an R group; however, mixtures of diastereomers of **101a** were observed (from 20:1 to 6:1 with *cis*-isomer being a major product).

Transition metal-catalyzed hydrostannation of cyclopropenes. In contrast to the *trans*-selective radical-initiated hydrostannation, transition metal-catalyzed addition of tin species across the double bond of cyclopropenes proceeds highly *cis*-selectively to produce multisubstituted cyclopropane derivatives in very good yields (Scheme 35).⁶⁷ A number of transition metals (Ru, Rh, Pt, Pd) were shown to catalyze this reaction; however, palladium catalysts appeared to be superior over other metals: the reaction proceeded extremely fast at temperatures as low as -78°C and allowed for efficient synthesis of up to pentasubstituted cyclopropylstannanes. Great functional group tolerance was demonstrated on substrates bearing ester, ether, silyl, and allyl functionalities. It was shown that the addition across the double bond of cyclopropene is generally controlled by steric factors and proceeds from the least hindered face regardless of the substituents at the tin atom (Me, Bu, Ph). Remarkably, alkoxyethyl substituents displayed a significant directing effect in the hydrostannation of 3,3-disubstituted cyclopropenes preferentially affording

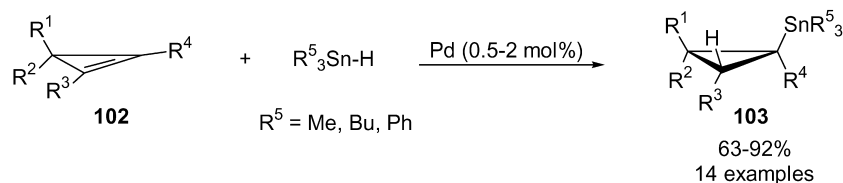
addition products with *syn* orientation of alkoxyethyl and tin substituents.

2.4.2. Addition of ditiin and silicon–tin species to cyclopropenes. De Meijere's protocol for silastannation of methylenecyclopropenes (see below) was adapted to sila- and stannastannation of 3,3-disubstituted cyclopropenes (Scheme 36).⁶⁷ Palladium acetate–*tert*-isooctyl isocyanide⁶⁸ (Walborsky's ligand) catalyst combination effected facile addition of the bimetallic species, which was shown to be entirely sterically controlled.

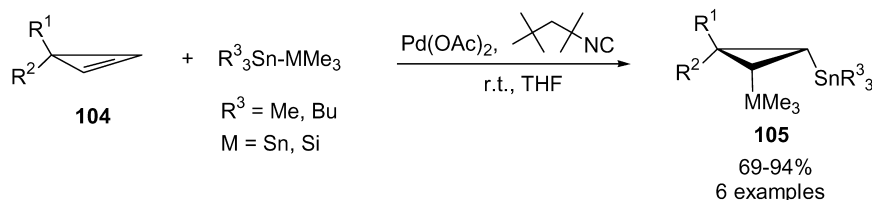
2.4.3. Addition of tin–metal species to methylenecyclopropanes. De Meijere showed that palladium acetate-catalyzed addition of silastannanes to bicyclic propylidene **106** proceeded smoothly in the presence of *tert*-isooctyl isocyanide complex to form stannyl bis-cyclopropanes **107** and **108** (Scheme 37).⁶⁹ It was shown that employment of palladium tetrakis (Pd(PPh₃)₄) in this reaction led to opening of cyclopropyl ring. Interestingly, disproportionation to form disilanes and distannanes occurred, when trimethylsilyl(trimethyltin) was employed (R=Me), resulting in formation and subsequent addition of hexamethyl-ditin to the double bond to give **108** (Scheme 37).⁶⁹

2.5. Miscellaneous

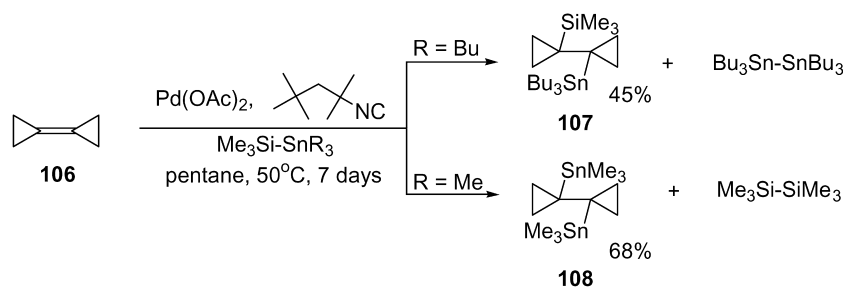
2.5.1. Kulinkovich reaction. A highly diastereoselective synthesis of cyclopropylstannanes using the Kulinkovich cyclopropanation reaction⁷⁰ was reported by Cha



Scheme 35.



Scheme 36.



Scheme 37.

(Scheme 38).⁷¹ Cyclopropanation of carboxamides afforded higher yields than that of corresponding esters, which was explained by higher stability of amides toward nucleophilic attack by Grignard reagents. Furthermore, due to the high propensity of β -stannylcyclopropanols toward ring-opening, silyl protection was necessary to isolate these compounds. Interestingly, esters and carboxamides afforded *cis*- and *trans*-products, respectively, and the stereochemical outcome of this reaction for both esters and amides was opposite to that for alkyl-substituted olefins.^{72,73} The reason for this effect remains unclear and is believed partly to originate from steric effect of the bulky tributyltin moiety. Overall, the method provides reasonable to good yields of amides **111**; however, the reaction with esters suffers from substantial formation of ring-opening products.

2.5.2. Substitution at cyclopropyl ring with tin nucleophiles. When optically active cyclopropylbromide **112** was treated with trimethylstannyl lithium, two products, **113** and **114**, were obtained (Scheme 39).^{74,75} The absolute configuration at C1 for both, **113** and **114**, remained unchanged with no racemization occurred. As a possible route to the formation of by-product **114**, the authors suggested involvement of the cyclopropyllithium intermediate **116**, which resulted from transition complex **115** via metal-halogen exchange. However, all attempts to prove the above assumption by trapping **116** with any other electrophiles failed.

The reaction of tributylstannyl lithium with the magnesium salt of 1-ethoxycyclopropanol **118**, obtained from hemiacetal **117**, proceeded very slowly to afford a low yield of stannylcyclopropyl MOM ether **119** (Scheme 40). The

authors explained the low efficiency of this reaction by competitive decomposition of the tributylstannyl lithium reagent.³⁵

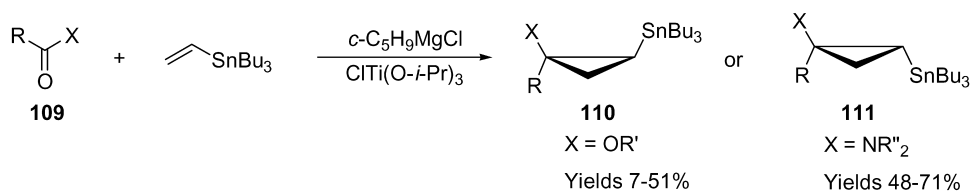
2.6. Cyclopropenylstannanes (synthesis and applications)

Cyclopropenes display comparable reactivity to that observed for terminal acetylenes, towards deprotonation reactions. The increased acidity of the olefinic protons in cyclopropenes is attributed to a high degree of *s*-character of the C–H bond, which results from significant ring strain.⁷⁶

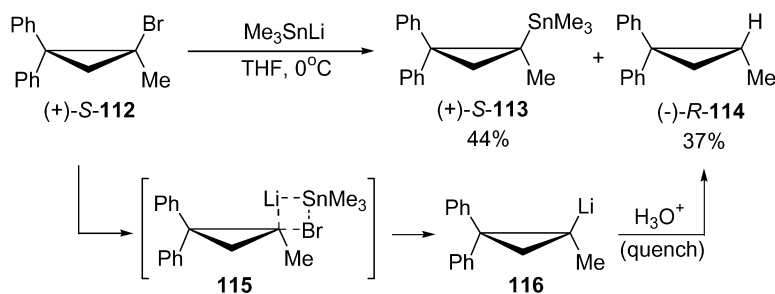
Thus, metalation of both olefinic carbon atoms in cyclopropene **120** by LDA followed by trapping with a metal electrophile afforded disilyl-, distannyl-, and digermyl-cyclopropenes **121a–c**. The yields of bis-silylcyclopropene **121a** obtained by this method was good, whereas preparation of tin (**121b**) and germanium (**121c**) analogs was less efficient (Scheme 41).⁷⁷ Low yields of **121b,c** were attributed to their low stability during isolation due to more labile C–Sn and C–Ge bonds in cyclopropenes.

Efficient monometalation of cyclopropenone acetal **122** was achieved by Nakamura by employment of 1 equiv. of *n*-BuLi at -70°C in THF in the presence of HMPA (Scheme 42).⁷⁸ The latter was shown to be necessary for stabilization of cyclopropenyllithium **123**, and thus for obtaining higher yields of the products.

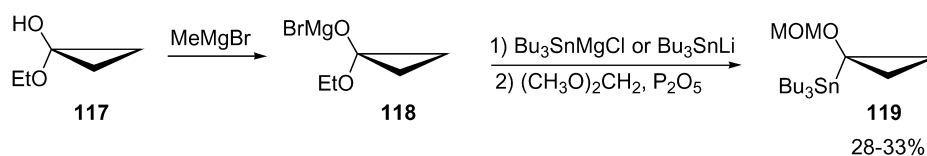
It was found that addition of allylzinc reagents to the stannyl cyclopropenone acetals (CPA), as well as to their silyl and germyl analogs, proceeded much faster than that to



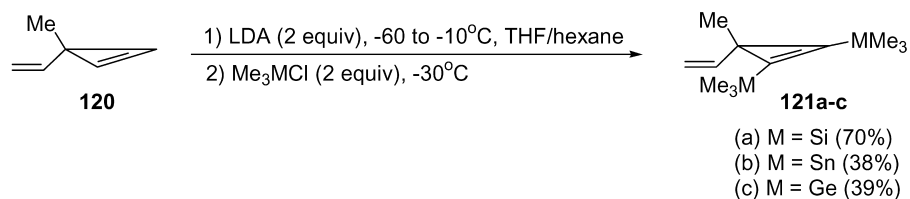
Scheme 38.



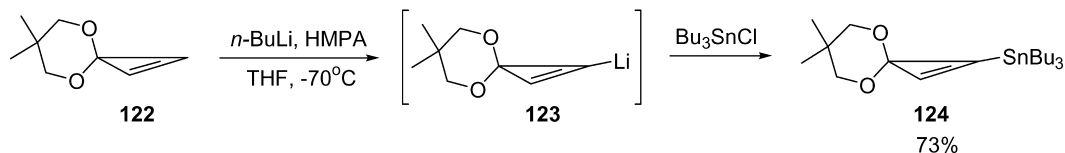
Scheme 39.



Scheme 40.



Scheme 41.



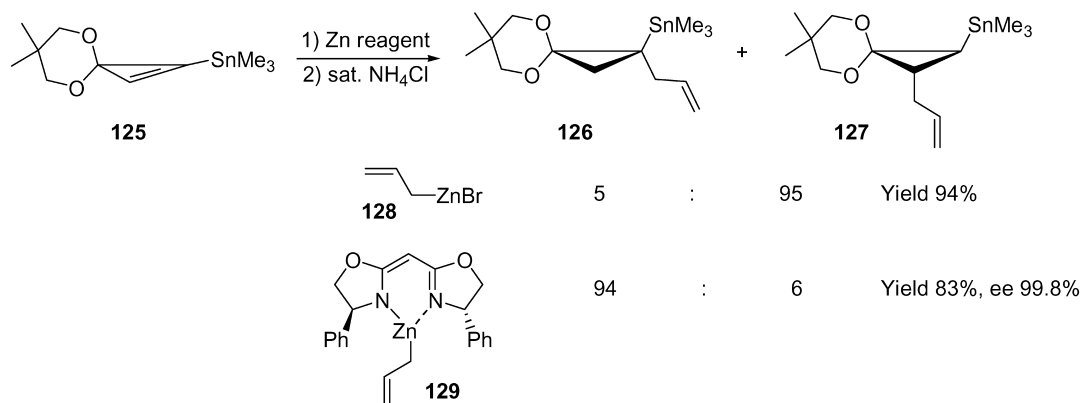
Scheme 42.

carbon-substituted CPAs (Scheme 43).⁷⁹ This observation is in agreement with previously obtained results on carbometalation of olefins.⁸⁰ Addition of allylzinc bromide to trimethylstannyl CPA provided a mixture of two regioisomers **126** and **127** in excellent yield with 95:5 selectivity favoring formation of the β -addition product **127**. The observed regioselectivity was attributed to electrostatic interactions between the Lewis acidic zinc atom and the partially negatively charged carbon atom adjacent to tin. However, the regioselectivity was completely reversed, favoring the geminal product **126**, when allylzinc reagent **129**, bearing a chiral bisoxazoline ligand, was used (Scheme 43). The opposite regioselectivity observed in this case was explained by unfavorable steric interactions between bulky bisoxazoline ligand and trimethyltin substituent. High yields, and very good regioselectivity, taken together with excellent enantioselectivity obtained in the reaction with **129**, makes it a very useful method for the

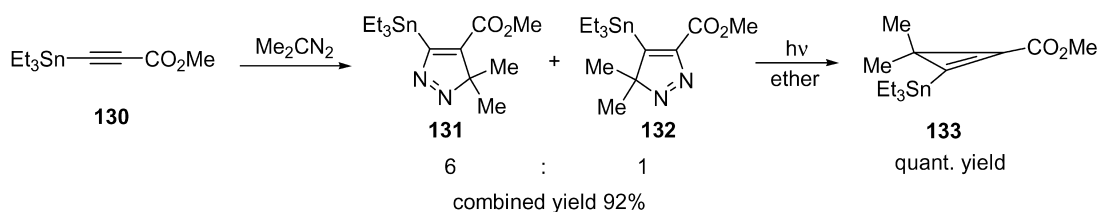
synthesis of allyl-substituted (trimethylstannyl)cyclopropanone acetals.

Guillerm reported a single example of dipolar [2+3] cycloaddition of diazopropane to methyl triethylstannylpropiolate (Scheme 44).⁸¹ The reaction proceeds in very high yield to form isomeric pyrazolines, which undergo extrusion of nitrogen upon irradiation to produce (triethylstannyl)cyclopropenyl carboxylate **133** in quantitative yield.

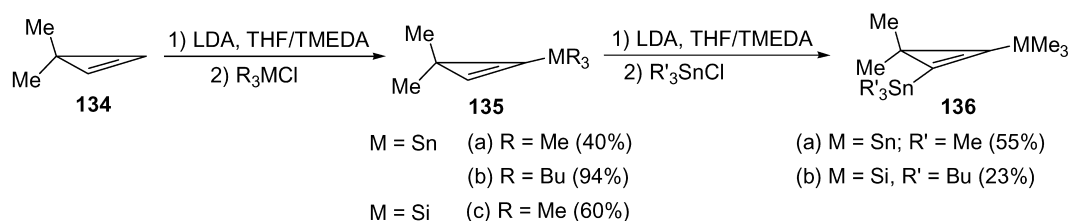
De Meijere reported synthesis of mono- (**135**) and dimetalated cyclopropenes (**136**) using sequential deprotonation/electrophile trapping (Scheme 45).^{82–84} It was recognized that use of LDA as the deprotonating agent allows to avoid undesirable addition of alkyl lithium reagent across the double bond of cyclopropene. Lower yields obtained for monometalated compounds **135a** and **135c** are probably due to volatility of these products (Scheme 45).⁸²



Scheme 43.



Scheme 44.



Scheme 45.

Cyclopropenylstannane **136b** was tested in the Stille cross-coupling reaction with various halides and triflates (Scheme 46). However, good results were obtained only in the reactions with phenyl iodide (98%) and bromide (63%), whereas employment of triflates proved inefficient.⁸⁴ A two-fold coupling of phenyl iodide with distannane **138** afforded diphenylcyclopropene **139**, albeit in low yield (Scheme 46).

3. Applications

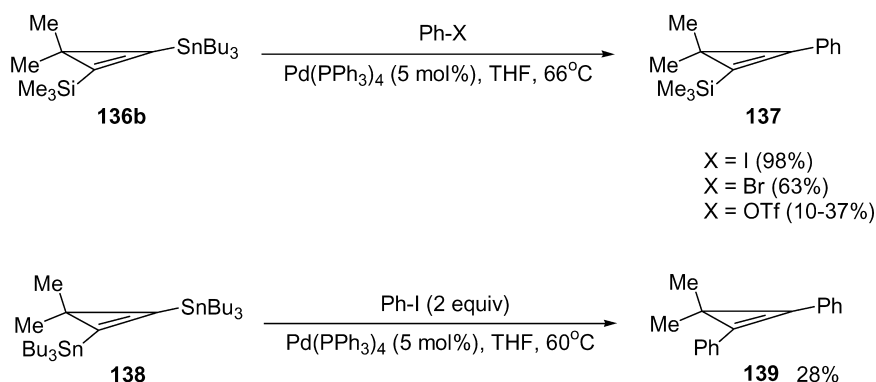
3.1. Transformations with preservation of the cyclopropyl ring

3.1.1. Reactions involving tin–lithium exchange. To date, among all applications, the tin–lithium exchange reaction represents the most important and most extensively used transformation of cyclopropylstannanes. Facile transmetalation with organolithium reagents at temperatures as low as -100°C makes cyclopropylstannanes a convenient precursor of reactive stereodefined (vide infra) cyclopropyllithium species. A few features of this transformation are worth emphasizing. First, while tributyltin group can undergo smooth tin–lithium exchange at geminally unsubstituted and substituted cyclopropylstannanes, transmetalation of the trimethyltin group of the latter proved

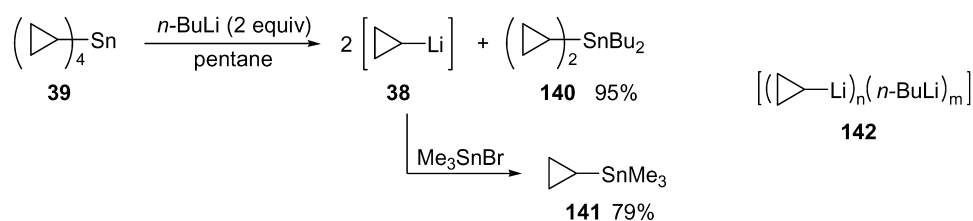
unsuccessful. Second, *syn*-oriented directing groups, such as alkoxyethyl- or carbonyl-containing substituents, facilitate transmetalation; however, generally, bulky *syn*-substituents significantly impede or completely suppress tin–lithium exchange. The resulting cyclopropyllithium species are normally configurationally stable at temperatures as high as 0°C , however, partial or complete epimerization can occur at this temperature if an *anti*-oriented directing substituent is present at the cyclopropyl ring.

The very first experiments on tin–lithium exchange on cyclopropyl series was performed by Seyferth in early 60s (Scheme 47).^{15,85} Solid cyclopropyllithium **38** was obtained via reaction of tetracyclopropylstannane **39** with 2 equiv. of *n*-BuLi in pentane. Cyclopropyllithium **38**, which precipitated from the reaction mixture, was treated with trimethyltin bromide to provide cyclopropyltrimethylstannane **141** in 79% yield. In all reactions performed, isolated solid cyclopropyllithium contained small amounts of *n*-BuLi, which upon quenching with Me_3SnBr produced BuSnMe_3 (2–4%). The presence of *n*-BuLi in the cyclopropyllithium precipitate was explained by the formation of mixed organolithium polymer of type **142**.

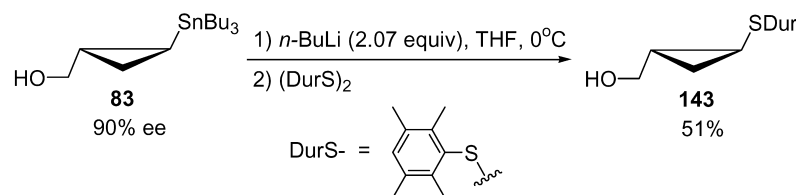
Lithiodestannylation of **83** was performed to introduce an arylthio-substituent in the cyclopropyl ring (Scheme 48).^{52,54}



Scheme 46.



Scheme 47.



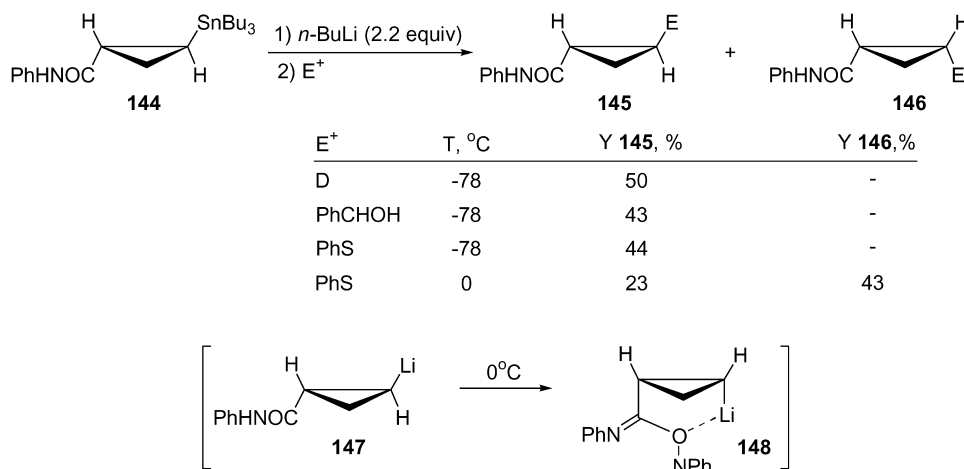
Scheme 48.

Interestingly, although the reaction of **83** was carried out at 0 °C, no epimerization occurred in this case despite the presence of the potentially directing hydroxymethyl substituent.

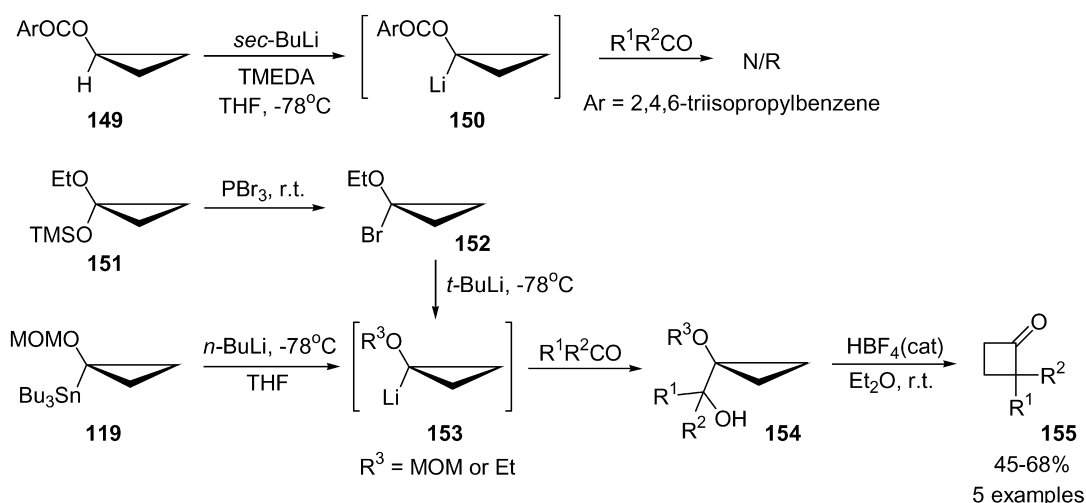
In contrast, Tanaka demonstrated that tin–lithium exchange with **144** proceeds with retention of configuration at low temperature; however, when warmed up to 0 °C, *trans*-**147** isomerizes into *cis*-cyclopropyllithium to form stabilized lithium chelate species **148** (Scheme 49). Experiments involving optically active **144** revealed that tin–lithium exchange performed at –78 °C did not compromise either of the chiral centers of the molecule.⁸⁶

Gadwood investigated various approaches to generation of (1-alkoxycyclopropyl)lithium reagents en route to cyclo-

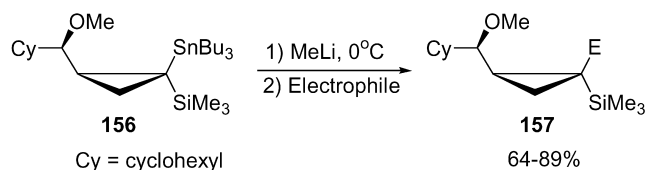
butanone derivatives **155** (Scheme 50).³⁵ Three methods have been explored: deprotonation of hindered cyclopropyl benzoates, halogen–metal exchange of α -haloethers, and transmetalation of alkoxy-cyclopropylstannanes. Direct deprotonation of cyclopropylbenzoate **149** can be easily accomplished with *sec*-BuLi/TMEDA, but the derived organolithium compound did not react with ketones, probably due to steric hindrance. In contrast, easily available 1-bromoethoxycyclopropane **152** has been found to be a convenient precursor for reactive (1-alkoxycyclopropyl)lithium reagents. Metal–halogen exchange between **152** and *t*-BuLi occurred rapidly at low temperature, and the resulting organolithium compound **153** reacted cleanly with a variety of aldehydes and ketones. Likewise, cyclopropylstannane **119** also underwent transmetalation smoothly, leading to desired lithium intermediate **153**. However, the



Scheme 49.



Scheme 50.



Scheme 51.

synthetic usefulness of this route is questionable due to the relative inaccessibility of starting cyclopropylstannane **119**.³⁵

Lautens performed systematic studies on the tin–lithium exchange using a series of different geminal bimetallic cyclopropylstannanes (Scheme 51).^{43,47,48} Investigation of solvent effect on the reaction rate revealed that the transmetalation of cyclopropylstannanes occurred extremely efficiently in a matter of a few minutes when THF or DME were used as solvents: only 1.05 equiv. of methyl-lithium were enough for complete rapid transmetalation in these solvents. Interestingly, the corresponding reactions in ether and hexane were unsuccessful. The analogous reaction with *n*-BuLi (30 equiv.) was complete only after 10 h in THF, and it was considerably slower in DME and did not proceed in Et₂O or hexane at all.⁴³ A number of electrophiles (R₃MCl (M=Sn, Si), CO₂, PhSPh, CHO) were tested to demonstrate the synthetic utility of this reaction (Scheme 51). In most cases, good to high yields of corresponding functionalized cyclopropanes were obtained. Surprisingly, attempts to trap the resulting cyclopropyl-lithium species with TMSCl were unsuccessful.⁴³

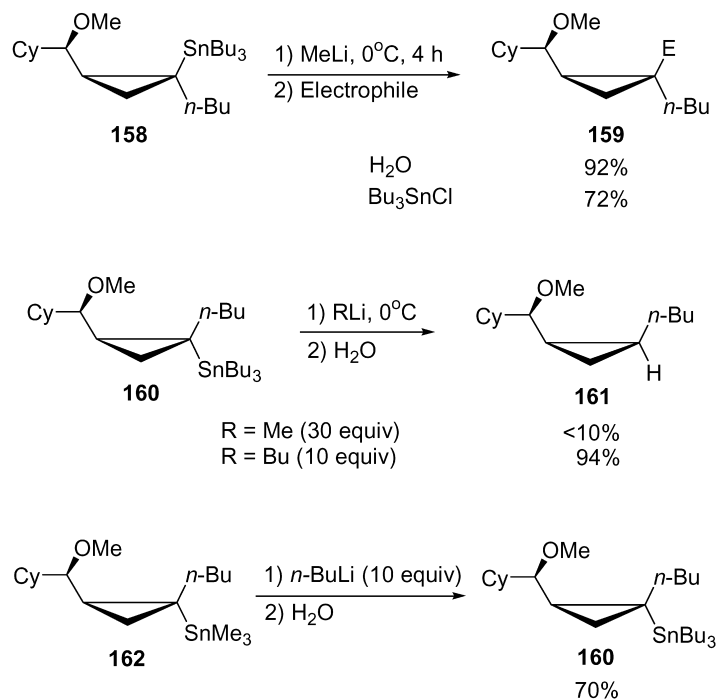
Replacement of a silyl moiety for an alkyl group has a significant effect on the transmetalation rate. Tin–lithium exchange of **158** required 4 h, versus bimetallic stannyl-silylcyclopropane **156** which reacted in 25 min (Scheme 52). The authors suggest that the ability of the silyl group to

stabilize an α-carbanion is responsible for the observed dramatic difference in the reaction rates of **156** versus **158**. The relative stereochemistry of the tributylstannyl group and alkoxyethyl substituent at C-2 was shown to have a significant influence on the rate of transmetalation. In contrast to smooth tin–lithium exchange of *Z*-stannyl-cyclopropane **158** with methyl-lithium, the isomeric *E*-**160** did not undergo transmetalation even with a large excess of MeLi. However, complete transmetalation was achieved with 10 equiv. of *n*-BuLi in THF (Scheme 52). To determine whether the less sterically hindered tin moiety would undergo transmetalation more readily than its tributylstannyl-substituted analog, the reaction with trimethylstannylcyclopropane **162** was attempted. No reaction of **162** with MeLi was observed; however, treatment of **162** with 10 equiv. of *n*-BuLi resulted in unexpected complete methyl to butyl group exchange at the tin moiety (Scheme 52).⁴³

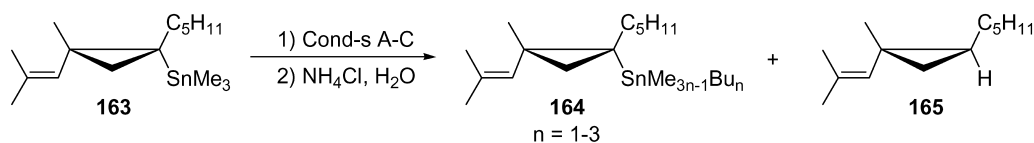
Analogously, lithiodestannylation of tetrasubstituted trimethylstannylcyclopropane **163** also proved unsuccessful (Scheme 53).³⁸ The reaction did not proceed in any conditions tried (methods A–C); instead, methyl to butyl substitution occurred leading to mixtures of products **164**.³⁸

Sensitivity of tin–lithium exchange to facial steric hindrance was studied using diastereomeric cyclopropylstannanes **166** and **168** (Scheme 54). While the substrate bearing less bulky *cis*-methyl group underwent smooth transmetalation with *n*-BuLi at –30 °C,⁸⁷ more sterically hindered **168** with a *cis*-phenyl substituent did not undergo this reaction even at room temperature.⁸⁸

Lautens has also found an interesting example of a retro-Brook type rearrangement⁸⁹ in cyclopropyl series: the silyl group underwent smooth 1,4-migration to C-1 of the cyclopropane under treatment of **169** with MeLi followed



Scheme 52.

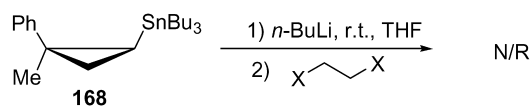
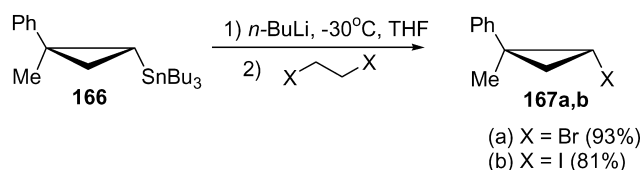


A: *n*-BuLi (2.05 equiv); **163** : **164** : **165** = 15 : 70 : 15

B: MeLi; N/R

C: *n*-BuLi (10 equiv); **164** (*n* = 3) : **165** = 75 : 5

Scheme 53.

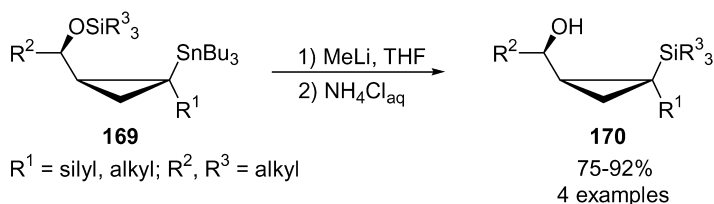


Scheme 54.

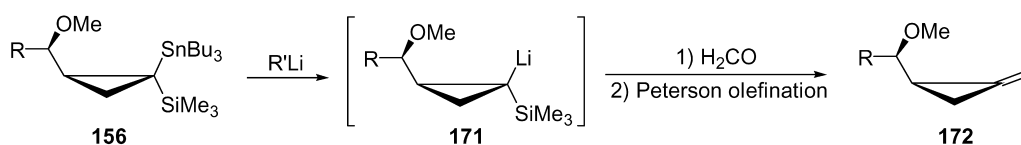
by hydrolytic workup (Scheme 55). Protonation of lithium alkoxide then provided a hydroxyl moiety, which can be used for further transformations.^{43,47}

Another application of bimetallic cyclopropanes en route to cyclopropylidenes has been reported by Lautens. Tin–lithium exchange followed by trapping with electrophile and subsequent Peterson olefination afforded product **172** in unspecified yield (Scheme 56).⁴⁶

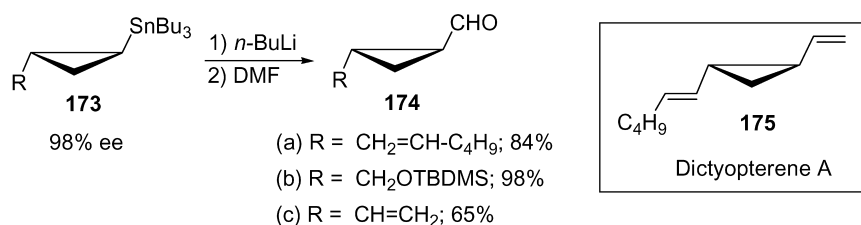
Optically active tributylstannylcyclopropyl synthons **173**



Scheme 55.



Scheme 56.

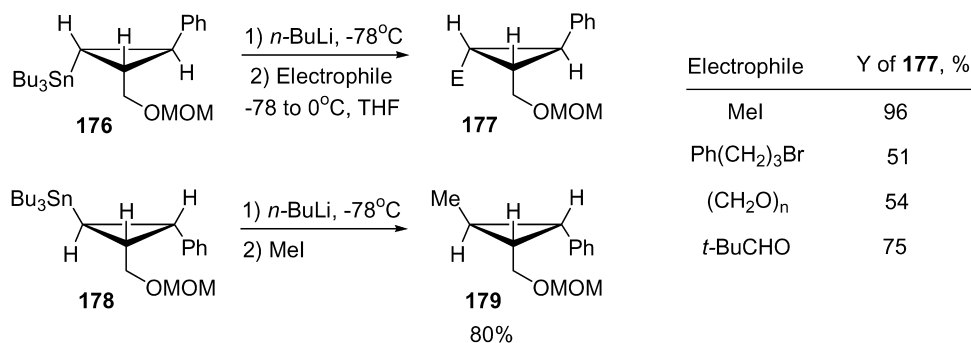


Scheme 57.

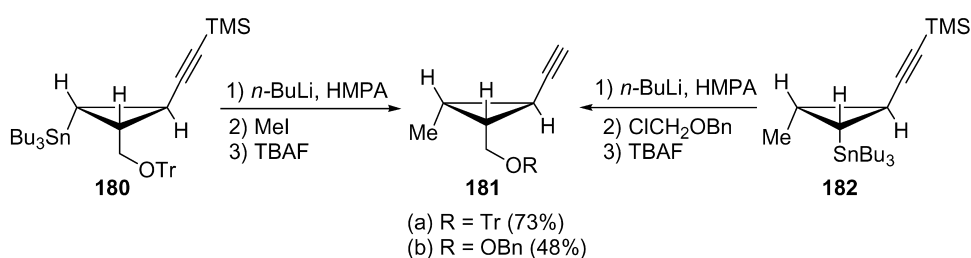
were used as key intermediates in the synthesis of Dictyoptere A (**175**, Scheme 57).⁵³ Transmetalation—trapping with electrophile occurred smoothly in case of all three compounds, providing cyclopropylaldehydes **174** in good to very high yields (Scheme 57).

Mori investigated transmetalation of 1,2,3-trisubstituted cyclopropanes **176** and **178**, and subsequent trapping of the resulting cyclopropyllithium species with various electrophiles (Scheme 58).²⁶ It was shown that quenching with MeI proceeded smoothly affording a very high yield of the methylated product, whereas other electrophiles required addition of HMPA, still providing moderate to good yields of the products. The fact that cyclopropylstannane **176** also undergoes methylation producing **177** in high yield indicates that transmetalation tolerates *cis*-oriented alkoxy-methyl substituents.

The extension of this methodology was demonstrated later by Mori in synthetic studies toward Ambruticin (Scheme 59).²⁷ Two alternative approaches to the required key intermediate **181** employing different flavors of the tin–lithium exchange motif at the cyclopropyl ring were explored. Thus, tributylstannylcyclopropane **180** was



Scheme 58.



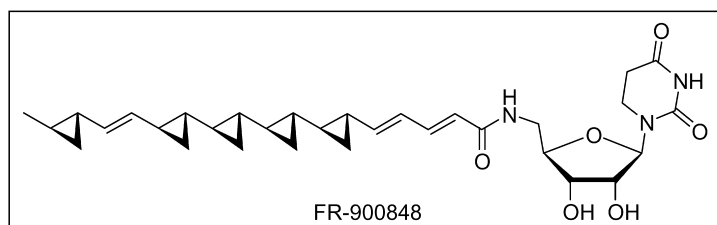
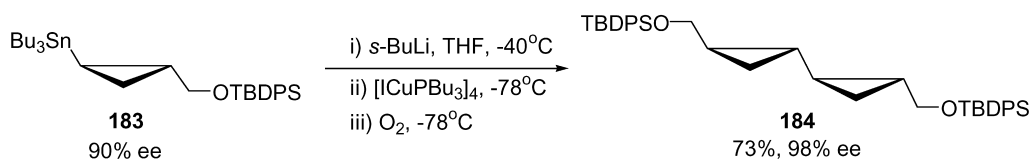
Scheme 59.

treated with *n*-butyllithium followed by trapping with MeI and desilylation to provide **181a** in 73% yield. Alternatively, lithiodestannylation of cyclopropane **182** produced lithium derivative, which upon alkylation with chloromethylbenzyl ether and deprotection with TBAF afforded **181b** in 48% overall yield (Scheme 59).

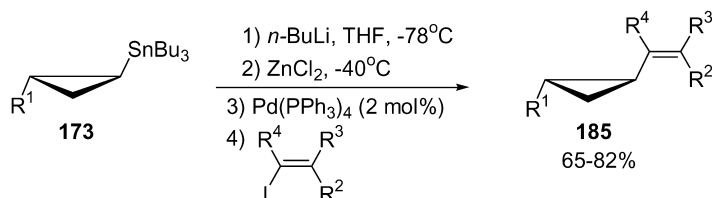
Tin–lithium exchange followed by oxidative homo-coupling of two cyclopropyllithium species was employed by Falck as an efficient protocol in the assembly of polycyclopropane framework of antibiotic FR-900848 (Scheme 60).⁵⁰ Tin group of silylated cyclopropylmethanol

183 was transmetalated with *sec*-BuLi and the resulting lithium anion was treated with [ICuPBu₃]₄ and then subjected to an oxygen-induced dimerization at low temperature to give *syn-trans*-bis-cyclopropane **184**. The observed enrichment in enantiomeric excess is a result of a statistical distribution of products and represents a variant of the Horeau amplification principle.⁹⁰

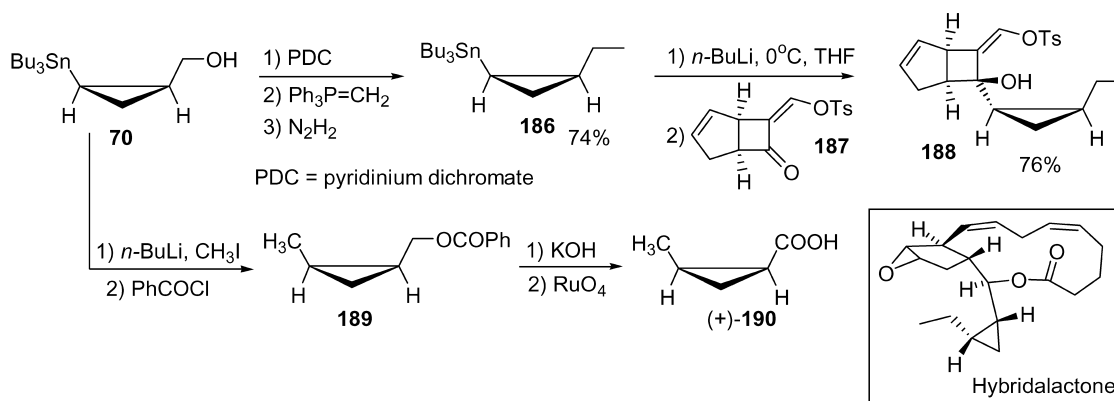
In synthetic studies toward sesquiterpenoids (±)-prezizanol and (±)-prezizaene, Piers demonstrated that cyclopropylstannanes **173** can efficiently be employed as remote precursors for Negishi cross-coupling reactions with various



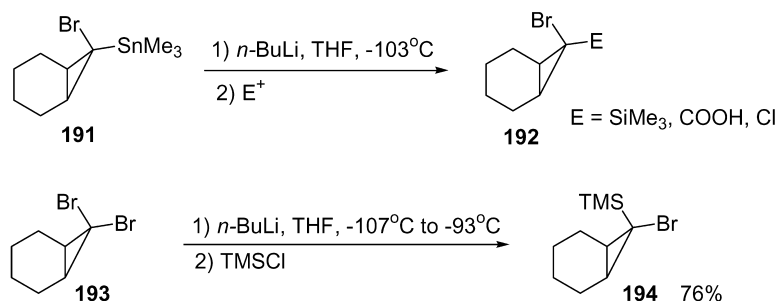
Scheme 60.



Scheme 61.



Scheme 62.



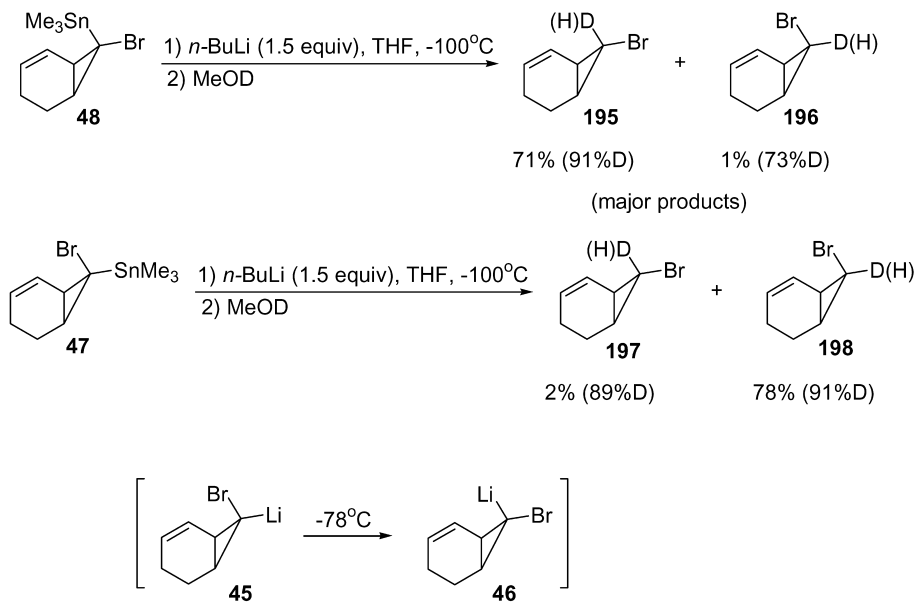
Scheme 63.

alkenyl iodides (Scheme 61).⁹¹ Tin–lithium exchange followed by Li–Zn transmetalation afforded cyclopropylzinc halide species, which smoothly underwent stereoselective Pd-catalyzed coupling with vinyl iodides to efficiently produce corresponding vinylcyclopropanes **185**.

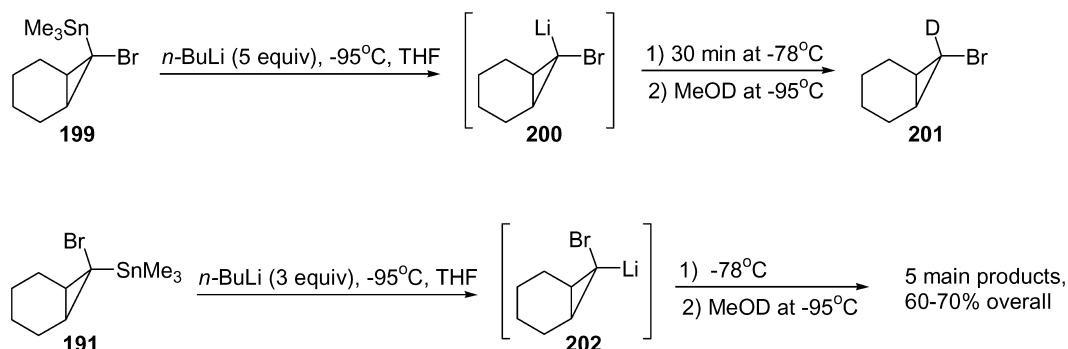
Corey took advantage of the facile tin–lithium exchange of *cis*-tributylstannylcyclopropane **186** in the total synthesis of Hybridalactone (Scheme 62).^{40,41} A coupling reaction between β -tosyloxyenone **187** and cyclopropyllithium generated from **186**, afforded a good yield of one of the

key intermediates **188**. To unambiguously establish the absolute configuration of the starting stannylcyclopropane **70**, the sequence involving tin–lithium exchange, electrophile trapping, esterification and oxidation was realized to provide known acid (+)-**190**.

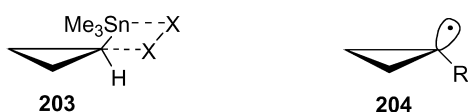
Seyferth demonstrated for the first time the possibility of performing a stereoselective transmetalation of tin in the presence of a geminal bromine substituent (Scheme 63).¹¹ Thus, transmetalation of *syn*-7-bromo-*anti*-7-trimethylstannylnorcaradiene **191** followed by trapping with electrophile produced *anti*-TMS-norcaradiene **192** as a sole



Scheme 64.



Scheme 65.



Scheme 66.

stereoisomer. Alternatively, isomeric *anti*-7-bromo-*syn*-7-TMS-norcarane **194** can stereospecifically be prepared by the metal–halogen exchange of dibromide **193** with $n\text{-BuLi}$, followed by treatment with TMSCl .

Analogously, Warner demonstrated that treatment of either epimer **48** or **47** with $n\text{-BuLi}$ at -100°C followed by MeOD workup provided deuteriodestannylated products with retention of configuration with trace amounts of inverted isomers detected (Scheme 64).²⁴ However, when lithium derivatives obtained from **48** or **47** were allowed to warm up to -78°C prior to MeOD quenching, mixtures of several products with variable ratios, depending upon reaction time, were obtained. It was proposed that irreversible isomerization of **45** into **46** takes place at this temperature thereby providing mixtures of *syn*- and *anti*-isomers along with some amounts of dimeric products (Scheme 64).²⁴

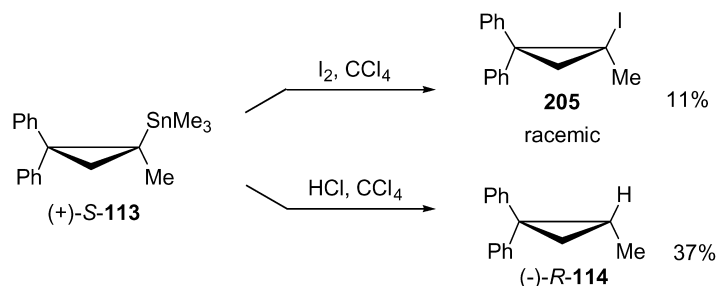
Likewise, lithium derivatives **200** and **202**, obtained from stannanes **199** and **191**, respectively, displayed different stability when allowed to warm up from -95 to -78°C (Scheme 65).⁹² Under these conditions, **200** provided single product **201**, whereas **202** produced, depending on reaction time, up to five main products. The results of these experiments confirmed that, although being relatively slow, the isomerization **202** to **200** takes place; however, its mechanism is unclear. These results are in accord with those obtained on the unsaturated series (see above).

3.1.2. Tin–halogen exchange reactions. While tin–

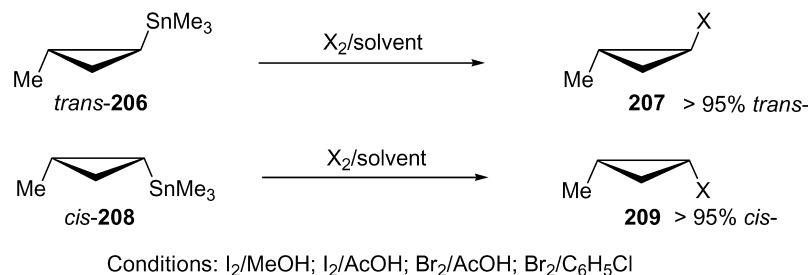
lithium exchange of cyclopropylstannanes proceeded with complete retention of configuration, regardless of the substitution pattern, a dramatic difference was observed in the stereochemical outcome of the tin–halogen exchange reactions. Thus, when α -unsubstituted cyclopropylstannanes provided corresponding halogenated products with complete retention of configuration at the reaction center, the α -substituted analogs normally led to racemic products. It was proposed that these two types of cyclopropylstannanes undergo tin–halogen exchange via different mechanisms. An ionic pathway via a four-centered transition state **203** leading to retention of configuration was proposed for α -unsubstituted substrates (Scheme 66). Formation of tertiary radical species of type **204**, capable to undergo epimerization leading to racemic mixtures, was suggested for reaction involving α -substituted analogs. While the former pathway was supported experimentally, no studies were performed to confirm the latter pathway.

First experiments on tin–halogen exchange were performed by Sisido in 1967.⁷⁴ The authors observed complete racemization when optically active **113** was subjected to iodine in carbon tetrachloride (Scheme 67). Reaction of **113** with hydrogen chloride, however, resulted in formation of protiodestannylated product **114** with complete retention of configuration. Homolytic cleavage of the tin–carbon bond and formation of configurationally unstable cyclopropyl radical species were proposed to account for racemization observed for the iodination reaction. Protiodestannylation of **113** was believed to proceed via an ionic mechanism.⁷⁴

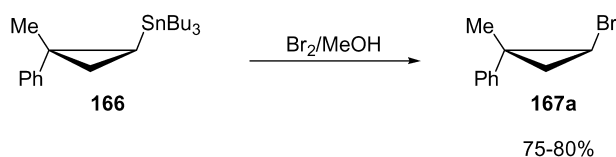
Shortly after Sisido's report, Baekelmans published his results on tin–halogen exchange using geminally unsubstituted *trans*- and *cis*-cyclopropylstannanes **206** and **208** (Scheme 68).^{93,94} Both reactions proceeded with retention of configuration regardless of the solvent or



Scheme 67.



Scheme 68.



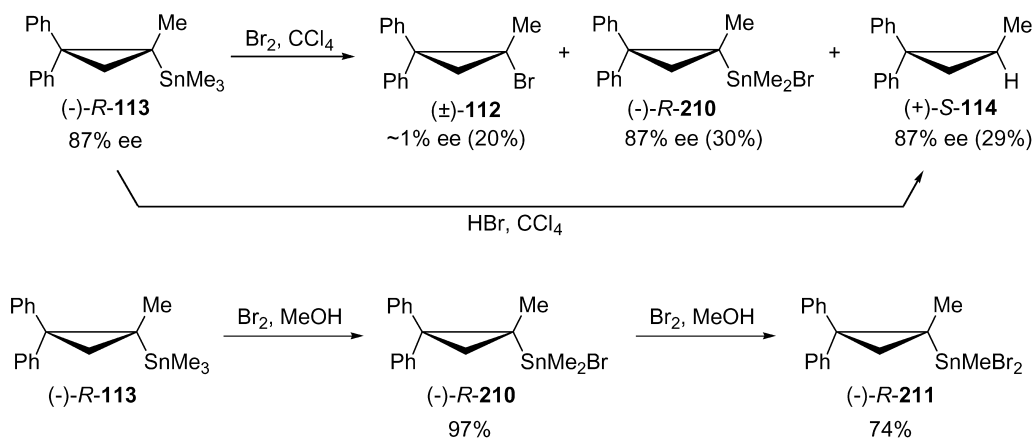
Scheme 69.

halogen source used. However, a dramatic solvent effect on the rate of halodemetalation was observed; the reaction proceeded very quickly in chlorobenzene, and considerably slower in methanol.

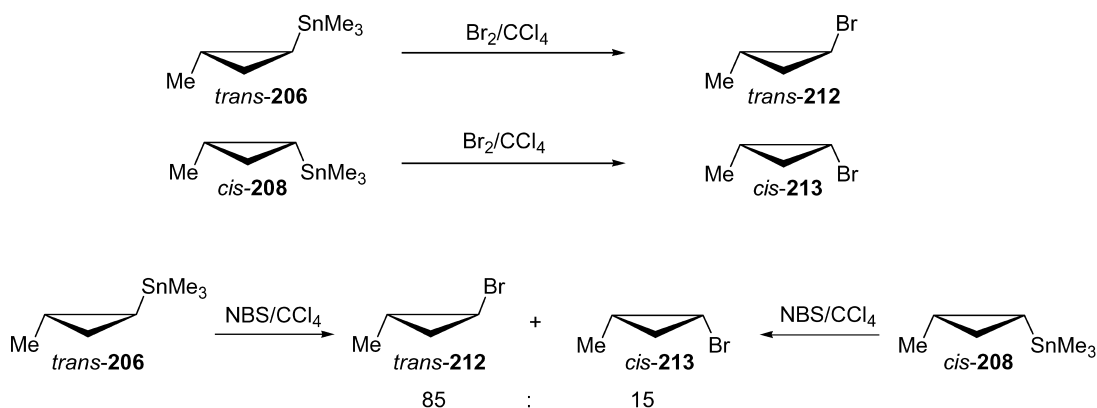
Analogously, the tributyltin group in trisubstituted **166** smoothly underwent tin–bromine exchange upon treatment with bromine in methanol to produce bromocyclopropane

167a with complete retention of configuration (Scheme 69).⁸⁸

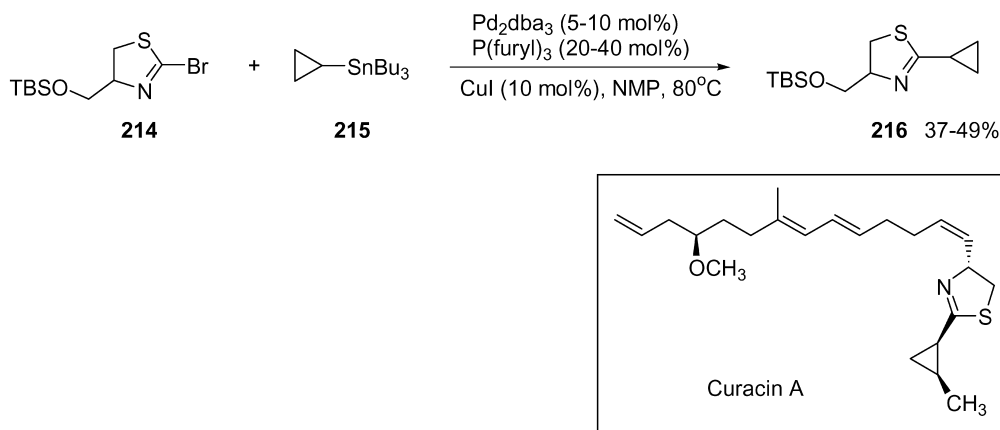
Baekelmans' results prompted Sisido to reinvestigate the halodestannylation reaction of **113** (Scheme 70).⁷⁵ Again, treatment of **113** with bromine in carbon tetrachloride resulted in racemic product **112** along with bromodimethylcyclopropylstannane **210** and protiodestannylated product **114**; formation of the latter resulted from the reaction of **113** with HBr, formed in situ. When the reaction of **113** with bromine was carried out in methanol, a selective cleavage of the tin–methyl bond occurred to produce **210** in nearly quantitative yield. Treatment of **113** with two equivalents of bromine resulted in exchange of an additional methyl group with bromine to give **211**. No racemization occurred during these transformations.



Scheme 70.



Scheme 71.



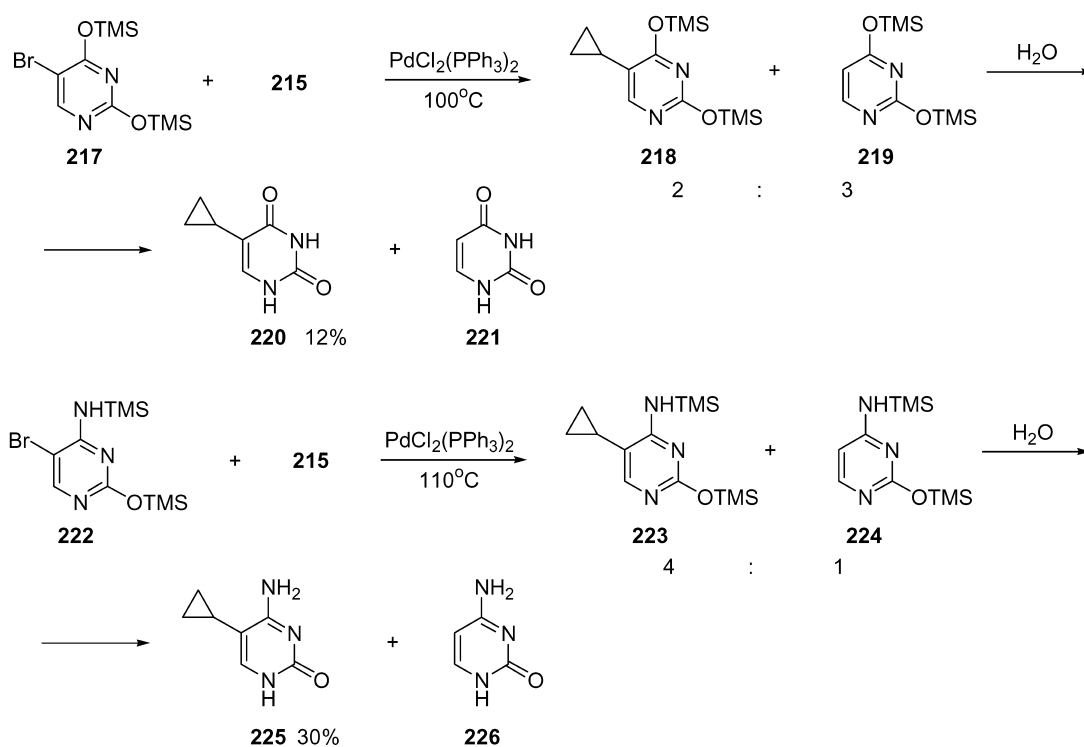
Scheme 72.

However, in the analogous reaction with geminally unsubstituted cyclopropyl derivatives **206** and **208** under the same reaction conditions, complete retention of configuration was observed (Scheme 71).⁹⁵ Sisido speculated that formation of a stable, tertiary cyclopropyl radical in case of **113** favored a radical pathway via intermediate **204**, whereas **206** and **208** reacted via a four-centered transition state **203** (Scheme 66). Under conditions of radical brominolysis (NBS, AIBN), a 85:15 mixture of *trans*-**212** and *cis*-**213** was produced regardless on whether *cis*-**208** or *trans*-**206** were employed (Scheme 71).

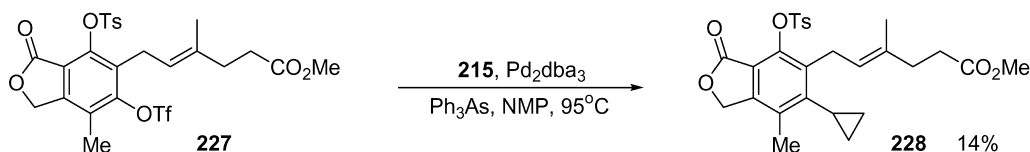
3.1.3. Cross-coupling reactions. Introduction of cyclopropyl moiety via the Pd-catalyzed cross-coupling reaction of cyclopropylstannanes with electrophilic counterparts potentially can serve as a very attractive approach to synthesis of complex cyclopropane-containing molecules.

Although a number of reports document attempts on Stille cross-coupling reactions of cyclopropylstannanes with different halides and triflates, unfortunately, most of the known examples provide unsatisfactory low yields of the coupling products. In contrast to cyclopropylboronate analogs, which are well-known to readily undergo Suzuki cross-coupling reaction,⁹⁶ cyclopropylstannanes display very poor reactivity primarily as a result of sluggish transmetalation of a weakly nucleophilic cyclopropyltin moiety.

Thus, in studies toward Curacin A, Romo investigated the possibility of installing a cyclopropyl moiety in thiazoline ring using Stille cross-coupling reaction (Scheme 72).⁹⁷ Under standard Stille coupling conditions 2-cyclopropylthiazoline **216** was obtained as an inseparable mixture with pyrroline (~4:1) in low yield. Addition of copper iodide allowed for increasing yields of reactions and



Scheme 73.



Scheme 74.

improving selectivity providing **216** in moderate yields (Scheme 72).

Cyclopropyluracil **220** and cyclopropylcytosine **225** were prepared by Stille coupling of pyrimidine **217** and trimethylcytosine **222** with tributylstannylcyclopropane **215** (Scheme 73). Both reactions provided low yields of desired cyclopropane derivatives **220** (12%) and **225** (30%), and were accompanied by formation of substantial amounts of dehalogenated by-products **221** and **226**, respectively.⁹⁸

The coupling of triflate **227** with tributylstannylcyclopropane provided poor results despite the use of a labile triphenylarsine ligand (Scheme 74). Apart from slow transmetalation at cyclopropyltin, the significant steric bulk created by two *ortho*-substituents at the aryl ring may also impede the oxidative addition step in this reaction, thus additionally accounting for the very low yield of coupling product **228**.⁹⁹

Cross-coupling of neat tributylstannylcyclopropane with very electron poor aryl iodide **229** under various conditions was unsuccessful (Scheme 75).¹⁰⁰ Reaction of **229** with tetracyclopropylstannane **39** was also unsuccessful with a series of different solvents and palladium catalysts. Attempted cross-coupling with triflate **230** led to the triflate cleavage to form the corresponding phenol only.

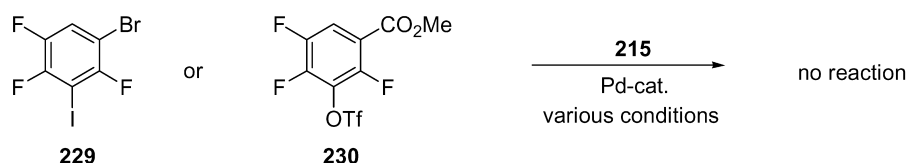
Cross-coupling reaction of triflate **231** with **215** also proved inefficient; harsh reaction conditions as well as a compli-

cated isolation procedure allowed for synthesis of coupling product **232** in trace amounts only (Scheme 76).¹⁰¹

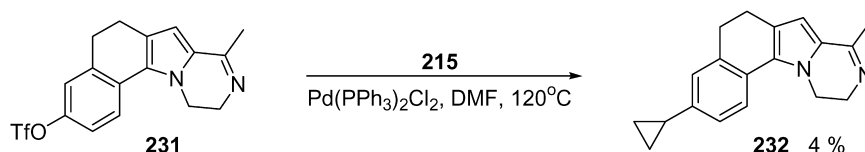
While Stille cross-coupling reaction on cyclopropylstannanes normally provides poor yields or no product at all, the oxidative homocoupling of two cyclopropyltin derivatives appeared to be a much more efficient method, as demonstrated by Itoh.³⁷ Conditions, originally reported by Liebeskind for the palladium-catalyzed oxidative dimerization of stannylquinones,¹⁰² were successfully applied for coupling of **233** furnishing the corresponding bis-cyclopropane **234** in 66% yield (Scheme 77).

3.1.4. Miscellaneous. Addition of dihalocarbenes to 2-trimethylstannyl methylenecyclopropane **12** occurs stereospecifically from the less hindered site to form *anti*-**235** as a single product (Scheme 78).⁶ However, addition of dichlorocarbene to methylenecyclopropane **237** bearing bulky cyclopropyl substituents at the double bond produces a mixture of *syn*- and *anti*-products **238** and **239**, respectively, with the *anti*-isomer being a major component.¹⁰³ Interestingly, with other substituents in place of the trimethyltin group in **237** (i.e., TMS, Br, alkyl) the reaction was completely stereospecific, affording the corresponding *anti*-product only. These results are explained by the greater length of the C–Sn bond, which makes the steric effect of this substituent less pronounced.

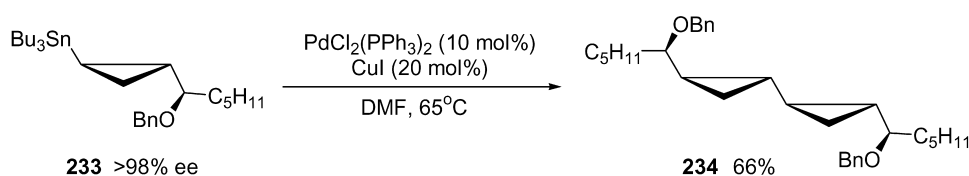
In the [2+2] cycloaddition reaction of dichloroketene with **240**, formation of more hindered isomer **242** was observed



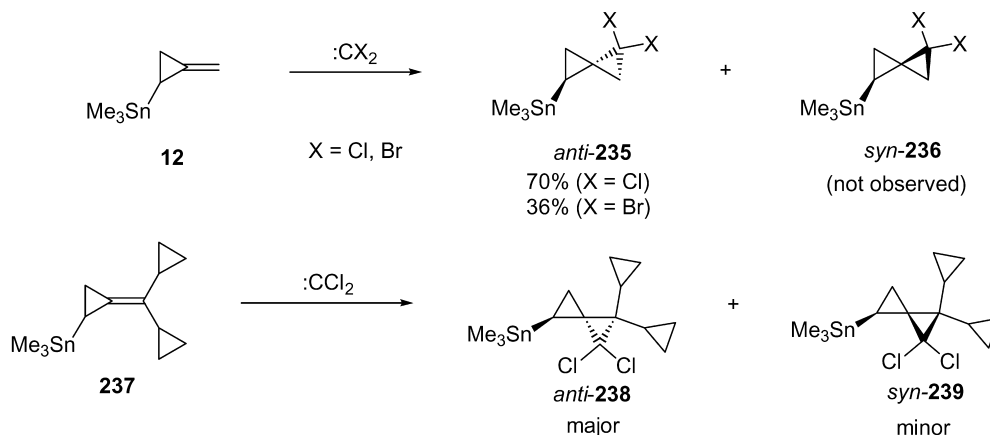
Scheme 75.



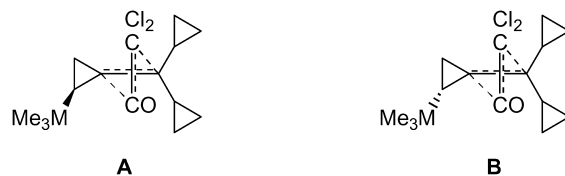
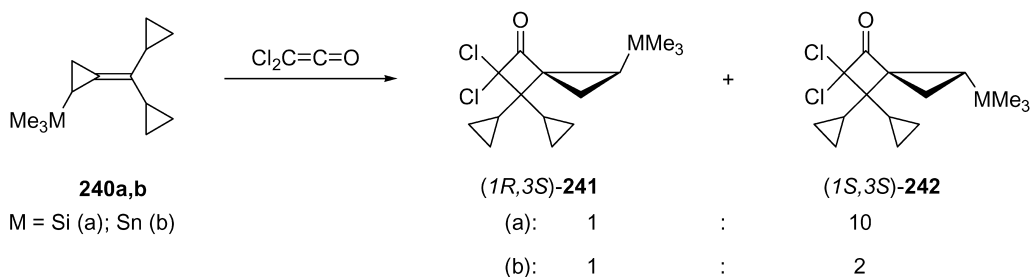
Scheme 76.



Scheme 77.



Scheme 78.

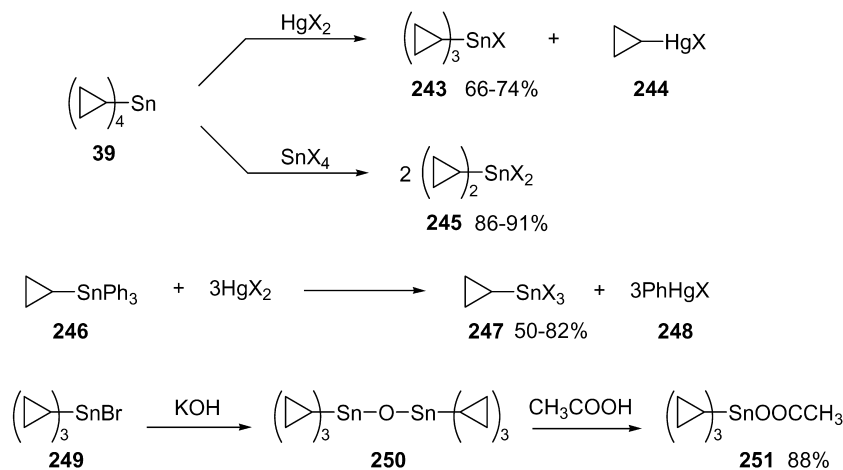


Scheme 79.

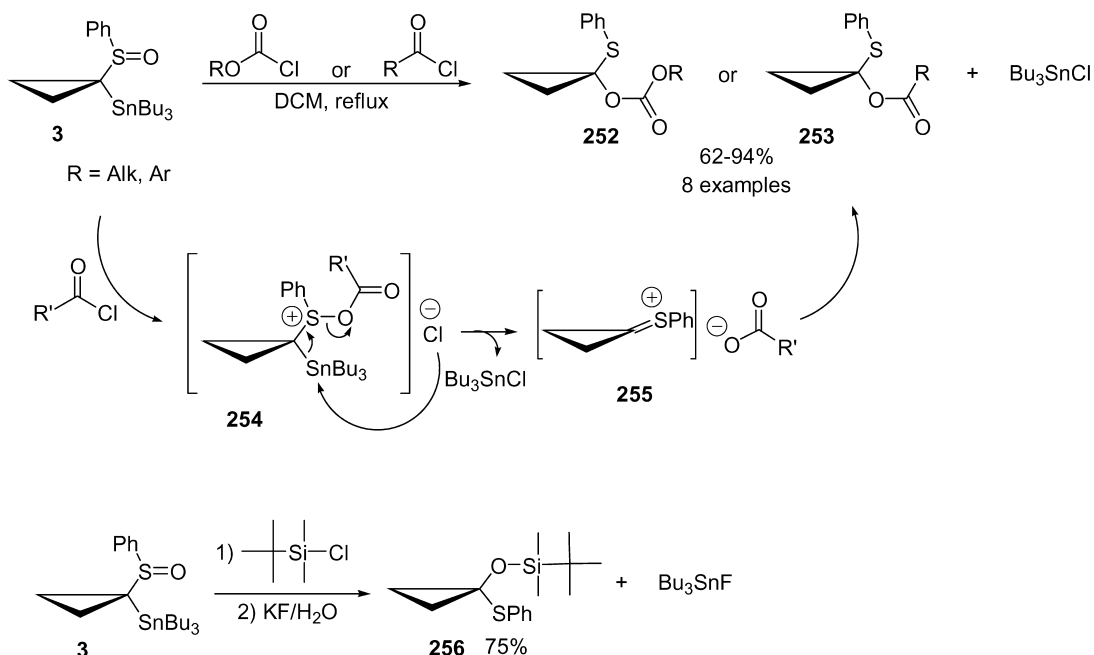
in case of both trimethylsilyl and trimethylstannyl substituents (Scheme 79). As expected,¹⁰⁴ such stereoselectivity is a result of a more favorable transition state **B**, in which dichloroketene is approaching from the face opposite to that occupied by a bulky substituent. Relatively strong steric control observed for **240a** deteriorated in the case of tin analog **240b**, which again is attributed to the

greater length of the carbon–tin bond as compared to that for the carbon–silicon bond.¹⁰⁵

Seyferth demonstrated that tetracyclopropyltin **39** can undergo disproportionation reactions with mercury or tin halides to produce corresponding cyclopropylmercuric **244** and -tin chlorides **243** and **245**, respectively (Scheme 80).¹⁰⁶



Scheme 80.

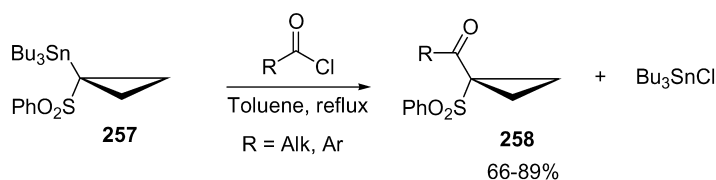


Scheme 81.

The reaction with **246** confirms that phenyl group is cleaved from tin much more readily than is the cyclopropyl group. Tricyclopropyltin acetate **251** was obtained in 88% yield by the reaction of **249** with potassium hydroxide followed by treatment with glacial acetic acid (Scheme 80).

Pohmakotr reported the destannylation Pummerer-type rearrangement of 1-phenylsulfinyl-1-tributylstannylcyclopropane **3** (Scheme 81).^{29,107} The reaction proceeds analogously to the previously reported rearrangement of α -silyl substituted cyclopropylsulfoxides¹⁰⁸ and allows for good to high yields of acyl derivatives **252** or **253**. The mechanism of this reaction involves acylation of α -stannyl sulfoxide to form acylsulfoxonium species **254** followed by the attack of chloride ion at the tin moiety, providing thionium salt **255**. The recombination of the thionium ion with the carboxylate gives products **252** or **253**. Following essentially the same pathway, α -siloxy cyclopropane **256** was obtained from **3** in the presence of TBDMS-Cl in 75% yield (Scheme 81).

Acyldestannylation of α -stannylsulfone **257** proceeded smoothly in refluxing toluene affording 1-acyl-1-sulfonylcyclopropanes **258** (Scheme 82).⁴ While acyl chlorides provided good yields of the corresponding products, the less reactive chloroformates did not undergo this transformation at all.



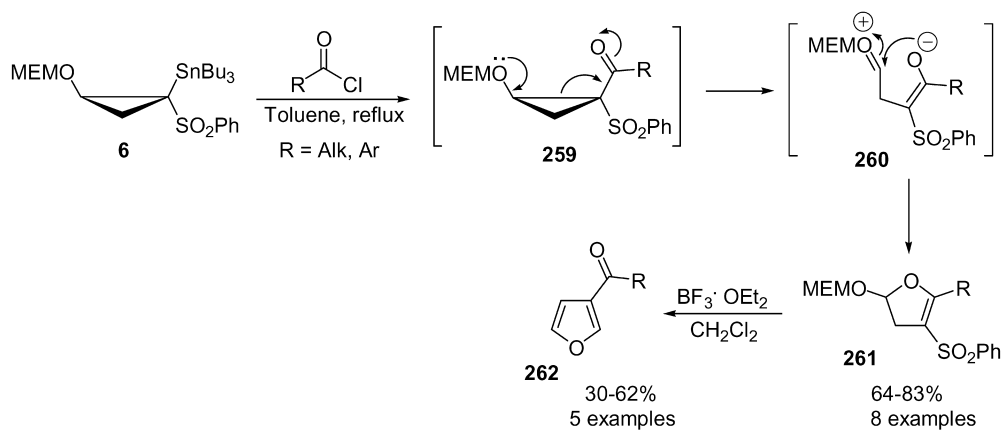
Scheme 82.

3.2. Reactions involving opening of the cyclopropyl ring

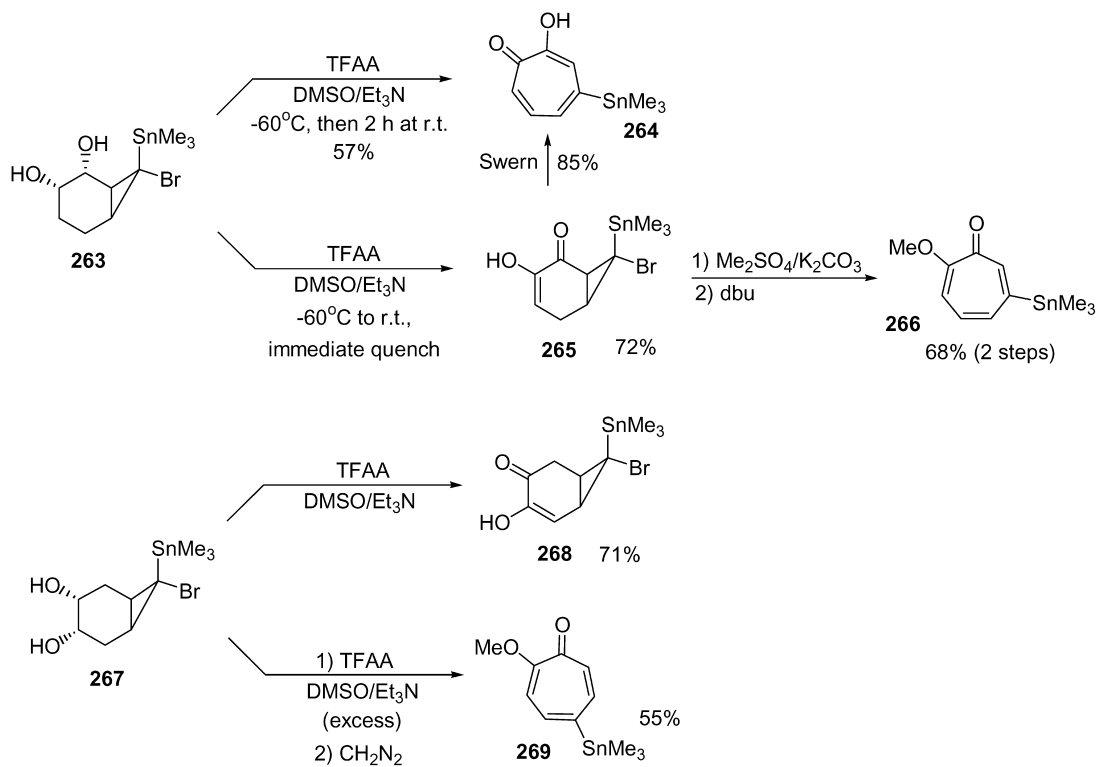
3.2.1. Ring opening reactions involving ionic intermediates. Destannylation acylation of MEM-protected cyclopropanol **6** followed by a facile ring opening of the resulting 1,2-donor–acceptor substituted cyclopropane **259** and subsequent cyclization of zwitterionic intermediate **260**, provided good yields of dihydrofurans **261** (Scheme 83).³ Treatment of the latter with $\text{BF}_3\text{-OEt}_2$ resulted in the formation of furans **262** in moderate yields.

In the synthesis of series of stannylated troponoids, Banwell applied a modified Swern oxidation protocol (with trifluoroacetic anhydride, TFAA) to dihydroxynorcaranes **263** and **267** (Scheme 84).¹⁸ Under these conditions, significant amounts of bicyclic hydroxyenones **265** and **268** were obtained. However, prolonged reaction times or excess of oxidant effected ring expansion/dehydrobromination of the intermediate hydroxyenones leading to troponoids **264** and **269**, respectively. Alternatively, methylation of **265** with dimethylsulfate followed by treatment with 1,8-diazabicyclo[5.4.0]undec-5-ene (DBU) afforded tropolone **266** in good yield (Scheme 84).

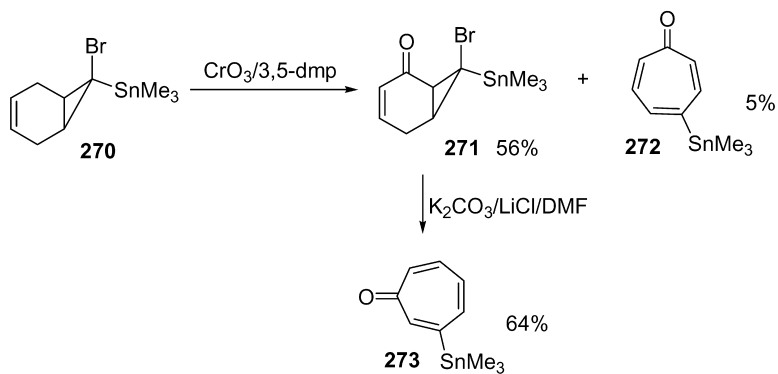
Synthesis of 3-stannyltropolone **273** was achieved by subjecting **270** to allylic oxidation conditions with chromium trioxide–3,5-dimethylpyrazole (3,5-dmp) complex, which provided enone **271** accompanied with trace



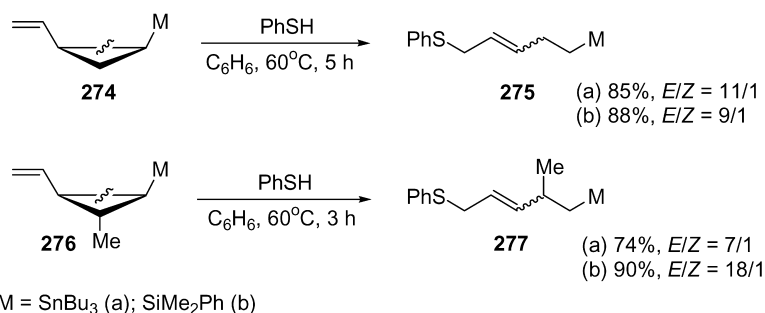
Scheme 83.



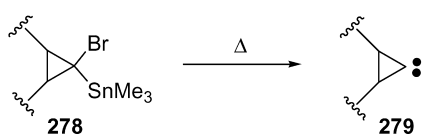
Scheme 84.



Scheme 85.



Scheme 86.



Scheme 87.

amount of tropolone **272** (Scheme 85). While treatment of **271** with DBU failed to provide any isolable products, reaction of this substrate with potassium carbonate and lithium chloride in DMF resulted in dehydrobrominative ring expansion to give **273** in 64% yield. It was pointed out that the use of either isomer (with *syn* or *anti* orientation of bromine) did not affect the reaction course. The resulting stannylated tropolones were successfully employed in further transformations including Stille cross-coupling reactions with aryl halides and in electrophilic substitution reactions.¹⁸

3.2.2. Radical-initiated ring opening. Radical-induced ring opening reactions of trialkylsilyl- and tributylstannyl-cyclopropanes **274** and **276** were investigated by Oshima and Utimoto (Scheme 86).³⁹ Both silicon and tin analogs provided homoallylic silanes or stannanes, respectively. A selective cleavage of the proximal bond occurred in this reaction, regardless of the metal and substitution pattern at cyclopropanes, which can be explained by a formation of the more stable α -stannyl or α -silyl radicals. In all cases predominant formation of the thermodynamically more favorable *E*-olefin was observed.

3.2.3. Ring opening via α -elimination. Seyferth and Lambert first proposed that α -halocyclopropylstannanes **278** can undergo thermolysis, potentially, via formation of

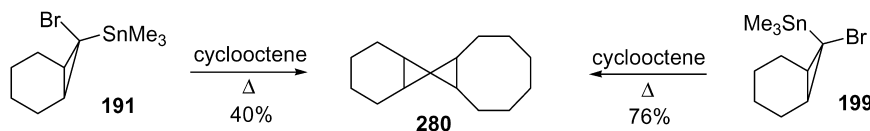
cyclopropylidene **279** (Scheme 87).¹⁰⁹ Although most α -halocyclopropylstannanes tested underwent ring-opening reactions providing allenes, norcaranes **191** and **199** produced insertion products of putative carbene species of type **279**.

Thus, the reaction with pure *syn*-isomer **199** in refluxing cyclooctene afforded after 6 h tetracyclic product **280** in 76% yield, while 40% of **280** only was produced from the *anti*-isomer **191** after 23 h (Scheme 88).

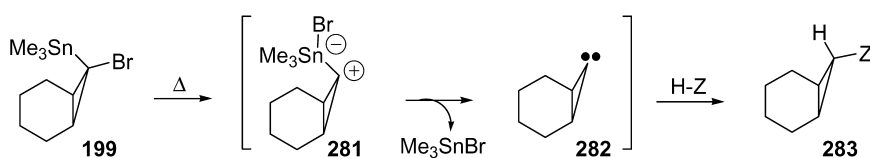
Having obtained some data supporting formation of cyclopropylidene **279**, the authors, however, stated that the exact mechanism of α -elimination was unclear, as there remained a number of uncertainties, such as different reactivity of *syn*- and *anti*-isomers and irreversible decomposition of only one, less reactive *anti*-isomer **191**.¹⁰⁹

Mechanistic studies on the thermolysis of **191** and **199**, performed later by Warner,²⁰ suggested that the more reactive **199** decomposes via initial C–Br heterolysis to give an ylide **281**, which upon loss of Me₃SnBr produces norcaranylidene **282**, which then undergoes addition/insertion reactions (Scheme 89). In contrast, thermolysis of less reactive **191** proceeds primarily or solely via an ionic, non-carbenic process, similar to that shown for unsaturated analog **47** (see below).

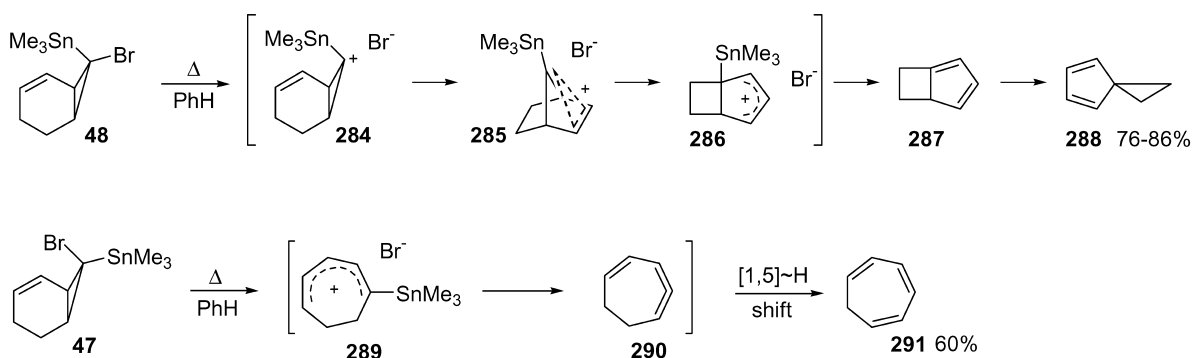
Warner further demonstrated that both isomeric norcaranes **48** and **47** undergo α -elimination, most likely, via ionization rather than via the formation of cyclopropylidene species.¹¹⁰ He found that pyrolysis of norcarane **48**, carried out at temperatures of 100–160 °C, produced good yields of spirodiene **288**, presumably, via a Scattebol-type



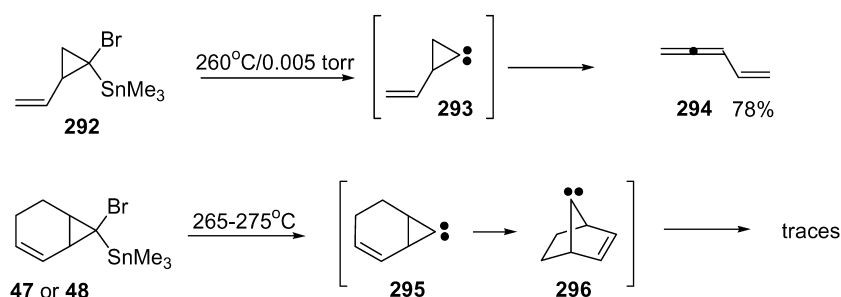
Scheme 88.



Scheme 89.



Scheme 90.



Scheme 91.

rearrangement.¹¹¹ Similar treatment of **47** afforded, via facile ionization of *syn*-oriented halogen and subsequent ring-opening, cycloheptatriene **291** accompanied by dimers and trimers of cyclic allene **290** (Scheme 90).¹¹⁰

Brinker employed flash vacuum pyrolysis to generate carbene species from α -bromocyclopropylstannane **292** and a norcarene of unknown configuration (**47** or **48**) (Scheme 91).²¹ It was found that thermal decomposition of vinylcyclopropane **292**, carried out at 260 °C, afforded vinyl allene **294** in 78% yield, accompanied by traces of isomeric enynes. In contrast, pyrolysis of the parent norcarene (**47** or **48**) proved unsuccessful. The high temperatures required for the decomposition of the latter appeared to be a major problem of this reaction (Scheme 91).²¹

4. Conclusion

Cyclopropylstannanes, versatile building blocks, have found numerous applications in synthetic organic chemistry. Being convenient, rather reactive yet stable synthons, cyclopropylstannanes allow for easy incorporation of a three-membered unit into more complex molecules via tin–lithium exchange combined with a variety of coupling protocols. Furthermore, as discussed above, the tin moiety in cyclopropylstannanes can be readily replaced with a broad range of functional groups with preservation of configuration. Cyclopropylstannanes are also suitable substrates for a number of transformations involving ring expansions. Not surprisingly, development of synthetic methods towards cyclopropylstannanes has attracted a great deal of attention from the synthetic community. Numerous approaches including well-established cyclopropanation procedures as well as func-

tional group transformations at cyclopropyl precursors have been successfully employed for the preparation of cyclopropylstannanes. With new methods being developed, the chemistry of cyclopropylstannanes will continue to fuel future synthetic applications and will open new opportunities for synthetic organic chemistry.

Acknowledgements

The support of the National Science Foundation (CHE-0096889) is gratefully acknowledged.

References and notes

- Alkorta, I.; Elguero, J. *Tetrahedron* **1997**, *53*, 9741–9748.
- Pohmakotr, M.; Sithikanchanakul, S. *Synth. Commun.* **1989**, *19*, 3011–3020.
- Pohmakotr, M.; Takampon, A. *Tetrahedron Lett.* **1996**, *37*, 4585–4588.
- Pohmakotr, M.; Khosavanna, S. *Tetrahedron* **1993**, *49*, 6483–6488.
- Paetow, M.; Kotthaus, M.; Grehl, M.; Fröhlich, R.; Hoppe, D. *Synlett* **1994**, 1034–1036.
- Akhachinskaya, T. V.; Donskaya, N. A.; Kalyakina, I. V.; Oprunenko, Yu. F.; Shabarov, Yu. S. *J. Org. Chem. USSR* **1989**, *25*, 1485–1489.
- Della, E. W.; Patney, H. K. *Aust. J. Chem.* **1979**, *32*, 2243–2248.
- Taylor, R. T.; Paquette, L. A. *J. Org. Chem.* **1978**, *43*, 242–250.
- Seyferth, D.; Cohen, H. M. *Inorg. Chem.* **1962**, *1*, 913–916.
- Seyferth, D.; Lambert, R. L., Jr. *J. Organomet. Chem.* **1975**, *88*, 287–301.

11. Seyferth, D.; Lambert, R. L., Jr. *J. Organomet. Chem.* **1973**, *55*, C53–C57.
12. Seebach, D.; Stucky, G.; Pfammatter, E. *Chem. Ber.* **1989**, *122*, 2377–2389.
13. Vu, V. A.; Ilan, M.; Polborn, K.; Knochel, P. *Angew. Chem. Int. Ed.* **2002**, *41*, 351–352.
14. Seyferth, D.; Dagani, D. D. *Synth. React. Inorg. Met.-Org. Chem.* **1980**, *10*, 137–145.
15. Seyferth, D.; Cohen, H. M. *J. Organomet. Chem.* **1963**, *1*, 15–21.
16. Doyle, M. P.; Austin, R. E.; Bailey, A. S.; Dwyer, M. P.; Dyatkin, A. B.; Kalinin, A. V.; Kwan, M. M. Y.; Liras, S.; Oalman, C. J.; Pieters, R. J.; Protopopova, M. N.; Raab, C. E.; Roos, G. H. P.; Zhou, Q.-L.; Martin, S. F. *J. Am. Chem. Soc.* **1995**, *117*, 5763–5775.
17. Martin, S. F.; Dwyer, M. P. *Tetrahedron Lett.* **1998**, *39*, 1521–1524.
18. Banwell, M. G.; Cameron, J. M.; Collis, M. P.; Gravatt, G. L. *Aust. J. Chem.* **1997**, *50*, 395–407.
19. Seyferth, D.; Lambert, R. L., Jr.; Massol, M. *J. Organomet. Chem.* **1975**, *88*, 255–286.
20. Warner, P. M.; Herold, R. D.; Chu, I.-S.; Lessman, J. *J. Org. Chem.* **1988**, *53*, 942–950.
21. Brinker, U. H.; Ritzer, J. *J. Am. Chem. Soc.* **1981**, *103*, 2116–2119.
22. Brinker, U. H.; Fleischhauer, I. *Chem. Ber.* **1986**, *119*, 1244–1268.
23. Warner, P.; Chang, S.-C. *Tetrahedron Lett.* **1979**, *20*, 4141–4144.
24. Warner, P. M.; Herold, R. D. *J. Org. Chem.* **1983**, *48*, 5411–5412.
25. Isono, N.; Mori, M. *Tetrahedron Lett.* **1995**, *36*, 9345–9348.
26. Isono, N.; Mori, M. *J. Org. Chem.* **1996**, *61*, 7867–7872.
27. Wakamatsu, H.; Isono, N.; Mori, M. *J. Org. Chem.* **1997**, *62*, 8917–8922.
28. Beak, P.; Wu, S.; Yum, E. K.; Jun, Y. M. *J. Org. Chem.* **1994**, *59*, 276–277.
29. Pohmakotr, M.; Sithikanchanakul, S.; Khosavanna, S. *Tetrahedron* **1993**, *49*, 6651–6660.
30. Tanaka, K.; Minami, K.; Kaji, A. *Chem. Lett.* **1987**, 809–810.
31. Lebel, H.; Marcoux, J.-F.; Molinaro, C.; Charette, A. B. *Chem. Rev.* **2003**, *103*, 977–1050.
32. Funaki, I.; Bell, R. P. L.; Thijs, L.; Zwanenburg, B. *Tetrahedron* **1996**, *52*, 12253–12274.
33. Seyferth, D.; Dertouzos, H.; Suzuki, R.; Mui, J. Y.-P. *J. Org. Chem.* **1967**, *32*, 2980–2984.
34. Seyferth, D.; Jula, T. F.; Dertouzos, H.; Pereyre, M. *J. Organomet. Chem.* **1968**, *11*, 63–76.
35. Gadwood, R. C.; Rubino, M. R.; Nagarajan, S. C.; Michel, S. T. *J. Org. Chem.* **1985**, *50*, 3255–3260.
36. Charette, A. B.; Beauchemin, A. *Org. React.* **2001**, *58*, 1–415.
37. Itoh, T.; Emoto, S.; Kondo, M. *Tetrahedron* **1998**, *54*, 5225–5232.
38. Piers, E.; Coish, P. D. *Synthesis* **2001**, 251–261.
39. Miura, K.; Oshima, K.; Utimoto, K. *Bull. Chem. Soc. Jpn* **1990**, *63*, 1665–1677.
40. Corey, E. J.; Eckrich, T. M. *Tetrahedron Lett.* **1984**, *23*, 2415–2418.
41. Corey, E. J.; De, B. *J. Am. Chem. Soc.* **1984**, *106*, 2735–2736.
42. Lautens, M.; Ren, Y. *J. Org. Chem.* **1996**, *61*, 2210–2214.
43. Lautens, M.; Delanghe, P. H. M.; Goh, J. B.; Zhang, C. H. *J. Org. Chem.* **1995**, *60*, 4213–4227.
44. Lautens, M.; Delanghe, P. H. M. *J. Org. Chem.* **1995**, *60*, 2474–2487.
45. Delanghe, P. H. M.; Lautens, M. *Tetrahedron Lett.* **1994**, *35*, 9513–9516.
46. Lautens, M.; Delanghe, P. H. M. *J. Org. Chem.* **1993**, *58*, 5037–5039.
47. Lautens, M.; Delanghe, P. H. M.; Goh, J. B.; Zhang, C. H. *J. Org. Chem.* **1992**, *57*, 3270–3272.
48. Lautens, M.; Delanghe, P. H. M. *J. Org. Chem.* **1992**, *57*, 798–800.
49. Mitchell, T. N.; Kowall, B. *J. Organomet. Chem.* **1995**, *490*, 239–242.
50. Falck, J. R.; Mekonnen, B.; Yu, J.; Lai, J.-Y. *J. Am. Chem. Soc.* **1996**, *118*, 6096–6097.
51. Charette, A. B.; Juteau, H.; Lebel, H.; Molinaro, C. *J. Am. Chem. Soc.* **1998**, *120*, 11943–11952.
52. Hoffmann, R. W.; Koberstein, R. *J. Chem. Soc. Perkin Trans. 2* **2000**, 592–602.
53. Itoh, T.; Inoue, H.; Emoto, S. *Bull. Chem. Soc. Jpn* **2000**, *73*, 409–416.
54. Hoffmann, R. W.; Koberstein, R. *Chem. Commun.* **1999**, 33–34.
55. Imai, N.; Sakamoto, K.; Takahashi, H.; Kobayashi, S. *Tetrahedron Lett.* **1994**, *35*, 7045–7048.
56. Imai, N.; Sakamoto, K.; Maeda, M.; Kouge, K.; Yoshizane, K.; Nokami, J. *Tetrahedron Lett.* **1997**, *38*, 1423–1426.
57. For recent reviews, see: (a) Davies, H. M. L.; Antoulinakis, E. G. *Org. React.* **2001**, *57*, 1–326. (b) Doyle, M. P.; Protopopova, M. N. *Tetrahedron* **1998**, *54*, 7919–7946.
58. Doyle, M. P.; Pieters, R. J.; Martin, S. F.; Austin, R. E.; Oalman, C. J.; Müller, P. *J. Am. Chem. Soc.* **1991**, *113*, 1423–1424.
59. Schöllkopf, U.; Rieber, N. *Angew. Chem. Int. Ed.* **1967**, *6*, 884.
60. Schöllkopf, U.; Bánhidai, B.; Scholz, H.-U. *Liebigs Ann. Chem.* **1972**, *761*, 137–149.
61. Olofson, R. A.; Hoskin, D. H.; Lotts, K. D. *Tetrahedron Lett.* **1978**, *19*, 1677–1680.
62. Emig, N.; Tejada, J.; Réau, R.; Bertrand, G. *Tetrahedron Lett.* **1995**, *36*, 4231–4234.
63. Nakamura, M.; Isobe, H.; Nakamura, E. *Chem. Rev.* **2003**, *103*, 1295–1326.
64. Baird, M. S. *Cyclopropenes: transformations: addition reactions. Houben-Weyl*; Thieme: Stuttgart, 1997; E17d/2. p 2794.
65. Nakamura, E.; Machii, D.; Inubushi, T. *J. Am. Chem. Soc.* **1989**, *111*, 6849–6850.
66. Yamago, S.; Ejiri, S.; Nakamura, E. *Chem. Lett.* **1994**, 1889–1892.
67. Rubina, M.; Rubin, M.; Gevorgyan, V. *J. Am. Chem. Soc.* **2002**, *124*, 11566–11567.
68. Suginome, M.; Ito, Y. *Chem. Rev.* **2000**, *100*, 3221–3256.
69. Pohlmann, T.; de Meijere, A. *Org. Lett.* **2000**, *2*, 3877–3879.
70. Kulinkovich, O. G. *Chem. Rev.* **2003**, *103*, 2597–2632.
71. Lee, K.; Kim, S.-I.; Cha, J. K. *J. Org. Chem.* **1998**, *63*, 9135–9138.
72. Lee, J.; Kim, H.; Cha, J. K. *J. Am. Chem. Soc.* **1996**, *118*, 4198–4199.
73. Lee, J.; Cha, J. K. *J. Org. Chem.* **1997**, *62*, 1584–1585.
74. Sisido, K.; Kozima, S.; Takizawa, K. *Tetrahedron Lett.* **1967**, *8*, 33–36.

75. Sisido, K.; Miyanisi, T.; Isida, T.; Kozima, S. *J. Organomet. Chem.* **1970**, *23*, 117–122.
76. Closs, G. L.; Closs, L. E. *J. Am. Chem. Soc.* **1961**, *83*, 1003–1004.
77. Eckert-Maksić, M.; Golić, M.; Paša-Tolić, L. *J. Organomet. Chem.* **1995**, *489*, 35–41.
78. Isaka, M.; Ejiri, S.; Nakamura, E. *Tetrahedron* **1992**, *48*, 2045–2057.
79. Nakamura, M.; Inoue, T.; Sato, A.; Nakamura, E. *Org. Lett.* **2000**, *2*, 2193–2196.
80. Nakamura, M.; Hara, K.; Sakata, G.; Nakamura, E. *Org. Lett.* **1999**, *1*, 1505–1507.
81. Guillermin, G.; l'Honoré, A.; Veniard, L.; Pourcelot, G.; Benaim, J. *Bull. Soc. Chim. Fr.* **1973**, 2739–2746.
82. Kirms, M. A.; Primke, H.; Stohlmeier, M.; de Meijere, A. *Recl. Trav. Chim. Pays-Bas* **1986**, *105*, 462–464.
83. Eckert-Maksić, M.; Elbel, S.; Stohlmeier, M.; Untiedt, S.; de Meijere, A. *Chem. Ber.* **1996**, *129*, 169–174.
84. Untiedt, S.; de Meijere, A. *Chem. Ber.* **1994**, *127*, 1511–1515.
85. Seyferth, D.; Cohen, H. M. *Inorg. Chem.* **1963**, *2*, 625–629.
86. Tanaka, K.; Minami, K.; Funaki, I.; Suzuki, H. *Tetrahedron Lett.* **1990**, *31*, 2727–2730.
87. See Supporting Information in Ref. 67.
88. Rubina, M.; Rubin, M.; Gevorgyan, V. Unpublished results.
89. (a) For the Brook rearrangement, see: Brook, A. G.; Pascoe, J. D. *J. Am. Chem. Soc.* **1971**, *93*, 6224–6227. (b) For the retro-Brook rearrangement, see: Linderman, R. J.; Ghannam, A. *J. Am. Chem. Soc.* **1990**, *112*, 2392–2398.
90. For a discussion of the Horeau amplification principle, see: Rautenstrauch, V. *Bull. Chem. Soc. Fr.* **1994**, *131*, 515–524.
91. Piers, E.; Jean, M.; Marrs, P. S. *Tetrahedron Lett.* **1987**, *28*, 5075–5078.
92. Warner, P. M.; Chang, S.-C.; Koszewski, N. J. *Tetrahedron Lett.* **1985**, *26*, 5371–5374.
93. Baelkelmans, P.; Gielen, M.; Nasielski, J. *Tetrahedron Lett.* **1967**, *8*, 1149–1151.
94. Gielen, M.; Baekelmans, P.; Nasielski, J. *J. Organomet. Chem.* **1972**, *34*, 329–339.
95. Sisido, K.; Ban, K.; Isida, T.; Kozima, S. *J. Organomet. Chem.* **1971**, *29*, C7–C8.
96. For application of cyclopropyl boronates in the Suzuki cross-coupling reaction, see for example: (a) Zhou, S.-M.; Deng, M.-Z.; Xia, L.-J.; Tang, M.-H. *Angew. Chem. Int. Ed.* **1998**, *37*, 2845–2847. (b) Luithle, J. E. A.; Pietruszka, J. *J. Org. Chem.* **2000**, *65*, 9194–9200. (c) Rubina, M.; Rubin, M.; Gevorgyan, V. *J. Am. Chem. Soc.* **2003**, *125*, 7198–7199.
97. Schmitz, W. D.; Romo, D. *Tetrahedron Lett.* **1996**, *37*, 4857–4860.
98. Peters, D.; Hörnfeldt, A.-B.; Gronowitz, S. *J. Heterocycl. Chem.* **1991**, 1629–1631.
99. Nelson, P. H.; Carr, S. F.; Devens, B. H.; Eugui, E. M.; Franco, F.; Gonzalez, C.; Hawley, R. C.; Loughhead, D. G.; Milan, D. J.; Papp, E.; Patterson, J. W.; Rouhafza, S.; Sjögren, E. B.; Smith, D. B.; Stephenson, R. A.; Talamas, F. X.; Waltos, A.-M.; Weikert, R. J.; Wu, J. C. *J. Med. Chem.* **1996**, *39*, 4181–4196.
100. Turner, W. R.; Suto, M. J. *Tetrahedron Lett.* **1993**, *34*, 281–284.
101. Branca, Q.; Jakob-Røtne, R.; Kettler, R.; Röver, S.; Scalone, M. *Chimia* **1995**, 381–385.
102. Liebeskind, L. S.; Riesinger, S. W. *Tetrahedron Lett.* **1991**, *32*, 5681–5682.
103. Akhachinskaya, T. V.; Grishin, Yu. K.; Donskaya, N. A.; Roznyatovskii, V. A.; Shulishov, E. V.; Yusipovich, N. F.; Shabarov, Yu. S. *J. Org. Chem. USSR* **1987**, *23*, 2076–2085.
104. Dunkelblum, E. *Tetrahedron* **1976**, *32*, 975–978.
105. Donskaya, N. A.; Grishin, Yu. K.; Lukovskii, B. A.; Beletskaya, I. P. *Russ. J. Org. Chem.* **1994**, *30*, 18–24.
106. Seyferth, D.; Cohen, H. M. *Inorg. Chem.* **1963**, *2*, 652–654.
107. Pohmakotr, M.; Sithikanchanakul, S. *Tetrahedron Lett.* **1989**, *30*, 6773–6776.
108. Cohen, T.; Bhupathy, M. *Tetrahedron Lett.* **1987**, *28*, 4793–4796.
109. Seyferth, D.; Lambert, R. L., Jr. *J. Organomet. Chem.* **1975**, *91*, 31–45.
110. Warner, P. M.; Herold, R. D. *Tetrahedron Lett.* **1984**, *25*, 4897–4900.
111. Holm, K. H.; Skattebol, L. *J. Am. Chem. Soc.* **1977**, *99*, 5480–5481.

Biographical sketch



Marina Rubina was born in Syktyvkar, Russia in 1974. She received her BSc from Syktyvkar State University in 1996. She spent 4 years (1995–1999) at The Moscow State University first as an undergraduate researcher and then as a graduate student. Marina is currently a graduate student in Professor Gevorgyan's group at The University of Illinois at Chicago. She is a recipient of the University of Illinois Graduate Fellowship (AY 2002–2003). Her graduate research is focused on the development of new catalytic transformations involving cyclopropenes and investigation of the Pd-catalyzed benzannulation reaction.



Vladimir Gevorgyan was born in Krasnodar, Russia in 1956. He received his BSc from Kuban State University in 1978 and his PhD from the Latvian Institute of Organic Synthesis in 1984, where he was promoted to Group Leader in 1986. He spent 2 years (1992–1994) in Tohoku University in Sendai, Japan, first as a JSPS Postdoctoral Fellow and then as a Ciba-Geigy International Postdoctoral Fellow. In the following year (1995), he worked as a Visiting Professor at CNR, Bologna, Italy. He returned to Tohoku University in 1996 as an Assistant Professor and was promoted to Associate Professor in 1997. In 1999, he moved to The University of Illinois at Chicago as an Associate Professor. He was promoted to the rank of Full Professor in 2003. Professor Gevorgyan's current research interests cover four main areas. The first is concerned with development of highly selective Pd-catalyzed benzannulation reactions. The second area of interest focuses on development of novel transition metal-catalyzed methods for the synthesis of heterocyclic and naturally occurring compounds. The third area of interest covers the development of selective Lewis acid-catalyzed bond formation and cleavage reactions. The fourth deals with the chemistry of strained ring systems.



Convergent approach to the maduropeptin chromophore: aryl ether formation of (*R*)-3-aryl-3-hydroxypropanamide and cyclization of macrolactam

Nobuki Kato, Satoshi Shimamura, Safraz Khan, Fumiyo Takeda, Yoko Kikai and Masahiro Hirama*

Department of Chemistry, Graduate School of Science, Tohoku University, Sendai 980-8578, Japan

Received 2 December 2003; revised 10 February 2004; accepted 12 February 2004

Abstract—Efficient enantioselective syntheses of the functionalized phenol and diethynylcyclopentene moiety of the maduropeptin chromophore were achieved. Their CsF-mediated coupling yielded a sterically congested aryl propargyl ether. The subsequent intramolecular Sonogashira coupling reaction between the vinyl iodide and diethynyl groups occurred at the appropriate position to yield a macrolactam, which was accompanied by Pd-mediated enyne-yne benzannulation.

© 2004 Elsevier Ltd. All rights reserved.

1. Introduction

Maduropeptin, isolated from the broth filtrate of *Actinomadura madura*, consists of a 1:1 complex of an acidic carrier apoprotein (32 kDa) and a 9-membered enediyne chromophore, and exhibits potent antibacterial and antitumor activities.¹ The structure of the intact chromophore has not been concluded because it was too labile for isolation, and instead methanol adduct **1** was isolated from the methanol extract and characterized with the exception of the absolute stereochemistry.^{1b} Compound **1** possesses a labile 9-membered diyne core, a macrolactam ansa-bridge, and an amino sugar. While there are several possibilities for the structure of the parent chromophore, the mechanism of action for **1** was proposed as shown in Scheme 1 on the basis of the isolation of cycloaromatization product **4**, as well as the enhancement of DNA cleavage under basic conditions. The amide nitrogen of **1** would attack C13, causing an S_N2' displacement of methoxy group to afford labile enediyne **2**, which undergoes cycloaromatization to *p*-benzyne biradical **3** capable of proton abstraction and DNA scission. The potent bioactivity and the novel structure of **1**, as well as the exploration of the structure of the intact chromophore stimulated the synthetic studies of **1**.²

The target of this study was *ent*-**1**, an enantiomer of the compound arbitrarily described in the literature,^{1b} due to the

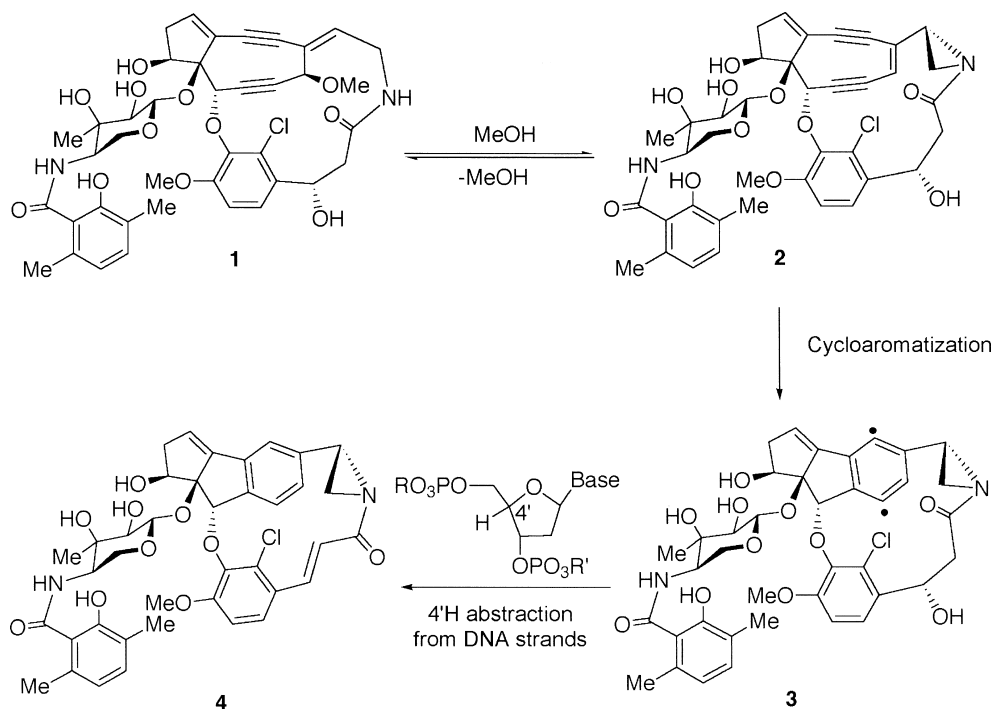
structural similarity of **1** to the related chromophores of C-1027³ and kedarcidin.^{4–6} The retrosynthetic analysis of *ent*-**1** is outlined in Scheme 2. The construction of *ent*-**1** was thought to be accomplished by macro-ring cyclization using intramolecular Sonogashira coupling⁷ of **5** and a subsequent internal addition of an alkyne to the aldehyde. The intermediate **5** was split into two fragments, 3-aryl-3(*R*)-hydroxypropanamide **6** and diethynylepoxycyclopentene **7** by disconnection of the aryl ether bond. The fragment **6** could be constructed from 3-aryl-3(*R*)-hydroxypropanoic acid **8** and amine **9**. The functionalized cyclopentene moiety **7** is to be generated from the previously synthesized chiral dihydroxycyclopentylidene **10**.^{2f,8} In this paper, the enantioselective synthesis of **5**, through the efficient CsF-mediated aryl ether bond formation⁹ between the sterically hindered phenol **6** and epoxide **7**, as well as macro-ring cyclization of **5**, is reported.

2. Results and discussion

Synthesis of allyl amine **15** is summarized in Scheme 3. Here, vinyl iodide **11**, prepared from 1,4-butanediol according to the literature procedure^{2c} was treated with MPMBBr in the presence of NaH to afford MPM ether **12** in a 60% yield. It is important to add NaH into a solution of **11** and MPMBBr in small portions. An excess of NaH results in the production of bis-TBS ether, subsequently decreasing the yield of **12**. Deprotection of the TBS group of **12** and subsequent formation of phthalimide **14** via Mitsunobu reaction¹⁰ followed by cleavage of the phthaloyl group with

Keywords: Maduropeptin chromophore; Aryl ether formation; Enantioselective synthesis; Macrolactam; Benzannulation.

* Corresponding author. Tel.: +81-22-217-6563; fax: +81-22-217-6566; e-mail address: hirama@ykbcs.chem.tohoku.ac.jp

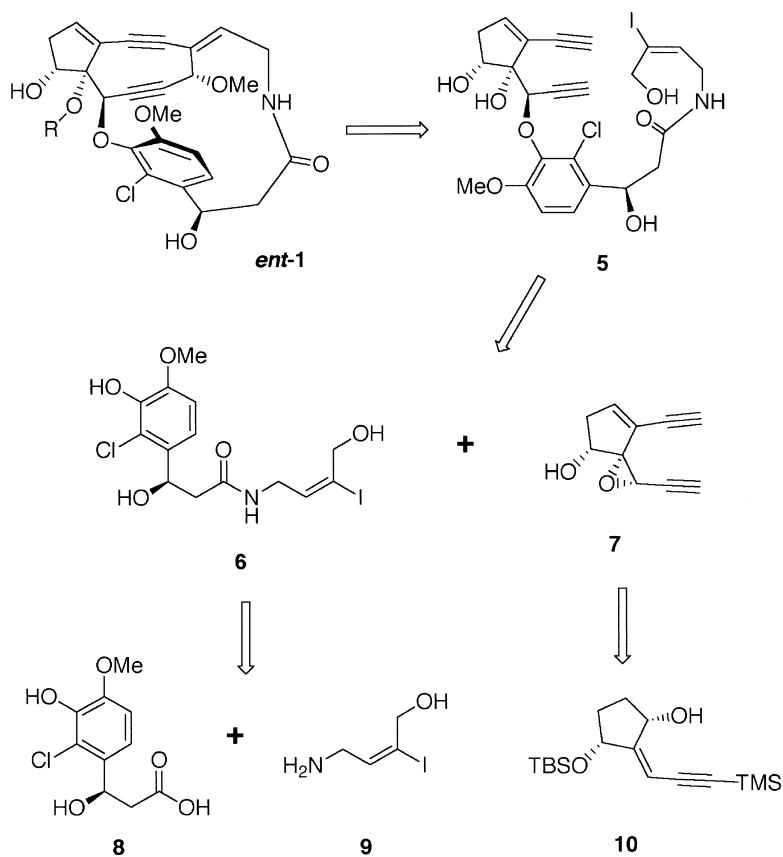


Scheme 1. Mechanism of action of methanol adduct **1** of the maduropeptin chromophore proposed by Schroeder et al.^{1b}

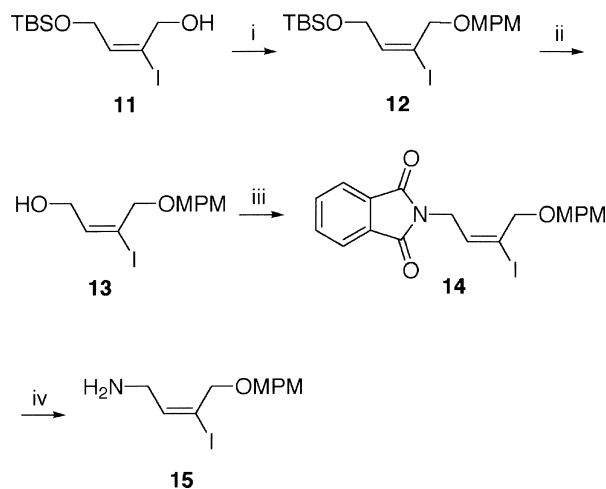
hydrazine monohydrate gave allyl amine **15**, which was used for the next reaction without purification.

Synthesis of 3-aryl-3(*R*)-hydroxypropanamide fragment **21** began with readily available chloroisovanilin **16**¹¹

(Scheme 4). The phenol of **16** was protected as TBS ether **17** in 98% yield, and then subjected to asymmetric Mukaiyama aldol reaction with 3-acetylthiazolidine-2-thione in the presence of (*R*)-chiral diamine **18**¹² to afford (*R*)-aldol product **19** as a major enantiomer (75% ee by



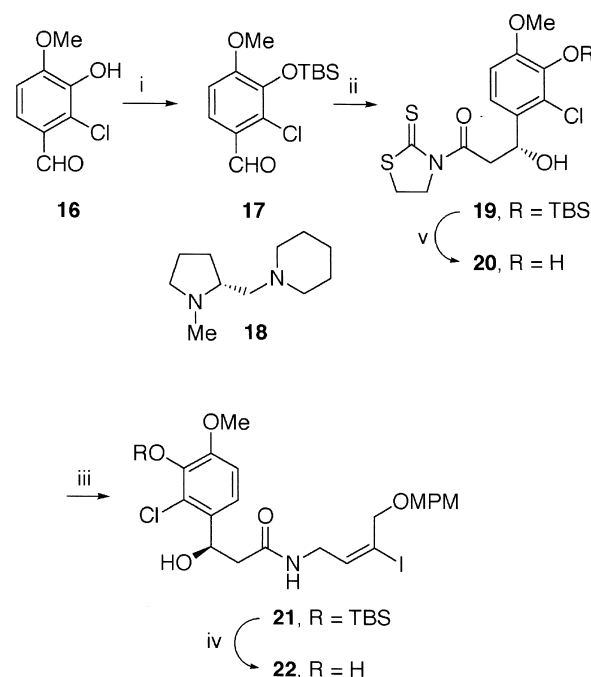
Scheme 2. Retrosynthesis of artifact *ent-1* of the maduropeptin chromophore.



Scheme 3. Reagents and conditions: (i) MPMBBr, NaH, THF/DMF (1:1), room temperature, 1 h, 60%; (ii) TBAF, THF, room temperature, 30 min, 87%; (iii) DEAD, PPh₃, phthalimide, THF, room temperature, 30 min, 98%; (iv) H₂NNH₂·H₂O, THF, room temperature, 6 h, 99%.

HPLC analysis). One recrystallization of thus obtained **19** yielded enantiomerically pure **19** in 49% yield. The absolute stereochemistry of **19** was unambiguously assigned by X-ray crystallographic analysis of **20**¹³ after deprotection of the TBS ether. The activated ester **19** was directly treated with the amine **15** to afford amide **21** in 99% yield¹⁴ and subsequent deprotection of the TBS group of **21** yielded **22** (85% yield).

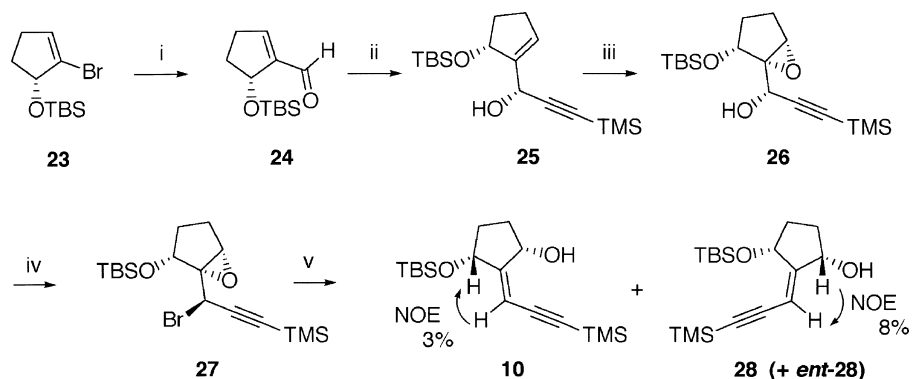
Although several syntheses of compounds related to the enyne **10** have been achieved by trapping enols as triflates followed by Sonogashira coupling,⁸ an alternative strategy is required for the syntheses of functionalized **10**. An efficient stereoselective route to **10** has been developed.^{2f} Synthesis of **10** started from a readily available 2-bromo-3(*R*)-cyclopentenol derivative **23**,¹⁵ which was formylated in the presence of BuLi and DMF¹⁶ to afford unstable aldehyde **24** (Scheme 5). The aldehyde **24** was treated with lithium trimethylsilylacetylide without purification to give a single diastereomer of allylic alcohol **25** in an 88% yield. This stereoselectivity can be accounted by the transition state model shown in Figure 1, where the conjugated enal system of **24** should be almost planar. The *s-cis* enal conformation **A** is expected to be favored over that of the *s-trans* **B**, because **B** may exhibit some steric repulsion between the TBS ether group and the carbonyl oxygen



Scheme 4. Reagents and conditions: (i) TBSCl, imidazole, DMF, room temperature, 40 min, 96%; (ii) (*R*)-**18**, Sn(OTf)₂, 3-acetylthiazolidine-2-thione, *N*-ethylpiperidine, CH₂Cl₂, -95 °C, 10 h, 72%, 75% ee; recrystallization (AcOEt/hexane=1:50), 64%, >99% ee; (iii) **15**, CH₂Cl₂, room temperature, 2 h, 88%; (iv) TBAF, THF, room temperature, 30 min, 85%; (v) HF-pyridine, THF, room temperature, 12 h, 81%.

coordinated with the lithium reagent. Epoxidation of **25** with *m*CPBA resulted in a 5:1 mixture of diastereomers in favor of **26**. On the other hand, Sharpless asymmetric epoxidation with (+)-DET¹⁷ yielded **26** as the sole product. Under these conditions, a kinetic resolution occurred and the epoxy alcohol **26** was produced in enantiomerically pure form. The stereochemistry of **26** was unambiguously assigned by X-ray crystallographic analysis (Fig. 2).¹⁸ The alcohol **26** was further converted to bromide **27** with a complete stereochemical inversion, using CBr₄ and PPh₃ in dry CH₂Cl₂. If the solvent was not dried, a dibromo alcohol (~20%) was formed via addition of HBr to the epoxide **27**.¹⁹

The subsequent reductive opening of the α -bromoepoxide **27** was attempted based on the assumption that anti-elimination using zinc would occur (Table 1).^{20,21} Treatment with Zn–NaI in MeOH at -40 °C gave **10** and **28**



Scheme 5. Reagents and conditions: (i) BuLi, THF, -78 °C, 30 min; DMF, -78 °C, 30 min.; (ii) TMSCLi, THF, -78 °C, 1.5 h, 95% (2 steps); (iii) (+)-DET, Ti(*O*-*i*-Pr)₄, TBHP, MS4A, CH₂Cl₂, -20 °C, 10 h, 72%; (iv) CBr₄, PPh₃, CH₂Cl₂, 2 h, 89%; (v) see Table 1.

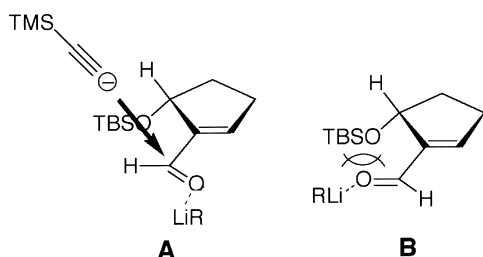


Figure 1. Stereoselective addition of lithium trimethylacetylide to the preferred *s-cis* enal conformation **A** of **24**.

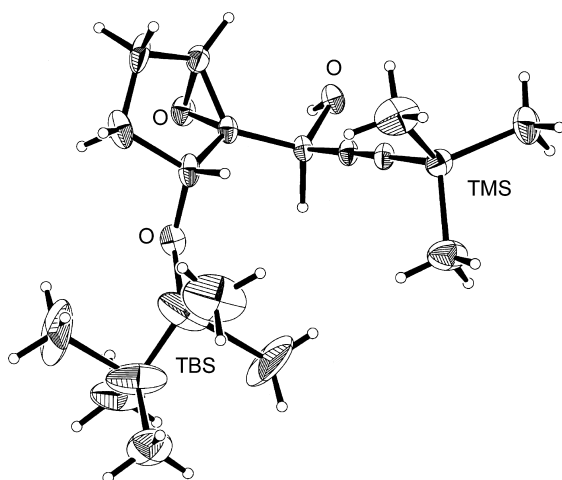
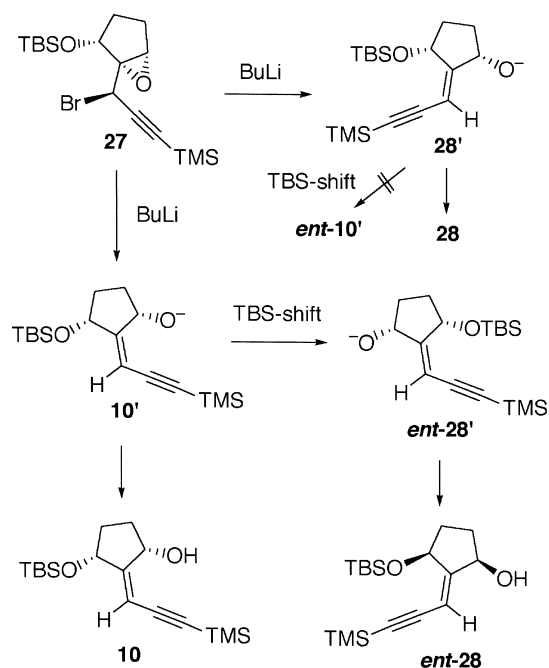


Figure 2. ORTEP drawing of **26**.

in a 2.7:1 ratio with 70% yield (entry 1). The *E* and *Z* stereochemistry was assigned based on the results of NOE experiments. A slightly higher ratio (3.1:1) was obtained with Zn–Cu in refluxing ethanol (entry 2). The best result (**10**–**28**=6.5–7:1, 99% yield) was achieved using BuLi at –90 °C in THF (entry 3). If a migration of TBS group occurs between the pseudo-axial hydroxyl groups under the basic reaction conditions, the alkoxide **10'** would produce *ent*-**28'** and the alkoxide **28'** would afford *ent*-**10'** (Scheme 6). Therefore, the enantiomeric purities of **10** and **28** were determined by HPLC with a chiral column. Interestingly, the major product **10** was always enantiomerically pure and the absolute configuration of **10** corresponded to that of **26**,²² whereas **28** was not enantiomerically pure; the ratio of **28** and *ent*-**28** greatly varied from 3:1 to 1:2. These results indicated that the only alkoxide **10'** underwent the TBS group migration. No simple explanation for the different migration reactivity observed between the alkoxides **10'** and **28'** can be offered at present. A reductive anti-elimination leading to **10** predominated in the reaction of α -bromoepoxide **27** with BuLi.

Thus obtained **10** was stereoselectively converted to epoxide **29** by hydroxy-directed *m*CPBA epoxidation in an 86% yield (Scheme 7). The stereochemistry of **29** was



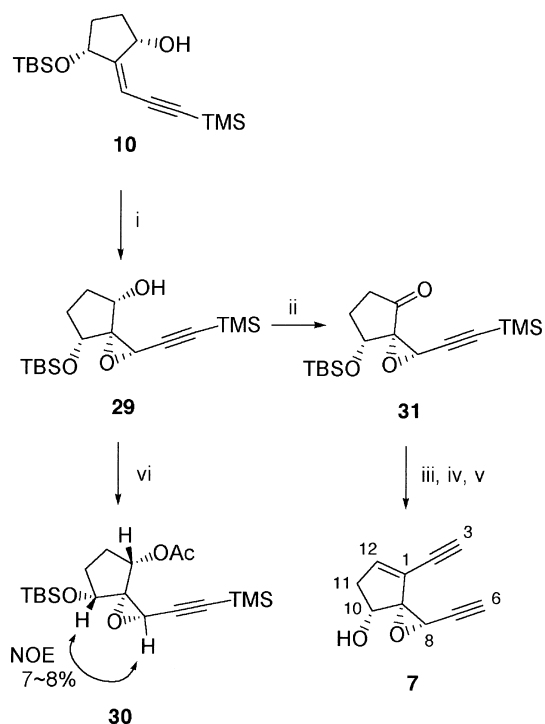
Scheme 6. Proposed reaction pathways to produce **10**, **28**, and *ent*-**28** in the BuLi-mediated reductive opening of α -bromoepoxide **27**.

confirmed by NOE experiments for acetate **30**. Dess–Martin oxidation²³ of **29** gave ketone **31** (84%), to which lithium trimethylsilylacetylide was added and the resulting epimeric mixture of alcohols were dehydrated with methanesulfonyl anhydride in the presence of triethylamine at 40 °C. Subsequent removal of the silyl groups with TBAF yielded diethynylcyclopentene **7** from **31** in a 57% overall yield. The absolute configuration of enantiomerically pure **7** was confirmed by NMR comparison of the corresponding (*S*)- and (*R*)-MTPA esters.²²

The two key fragments **7** and **22** in hand were then assembled. Our coupling method,^{9a,b} employing CsF in DMF at 60 °C, proved to be effective for the sterically congested *o,o,m*-tri-substituted phenol **22**. The coupling of these compounds resulted into aryl ether **32** in a 50% yield (Scheme 8). Thus obtained diyne alkenyl iodide **32** was subjected to the most critical step in this study, an intramolecular Sonogashira reaction under the previously established optimized conditions.⁷ A regioselective cyclization between C3 and C4 forming a 16-membered ring was expected to be favored over the formation of the more strained 14-membered ansa-macro ring through C4–C6 coupling. The reaction at room temperature for 3.5 h afforded product in a 7% yield. The reaction mixture was subsequently heated at 60 °C to increase the yield of the product to 40% yield. This product was not the desired **33**. The product was deduced to be **34** by detailed NMR analysis using HMBC (see Experimental), HMQC, and NOE

Table 1. Reductive opening of the α -bromoepoxide **27**

Entry	Reaction conditions	Product ratio (10/28)	Combined yield (%)
1	Zn (3.0 equiv.), NaI (1.7 equiv.), MeOH, –40 °C, 1 h	73/27	70
2	Zn–Cu (3.0 equiv.), EtOH, reflux, 30 min	76/24	90
3	BuLi (1.5 equiv.), THF, –90 °C, 15 min	87/13	99



Scheme 7. Reagents and conditions: (i) *m*CPBA, Na₂HPO₄, CH₂Cl₂, room temperature, 16 h, 86%; (ii) Dess–Martin periodinane, room temperature, 30 min, 84%; (iii) TMSOCl, −78 °C, THF, 3 h; (iv) Ms₂O, Et₃N, dichloroethane, 40 °C, 3 h; (v) TBAF, THF, room temperature, 0 °C, 57% (3 steps); (vi) Ac₂O, pyridine, 50 °C, 11 h, 73%.

experiments (Fig. 3). The product **34**, however, clearly indicated the intermediacy of **33**, which underwent a concomitant Pd-mediated benzannulation reaction between the enyne and alkyne functionalities.²⁴

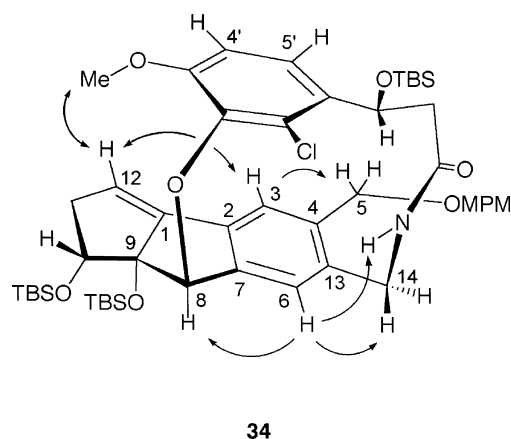
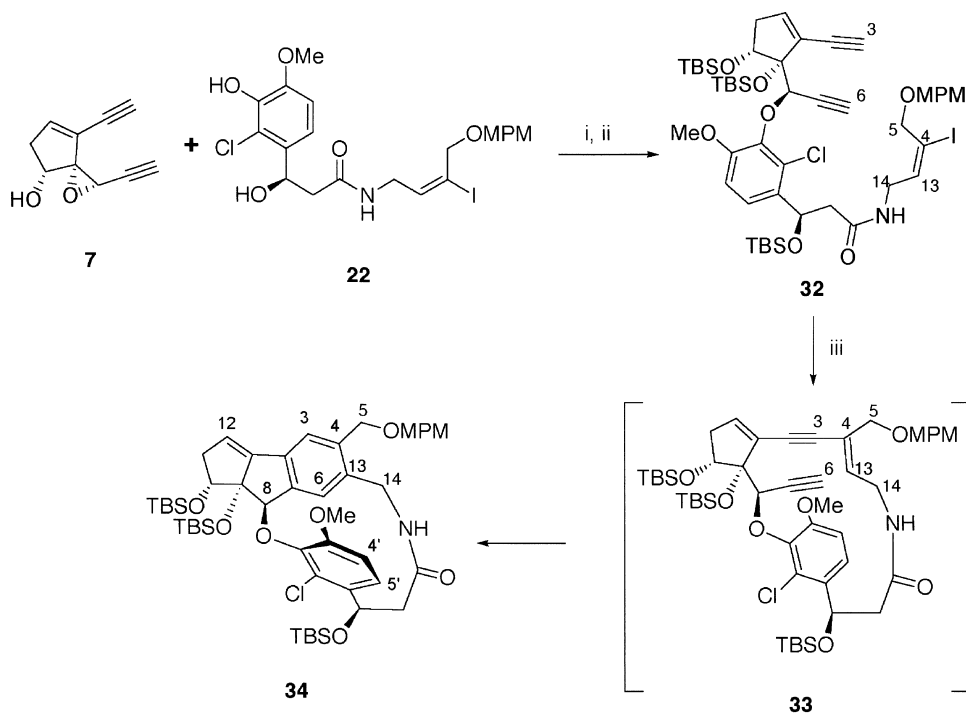


Figure 3. NOEs observed for **34**.

3. Conclusion

An enantioselective synthesis of (*R*)-3-aryl-3-hydroxypropanamide fragment **22** of maduropeptin chromophore artifact *ent*-**1** was achieved via asymmetric Mukaiyama aldol reaction, whereas a stereoselective route to diethynylcyclopentene moiety **7** was developed using a novel BuLi-mediated reductive opening of α -bromoepoxide **27**. The CsF-mediated coupling strategy between highly congested phenol derivative **22** and epoxide **7** successfully constructed a key aryl ether structure **32**. A critical intramolecular Sonogashira macro-ring cyclization of diene vinyl iodide **32** was demonstrated to proceed in the desired manner forming the 16-membered ring intermediate **33**, which underwent a concomitant Pd-mediated benzannulation of an enyne–yne system, leading to the 13-membered lactam **34**. Based on the chemistry described



Scheme 8. Synthesis of **32** and Pd-catalyzed macrocyclization. Reactions and conditions: (i) CsF, DMF, 60 °C, 8 h, 50%; (ii) TBSOTf, 2,6-lutidine, CH₂Cl₂, room temperature, 77%; (iii) Pd₂(dba)₃·CHCl₃, CuI, *i*-Pr₂NEt, DMF, 60 °C, 3 h, 40%.

herein, further studies directed toward the total synthesis of *ent*-**1** are currently underway.

4. Experimental

4.1. General

All reactions sensitive to air or moisture were carried out under argon or nitrogen atmosphere in dry, freshly distilled solvents under anhydrous conditions, unless otherwise noted. THF was distilled from sodium/benzophenone just prior to use. CH₂Cl₂, DMF and dichloroethane were distilled from calcium hydride. All other reagents were used as supplied unless otherwise stated. Analytical thin-layer chromatography (TLC) was performed using E. Merck Silica Gel 0.25 mm pre-coated plates (60F-254). Column chromatography was performed using Silica Gel 60 (E. Merck, 70–230 mesh) or 100–210 μm Silica Gel 60N (Kanto Chemical Co., Inc.), and for flash column chromatography 40–50 μm Silica Gel 60N (Kanto Chemical Co., Inc.) was used. HPLC was performed on Hitachi D-7000 HPLC System using a UV detector (254 nm).

¹H- and ¹³C NMR spectra were recorded on a Varian INOVA 500 or a JEOL α-500 spectrometer. Chemical shifts are reported in δ (ppm) using residual CHCl₃ as an internal standard of δ 7.26 and 76.9 for ¹H and ¹³C NMR, respectively. IR spectra were recorded on a Perkin–Elmer Spectrum BX FT-IR spectrometer. MALDI-TOF mass spectra were recorded on a Applied Biosystems Voyager DE STR SI-3 instrument, and ESI-TOFMS were on a Applied Biosystems Mariner. Optical rotations were recorded on a JASCO DIP-370 polarimeter. Elemental analysis was conducted with a Yanaco CHN corder MT-5. Melting points were measured on a Yanaco MP-S3 micro melting point apparatus.

4.1.1. MPM ether 12. To a solution of **11** (1.98 g, 6.04 mmol) and MPMBR (3.04 g, 15.1 mmol) in DMF–THF (1:1, 20 ml) was slowly added NaH (60% dispersion in mineral oil, 400 mg, 16.7 mmol) in small portions at 0 °C. After stirring for 1 h at room temperature, to the reaction mixture were added MeOH (2 ml) and sat. NH₄Cl aq. The aqueous layer was extracted with hexane. The combined organic layer was washed with brine, dried over Na₂SO₄, and concentrated in vacuo. The residue was purified by silica-gel column chromatography (hexane/AcOEt=20:1) to afford **12** (1.63 g, 60%) as a colorless oil. IR (neat) ν 2954, 2930, 2856, 1613, 1514, 1250, 1088, 1037, 837, 778 cm⁻¹. ¹H NMR (500 MHz, CDCl₃) δ 0.05 (s, 6H), 0.88 (s, 9H), 3.81 (s, 3H), 4.13 (brs, 2H), 4.15 (d, 2H, *J*=6.4 Hz), 4.43 (s, 2H), 6.55 (brd, 1H, *J*=6.4 Hz), 6.89 (d, 2H, *J*=8.7 Hz), 7.30 (d, 2H, *J*=8.7 Hz). ¹³C NMR (125 MHz, CDCl₃) δ -5.38, 18.17, 25.73, 55.16, 61.09, 70.98, 71.19, 100.13, 113.72, 129.24, 129.53, 144.25, 159.25. MALDI-TOFMS (positive-ion) calcd for C₁₈H₂₉IO₃SiNa: (M+Na)⁺ 471.0828; found: 471.0606.

4.1.2. TBS ether 13. To a solution of **12** (3.20 g, 7.14 mmol) in THF (50 ml) was added to TBAF (1.0 M THF solution, 11 ml, 11.0 mmol) at 0 °C. After stirring for 30 min, the reaction quenched with sat. NH₄Cl aq. The

water layer was extracted with ethyl acetate. The combined organic layer was washed with brine, dried over Na₂SO₄, and concentrated in vacuo. The residue was purified by silica-gel column chromatography (hexane/AcOEt=3:1) to afford **13** (2.07 g, 87%) as a colorless oil. IR (neat) ν 3418, 2933, 1614, 1515, 1249, 1175, 1033, 820, 759 cm⁻¹. ¹H NMR (500 MHz, CDCl₃) δ 2.18 (brs, 1H), 3.81 (s, 3H), 4.08 (brd, 2H, *J*=6.7 Hz), 4.19 (s, 2H), 4.46 (s, 2H), 6.63 (t, 1H, *J*=6.7 Hz), 6.89 (d, 2H, *J*=8.4 Hz), 7.29 (d, 2H, *J*=8.4 Hz). ¹³C NMR (125 MHz, CDCl₃) δ 55.16, 60.28, 71.45, 71.92, 101.26, 113.77, 129.14, 129.56, 143.37, 159.32. ESI-TOFMS (positive-ion) calcd for C₁₂H₁₅IO₃H: (M+H)⁺ 335.0144; found: 335.0126, calcd for C₁₂H₁₅IO₃NH₄: (M+NH₄)⁺ 352.0140; found: 352.0464, calcd for C₁₂H₁₅IO₃Na: (M+Na)⁺ 356.9964; found: 357.0032, calcd for C₁₂H₁₅IO₃K: (M+K)⁺ 372.9703; found: 372.9713.

4.1.3. Phthalimide 14. To a solution of **13** (2.95 g, 8.81 mmol), PPh₃ (3.50 g 13.3 mmol) and phthalimide (1.98 g, 13.5 mmol) in dry THF (20 ml) was added DEAD (5.5 ml, 72.4 mmol) at 0 °C under argon, and the mixture was stirred at room temperature for 30 min. The solvent was removed, and the residue was added diethyl ether. Then, the precipitate was removed by filtration and concentrated in vacuo. The residue was purified by silica-gel column chromatography (hexane/AcOEt=7:1) to afford **14** (4.00 g, 98%) as needles. Mp 78–80 °C (from hexane/AcOEt). IR (film) ν 2835, 2066, 1722, 1714, 1611, 1513, 1393, 1248, 1087, 1033, 721, 529 cm⁻¹. ¹H NMR (500 MHz, CDCl₃) δ 3.80 (s, 3H), 4.29 (d, 2H, *J*=7.4 Hz), 4.37 (s, 2H), 4.51 (s, 2H), 6.48 (t, 1H, *J*=7.4 Hz), 6.90 (d, 2H, *J*=6.9 Hz), 7.36 (d, 2H, *J*=6.9 Hz), 7.72 (dd, 2H, *J*=5.9, 3.3 Hz), 7.84 (dd, 2H, *J*=5.9, 3.3 Hz). ¹³C NMR (125 MHz, CDCl₃) δ 36.83, 55.17, 71.33, 104.54, 113.75, 123.29, 129.58, 131.87, 134.02, 137.08, 159.25, 167.41. ESI-TOFMS (positive-ion) calcd for C₂₀H₁₈INO₄NH₄: (M+NH₄)⁺ 481.0624; found: 481.0462, calcd for C₂₀H₁₈INO₄Na: (M+Na)⁺ 486.0178; found: 486.0185, calcd for C₂₀H₁₈INO₄K: (M+K)⁺ 501.9918; found: 501.9926. Anal. Calcd for C₂₀H₁₈INO₄: C, 51.85; H, 3.92; N, 3.02. Found: C, 51.80; H, 4.06; N, 2.85.

4.1.4. Amine 15. To a solution of **14** (185 mg, 0.399 mmol) in THF (5 ml) was added hydrazine monohydrate (150 μl, 3.09 mmol), and the mixture was stirred at room temperature. After stirring for 30 min, the solvent was removed in vacuo. The residue was treated with sat. NaOH aq. and extracted with CH₂Cl₂. The combined organic layers were washed with brine, dried over Na₂SO₄, and concentrated in vacuo to afford **15** (132 mg, 99%) as a pale yellow oil. IR (neat) ν 3364, 2999, 2906, 2856, 1613, 1514, 1249, 1174, 1085, 1033, 820 cm⁻¹. ¹H NMR (500 MHz, CDCl₃) δ 1.74 (brs, 2H), 3.28 (d, 2H, *J*=7.3 Hz), 3.79 (s, 3H), 4.13 (s, 2H), 4.43 (s, 2H), 6.52 (t, 1H, *J*=7.3 Hz), 6.87 (d, 2H, *J*=8.6 Hz), 7.28 (d, 2H, *J*=8.6 Hz). ¹³C NMR (125 MHz, CDCl₃) δ 41.65, 55.11, 71.04, 71.10, 99.71, 113.67, 129.40, 145.63, 159.20. ESI-TOFMS (positive-ion) calcd for C₁₂H₁₆INO₂H: (M+H)⁺ 334.0304; found: 334.0295.

4.1.5. TBS ether 17. To a solution of **16** (3.42 g, 18.4 mmol) and imidazole (2.83 g, 42.2 mmol) in DMF (20 ml) was added TBSCl (3.68 g, 24.5 mmol) at 0 °C, and the mixture was stirred at room temperature for 45 min. The

reaction quenched with sat. NH_4Cl aq. The aqueous layer was extracted with hexane, and the combined organic layer was dried over MgSO_4 , and concentrated in vacuo. The residue was purified by silica-gel column chromatography (hexane/ AcOEt =20:1) to afford **17** (4.24 g, 96%) as a colorless oil. Mp 41–43 °C (from $\text{MeOH}/\text{H}_2\text{O}$). IR (film) ν 2931, 2858, 1689, 1580, 1494, 1312, 1282, 1043, 875, 838, 785 cm^{-1} . ^1H NMR (500 MHz, CDCl_3) δ 0.21 (s, 6H), 1.05 (s, 9H), 3.89 (s, 3H), 6.86 (d, 1H, J =8.7 Hz), 7.59 (d, 1H, J =8.7 Hz), 10.35 (s, 1H). ^{13}C NMR (125 MHz, CDCl_3) δ -4.09, 18.78, 25.75, 55.38, 109.23, 122.66, 126.42, 129.56, 141.71, 156.10, 189.36. ESI-TOFMS (positive-ion) calcd for $\text{C}_{14}\text{H}_{21}\text{ClO}_3\text{SiH}$: ($\text{M}+\text{H}$)⁺ 301.1027; found: 301.0943. Anal. Calcd for $\text{C}_{14}\text{H}_{21}\text{ClO}_3\text{Si}$: C, 55.89; H, 7.04; Cl, 11.78. Found C, 55.73; H, 7.05; Cl, 11.68.

4.1.6. Thiazolidinethione 19. To a suspension of stannous triflate (1.02 g, 2.45 mmol) and *N*-ethyl piperidine (386 μl , 2.85 mmol) in CH_2Cl_2 (10 ml) was dropwise added 3-acetylthiazolidine-2-thione (637 mg, 3.96 mmol) in CH_2Cl_2 (1.5 ml) at -78 °C under argon. After the mixture was stirred for (*R*)-**18** (501 mg, 2.75 mmol) in CH_2Cl_2 (1.5 ml) was added dropwise, and the mixture was stirred for 5 min at this temperature. Then the mixture was cooled to -95 °C and **17** (598 mg, 2.21 mmol) in CH_2Cl_2 (1.5 ml) was added dropwise. The mixture was further stirred for 1 h at this temperature, and then quenched with 0.1 M HCl. The organic layer was extracted with diethyl ether and the extracts were washed with brine, and dried over MgSO_4 . After evaporation of the solvent, the residue was purified by silica-gel column chromatography (hexane/ AcOEt =20:1) to afford **19** (673 mg, 72%) as a yellow solid. To a solution of **19** (673 mg, 75% ee) in ethyl acetate (1 ml) was added hexane (50 ml) at 50 °C, and the mixture was allowed to stand at room temperature for 3 h. The mixture was filtered through a sintered-glass funnel, and the crystals were repeatedly rinsed with hexane (3 \times 30 ml) to afford enantiomerically pure **19** (431 mg, 64%, >99% ee) as yellow needles. Mp 119–121 °C. $[\alpha]_{\text{D}}^{23}$ =+73.7 (*c* 0.88, CHCl_3). IR (film) ν 3500, 2930, 2857, 1694, 1494, 1277, 1157, 1046, 829 cm^{-1} . ^1H NMR (500 MHz, CDCl_3) δ 0.18 (s, 3H), 0.20 (s, 3H), 1.02 (s, 9H), 3.32 (t, 2H, J =7.6 Hz), 3.34 (d, 1H, J =2.8 Hz), 3.59 (dd, 1H, J =18.0, 9.2 Hz), 3.66 (dd, 1H, J =18.0, 2.8 Hz), 3.80 (s, 3H), 4.63 (t, 2H, J =7.6 Hz), 5.53 (dt, 1H, J =9.2, 2.8 Hz), 6.81 (d, 1H, J =8.8 Hz), 7.15 (d, 1H, J =8.8 Hz). ^{13}C NMR (125 MHz, CDCl_3) δ -4.16, -4.07, 18.78, 25.80, 28.30, 46.06, 55.19, 55.55, 67.06, 109.78, 118.47, 123.50, 132.51, 141.34, 150.44, 173.55, 201.48. ESI-TOFMS (positive-ion) calcd for $\text{C}_{19}\text{H}_{28}\text{ClNO}_4\text{S}_2\text{SiH}$: ($\text{M}+\text{H}$)⁺ 462.0996; found: 462.1161, calcd for $\text{C}_{19}\text{H}_{28}\text{ClNO}_4\text{S}_2\text{SiNH}_4$: ($\text{M}+\text{NH}_4$)⁺ 479.1261; found: 479.1351, calcd for $\text{C}_{19}\text{H}_{28}\text{ClNO}_4\text{S}_2\text{SiNa}$: ($\text{M}+\text{Na}$)⁺ 484.0815; found: 484.0904, calcd for $\text{C}_{19}\text{H}_{28}\text{ClNO}_4\text{S}_2\text{SiK}$: ($\text{M}+\text{K}$)⁺ 500.0555; found 500.0643. Anal. Calcd for $\text{C}_{19}\text{H}_{28}\text{ClNO}_4\text{S}_2\text{Si}$: C, 49.38; H, 6.11; N, 3.03. Found C, 49.25; H, 6.27; N, 3.01.

The ee of **19** was determined as follows. To a solution of chromatographically purified **19** (46.4 mg, 108 μmol) in MeOH (3 ml) was added K_2CO_3 (8.4 mg, 60.9 μmol) and the mixture was stirred at room temperature for 20 min, then added NaCl. The organic layer was extracted with ether and the extracts were washed with brine, and dried over MgSO_4 .

The residue was purified by silica-gel column chromatography (hexane/ AcOEt =4:1) to afford methyl ester (30.3 mg, 82%) as a colorless oil, which was analyzed to be 75% ee by HPLC using Chiralcel OJ-R column 4.6 ϕ \times 150 mm ($\text{MeOH}/\text{H}_2\text{O}$ =7:3): $[\alpha]_{\text{D}}^{20}$ =+54.6 (2.62, CHCl_3). IR (neat) ν 3500, 2931, 2858, 1731, 1592, 1494, 1258, 1046, 830 cm^{-1} . ^1H NMR (500 MHz, CDCl_3) δ 0.18 (s, 3H), 0.19 (s, 3H), 1.02 (s, 9H), 2.58 (dd, 1H, J =16.5, 9.2 Hz), 2.83 (dd, 1H, J =16.5, 2.4 Hz), 3.40 (brd, 1H, J =3.4 Hz, OH), 3.73 (s, 3H), 3.79 (s, 3H), 5.42 (ddd, 1H, J =9.2, 3.4, 2.4 Hz), 6.79 (d, 1H, J =8.8 Hz), 7.14 (d, 1H, J =8.8 Hz). ^{13}C NMR (125 MHz, CDCl_3) δ -4.20, -4.14, 18.75, 25.77, 41.36, 51.75, 55.14, 67.07, 109.68, 118.11, 123.34, 132.64, 141.32, 150.38, 172.87. ESI-TOFMS (positive-ion) calcd for $\text{C}_{17}\text{H}_{27}\text{ClO}_5\text{SiNH}_4$: ($\text{M}+\text{NH}_4$)⁺ 392.1600; found: 392.1509.

4.1.7. Propanamide 21. To a solution of **15** (3.52 g, 28.9 mmol) in CH_2Cl_2 (20 ml) was added **19** (5.5 ml, 72.4 mmol), and the mixture was stirred at room temperature for 2 h. The reaction mixture was quenched with sat. NH_4Cl aq. The water layer was extracted with CHCl_3 , and the combined organic layers were washed with brine, dried over MgSO_4 , and concentrated in vacuo. The residue was purified by silica-gel column chromatography (hexane/ AcOEt =3:2) to afford **21** (3.89 g, 88%) as a colorless oil. $[\alpha]_{\text{D}}^{26}$ =+49.9 (*c* 1.6, CHCl_3). IR (film) ν 3313, 2930, 2856, 1651, 1514, 1493, 1250, 1045, 839 cm^{-1} . ^1H NMR (500 MHz, CDCl_3) δ 0.18 (s, 3H), 0.19 (s, 3H), 1.02 (s, 9H), 2.39 (dd, 1H, J =15.1, 8.7 Hz), 2.61 (dd, 1H, J =15.1, 2.3 Hz), 3.76–3.82 (m, 7H), 3.87 (ddd, 1H, J =15.0, 6.6, 5.8 Hz), 4.19 (s, 2H), 4.30 (brs, 1H), 4.45 (s, 2H), 5.32 (dd, 1H, J =8.7, 2.3 Hz), 5.96 (brs, 1H), 6.36 (t, 1H, J =6.6 Hz), 6.81 (d, 1H, J =8.7 Hz), 6.88 (d, 2H, J =8.7 Hz), 7.11 (d, 1H, J =8.7 Hz), 7.29 (dd, 2H, J =8.7 Hz). ^{13}C NMR (125 MHz, CDCl_3) δ -4.17, -4.07, 18.79, 25.81, 38.76, 42.20, 55.16, 55.19, 67.69, 71.56, 71.93, 101.89, 109.73, 113.82, 118.29, 122.13, 129.30, 129.51, 132.87, 139.72, 141.32, 150.37, 159.38, 171.56. ESI-TOFMS (positive-ion) calcd for $\text{C}_{28}\text{H}_{39}\text{ClINO}_6\text{SiH}$: ($\text{M}+\text{H}$)⁺ 676.1358; found: 676.1198, calcd for $\text{C}_{28}\text{H}_{39}\text{ClINO}_6\text{SiNa}$: ($\text{M}+\text{Na}$)⁺ 698.1178; found: 698.0712, calcd for $\text{C}_{28}\text{H}_{39}\text{ClINO}_6\text{SiK}$: ($\text{M}+\text{K}$)⁺ 714.0917; found 714.0647.

4.1.8. Phenol propanamide 22. To a solution of **21** (1.48 g, 4.45 mmol) in THF (10 ml) was added to TBAF (1.0 M THF solution, 5.6 ml, 5.60 mmol) at 0 °C. After stirring at same temperature for 30 min, the reaction quenched with phosphate buffer (pH 7.0). The water layer was extracted with ethyl acetate. The combined organic layer was washed with brine, dried over MgSO_4 , and concentrated in vacuo. The reaction mixture was purified by silica-gel column chromatography (hexane/ AcOEt =1:1) to afford **22** (2.08 g, 85%) as a white solid. $[\alpha]_{\text{D}}^{26}$ =+44.4 (*c* 1.4, CHCl_3). IR (film) ν 3340, 2937, 1650, 1612, 1513, 1493, 1282, 1249, 1041 cm^{-1} . ^1H NMR (500 MHz, CDCl_3) δ 2.47 (dd, 1H, J =15.1, 8.3 Hz), 2.61 (dd, 1H, J =15.1, 3.1 Hz), 3.76–3.82 (m, 4H), 3.85–3.90 (m, 4H), 4.19 (s, 2H), 4.45 (s, 2H), 5.32 (dd, 1H, J =8.3, 3.1 Hz), 5.98 (brs, 1H), 6.01 (brt, 1H, J =5.7 Hz), 6.35 (t, 1H, J =7.3 Hz), 6.83 (d, 1H, J =8.8 Hz), 6.87 (d, 2H, J =8.3 Hz), 7.08 (d, 1H, J =8.8 Hz), 7.28 (d, 2H, J =8.3 Hz). ^{13}C NMR (125 MHz, CDCl_3) δ 38.74, 42.11, 55.15, 56.24, 67.39, 71.53, 71.86, 101.80, 109.08, 113.79,

116.91, 117.12, 129.28, 129.48, 133.06, 139.77, 141.73, 146.46, 159.31, 171.48. ESI-TOFMS (positive-ion) calcd for $C_{22}H_{25}ClINO_6H$: $(M+H)^+$ 562.0493; found: 562.0275, calcd for $C_{22}H_{25}ClINO_6Na$: $(M+Na)^+$ 584.0313; found: 583.9929, calcd for $C_{22}H_{25}ClINO_6K$: $(M+K)^+$ 600.0052; found 599.9821.

4.1.9. Phenol thiazolidinethione 20. To a solution of **19** (88.7 mg, 0.191 mmol) in THF (3.5 ml) was added to HF-pyridine (280 μ l) at 0 °C. After stirring at room temperature for 12 h, the reaction quenched with sat. KF aq. The water layer was extracted with ethyl acetate. The combined organic layers were washed with brine, dried over Na_2SO_4 , and concentrated in vacuo. The reaction mixture was purified by silica-gel column chromatography (hexane/AcOEt=4:1) to afford **20** (53.8 mg, 81%) as yellow needles. Mp 160–162 °C (from hexane/AcOEt). $[\alpha]_D^{25}=+92.7$ (*c* 0.51, EtOH). IR (film) ν 3304, 1673, 1497, 1349, 1288, 1162, 1036 cm^{-1} . 1H NMR (500 MHz, $CDCl_3$) δ 3.32 (t, 2H, *J*=7.5 Hz), 3.38 (brd, 1H, *J*=3.3 Hz), 3.59 (dd, 1H, *J*=17.5, 9.2 Hz), 3.68 (dd, 1H, *J*=17.5, 3.3 Hz), 3.91 (s, 3H), 4.63 (t, 2H, *J*=7.5 Hz), 5.54 (dt, 1H, *J*=9.2, 3.3 Hz), 5.91 (s, 1H), 6.84 (d, 1H, *J*=8.6 Hz), 7.13 (d, 1H, *J*=8.6 Hz). ^{13}C NMR (125 MHz, $CDCl_3$) δ 28.29, 46.11, 55.53, 56.23, 66.73, 109.12, 117.23, 117.37, 132.67, 141.76, 146.53, 173.41, 201.55. ESI-TOFMS (positive-ion) calcd for $C_{13}H_{14}ClINO_4S_2Na$: $(M+Na)^+$ 369.9950; found: 369.9979, calcd for $C_{13}H_{14}ClINO_4S_2K$: $(M+K)^+$ 385.9690; found 385.9736. Anal. Calcd for $C_{13}H_{14}ClINO_4S_2$: C, 44.89; H, 4.06; N, 4.03. Found C, 44.96; H, 4.30; N, 3.88.

4.1.10. Aldehyde (24). To a solution of **23** (33.9 g, 122 mmol, ~90% ee) in THF (100 ml) was slowly added *n*-BuLi (1.61 M hexane solution, 91.0 ml, 147 mmol) at –78 °C. After stirred for 30 min at the same temperature, DMF (15 ml, 194 mmol) was added and the mixture was stirred at –78 °C for 1 h. The reaction mixture was quenched with sat. NH_4Cl aq. The water layer was extracted with hexane. The combined organic layer was washed with brine, dried over $MgSO_4$, and concentrated in vacuo to afford **24** (27.8 g, crude) as a pale yellow oil. $[\alpha]_D^{27}=-6.8$ (*c* 0.50, $CHCl_3$). IR (neat) ν 2955, 2930, 2856, 1693, 1251, 1075, 837, 778 cm^{-1} . 1H NMR (500 MHz, $CDCl_3$) δ 0.10 (s, 3H), 0.14 (s, 3H), 0.87 (s, 9H), 1.83–1.89 (m, 1H), 2.20–2.27 (m, 1H), 2.41–2.48 (m, 1H), 2.72–2.80 (m, 1H), 5.09 (dt, 1H, *J*=7.4, 2.4 Hz), 6.94 (t, 1H, *J*=2.4 Hz), 9.78 (s, 1H). ^{13}C NMR (125 MHz, $CDCl_3$) δ –5.09, –5.00, 18.10, 25.67, 31.16, 34.33, 73.35, 148.40, 153.68, 188.75. ESI-TOFMS (positive-ion) calcd for $C_{12}H_{22}O_2SiNa$: $(M+Na)^+$ 249.1287; found: 249.1286, calcd for $C_{12}H_{22}O_2SiK$: $(M+K)^+$ 265.1026; found 265.1048.

4.1.11. Alkyne (25). To a solution of trimethyl acetylene (35.0 ml, 245 mmol) in THF (100 ml) was added dropwise *n*-BuLi (1.61 M hexane solution, 115 ml, 185 mmol) at –78 °C and stirred at –78 °C for 20 min. To the acetylide solution, a solution of **24** (27.8 g, crude) prepared above in THF (100 ml) added slowly at –78 °C and the mixture was stirred at –78 °C for 1.5 h. The reaction mixture was quenched with sat. NH_4Cl aq. The aqueous layer was extracted with hexane. The combined organic layers were washed with brine, dried over $MgSO_4$, and concentrated in

vacuo. The residue was purified by silica-gel column chromatography (hexane/AcOEt=25:1) to afford **25** (37.5 g, 2 steps 95%) as a pale yellow oil: $[\alpha]_D^{24}=+4.3$ (*c* 0.62, $CHCl_3$). IR (neat) ν 3416, 2957, 2929, 1250, 1065, 841, 776 cm^{-1} . 1H NMR (500 MHz, $CDCl_3$) δ 0.10 (s, 3H), 0.13 (s, 3H), 0.18 (s, 9H), 0.89 (s, 9H), 1.76 (ddt, 1H, *J*=12.6, 9.1, 6.3 Hz), 2.21–2.35 (m, 2H), 2.45 (ddq, 1H, *J*=15.9, 9.1, 1.9 Hz), 3.29 (d, 1H, *J*=2.9 Hz), 4.94 (brt, 1H, *J*=6.3 Hz), 5.05 (brs, 1H), 6.05 (brs, 1H). ^{13}C NMR (125 MHz, $CDCl_3$) δ –5.10, –4.29, –0.26, 17.76, 25.65, 29.41, 34.84, 61.15, 79.36, 89.84, 103.60, 129.56, 143.29. ESI-TOFMS (positive-ion) calcd for $C_{17}H_{32}O_2Si_2Na$: $(M+Na)^+$ 347.1839; found: 347.1828, calcd for $C_{17}H_{32}O_2Si_2K$: $(M+K)^+$ 363.1578; found 363.1584.

4.1.12. Epoxide (26). Activated MS4A (1.21 g) suspended in CH_2Cl_2 (5 ml) was vigorously stirred at –20 °C under argon for 10 min. (+)-DET (68 μ l, 0.40 μ mol) and $Ti(O-i-Pr)_4$ (75 μ l, 0.25 mmol) were added sequentially with stirring. The reaction mixture was stirred at –20 °C as TBHP (5.2 M CH_2Cl_2 solution, 1.2 ml, 6.03 mmol) was added. The resulting mixture was stirred at –20 °C for 30 min. **25** (1.63 g, 5.03 mmol), dissolved in CH_2Cl_2 (5 ml), was slowly added at –20 °C and the reaction mixture was stirred at –20 °C for 10 h. The reaction mixture was quenched with 30% NaOH in saturated brine. The water layer was extracted with CH_2Cl_2 . The combined organic layer was washed with brine, and dried over $MgSO_4$, and concentrated in vacuo. The residue was purified by silica-gel column chromatography (hexane/AcOEt=20:1) to afford **26** (1.22 g, 72%) as colorless needles. Mp 132 °C (from hexane/AcOEt). $[\alpha]_D^{25}=-25.8$ (*c* 0.97, $CHCl_3$). IR (film) ν 3512, 2956, 2360, 2178, 1249, 1073, 846, 776, 668 cm^{-1} . 1H NMR (500 MHz, $CDCl_3$) δ 0.07 (s, 3H), 0.10 (s, 3H), 0.17 (s, 9H), 0.89 (s, 9H), 1.46 (t, 1H, *J*=8.4, 7.8 Hz), 1.63 (dddd, 1H, *J*=14.2, 12.0, 8.4, 1.1 Hz), 1.85 (dt, 1H, *J*=12.0, 7.8 Hz), 2.03 (dd, 1H, *J*=14.2, 8.4 Hz), 2.38 (brs, 1H), 3.56 (s, 1H), 4.50 (t, 1H, *J*=7.8 Hz), 4.91 (s, 1H). ^{13}C NMR (125 MHz, $CDCl_3$) δ –5.06, –4.63, –0.38, 17.94, 24.29, 25.68, 28.13, 58.02, 58.61, 69.45, 72.19, 91.57, 101.44. ESI-TOFMS (positive-ion) calcd for $C_{17}H_{32}O_3Si_2H$: $(M+H)^+$ 341.1968; found: 341.1920, calcd for $C_{17}H_{32}O_3Si_2NH_4$: $(M+NH_4)^+$ 358.2234; found 358.2132. Anal. Calcd for $C_{17}H_{32}O_3Si_2$: C, 59.95; H, 9.47. Found C, 59.97; H, 4.40.

4.1.13. Bromide (27). To a solution of **26** (14.2 g, 41.8 mmol) and CBr_4 (17.1 g, 51.7 mmol) in CH_2Cl_2 (120 ml) was added PPh_3 (22.0 g, 83.4 mmol) at room temperature under argon, and the mixture was stirred at room temperature for 2 h. The reaction mixture was added ether and filtered through Celite. After evaporation of the solvent, the residue was purified by silica-gel column chromatography (hexane/AcOEt=50:1) to afford **27** (15.0 g, 89%) as a pale yellow oil. $[\alpha]_D^{23}=-20.1$ (*c* 0.50, $CHCl_3$). IR (neat) ν 2957, 2858, 2360, 2179, 1472, 1373, 1250, 1118, 846 cm^{-1} . 1H NMR (500 MHz, $CDCl_3$) δ 0.08 (s, 3H), 0.13 (s, 3H), 0.17 (s, 9H), 0.90 (s, 9H), 1.46 (ddt, 1H, *J*=14.0, 11.0, 7.8 Hz), 1.63 (ddd, 1H, *J*=11.0, 8.6, 7.8 Hz), 1.83 (dt, 1H, *J*=12.2, 7.8 Hz), 2.00 (dd, *J*=14.0, 8.6 Hz), 3.59 (s, 1H), 4.70 (t, 1H, *J*=7.8 Hz), 4.88 (s, 1H). ^{13}C NMR (125 MHz, $CDCl_3$) δ –4.81, –4.53, –0.48, 17.91, 24.39, 25.71, 28.34, 33.53, 60.56, 66.77, 70.92,

93.86, 99.21. MALDI-TOFMS (positive-ion) calcd for $C_{17}H_{31}BrO_2Si_2K$: (M+K)⁺ 441.0683; found: 441.0239.

4.1.14. Enynes (10 and 28). To a solution of **27** (3.48 g, 8.64 mmol) in THF (30 ml) was added *n*-BuLi (1.61 M hexane solution, 8 ml, 12.9 mmol) at -90°C under argon, and the mixture was stirred at this temperature for 15 min. The mixture was quenched with sat. NH_4Cl aq. The aqueous layer was extracted with hexane. The combined organic layer was washed with sat. NH_4Cl aq. solution, brine, and dried over MgSO_4 , and concentrated in vacuo. The residue was purified by silica-gel column chromatography (hexane/AcOEt=50:1) to afford **10** (2.42 g, 86%) and **28** (0.366 g, 13%). The enantiomeric purities of **10** and **28** were determined by HPLC with CHIRALCEL OJ-R column (4.6 ϕ ×150 mm; MeOH/water=75:25) and CHIRALCEL OD-R column (4.6 ϕ ×250 mm; MeOH/water=80:20), respectively. **Compound 10.** Pale yellow oil. $[\alpha]_D^{24}=+71.2$ (*c* 0.60, CHCl_3); 100% ee. IR (neat) ν 3352, 2957, 2857, 2131, 1722, 1620, 1471, 1360, 1250, 1161, 842 cm^{-1} . ^1H NMR (500 MHz, CDCl_3) δ 0.07 (s, 3H), 0.08 (s, 3H), 0.19 (s, 9H), 0.90 (s, 9H), 1.74–1.88 (m, 4H), 2.86 (brs, 1H), 4.42 (ddd, 1H, *J*=8.2, 4.7, 2.0 Hz), 4.78 (brdd, 1H, *J*=5.0, 2.0 Hz), 5.66 (t, 1H, *J*=2.0 Hz). ^{13}C NMR (125 MHz, CDCl_3) δ -4.93, -4.64, -0.29, 18.01, 25.69, 29.68, 32.64, 70.56, 74.85, 101.33, 101.51, 104.68, 164.18. ESI-TOFMS (positive-ion) calcd for $C_{17}H_{32}O_2Si_2H$: (M+H)⁺ 325.2019; found: 325.1832, calcd for $C_{17}H_{32}O_2Si_2NH_4$: (M+NH₄)⁺ 342.2285; found 342.2111. **Compound 28.** Pale yellow oil. $[\alpha]_D^{23}=-66.4$ (*c* 0.66, CHCl_3); 50% ee. IR (neat) ν 3348, 2957, 2930, 1250, 842 cm^{-1} . ^1H NMR (500 MHz, CDCl_3) δ 0.16 (s, 6H), 0.19 (s, 9H), 0.89 (s, 9H), 1.63–1.66 (m, 1H), 1.84–1.88 (m, 2H), 1.99–2.03 (m, 1H), 2.30 (brs, 1H), 4.30 (brdd, 1H, *J*=6.6, 4.3 Hz), 4.78 (d, 1H, *J*=4.5 Hz), 5.72 (brs, 1H). ^{13}C NMR (125 MHz, CDCl_3) δ -4.91, -4.54, -0.22, 17.84, 25.70, 32.73, 32.85, 72.03, 74.58, 99.57, 101.64, 106.63, 159.51. ESI-TOFMS (positive-ion) calcd for $C_{17}H_{32}O_2Si_2H$: (M+H)⁺ 325.2019; found: 325.2039, calcd for $C_{17}H_{32}O_2Si_2Na$: (M+Na)⁺ 347.1839; found 347.1805.

4.1.15. Epoxide (29). To a solution of **10** (2.56 g, 7.90 mmol) in CH_2Cl_2 (30 ml) was added Na_2HPO_4 (4.71 g, 33.2 mmol). After stirring for 10 min at room temperature, *m*CPBA (3.27 g, 19.0 mmol) was added to the white suspension and stirring continued at this temperature for 16 h. The reaction mixture was quenched with sat. Na_2SO_3 aq. The aqueous layer was extracted with hexane, and the combined organic layer was washed with brine, dried over MgSO_4 , and concentrated in vacuo to afford **29** (2.31 g, 86%) as a white solid. $[\alpha]_D^{25}=-6.0$ (*c* 0.50, CHCl_3). IR (film) ν 3555, 2958, 2361, 2183, 1473, 1252, 1062, 845, 778 cm^{-1} . ^1H NMR (500 MHz, CDCl_3) δ 0.03 (s, 3H), 0.04 (s, 3H), 0.17 (s, 9H), 0.86 (s, 9H), 1.83 (dtd, 1H, *J*=12.9, 7.2, 5.4 Hz), 1.90 (dddd, 1H, *J*=12.9, 7.8, 7.2, 5.4 Hz), 1.98–2.02 (m, 2H), 2.27 (d, 1H, *J*=4.8 Hz), 3.49 (s, 1H), 3.93 (t, 1H, *J*=5.4 Hz), 4.09 (dd, 1H, *J*=9.8, 4.8 Hz). ^{13}C NMR (125 MHz, CDCl_3) δ -4.96, -4.92, -0.47, 18.02, 25.59, 30.21, 30.89, 48.88, 68.71, 71.23, 72.64, 92.96, 99.19. ESI-TOFMS (positive-ion) calcd for $C_{17}H_{32}O_3Si_2H$: (M+H)⁺ 341.1968; found: 341.1961, calcd for $C_{17}H_{32}O_3Si_2NH_4$: (M+NH₄)⁺ 358.2234; found 358.2241, calcd for $C_{17}H_{32}O_3Si_2Na$: (M+Na)⁺ 363.1788; found: 363.1779,

calcd for $C_{17}H_{32}O_3Si_2K$: (M+K)⁺ 379.1527; found 379.1561.

4.1.16. Acetate (30). To a solution of **29** (108 mg, 0.317 mmol) in pyridine (3 ml) was added Ac_2O (1.5 ml) at room temperature and the mixture was stirred at 50°C for 11 h. The reaction mixture was quenched with saturated NH_4Cl solution. The aqueous layer was extracted with hexane, and the combined organic layer was washed with brine, dried over Na_2SO_4 , and concentrated in vacuo to afford **30** (88.6 mg, 73%) as a colorless oil: $[\alpha]_D^{21}=+36.1$ (*c* 0.48, CHCl_3). IR (film) ν 2956, 2929, 1743, 1250, 1060, 844 cm^{-1} . ^1H NMR (500 MHz, CDCl_3) δ 0.00 (s, 3H), 0.05 (s, 3H), 0.15 (s, 9H), 0.87 (s, 9H), 1.76 (dddd, 1H, *J*=13.1, 8.8, 8.0, 5.0 Hz), 1.85 (ddt, 1H, *J*=13.1, 8.8, 5.0 Hz), 1.99 (ddt, 1H, *J*=14.1, 5.0, 8.0 Hz), 2.04 (s, 3H), 2.23 (dddd, 1H, *J*=14.1, 8.0, 7.6, 5.0 Hz), 3.41 (s, 1H), 3.83 (t, 1H, *J*=5.0 Hz), 5.17 (dd, 1H, *J*=7.6, 5.0 Hz). ^{13}C NMR (125 MHz, CDCl_3) δ -5.11, -4.85, -0.54, 18.02, 21.00, 25.55, 29.18, 30.91, 49.16, 69.68, 70.37, 72.78, 92.90, 98.88, 170.08. ESI-TOFMS (positive-ion) calcd for $C_{19}H_{34}O_4Si_2H$: (M+H)⁺ 383.2074; found: 383.2034, calcd for $C_{19}H_{34}O_4Si_2NH_4$: (M+NH₄)⁺ 400.2339; found 400.2313, calcd for $C_{19}H_{34}O_4Si_2Na$: (M+Na)⁺ 405.1893; found: 405.1864, calcd for $C_{19}H_{34}O_4Si_2K$: (M+K)⁺ 421.1633; found 421.1612.

4.1.17. Ketone (31). To a solution of **29** (4.32 g, 12.7 mmol) in CH_2Cl_2 (30 ml) was added Dess–Martin periodinane (8.08 g, 19.1 mmol) and the mixture was stirred at room temperature for 1 h. The reaction was quenched with saturated aqueous NaHCO_3 . The aqueous layer was extracted with hexane, and the combined organic layer was dried over MgSO_4 , and concentrated in vacuo. The residue was purified by silica-gel column chromatography (hexane/AcOEt=30:1) to afford **31** (3.59 g, 84%) as needles. Mp 112–113 $^\circ\text{C}$ (from hexane/AcOEt) $[\alpha]_D^{23}=-121.3$ (*c* 0.50, CHCl_3). IR (film) ν 2955, 2853, 1747, 1401, 1249, 838 cm^{-1} . ^1H NMR (500 MHz, CDCl_3) δ 0.03 (s, 3H), 0.03 (s, 3H), 0.16 (s, 9H), 0.84 (s, 9H), 2.15–2.21 (m, 2H), 2.37 (dtd, 1H, *J*=18.9, 3.7, 3.0 Hz), 2.64 (dt, 1H, *J*=18.9, 10.5 Hz), 3.66 (s, 1H), 4.07 (brt, 1H, *J*=1.8 Hz). ^{13}C NMR (125 MHz, CDCl_3) δ -5.31, -4.83, -0.56, 17.99, 25.48, 28.06, 33.12, 50.57, 69.89, 71.68, 93.33, 96.61, 207.69. ESI-TOFMS (positive-ion) calcd for $C_{17}H_{30}O_3Si_2H$: (M+H)⁺ 339.1812; found: 339.1636. Anal. Calcd for $C_{17}H_{30}O_3Si_2$: C, 60.30; H, 8.93. Found C, 60.11; H, 8.95.

4.1.18. Diyne (7). To a solution of trimethylsilylacetylene (320 μl , 2.24 mmol) in THF (4 ml) was added dropwise *n*-BuLi (1.61 M hexane solution, 990 μl , 1.60 mmol) at -78°C and stirred at -78°C for 50 min. A solution of **31** (261 mg, 77.1 μmol) in THF (4 ml) was then slowly added at -78°C and the reaction mixture was stirred at -78°C for 3 h. The reaction mixture was quenched with sat. NH_4Cl aq. The aqueous layer was extracted with hexane. The combined organic layer was washed with brine, dried over Na_2SO_4 , and concentrated in vacuo to afford a crude mixture of epimeric alcohols (304 mg) as a yellow oil. To the mixture in dichloroethane (2 ml) were added Et_3N (600 μl , 7.64 mmol) and Ms_2O (274 mg, 1.57 mmol) at room temperature and the reaction mixture was stirred at

40 °C for 3 h. The reaction quenched with sat. NH₄Cl aq. The aqueous layer was extracted with hexane. The combined organic layer was washed with brine, dried over Na₂SO₄, and concentrated in vacuo to afford a crude mixture of mesylates (330 mg). To a solution of the mixture in THF (10 ml) was added TBAF (1.0 M THF solution, 3.5 ml, 3.50 mmol) at 0 °C. After stirring at the same temperature for 20 min, the reaction quenched with phosphate buffer (pH 7.0). The aqueous layer was extracted with ethyl acetate. The combined organic layer was washed with brine, dried over Na₂SO₄, and concentrated in vacuo. The reaction mixture was purified by silica-gel column chromatography (hexane/AcOEt=1:1) to afford **7** (70.6 mg, 57% in 2 steps) as colorless plates. Mp 86 °C (from hexane/AcOEt). $[\alpha]_D^{20} = +36.6$ (c 0.36, CHCl₃). IR (film) ν 3263, 905, 644 cm⁻¹. ¹H NMR (500 MHz, CDCl₃) δ 2.21 (brs, 1H), 2.50 (dt, 1H, *J*=19.1, 2.6 Hz), 2.53 (d, 1H, *J*=2.0 Hz), 2.83 (ddd, 1H, *J*=19.1, 6.3, 2.6 Hz), 3.04 (s, 1H), 3.74 (d, 1H, *J*=2.0 Hz), 4.20 (dd, 1H, *J*=6.3, 2.6 Hz), 6.62 (t, 1H, *J*=2.6 Hz), ¹³C NMR (125 MHz, CDCl₃) δ 38.42, 50.23, 69.70, 72.96, 76.41, 76.70, 77.06, 82.31, 119.95, 145.73. ESI-TOFMS (positive-ion) calcd for C₁₀H₈O₂NH₄: (M+NH₄)⁺ 178.0868; found: 178.0699, calcd for C₁₀H₈O₂Na: (M+Na)⁺ 183.0422; found: 183.0216, calcd for C₁₀H₈O₂K: (M+K)⁺ 199.0161; found 198.9940.

The absolute configuration of **7** was confirmed by the modified Mosher method using (*R*)- and (*S*)-MTPA esters of **7**:

Position	(<i>R</i>)-MTPA- 7 δ (ppm)	(<i>S</i>)-MTPA- 7 δ (ppm)	$\Delta\delta = \delta_S - \delta_R$
H-3	3.050	3.062	0.012
H-6	2.505	2.513	0.007
H-8	4.000	4.017	0.017
H-11	2.739	2.543	-0.196
H-11	3.043	2.955	-0.088
H-12	6.582	6.542	-0.040

4.1.19. Aryl ether (32). To a solution **7** (52.0 mg, 0.324 mmol) and CsF (53.0 mg, 0.349 mmol) in DMF (2 ml) was added a solution of **22** (97.0 mg, 0.173 mmol) in DMF (2 ml) at room temperature and the mixture was stirred at 60 °C for 12 h. The reaction was quenched with phosphate buffer (pH 7.0) at room temperature. The aqueous layer was extracted with ethyl acetate. The combined organic layer was washed with brine, dried over Na₂SO₄, and concentrated in vacuo. The reaction mixture was purified by silica-gel column chromatography (hexane/AcOEt=1:4) to afford triol (62.0 mg, 50%): $[\alpha]_D^{23} = -2.9$ (c 0.92, CHCl₃). IR (film) ν 3287, 1651, 1514, 1487, 1249, 1037 cm⁻¹. ¹H NMR (500 MHz, CDCl₃) δ 2.33 (dd, 1H, *J*=15.2, 8.3 Hz), 2.41 (d, 1H, *J*=2.0 Hz), 2.47 (ddd, 1H, *J*=17.8, 5.3, 2.0 Hz), 2.58 (dd, 1H, *J*=15.2, 3.1 Hz), 2.82 (ddd, 1H, *J*=17.8, 7.3, 3.1 Hz), 3.04 (s, 1H), 3.37 (brd, 1H, *J*=2.4 Hz), 3.72–3.79 (m, 4H), 3.83–3.89 (m, 4H), 4.11 (s, 1H), 4.15 (d, 1H, *J*=13.0 Hz), 4.18 (d, 1H, *J*=13.0 Hz), 4.43 (s, 2H), 4.79 (brd, 1H, *J*=3.1 Hz), 4.94 (ddd, 1H, *J*=7.3, 5.3, 2.4 Hz), 5.27 (dt, 1H, *J*=8.3, 3.1 Hz), 5.53 (d, 1H, *J*=2.0 Hz), 6.31 (t, 1H, *J*=7.0 Hz), 6.32 (dd, 1H, *J*=3.1, 2.0 Hz), 6.36 (t, 1H, *J*=5.8 Hz), 6.86 (d, 3H, *J*=8.8 Hz),

7.27 (d, 2H, *J*=8.8 Hz), 7.29 (d, 1H, *J*=8.8 Hz). ¹³C NMR (125 MHz, CDCl₃) δ 38.33, 38.68, 41.74, 55.12, 56.00, 67.30, 71.12, 71.47, 71.66, 76.33, 77.46, 77.59, 78.30, 80.47, 84.27, 101.81, 110.38, 113.73, 122.19, 124.52, 125.72, 129.18, 129.50, 133.12, 139.76, 141.12, 141.61, 152.21, 159.25, 171.57. ESI-TOFMS (positive-ion) calcd for C₃₂H₃₃ClINO₈H: (M+H)⁺ 722.1018; found: 722.0996, calcd for C₃₂H₃₃ClINO₈NH₄: (M+NH₄)⁺ 739.1283; found 739.1238, calcd for C₃₂H₃₃ClINO₈Na: (M+Na)⁺ 744.0837; found: 744.0787, calcd for C₃₂H₃₃ClINO₈K: (M+K)⁺ 760.0577; found 760.0441.

To a solution of the above triol (53.3 mg, 73.8 μ mol) and 2,6-lutidine (130 μ l, 1.12 mmol) in CH₂Cl₂ (1 ml) was added a solution of TBSOTf (100 μ l, 435 μ mol) at -78 °C and the mixture was stirred at room temperature for 12 h. The reaction was quenched with phosphate buffer (pH 7.0). The aqueous layer was extracted with ethyl acetate. The combined organic layer was washed with brine, dried over Na₂SO₄, and concentrated in vacuo. The reaction mixture was purified by silica-gel column chromatography (hexane/AcOEt=1:1) to afford **32** (60.2 mg, 77%) as amorphous solid: $[\alpha]_D^{23} = +34.5$ (0.60, CHCl₃). IR (film) ν 3311, 2954, 2930, 2856, 1659, 1651, 1514, 1487, 1251, 837, 778 cm⁻¹. ¹H NMR (500 MHz, CDCl₃) δ -0.19 (s, 3H), 0.02 (s, 3H), 0.04 (s, 3H), 0.08 (s, 3H), 0.12 (s, 3H), 0.21 (s, 3H), 0.86 (s, 9H), 0.89 (s, 9H), 0.92 (s, 9H), 2.21 (d, 1H, *J*=2.6 Hz), 2.32 (dd, 1H, *J*=14.1, 8.8 Hz), 2.39 (ddd, 1H, *J*=16.7, 7.3, 2.6 Hz), 2.53 (dd, 1H, *J*=14.1, 3.0 Hz), 2.62 (ddd, 1H, *J*=16.7, 7.3, 2.6 Hz), 3.04 (s, 1H), 3.79–3.94 (m, 8H), 4.21 (s, 2H), 4.46 (s, 2H), 4.63 (t, 1H, *J*=7.3 Hz), 5.36 (d, 1H, *J*=2.6 Hz), 5.43 (dd, 1H, *J*=8.8, 3.0 Hz), 6.12 (t, 1H, *J*=5.8 Hz), 6.33 (t, 1H, *J*=2.6 Hz), 6.44 (t, 1H, *J*=7.2 Hz), 6.84 (d, 1H, *J*=8.6 Hz), 6.89 (d, 2H, *J*=8.3 Hz), 7.17 (d, 1H, *J*=8.6 Hz), 7.31 (d, 2H, *J*=8.3 Hz). ¹³C NMR (125 MHz, CDCl₃) δ -5.45, -5.03, -4.78, -4.57, -2.63, -2.61, 17.95, 18.07, 18.71, 25.66, 25.95, 25.99, 38.80, 38.82, 45.74, 55.14, 55.52, 68.58, 71.35, 71.40, 72.42, 73.61, 76.48, 79.63, 79.88, 81.73, 85.14, 102.10, 110.09, 113.75, 121.89, 126.27, 127.12, 129.39, 129.52, 130.71, 140.28, 141.60, 142.07, 152.53, 159.27, 169.93. MALDI-TOFMS (positive-ion) calcd for C₅₀H₇₅ClINO₈Si₃Na: (M+Na)⁺ 1086.3431; found: 1086.3484, calcd for C₅₀H₇₅ClINO₈Si₃K: (M+K)⁺ 1102.3171; found 1102.3180.

4.1.20. Macrolactam (34). To a degassed solution of Pd₂(dba)₃·CHCl₃ (26.9 mg, 26.0 μ mol) and CuI (9.9 mg, 52.0 μ mol) in DMF (13 ml) was added a degassed solution of **32** (27.7 mg, 26.0 μ mol) and (*i*-Pr)₂NEt (160 μ l) in DMF (13 ml) at 60 °C. The mixture was stirred at 60 °C for 3 h. The reaction mixture was quenched with saturated NH₄Cl solution. The aqueous layer was extracted with ethyl acetate, and the combined organic layer was dried over Na₂SO₄, and concentrated in vacuo. The residue was purified by silica-gel column chromatography to afford **34** (9.7 mg, 40%) as colorless needles, mp 210–213 °C (from hexane/AcOEt): $[\alpha]_D^{20} = -35.5$ (0.16, CHCl₃). IR (film) ν 3287, 2929, 2856, 1634, 1253, 1090, 1072, 837, 778 cm⁻¹. ¹H NMR (500 MHz, CDCl₃) δ -0.38 (s, 3H), -0.14 (s, 3H), -0.05 (s, 3H), 0.10 (s, 3H), 0.15 (s, 3H), 0.21 (s, 3H), 0.77 (s, 9H), 0.83 (s, 9H), 0.95 (s, 9H), 2.02 (t, 1H, *J*=10.7 Hz), 2.82–2.87 (m, 2H), 2.94 (ddd, 1H, *J*=15.5, 7.8, 1.4 Hz), 3.30 (s, 3H, C3'-OMe), 3.57 (dd, 1H, *J*=14.1,

2.3 Hz, CH₂N), 3.83 (s, 3H), 4.19 (d, 1H, *J*=11.7 Hz, CH₂OMPM), 4.20 (d, 1H, *J*=11.2 Hz), 4.27 (d, 1H, *J*=11.2 Hz), 4.62 (d, 1H, *J*=11.7 Hz, CH₂OMPM), 4.88 (dd, 1H, *J*=14.1, 10.8 Hz, CH₂N), 5.00 (dd, 1H, *J*=10.8, 2.3 Hz, NH), 5.22 (t, 1H, *J*=7.8 Hz), 5.35 (s, 1H, H-8), 5.61 (dd, 1H, *J*=10.7, 4.8 Hz), 5.87 (dd, 1H, *J*=3.5, 1.4 Hz, H-12), 6.34 (d, 1H, *J*=8.3 Hz, H-4'), 6.86 (d, 1H, *J*=8.3 Hz, H-5'), 6.92 (d, 2H, *J*=8.8 Hz), 7.04 (s, 1H, H-3), 7.18 (d, 2H, *J*=8.8 Hz), 7.30 (s, 1H, H-6). ¹³C NMR (125 MHz, CDCl₃) δ -5.17, -5.03, -4.77, -4.39, -3.21, -3.06, 17.77, 18.13, 18.42, 25.61, 25.66, 26.00, 38.47 (C14), 43.55, 48.98, 54.88, 55.24, 67.54, 70.39 (C5), 70.57, 70.79, 83.76 (C8), 92.45 (C9), 110.19, 113.88, 120.24, 121.91 (C3), 122.10, 128.97, 129.21, 129.72, 131.44 (C6), 133.47, 135.81 (C4), 136.12 (C2), 138.96 (C13), 142.33, 144.30 (C7), 150.06 (C1), 153.95, 159.33, 168.34. HMBC correlations: H3–C1, H3–C7, H3–C5, H3–C13; H5–C3, H5–C4, H5–C13; H6–C2, H6–C4, H6–C8, H6–C14. MALDI-TOFMS (positive-ion) calcd for C₅₀H₇₄ClNO₈Si₃-Na: (M+Na)⁺ 958.4308; found: 958.4375, calcd for C₅₀H₇₄ClNO₈Si₃K: (M+K)⁺ 974.4048; found 974.4182.

Acknowledgements

This work was supported by CREST, Japan Science and Technology Corporation (JST). We thank Dr. Chizuko Kabuto for her assistance in X-ray crystallographic analysis, and Mr. Kazuo Sasaki for his detailed NMR spectroscopic analysis. A fellowship to N. K. from the Japanese Society for the Promotion of Science (JSPS) for Young Japanese Scientists and a postdoctoral fellowship to S. K. from JSPS are gratefully acknowledged. We are grateful to ZEON CORPORATION for cyclopentenone.

References and notes

- For maduropeptin, see: (a) Hanada, M.; Ohkuma, H.; Yonemoto, T.; Tomita, K.; Ohbayashi, M.; Kamei, H.; Miyaki, T.; Konishi, M.; Kawaguchi, H.; Forenza, S. *J. Antibiot.* **1991**, *44*, 403. (b) Schroeder, D. R.; Colson, K. L.; Klohr, S. E.; Zein, N.; Langley, D. R.; Lee, M. S.; Matson, J. A.; Doyle, T. W. *J. Am. Chem. Soc.* **1994**, *116*, 9351. (c) Zein, N.; Solomon, W.; Colson, K. L.; Schroeder, D. R. *Biochemistry* **1995**, *34*, 11591. (d) Zein, N.; Reiss, P.; Bernatowicz, M.; Bolger, M. *Chem. Biol.* **1995**, *2*, 451.
- For synthetic studies of the maduropeptin chromophore: (a) Nicolaou, K. C.; Koide, K. *Tetrahedron Lett.* **1997**, *38*, 3667. (b) Nicolaou, K. C.; Koide, K.; Xu, J.; Izraelewicz, M. H. *Tetrahedron Lett.* **1997**, *38*, 3671. (c) Suffert, J.; Toussaint, D. *Tetrahedron Lett.* **1997**, *38*, 5507. (d) Roger, C.; Grierson, D. S. *Tetrahedron Lett.* **1998**, *39*, 27. (e) Dai, W.-M.; Fong, K. C.; Lau, C. W.; Zhou, L.; Hamaguchi, W.; Nishimoto, S. *J. Org. Chem.* **1999**, *64*, 682. (f) Khan, S.; Kato, N.; Hiram, M. *Synlett* **2000**, 1494.
- Iida, K.; Fukuda, S.; Tanaka, T.; Hiram, M.; Imajo, S.; Ishiguro, M.; Yoshida, K.; Otani, T. *Tetrahedron Lett.* **1996**, *37*, 4997. (b) Minami, Y.; Yoshida, K.; Azuma, R.; Saeki, M.; Otani, T. *Tetrahedron Lett.* **1993**, *34*, 2633. (c) Yoshida, K.; Minami, Y.; Azuma, R.; Saeki, M.; Otani, T. *Tetrahedron Lett.* **1993**, *34*, 2637.
- Kawata, S.; Ashizawa, S.; Hiram, M. *J. Am. Chem. Soc.* **1997**, *119*, 12012. (b) Leet, J. E.; Schroeder, D. R.; Langley, D. R.; Colson, K. L.; Huang, S.; Klohr, S. E.; Lee, M. S.; Golik, J.; Hofstead, S. J.; Doyle, T.; Matson, J. A. *J. Am. Chem. Soc.* **1993**, *115*, 8432. (c) Leet, J. E.; Schroeder, D. R.; Hofstead, S. J.; Golik, J.; Colson, K. L.; Huang, S.; Klohr, S. E.; Doyle, T. W.; Matson, J. A. *J. Am. Chem. Soc.* **1992**, *114*, 7946.
- For reviews on enediyne antibiotics, see: (a) Maeda, H.; Edo, K.; Ishida, N., Eds.; Springer: Tokyo, **1997**. (b) Xi, Z.; Goldberg, I. H. *Comprehensive natural products chemistry*; Barton, D. H. R., Nakanishi, K., Eds.; Elsevier: Amsterdam, 1999; Vol. 7, p 533. (c) Nicolaou, K. C.; Dai, W.-M. *Angew. Chem. Int. Ed. Engl.* **1991**, *30*, 1387. (d) Grissom, J. W.; Gunawardena, G. U.; Klingberg, D.; Huang, D. *Tetrahedron* **1996**, *52*, 6453. (e) Smith, A. L.; Nicolaou, K. C. *J. Med. Chem.* **1996**, *39*, 2103.
- For recent synthetic studies on nine-membered endiynes antibiotics, see: (a) Myers, A. G.; Hogan, P. C.; Hurd, A. R.; Goldberg, S. D. *Angew. Chem. Int. Ed. Engl.* **2002**, *41*, 1062. (b) Myers, A. G.; Glatthar, R.; Hammond, M.; Harrington, P. M.; Kuo, E. Y.; Liang, J.; Schaus, S. E.; Wu, Y.; Xiang, J.-N. *J. Am. Chem. Soc.* **2002**, *124*, 5380. (c) Kobayashi, S.; Ashizawa, S.; Takahashi, Y.; Sugiura, Y.; Nagaoka, M.; Lear, M. J.; Hiram, M. *J. Am. Chem. Soc.* **2001**, *123*, 11294. (d) Kobayashi, S.; Reddy, R. S.; Sugiura, Y.; Sasaki, D.; Miyagawa, N.; Hiram, M. *J. Am. Chem. Soc.* **2001**, *123*, 2887. (e) Myers, A. G.; Liang, J.; Hammond, M.; Harrington, P. M.; Wu, Y.; Kuo, E. Y. *J. Am. Chem. Soc.* **1998**, *120*, 5319. (f) Myers, A. G.; Goldberg, S. D. *Angew. Chem. Int. Ed. Engl.* **2000**, *39*, 2732. (g) Magnus, P.; Carter, R.; Davies, M.; Elliott, J.; Pitterna, T. *Tetrahedron* **1996**, *52*, 6283. (h) Caddick, S.; Delisser, V. M.; Doyle, V. E.; Khan, S.; Avent, A. G.; Vile, S. *Tetrahedron* **1999**, *55*, 2737. (i) Tanaka, H.; Yamada, H.; Matsuda, A.; Takahashi, T. *Synlett* **1997**, 381, and references cited therein.
- Yoshimura, F.; Kawata, S.; Hiram, M. *Tetrahedron Lett.* **1999**, *40*, 8281.
- Related synthetic studies, see: (a) Nakatani, K.; Arai, K.; Hirayama, N.; Matsuda, F.; Terashima, S. *Tetrahedron Lett.* **1990**, *31*, 2323. (b) Nakatani, K.; Arai, K.; Yamada, K.; Terashima, S. *Tetrahedron Lett.* **1991**, *32*, 3405. (c) Nakatani, K.; Arai, K.; Hirayama, N.; Matsuda, F.; Terashima, S. *Tetrahedron* **1992**, *48*, 633. (d) Nakatani, K.; Arai, K.; Terashima, S. *J. Chem. Soc., Chem. Commun.* **1992**, 289. (e) Nakatani, K.; Arai, K.; Yamada, K.; Terashima, S. *Tetrahedron* **1992**, *48*, 3045. (f) Nakatani, K.; Arai, K.; Terashima, S. *Tetrahedron* **1993**, *49*, 1901. (g) Brückner, R.; Scheuplein, S. W.; Suffert, J. *Tetrahedron Lett.* **1991**, *32*, 1449. (h) Suffert, J.; Brückner, R. *Tetrahedron Lett.* **1991**, *32*, 1453. (i) Scheuplein, S. W.; Harms, K.; Brückner, R.; Suffert, J. *Chem. Ber.* **1992**, *125*, 271. (j) Suffert, J.; Eggers, A.; Scheuplein, S. W.; Brückner, R. *Tetrahedron Lett.* **1993**, *34*, 4177. (k) Dai, W.-M.; Wu, J. *Tetrahedron* **1997**, *53*, 9107.
- Kawata, S.; Hiram, M. *Tetrahedron Lett.* **1998**, *39*, 8707. (b) Sato, I.; Kikuchi, T. *Hirama. Chem. Lett.* **1999**, 511. (c) Kitaori, K.; Furukawa, Y.; Yoshimoto, H.; Otera, J. *Tetrahedron Lett.* **1998**, *39*, 3173. (d) Nambu, Y.; Endo, T. *Tetrahedron Lett.* **1990**, *31*, 1723.
- For a review, see: Mitunobu, O. *Synthesis* **1981**, 1.
- Ginsburg, D. *J. Am. Chem. Soc.* **1951**, *73*, 703.
- Iwasawa, N.; Mukaiyama, T. *Chem. Lett.* **1983**, 297. (b) Mukaiyama, T.; Iwasawa, N.; Stevens, R. W.; Haga, T.

- Tetrahedron* **1984**, *40*, 1381. (c) Iwasawa, N.; Mukaiya, T. *Chem. Lett.* **1982**, 1441.
- Crystal data: $C_{13}H_{14}ClNO_4S_2$, $M=347.83$, monoclinic, space group $P2_1$, $D_c=1.567\text{ g/cm}^3$, $Z=2$, $a=4.562(1)\text{ \AA}$, $b=14.341(4)\text{ \AA}$, $c=11.433(3)\text{ \AA}$, $\alpha=99.743(6)^\circ$, $\beta=737.2(3)^\circ$, $F(000)=360.00$, $\mu(\text{Mo K}\alpha)=5.56\text{ cm}^{-1}$, $R=0.026$, $R_w=0.033$. Crystallographic data for the structures in this paper have been deposited with Cambridge Crystallographic Data Centre as supplementary publication numbers CCDC 226183 (20) and CCDC 226184 (26) in CIF format. Copies of the data can be obtained, free of charge, on application of CCDC, 12 Union Road, Cambridge CB2 1EZ, UK [fax:+44(0)-1223-336033 or e-mail deposit@ccdc.cam.ac.uk].
 - Fujita, E. *Pure Appl. Chem.* **1981**, *53*, 1141.
 - Corey, E. J.; Rao, K. S. *Tetrahedron Lett.* **1991**, *32*, 4623.
 - Smith, A. B., III; Branca, S. J.; Guaciaro, M. A.; Wovkulich, P. M.; Korn, A. *Org. Synth.* **1983**, *61*, 65.
 - Katsuki, T.; Sharpless, K. B. *J. Am. Chem. Soc.* **1980**, *102*, 5974. (b) Gao, Y.; Hanson, R. M.; Klunder, J. M.; Ko, S. Y.; Masamune, H.; Sharpless, K. B. *J. Am. Chem. Soc.* **1987**, *109*, 5765.
 - Crystal data: $C_{17}H_{32}O_3Si_2$, $M=340.61$, monoclinic, space group $C2/c$, $D_c=1.041\text{ g/cm}^3$, $Z=8$, $a=28.247(7)\text{ \AA}$, $b=7.798(3)\text{ \AA}$, $c=24.593(7)\text{ \AA}$, $\alpha=126.65(1)^\circ$, $\beta=4326(2)\text{ \AA}^3$, $F(000)=1488.00$, $\mu(\text{Mo K}\alpha)=1.72\text{ cm}^{-1}$, $R=0.089$, $R_w=0.088$. See also Ref. 13.
 - Afonso, A. M.; Vieira, N. M. L.; Motherwell, W. B. *Synlett* **2000**, 382.
 - For stereochemistry, see: (a) Corey, L. D.; Singh, S. M.; Oehlschlager, A. C. *Can. J. Chem.* **1987**, *65*, 1821. (b) Sarandeses, L. A.; Mourino, A.; Luche, J.-L. *J. Chem. Soc., Chem. Commun.* **1991**, 818.
 - For synthetic utility, see: (a) Nicolaou, K. C.; Duggan, M. E.; Ladduwahetty, T. *Tetrahedron Lett.* **1984**, *25*, 2069. (b) Balmer, E.; Germain, A.; Jackson, W. P.; Lygo, B. *J. Chem. Soc. Perkin Trans. 1* **1993**, 399. (c) Barluenga, J.; Llavona, L.; Bernad, P. L.; Concellon, J. M. *Tetrahedron Lett.* **1993**, *34*, 3173.
 - The absolute configuration of **10** was confirmed by the modified Mosher method (Ohtani, I.; Kusumi, T.; Kashman, Y.; Kakisawa, H. *J. Am. Chem. Soc.* **1991**, *60*, 504) using (*S*)- and (*R*)-MTPA esters of **7**. See Section 4.
 - Dess, D. B.; Martin, J. C. *J. Am. Chem. Soc.* **1991**, *113*, 7277. (b) Dess, D. B.; Martin, J. C. *J. Org. Chem.* **1983**, *48*, 4156. (c) Ireland, R. E.; Liu, L. *J. Org. Chem.* **1993**, *58*, 2899.
 - For review, see: Saito, S.; Yamamoto, Y. *Chem. Rev.* **2000**, *100*, 2901.

Pentaspiranes and hexaspiranes with 1,3-dioxane or 1,3-oxathiane rings: synthesis and stereochemistry

Anamaria Terec,^a Ion Grosu,^{a,*} Eric Condamine,^b Livain Breau,^c Gérard Plé,^b Yvan Ramondenc,^b Fernande D. Rochon,^c Valérie Peulon-Agasse^b and Dorina Opris^a

^aOrganic Chemistry Department and CSOFSTM, "Babes-Bolyai" University, 11 Arany Janos str., RO-400028 Cluj-Napoca, Romania

^bFaculté des Sciences, Université de Rouen, IRCOF, UMR 6014, 76821 Mont Saint-Aignan, Cedex, France

^cUniversité du Québec à Montréal, CP 8888, Succ. Centre Ville, Montréal, Que., Canada H3C 3P8

Received 25 November 2003; revised 2 February 2004; accepted 12 February 2004

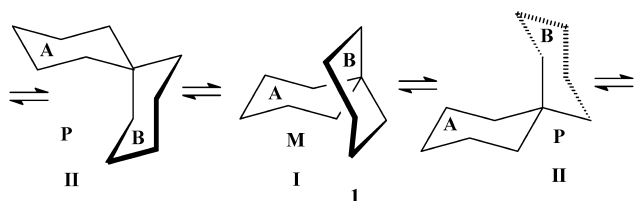
Abstract—The synthesis and stereochemistry of the first reported pentaspiro- and hexaspiro-1,3-dioxane and polyspiro-1,3-oxathiane (from dispiro to hexaspiro) derivatives are described. The crystal structures of a dispiro- and tetraspiro-1,3-oxathiane were determined by X-ray diffraction methods. NMR and chiral column HPLC investigations in solution revealed flexible and semiflexible structures for which *syn-anti*, *cis-trans* and *d,l* isomers were observed.

© 2004 Elsevier Ltd. All rights reserved.

1. Introduction

Our previous investigations^{1–4} of the stereochemistry of spiro-1,3-dioxanes dealt with the helical chirality of those spiranes with six-membered rings. The sequence of a helix which exhibits P or M configuration repeats after every fourth six-membered ring.

The parent compound, spiro[5.5]undecane **1** exhibits a flexible structure in which ring flip (A and B, Scheme 1) causes enantiomeric inversion. [I(M)⇌II(P)].



Scheme 1.

The dispiranes, as well as the higher members of the polyspirane series, can be built up by merging the corresponding monospirane units. For example, dispirane **2** (Scheme 2, Table 1), is made up of monospiranes AB and BC. If the two merged units have the same helix configuration, a dispirane with a M (III) or P (V) configuration is obtained, but if they have different helix

configurations, the achiral form (IV) of the dispirane is generated. At the same time marginal rings A and C can be oriented on the same side of the best plane of ring B (defined by bonds C⁶–C¹ and C⁶–C⁵ or C⁹–C¹⁰ and C⁹–C¹⁴) for which the structures are named 6,9-*syn*. If they are on opposite sides of the reference plane the isomer is 6,9-*anti*. The *syn* or *anti* orientations of marginal rings A and C can be deduced from the values of the dihedral angle described by the planes formed by bonds C¹⁰–C¹¹, C¹³–C¹⁴ and C¹–C², C⁴–C⁵. The dihedral angle is close to 0° for the *anti* isomer, while for the *syn* isomers the two reference planes are perpendicular. The *syn* isomers are chiral and exhibit M or P configurations while the *anti* isomer is achiral, being centrosymmetric.

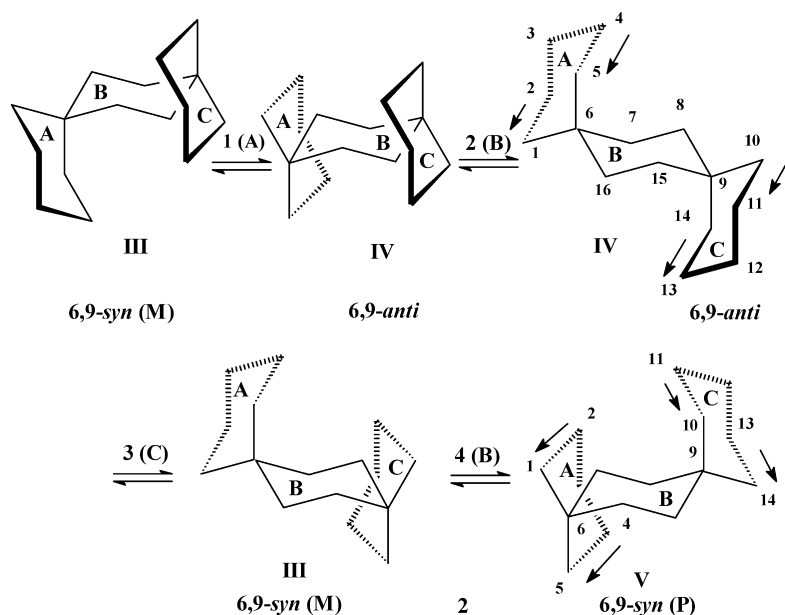
The possible stereoisomers of trispirane **3** and tetraspirane **4** (Scheme 3, Table 1) and their chirality may be deduced from the configurations of the three (or four) constituent monospiro units (Table 1). For an odd number of monospiro units all the possible stereoisomers are chiral, while in the case of an even number of monospiro units, achiral forms are also present.

The number of possible stereoisomers increases with the number of monospirane units. The number of possible structures of trispirane **3** is 6 and the tetraspirane **4** and the pentaspirane **5** exhibit 10 and 20 isomers, respectively (Table 1).

Hexaspirane **6** shows 36 possible conformers of the spirane skeleton (found by extending the algorithm discussed for compounds **1–5**) four of them being achiral (6,9-*syn*-9,12-*syn*-12,15-*anti*-15,18-*syn*-18,21-*syn*; 6,9-*syn*-9,12-*anti*-12,

Keywords: Polyspiranes; Conformational analysis; Helical and axial chirality.

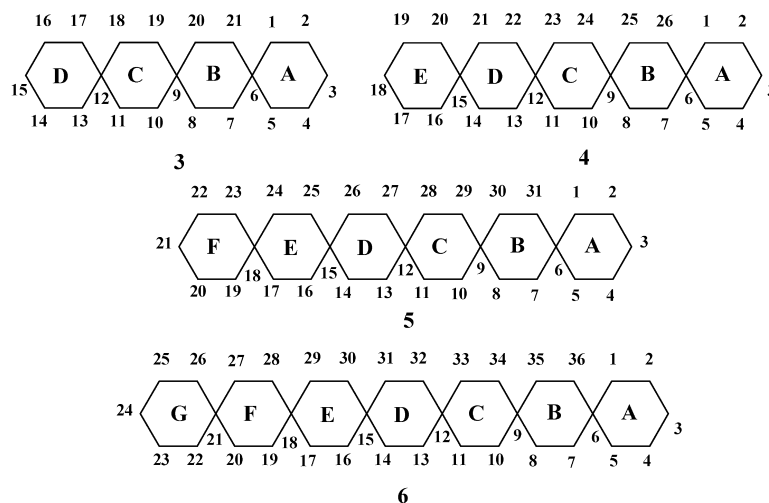
* Corresponding author. Tel.: +40-6459-3833; fax: +40-6459-0818; e-mail address: igrosu@chem.ubbcluj.ro



Scheme 2.

Table 1. Possible stereoisomers of spiro (from mono to penta) compounds with six-membered rings

Isomer	Rings orientation 6,9-9,12-12,15-15,18	AB	BC	CD	DE	EF	Helix
I	—	M	—	—	—	—	M
II	—	P	—	—	—	—	P
III	<i>syn</i>	M	M	—	—	—	M
IV	<i>anti</i>	P(M)	M(P)	—	—	—	—
V	<i>syn</i>	P	P	—	—	—	P
VI	<i>syn-syn</i>	M	M	M	—	—	M
VII	<i>syn-syn</i>	P	P	P	—	—	P
VIII	<i>syn-anti</i>	P	P	M	—	—	P
IX	<i>syn-anti</i>	M	M	P	—	—	M
X	<i>anti-anti</i>	P	M	P	—	—	P
XI	<i>anti-anti</i>	M	P	M	—	—	M
XII	<i>syn-syn-syn</i>	P	P	P	P	—	P
XIII	<i>syn-syn-syn</i>	M	M	M	M	—	M
XIV	<i>syn-syn-anti</i>	P	P	P	M	—	P
XV	<i>syn-syn-anti</i>	M	M	M	P	—	M
XVI	<i>anti-syn-anti</i>	M	P	P	M	—	P
XVII	<i>anti-syn-anti</i>	P	M	M	P	—	M
XVIII	<i>anti-anti-syn</i>	P	M	P	P	—	P
XIX	<i>anti-anti-syn</i>	M	P	M	M	—	M
XX	<i>anti-anti-anti</i>	M(P)	M(P)	P(M)	P(M)	—	—
XXI	<i>anti-anti-anti</i>	M(P)	P(M)	M(P)	P(M)	—	—
XXII	<i>syn-syn-syn-syn</i>	M	M	M	M	M	M
XXIII	<i>syn-syn-syn-syn</i>	P	P	P	P	P	P
XXIV	<i>syn-syn-syn-anti</i>	M	M	M	M	P	M
XXV	<i>syn-syn-syn-anti</i>	P	P	P	P	M	P
XXVI	<i>syn-syn-anti-syn</i>	M	M	M	P	P	M
XXVII	<i>syn-syn-anti-syn</i>	P	P	P	M	M	P
XVIII	<i>syn-syn-anti-anti</i>	M	M	M	P	M	M
XXIX	<i>syn-syn-anti-anti</i>	P	P	P	M	P	P
XXX	<i>syn-anti-syn-anti</i>	M	M	P	P	M	M
XXXI	<i>syn-anti-syn-anti</i>	P	P	M	M	P	P
XXXII	<i>syn-anti-anti-syn</i>	M	M	P	M	M	M
XXXIII	<i>syn-anti-anti-syn</i>	P	P	M	P	P	P
XXXIV	<i>anti-syn-syn-anti</i>	M	P	P	P	M	P
XXXV	<i>anti-syn-syn-anti</i>	P	M	M	M	P	M
XXXVI	<i>syn-anti-anti-anti</i>	M	M	P	M	P	M
XXXVII	<i>syn-anti-anti-anti</i>	P	P	M	P	M	P
XXXVIII	<i>anti-syn-anti-anti</i>	M	P	P	M	P	P
XXXIX	<i>anti-syn-anti-anti</i>	P	M	M	P	M	M
XL	<i>anti-anti-anti-anti</i>	M	P	M	P	M	M
XLI	<i>anti-anti-anti-anti</i>	P	M	P	M	P	P



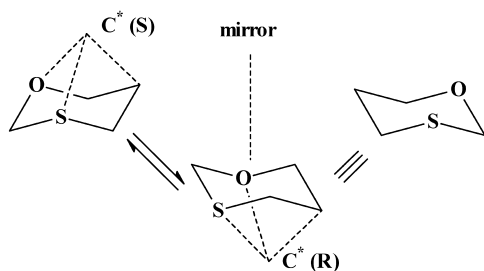
Scheme 3.

15-*anti*-15,18-*anti*-18,21-*syn*; 6,9-*anti*-9,12-*syn*-12,15-*anti*-15,18-*syn*-18,21-*anti* and 6,9-*anti*-9,12-*anti*-12,15-*anti*-15,18-*anti*-18,21-*anti*).

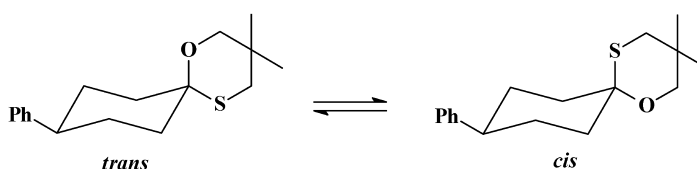
Earlier studies^{5,6} of the monocycle and spiro-1,3-oxathianes determined that the peculiar chirality of the unsubstituted heterocycle involves a virtual tricoordinated chiral center (Scheme 4)⁵ and we also disclosed *cis*–*trans* equilibration of some of the spiro-derivatives via ring-chain tautomerism (Scheme 5).⁶

We decided to extend our structural investigation to include the synthesis of a new series of compounds involving larger

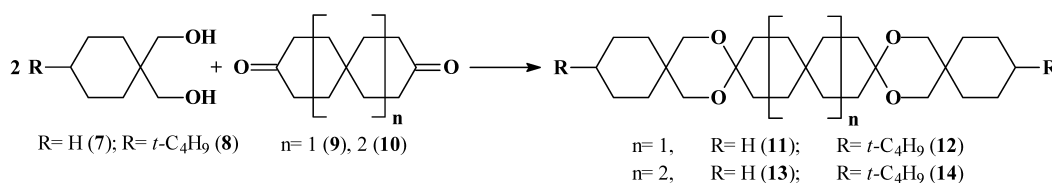
spiro-1,3-dioxane (penta and hexaspiro) and polypspiro-1,3-oxathiane derivatives (up to hexaspiro) given the interesting configurational and conformational aspects (revealed by variable temperature NMR experiments) of six-membered ring spiro compounds observed in previous studies. These were performed with spiro-1,3-dioxanes, spiro-1,3-oxathiane and polypspiro-1,3-dioxanes (up to tetraspiro-anes).^{1–10} Also we wished to gain a better understanding of the observations concerning the stereochemistry of these derivatives. As far as we know, only a few penta and hexaspiro-anes have already been reported^{11–25} (all of them from the ‘rotan’ family; i.e., all spiro atoms being located on the same ring) and no studies of the higher spiranes were found. Our target spiranes are among the largest described in the literature and the first ones of this size to have 1,3-dioxane or 1,3-oxathiane rings.



Scheme 4.



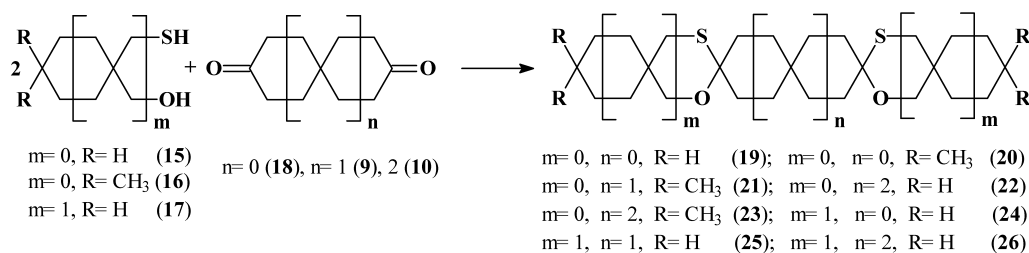
Scheme 5.



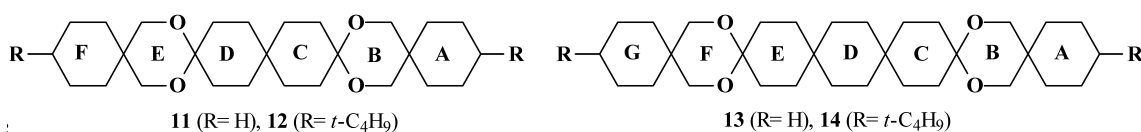
Scheme 6.

2. Results and discussion

New polypspiro 1,3-dioxanes **11–14** and oxathianes **19–26** were obtained by condensation reactions of a dicarbonyl compound with a 1,3-diol or a 3-mercapto-alcohol (Schemes 6 and 7).



Scheme 7.



Scheme 8.

2.1. Penta and hexaspiro-1,3-dioxanes

Compounds **11** and **13** have flexible structures (R=H, Scheme 8). All the rings are flipping and all the possible structures of the spirane are in equilibrium. The NMR spectra of these compounds at rt show singlets for the methylene protons of the 1,3-dioxane rings (Table 2). At low temperature (180 K), the changes in the shape of the spectra (broad bands instead of the singlets) suggest that ring flip is frozen.

Table 2. NMR data (CH₂–O moiety, CD₂Cl₂) for **11–14**

Compound	11	12	13	14
δ (–CH ₂ –), ppm	3.54	3.38 3.67	3.46	3.38 3.67

Compounds **12** and **14** (Scheme 8, R=*t*-C₄H₉) exhibit semiflexible structures, the marginal rings being anacomeric²⁶ ('rigid') while the middle part of the spiranes is flipping (**12**: rings B, C, D, E; **14**: B, C, D, E, F; Scheme 8). The conformational equilibria in **12** involve, on one side, 10 possible structures XXII, XXV, XXVI, XXIX, XXX, XXXIII, XXXV, XXXVI, XXXIX and XL and, on the other side, the other 10 possible conformers (Table 1). To transform a structure of one of these groups into a structure belonging to the other group it is necessary to break and to remake bonds with the opposite stereochemistry. This transformation is not possible via conformational equilibrium, so two separable stereoisomers are possible. A comparison of the configuration of the chiral elements of the isomers of **12** shows that they are enantiomers.

In order to observe the enantiomers of **12**, the compound (racemate) was subjected to resolution on chiral column HPLC. A partial resolution ($t_{R1}=24.9$ min and $t_{R2}=25.8$ min) was observed on CHIRALCEL OD column, using an isocratic mobile phase (*n*-hexane) and polarimetric, mass spectrometry (ESI-MS) and evaporative light scattering detection (ELSD).

Investigations of the conformational equilibria of **14** demonstrated the possibility of having two separable

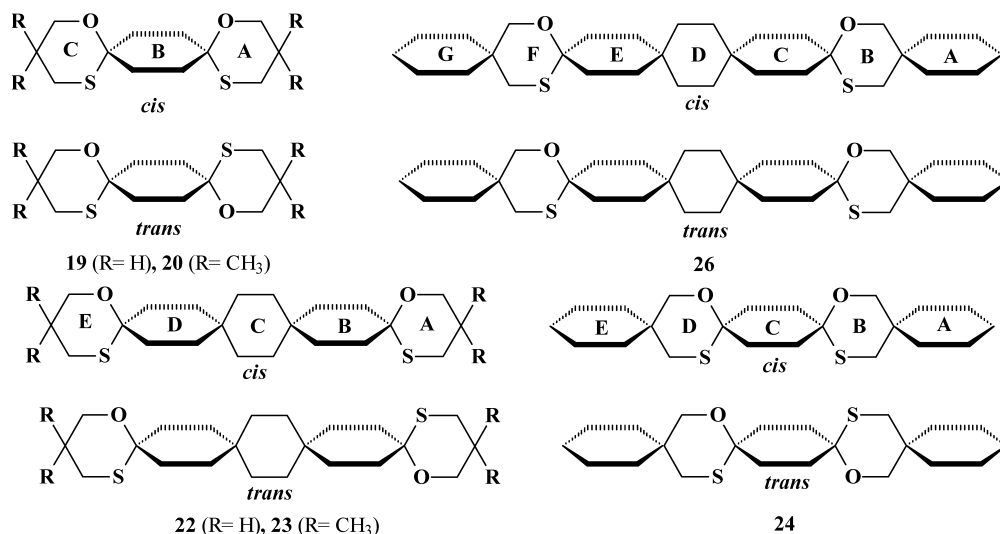
diastereoisomers (as can be deduced from the configurations of the chiral elements). As for **12**, there are two groups of conformers (one of 19 and the other of 17 possible structures for a total of 36). To transform one member of a group into another of the same group, ring flips are sufficient, while to change from a structure of one group into one of the other requires the breaking and remaking of bonds with inverted stereochemistry. The pentaspiro with fixing groups at its extremities and other substituted spiranes with an odd number of spiro units (e.g., monospiro and trispiro),^{1,2} have separable enantiomers, while those with an even number of spiro units (e.g., substituted dispiro, tetraspiro and hexaspiro)^{3,4} exhibit separable diastereoisomers. In the NMR spectra of **12** and **14** (mixtures of diastereoisomers), recorded at rt, the protons of the 1,3-dioxane rings show up as two singlets (Table 2). The low temperature spectra (180 K, CD₂Cl₂) of these compounds reveal that the flipping of the rings is frozen and rather than the above two singlets, four groups of unresolved signals (bands) are observed from 3.0 to 4.2 ppm. These signals belong to the axial and equatorial protons of the various structurally frozen diastereoisomers.

2.2. Polyspiro-1,3-oxathianes

The stereochemistry of polyspiro-1,3-oxathianes **19–26** correlates with the total number of spiro units and with the number of cyclohexane rings separating the two heterocycles. If the two 1,3-oxathiane rings are separated by an odd number of carbocycles, the compound exhibits *cis* and *trans* isomers, whereas, if the number of intervening cyclohexane rings is even, the polyspiro-1,3-oxathiane has separable enantiomers.

2.2.1. Stereochemistry of compounds **19**, **20**, **22–24** and **26**

Compounds **19**, **20**, **22–24** and **26** were separated by flash-chromatography into the two possible diastereoisomers (*cis* and *trans*, Scheme 9) and these were investigated as single compounds. In most of the syntheses, the major isomer was *trans* (Table 3). The two isomers have very similar NMR spectra and, in the majority of cases, they could not be differentiated (in their mixture) by NMR. The ratios were calculated using the already determined amounts of separated isomers.



Scheme 9.

Table 3. *trans/cis* or (D^1/D^2)^a ratio of compounds **19**, **20**, **22–24** and **26**

Compound	19	20	22	23	24	26
<i>trans/cis</i> (D^1/D^2)	0.94	1.35	1.44	1.52	1.50	1.04

The assignment for the *trans* and *cis* structures could not be performed unambiguously; D^1 for **23** and **26** is only assumed to be the *trans* isomer.

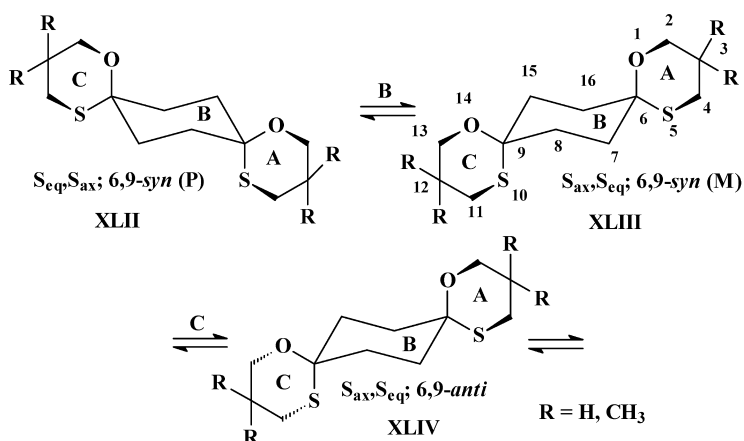
The possible conformational equilibria for the *cis* and *trans* isomers of dispiroanes **19** and **20** are shown in Schemes 10 and 11. There are three *cis* structures corresponding to the *syn* (P and M helix) and *anti* orientations of the spirane skeleton. In all of these structures one of the sulfur atoms (on the middle cyclohexane ring) is equatorial and the other, axial. Sulfur is the reference atom since it has priority. The number of possible conformers for the *trans* isomers of **19** and **20** is higher (six) because both sulfur atoms must either be equatorial (main case) or axial (minor case), and each of these is either *syn* (P or M configuration) or *anti*.

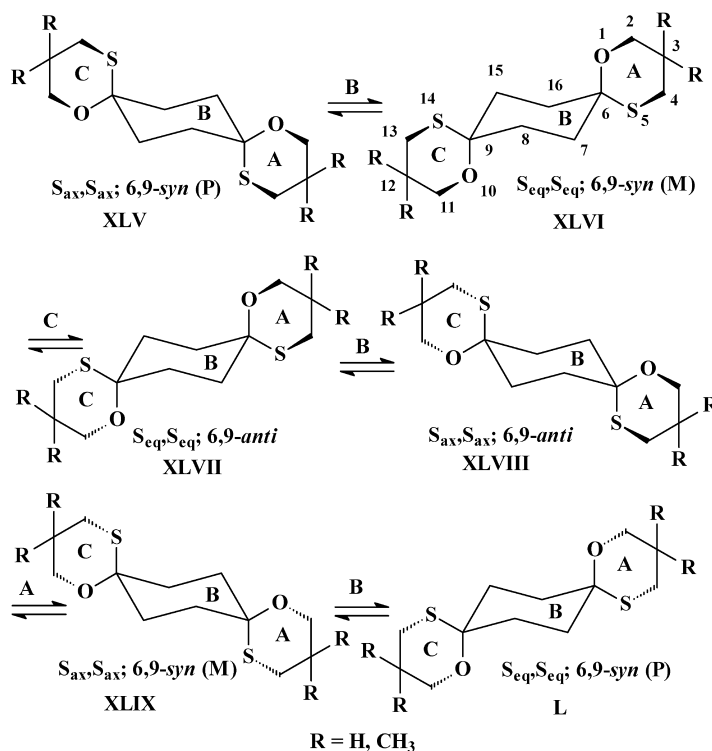
At rt, all possible conformers of each diastereoisomer (*cis* or *trans*) are in equilibrium. The NMR spectra recorded at this temperature are very simple (e.g., the spectra of the *trans* and *cis* isomers of **20** only show two singlets for the protons

of the heterocycles; *trans*: $\delta_{O-CH_2}=3.40$ ppm and $\delta_{S-CH_2}=2.61$ ppm; *cis*: $\delta_{O-CH_2}=3.42$ ppm and $\delta_{S-CH_2}=2.59$ ppm; Table 4). The 1H NMR spectra of the *cis* and *trans* isomers of dispiro-1,3-oxathianes are very similar. Nonetheless, some differences were observed for the protons of the middle cyclohexane ring. The flipping of the rings in both isomers produces isochronous carbon resonances at positions 7, 8, 15 and 16 (one signal in ^{13}C NMR spectra). However, the protons at these positions are not all equivalent in the conformational equilibrium (Scheme 12).

Four of the eight protons at these positions are *pro-cis* (denoted with c), being oriented on the same side of the middle ring as the two sulfur atoms in the *cis* isomer or on the same side as the closer sulfur atom in the *trans* isomer. The other four protons are oriented on opposite sides of the middle ring with respect to the reference sulfur atoms and, thus, are *pro-trans* (denoted with t).

In the NMR spectrum of the *trans* isomer, the protons of the cyclohexane ring correspond to two doublets at δ 1.80 and 2.1 ppm with an average coupling constant of 10.0 Hz, while in the spectrum of the *cis* isomer, the signals at δ 1.85–2.05 ppm are unresolved doublets of doublets (Figs. 1a and 2a). The low temperature spectra of the isomers of

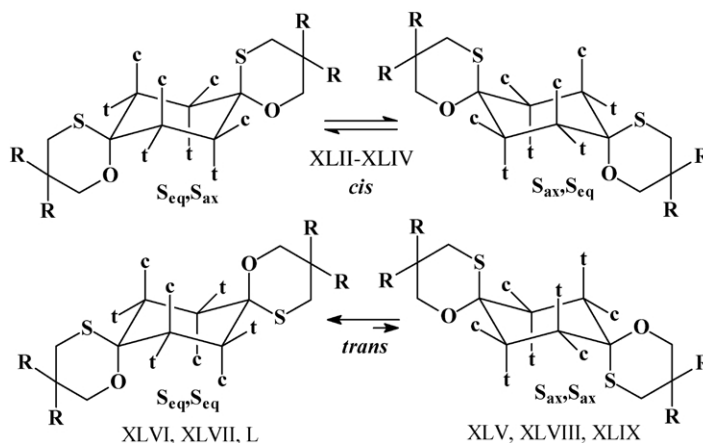
Scheme 10. Conformational equilibria for *cis* isomers of **19** and **20**.

Scheme 11. Conformational equilibria for *trans* isomers of **19** and **20**.Table 4. NMR data (rt, CD₂Cl₂, δ , ppm) of compounds **19**–**26**

Compound	Isomer	O–CH ₂	S–CH ₂	CH ₃
19	<i>cis</i>	3.88	2.83	—
	<i>trans</i>	3.85	2.86	—
20	<i>cis</i>	3.42	2.59	1.05
	<i>trans</i>	3.40	2.61	1.05
21	—	3.39	2.57	1.02
22	<i>cis</i>	3.74	2.72	—
	<i>trans</i>	3.74	2.72	—
23 *	D ²	3.30	2.49	0.93
	D ¹	3.30	2.48	0.93
24	<i>cis</i>	3.47	2.66	—
	<i>trans</i>	3.45	2.68	—
25	—	3.47	2.65	—
26 *	D ²	3.46	2.65	—
	D ¹	3.46	2.65	—

20 (Figs. 1b and 2b) show the signals arising from the frozen diastereoisomers.

The ¹H NMR spectrum of the *trans* isomer run at 187 K (Fig. 1) exhibits four sets of signals with different intensities assigned to the six frozen conformations (four which form two pairs of enantiomers) of this isomer. Two sets of high intensity signals were assigned to the *syn* (XLVI, L) and *anti* (XLVII) conformers bearing the equatorial sulfur atoms on the middle cyclohexane ring while the other two sets of low intensity signals belong to the minor conformers for which the sulfur atoms are axial (*syn*: XLV, XLIX; *anti*: XLVIII). The *syn* and *anti* conformers could not be differentiated due to the overlap of the signals belonging to the protons of the cyclohexane rings. This is despite the theoretically different shapes of the spectra anticipated for these protons. In both conformers of the *trans* isomer (*syn* and *anti*), the two heterocycles of the spirane are equivalent.



Scheme 12.

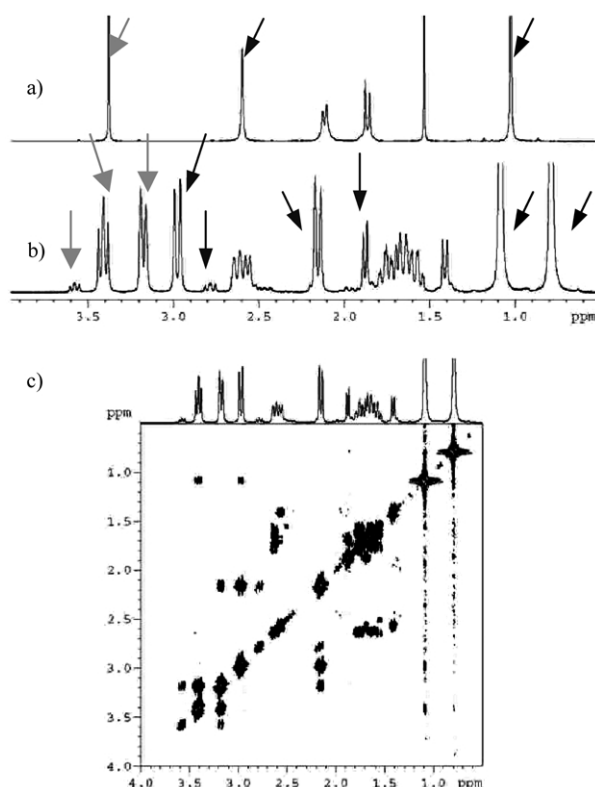


Figure 1. ^1H NMR spectra of the *trans* of **20**; (a) at rt; (b) at 187 K; (c) COSY at 187 K.

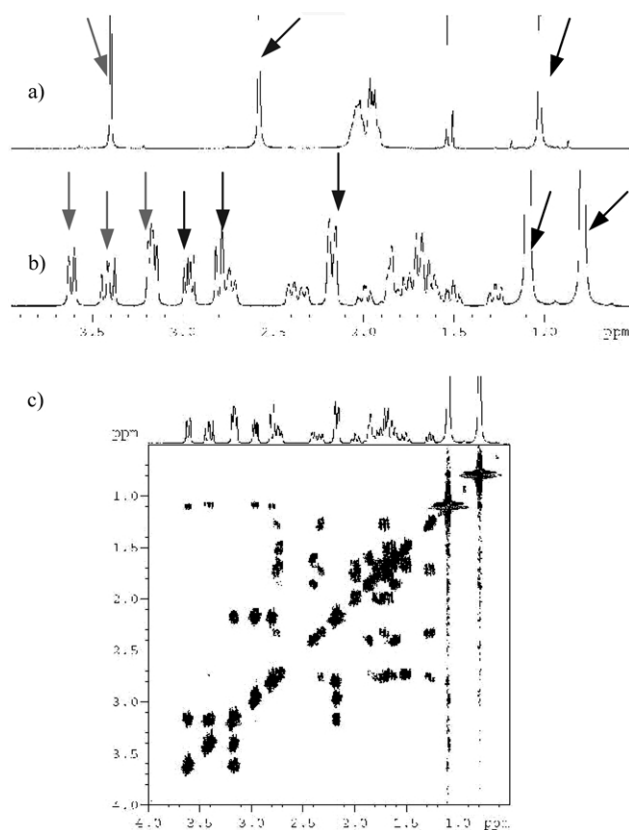


Figure 2. ^1H NMR spectra of the *cis* of **20**; (a) at rt; (b) at 187 K; (c) COSY at 187 K.

The part of the spectrum belonging to the protons of the heterocycles shows, for each diastereoisomer, two AB (AX) systems which were assigned to the axial and equatorial protons of the O-CH₂ and S-CH₂ moieties, respectively (Fig. 1, Table 5). At low temperature, well separated signals were observed which could be attributed to axial (δ_{ax} =1.080, 1.085 ppm) and equatorial (δ_{eq} =0.789 ppm) protons. However, it was not possible to differentiate the signals belonging to the different stereoisomers.

The ^1H NMR spectrum of *cis* isomer run at 187 K (Fig. 2) is as complex as the spectrum recorded for *trans* isomer, despite the lower number of stereoisomers (in fact only two, the *syn* and *anti* diastereoisomers, which are present in an almost 1/1 ratio). The complexity of the spectrum is due to the non-equivalence of the two 1,3-oxathiane rings A and C. Each isomer has one 1,3-oxathiane ring with an axial sulfur atom while the other one has an equatorial sulphur. The low temperature spectrum shows four sets of signals of similar intensity (some of which overlapped).

The NMR spectra recorded at rt for the *cis* and *trans* isomers of **24** exhibit, for the heterocyclic protons as well as for those of the middle cyclohexane ring, sets of signals similar to those of **20**. Low temperature spectra of the isomers of **24** are more complex due to the higher number of possible structures, but the part of the spectra belonging to the protons of the heterocycles shows groups of signals similar to those attributed to the diastereoisomers of **20**.

The differences observed between the spectra (either at rt or at low temperature) of the *cis* and *trans* isomers of **22**, **23** and **26** are not as significant as those for **19**, **20** and **24**. Thus, structural assignment (*cis* and *trans*), by NMR, for the two isolated isomers of each compound was not possible. However, an assignment was possible for compound **22** via the X-ray diffraction of the crystalline *trans* isomer. In the other cases (compounds **23** and **26**) it was assumed that the less polar product (i.e., the highest R_f on silica gel) was the *trans* isomer (as in the case for **19**, **20**, **22** and **24**). However, without other experimental support, it was preferred to mark the isolated isomers as D¹ and D² (in the order of their elution on silica gel, they are assumed to be either the *trans* or the *cis* form of a compound).

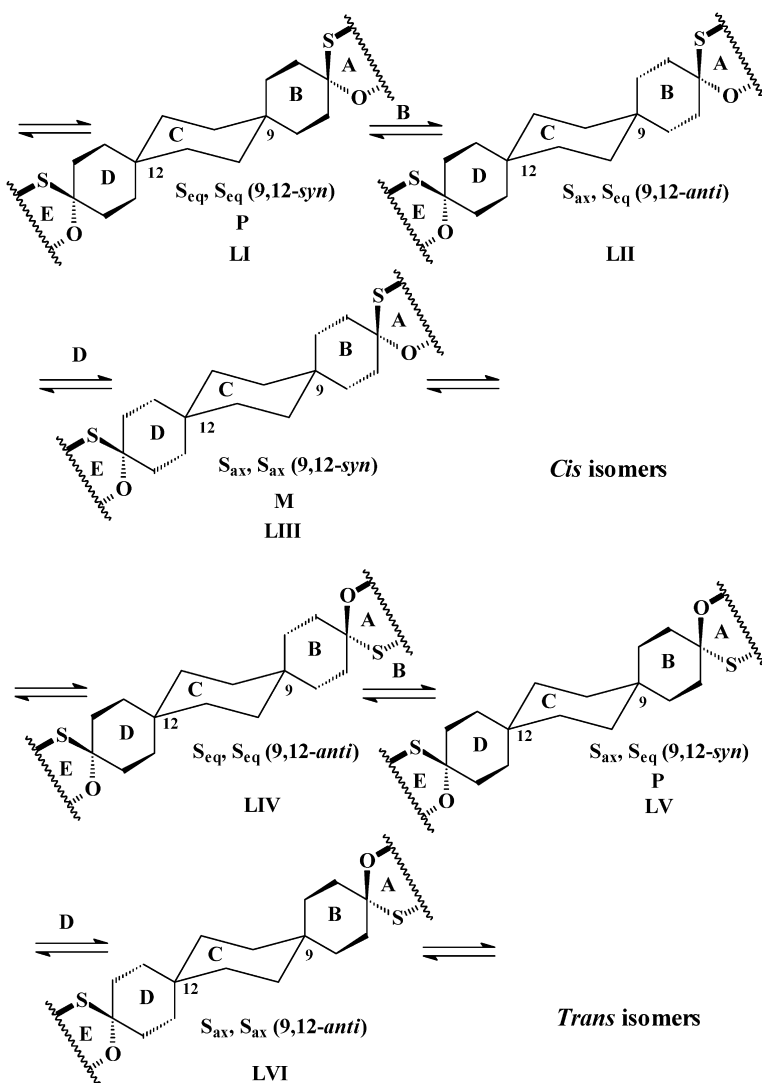
Conformational analysis (Scheme 13) of the middle part of the tetra- (rings B, C and D) and hexaspiranes (rings C, D and E) had markedly different results than those of **19**, **20** and **24**.

The conformational equilibria for the *cis* and *trans* diastereoisomers involving the flipping of rings B, C and D (compounds **22** and **23**, Scheme 13) or C, D and E (compound **26**) lead to conformations in which both sulphur atoms are either both equatorial or both axial or in which there is one axial and one equatorial sulphur (Scheme 13). The different axial and equatorial positions of the sulphur atoms (which dictate the differences in NMR spectra) observed for the *cis* and *trans* isomers of **19**, **20** and **24** do not exist for the *cis* and *trans* isomers of **22**, **23** and **26**. The small steric differences between the *cis* and *trans* isomers of these compounds explain their very similar NMR spectra

Table 5. NMR data^a (187 K, CD₂Cl₂, δ , ppm) of *trans* and *cis* isomers of **20**

Isomer	O-CH ₂		S-CH ₂		CH ₃	
	eq	ax	eq	Ax	eq	ax
<i>trans</i> (major) <i>syn</i> and <i>anti</i>	3.17	3.42, 3.39	2.15	2.97	1.085, 1.080	0.789
<i>trans</i> (major) <i>syn</i> and <i>anti</i>	3.17	3.59, 3.56	2.17	2.79, 2.77	1.08	0.79
<i>cis</i> (all rings of <i>syn</i> and <i>anti</i> structures)	3.15, 3.17	3.61, 3.43, 3.39	2.16	2.97, 2.95, 2.80	1.097, 1.083	0.795, 0.784

^a The COSY spectra show long range couplings of the axial proton of the heterocycles with the axial methyl groups (the more deshielded ones).

**Scheme 13.**

(some minor differences are observed for the signals assigned to the cyclohexane).

The low temperature spectra (180 K) of the isomers of compounds **22**, **23** and **26** do not allow for the differentiation of the signals belonging to their many frozen structures, related to the three different arrangements of the sulfur atoms (eq.,eq.; eq.,ax.; and ax.,ax.). Nonetheless, they do show separate signals for the protons of the 1,3-oxathiane rings with both axial or equatorial sulfur atoms. Thus, the low temperature spectra of these compounds show two sets of signals of different intensities (ratio 3/2). The main set

belongs to the protons of the heterocycles bearing an equatorial sulfur atom on the neighbouring cyclohexane ring. This finding is consistent with a higher *A*-value for the cyclohexane ring having the S-R group than for that having the O-R group²⁷ and it is in agreement with the results of previous conformational determinations involving mono-spiro-1,3-oxathianes.⁶ However, the low temperature spectra of compounds **22** and **23** (Figs. 3 and 4) are quite different. It is known that the presence of geminal methyl groups at position 5 of the 1,3-oxathiane ring increases the barrier for the flipping of the heterocycle. This is contrary to geminal substitution at position 2 which diminishes $\Delta^{\ddagger}G^{\circ}$

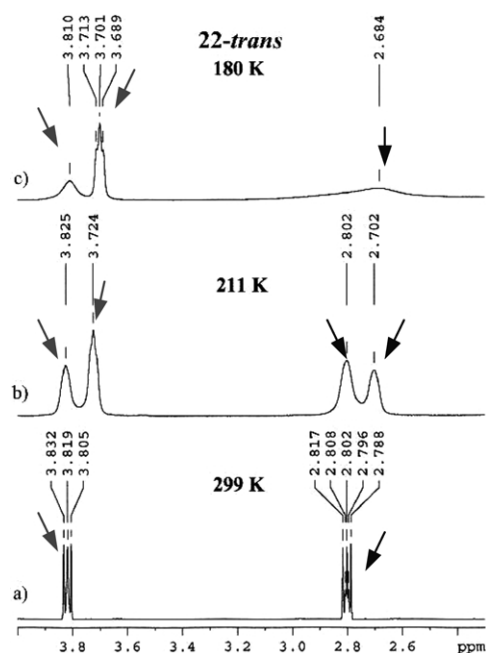


Figure 3. Variable NMR spectra (CD_2Cl_2) of *trans* isomer of compound **22**: (a) 299 K, (b) 211 K and (c) 180 K.

(e.g., the $\Delta^\ddagger G^\circ$ values for 1,3-oxathiane, for 2,2-dimethyl-1,3-oxathiane and 5,5-dimethyl-1,3-oxathiane are 38.9, 33.4 and 43.5 kJ/mol, respectively).²⁸ Two factors determine the amount of ring flip for these compounds: an increase in the energy of the ground state (which lowers the barrier of inversion due to the axial substituent) and an increase in the energy of the transition state (half-chair conformations, which increase the barrier of inversion) due to greater steric hindrance. The *A*-values for a methyl group at position 5 of the 1,3-oxathiane ring ($A=2.7\text{--}3.7$ kJ/mol)^{29,30} are con-

siderably lower than for that at position 2 ($A=13.6$ kJ/mol)^{29,30} which explains the differences between the values for the inversion barriers. As has been previously observed for the higher barrier of inversion of 5,5-dimethyl-1,3-oxathiane versus 1,3-oxathiane itself the conformational behaviours of compounds **22** and **23** are indeed different. The inversion barrier of the 1,3-oxathiane rings in **23** is high enough that the flipping of the heterocycle freezes at 180 K. This effect can be attributed to the presence of methyl groups. On the other hand, the NMR spectrum of **22** at the same temperature, shows only the beginning of the coalescence related to conformational equilibrium. Variable temperature NMR experiments of the *trans* isomer of **22** (Fig. 3) revealed that the flipping of the cyclohexane part of the spirane (rings B, C and D) froze at 211 K. Two sets of broad and unresolved signals are obtained instead of the two multiplets recorded at 299 K ($\delta_{\text{CH}_2\text{-O}}=3.81$ ppm and $\delta_{\text{CH}_2\text{-S}}=2.80$ ppm). The set of higher intensity signals ($\delta_{\text{CH}_2\text{-O}}=3.72$ ppm and $\delta_{\text{CH}_2\text{-S}}=2.80$ ppm) corresponds to those 1,3-oxathiane rings with an equatorial sulfur atom on the neighboring cyclohexane ring, while the set of lower intensity signals ($\delta_{\text{CH}_2\text{-O}}=3.82$ ppm and $\delta_{\text{CH}_2\text{-S}}=2.70$ ppm) belong to 1,3-oxathiane rings bearing an axial sulfur. The spectrum run at 180 K shows the coalescence of the signals due to the heterocycles and thus the freezing in space of the 1,3-oxathiane rings.

Variable temperature NMR experiments of diastereomer **D**¹ of compound **23** show the freezing in space of both the cyclohexane and the 1,3-oxathiane rings. The two singlets recorded at 299 K ($\delta_{\text{CH}_2\text{-O}}=3.38$ ppm and $\delta_{\text{CH}_2\text{-S}}=2.56$ ppm), which may be attributed to the protons of the heterocycles, change in the spectrum run at 180 K. Signals belonging to the two types of 1,3-oxathiane rings (equatorial sulfur atom, main case; axial sulfur atom, minor case) and to the axial and equatorial positions of these protons are observed. The signals assigned to the axial protons of each moiety are well separated for each type of ring ($\text{CH}_2\text{-O}$ moiety: $\delta_{\text{ax}}=3.40$ ppm (S_{eq} rings), $\delta_{\text{ax}}=3.62$ ppm (S_{ax} rings); $\text{CH}_2\text{-S}$ moiety: $\delta_{\text{ax}}=2.97$ ppm (S_{eq} rings), $\delta_{\text{ax}}=2.77$ ppm (S_{ax} rings), while those due to the equatorial protons overlapped ($\text{CH}_2\text{-O}$ moiety: $\delta_{\text{eq}}=3.13$ ppm; $\text{CH}_2\text{-S}$ moiety: $\delta_{\text{eq}}=2.12$ ppm). The other two signals ($\delta=2.57$ ppm and 2.31 ppm) of Figure 4 belong to the protons of the cyclohexane rings. The conclusion that freezing of the flipping of the 1,3-oxathiane rings has occurred was also supported by the recording of different signals for the axial ($\delta_{\text{ax}}=1.11, 1.09$ ppm) versus equatorial ($\delta_{\text{eq}}=0.80$ ppm) methyl groups at the extremities of the spirane. Variable temperature experiments of the other isomers of **22** and **23** gave similar results.

Low temperature spectra of the isomers of **26** were similar to those observed for the isomers of **23**. That is, the freezing in space of the 1,3-oxathiane rings as well as the central carbocycle occur.

Crystals of the *trans* isomers of compounds **20** and **22** were investigated by X-ray diffraction methods. The ORTEP diagrams (Figs. 5 and 6) show a chair conformation for all six-membered rings, a 6,9-*anti* conformation for dispirane **20** and a 6,9-*syn*-9,12-*anti*-12,15-*syn* conformation of the spirane skeleton for **22**.

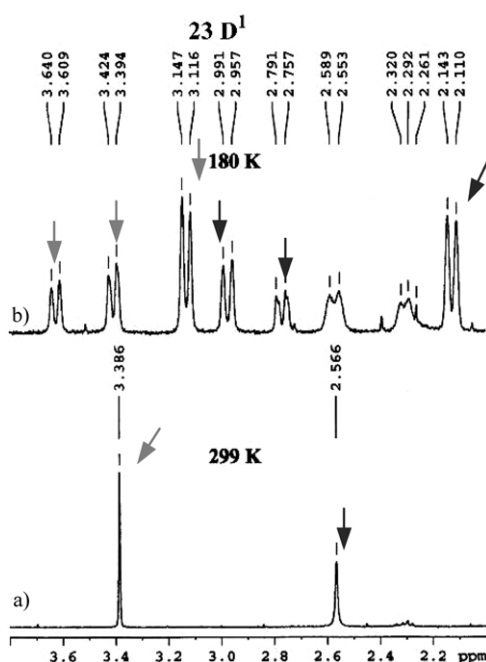


Figure 4. Variable temperature NMR spectra of **D**¹ isomer of compound **23**: (a) 299 K and (b) 180 K.

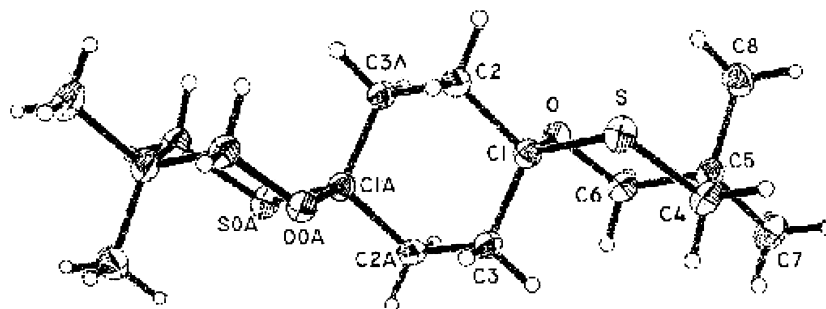


Figure 5. Labeled diagram of the *trans* isomer of compound 20.

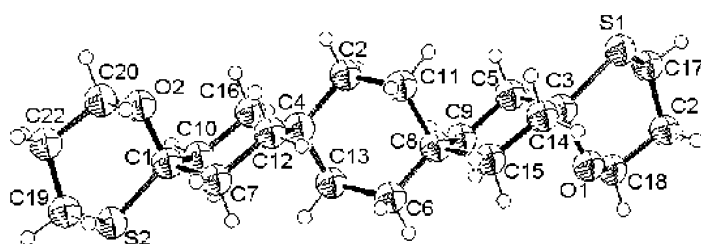
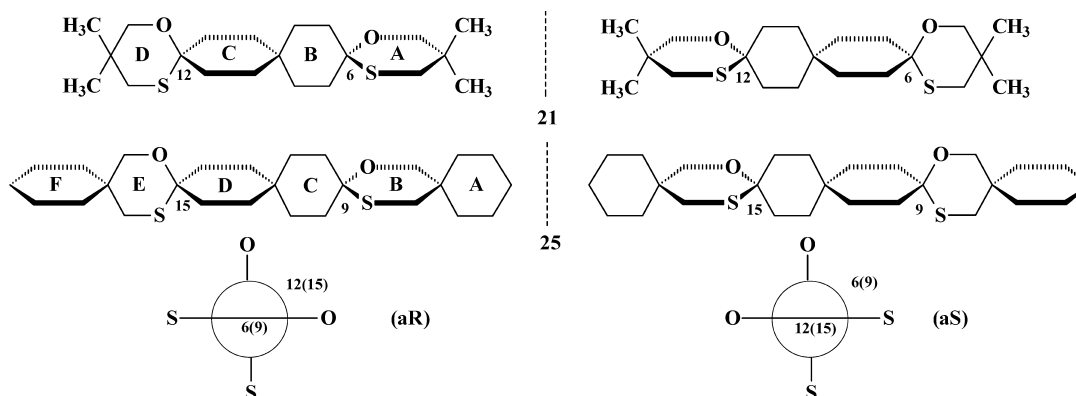


Figure 6. ORTEP diagram of *trans* isomer of compound 22.



Scheme 14.

These conformations were determined from the values of the reference dihedral angles [**20**: $C^4SC^6O/C^4AS^AC^6AO=0.0^\circ$ (the molecule is centrosymmetric); **22**: $(C^{18}O^1S^1C^{17}/C^2C^{11}C^6C^{13}=99.6^\circ$; $C^5C^9C^{14}C^{15}/C^7C^{12}C^{10}C^{16}=17.9^\circ$; $C^2C^{11}C^{13}C^6/C^{20}O^2S^2C^{19}=96.9^\circ$].

2.2.2. Stereochemistry of compounds 21 and 25. Compounds **21** and **25** exhibit separable enantiomers (Scheme 14). In addition to the chiral elements specific to the spirane skeleton (helical chirality) and those specific to the 1,3-oxathiane ring (a virtual tricoordinated chiral center) these compounds also contain a chiral axis (C^6-C^{12} for compound **21** and C^9-C^{15} for compound **25**). The best planes of rings A and D in **21** and B and E in **25** remain perpendicular regardless of the ring flips producing conformational equilibria.

The presence of different heteroatoms (oxygen and sulfur) in these cycles gives the parent structures axial chirality. In fact, the chirality of these molecules is similar to that of

spiro[5.5]undecane derivatives bearing different substituents at their extremities.

The different configurations arising from helicity and the virtual chiral center are inverted during ring flip, while the configuration of the chiral axis remains unchanged and compounds **21** and **25** exhibit only enantiomers. The racemic of **25** was solved on HPLC using a chiral column (Fig. 8). The flexible behaviour of the compounds was seen in the NMR spectra which show singlets for the CH_2-O (**21**: $\delta=3.38$ ppm; **25**: $\delta=3.46$ ppm) and the CH_2-S (**21**: $\delta=2.56$ ppm; **25**: $\delta=2.65$ ppm) moieties (Fig. 7). All methyl groups in **21** are detected as one singlet at $\delta=1.01$ ppm (Fig. 8).

Stereochemical analysis of the moiety containing the middle part of the spiranes and the heteroatoms (Scheme 15) reveals that, for each enantiomer, three arrangements are feasible. These would correspond to the axial–axial, equatorial–equatorial or axial–equatorial orientations of

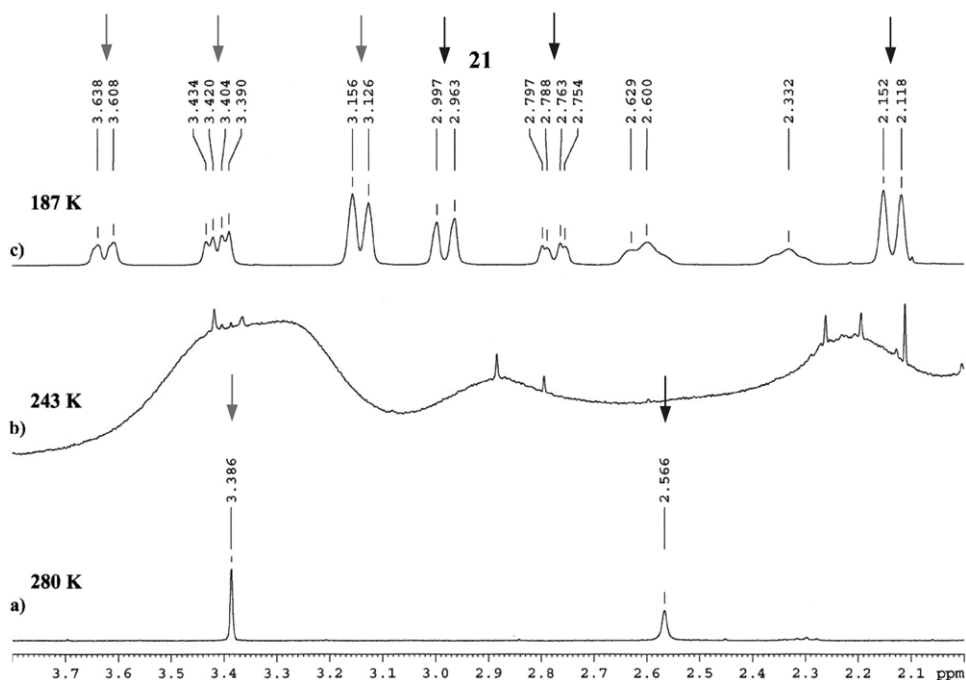


Figure 7. Variable temperature NMR spectra (CD_2Cl_2) of **19**: (a) 280 K, (b) 243 K and (c) 187 K.

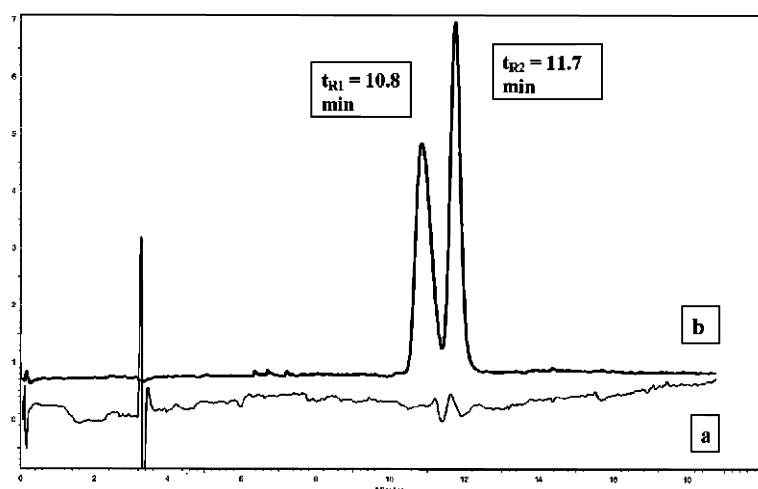


Figure 8. Chromatograms of the resolution of **25** on a CHIRACEL OD column using a chiral detector (polarimeter, a) and evaporative light scattering detection (b).

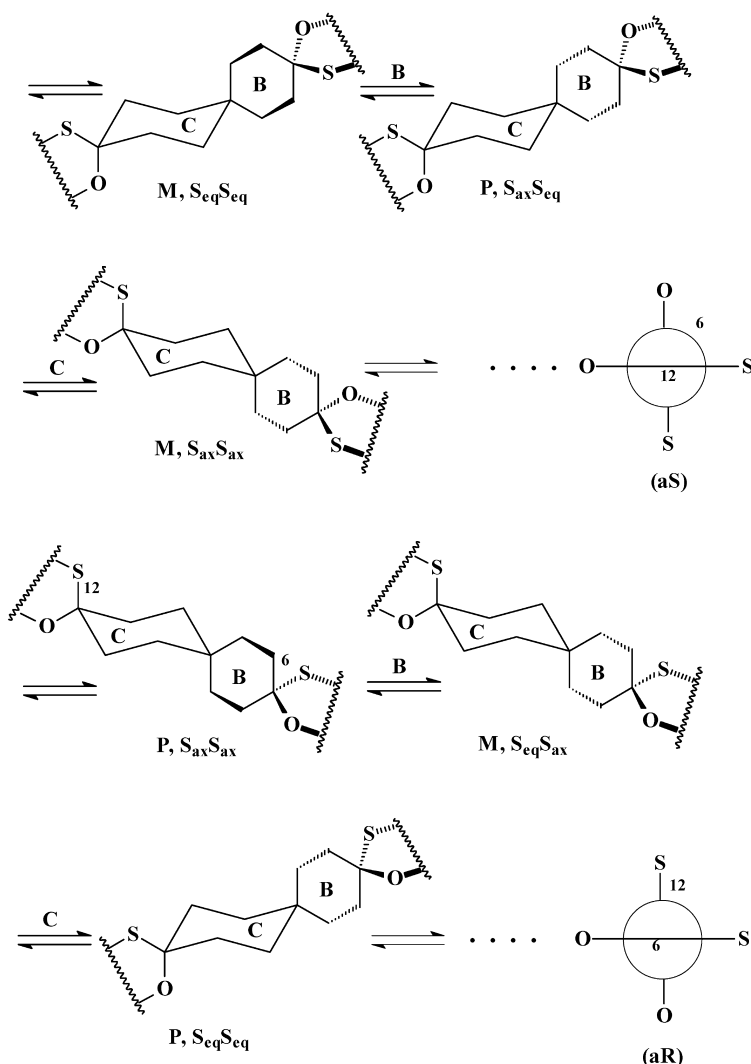
the sulphur atoms. Low temperature NMR spectra could not differentiate between the large number of stereoisomers of the frozen structures. Nonetheless, different signals for the two types of 1,3-oxathiane rings, that is, either having an equatorial (main case) or axial (minor case) sulfur atom, are observed. The ratio for the two types of rings is about 3/2. The signal for the axial protons of each moiety are well separated for each type of ring ($\text{CH}_2\text{-O}$ moiety: $\delta_{ax}=3.41$, 3.40 ppm (S_{eq} rings), $\delta_{ax}=3.62$ ppm (S_{ax} rings); $\text{CH}_2\text{-S}$ moiety: $\delta_{ax}=2.98$ ppm (S_{eq} rings), $\delta_{ax}=2.77$, 2.28 ppm (S_{ax} rings). On the other hand, the equatorial protons belonging to different type of rings overlapped ($\text{CH}_2\text{-O}$ moiety: $\delta_{eq}=3.14$ ppm; $\text{CH}_2\text{-S}$ moiety: $\delta_{eq}=2.13$ ppm). The axial and equatorial methyl groups produce different signals. ($\delta_{ax}=1.16$, 1.17 ppm; $\delta_{eq}=0.86$ ppm).

The low temperature spectra of compound **25**, while

showing evidence that conformational equilibrium freezes, are more complex. The complexity arises from the higher number of isomers and greater differentiation between the many types of 1,3-oxathiane rings.

3. Conclusions

The good yielding synthesis of the first reported polyspiro-1,3-oxathianes, from di to hexaspiro, and of the first penta and hexaspiro-1,3-dioxanes is reported. The *cis* and *trans* isomers of oxathiane derivatives were separated by column chromatography and were investigated as single compounds. The first crystal structures of polyspiro-1,3-oxathiane derivatives (one dispiro- and another one tetraspiro) were determined by X-ray diffraction and the 6,9-*anti* disposition of the dispiroane (**20**) and the



Scheme 15.

6,9-*syn*-9,12-*anti*-12,15-*syn* (**22**) arrangement of the tetraspiroane skeleta were revealed. The variable temperature NMR experiments showed the flexible or the semiflexible structure of the investigated polyspiro-1,3-dioxane or polyspiro-1,3-oxathiane derivatives. The semiflexible 1,3-dioxane spiranes bearing an odd number of spirane units were found to have separable enantiomers, while those with an even number of spiro units have separable diastereoisomers. The polyspiro-1,3-oxathiane compounds exhibiting two 1,3-oxathiane rings separated by an odd number of cyclohexane rings have separable *cis* and *trans* isomers, but if the respective number of cyclohexane rings is even, the polyspiroane shows separable enantiomers. The chiral HPLC resolution of polyspiroanes (pentaspiro-1,3-dioxane and tetraspiro-1,3-oxathiane) is also reported.

4. Experimental

4.1. General remarks

^1H and ^{13}C NMR spectra were recorded in CD_2Cl_2 (CDCl_3) as solvent in 5 mm tubes on a Bruker AM 400 (Varian

Gemini) NMR spectrometer equipped with a dual ^{13}C – ^1H (multinuclear) head operating at 400 (300) MHz for protons and 100 (75) MHz for carbon atoms. IR spectra were recorded on a JASCO FT-IR 615 spectrometer. Melting points were measured with a Kleinfeld APOTEC melting point apparatus and are uncorrected. Elemental analyses were obtained at the University of Medicine and Pharmaceuticals, Cluj-Napoca, Romania or at Université de Rouen, France. The results agreed favorably with the calculated values. Thin-layer chromatography was performed on Merck silica gel 60 F 254. Silica gel Merck (40–63 μm) was used for flash chromatography.

HPLC separations were carried out at 15 °C using a quaternary gradient pump (Spectra Physics P4000) with a Rheodyne Model 7725 injection valve (20 μL sample loop) and a column of 250 mm length and 4.6 mm i.d. containing a CHIRALCEL OD phase (DAICEL Chemical Industries, 10 μm particles). Detection was performed by a DDL 31 Evaporative Light Scattering Detector (ELSD) (Eurosep Instrument), ESI-MS and a chiral detector (polarimeter JASCO Model OR 1590). The sensitivity on the ELSD was adjusted via the photomultiplier gain at 600 V (HT PM

Table 6. Crystal data and data collection information for **20** and **22**

Compound	20	22
Empirical formula	C ₁₆ H ₂₈ O ₂ S ₂	C ₂₂ H ₃₆ O ₂ S ₂
Formula weight	316.50	396.63
Temperature (K)	293(2)	297(2)
Wavelength (Å)	0.71073	0.71073
Crystal system	Orthorhombic	Triclinic
Space group	<i>Pbca</i>	<i>P1</i> (no. 1)
Unit cell dimensions		
<i>a</i> (Å)	9.8770(10)	6.0808(7)
<i>b</i> (Å)	7.8200(10)	
<i>c</i> (Å)	21.739(2)	9.9635(12)
α (°)	90	112.061(2)
β (°)	90	105.678(2)
γ (°)	90	92.743(2)
Volume (Å ³)	1679.1(3)	525.04(11)
<i>Z</i>	4	1
<i>D</i> _{calc} (g/cm ³)	1.252	1.254
Absorption coefficient (mm ⁻¹)	0.317	0.267
<i>F</i> (000)	688	216
Crystal size (mm)	0.29×0.42×0.31	0.37×0.37×0.48
θ range for the data collection (°)	1.87–2.75	2.26–28.1
Reflections collected	14,189	4004
Independent reflections	1927	1980
Refinement method	Full-matrix on <i>F</i> ²	Full-matrix on <i>F</i> ²
Data/restraints/parameters	1927/0/92	1980/0/235
Goodness-of-fit on <i>F</i> ²	1.059	1.089
Final <i>R</i> indices [<i>F</i> ² >2 σ (<i>F</i> ²)]	<i>R</i> ₁ =0.0321, <i>wR</i> ₂ =0.0755	<i>R</i> ₁ 0.0349, <i>wR</i> ₂ =0.0896
<i>R</i> indices (all data)	<i>R</i> ₁ =0.0397	<i>R</i> ₁ =0.0380
Largest difference peak and hole (e Å ⁻³)	0.279 and -0.146	0.19 and -0.21

600). Nitrogen (pressure 1.3 bar) was chosen to nebulise the effluent coming from column and the evaporation temperature was set at 50 °C. The samples were prepared in *n*-hexane. The solutes were analyzed with an isocratic mobile phase (100% *n*-hexane) at a flow rate of 0.7 mL/min. *n*-Hexane (HPLC grade) was obtained from ACROS (Geel, Belgium). A Finnigan Navigator LC–MS system (Manchester, UK) with a Spectra Physics pump (P1000) was used in the Atmospheric Pressure Chemical Ionisation in positive mode (APCI+) for compounds identification in these conditions: source heater=130 °C, APCI heater=550 °C, cone voltage 30 V.

4.2. X-ray crystallographic data

The molecular structure of **20** was determined at Université du Québec à Montréal, Québec, Canada, while the structure of **22** was determined at the National Laboratory of X-ray Diffraction, ‘Babes-Bolyai’ University, Cluj-Napoca, Romania. The details of the crystal structure determination and refinement for compounds **20** and **22** are given in Table 6.

The crystals were studied on a Siemens P4 diffractometer (**20**) and on a Bruker SMART-APEX diffractometer (**22**), using graphite-monochromatised Mo K α radiation. Crystal (**22**) was attached with silicon grease to a cryoloop. The data were collected using the XSCANS program for crystal **20**. The structures were solved by direct methods, and all the other non-hydrogen atoms were found by the usual Fourier methods. The structures were refined with anisotropic thermal parameters. The hydrogen atoms were fixed in a riding model with mutual isotropic thermal parameters. The resolution and

the refinement of the structures were done using the Siemens SHELXTL system (**20**)³¹ and a software package SHELX-97 (**22**).^{32,33} The drawings were created with the Siemens SHELXTL system (**20**) and Ortep program (**22**).³⁴

The CIF tables have been deposited with the Cambridge Crystallographic Data File Centre as supplementary publication no. CCDC-2158555 (**20**) and 215677 (**22**). Copies of the data can be obtained free of charge on application to CCDC, 12 Union Road, Cambridge CB2 1EZ, UK [fax: int. code +44(1223)336-033; e-mail: deposit@ccdc.cam.ac.uk].

4.3. General procedure for the synthesis of compounds 11–14 containing 1,3-dioxane rings

To a solution of 4.4 mmol of diol (**7** or **8**) in 20 mL of toluene and 2 mL of DMSO were added 2.0 mmol of the corresponding diketone (**9** and **10**, respectively) and 0.02 g of *p*-toluenesulfonic acid. The mixture was refluxed and the water that resulted from the reaction was removed using a Dean–Stark trap. When the theoretical amount of water was separated, after cooling at room temperature, the catalyst was neutralised (with stirring) with excess powdered CH₃COONa (ca. 0.05 g). The reaction mixture was washed twice with 20 mL water. The organic layer was dried over Na₂SO₄, then toluene was removed under reduced pressure and the spiro compounds were purified by flash-chromatography on silica gel or by crystallisation from acetone.

The syntheses of the starting diol, **8**, and mercaptoalcohol **17** were devised by our group³⁵ (being new compounds), while the syntheses of diol **7**³⁶ and of diketones **9**^{37–39} and **10**⁴⁰ were performed using procedures described in the literature

4.3.1. 8,16,25,30-Tetraoxapentasp[5.2.2.2.5.2.2.2.2]hentriacontane (11). White crystals (0.2 g, 24%), mp 180–182 °C. (Found: C, 74.99; H, 10.32. $C_{27}H_{44}O_4$ requires: C, 74.96; H, 10.25%); δ_H (400 MHz; CD_2Cl_2) 1.25–1.45 (28H, overlapped peaks, 1-H₂, 5-H₂, 19-H₂, 23-H₂; 2-H₂, 4-H₂, 20-H₂, 22-H₂; 3-H₂, 21-H₂; 11-H₂, 13-H₂, 27-H₂, 28-H₂), 1.69 (8H, broad triplet (AA'BB' system), $^3J=6.0$ Hz, 10-H₂, 14-H₂, 26-H₂, 29-H₂) and 3.54 (8H, s, 7-H₂, 17-H₂, 24-H₂, 31-H₂); δ_C (100 MHz; CD_2Cl_2) 21.98, 27.24, 28.64, 32.08, 32.30, 32.49, 32.99 (C-1, C-5, C-19, C-23; C-2, C-4, C-20, C-22; C-3, C-21; C-6, C-18; C-10, C-14, C-26, C-28; C-11, C-13, C-27, C-28), 68.46 (C-7, C-17, C-24, C-31) and 98.91 (C-9, C-15).

4.3.2. 3,21-Di-*t*-butyl-8,16,25,30-tetraoxapentasp[5.2.2.2.5.2.2.2.2]hentriacontane (12). White crystals (0.19 g, 18%), mp 290–292 °C. (Found: C, 77.30; H, 11.21. $C_{35}H_{60}O_4$ requires: C, 77.15; H, 11.10%); δ_H (400 MHz; CD_2Cl_2) 0.84 (18H, s, 3-C(CH₃)₃, 21-C(CH₃)₃), 0.91–1.11 (10H, overlapped peaks, 3-H, 21-H; 2-H₂, 4-H₂, 20-H₂, 22-H₂), 1.35 (8H, m, 11-H₂, 13-H₂, 27-H₂, 28-H₂), 1.59 (4H, m, 1-H_{ax}, 5-H_{ax}, 19-H_{ax}, 23-H_{ax}), 1.69 (8H, m, 10-H₂, 14-H₂, 26-H₂, 29-H₂), 1.87 (4H, m, 1-H_{eq}, 5-H_{eq}, 19-H_{eq}, 23-H_{eq}), 3.38 (4H, s, 7-H₂, 24-H₂) and 3.67 (8H, s, 17-H₂, 31-H₂); δ_C (100 MHz; CD_2Cl_2) 22.68, 28.66, 32.31, 32.49, 32.69, 32.84 (C-1, C-5, C-19, C-23; C-2, C-4, C-20, C-22; 3-C(CH₃)₃, 21-C(CH₃)₃; C-6, C-18; C-10, C-14, C-26, C-28; C-11, C-13, C-27, C-28), 27.81 (3-C(CH₃)₃, 21-C(CH₃)₃), 49.14 (C-3, C-21), 64.99 (C-7, C-17, C-24, C-31) and 98.92 (C-9, C-15).

4.3.3. 8,19,28,35-Tetraoxahexaspiro[5.2.2.2.2.5.2.2.2.2]hexatriacontane (13). White crystals (0.27 g, 26%), mp 309–311 °C. (Found: C, 76.82; H, 10.99. $C_{33}H_{56}O_4$ requires: C, 76.69; H, 10.92%); δ_H (400 MHz; CD_2Cl_2) 1.25–1.45 (36H, overlapped peaks, 1-H₂, 5-H₂, 22-H₂, 26-H₂; 2-H₂, 4-H₂, 23-H₂, 25-H₂; 3-H₂, 24-H₂; 11-H₂, 16-H₂, 30-H₂, 33-H₂; 13-H₂, 14-H₂, 31-H₂, 32-H₂), 1.69 (8H, m, 10-H₂, 17-H₂, 29-H₂, 34-H₂) and 3.46 (8H, s, 7-H₂, 20-H₂, 27-H₂, 36-H₂); δ_C (100 MHz; CD_2Cl_2) 21.98, 27.24, 28.45, 29.30, 30.27, 32.08, 32.79, 32.99 (C-1, C-5, C-22, C-26; C-2, C-4, C-23, C-25; C-3, C-24; C-6, C-21; C-10, C-17, C-29, C-34; C-11, C-16, C-30, C-33; C-12, C-15; C-13, C-14, C-31, C-32), 68.44 (C-7, C-20, C-27, C-36) and 99.01 (C-9, C-18).

4.3.4. 3,24-Di-*t*-butyl-8,19,28,35-tetraoxahexaspiro[5.2.2.2.2.5.2.2.2.2]hexatriacontane (14). White crystals (0.41 g, 33%), mp 310–312 °C. (Found: C, 78.15; H, 11.66. $C_{41}H_{72}O_4$ requires: C, 78.29; H, 11.54%); mixture of diastereoisomers. δ_H (400 MHz; CD_2Cl_2) 0.84 (18H, s, 3-C(CH₃)₃, 24-C(CH₃)₃), 0.91–1.10 (10H, overlapped peaks, 3-H, 24-H; 2-H₂, 4-H₂, 23-H₂, 25-H₂), 1.29 (8H, s, 13-H₂, 14-H₂, 31-H₂, 32-H₂), 1.33 (8H, m, 11-H₂, 16-H₂, 30-H₂, 33-H₂), 1.58 (4H, m, 1-H_{ax}, 5-H_{ax}, 19-H_{ax}, 23-H_{ax}), 1.68 (8H, m, 10-H₂, 17-H₂, 29-H₂, 34-H₂), 1.87 (4H, m, 1-H_{eq}, 5-H_{eq}, 19-H_{eq}, 23-H_{eq}) and 3.38 (4H, s, 7-H₂, 27-H₂), 3.67 (8H, s, 22-H₂, 36-H₂); δ_C (100 MHz; CD_2Cl_2) 22.67, 28.46, 32.07, 32.48, 32.69, 32.99, 32.79, 32.84 (C-1, C-5, C-22, C-26; C-2, C-4, C-23, C-25; 3-C(CH₃)₃, 24-C(CH₃)₃; C-6, C-21; C-10, C-17, C-29, C-34; C-11, C-16, C-30, C-33; C-12, C-15; C-13, C-14, C-31, C-32), 27.80 (3-C(CH₃)₃, 24-C(CH₃)₃), 49.14 (C-3, C-24), 64.97 (C-7, C-20, C-27, C-36) and 99.04 (C-9, C-18).

4.4. General procedure for the synthesis of compounds 19–26 containing 1,3-oxathiane rings

A solution of 4.4 mmol of 3-mercapto-propan-1-ol (**15–17**), the corresponding diketone (**9**, **10**, **18**) (2.0 mmol) and 0.05 g of *p*-toluenesulfonic acid in 20 mL of toluene was refluxed and the water generated in the reaction was removed using a Dean–Stark trap. When the theoretical water was separated, after cooling at rt, the catalyst was neutralised (with stirring) with an excess of 0.1 M KOH (in order to remove the remaining thiol). The organic layer was then washed twice with water (20 mL). After drying over Na₂SO₄, the toluene was removed under reduced pressure and the oxathianes were purified by flash-chromatography or by crystallisation from acetone.

4.4.1. 5,14-Dioxa-1,10-dithiadispiro[5.2.5.2]hexadecane (19). White crystals (0.43 g, 83%), mixture of *trans* and *cis* isomers, subjected to column chromatography (dichloromethane–petroleum ether–ethyl acetate 5/12/1, $\Delta R_f=0.14$, *trans* isomer with $R_f=0.54$ and *cis* isomer with $R_f=0.40$).

trans Isomer. White crystals (0.18 g, 35%), mp 187–188 °C. (Found: C, 55.32; H, 7.56; S, 24.88. $C_{12}H_{20}O_2S_2$ requires: C, 55.35; H, 7.74; S, 24.63%); δ_H (300 MHz, $CDCl_3$) 1.78–1.86 (4H, m, 3-H₂, 12-H₂), 2.00 (4H, d, $^2J=10.0$ Hz, 7-HH', 8-HH', 15-HH', 16-HH'), 2.12 (4H, d, $^2J=10.0$ Hz, 7-HH', 8-HH', 15-HH', 16-HH'), 2.86 (4H, m, 2-H₂, 11-H₂) and 3.85 (4H, m, 4-H₂, 13-H₂); δ_C (75 MHz, $CDCl_3$) 24.08 (C-3, C-12), 25.51 (C-7, C-8, C-15, C-16), 31.78 (C-2, C-11), 61.63 (C-4, C-13) and 80.19 (C-6, C-9).

cis Isomer. White crystals (0.19 g, 37%), mp 119–120.2 °C. (Found: C, 55.54; H, 7.58; S, 24.72. $C_{12}H_{20}O_2S_2$ requires: C, 55.35; H, 7.74; S, 24.63%); δ_H (300 MHz, $CDCl_3$) 1.78–1.86 (4H, m, 3-H₂, 12-H₂), 1.98–2.16 (8H, m, 7-H₂, 8-H₂, 15-H₂, 16-H₂), 2.83 (4H, m, 2-H₂, 11-H₂) and 3.88 (4H, m, 4-H₂, 13-H₂); δ_C (75 MHz, $CDCl_3$) 24.12 (C-3, C-12), 25.64 (C-7, C-8, C-15, C-16), 32.37 (C-2, C-11), 61.37 (C-4, C-13) and 80.91 (C-6, C-9).

4.4.2. 3,3,12,12-Tetramethyl-5,14-dioxa-1,10-dithiadispiro[5.2.5.2]hexadecane (20). White crystals (0.5 g, 79%), mixture of *trans* and *cis* isomers, subjected to column chromatography (petroleum ether–ethyl acetate 12/1, $\Delta R_f=0.11$, *trans* isomer with $R_f=0.52$ and *cis* isomer with $R_f=0.41$).

trans Isomer. White crystals (0.26 g, 42%), mp 192–193 °C. (Found: C, 60.85; H, 8.99; S, 20.16. $C_{16}H_{28}O_2S_2$ requires: C, 60.71; H, 8.92; S, 20.26%); δ_H (300 MHz, $CDCl_3$) 1.05 (12H, s, 3-CH₃, 12-CH₃), 1.94 (4H, d, $^2J=10.0$ Hz, 7-HH', 8-HH', 15-HH', 16-HH'), 2.13 (4H, d, $^2J=10.0$ Hz, 7-HH', 8-HH', 15-HH', 16-HH'), 2.61 (4H, s, 2-H₂, 11-H₂) and 3.40 (4H, s, 4-H₂, 13-H₂); δ_C (75 MHz, $CDCl_3$) 24.92 (3-CH₃, 12-CH₃), 28.04 (C-3, C-12), 31.62 (C-7, C-8, C-15, C-16), 36.75 (C-2, C-11), 71.25 (C-4, C-13) and 80.05 (C-6, C-9).

cis Isomer. White crystals (0.19 g, 31%), mp 156 °C. (Found: C, 55.29; H, 7.68; S, 24.81. $C_{16}H_{28}O_2S_2$ requires: C, 60.71; H, 8.92; S, 20.26%); δ_H (300 MHz, $CDCl_3$) 1.05 (12H, s, 3-CH₃, 12-CH₃), 1.92–2.14 (8H, m, 7-H₂, 8-H₂,

15-H₂, 16-H₂), 2.59 (4H, s, 2-H₂, 11-H₂) and 3.42 (4H, s, 4-H₂, 13-H₂); δ_C (75 MHz, CDCl₃) 24.93 (3-CH₃, 12-CH₃), 28.09 (C-3, C-12), 32.20 (C-7, C-8, C-15, C-16), 36.81 (C-2, C-11), 71.16 (C-4, C-13) and 80.70 (C-6, C-9).

4.4.3. 3,3,15,15-Tetramethyl-5,17-dioxa-1,13-dithia-trispiro[5.2.2.5.2.2]hencosane (21). White crystals (0.21 g, 27%), mp 189–191 °C. (Found C, 65.64; H, 9.37; S, 16.44. C₂₁H₃₆O₂S₂ requires: C, 65.57; H, 9.43; S, 16.67%); δ_H (400 MHz; CD₂Cl₂) 1.02 (12H, s, 3-CH₃, 15-CH₃), 1.25–1.50 (8H, m, 8-H₂, 10-H₂, 19-H₂, 20-H₂), 1.81 (4H, m, 7-HH', 11-HH', 18-HH', 21-HH'), 1.98 (4H, m, 7-HH', 11-HH', 18-HH', 21-HH'), 2.57 (4H, s, 2-H₂, 14-H₂) and 3.39 (4H, s, 4-H₂, 16-H₂); δ_C (100 MHz; CD₂Cl₂) 28.40, 29.94, 32.20, 33.13 (C-3, C-5; C-7, C-11, C-18, C-21; C-8, C-10, C-19, C-20; C-9), 25.14 (3-CH₃, 15-CH₃), 37.09 (C-2, C-14), 71.42 (C-4, C-16) and 82.19 (C-6, C-12).

4.4.4. 5,20-Dioxa-1,16-dithiatetraspiro[5.2.2.2.5.2.2.2]-hexacosane (22). White crystals (0.56 g, 71%), mixture of *trans* and *cis* isomers, subjected to column chromatography (toluene–dichloromethane–ethyl acetate 8/2/0.5, $\Delta R_f=0.10$, *trans* isomer with $R_f=0.34$ and *cis* isomer with $R_f=0.23$).

trans Isomer. White crystals (0.33 g, 42%), mp 215–217 °C. (Found: C, 66.78; H, 9.12; S, 16.14. C₂₂H₃₆O₂S₂ requires: C, 66.62; H, 9.15; S, 16.17%); δ_H (400 MHz, CDCl₃) 1.33–1.58 (16H, overlapped peaks, 8-H₂, 13-H₂, 22-H₂, 25-H₂; 10-H₂, 11-H₂, 23-H₂, 24-H₂), 1.64–1.78 (8H, overlapped peaks, 3-H₂, 18-H₂; 7-HH', 14-HH', 21-HH', 26-HH'), 1.86 (4H, m, 7-HH', 14-HH', 21-HH', 26-HH'), 2.72 (4H, m, 2-H₂, 17-H₂) and 3.74 (4H, m, 4-H₂, 19-H₂); δ_C (100 MHz, CDCl₃) 24.47, 26.39, 30.26, 32.52, 32.74 (C-2, C-17; C-3, C-18; C-7, C-14, C-21, C-26; C-8, C-13, C-22, C-25; C-9, C-12; C-10, C-11, C-23, C-24), 61.61 (C-4, C-19) and 82.52 (C-6, C-15).

cis Isomer. White crystals (0.23 g, 29%), mp 206–208 °C. (Found: C, 66.55; H, 9.26; S, 16.30. C₂₂H₃₆O₂S₂ requires: C, 66.62; H, 9.15; S, 16.17%); δ_H (400 MHz, CDCl₃) 1.19 (4H, s, 10-H₂, 23-H₂), 1.24 (4H, s, 11-H₂, 24-H₂), 1.28–1.34 (8H, overlapped peaks, 8-H₂, 13-H₂, 22-H₂, 25-H₂), 1.64–1.78 (8H, overlapped peaks, 3-H₂, 18-H₂; 7-HH', 14-HH', 21-HH', 26-HH'), 1.86 (4H, m, 7-HH', 14-HH', 21-HH', 26-HH'), 2.72 (4H, m, 2-H₂, 17-H₂) and 3.74 (4H, m, 4-H₂, 19-H₂); δ_C (100 MHz, CDCl₃) 24.47, 26.39, 30.26, 32.52, 32.74 (C-2, C-17; C-3, C-18; C-7, C-14, C-21, C-26; C-8, C-13, C-22, C-25; C-9, C-12; C-10, C-11, C-23, C-24), 61.61 (C-4, C-19) and 82.52 (C-6, C-15).

4.4.5. 3,3,18,18-Tetramethyl-5,20-dioxa-1,16-dithiate-trispiro[5.2.2.2.5.2.2.2]hexacosane (23). White crystals (0.57 g, 63%), mixture of *trans* and *cis* isomers, subjected to column chromatography (toluene–dichloromethane–ethyl acetate 60/1/0.15, $\Delta R_f=0.09$, D¹ isomer with $R_f=0.29$ and D² isomer with $R_f=0.20$).

D¹ isomer. White crystals (0.32 g, 35%), mp 225–227 °C. (Found: C, 68.89; H, 9.61; S, 14.33. C₂₆H₄₄O₂S₂ requires: C, 68.97; H, 9.80; S, 14.16%); δ_H (400 MHz, CDCl₃) 0.93 (12H, s, 3-CH₃, 18-CH₃), 1.16–1.35 (16H, overlapped peaks, 8-H₂, 13-H₂, 22-H₂, 25-H₂; 10-H₂, 11-H₂, 23-H₂,

24-H₂), 1.73 (4H, m, 7-HH', 14-HH', 21-HH', 26-HH'), 1.84 (4H, m, 7-HH', 14-HH', 21-HH', 26-HH'), 2.48 (4H, s, 2-H₂, 17-H₂) and 3.30 (4H, s, 4-H₂, 19-H₂); δ_C (100 MHz, CDCl₃) 28.40, 32.11, 32.74 (C-3, C-18; C-7, C-14, C-21, C-26; C-8, C-13, C-22, C-25; C-9, C-12; C-10, C-11, C-23, C-24), 25.14 (3-CH₃, 18-CH₃), 37.10 (C-2, C-17), 71.40 (C-4, C-19) and 82.38 (C-6, C-15).

D² isomer. White crystals (0.21 g, 23%), mp 206–208 °C. (Found: C, 68.99; H, 9.64; S, 14.31. C₂₆H₄₄O₂S₂ requires: C, 68.97; H, 9.80; S, 14.16%); δ_H (400 MHz, CDCl₃) 0.93 (12H, s, 3-CH₃, 18-CH₃), 1.19 (4H, s, 10-H₂, 23-H₂), 1.23 (4H, s, 11-H₂, 24-H₂), 1.27–1.35 (8H, overlapped peaks, 8-H₂, 13-H₂, 22-H₂, 25-H₂), 1.73 (4H, m, 7-HH', 14-HH', 21-HH', 26-HH'), 1.84 (4H, m, 7-HH', 14-HH', 21-HH', 26-HH'), 2.49 (4H, s, 2-H₂, 17-H₂) and 3.30 (4H, s, 4-H₂, 19-H₂); δ_C (100 MHz, CDCl₃) 28.40, 30.26, 31.15, 32.13, 32.74 (C-3, C-18; C-7, C-14, C-21, C-26; C-8, C-13, C-22, C-25; C-9, C-12; C-10, C-11, C-23, C-24), 25.15 (3-CH₃, 18-CH₃), 37.10 (C-2, C-17), 71.40 (C-4, C-19) and 82.39 (C-6, C-15).

4.4.6. 22,25-Dioxa-8,13-dithiatetraspiro[5.2.2.2.5.2.2.2]-hexacosane (24). White crystals (0.49 g, 62%), mixture of *trans* and *cis* isomers, subjected to column chromatography (toluene–dichloromethane–ethyl acetate 24/2/0.25, $\Delta R_f=0.15$, *trans* isomer with $R_f=0.43$ and *cis* isomer with $R_f=0.28$).

trans Isomer. White crystals (0.26 g, 33% yield), mp 217–219 °C. (Found: C, 66.47; H, 9.22; S, 16.21. C₂₂H₃₆O₂S₂ requires: C, 66.62; H, 9.15; S, 16.17%); δ_H (400 MHz, CDCl₃) 1.33–1.58 (20H, overlapped peaks, 1-H₂, 5-H₂, 16-H₂, 20-H₂; 2-H₂, 4-H₂, 17-H₂, 19-H₂; 3-H₂, 18-H₂), 1.85 (4H, d, $^2J=10$ Hz, 10-HH', 11-HH', 23-HH', 24-HH'), 2.10 (4H, d, $^2J=10$ Hz, 10-HH', 11-HH', 23-HH', 24-HH'), 2.68 (4H, s, 7-H₂, 14-H₂) and 3.45 (4H, s, 21-H₂, 26-H₂); δ_C (100 MHz, CDCl₃) 21.74, 27.17, 30.66, 32.95, 33.56 (C-1, C-5, C-16, C-20; C-2, C-4, C-17, C-19; C-3, C-18, C-6, C-15; C-10, C-11, C-23, C-24), 34.31 (C-7, C-14), 70.69 (C-21, C-26) and 81.77 (C-9, C-12).

cis Isomer. White crystals (0.17 g, 22%), mp 196–198 °C. (Found: C, 66.38; H, 9.18; S, 16.11. C₂₂H₃₆O₂S₂ requires: C, 66.62; H, 9.15; S, 16.17%); δ_H (400 MHz, CDCl₃) 1.35–1.60 (20H, overlapped peaks, 1-H₂, 5-H₂, 16-H₂, 20-H₂; 2-H₂, 4-H₂, 17-H₂, 19-H₂; 3-H₂, 18-H₂), 1.90–2.07 (8H, overlapped peaks, 10-H₂, 11-H₂, 23-H₂, 24-H₂), 2.66 (4H, s, 7-H₂, 14-H₂) and 3.47 (4H, s, 21-H₂, 26-H₂); δ_C (100 MHz, CDCl₃) 21.74, 27.18, 30.60, 32.39, 33.55 (C-1, C-5, C-16, C-20; C-2, C-4, C-17, C-19; C-3, C-18, C-6, C-15; C-10, C-11, C-23, C-24), 34.23 (C-7, C-14), 70.80 (C-21, C-26) and 81.08 (C-9, C-12).

4.4.7. 24,31-Dioxa-7,17-dithia-pentaspairo[5.2.2.2.2.5.2.2.2]hentriacontane (25). White crystals (0.19 g, 21%), mp 250–252 °C. (Found: C, 69.95; H, 9.45; S, 13.88. C₂₇H₄₄O₂S₂ requires: C, 69.77; H, 9.54; S, 13.80%); δ_H (400 MHz; CD₂Cl₂) 1.32–1.58 (28H, overlapped peaks, 1-H₂, 5-H₂, 19-H₂, 23-H₂; 2-H₂, 4-H₂, 20-H₂, 22-H₂; 3-H₂, 21-H₂; 11-H₂, 13-H₂, 27-H₂, 28-H₂), 1.80 (4H, m, 10-HH', 14-HH', 26-HH', 29-HH'), 1.93 (4H, m, 10-HH', 14-HH', 26-HH', 29-HH'), 2.65 (4H, s, 7-H₂, 17-H₂) and 3.46 (4H, s,

24-H₂, 31-H₂); δ_C (100 MHz; CD₂Cl₂) 21.76, 27.20, 30.67, 32.18, 32.29, 32.39, 33.60 (C-1, C-5, C-19, C-23; C-2, C-4, C-20, C-22; C-3, C-21; C-6, C-18; C-10, C-14, C-26, C-28; C-11, C-13, C-27, C-28), 34.19 (C-7, C-17), 70.53 (C-24, C-31) and 82.80 (C-9, C-15).

4.4.8. 27,36-Dioxa-7,20-dithia-hexaspiro[5.2.2.2.2.5.2.2.2.2]hexatriacontane (26). White crystals (0.62 g, 57% yield), mixture of *trans* and *cis* isomers, subjected to column chromatography (toluene–dichloromethane–ethyl acetate 24/2/0.25, $\Delta R_f=0.13$, D¹ isomer with $R_f=0.38$ and D² isomer with $R_f=0.25$).

D¹ isomer. White crystals (0.24 g, 22% yield), mp 315–317 °C. (Found: C, 72.41; H, 10.11; S, 11.82. C₃₃H₅₆O₂S₂ requires: C, 72.20; H, 10.28; S, 11.68%); δ_H (400 MHz, CDCl₃) 1.28–1.49 (36H, overlapped peaks, 1-H₂, 5-H₂, 22-H₂, 26-H₂; 2-H₂, 4-H₂, 23-H₂, 25-H₂; 3-H₂, 24-H₂; 11-H₂, 16-H₂, 30-H₂, 33-H₂; 13-H₂, 14-H₂, 31-H₂, 32-H₂), 1.80 (4H, m, 10-HH', 17-HH', 29-HH', 34-HH'), 1.84 (4H, m, 10-HH', 17-HH', 29-HH', 34-HH'), 2.65 (4H, s, 7-H₂, 20-H₂) and 3.46 (4H, s, 27-H₂, 36-H₂).

D² isomer. White crystals (0.23 g, 21%), mp 324–326 °C. (Found: C, 72.34; H, 10.11; S, 11.81. C₃₃H₅₆O₂S₂ requires: C, 72.20; H, 10.28; S, 11.68%); δ_H (400 MHz, CDCl₃) 1.27–1.48 (36H, overlapped peaks, 1-H₂, 5-H₂, 22-H₂, 26-H₂; 2-H₂, 4-H₂, 23-H₂, 25-H₂; 3-H₂, 24-H₂; 11-H₂, 16-H₂, 30-H₂, 33-H₂; 13-H₂, 14-H₂, 31-H₂, 32-H₂), 1.80 (4H, m, 10-HH', 17-HH', 29-HH', 34-HH'), 1.84 (4H, m, 10-HH', 17-HH', 29-HH', 34-HH'), 2.65 (4H, s, 7-H₂, 20-H₂) and 3.46 (4H, s, 27-H₂, 36-H₂).

Acknowledgements

The work was supported by grants from CNCSIS (33/2002 and 34/2002) and by AUPELF-UREF (Agence Universitaire de la Francophonie) (PAS 26/2001). Special thanks to Kelly Walsh for providing assistance with editing of this manuscript.

References and notes

- Grosu, I.; Mager, S.; Plé, G.; Horn, M. *J. Chem. Soc., Chem. Commun.* **1995**, 167–168.
- Grosu, I.; Mager, S.; Plé, G. *J. Chem. Soc., Perkin Trans. 2* **1995**, 1351–1357.
- Grosu, I.; Mager, S.; Plé, G.; Mesáros, E. *Tetrahedron* **1996**, *52*, 12783–12798.
- Opris, D.; Grosu, I.; Toupet, L.; Plé, G.; Terec, A.; Mager, S.; Muntean, L. *J. Chem. Soc., Perkin Trans. 1* **2001**, 2413–2420.
- Grosu, I.; Mager, S.; Plé, G.; Martínez, R. *Chirality* **1996**, *8*, 311–315.
- Terec, A.; Grosu, I.; Muntean, L.; Toupet, L.; Plé, G.; Socaci, C.; Mager, S. *Tetrahedron* **2001**, *57*, 8751–8758.
- Greenberg, A.; Laszlo, P. *Tetrahedron Lett.* **1970**, 2641–2644.
- Mursakulov, I. G.; Ramazanov, E. A.; Guseinov, M. M.; Zefirov, N. S.; Samoshin, V. V.; Eliel, E. L. *Tetrahedron* **1980**, *36*, 1885–1890.
- Dodziuk, H. *J. Chem. Soc., Perkin Trans. 2* **1986**, 249–252.
- Dodziuk, H.; Sitkowski, J.; Stefanian, I.; Mursakulov, I. G.; Guseinov, M. M.; Kurbanova, V. A. *Struct. Chem.* **1992**, *3*, 269–276.
- Fitjer, L.; Klages, U.; Wehle, D.; Giersig, M.; Schormann, N.; Clegg, W.; Stephenson, D. S.; Binsch, G. *Tetrahedron* **1988**, *44*, 405–416.
- Giersig, M.; Wehle, D.; Fitjer, L.; Schormann, N.; Clegg, W. *Chem. Ber.* **1988**, *121*, 525–532.
- Fitjer, L.; Kuehn, W.; Klages, U.; Egert, E.; Clegg, W.; Schormann, N.; Sheldrick, G. M. *Chem. Ber.* **1984**, *117*, 3075–3092.
- Fitjer, L.; Giersig, M.; Clegg, W.; Schormann, N. *Tetrahedron Lett.* **1983**, *24*, 5351–5354.
- Fitjer, L.; Wehle, D.; Noltemeyer, J.; Egert, E.; Sheldrick, G. M. *Chem. Ber.* **1984**, *117*, 203–221.
- de Meijere, A.; Kozhushkov, S. I.; von Seebach, M.; Boese, R.; Benet-Buchholz, J.; Yufit, D. S.; Howard, J. A. K. *Angew. Chem., Int. Ed.* **2000**, *39*, 2495–2498.
- Shizuma, M.; Kadoya, Y.; Takai, Y.; Imamura, H.; Yamada, H.; Takeda, T.; Arakawa, R.; Takahashi, S.; Sawada, M. *J. Org. Chem.* **2002**, *67*, 4795–4807.
- Rablen, P. R.; Paquette, L. A.; Borden, W. T. *J. Org. Chem.* **2000**, *65*, 9180–9185.
- de Meijere, A.; Kozhushkov, S. I.; Puls, C.; Haumann, T.; Boese, R. *Angew. Chem.* **1994**, *106*, 934–936.
- Wulf, K.; Klages, U.; Rissom, B.; Fitjer, L. *Tetrahedron* **1997**, *53*, 6011–6018.
- Yufit, D. S.; Struchkov, Y. T.; Kozhushkov, S. I.; de Meijere, A. *Acta Crystallogr. Sect. C: Cryst. Struct. Commun.* **1993**, *49*, 1517–1519.
- Fitjer, L.; Justus, K.; Puder, P.; Dittmer, M.; Hassler, C.; Noltemeyer, J. *Angew. Chem.* **1991**, *103*, 431–433.
- de Meijere, A.; Jaekel, F.; Simon, A.; Borrmann, H.; Koehler, J.; Johnels, D.; Scott, L. T. *J. Am. Chem. Soc.* **1991**, *113*, 3935–3941.
- Fitjer, L.; Giersig, M.; Wehle, D.; Dittmer, M.; Koltermann, G.-W.; Schormann, N.; Egert, E. *Tetrahedron* **1988**, *44*, 393–404.
- Fitjer, L.; Klages, U.; Kuehn, W.; Stephenson, D. S.; Binsch, G.; Noltemeyer, J.; Egert, E.; Sheldrick, G. M. *Tetrahedron* **1984**, *40*, 4337–4350.
- Eliel, E. L.; Wilen, S. *Stereochemistry of organic compounds*; Wiley: New York, 1994; p 1191.
- Buchweller, C. H. In *Stereodynamics of cyclohexane and substituted cyclohexanes. Substituent A values in conformational behavior of six-membered ring*; Juaristi, E., Ed.; VCH: New York, 1995; p 42.
- Friebolin, H.; Schmid, H. G.; Kabuss, S.; Faisst, W. *Org. Magn. Reson.* **1969**, *1*, 67–86.
- Pihlaja, K.; Pasanen, P.; Wähäsilta, J. *Org. Magn. Reson.* **1979**, *12*, 331–336.
- Pasanen, P.; Pihlaja, K. *Tetrahedron* **1972**, *28*, 2617–2626.
- Siemens XSCANS, SHELXS-97, SHELXL-97 and Siemens SHELXTL programs.
- Sheldrick, G. M. SHELX-97; Universität Göttingen, Germany, 1997.
- Bruker. SMART (Version 5.611), SAINT (Version 6.02a), SHELXTL (Version 5.10) and SADABS; Bruker AXS Inc., Madison, Wisconsin, 1999. Claridge, J. B.; Layland, R. C.; zur Loye, H.-C. *Acta Crystallogr. Sect. C* **1997**, *53*, 1740.
- Farrugia, L. J. *J. Appl. Crystallogr.* **1997**, *30*, 565.

35. Terec, A. Ph.D. Thesis, Babes-Bolyai University, 2003.
36. Campbell, T. W.; Foldi, V. S. *J. Org. Chem.* **1961**, *26*, 4654–4658.
37. Jung, M. E.; McCombs, C. A. *Org. Synth.* **1979**, *58*, 163–164.
38. Rigby, J. H.; Kotnis, A.; Kramer, J. *J. Org. Chem.* **1990**, *55*, 5078–5088.
39. Anteunis, M.; Geens, A.; van Cauwenberghe, R. *Bull. Soc. Chim. Belg.* **1973**, *82*, 573–590.
40. Feuerbacher, N.; Vögtle, F.; Windscheidt, J.; Poetsch, E.; Nieger, M. *Synthesis* **1999**, 117–120.



Influence of the metal and chiral diamine on metal(II)salen catalysed, asymmetric synthesis of α -methyl α -amino acids

Yuri N. Belokon,^b Jose Fuentes,^a Michael North^{a,*} and Jonathan W. Steed^a

^aDepartment of Chemistry, King's College London, Strand, London WC2R 2LS, UK

^bA.N. Nesmeyanov Institute of Organo-Element Compounds, Russian Academy of Sciences, Vavilov 28, 117813 Moscow, Russian Federation

Received 24 November 2003; revised 16 January 2004; accepted 12 February 2004

Abstract—The influence of the metal ion and chiral diamine used to form a metal(salen) complex on the catalytic activity of the complex in the asymmetric benzylation of an alanine enolate was investigated. Only metal ions which could form square-planar complexes gave catalytically active complexes, and best results were obtained with metal ions from the first row of transition metals, particularly copper(II) and cobalt(II). Salen ligands derived from acyclic, chiral 1,2-diamines were found to generate poor catalysts, an effect which seems to correlate with the ability of the substituents within the diamine to adopt a conformation in which they are *anti* to one another. Complexes derived from a variety of 5- and 6-membered cyclic 1,2-diamines did form active catalysts, but the enantioselectivity was always far lower than that of the parent cyclohexane-1,2-diamine derived complex.

© 2004 Elsevier Ltd. All rights reserved.

1. Introduction

There is currently considerable interest in the asymmetric synthesis of α -amino acids and α,α -disubstituted amino acids by the alkylation of a prochiral enolate derived from glycine or an α -substituted amino acid in the presence of a chiral catalyst. Most of this work is carried out under phase-transfer conditions, with the chiral catalyst acting as a phase transfer catalyst.¹

The first results in this area came from the group of O'Donnell and used quaternary ammonium salts derived from cinchona alkaloids to catalyse the asymmetric alkylation of a glycine derived enolate, leading to α -amino acids with moderate enantiomeric excesses.² The main problem with this chemistry was the inadequate enantioselectivity, but recently the groups of Lygo³ and Corey,⁴ have shown that the use of a 9-anthracenylmethyl group to quaternize the cinchona alkaloid resulted in a catalyst that exhibited significantly enhanced enantioselectivity, and allowed the synthesis of α -amino acids with >95% enantiomeric excess.⁵ Attempts to extend this chemistry to enolates derived from other amino acids, thus allowing the synthesis of α,α -disubstituted amino acids were less successful due to the lower enantioselectivity observed.⁶ The same catalyst can also be used to catalyse the alkylation of other enolates,⁷ Michael additions,^{8,9} aldol

reactions,¹⁰ and enone epoxidations.¹¹ It can also be used in conjunction with achiral palladium complexes to induce the asymmetric allylation of enolates.¹² Recently, polymer supported^{9,13} and oligomeric¹⁴ versions of the cinchona derived phase transfer catalysts have been developed and used for asymmetric amino acid synthesis. The catalysts have also been used under micellar conditions.¹⁵

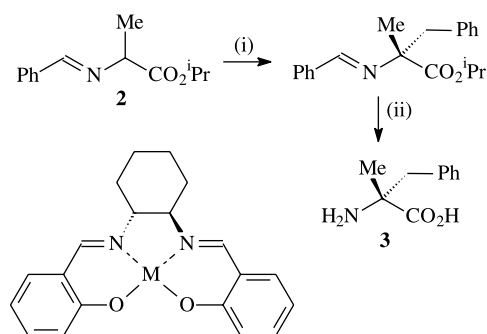
Synthetic quaternary ammonium salts derived from binaphthol have been developed by Maruoka.¹⁶ These salts have been shown to act as asymmetric phase transfer catalysts for both the alkylation and dialkylation (with two different alkylating agents) of a glycine derived imine, leading to both α -amino acids and α,α -disubstituted amino acids with excellent enantiomeric excesses. The asymmetric alkylation of β -keto-esters¹⁷ and aldol reactions are also catalysed by these chiral ammonium salts.¹⁸ Other groups have also investigated the use of synthetic phase transfer catalysts derived from ammonium¹⁹ or guanidinium²⁰ salts and crown ethers.²¹

All the above work is based on the use of purely organic catalysts as asymmetric phase transfer catalysts. It was not until 1998 that Belokon⁷ and Kagan first demonstrated that a metal complex could act as an asymmetric phase transfer catalyst. The sodium salt of TADDOL was found to catalyse the alkylation of alanine derivatives leading to α -methyl- α -amino acids with up to 82% enantiomeric excess.²² It was subsequently shown that the sodium salts of both NOBIN²³ and BINOLAM²⁴ could act as asymmetric phase transfer catalysts for the same reaction.

Keywords: Phase-transfer-catalysis; α -Amino acid; Alkylation; Diamine.

* Corresponding author. Tel.: +44-207-848-1164; fax: +44-870-131-3783; e-mail address: michael.north@kcl.ac.uk

Chiral transition metal complexes have been used to catalyse a wide range of asymmetric transformations, and we have shown that they can be used to catalyse the asymmetric alkylation of amino acid enolates under phase transfer conditions. In 1999, we reported that nickel(II)salen complex **1a** (10 mol%) would catalyse the asymmetric benzylation of alanine enolate **2** leading to α -methyl phenylalanine **3** (Scheme 1) with 30% enantiomeric excess.²⁵ The corresponding copper(II)salen complex **1b** was found to be a far more effective catalyst and 2 mol% of this complex was sufficient to catalyse the formation of compound **3** with 88% enantiomeric excess. Complex **1b** also catalysed the asymmetric alkylation of compound **2** with other alkyl halides, giving α -methyl α -amino acids with 75–90% enantiomeric excess.²⁵ These reactions are carried out under solid–liquid phase transfer conditions with solid sodium hydroxide as the base, and both enantiomers of catalyst **1b** are equally readily available, thus allowing the synthesis of either enantiomer of an α -methyl α -amino acid.



1a: M = Ni **1b:** M = Cu
1c: M = Mn **1d:** M = Fe
1e: M = Co **1f:** M = Zn
1g: M = Rh **1h:** M = Pd
1i: M = Pt **1j:** M = Co-I
1k: M = Co⁺ PF₆⁻
1l: M = Co-Na

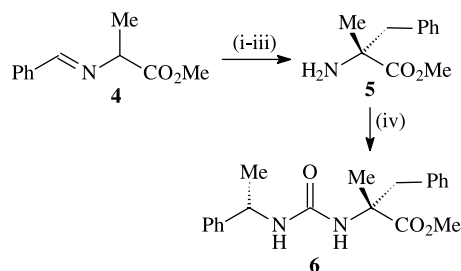
Scheme 1. Reagents: (i) **1a,b** (2–10 mol%)/NaOH (solid)/BnBr; (ii) H₃O⁺/Δ.

In subsequent work, we have studied the effect that substituents on the aromatic rings of catalyst **1b** have on the enantioselectivity of the catalyst,^{25,26} and optimized the reaction conditions and the structure of the imine within substrate **2**.²⁶ We have also demonstrated that under appropriate reaction conditions, it is possible to use the readily available methyl ester analogue **4** of substrate **2**.²⁷ Most recently, we have shown that the chemistry shown in Scheme 1 can be applied to amino acids other than alanine, thus allowing the synthesis of a range of non-racemic α,α -disubstituted α -amino acids.²⁸

In this paper, we report the results of a study aimed at better understanding the influence of various factors on the enantioselectivity of this reaction. In particular, we have prepared catalysts from a range of transition metals and from both cyclic and acyclic chiral diamines.

2. Results and discussion

The first factor that we studied was the effect of the central transition metal. Since the nickel(II) and copper(II) complexes **1a,b** had already been found to be catalytically active,²⁵ a range of other (salen)M²⁺ complexes were prepared and tested for catalytic activity in the model reaction shown in Scheme 2. The substrate **4** used in this work does not have the optimized *para*-chlorobenzylidene imine as this optimisation had not been discovered at the start of this project.²⁶ Substrate **4** was subsequently used throughout the work described in this paper to allow the results to be compared. The enantiomeric excess of the α -methyl-phenylalanine methyl ester product **5** was determined by reaction with an excess of (*S*)- α -methyl benzylisocyanate to give a pair of diastereomeric ureas **6**. The diastereotopic benzylic protons (PhCH₂) of compounds **6** give rise to a series of four well resolved doublets in the ¹H NMR spectrum. Integration of these doublets allowed the diastereomeric excess of ureas **6** and hence the enantiomeric excess of amine **5** to be determined once the conversion of **5** to **6** had gone to completion.



Scheme 2. Reagents: (i) **1a-i** (2 mol%)/NaOH (solid)/BnBr; (ii) MeOH/AcCl; (iii) SiO₂; (*S*)-PhCH(Me)N=C=O.

Initially, first row transition metal complexes were studied. Complexes **1c-e** could be prepared and isolated by reaction of the salen ligand with the appropriate metal acetate. However, all attempts to isolate complex **1f** using zinc bromide or diethylzinc (in thf, toluene or hexane) as the metal source were completely unsuccessful.²⁹ Therefore, this complex was prepared in situ from the salen ligand and diethylzinc. Manganese(II)salen^{30,31} and iron(II)salen^{31,32} complexes **1c** and **1d** were found to be catalytically inactive (Table 1: entries 1 and 2). These complexes would not be

Table 1. The effect of the metal in complexes **1** on enantioselectivity^a

Entry	Metal	Complex	Yield (%)	Enantioselectivity (%) ^b
1	Mn ²⁺	1c	15	1
2	Fe ²⁺	1d	34	3
3	Co ²⁺	1e	83	80
4 ^c	Ni ²⁺	1a	34	30
5	Cu ²⁺	1b	91	81
6	Zn ²⁺	1f	39	1
7	Rh ²⁺	1g	92	14
8	Pd ²⁺	1h	56	1
9	Pt ²⁺	1i	55	0
10	Co ³⁺	1j	46	7
11	Co ³⁺	1k	66	0
12	Co ¹⁺	1l	21	0

^a Reactions were carried out under the conditions described in Scheme 2.

^b The error in this measurement is estimated to be $\pm 3\%$.

^c Data taken from Ref. 25 for substrate **2** and using 10 mol% of complex **1a**.

expected to be square-planar. The 15–34% yield of essentially racemic compound **5** obtained in these reactions presumably arises from an uncatalysed background reaction as we have previously shown that even in the absence of any catalyst, racemic α -methyl-phenylalanine is formed under the reaction conditions.³³

Cobalt(II)salen complex³⁴ **1e** was found to be as active a catalyst as the copper(II)salen complex **1b** (Table 1: entries 3 and 5), which is the best previously known salen complex for this reaction. To further investigate the relationship between complexes **1e** and **1b**, the X-ray structure³⁵ of complex **1e** was obtained for comparison with the known structure of complex **1b**.³⁶ The structure of complex **1e** is shown in Figure 1, and as expected the complex was found to be square-planar.³⁷ Comparison of the bond lengths and bond angles within the X-ray structures of complexes **1b** and **1e** revealed that the structures were essentially superimposable. The asymmetric unit of compound **1e** contains two essentially identical, independent, homochiral molecules that form discrete, face-to-face dimers in the solid state with a Co···Co distance of 3.326(1) Å. Symmetry-related dimers interact via CH···O hydrogen bonds.

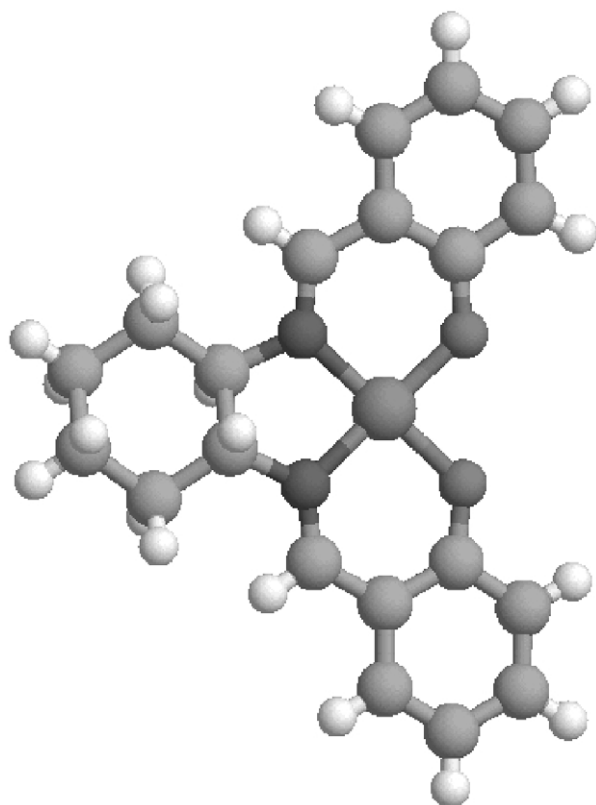


Figure 1. The X-ray structure of complex **1e**.

In situ prepared zinc(II)salen complex **1f** did not give an active catalyst (Table 1: entry 6). A survey of the Cambridge X-ray database revealed that Zn(salen) complexes tend not to be four-coordinate in the solid state. Instead, trigonal bipyramidal, five-coordinate complexes are formed by intermolecular association involving the salen oxygen atoms.²⁹

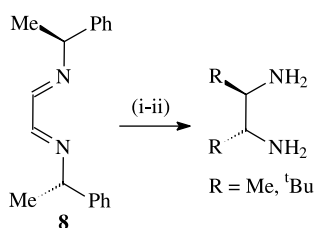
The results from the first row of transition metal M^{2+} (salen) complexes clearly show that a square-planar complex is essential for catalytic activity. It is also notable that complexes **1b** and **1e** which are both paramagnetic ($17e^-$ and $15e^-$ systems respectively) are significantly more active than the nickel(II)salen complex **1a** which is diamagnetic ($16e^-$ system), despite the fact that all three complexes are known to be square-planar.^{36,38} This suggests that the mechanism may involve a single electron transfer process.

Three other M^{2+} (salen) complexes were prepared from group 9/10 metals in the second and third rows of transition metals. Rh(II)salen complex **1g** was prepared from rhodium(II) acetate and was found to be catalytically active, but gave product **5** with only 14% enantiomeric excess (Table 1: entry 7). An attempt to increase the enantioselectivity by using 10 mol% of catalyst **1g** was unsuccessful, giving product **5** with an unchanged 13% enantiomeric excess. Interestingly however, complex **1g** gave the (*S*)-enantiomer of compound **5** as the major product, whilst every other complex tested gave predominantly the (*R*)-enantiomer of the product. The reason for this difference in enantioselectivity is not known, but it may be relevant that rhodium(II)salen complexes are known to be bimetallic with a Rh–Rh bond.³⁹ Palladium(II)salen complex^{40,41} **1h** (prepared from palladium(II) acetate) and platinum(II)salen complex^{41,42} **1i** (prepared from platinum(II) chloride) were both catalytically inactive, giving racemic product **5** (Table 1: entries 8 and 9). These three results again show the superiority of complexes from group 9 over complexes from group 10 as asymmetric phase transfer catalysts. Complexes **1h** and **1i** were also tested as catalysts in conjunction with potassium hydroxide rather than sodium hydroxide as the base. Our model to explain the asymmetric induction in these reactions^{25,28} envisages the formation of a bimetallic complex, with the alkali metal coordinated between the oxygen atoms of the salen ligand. Increasing the size of the transition metal within the salen complex was anticipated to increase the distance between these two oxygen atoms so that they would prefer to coordinate to a larger alkali metal. However, palladium complex **1h** gave just a 13% yield of racemic **5** under these conditions, and platinum complex **1i** gave no product. As a result of these results we concluded that only first row transition metal complexes formed useful catalysts and our subsequent work was concentrated on these species.

All of the above work was carried out with metal ions in the +2 oxidation state. Two Co(III) complexes were also prepared and tested. Iodo complex **1j** was prepared by treatment of Co(II)salen complex **1e** with iodine in dichloromethane as reported for the preparation of other iodocobalt(III)salen complexes.⁴³ Complex **1k** was obtained by treatment of complex **1e** with ferrocinium hexafluorophosphate in acetonitrile.⁴⁴ By analogy with the known X-ray structures⁴⁵ of other 5-coordinate Co(III)salen complexes, complex **1j** is expected to have a square-based pyramidal structure with the salen ligand forming the square base. Complex **1k**, with a non-coordinating anion will however be square-planar.⁴⁶ Both of these complexes displayed little or no catalytic activity (Table 1, entries 10 and 11).

Finally, the use of salen complexes of metals in the +1 oxidation state was investigated. Attempts to prepare the Cu(I)salen complex from copper(I) acetate and the salen ligand were unsuccessful as only the Cu(II)salen complex **1b** could be isolated from these reactions. The preparation of Co(I)salen complexes by the reduction of the corresponding Co(II)salen complexes using sodium amalgam is however a well known process.⁴⁷ Cobalt(I)salen complexes are known to be square-planar and to be capable of coordinating a sodium ion between the two phenolic oxygens.⁴⁸ Therefore, complex **1e** was treated with sodium amalgam in thf to generate the corresponding Co(I)salen complex³⁴ **11**. This complex was used without purification due to the known sensitivity of Co(I)salen complexes to air, but was not found to display any catalytic activity. Reactions involving complex **11** were far less clean than those involving complexes **1b,e**, produced only a small amount of product and gave only racemic product (Table 1: entry 12).

Having determined that Co²⁺ and Cu²⁺ were the optimal metals, the structure of the diamine was next investigated. Four complexes (**7a–d**) derived from three C₂-symmetric acyclic diamines with different steric properties were prepared. The (*R,R*)-1,2-diphenyl-ethane-1,2-diamine needed for the preparation of complexes **7b,c** was commercially available^{49,50} and the corresponding diamines needed for the preparation of complexes **7a,d** were prepared by a literature route involving the addition of the appropriate Grignard reagent to imine **8** (Scheme 3).^{51,52} As the results in Table 2 show, all of these ligands formed copper(II) complexes which were less catalytically active than complex **1b**. The most active of these complex was **7a** (Table 2: entry 1) derived from (*R,R*)-butane-2,3-diamine, and complex **7d** was catalytically inactive (Table 2: entry 4) as indicated by the absence of any enantioselectivity. The chemical yield in this case is probably due to the uncatalysed background reaction.³³

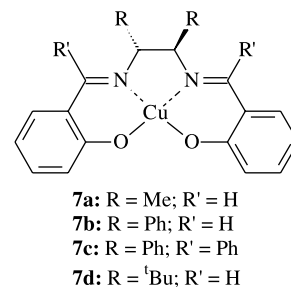


Scheme 3. Reagents: (i) RMgBr then H₃O⁺; (ii) Pd(OH)₂/HCO₂NH₄/EtOH/Δ.

Table 2. The effect of acyclic diamines on catalytic activity^a

Entry	Complex	Yield (%)	Enantioselectivity (%)
1	7a	73	36
2	7b	21	25
3	7c	54	5
4	7d	27	0

^a Reactions were carried out under the conditions described in Scheme 2.



The R-groups in complexes **7a–d** can adopt locations which are either *gauche*- or *anti*- to one another as shown by the Newman projections in Figure 2. Cyclic diamines (such as (*R,R*)-cyclohexane-1,2-diamine) can only adopt the *gauche*-conformation, but for acyclic diamines the *anti*-conformation is generally thermodynamically more stable as it minimizes steric repulsions between the R-groups. The X-ray structure of the square-planar cobalt(II) complex derived from ligand **7a** has previously been determined⁵³ and shows that the methyl groups are indeed *anti* to one another.

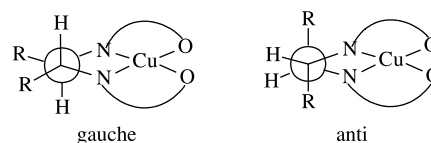


Figure 2. *gauche*- and *anti*-Conformations of salen complexes.

Complex **7b** derived from (*R,R*)-1,2-diphenyl-ethane-1,2-diamine was less active than complex **7a** (Table 2: compare entries 1 and 2). X-ray structures of square-planar nickel(II)salen complexes derived from this ligand have been reported in which the phenyl rings are *gauche*- or *anti*- to one another.^{54,55} In contrast, the X-ray structure of the square-planar cobalt(II) complex analogous to **7c** shows that the phenyl rings on the ethylenediamine unit are in this case locked into the *anti*-conformation to avoid steric interactions with the two additional phenyl rings on the imine part of the ligand.⁵⁶ Complex **7c** was found exhibit only a very low enantioselectivity (Table 2: entry 3).

To investigate why complex **7d** was totally inactive, an X-ray structure analysis of this complex was undertaken.⁵⁷ This compound also contains two independent molecules in the asymmetric unit, although a face-to-face interaction as in **1e** is precluded by the bulk of the *tert*-butyl substituents. Intermolecular association is again via CH^{δ+}⋯O interactions and, as in **1e**, the geometry at both independent Cu(II) ions is square-planar. The structure also revealed (Fig. 3) that the *tert*-butyl groups adopted *anti*-positions on the five-membered chelate ring to minimize steric repulsions between them. The effect of this is that the *tert*-butyl groups extend over and below the copper ion as shown in the space filling model illustrated in Figure 4. This would prevent substrate **4** from complexing to the copper ion, and hence prevent complex **7d** from exhibiting any catalytic activity.

The results obtained with complexes **7a–d** strongly suggest that for a complex to be catalytically active, the substituents

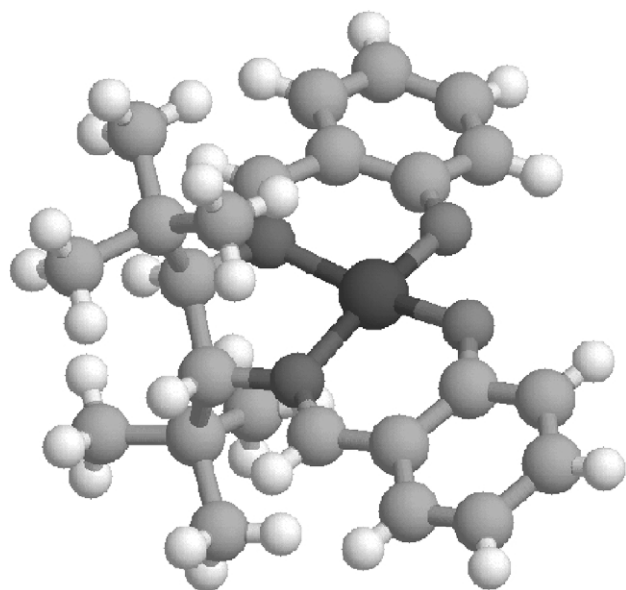


Figure 3. The X-ray structure of complex **7d**.

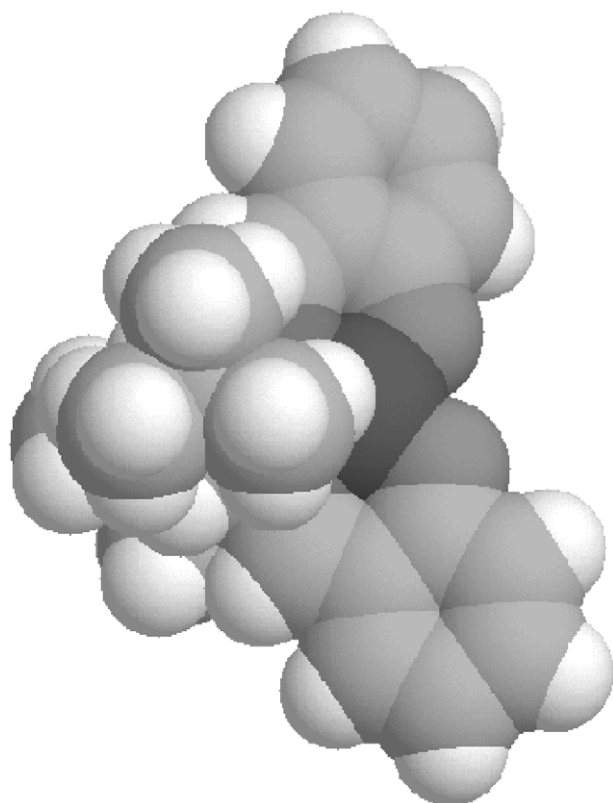
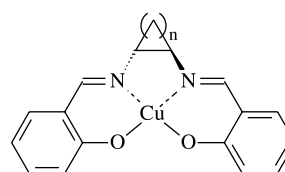


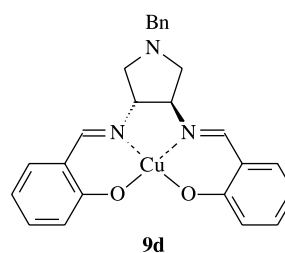
Figure 4. A space-filling model of complex **7d** showing the *tert*-butyl group protruding over the copper ion.

on the ethylenediamine part of the salen ligand must adopt a *gauche*-conformation. Complexes **7c,d** where this is not possible are inactive, whilst complexes **7a,b** which are expected to exist as an equilibrium mixture of *anti*- and *gauche*-conformations are active. Complex **7a** with small methyl substituents would be expected to have a greater percentage of molecules in the *gauche*-conformation than complex **7b** and hence to be more catalytically active. This matches the observed results.

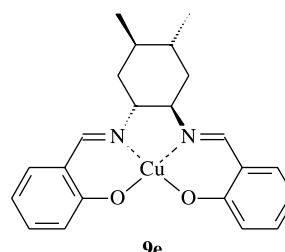
To restrict the ligands to a *gauche*-conformation whilst varying the size of the substituents within the ethylenediamine unit, a series of complexes derived from cyclic diamines was prepared. First, the systematic replacement of the cyclohexyl ring within catalyst **1b** with cyclopropyl, cyclobutyl- and cyclopentyl- rings to give complexes **9a-c** was investigated. The enantiomerically pure diamines required for this work were prepared by literature procedures.^{58,59} The catalytic activity observed which should be with each of these complexes is presented in Table 3.



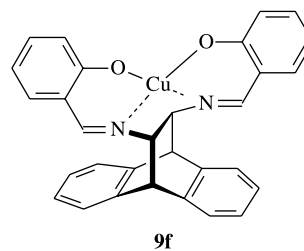
9a: n = 1
9b: n = 2
9c: n = 3



9d



9e



9f

Table 3. The effect of cyclic diamines on catalytic activity^a

Entry	Complex	Yield (%)	Enantioselectivity (%)
1	9a	69	0
2	9b	60	0
3	9c	84	25
4	9d	59	37
5	9e	52	32
6	9f	85	32

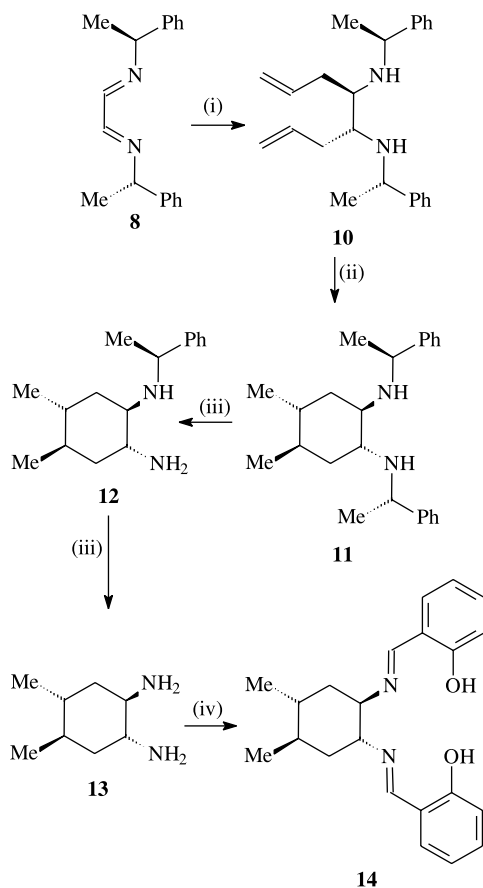
^a Reactions were carried out under the conditions described in Scheme 2.

In the case of compounds **9a** and **9b**, whilst we were able to prepare the required enantiomerically pure 1,2-diamines, and the salen ligand, it was not possible to isolate the copper

complexes **9a,b**. It may be that the torsional angles around the 3- or 4-membered ring prevent the heteroatoms within the salen ligand from adopting suitable locations to form a square-planar complex. However, the crude product obtained by mixing the ligand and copper(II) bromide was tested, though no enantioselectivity was observed (Table 3: entries 1 and 2).

Cyclopentane derivative **9c** was prepared by the literature route,⁵⁹ and the corresponding *N*-benzyl pyrrolidine derived ligand was also prepared by a modification of the literature procedure.⁶⁰ Thus, *N*-benzyl-(3*S*,4*S*)-3,4-dihydroxy-pyrrolidine was prepared from (*R,R*)-tartaric acid. However, in our hands the conversion of this diol into the corresponding bis-azide by a Mitsunobu procedure⁶⁰ was problematic. In contrast, conversion of the diol to the corresponding bis-mesylate⁶¹ and then conversion to the bis-azide using the procedure reported for 1,2-diazidocyclopentane⁶² worked smoothly. Subsequent reduction of the bis-azide to the corresponding diamine, formation of the salen ligand and synthesis and isolation of complex **9d** occurred as expected. However, whilst complexes **9c** and **9d** did form active catalysts (Table 3: entries 3 and 4), the asymmetric induction observed with them was only about one third that observed with the corresponding cyclohexane derivative **1b**.

The 1,2-diamino-4,5-dimethylcyclohexane required for the synthesis of complex **9e** was prepared by a modification of a literature procedure. Addition of allylmagnesium bromide



Scheme 4. Reagents: (i) allylMgBr then H₃O⁺; (ii) BuMgBr (5 equiv.)/Cp₂ZrCl₂ (20 mol%); (iii) Pd(OH)₂/C/H₂, 3 atm; (iv) salicylaldehyde.

to imine **8** gave diamine⁶³ **10** as shown in Scheme 4. Treatment of diamine **10** with butylmagnesium chloride and catalytic bis-(cyclopentadienyl)zirconium dichloride resulted in reductive cyclisation to cyclohexane derivative⁶⁴ **11**. However, the order of addition of the reagents was found to be critical to control the stereochemistry of the cyclisation. Only when the butylmagnesium chloride and (cyclopentadienyl)zirconium dichloride were premixed followed by addition of diamine **10** was compound **11** obtained as the major stereoisomer. In our hands, all other conditions gave unreacted starting material. Hydrogenolysis of compound **11** was carried out using 20% Pd(OH)₂ on carbon at three atmospheres pressure of hydrogen for 24 h, and gave the partially deprotected compound **12**. Compound **12** was resubjected to the same hydrogenolysis conditions to give diamine **13**. Treatment of diamine **13** with salicylaldehyde gave the required salen ligand **14** which could be complexed to copper to give complex **9e**.

In complex **9e**, the formation of the chelate forces both amino groups to adopt equatorial positions on the cyclohexane ring, and this in turn means that both methyl groups are in axial positions. It was hoped that the methyl groups would be able to interact with a coordinated substrate, but disappointingly, complex **9e** only exhibited 32% enantioselectivity (Table 3: entry 5), compared to 81% for complex **1b** (Table 1: entry 5) which does not have the two methyl groups on the cyclohexane ring. The acyclic diamine derived ligands **7a-d** demonstrated that axial groups on the carbon adjacent to the nitrogen atoms were detrimental to the enantioselectivity of the catalysts. The result obtained with complex **9e** suggests that this effect extends all the way across the cyclohexane ring.

The enantiomerically pure anthracene derived diamine required for the preparation of complex **9f** was prepared from anthracene and fumaric acid by the literature route.⁶⁵ Condensation of this diamine with salicylaldehyde gave the required salen ligand⁴⁹ which could be complexed to copper to give complex **9f**. In complex **9f**, the cyclohexane ring is forced to adopt a boat conformation, and this was found to have a detrimental effect on the enantioselectivity of the catalyst (Table 3: entry 6) as the complex converted compound **4** into product **5** with just 32% enantiomeric excess.

3. Conclusions

Of the metal(salen) complexes studied as asymmetric phase transfer catalysts in this work, only the Cu(II) and Co(II) complexes were found to give high levels of asymmetric induction. These two complexes are both square-planar and paramagnetic. Variation of the original cyclohexane-1,2-diamine derived salen ligand did not increase the asymmetric induction. Complexes derived from acyclic diamines exist predominantly in an *anti*-conformation which may account for their reduced catalytic activity. It was not possible to isolate copper complexes of cyclopropyldiamine and cyclobutyldiamine derived ligands. The cyclopentyl-diamine and cyclohexyldiamine derived ligands studied, were catalytically active, but gave lower asymmetric

induction than the parent cyclohexane diamine derived complex.

4. Experimental

4.1. General

^1H NMR, ^{13}C NMR, ^{19}F NMR and ^{31}P NMR spectra were recorded on a Bruker Avance 360 Spectrometer, (^1H 360 MHz, ^{13}C 90 MHz, ^{19}F 338 MHz and ^{31}P 145 MHz). The solvent for a particular spectrum is given in parentheses. ^1H and ^{13}C NMR Spectra were referenced to TMS and chemical-shift (δ) values, expressed in parts per million (ppm), are reported downfield of TMS. Chemical-shift values for ^{31}P spectra are reported downfield of phosphoric acid, and chemical-shift values for ^{19}F spectra are relative to CFCl_3 . The multiplicity of signals is reported as singlet (s), doublet (d), triplet (t), quartet (q), multiplet (m), broad (br) or a combination of any of these. For ^{13}C NMR spectra, the peak assignments were made with the assistance of DEPT experiments.

Infrared spectra were recorded on a Perkin–Elmer FT-IR Paragon 1000 spectrometer, as a thin film between NaCl plates in the reported solvent, or as KBr disks. The characteristic absorption is reported as broad (br), strong (s), medium (m) or weak (w). Low and high resolution mass spectra were recorded at the EPSRC national service at the University of Wales, Swansea, or on a Bruker Apex III FTMS or Jeol AX505W spectrometer within the chemistry department at King's College. The sample was ionized by electron ionization (EI), chemical ionisation (CI) fast atom bombardment (FAB) or electrospray ionization (ESI). The major fragment ions are reported and only the molecular ions are assigned.

Optical rotations were recorded on a Perkin–Elmer 343 polarimeter in a thermostated cell of length 1 dm at 20 °C using the sodium D-line, and a suitable solvent that is reported along with the concentration (in g/100 ml). Melting points were determined with a Buchi Melting Point apparatus N° 520092 and are uncorrected. Elemental analyses were performed by the London School of Pharmacy.

Chromatographic separations were performed with silica gel 60 (230–400 mesh) and thin-layer chromatography was performed on polyester backed sheets coated with silica gel 60 F254, both supplied by Merck. Toluene was distilled from sodium prior to use.

Crystals were mounted on a thin glass fibre using epoxy resin and cooled on the diffractometer to 120 K using an Oxford Cryostream low temperature attachment. Approximate unit cell dimensions were determined by the Nonius Collect program⁶⁶ from 5 index frames of width 2° in ϕ using a Nonius $\text{K}\alpha$ CCD diffractometer, with a detector to crystal distance of 30 mm. The Collect program was then used to calculate a data collection strategy to 99.5% completeness for $\theta=27.5^\circ$ using a combination of 2° ϕ and ω scans of 10–120 s deg^{-1} exposure time (depending on crystal quality). Crystals were indexed using the

DENZO-SMN package⁶⁷ and positional data were refined along with diffractometer constants to give the final unit cell parameters. Integration and scaling (DENZO-SMN, Scale-pack⁶⁷) resulted in unique data sets corrected for Lorentz and polarisation effects and for the effects of crystal decay and absorption by a combination of averaging of equivalent reflections and an overall volume and scaling correction. Structures were solved using SHELXS-97⁶⁸ and developed via alternating least squares cycles and difference Fourier synthesis (SHELXL-97⁶⁸) with the aid of the program XSeed.⁶⁹ All non-hydrogen atoms were modelled anisotropically, while hydrogen atoms are assigned an isotropic thermal parameter 1.2 times that of the parent atom (1.5 for terminal atoms) and allowed to ride. All calculations were carried out with IBM compatible PCs.

4.1.1. Manganese(II)salen complex 1c. To a solution of (*R,R*)-[*N,N'*-bis-(2'-hydroxybenzylidene)]-1,2-diamino-cyclohexane (476 mg, 1.48 mmol) in ethanol (15 ml), was added KOH (166 mg, 2.96 mmol) dissolved in ethanol (4 ml). To the resulting yellow solution was added a suspension of anhydrous manganese acetate (256 mg, 1.48 mmol) in ethanol (4 ml) and the reaction was refluxed at 100–120 °C for 2 h under a nitrogen atmosphere. The solution was allowed to reach room temperature and then concentrated in vacuo. The resulting black solid was taken up with dichloromethane, filtered and evaporated in vacuo to leave a black solid which was recrystallized from dichloromethane/hexane to afford compound **1c** (461 mg, 83%) as black crystals. Mp >250 °C. $[\alpha]_{\text{D}}^{20} = -1233$ (*c* 0.012, CHCl_3); ν_{max} (KBr) 3022 (w), 2934 (m), 2859 (w), 1632 (s), 1600 (s) and 1537 cm^{-1} (s); *m/z* (ESI) 375 (M^+ , 100). Found (ESI) 375.0900 (M^+), $\text{C}_{20}\text{H}_{20}\text{N}_2\text{O}_2\text{Mn}$ requires 375.0880.

4.1.2. Iron(II)salen complex 1d.³² (*R,R*)-[*N,N'*-Bis-(2'-hydroxybenzylidene)]-1,2-diamino-cyclohexane (847 mg, 2.63 mmol) and anhydrous iron(II) acetate (457 mg, 2.63 mmol) were stirred in ethanol (8 ml) at 75 °C for 1 h under a nitrogen atmosphere. A dark orange solid precipitated. The mixture was allowed to cool to room temperature and then filtered and washed with hexane under a nitrogen atmosphere. The orange precipitate was purified by suspension in refluxing ethanol under a nitrogen atmosphere, followed by filtration and washing with hexane to give compound **1d** (494 mg, 50%) as an orange solid. Mp >270 °C; $[\alpha]_{\text{D}}^{20} = -714$ (*c* 0.017, CHCl_3); ν_{max} (KBr) 3024 (w), 2926 (m), 2855 (w), 1614 (s) and 1539 cm^{-1} (s); *m/z* (ESI) 376 (M^+ , 100). Found (ESI) 376.0846 (M^+), $\text{C}_{20}\text{H}_{20}\text{N}_2\text{O}_2\text{Fe}$ requires 376.0869.

4.1.3. Cobalt(II)salen complex 1e.³⁴ (*R,R*)-[*N,N'*-Bis-(2'-hydroxybenzylidene)]-1,2-diamino-cyclohexane (1.61 g, 5.0 mmol) and anhydrous cobalt(II) acetate (1.25 g, 5.0 mmol) were stirred in ethanol (16 ml) at 70 °C for 1 h under an argon atmosphere. During this time an orange solid precipitated. The reaction was allowed to cool to room temperature and then filtered and washed with hexane under a nitrogen atmosphere. The orange precipitate was purified by suspension in refluxing ethanol under an argon atmosphere, followed by filtration and washing with hexane to obtain a crimson solid (543 mg, 29%). Crystals suitable for X-ray analysis were obtained by recrystallisation from hexane/dichloromethane. Mp >270 °C; $[\alpha]_{\text{D}}^{20} = -1420$ (*c*

0.050, CHCl₃); ν_{\max} (KBr) 3019 (w), 2930 (w), 2855 (w), 1603 (s) and 1531 cm⁻¹ (m); m/z (FAB) 380 (MH⁺, 70%), 379 (M⁺, 66), 307 (26), 154 (100), 136 (69). Crystal data: C₂₀H₂₀CoN₂O₂, $M=379.31$, red cube, 0.30×0.30×0.30 mm³, monoclinic, space group $P2_1$ (No. 4), $a=11.1089(7)$, $b=12.3377(6)$, $c=12.3903(10)$ Å, $\beta=97.133(3)^\circ$, $V=1685.05(19)$ Å³, $Z=4$, $D_c=1.495$ g/cm³, $F_{000}=788$, KappaCCD, Mo K α radiation, $\lambda=0.71073$ Å, $T=120(2)$ K, $2\theta_{\max}=55.0^\circ$, 10999 reflections collected, 6940 unique ($R_{\text{int}}=0.0610$). Final GooF=0.996, $R1=0.0534$, $wR2=0.0871$, R indices based on 5011 reflections with $I>2\sigma(I)$ (refinement on F^2), 452 parameters, 1 restraint. Lp and absorption corrections applied, $\mu=1.034$ mm⁻¹. Absolute structure parameter=-0.009(17).⁷⁰

4.1.4. Rhodium(II)salen complex 1g. (*R,R*)-[*N,N'*-Bis-(2'-hydroxybenzylidene)]-1,2-diamino-cyclohexane (116 mg, 0.36 mmol) and sodium methoxide (39 mg, 0.72 mmol) were dissolved in methanol (7 ml). The yellow solution was stirred at room temperature for 5 min, then [Rh(OAc)₂]₂·2H₂O (86 mg, 0.18 mmol) was added as a slurry in MeOH (2 ml). The resulting green solution was stirred and heated to 60 °C for 4 h, under an argon atmosphere. Subsequently, the dark brown mixture was allowed to cool to room temperature and then evaporated in vacuo. The crude product was dissolved in dichloromethane (7 ml) and diethyl ether (10 ml) was added until a pale brown solid precipitated. The precipitate was collected by suction filtration, washed with diethyl ether (5 ml) and dried in vacuo to leave complex **1g** (150 mg, 98%) as a pale brown solid. Mp >270 °C; $[\alpha]_D^{20}=-8$ (c 0.025, MeOH); ν_{\max} (CHCl₃) 2942 (m), 2863 (w), 1635 (s), 1602 (s) and 1536 cm⁻¹ (w); m/z (ESI) 423 (M⁺, 100). Found (ESI) 423.0572 (M⁺), C₂₀H₂₀N₂O₂Rh requires 423.0574.

4.1.5. Palladium(II)salen complex 1h.⁴⁰ (*R,R*)-[*N,N'*-Bis-(2'-hydroxybenzylidene)]-1,2-diamino-cyclohexane (122 mg, 0.378 mmol) and sodium methoxide (49 mg, 0.91 mmol) were dissolved in methanol (29 ml). The yellow solution was stirred at room temperature for 5 min, then anhydrous palladium acetate (85 mg, 0.378 mmol) was added and the reaction stirred for 2 h. The precipitate was collected by vacuum filtration, washed with cold methanol and dried in vacuo with gentle heating for several hours to provide complex **1h** (127 mg, 79%) as a yellow solid. Mp >270 °C; $[\alpha]_D^{20}=-504$ (c 0.025, CHCl₃); ν_{\max} (KBr) 3045 (w), 2932 (m), 2857 (w), 1632 (s), 1601 (s) and 1531 cm⁻¹ (s); δ_H (CDCl₃) 1.3–2.4 (4H, m, CH₂CH₂), 3.6–3.7 (1H, m, CH–N), 6.4–7.3 (4H, m, ArCH), 7.31 (1H, s, HC=N); δ_C (CDCl₃) 24.9 (CH₂), 28.8 (CH₂), 72.7 (CH), 115.0 (ArCH), 121.2 (ArC), 122.2 (ArCH), 135.0 (ArCH), 135.2 (ArCH), 155.6 (CH=N), 165.9 (ArC); m/z (ESI) 426 (M⁺, 100). Found (ESI) 426.0644 (M⁺), C₂₀H₂₀N₂O₂Pd requires 426.0648. Found: C, 56.4%; H, 4.5%; N, 6.3%. C₂₀H₂₀N₂O₂Pd requires: C, 56.3%; H, 4.7%; N, 6.6%.

4.1.6. Platinum(II)salen complex 1i.⁴¹ (*R,R*)-[*N,N'*-Bis-(2'-hydroxybenzylidene)]-1,2-diamino-cyclohexane (200 mg, 0.62 mmol), PtCl₂ (165 mg, 0.62 mmol) and NaOMe (67 mg, 1.24 mmol) were added to methanol (5 ml) stirred for 4 h at room temperature and then the solvent was removed in vacuo. The residue was first purified by

chromatography on LH-20 using EtOH/toluene (1:3) as eluent to give a mixture of complex **1i** and unreacted ligand. The mixture was washed with diethyl ether (3×4 ml) to leave complex **1i** (60 mg, 19%) as a yellow solid. Mp 180–190 °C (decomp.); $[\alpha]_D^{20}=-192$ (c 0.017, CHCl₃); ν_{\max} (KBr) 2932 (m), 1607 (s) and 1535 cm⁻¹ (m); δ_H (CDCl₃) 1.3–2.4 (4H, m, CH₂CH₂), 3.6–3.7 (1H, m, CH–N), 6.4–7.4 (4H, m, ArCH), 7.63 (1H, s, H–CN); δ_C (CDCl₃) 25.0 (CH₂), 28.1 (CH₂), 74.1 (CH), 116.2 (ArCH), 122.5 (ArC), 122.7 (ArCH), 134.1 (ArCH), 134.3 (ArCH), 151.2 (CH=N), 163.8 (ArC); m/z (ESI) 538 (M+Na⁺). Found (ESI) 1053.2262 (2M+Na⁺), C₄₀H₄₀N₄O₄Pt₂Na requires 1053.2237.

4.1.7. Cobalt(III)salen complex 1j. To a solution of complex **1e** (100 mg, 0.26 mmol) in dichloromethane (53 ml) was added a solution of iodine (34 mg, 0.13 mmol) in dichloromethane (1 ml). The mixture was stirred at room temperature for 1 h during which time the red colour of the solution disappeared and a brown solid precipitated. The solution was evaporated to dryness to give complex **1j** (128 mg, 96%) as a brown solid which was used without further purification. Mp 260 °C; $[\alpha]_D^{20}=-1000$ (c 0.001, CHCl₃); ν_{\max} (KBr) 3052 (w), 2933 (w), 2859 (w), 1628 (s), 1595 (s) and 1535 cm⁻¹ (m); δ_H (DMSO-*d*₆) 1.5–3.1 (4H, m, CH₂CH₂), 3.6–3.7 (1H, m, CHN), 6.5–7.6 (4H, m, ArCH), 8.03 (1H, s, HC=N); δ_C (DMSO-*d*₆) 24.5 (CH₂), 29.8 (CH₂), 69.9 (CH), 115.5 (ArCH), 119.3 (ArC), 123.0 (ArCH), 135.1 (ArCH), 135.5 (ArCH), 164.4 (CH=N), 165.6 (ArC). Found (ESI) 379 (M–I⁺, 100). Found (ESI) 379.0831 (M–I⁺), C₂₀H₂₀N₂O₂Co requires 379.0857.

4.1.8. Cobalt(III)salen complex 1k. A solution of ferrocenium hexafluorophosphate (66 mg, 0.20 mmol) in acetonitrile (4 ml) was added to a solution of complex **1e** (75 mg, 0.20 mmol) in acetonitrile (4 ml) at room temperature. The mixture was stirred for 19 h and then was concentrated in vacuo. The crystalline residue was washed with hexane to remove ferrocene and dried in vacuo to afford complex **1k** (104 mg, 99%) as a black crystalline solid. Mp >250 °C; $[\alpha]_D^{20}=-3005$ (c 0.033, MeOH); ν_{\max} (KBr): 2939 (w), 1637 (s), 1604 (m), and 1544 cm⁻¹ (m); δ_H (DMSO-*d*₆) 1.6–2.1 (4H, m, CH₂CH₂), 3.0–3.1 (1H, m, CHN), 6.7–7.6 (4H, m, ArCH), 8.02 (1H, s, HC=N); δ_C (DMSO-*d*₆) 24.5 (CH₂), 29.8 (CH₂), 69.8 (CH), 115.5 (ArCH), 119.2 (ArC), 123.0 (ArCH), 135.1 (ArCH), 135.5 (ArCH), 164.4 (CH=N), 165.6 (ArC); δ_F (DMSO-*d*₆) –70.5 (d ¹J_{PF}=711 Hz, PF₆); δ_P (DMSO-*d*₆) –143 (hept. ¹J_{PF}=711 Hz, PF₆); m/z (ESI) 379 (M–PF₆)⁺. Found (ESI) 379.0821 (M–PF₆)⁺, C₂₀H₂₀N₂O₂Co requires 379.0851.

4.1.9. Copper(II)salen complex 7a. (+)-[*N,N'*-Bis-(2'-hydroxybenzylidene)]-2,3-diamino-butane⁵³ (80 mg, 0.3 mmol), copper(II) bromide (67 mg, 0.3 mmol) and sodium methoxide (33 mg, 0.6 mmol) were dissolved in methanol (5 ml) and stirred for 18 h at room temperature. The solvent was evaporated in vacuo and the residue was purified by chromatography on LH-20 using EtOH/toluene (1:3) to give complex **7a** (74 mg, 69%), as a dark brown solid. Mp 258–260 °C; $[\alpha]_D^{20}=-582$ (c 0.014, CHCl₃); ν_{\max} (CHCl₃) 2964 (w), 1622 (s), 1600 (m) and 1536 cm⁻¹ (m); m/z (CI) 358 (MH⁺, 55), 297 (63), 148 (89), 122 (100), 72

(61). Found (ESI) 358.0743 (MH⁺), C₁₈H₁₉N₂O₂Cu requires 358.0737.

4.1.10. [N,N'-Bis-(2'-hydroxyphenyl)phenylmethylidene]-(R,R)-1,2-diamino-1,2-diphenylethane and [N-(2'-hydroxyphenyl)phenylmethylidene]-(R,R)-1,2-diamino-1,2-diphenylethane. To a solution of (R,R)-1,2-diamino-1,2-diphenylethane (220 mg, 1.04 mmol) in ethanol (10 ml), 2-hydroxybenzophenone (410 mg, 2.07 mmol) was added at room temperature. The resulting bright yellow solution was stirred under reflux for 44 h, then it was allowed to cool to room temperature and allowed to stand overnight. The resulting precipitate was filtered, washed with cold ethanol (2 ml), dried by suction filtration and then in vacuo to leave [N,N'-bis-(2'-hydroxyphenyl)phenylmethylidene]-(R,R)-1,2-diamino-1,2-diphenylethane⁷¹ (300 mg, 51%) as a yellow solid. Mp 215–217 °C; [α]_D²⁰=+178 (c 0.55, CHCl₃); ν_{max} (CHCl₃) 3064 (w), 3032 (w), 2913 (w) and 1606 cm⁻¹ (s); δ_H (CDCl₃) 4.68 (1H, s, CH), 6.50–7.37 (14H, m, ArCH), 15.42 (1H, s, OH); δ_C (CDCl₃) 72.5 (CH), 117.9 (ArCH), 118.4 (ArCH), 120.4 (ArC), 127.4 (ArCH), 127.7 (ArCH), 128.0 (ArCH), 128.3 (ArCH), 128.5 (ArCH), 128.7 (ArCH), 128.9 (ArCH), 129.2 (ArCH), 132.4 (ArCH), 132.9 (ArCH), 134.3 (ArC), 140.3 (ArC), 163.2 (ArC), 175.4 (C=N); m/z (CI) 573 (MH⁺, 5), 286 (31), 198 (73), 106 (100). Found (ESI) 573.2549 (MH⁺), C₄₀H₃₃N₂O₂ requires 573.2536. The mother liquors from the crystallisation were evaporated in vacuo, and the resulting yellow residue was purified by chromatography using Et₂O/hexane (3:7) to give [N-(2'-hydroxyphenyl)phenylmethylidene]-(R,R)-1,2-diamino-1,2-diphenylethane (142 mg, 35%) as a yellow solid. Mp 61–64 °C; [α]_D²⁰=+48 (c 0.5, CHCl₃); ν_{max} (CHCl₃) 3384 (w), 3062 (m), 3030 (m), 2908 (w), 1607 (s) and 1572 cm⁻¹ (m); δ_H (CDCl₃) 1.55 (2H, brs, NH₂), 4.32 (1H, d, J=5.5 Hz, CH), 4.39 (1H, d, J=5.5 Hz, CH), 6.51–7.31 (19H, m, ArCH), 15.90 (1H, s, OH); δ_C (CDCl₃) 62.8 (CH), 72.7 (CH), 117.9 (ArCH), 118.4 (ArCH), 120.3 (ArC), 127.6 (ArCH), 127.7 (ArCH), 127.5 (ArCH), 127.9 (ArCH), 128.1 (ArCH), 128.5 (ArCH), 128.6 (ArCH), 128.8 (ArCH), 129.3 (ArCH), 132.3 (ArCH), 133.1 (ArCH), 133.9 (ArC), 141.0 (ArC), 142.6 (ArC), 163.7 (ArC), 175.4 (C=N); m/z (CI) 393 (MH⁺, 20), 287 (100), 270 (99), 167 (15), 106 (55). Found (ESI) 393.1961 (MH⁺), C₂₇H₂₅N₂O requires 393.1961.

4.1.11. Copper(II)salen complex 7b.⁵⁰ (R,R)-[N,N'-Bis-(2'-hydroxybenzylidene)]-1,2-diamino-1,2-diphenylethane, (140 mg, 0.33 mmol), CuBr₂ (74 mg, 0.33 mmol) and NaOMe (36 mg, 0.67 mmol) in methanol (4 ml) were stirred for 4 h at room temperature and then the solvent was removed in vacuo. The crude residue was purified by chromatography on LH-20 using EtOH/toluene (1:3) to give complex **7b** (109 mg, 69%) as a purple solid. Mp >270 °C; [α]_D²⁰=-310 (c 0.010, CHCl₃); ν_{max} (CHCl₃) 3028 (w), 1619 (s), and 1535 cm⁻¹ (m); m/z (FAB) 504 (M+Na⁺, 100%), 482 (MH⁺, 69), 481 (M⁺, 21). Found (ESI) 482.1053 (MH⁺), C₂₈H₂₃N₂O₂Cu requires 482.1056. Found: C, 70.0%; H, 4.4%; N, 5.5%. C₂₈H₂₂N₂O₂Cu requires: C, 69.8%; H, 4.6%; N, 5.8%.

4.1.12. Copper(II)salen complex 7c. [N,N'-Bis-(2'-hydroxyphenyl)phenylmethylidene]-(R,R)-1,2-diamino-1,2-diphenylethane⁷¹ (173 mg, 0.3 mmol), copper(II) bromide (67 mg, 0.3 mmol) and sodium methoxide (33 mg,

0.6 mmol) were dissolved in methanol (8 ml) and stirred for 3 h at room temperature. The solvent was evaporated in vacuo and the residue was purified by chromatography on LH-20 using EtOH/toluene (1:3) to give complex **7c** (186 mg, 98%), as a brown solid. Mp >270 °C; [α]_D²⁰=-60 (c 0.025, CHCl₃); ν_{max} (KBr) 3057 (w), 2926 (w), 1600 (m), 1568 (s) and 1521 cm⁻¹ (s); m/z (CI) 634 (MH⁺, 100), 573 (33), 286 (56), 106 (92). Found (ESI) 634.1680 (MH⁺), C₄₀H₃₁N₂O₂Cu requires 634.1676.

4.1.13. [N,N'-Bis-(2'-hydroxybenzylidene)]-(R,R)-3,4-diamino-2,2,5,5-tetramethylhexane. To a solution of (R,R)-3,4-diamino-2,2,5,5-tetramethylhexane⁵² (270 mg, 1.6 mmol) in ethanol (20 ml), was added salicylaldehyde (380 mg, 3.2 mmol). The resulting bright yellow solution was stirred under reflux for 5 h. Subsequently the solution was allowed to reach room temperature and then evaporated in vacuo. The residue was recrystallized from hexane-isopropanol to leave the desired product (340 mg, 56%) as yellow crystals. Mp 117–119 °C; [α]_D²⁰=+185 (c 0.083, CHCl₃); ν_{max} (CHCl₃) 3060 (w), 2963 (s), 2871 (m), 1626 (s) and 1582 cm⁻¹ (m); δ_H (CDCl₃) 0.83 (9H, s, C(CH₃)₃), 3.31 (1H, s, CH-N), 6.8–7.3 (4H, m, ArCH), 8.30 (1H, s, HC=N), 13.58 (1H, s, OH); δ_C (CDCl₃): 28.0 (CH₃), 36.3 (CMe₃), 77.7 (CHN), 118.0 (ArCH), 118.6 (ArCH), 118.9 (ArC), 131.7 (ArCH), 132.8 (ArCH), 162.3 (ArC), 165.8 (CH=N); m/z (CI) 381 (MH⁺, 100), 262 (8), 122 (12). Found (ESI) 381.2541 (MH⁺), C₂₄H₃₃N₂O₂ requires 381.2542. Found: C, 75.9%; H, 8.6%; N, 7.2%. C₂₄H₃₂N₂O₂ requires: C, 75.8%; H, 8.5%; N, 7.4%.

4.1.14. Copper(II)salen complex 7d. [N,N'-Bis-(2'-hydroxybenzylidene)]-(R,R)-3,4-diamino-2,2,5,5-tetramethylhexane (140 mg, 0.37 mmol), copper(II) bromide (82 mg, 0.37 mmol) and sodium methoxide (40 mg, 0.74 mmol) were added to methanol (2 ml) and stirred for 3 h at room temperature. The solvent was evaporated in vacuo and the residue was purified by chromatography on LH-20 using EtOH/toluene (1:3) to give complex **7d** as a black solid. Recrystallisation from hexane-dichloromethane gave complex **7d** (111 mg, 68%) as black crystals. Mp >270 °C; [α]_D²⁰=-1200 (c 0.025, CHCl₃); ν_{max} (KBr) 3021 (w), 2963 (s), 2870 (w), 1614 (s), and 1533 cm⁻¹ (s); m/z (FAB) 464 (M+Na⁺, 100), 442 (MH⁺, 66), 350 (24), 328 (52). Found (ESI) 442.1682 (MH⁺), C₂₄H₃₁N₂O₂Cu requires 442.1681. Found: C, 65.1%; H, 7.0%; N, 6.2%. C₂₄H₃₀N₂O₂Cu requires: C, 65.2%; H, 6.8%; N, 6.3%. Crystal data: C₂₄H₃₀N₂O₂Cu, M=442.04, blue needle, 0.40×0.15×0.15 mm³, monoclinic, space group P₂₁ (No. 4), a=11.2350(4), b=18.1208(5), c=11.5127(4) Å, β=108.019(2)°, V=2228.88(13) Å³, Z=4, D_c=1.317 g/cm³, F₀₀₀=932, KappaCCD, Mo K_α radiation, λ=0.71073 Å, T=120(2) K, 2θ_{max}=55.0°, 14897 reflections collected, 8895 unique (R_{int}=0.0872). Final GooF=1.012, R1=0.0527, wR2=0.1067, R indices based on 7186 reflections with I>2σ(I) (refinement on F²), 535 parameters, 1 restraint. Lp and absorption corrections applied, μ=1.001 mm⁻¹. Absolute structure parameter=-0.007(12).⁷⁰

4.1.15. (-)-(R,R)-[N,N'-Bis-(2'-hydroxybenzylidene)]-1,2-diaminocyclopropane. To a solution of (-)-trans-1,2-diaminocyclopropane dihydrochloride⁵⁸ (190 mg, 1.3 mmol) in dichloromethane (10 ml), salicylaldehyde (351 mg, 2.9 mmol) was added at room temperature. The

resulting bright yellow solution was stirred at reflux for 23 h, and then evaporated in vacuo to give a dark yellow syrup. The residue was dissolved in dichloromethane and hexane was added to precipitate impurities. The solution was filtered and evaporated in vacuo to give the desired compound^{72,73} (148 mg, 40%) as a bright yellow solid. Mp 109–111 °C; $[\alpha]_D^{20} = -563$ (*c* 1.6, CHCl₃); ν_{\max} (CHCl₃) 3057 (w), 2986 (w), 2883 (w), 1625 (s) and 1580 cm⁻¹ (m); δ_H (CDCl₃) 1.59 (2H, t *J*=6.3 Hz, CH₂), 3.32 (1H, t *J*=6.3 Hz, CH), 6.8–6.9 (2H, m, ArCH), 7.1–7.3 (2H, m, ArCH), 8.40 (1H, s, H–CN), 12.37 (1H, brs, OH); δ_C (CDCl₃) 20.4 (CH₂), 50.6 (CHN), 117.3 (ArCH), 119.3 (ArC), 119.4 (ArCH), 131.5 (ArCH), 132.5 (ArCH), 160.7 (ArC), 164.0 (CH=N); *m/z* (FAB) 281 (MH⁺, 50), 160 (55), 148 (100), 132 (72), 105 (80). Found (ESI) 281.1286 (MH⁺) C₁₇H₁₇N₂O₂ requires 281.1290.

4.1.16. (+)-[N,N'-Bis-(2'-hydroxybenzylidene)]-1,2-diaminocyclobutane. To a solution of (+)-*trans*-1,2-diaminocyclobutane⁵⁹ (112 mg, 1.3 mmol) in dichloromethane (10 ml), salicylaldehyde (317 mg, 2.6 mmol) was added at room temperature. The resulting bright yellow solution was stirred at room temperature for 19 h, and then evaporated in vacuo to give the desired product⁷³ (233 mg, 61%) as a yellow gel. $[\alpha]_D^{20} = +565$ (*c* 1.2, CHCl₃); ν_{\max} (CHCl₃) 3057 (w), 2990 (w), 2948 (w), 2875 (w), 1625 (s) and 1580 cm⁻¹ (m); δ_H (CDCl₃) 1.9–2.3 (2H, m, CH₂CH₂), 4.0–4.1 (1H, m, CH), 6.8–7.3 (4H, m, ArCH), 8.21 (1H, s, HC=N), 13.21 (1H, brs, OH); δ_C (CDCl₃) 24.4 (CH₂), 69.5 (CHN), 117.4 (ArCH), 119.0 (ArC), 119.2 (ArCH), 132.1 (ArCH), 132.9 (ArCH), 161.4 (ArC), 164.2 (CH=N); *m/z* (CI) 295 (MH⁺, 100), 191 (10), 148 (6), 122 (6). Found (ESI) 317.1243 (M+Na)⁺, C₁₈H₁₈N₂O₂Na requires 317.1261.

4.1.17. (-)-(R,R)-[N,N'-Bis-(2'-hydroxybenzylidene)]-1,2-diaminocyclopentane. To a solution of (-)-(R,R)-*trans*-1,2-diaminocyclopentane⁵⁹ (179 mg, 1.8 mmol) in dichloromethane (10 ml), salicylaldehyde (437 mg, 3.6 mmol) was added at room temperature. The resulting bright yellow solution was stirred at room temperature for 21 h, then evaporated in vacuo, and dried in vacuo with gentle heating for several hours to give the desired product (433 mg, 78%) as a yellow gel. $[\alpha]_D^{20} = -467$ (*c* 0.535, CHCl₃); ν_{\max} (neat) 3057 (w), 2959 (m), 2873 (m), 1626 (s) and 1580 cm⁻¹ (m); δ_H (CDCl₃) 1.8–2.2 (3H, m, CH₂CH₂–CH₂), 3.6–3.7 (1H, m, NCH), 6.8–7.2 (4H, m, ArCH), 8.19 (1H, s, HC=N), 13.24 (1H, s, OH); δ_C (CDCl₃) 22.3 (CH₂), 33.4 (CH₂), 76.9 (CHN), 117.2 (ArCH), 119.0 (ArC), 119.1 (ArCH), 131.8 (ArCH), 132.7 (ArCH), 161.3 (ArC), 165.1 (CH=N); *m/z* (CI) 308 (M⁺, 56), 187 (100), 147 (14), 122 (22). Found (ESI) 309.1593 (MH⁺) C₁₉H₂₁N₂O₂ requires 309.1598.

4.1.18. Copper(II) complex 9c. (-)-(R,R)-[N,N'-Bis-(2'-hydroxybenzylidene)]-1,2-diamino-cyclopentane (213 mg, 0.69 mmol), CuBr₂ (154 mg, 0.69 mmol) and NaOMe (75 mg, 1.38 mmol) were added to methanol (5 ml) and stirred for 5 h at room temperature. The solvent was evaporated in vacuo and the residue was purified by gel permeation chromatography on LH-20 using CH₂Cl₂ as eluent. Recrystallization from dichloromethane gave complex **9c** (104 mg, 41%) as small green needles. Mp >270 °C; $[\alpha]_D^{20} = -177.8$ (*c* 0.016, CHCl₃); ν_{\max} (KBr) 2933

(w), 1639 (s), 1601 (m) and 1534 cm⁻¹ (m); *m/z* (ESI) 370 (MH⁺). Found (ESI) 739.1402 (2M+H⁺), C₃₈H₃₇N₄O₄Cu₂ requires 739.1401.

4.1.19. Copper(II) complex 9d. (3*R*,4*R*)-[N,N'-Bis-(2'-hydroxybenzylidene)]-1-benzyl-3,4-diaminopyrrolidine⁶⁰ (65 mg, 0.16 mmol), CuBr₂ (36 mg, 0.16 mmol) and NaOMe (18 mg, 0.33 mmol) were added to methanol (6 ml) and stirred at room temperature for 3 h. The solvent was evaporated in vacuo and the residue was purified by gel permeation chromatography on LH-20 using EtOH/toluene (1:3) as eluent to give complex **9d** (34 mg, 45%) as a dark green solid. Mp 236–238 °C; $[\alpha]_D^{20} = -30$ (*c* 0.023, CHCl₃); ν_{\max} (KBr) 1637 (s) and 1536 cm⁻¹ (m); *m/z* (ESI) 461 (MH⁺, 55), 412 (100), 387 (31). Found (ESI) 461.1158 (MH⁺), C₂₂H₂₅N₂O₂Cu requires 461.1159.

4.1.20. N,N'-Bis-[(S)-1'-phenylethyl]-(1*R*,2*R*,4*R*,5*R*)-1,2-diamino-4,5-dimethyl-cyclohexane.⁶⁴ Bis-(cyclopentadienyl)zirconium dichloride (224 mg, 0.76 mmol) and dry diethyl ether (70 ml) were added to a three necked flask under a N₂ atmosphere. *n*-Butylmagnesium chloride (2 M in Et₂O, 9.4 ml, 18.7 mmol) was added with stirring and the mixture was allowed to react for 30 min. N,N'-Bis-[(S)-1'-phenylethyl]-(*R,R*)-4,5-diamino-1,7-octadiene (1.3 g, 3.74 mmol) dissolved in dry diethyl ether (5 ml) was then added dropwise and the resulting mixture was allowed to react for 44 h at room temperature. The reaction was quenched with saturated aqueous ammonium chloride (40 ml). The aqueous layer was extracted with diethyl ether (3×40 ml) and the combined organic layers were washed with brine (70 ml), dried over magnesium sulphate and concentrated in vacuo to give an orange oil (1.3 g) which contained a 6:1 ratio of the 4,5-(*R,R*) and 4,5-(*R,S*)-diastereomers. The diastereomers were separated by column chromatography using EtOAc/hexane (1:3) as eluent. The 4,5-(*R,R*)-diastereomer (790 mg, 60%) eluted first as a yellow oil, followed by the 4,5-(*R,S*)-diastereomer (134 mg, 10%) as a yellow oil. Spectroscopic data for both diastereomers were consistent with the literature data.⁶⁴

4.1.21. N-[(S)-1'-Phenylethyl]-(1*R*,2*R*,4*R*,5*R*)-1,2-diamino-4,5-dimethyl cyclohexane 12. A solution of N,N'-bis-[(S)-1'-phenylethyl]-(1*R*,2*R*,4*R*,5*R*)-1,2-diamino-4,5-dimethyl cyclohexane (350 mg, 1.0 mmol) in methanol (20 ml) was hydrogenated in the presence of 20% Pd(OH)₂ on carbon (150 mg) under hydrogen at three atmospheres pressure for 24 h. The reaction was filtered through Celite and concentrated in vacuo. The resulting pale yellow residue was purified by chromatography using ethyl acetate/methanol (5:1) to give compound **12** (115 mg, 47%) as a colourless oil. $[\alpha]_D^{20} = -96.7$ (*c* 0.55, CHCl₃); ν_{\max} (neat) 3301 (s), 3025 (w), 2960 (s), 2923 (s), 2872 (m) and 1584 cm⁻¹ (m); δ_H (CDCl₃) 0.79 (3H, d *J*=6.3 Hz, CH₃), 0.88 (3H, d *J*=6.3 Hz, CH₃), 1.27 (3H, d *J*=6.6 Hz, CH₃), 1.3–1.5 (4H, m, 2×CH₂), 1.75 (2H, brs, NH₂), 1.77 (1H, s, NH), 2.1–2.2 (1H, m, CH), 2.6–2.7 (1H, m, CH), 3.82 (1H, q *J*=6.6 Hz, CH), 7.1–7.3 (5H, m, ArCH); δ_C (CDCl₃) 20.4 (CH₃), 20.5 (CH₃), 25.6 (CH₃), 32.9 (CH), 33.5 (CH₂), 33.8 (CH), 37.1 (CH₂), 51.3 (CH), 55.3 (CH), 56.5 (CH), 127.1 (ArCH), 127.2 (ArCH), 128.8 (ArCH), 146.3 (ArC); *m/z* (CI) 247 (MH⁺, 100), 174 (10), 120 (43). Found (ESI) 247.2174 (MH⁺), C₁₆H₂₇N₂ requires 247.2174.

4.1.22. (1R,2R,4R,5R)-1,2-Diamino-4,5-dimethyl cyclohexane 13. A solution of compound **12** (236 mg, 0.96 mmol) in methanol (6 ml) was hydrogenated in the presence of 20% Pd(OH)₂ on carbon (150 mg) under hydrogen at three atmospheres pressure for 90 h. The reaction was filtered through Celite and concentrated in vacuo. The resulting pale yellow residue was purified by chromatography using dichloromethane/methanol (3:1) to give compound **13** (45 mg, 33%) as a colourless oil. Spectroscopic data were consistent with the literature data.⁶⁴

4.1.23. (1R,2R,4R,5R)-[N,N'-Bis-(2'-hydroxybenzylidene)]-1,2-diamino-4,5-dimethylcyclohexane 14. To a solution of (1R,2R,4R,5R)-4,5-dimethyl-cyclohexane-1,2-diamine⁶⁴ (35 mg, 0.25 mmol) in ethanol (6 ml), salicylaldehyde (61 mg, 0.50 mmol) was added at room temperature. The resulting bright yellow solution was refluxed for 19 h, then allowed to cool to room temperature and evaporated in vacuo. The residue was purified by column chromatography using ethyl acetate/hexane (1:2) as eluent to afford compound **14** (26 mg, 30%) as a yellow solid. Mp 93–95 °C; $[\alpha]_D^{20} = +245$ (c 1.3, CHCl₃); ν_{\max} (CHCl₃) 2957 (w), 2926 (m), 2875 (m), 1630 (s) and 1582 cm⁻¹ (m); δ_H (CDCl₃) 0.95 (3H, d $J=6.0$ Hz, CH₃), 1.5–1.7 (2H, m, CH₂), 1.7–1.9 (1H, m, CH), 3.4–3.5 (1H, m, CH), 6.8–6.9 (2H, m, ArCH), 7.1–7.3 (2H, m, ArCH), 8.32 (1H, s, HC=N), 13.51 (1H, brs, OH); δ_C (CDCl₃) 20.4 (CH₃), 33.8 (CH), 37.2 (CH₂), 70.0 (CHN), 117.3 (ArCH), 119.1 (ArCH), 119.2 (ArC), 131.8 (ArCH), 132.8 (ArCH), 161.5 (ArC), 164.6 (CH=N); m/z (CI) 351 (MH⁺, 100%), 247 (9), 232 (10), 122 (39). Found (ESI) 351.2063 (MH⁺), C₂₂H₂₇N₂O₂ requires 351.2067.

4.1.24. Copper(II) complex 9e. Ligand **14** (25 mg, 0.07 mmol), CuBr₂ (16 mg, 0.07 mmol) and NaOMe (8 mg, 0.142 mmol) were added to methanol (2 ml) and stirred at room temperature for 5 h. The solvent was evaporated in vacuo and the residue was purified by gel permeation chromatography on LH-20 using CH₂Cl₂/MeOH (1:1) as eluent. Recrystallization from dichloromethane/methanol gave complex **9e** (28 mg, 96%) as small purple needles. Mp >250 °C; $[\alpha]_D^{20} = -451$ (c 0.014, CHCl₃); ν_{\max} (CHCl₃) 2931 (w), 1630 (s), 1602 (m) and 1540 cm⁻¹ (m); m/z (EI) 411 (M⁺, 2), 132 (25), 91 (22), 44 (100). Found (ESI) 412.1204 (MH⁺), C₂₂H₂₅N₂O₂Cu requires 412.1207.

4.1.25. (+)-(11S,12S)-11,12-Diamino-9,10-dihydro-9,10-ethano-anthracene dihydrochloride.⁶⁵ (11S,12S)-9,10-Dihydro-9,10-ethanoanthracene-11,12-diacid chloride⁶⁵ (2.00 g, 6.04 mmol) dissolved in toluene (15 ml) was added dropwise to a cooled (ice bath) solution of sodium azide (1.37 g, 21.18 mmol) in water (15 ml). The mixture was stirred between 0 °C and room temperature for 4 h. The organic layer was separated and washed with dilute sodium hydrogen carbonate (15 ml) and water (2×10 ml), dried over anhydrous magnesium sulfate and filtered into a 50 ml round bottom flask to give a solution of the corresponding bis-azide. A reflux condenser and extra toluene (15 ml) were added to the flask, and the solution was stirred and heated to 80 °C for 1 h. Subsequently, the reaction was cooled to room temperature to give a solution of bis-isocyanate. To this

solution was added 6 N HCl (6 ml). The mixture was stirred and heated to 80 °C for 3 h and stirred at room temperature overnight. The two layers were separated and the aqueous phase was washed with toluene (2×10 ml). The aqueous phase was then concentrated in vacuo to give (+)-(11S,12S)-diamino-9,10-dihydro-9,10-ethano-anthracene dihydrochloride (970 mg, 40%) as a brownish solid. Mp >250 °C; $[\alpha]_D^{20} = +14$ (c 0.25, CHCl₃); ν_{\max} (KBr) 3406 (m), 2878 (br), 1578 (m) and 1527 cm⁻¹ (m); δ_H (CD₃OD) 3.66 (1H, brs, CH), 4.79 (1H, brs, CH), 7.3–7.4 (2H, m, ArCH), 7.5–7.6 (2H, m, ArCH); δ_C (CD₃OD) 48.0 (CH), 56.6 (CH), 126.8 (ArCH), 127.9 (ArCH), 129.5 (ArCH), 129.7 (ArCH), 138.1 (ArC), 141.3 (ArC); m/z (EI) 237 ((M–HCl–Cl)⁺, 100).

4.1.26. (11S,12S)-[N,N'-Bis-(2'-hydroxybenzylidene)]-11,12-diamino-9,10-dihydro-9,10-ethanoanthracene. To a solution of (+)-(11S,12S)-11,12-diamino-9,10-dihydro-9,10-ethanoanthracene dihydrochloride (280 mg, 0.9 mmol) in ethanol (20 ml), were added sodium methoxide (98 mg, 1.8 mmol) and salicylaldehyde (221 mg, 1.8 mmol). The resulting solution was stirred under reflux for 3 h. The solution was allowed to cool to room temperature and then evaporated in vacuo. The yellow residue was taken up in dichloromethane (20 ml) and washed with water (15 ml) and brine (15 ml). The organic layer was dried over anhydrous magnesium sulphate and evaporated to dryness to leave the desired compound (220 mg, 54%) as a yellow solid. Mp 102–104 °C; $[\alpha]_D^{20} = +250$ (c 1.4, CHCl₃); ν_{\max} (CHCl₃) 3024 (w), 2879 (w), 1628 (s) and 1579 cm⁻¹ (m); δ_H (CDCl₃) 3.45 (1H, s, CH), 4.23 (1H, s, CH), 6.7–6.8 (2H, m, ArCH), 7.1–7.3 (6H, m, ArCH), 8.21 (1H, s, HC=N), 12.41 (1H, s, OH); δ_C (CDCl₃) 52.0 (CH), 77.5 (CH), 117.5 (ArCH), 118.9 (ArC), 119.2 (ArCH), 124.6 (ArCH), 126.1 (ArCH), 127.1 (ArCH), 127.2 (ArCH), 131.9 (ArCH), 133.0 (ArCH), 140.2 (ArC), 140.7 (ArC), 161.2 (ArC), 164.9 (CH=N); m/z (ESI) 445 (MH⁺, 100). Found (ESI) 445.1907 (MH⁺), C₃₀H₂₅N₂O₂ requires 445.1911.

Acknowledgements

The authors thank the EPSRC mass spectrometry service at the University of Wales, Swansea for recording low and high resolution mass spectra.

References and notes

- Nelson, A. *Angew. Chem., Int. Ed.* **1999**, *38*, 1583.
- O'Donnell, M. J.; Drew, M. D.; Cooper, J. T.; Delgado, F.; Zhou, C. *J. Am. Chem. Soc.* **2002**, *124*, 9348. O'Donnell, M. J.; Delgado, F. *Tetrahedron* **2001**, *57*, 6641. O'Donnell, M. J.; Delgado, F.; Pottorf, R. S. *Tetrahedron* **1999**, *55*, 6347. O'Donnell, M. J.; Delgado, F.; Hostettler, C.; Schwesinger, R. *Tetrahedron Lett.* **1998**, *39*, 8775. O'Donnell, M. J.; Wu, Sh.; Hauffman, J. C. *Tetrahedron* **1994**, *50*, 4507. O'Donnell, M. J.; Bennet, W.; Wu, Sh. *J. Am. Chem. Soc.* **1989**, *111*, 2353.
- Lygo, B.; Andrews, B. I. *Tetrahedron Lett.* **2003**, *44*, 4499. Lygo, B.; Andrews, B. I.; Crosby, J.; Peterson, J. A. *Tetrahedron Lett.* **2002**, *43*, 8015. Lygo, B.; Humphreys, L. D. *Tetrahedron Lett.* **2002**, *43*, 6677. Lygo, B.; Crosby, J.;

- Peterson, J. A. *Tetrahedron* **2001**, *57*, 6447. Lygo, B.; Crosby, J.; Lowdon, T. R.; Peterson, J. A.; Wainwright, P. G. *Tetrahedron* **2001**, *57*, 2403. Lygo, B.; Crosby, J.; Lowdon, T. R.; Wainwright, P. G. *Tetrahedron* **2001**, *57*, 2391. Lygo, B.; Crosby, J.; Peterson, J. A. *Tetrahedron Lett.* **1999**, *40*, 1385. Lygo, B. *Tetrahedron Lett.* **1999**, *40*, 1389. Lygo, B.; Wainwright, P. G. *Tetrahedron Lett.* **1997**, *38*, 8595.
- Corey, E. J.; Noe, M. C.; Xu, F. *Tetrahedron Lett.* **1998**, *39*, 5347. Corey, E. J.; Xu, F.; Noe, M. C. *J. Am. Chem. Soc.* **1997**, *119*, 12414.
 - For other work on the use of monomeric N-alkylated cinchona alkaloid derivatives as asymmetric phase transfer catalysts see: Castle, S. L.; Srikanth, G. S. C. *Org. Lett.* **2003**, *5*, 3611. Jew, S.-s.; Jeong, B.-S.; Lee, J.-H.; Yoo, M.-S.; Lee, Y.-J.; Park, B.-s.; Kim, M. G.; Park, H.-g. *J. Org. Chem.* **2003**, *68*, 4514. Mazón, P.; Chinchilla, R.; Nájera, C.; Guillena, G.; Kreiter, R.; Gebbink, R. J. M. K.; Koten, G. van *Tetrahedron: Asymmetry* **2002**, *13*, 2181. Jew, S.-s.; Yoo, M.-S.; Jeong, B.-S.; Park, J. I.; Park, H.-g. *Org. Lett.* **2002**, *4*, 4245. Dehmlow, E. V.; Düttmann, S.; Neumann, B.; Stammler, H.-G. *Eur. J. Org. Chem.* **2002**, 2087.
 - For an application to alanine derived substrates see: Lygo, B.; Crosby, J.; Peterson, J. A. *Tetrahedron Lett.* **1999**, *40*, 8671.
 - For the alkylation of a non-amino acid derived enolate see: Corey, E. J.; Bo, Y.; Busch-Petersen, J. *J. Am. Chem. Soc.* **1998**, *120*, 13000.
 - O'Donnell, M. J.; Delgado, F.; Domínguez, E.; Blas, J. de; Scott, W. L. *Tetrahedron: Asymmetry* **2001**, *12*, 821. Zhang, F. Y.; Corey, E. J. *Org. Lett.* **2000**, *2*, 4257. Zhang, F. Y.; Corey, E. J. *Org. Lett.* **2000**, *2*, 1097.
 - Thierry, B.; Perrard, T.; Audouard, C.; Plaquevent, J.-C.; Cahard, D. *Synthesis* **2001**, 1742.
 - Horikawa, M.; Busch-Petersen, J.; Corey, E. J. *Tetrahedron Lett.* **1999**, *40*, 3843. Corey, E. J.; Zhang, F. Y. *Angew. Chem., Int. Ed.* **1999**, *38*, 1931.
 - Lygo, B.; Wainwright, P. G. *Tetrahedron* **1999**, *55*, 6289. Corey, E. J.; Zhang, F. Y. *Org. Lett.* **1999**, *1*, 1287.
 - Nakoji, M.; Kanayama, T.; Okino, T.; Takemoto, Y. *J. Org. Chem.* **2002**, *67*, 7418. Nakoji, M.; Kanayama, T.; Okino, T.; Takemoto, Y. *Org. Lett.* **2001**, *3*, 3329. Chen, G.; Deng, Y.; Gong, L.; Mi, A.; Cui, X.; Jiang, Y.; Choi, M. C. K.; Chan, A. S. C. *Tetrahedron: Asymmetry* **2001**, *12*, 1567.
 - Chinchilla, R.; Mazón, P.; Nájera, C. *Tetrahedron: Asymmetry* **2000**, *11*, 3277. Thierry, B.; Plaquevent, J.-C.; Cahard, D. *Tetrahedron: Asymmetry* **2003**, *14*, 1671.
 - Kim, S.; Lee, J.; Lee, T.; Park, H.-g.; Kim, D. *Org. Lett.* **2003**, *5*, 2703. Park, H.-g.; Jeong, B.-S.; Yoo, M.-S.; Lee, J.-H.; Park, B.-s.; Kim, M. G.; Jew, S.-s. *Tetrahedron Lett.* **2003**, *44*, 3497. Chinchilla, R.; Mazón, P.; Nájera, C. *Tetrahedron: Asymmetry* **2002**, *13*, 927. Park, H.-g.; Jeong, B.-s.; Yoo, M.-s.; Lee, J.-H.; Park, M.-k.; Lee, Y.-J.; Kim, M.-J.; Jew, S.-s. *Angew. Chem., Int. Ed.* **2002**, *41*, 3036. Park, H.-g.; Jeong, B.-s.; Yoo, M.-s.; Park, M.-k.; Huh, H.; Jew, S.-s. *Tetrahedron Lett.* **2001**, *42*, 4645.
 - Okino, T.; Takemoto, Y. *Org. Lett.* **2001**, *3*, 1515.
 - Ooi, T.; Kubota, Y.; Maruoka, K. *Synlett* **2003**, 1931. Hashimoto, T.; Tanaka, Y.; Maruoka, K. *Tetrahedron: Asymmetry* **2003**, *14*, 1599. Hashimoto, T.; Maruoka, K. *Tetrahedron Lett.* **2003**, *44*, 3313. Ooi, T.; Tayama, E.; Maruoka, K. *Angew. Chem., Int. Ed.* **2003**, *42*, 579. Ooi, T.; Kameda, M.; Maruoka, K. *J. Am. Chem. Soc.* **2003**, *125*, 5139. Ooi, T.; Uematsu, Y.; Maruoka, K. *Adv. Synth. Catal.* **2002**, *344*, 288. Ooi, T.; Doda, K.; Maruoka, K. *Org. Lett.* **2001**, *3*, 1273. Ooi, T.; Takeuchi, M.; Maruoka, K. *Synthesis* **2001**, 1716. Ooi, T.; Takeuchi, M.; Ohara, D.; Maruoka, K. *Synlett* **2001**, 1185. Ooi, T.; Takeuchi, M.; Kameda, M.; Maruoka, K. *J. Am. Chem. Soc.* **2000**, *122*, 5228. Ooi, T.; Tayama, E.; Doda, K.; Takeuchi, M.; Maruoka, K. *Synlett* **2000**, 1500. Ooi, T.; Kameda, M.; Tannai, H.; Maruoka, K. *Tetrahedron Lett.* **2000**, *41*, 8339. Ooi, T.; Kameda, M.; Maruoka, K. *J. Am. Chem. Soc.* **1999**, *121*, 6519.
 - Ooi, T.; Miki, T.; Taniguchi, M.; Shiraiishi, M.; Takeuchi, M.; Maruoka, K. *Angew. Chem., Int. Ed.* **2003**, *42*, 3796.
 - Ooi, T.; Doda, K.; Maruoka, K. *J. Am. Chem. Soc.* **2003**, *125*, 2054. Ooi, T.; Taniguchi, M.; Kameda, M.; Maruoka, K. *Angew. Chem., Int. Ed.* **2002**, *41*, 4542.
 - Lygo, B.; Allbutt, B.; James, S. R. *Tetrahedron Lett.* **2003**, *44*, 5629. Mase, N.; Ohno, T.; Hoshikawa, N.; Ohishi, K.; Morimoto, H.; Yoda, H.; Takabe, K. *Tetrahedron Lett.* **2003**, *44*, 4073. Shibuguchi, T.; Fukuta, Y.; Akachi, Y.; Sekine, A.; Ohshima, T.; Shibasaki, M. *Tetrahedron Lett.* **2002**, *43*, 9539. Arai, S.; Tsuji, R.; Nishida, A. *Tetrahedron Lett.* **2002**, *43*, 9535.
 - Kita, T.; Georgieva, A.; Hashimoto, Y.; Nakata, T.; Nagasawa, K. *Angew. Chem., Int. Ed.* **2002**, *41*, 2832.
 - Akiyama, T.; Hara, M.; Fuchibe, K.; Sakamoto, S.; Yamaguchi, K. *Chem. Commun.* **2003**, 1734.
 - Belokon', Y. N.; Kochetkov, K. A.; Churkina, T. D.; Ikonnikov, N. S.; Chesnokov, A. A.; Larionov, O. V.; Parmer, V. S.; Kumar, R.; Kagan, H. B. *Tetrahedron: Asymmetry* **1998**, *9*, 851. Belokon', Y. N.; Kochetkov, K. A.; Churkina, T. D.; Ikonnikov, N. S.; Chesnokov, A. A.; Larionov, O. V.; Kagan, H. B. *Russ. Chem. Bull.* **1999**, *48*, 917. Belokon', Y. N.; Kochetkov, K. A.; Churkina, T. D.; Ikonnikov, N. S.; Chesnokov, A. A.; Larionov, O. V.; Singh, I.; Parmer, V. S.; Vyskocil, S.; Kagan, H. B. *J. Org. Chem.* **2000**, *65*, 7041.
 - Belokon', Y. N.; Kochetkov, K. A.; Churkina, T. D.; Ikonnikov, N. S.; Vyskocil, S.; Kagan, H. B. *Tetrahedron: Asymmetry* **1999**, *10*, 1723. Belokon', Y. N.; Kochetkov, K. A.; Churkina, T. D.; Ikonnikov, N. S.; Larionov, O. V.; Harutyunyan, S. R.; Vyskocil, S.; North, M.; Kagan, H. B. *Angew. Chem., Int. Ed.* **2001**, *40*, 1948.
 - Casas, J.; Nájera, C.; Sansano, J. M.; González, J.; Saá, J. M.; Vega, M. *Tetrahedron: Asymmetry* **2001**, *12*, 699.
 - Belokon', Y. N.; North, M.; Kublitski, V. S.; Ikonnikov, N. S.; Krasik, P. E.; Maleev, V. I. *Tetrahedron Lett.* **1999**, *40*, 6105. Belokon', Y. N.; North, M.; Churkina, T. D.; Ikonnikov, N. S.; Maleev, V. I. *Tetrahedron* **2001**, *57*, 2491.
 - Belokon', Y. N.; Davies, R. G.; Fuentes, J. A.; North, M.; Parsons, T. *Tetrahedron Lett.* **2001**, *42*, 8093.
 - Belokon', Y. N.; Davies, R. G.; North, M. *Tetrahedron Lett.* **2000**, *41*, 7245.
 - Belokon', Y. N.; Bhave, D.; D'Addario, D.; Groaz, E.; Maleev, V.; North, M.; Pertosyan, A. *Tetrahedron Lett.* **2003**, *44*, 2045. Belokon', Y. N.; Bhave, D.; D'Addario, D.; Groaz, E.; North, M.; Tagliuzucca, V. *Tetrahedron* **2004**, *60*, 1849.
 - For zinc(II)salen complexes see: Sacconi, L.; Ciampolini, M.; Speroni, G. P. *J. Am. Chem. Soc.* **1965**, *87*, 3102. Cozzi, P. G. *Angew. Chem., Int. Ed.* **2003**, *42*, 2895. DiMauro, E. F.; Kozlowski, M. C. *Org. Lett.* **2001**, *3*, 3053. Wong, W.-K.; Liang, H.; Wong, W.-Y.; Cai, Z.; Li, K.-F.; Cheah, K.-W. *New J. Chem.* **2002**, *26*, 275. Hall, D.; Moore, F. H. *J. Chem. Soc. A* **1966**, 1822. Morris, G. A.; Zhou, H.; Stern, C. L.; Nguyen, S. T. *Inorg. Chem.* **2001**, *40*, 3222.
 - Ohi, A. R.; Hodgson, D. J. *Inorg. Chim. Acta* **1990**, *170*, 65. Hashihayata, T.; Punniyamurthy, T.; Irie, R.; Katsuki, T.;

- Akita, M.; Moro-oka, Y. *Tetrahedron* **1999**, *55*, 14599. Zhang, W.; Jacobsen, E. N. *J. Org. Chem.* **1991**, *56*, 2296.
31. Kessel, S. L.; Emberson, R. M.; Debrunner, P. G.; Hendrickson, D. N. *Inorg. Chem.* **1980**, *19*, 1170.
32. Hamaker, C. G.; Mirafzal, G. A.; Woo, L. K. *Organometallics* **2001**, *20*, 5171.
33. Belokon, Y. N.; Fuentes, J.; North, M. Unpublished results.
34. Aoi, H.; Ishimori, M.; Yoshikawa, S.; Tsuruta, T. *J. Organomet. Chem.* **1975**, *85*, 241.
35. X-ray data has been deposited with the Cambridge crystal structure database; deposition number CCDC 222155.
36. Bernard, K.; Leppard, S.; Robert, A.; Commenges, G.; Dahan, F.; Meunier, B. *Inorg. Chem.* **1996**, *35*, 387.
37. For the X-ray structure of the diastereomeric, achiral complex derived from *meso*-cyclohexanediamine see: Bresciani, N.; Calligaris, M.; Nardin, G.; Randaccio, L. *J. Chem. Soc., Dalton Trans.* **1974**, 1606.
38. For the X-ray structure of nickel(II)salen complex **1a** see: Castro, B. de; Freire, C.; Duarte, M. T.; Minas-da-Piedade, M. F.; Santos, I. C. *Acta Crystallogr., Sect. C* **2001**, *57*, 370. Woitczak, A.; Szlyk, E.; Jaskolski, M.; Larsen, E. *Acta Chem. Scand.* **1997**, *51*, 274.
39. Bunn, A. G.; Ni, Y.; Wei, M.; Wayland, B. B. *Inorg. Chem.* **2000**, *39*, 5576.
40. Miller, K. J.; Baag, J. H.; Abu-Omar, M. M. *Inorg. Chem.* **1999**, *38*, 4510.
41. Cesarotti, E.; Pasini, A.; Ugo, R. *J. Chem. Soc., Dalton Trans.* **1981**, 2147.
42. For the X-ray structure of an achiral platinum(II)salen complex see: Sawodny, W.; Thewalt, U.; Potthoff, E.; Ohl, R. *Acta Crystallogr., Sect. C* **1999**, *55*, 2060.
43. Fukuda, T.; Katsuki, T. *Tetrahedron* **1997**, *53*, 7201. Lee, S.-W.; Chang, S.; Kossakovski, D.; Cox, H.; Beauchamp, J. L. *J. Am. Chem. Soc.* **1999**, *121*, 10152. Blaauw, R.; Kingma, I. E.; Laan, J. H.; Baan, J. L. van der; Balt, S.; Bolster, M. W. G. de; Klumpp, G. W.; Smeets, W. J. J.; Spek, A. L. *J. Chem. Soc., Perkin Trans. 1* **2000**, 1199. Ikeno, T.; Iwakura, I.; Yamada, T. *J. Am. Chem. Soc.* **2002**, *124*, 15152. Mita, T.; Ohtsuki, N.; Ikeno, T.; Yamada, T. *Org. Lett.* **2002**, *4*, 2457. Floriani, C.; Puppis, M.; Calderazzo, F. *J. Organomet. Chem.* **1968**, *12*, 209. Breinbauer, R.; Jacobsen, E. N. *Angew. Chem., Int. Ed.* **2000**, *39*, 3604.
44. Janssen, K. B. M.; Laquiere, I.; Dehaen, W.; Parton, R. F.; Vankelecom, I. F. J.; Jacobs, P. A. *Tetrahedron: Asymmetry* **1997**, *8*, 3481.
45. Ready, J. M.; Jacobsen, E. N. *J. Am. Chem. Soc.* **1999**, *121*, 6086. Blaauw, R.; Baan, J. L. van der; Balt, S.; Bolster, M. W. G. de; Klumpp, G. W.; Kooijman, H.; Spek, A. L. *Chem. Commun.* **1998**, 1295. Chapman, J. J.; Day, C. S.; Welker, M. E. *Organometallics* **2000**, *19*, 1615. Blaauw, R.; Baan, J. L. van der; Balt, S.; Bolster, M. W. G. de; Klumpp, G. W.; Kooijman, H.; Spek, A. L. *Inorg. Chim. Acta* **2002**, *336*, 29. Wang, B.-C.; Huie, B. T.; Schaefer, W. P. *Acta Crystallogr.* **1979**, *35B*, 1232. Kingma, I. E.; Wiersma, M.; Baan, J. L. van der; Balt, S.; Bickelhaupt, F.; Bolster, M. W. G. de; Klumpp, G. W.; Spek, A. L. *J. Chem. Soc., Chem. Commun.* **1993**, 832. Arkel, B. van; Baan, J. L. van der; Balt, S.; Bickelhaupt, F.; Bolster, M. W. G. de; Kingma, I. E.; Klumpp, G. W.; Moos, J. W. E.; Spek, A. L. *J. Chem. Soc., Chem. Commun.* **1991**, 225. Arkel, B. van; Baan, J. L. van der; Balt, S.; Bickelhaupt, F.; Bolster, M. W. G. de; Kingma, I. E.; Klumpp, G. W.; Moos, J. W. E.; Spek, A. L. *J. Chem. Soc., Perkin Trans. 1* **1993**, 3023. Calligaris, M.; Minichelli, D.; Nardin, G.; Randaccio, L. *J. Chem. Soc. A* **1971**, 2721. Huilan, C.; Deyan, H.; Tian, L.; Hong, Y.; Wenxia, T.; Chen, J.; Zheng, P.; Chen, C. *Inorg. Chem.* **1996**, *35*, 1502.
46. For an X-ray structure of a cobalt(III) salen complex with two additional DMF molecules coordinated see: Gollas, B.; Speiser, B.; Stahl, H.; Sieglens, J.; Strahle, J. Z. *Naturforsch. Sect. B* **1996**, *51*, 388.
47. Gill, G. B.; Pattenden, G.; Reynolds, S. J. *J. Chem. Soc., Perkin Trans. 1* **1994**, 369.
48. Fachinetti, G.; Floriani, C.; Zanazzi, P. F.; Zanari, A. R. *Inorg. Chem.* **1979**, *18*, 3469. Gambarotta, S.; Arena, F.; Floriani, C.; Zanazzi, P. F. *J. Am. Chem. Soc.* **1982**, *104*, 5082. Arena, F.; Floriani, C.; Zanazzi, P. F. *J. Chem. Soc., Chem. Commun.* **1987**, 183.
49. For the synthesis of the salen ligand required for the synthesis of catalyst **7b** and an aryl substituted analogue of the ligand required for the synthesis of catalyst **9f** see: Wang, B.; Feng, X.; Huang, Y.; Liu, H.; Cui, X.; Jiang, Y. *J. Org. Chem.* **2002**, *67*, 2175.
50. For previous syntheses and applications of this ligand see: Müller, P.; Nury, P. *Helv. Chim. Acta* **2001**, *84*, 662. Zolezzi, S.; Decinti, A.; Spodine, E. *Polyhedron* **1999**, *18*, 897. Zolezzi, S.; Spodine, E.; Decinti, A. *Polyhedron* **2002**, *21*, 55. Jiang, Y.; Gong, L.; Feng, X.; Hu, W.; Pan, W.; Li, Z.; Mi, A. *Tetrahedron* **1997**, *53*, 14327.
51. Bambridge, K.; Begley, M. J.; Simpkins, N. S. *Tetrahedron Lett.* **1994**, *35*, 3391.
52. Roland, S.; Mangeney, P.; Alexakis, A. *Synthesis* **1999**, 228.
53. Calligaris, M.; Nardin, G.; Randaccio, L. *J. Chem. Soc., Dalton Trans.* **1973**, 419.
54. Hoshina, G.; Tsuchimoto, M.; Ohba, S. *Bull. Chem. Soc. Jpn* **2000**, *73*, 369.
55. Averseng, F.; Lacroix, P. G.; Malfant, I.; Dahan, F.; Nakatani, K. *J. Mater. Chem.* **2000**, *10*, 1013.
56. Hirotsu, M.; Kojima, M.; Nakajima, K.; Kashino, S.; Yoshikawa, Y. *Chem. Lett.* **1994**, 2183. Hirotsu, M.; Kojima, M.; Nakajima, K.; Kashino, S.; Yoshikawa, Y. *Bull. Chem. Soc. Jpn* **1996**, *69*, 2549.
57. X-ray data has been deposited with the Cambridge crystal structure database; deposition number CCDC 222156.
58. For the synthesis of 1,2-diaminocyclopropane see: Payne, G. B. *J. Org. Chem.* **1967**, *32*, 3351. Doering, W. Von E.; Sachdev, K. *J. Am. Chem. Soc.* **1974**, *96*, 1168. Witiak, D. T.; Lee, H. J.; Hart, R. W.; Gibson, R. E. *J. Med. Chem.* **1977**, *20*, 630. Villa, L.; Villa, A. M.; Pallavicini, M.; Romeo, S.; Valoti, E. *Farmaco* **1995**, *50*, 643.
59. For the synthesis of (*R,R*)-1,2-diaminocyclobutane and (*R,R*)-1,2-diaminopentane see: Daly, A. M.; Gilheany, D. G. *Tetrahedron: Asymmetry* **2003**, *14*, 127. Heintz, V. J.; Keiderling, T. A. *J. Am. Chem. Soc.* **1981**, *103*, 2395.
60. Reddy, D. R.; Thornton, E. R. *J. Chem. Soc., Chem. Commun.* **1992**, 172. Skarzewski, J.; Gupta, A. *Tetrahedron: Asymmetry* **1997**, *8*, 1861.
61. Nagel, U.; Kinzel, E.; Andrade, J.; Prescher, G. *Chem. Ber.* **1986**, *119*, 3326.
62. Gouin, S. G.; Gustin, J. F.; Joly, K.; Loussouarn, A.; Reliquet, A.; Meslin, J. C.; Deniaud, D. *Tetrahedron* **2002**, *58*, 1131.
63. Alvaro, G.; Grepioni, F.; Savoia, D. *J. Org. Chem.* **1997**, *62*, 4180. Neumann, W. L.; Rogic, M. M.; Dunn, T. J. *Tetrahedron Lett.* **1991**, *32*, 5865. Martelli, G.; Morri, S.; Savoia, D. *Tetrahedron* **2000**, *56*, 8367. Grilli, S.; Martelli, G.; Savoia, D. *Eur. J. Org. Chem.* **2001**, 2917.
64. Grepioni, F.; Grilli, S.; Martelli, G.; Savoia, D. *J. Org. Chem.*

- 1999, 64, 3679. Grilli, S.; Martelli, G.; Savoia, D.; Zazzetta, C. *Synthesis* **2003**, 1083.
65. Bachmann, W. E.; Scotter, L. B. *J. Am. Chem. Soc.* **1948**, 70, 1458. Briene, M. J.; Jacques, J. *Bull. Soc. Chim. Fr.* **1973**, 190. Hagishita, S.; Kuriyama, K. *Tetrahedron*. **1972**, 1435, Trost. Vranken, B. M.; Van, D. L.; Bingel, C. *J. Am. Chem. Soc.* **1992**, 114, 9327.
66. Hooft, R. *Collect*; Nonius B.V.: Delft, 1998.
67. Otwinowski, Z.; Minor, W. *Methods in enzymology*; Carter, C. W., Sweet, R. M., Eds.; Academic: New York, 1997; Vol. 276, p 307.
68. Sheldrick, G. M. *SHELXL-97*; University of Göttingen, 1997.
69. Barbour, L. J. *XSeed, A Program of the Manipulation and Display of Crystallographic Models*; University of Missouri—Columbia, 1999.
70. Flack, H. D. *Acta Crystallogr., Sect. A.* **1983**, 39, 876.
71. Hirotsu, M.; Nakajima, K.; Kojima, M.; Yoshikawa, Y. *Inorg. Chem.* **1995**, 34, 6173.
72. For references to the racemic cyclopropyl ligand see: Quast, H.; Stawitz, J. *Tetrahedron Lett.* **1977**, 31, 2709. Quast, H.; Seidenspinner, H.-M.; Stawitz, J. *Liebigs Ann. Chem.* **1983**, 1207.
73. For references to the racemic cyclopropyl and cyclobutyl ligands see: Staab, H. A.; Vögtle, F. *Chem. Ber.* **1965**, 98, 1359. Staab, V. *Chem. Ber.* **1965**, 98, 2691.

Preparation of aminals in water

Václav Jurčík and René Wilhelm*

Institut für Organische Chemie der Technischen Universität Clausthal, 38678 Clausthal-Zellerfeld, Germany

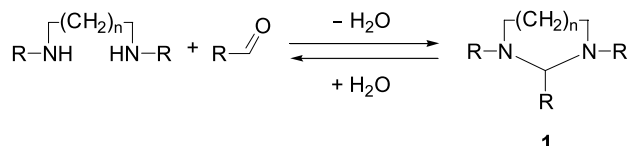
Received 5 December 2003; revised 9 February 2004; accepted 11 February 2004

Abstract—Aminals, which are used as protecting groups in syntheses and are part of many biologically active compounds, are normally prepared from aldehydes and diamines under conditions that remove water in order to shift the equilibrium to the side of the amina. Here we report for the first time that aminals can be prepared and isolated in pure water without a catalyst in high yield and purity.
© 2004 Elsevier Ltd. All rights reserved.

1. Introduction

Aminals,¹ which are also known under the term *N,N*-acetals, are the aminated equivalents of acetals. The aminals can be either open chained or cyclic like amina analogue **1**. Cyclic aminals can be used in synthesis as protecting groups for aldehydes.^{2–6} In addition, five-membered ring aminals (imidazolidines) are important parts of biologically active compounds, for example, folic acid derivatives.^{7–9} Six-membered ring aminals (hexahydro-pyrimidines) are also often incorporated in biologically active molecules.^{10,11}

Classical methods of preparing aminals involve the use of various drying agents, for example, potassium carbonate,¹² calcium sulfate,¹³ boric anhydride¹⁴ or removal of water by azeotropic distillation with benzene¹⁵ in order to shift the equilibrium to the product side as shown in Scheme 1. If the aminals are crystallizing easily, reactions are performed in methanol or ethanol in the presence of a small amount of acetic acid.² If formaldehyde is used in the reaction, often an ethanol–water mixture is used as the solvent.¹⁶



Scheme 1.

We noticed from the literature that imines can be conveniently prepared in pure water without the presence of a catalyst from corresponding amines and aldehydes.¹⁷

Since we were interested in preparing imidazolidines in a fast and easy way, we wanted therefore to investigate, if it would be also possible to prepare aminals in a similar way. So far aminals have never been synthesized and isolated in pure water. There is only one example known in the literature where the equilibrium constants for the formation of a few imidazolidines were measured in water via UV absorbance, however, no products were isolated.¹⁸ In addition an amina was prepared in a biphasic system of water and dichloromethane from diamines and glyoxal.¹⁹

The preparation of aminals in water is desirable, since reaction procedures, where water is used as a solvent instead of an organic solvent have become in recent years more and more important due to environmental consideration.^{20,21}

2. Results and discussion

In order to follow the procedure of Simion et al. for the preparation of imines in water,¹⁷ *N,N*-dibenzyl-ethane-1,2-diamine (**2**) was strongly stirred in water and benzaldehyde was added to the emulsion. During 3 h of stirring a white precipitate formed which was filtered off and washed with water. After drying under vacuum the desired product **3a** was obtained in 91% yield (Table 1, entry 1) in high purity according to NMR spectral data and CHN-analysis. In comparison, when **2** was refluxed with benzaldehyde and a catalytic amount of *p*-toluene sulfonic acid in benzene on a Dean–Stark apparatus, the reaction took 16 h and a flash column chromatography with deactivated silica gel had to be performed to get **3a** in proper purity. When the reaction was carried out in abs. ethanol the product had to be purified again via flash column chromatography or via recrystallisation, which gave the product in only 62% yield. Finally, benzaldehyde was added to neat diamine **2** and a strong exothermic reaction was observed, which was completed

Keywords: Aminals; Water; Solvent; Imidazolidines; Protecting group.

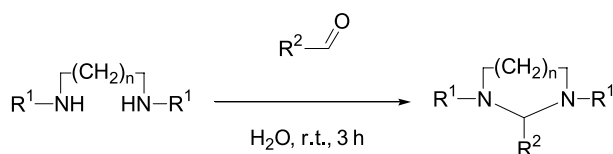
* Corresponding author. Tel.: +49-5323-723886; fax: +49-5323-722834; e-mail address: rene.wilhelm@tu-clausthal.de

Table 1. Preparation of amins

Entry	Diamine	Aldehyde	Aminal	Yield (%)
1	2 R ¹ =Bn, n=2	Benzaldehyde	3a R ² =C ₆ H ₅	91
2	2	2-Chlorobenzaldehyde	3b R ² =1-(2-Cl-C ₆ H ₄)	96
3	2	Pyridine-2-carbaldehyde	3c R ² =2-(C ₅ H ₄ N)	99
4	2	Thiophene-2-carbaldehyde	3d R ² =2-(C ₄ SH ₃ S)	99
5	2	2-Methoxybenzaldehyde	3e R ² =1-(2-MeO-C ₆ H ₄)	94
6 ^a	2	2,4-Dichlorobenzaldehyde	3f R ² =1-(2,4-Cl ₂ -C ₆ H ₃)	96
7	2	Pentafluorobenzaldehyde	3g R ² =1-(C ₆ F ₅)	92
8 ^a	2	4-Chlorobenzaldehyde	3h R ² =1-(4-Cl-C ₆ H ₄)	91
9 ^a	2	2,6-Dichlorobenzaldehyde	3i R ² =1-(2,6-Cl ₂ -C ₆ H ₃)	88
10 ^b	2	Propionaldehyde	3j R ² =CH ₂ CH ₃	85
11	4 R ¹ =Bn, n=3	Benzaldehyde	5a R ² =C ₆ H ₅	96
12	4	2-Chlorobenzaldehyde	5b R ² =1-(2-Cl-C ₆ H ₄)	88
13	4	Pyridine-2-carbaldehyde	5c R ² =2-(C ₅ H ₄ N)	93
14	6 R ¹ =Bn, n=4	2-Chlorobenzaldehyde	7a R ² =1-(2-Cl-C ₆ H ₄)	99
15 ^b	8 R ¹ =(<i>R</i>)-MeCHPh	2-Chlorobenzaldehyde	9a R ² =1-(2-Cl-C ₆ H ₄)	81
16 ^{a,b}	8	4-Chlorobenzaldehyde	9b R ² =1-(4-Cl-C ₆ H ₄)	80
17 ^a	10 R ¹ =Ph, n=2	2-Chlorobenzaldehyde	11a R ² =1-(2-Cl-C ₆ H ₄)	98
18 ^a	10	Acetaldehyde	11b R ² =CH ₃	42
19	12 R ¹ =Me, n=2	Benzaldehyde	13 R ² =C ₆ H ₅	67
20 ^c	14 Piperidine	2-Chlorobenzaldehyde	15	99
21	16 (±)- <i>N,N'</i> -Dibenzyl-1,2-cyclohexanediamine	Pyridine-2-carbaldehyde	17	95

^a Reaction temperature 80 °C.^b Reaction time 16 h.^c 2 equiv. piperidine.

after 15 min. However, due to the high temperature during the reaction many impurities next to **3a** were detected in the NMR spectra and again a flash column chromatography had to be carried out which gave the aminal **3a** in 60% yield. Given those results we concluded that for the preparation of aminal analogues of **3a** a reaction of diamines and benzaldehydes in water would be the most convenient and efficient procedure. The results are summarized in **Table 1** **Scheme 2**.

**Scheme 2.**

First diamine **2** was reacted with different benzaldehydes to give the corresponding imidazolidines (entries 1–9). In all cases the obtained yields were very high (between 91 and 99%) and the products were pure according to NMR spectra and CHN-analysis. Electron deficient (entries 1–3, 6–9) and electron rich (entries 4, 5) benzaldehydes gave similar results. Even the hindered 2,6-dichloro-benzaldehyde gave the corresponding aminal **3i** in a good yield of 88% (entry 9). In cases where the melting points of the benzaldehydes were higher than room temperature, the mixtures were heated to 80 °C in order to melt the aldehydes and ensure the

formation of an emulsion containing both reactants (entries 6, 8, 9, 16). When the benzaldehydes were not melted, yields were significantly lower.

In case of the polyfluorinated aminal **3g** (entry 7) the reaction was carried out in deoxygenated water under a nitrogen atmosphere. This was necessary to prevent the rapid oxidation of the aldehyde to the corresponding carboxylic acid before the formation of the desired aminal **3g** was finished. The product **3g** was isolated in a good yield of 92%. Since **3g** was a liquid, it was extracted from the reaction mixture with chloroform. To compare again methods, an attempt to prepare **3g** in benzene with a Dean–Stark apparatus under reflux was carried out, which gave no product at all. The same result was observed when abs. ethanol was chosen as a solvent for the reaction. When pentafluorobenzaldehyde was added to neat diamine **2** a strong exothermic reaction was observed, however no product was isolated, which may be due to the possible instability of either pentafluorobenzaldehyde or aminal **3g** at higher temperatures.

Aliphatic aldehydes can be applied in the described procedure also. Propionaldehyde gave with diamine **2** the expected aminal **3j** in 85% yield (entry 10). However, due to the lower reactivity of aliphatic aldehydes the reaction time had to be prolonged to 16 h. The scope of the reaction was extended with *N,N'*-dibenzyl-propane-1,3-diamine (**4**)^{17,22} and *N,N'*-dibenzyl-butane-1,3-diamine (**6**)²² which gave

with aldehydes cyclic amins with a six- or a seven-membered ring in good yields between 88 and 99% (entries 11–14).

Furthermore *N,N'*-bis-((*R*)1-phenyl-ethyl)-ethane-1,2-diamine (**8**)²³ was used in the reaction with 2- and 4-chlorobenzaldehydes in order to have a more hindered system next to the nitrogen atoms. The reactions were complete after 16 h and the liquid products were isolated via extraction with chloroform giving the amins **9a** and **9b** in 81 and 80% yield, respectively (entries 14, 15).

In addition *N,N'*-diphenyl-ethane-1,2-diamine (**10**) was forming with 2-chlorobenzaldehyde and acetaldehyde the amins **11a** and **11b** in 98 and 42% yield, respectively (entries 17, 18). Since the melting point of the diamine **10** is 70 °C the reaction mixture was heated to 80 °C to melt the diamine. Aminal **13** was obtained in 67% yield from *N,N'*-dimethyl-ethane-1,2-diamine (**12**) and benzaldehyde (entry 19). Open amins are also accessible as shown in entry 20, where 2 equiv. of piperidine (**14**) gave with 2-chlorobenzaldehyde the expected product in 99% yield (entry 20). Finally, the (\pm)-*trans*-cyclohexanediamine analogue **16** furnished with pyridine-2-carbaldehyde the aminal **17** in 95% yield (entry 21).

3. Conclusion

We were able to demonstrate a simple method to prepare cyclic amins with various ring sizes in high yield and high purity in pure water without the presence of a catalyst. In addition it was possible to get access to amins which could not be prepared via several different standard procedures.

4. Experimental

4.1. General experimental

N,N'-Dibenzyl-ethane-1,2-diamine (**2**), *N,N'*-diphenyl-ethane-1,2-diamine (**10**), *N,N'*-dimethyl-ethane-1,2-diamine (**12**), piperidine (**14**) and aldehydes were obtained from Aldrich and used without further purification. *N,N'*-Dibenzyl-propane-1,3-diamine (**4**),^{17,22} *N,N'*-dibenzyl-butane-1,3-diamine (**6**),²² *N,N'*-bis-((*R*)1-phenyl-ethyl)-ethane-1,2-diamine (**8**)²³ and (\pm)-*N,N'*-dibenzyl-1,2-cyclohexanediamine (**16**)²⁴ were prepared according to literature procedures. The reactions were carried out in dest. water.

Flash column chromatography²⁵ was performed on Sorbisil C-60. All reactions were monitored by TLC with Merck Silica gel 60 F₂₅₄ plates. Elemental analyses were carried out by the Microanalytical Laboratory of the Institut für Pharmazeutische Chemie der Universität Braunschweig. Infrared spectra were recorded on a Perkin–Elmer 2000 FT-IR System FTIR instrument. NMR spectra were performed in CDCl₃ at ambient temperature on a Bruker AMX 400 and a Bruker AC 200F. Mass spectra were recorded on Hewlett–Packard 5898B (at 70 eV). Melting points were taken with an apparatus after Dr Tottoli and are uncorrected.

4.2. Preparation of amins

General procedure. A diamine (1.00 mmol) was added to water (1.5 mL) and an aldehyde (1.00 mmol) was added. The mixture was vigorously stirred for 3 h at rt. For exceptions in temperature and reaction times see Table 1. The precipitate was isolated by filtration, washed with water (5 mL) and dried under vacuum to afford the desired product. In case the product was a liquid, the reaction mixture was extracted with CHCl₃ (3×5 mL) and the combined organic phases were dried (Na₂SO₄) and the solvent evaporated.

4.2.1. 1,3-Dibenzyl-2-phenyl-imidazolidine (3a). As a white solid (91%). Mp 97–98 °C (Lit.²⁶ 99 mp °C); MS (EI), *m/e* 328 (M⁺, 25%), 327 (M⁺–H, 25), 251 (M⁺–Ph, 100), 91 (80); IR (KBr) 2780s, 1490s, 1450s, 1161s, 700s cm⁻¹; ¹H NMR (200 MHz) δ 7.67–7.16 (m, 15H), 3.84 (s, 1H), 3.79 (d, *J*=13.0 Hz, 2H), 3.22–3.13 (m, 2H), 3.20 (d, *J*=13.2 Hz, 2H), 2.53–2.45 (m, 2H); ¹³C NMR (50 MHz) δ 140.3, 139.2, 129.5, 128.6, 128.2, 128.1, 126.8, 89.0, 56.9, 50.6. Anal. Calcd for C₂₃H₂₄N₂: C, 84.11; H, 7.36; N, 8.53, found: C, 83.80; H, 7.37; N, 8.48. The spectral data were consistent with literature values.^{27,28}

4.2.2. 1,3-Dibenzyl-2-(2-chloro-phenyl)-imidazolidine (3b). As a white solid (96%). Mp 96 °C (Lit.²⁹ 96–97 °C); MS (EI), *m/e* 361 (M⁺+H, 25%), 251 (100), 91 (75); IR (KBr) 2793m, 1365m, 1151s, 757vs, 698vs cm⁻¹; ¹H NMR (400 MHz) δ 8.14 (d, *J*=7.8 Hz, 1H), 7.45–7.25 (m, 13H), 4.70 (s, 1H), 3.85 (d, *J*=13.2 Hz, 2H), 3.41 (d, *J*=13.2 Hz, 2H), 3.26–3.23 (m, 2H), 2.64–2.61 (m, 2H); ¹³C NMR (100 MHz) δ 139.7, 138.2, 136.0, 131.8, 129.8, 129.3, 128.9, 128.6, 127.7, 127.3, 83.6, 57.3, 51.2. Anal. Calcd for C₂₃H₂₃ClN₂: C, 76.12; H, 6.39; N, 7.72, found: C, 75.82; H, 6.32; N, 7.55.

4.2.3. 2-(1,3-Dibenzyl-imidazolidin-2-yl)-pyridine (3c). As a white solid (99%). Mp 80–81 °C; MS (EI), *m/e* 329 (M⁺+H, 5%), 251 (100), 197 (10), 238 (10), 91 (80), 65 (10); IR (KBr) 2792m, 1493m, 1434s, 1360m, 1135m, 1148m, 781s, 749s, 696vs cm⁻¹; ¹H NMR (400 MHz) δ 8.56–8.55 (m, 1H), 8.01 (dt, *J*=8.0, 1.0 Hz, 1H), 7.79 (td, *J*=7.7, 1.8 Hz, 1H), 7.30–7.20 (m, 11H), 4.14 (s, 1H), 3.86 (d, *J*=13.4 Hz, 2H), 3.41 (d, *J*=13.4 Hz, 2H), 3.27–3.23 (m, 2H), 2.61–2.57 (m, 2H); ¹³C NMR (100 MHz) δ 161.8, 148.6, 139.4, 137.3, 128.9, 128.5, 127.2, 123.7, 123.5, 89.9, 57.4, 51.3. Anal. Calcd for C₂₂H₂₃N₃: C, 80.21; H, 7.04; N, 12.76, found: C, 79.89; H, 7.12; N, 12.88.

4.2.4. 1,3-Dibenzyl-2-thiophen-2-yl-imidazolidine (3d). As a white solid (99%). Mp 122 °C; MS (EI), *m/e* 333 (M⁺+H, 1%), 124 (50), 97 (30), 91 (100); IR (KBr) 1307s, 1161s, 744s, 717s, 698s cm⁻¹; ¹H NMR (400 MHz) δ 7.42–6.99 (m, 13H), 4.82 (s, 1H), 3.96 (d, *J*=12.9 Hz, 2H), 3.29 (d, *J*=12.9 Hz, 2H), 3.20–3.17 (m, 2H), 2.56–2.52 (m, 2H); ¹³C NMR (100 MHz) δ 146.4, 139.4, 129.0, 128.6, 128.0, 127.3, 127.1, 126.2, 84.0, 57.3, 50.7. Anal. Calcd for C₂₁H₂₂N₂S: C, 75.41; H, 6.63; N, 8.38, found: C, 75.41; H, 6.61; N, 8.77.

4.2.5. 1,3-Dibenzyl-2-(2-methoxy-phenyl)-imidazolidine (3e). As a white solid (94%). Mp 70 °C; MS (EI), *m/e* 357

($M^+ + H$, 20%), 251 (100), 148 (15), 121 (20), 91 (100), 65 (20); IR (KBr) 2795s, 2492s, 1380s, 1239s, 1153s, 752s, 698s cm^{-1} ; 1H NMR (400 MHz) δ 8.00 (dd, $J=7.6, 1.4$ Hz, 1H), 7.32–7.03 (m, 12H), 6.87 (d, $J=8.3$ Hz, 1H), 3.59 (s, 1H), 3.84 (s, 3H), 3.80 (d, $J=13.2$ Hz, 2H), 3.29 (d, $J=13.2$ Hz, 2H), 3.17–3.14 (m, 2H), 2.56–2.52 (m, 2H); ^{13}C NMR (100 MHz) δ 159.5, 140.0, 130.3, 129.5, 128.4, 121.5, 110.6, 80.1, 55.9, 51.1. Anal. Calcd for $C_{24}H_{26}N_2O$: C, 80.41; H, 7.31; N, 7.81, found: C, 80.3; H, 7.43; N, 7.71.

4.2.6. 1,3-Dibenzyl-2-(2,4-dichloro-phenyl)-imidazolidine (3f). As a yellow solid (96%). Mp 84 °C; MS (EI), m/e 395 ($M^+ + H$, 15%), 251 (100), 91 (80); IR (KBr) 2804s, 1337s, 1152s, 854s, 697vs cm^{-1} ; 1H NMR (400 MHz) δ 8.03 (d, $J=8.3$ Hz, 1H), 7.39–7.35 (m, 2H), 7.31–7.20 (m, 10H), 4.60 (s, 1H), 3.78 (d, $J=13.1$ Hz, 2H), 3.38 (d, $J=13.1$ Hz, 2H), 3.25–3.15 (m, 2H), 2.65–2.55 (m, 2H); ^{13}C NMR (100 MHz) δ 139.4, 137.2, 136.4, 134.7, 132.8, 128.9, 128.8, 128.6, 128.1, 127.3, 83.1, 57.2, 51.2. Anal. Calcd for $C_{23}H_{22}Cl_2N_2$: C, 69.52; H, 5.58; N, 7.05, found: C, 69.33; H, 5.46; N, 6.81.

4.2.7. 1,3-Dibenzyl-2-pentafluorophenyl-imidazolidine (3g). Reaction was carried out in deoxygenated water under a nitrogen atmosphere. The crude oily product was purified by flash chromatography (FCC) (eluant: 2.5% ethyl acetate – 0.5% triethylamine–hexane) through a short pad of silica to afford the title compound **3g** as a clear oil (92%). MS (EI), m/e 418 (M^+ , 10%), 251 (40), 91 (100); IR (KBr) 2795s, 1500s, 954s, 740s, 700s cm^{-1} ; 1H NMR (400 MHz) δ 7.22–7.18 (m, 10H), 4.61 (s, 1H), 3.75 (d, $J=13.3$ Hz, 2H), 3.66 (d, $J=13.2$ Hz, 2H), 3.32–3.29 (m, 2H), 2.72–2.69 (m, 2H); ^{13}C NMR (100 MHz) δ 138.8, 128.7, 128.5, 127.5, 79.8, 58.3, 52.0. Anal. Calcd for $C_{23}H_{19}N_2F_5$: C, 66.02; H, 4.58; N, 6.70, found: C, 65.67; H, 4.56; N, 6.55.

4.2.8. 1,3-Dibenzyl-2-(4-chloro-phenyl)-imidazolidine (3h). As a white solid (91%). Mp 106 °C (Lit.²⁹ 109 °C); MS (EI), m/e 361 ($M^+ + H$, 25%), 251 (75), 152 (20), 125 (20), 91 (100), 65 (20); IR (KBr) 2804m, 1493m, 1148m, 1186m, 822s, 698vs cm^{-1} ; 1H NMR (400 MHz) δ 7.64–7.61 (m, 2H), 7.44–7.38 (m, 2H), 7.33–7.22 (m, 10H), 4.01 (s, 1H), 3.79 (d, $J=13.2$ Hz, 2H), 3.28–3.20 (m, 4H), 2.57–2.53 (m, 2H); ^{13}C NMR (100 MHz) δ 139.6, 139.4, 134.6, 131.2, 128.9, 128.8, 128.6, 127.3, 88.6, 57.3, 51.1. Anal. Calcd for $C_{23}H_{23}ClN_2$: C, 76.12; H, 6.39; N, 7.72, found: C, 76.00; H, 6.39; N, 7.65.

4.2.9. 1,3-Dibenzyl-2-(2,6-dichloro-phenyl)-imidazolidine (3i). As a white solid (88%). Mp 145 °C; MS (EI), m/e 495 ($M^+ + H$, 5%), 251 (90), 91 (100); IR (KBr) 2792m, 1492m, 1436s, 1377m, 1337m, 1148m, 782m, 766m, 737vs, 698s cm^{-1} ; 1H NMR (400 MHz) δ 7.37–7.11 (m, 13H), 5.07 (s, 1H), 3.87 (d, $J=13.6$ Hz, 2H), 3.58 (d, $J=13.6$ Hz, 2H), 3.36–3.33 (m, 2H), 2.62–2.58 (m, 2H); ^{13}C NMR (100 MHz) δ 140.1, 137.7, 135.2, 129.5, 128.6, 128.5, 128.2, 127.1, 85.0, 58.2, 51.8. Anal. Calcd for $C_{23}H_{22}Cl_2N_2$: C, 69.52; H, 5.58; N, 7.06, found: C, 69.47; H, 5.59; N, 6.88.

4.2.10. 1,3-Dibenzyl-2-ethyl-imidazolidine (3j). The crude oil was purified by flash chromatography (FCC) (eluant: 2.5% ethyl acetate – 0.5% triethylamine–hexane) to afford the title compound **3j** as a clear oil. (85%). MS (EI), m/e 280

(M^+ , 5%), 251 ($M^+ - Et$, 100); IR (neat) 2925s, 2785s, 1495s, 1455s, 1345s, 1028s, 700s cm^{-1} ; 1H NMR (200 MHz) δ 7.29–7.19 (m, 10H), 3.98 (d, $J=13.1$ Hz, 2H), 3.38 (d, $J=13.3$ Hz, 2H), 3.14 (t, $J=3.8$ Hz, 1H), 2.99–2.86 (m, 2H), 2.47–2.38 (m, 2H), 1.73–1.60 (m, 2H), 1.11–0.92 (m, 3H); ^{13}C NMR (50 MHz) δ 139.8, 128.6, 128.2, 126.8, 85.6, 58.5, 50.6, 24.4, 8.16. The spectral data were consistent with literature values.^{27,28}

4.2.11. 1,3-Dibenzyl-2-phenyl-hexahydro-pyrimidine (5a). As a white solid (96%). Mp 113–114 °C (Lit.³⁰ 120 °C); MS (EI), m/e 341 ($M^+ - H$, 10%), 265 ($M^+ - Ph$, 100), 91 (95); IR (KBr) 2950s, 2795s, 1490s, 1450s, 1095s, 700s cm^{-1} ; 1H NMR (200 MHz) δ 7.69–7.13 (m, 15H), 3.612 (d, $J=13.2$ Hz, 2H), 3.608 (s, 1H), 3.02–2.95 (m, 2H), 2.85 (d, $J=13.1$ Hz, 2H), 2.11–1.41 (m, 4H); ^{13}C NMR (50 MHz) δ 141.9, 139.7, 129.6, 128.6, 128.3, 128.2, 128.0, 126.6, 89.0, 58.4, 51.8, 24.4. Anal. Calcd for $C_{24}H_{26}N_2$: C, 84.17; H, 7.65; N, 8.18, found: C, 84.20; H, 7.65; N, 8.13.

4.2.12. 1,3-Dibenzyl-2-(2-chloro-phenyl)-hexahydro-pyrimidine (5b). As a white solid (88%). Mp 94–96 °C; MS (EI), m/e 375 ($M^+ + H$, 5%), 365 (100), 91 (80); IR (KBr) 2923s, 1367s, 1098s, 756vs, 739vs, 698vs cm^{-1} ; 1H NMR (400 MHz) δ 8.19–8.16 (m, 1H), 7.41–7.19 (m, 13H), 4.34 (s, 1H), 3.58 (d, $J=13.2$ Hz, 2H), 3.03–2.99 (m, 4H), 2.15–2.08 (m, 2H), 1.92–1.83 (m, 1H), 1.51–1.47 (m, 1H); ^{13}C NMR (100 MHz) δ 139.9, 136.1, 131.3, 129.5, 128.9, 128.7, 128.5, 128.0, 127.7, 127.1, 83.2, 58.1, 51.3, 25.1. Anal. Calcd for $C_{24}H_{25}ClN_2$: C, 76.48; H, 6.69; N, 7.43, found: C, 76.08; H, 6.69; N, 7.36.

4.2.13. 1,3-Dibenzyl-2-pyridin-2-yl-hexahydro-pyrimidine (5c). As a white solid (93%). Mp 80–81 °C; MS (EI), m/e 344 ($M^+ + H$, 25%), 265 ($M^+ - pyridinyl$, 100), 91 (80); IR (KBr) 3060s, 2930s, 2790s, 1590s, 1490s, 1450s, 1440s, 1170s, 980s, 820s, 790s cm^{-1} ; 1H NMR (400 MHz) δ 8.58–8.56 (m, 1H), 8.07–8.04 (m, 1H), 7.77 (td, $J=7.6, 1.7$ Hz, 1H), 7.28–7.21 (m, 11H), 3.90 (s, 1H), 3.50 (d, $J=13.6$ Hz, 2H), 3.06 (d, $J=13.6$ Hz, 2H), 3.05–3.01 (m, 2H), 2.13 (td, $J=11.8, 2.8$ Hz, 2H), 1.94–1.85 (m, 1H), 1.56–1.52 (m, 1H); ^{13}C NMR (100 MHz) δ 163.1, 148.4, 139.7, 137.5, 129.0, 128.5, 127.1, 124.0, 123.6, 89.5, 58.7, 51.8, 25.0. Anal. Calcd for $C_{23}H_{25}N_3$: C, 80.43; H, 7.34; N, 12.23, found: C, 80.03; H, 7.28; N, 12.17.

4.2.14. 1,3-Dibenzyl-2-(2-chloro-phenyl)-[1,3]diazepane (7a). As a white solid (98%). Mp 67 °C; MS (EI), m/e 390 ($M^+ + H$, 1%), 160 (80), 91 (100); IR (KBr) 2791m, 1085s, 1070s, 762vs, 751vs, 697vs cm^{-1} ; 1H NMR (400 MHz) δ 8.10 (d, $J=4$ Hz, 1H), 7.45–7.19 (m, 13H), 5.04 (s, 1H), 3.90–3.84 (m, 2H), 3.70–3.66 (m, 2H), 3.02–2.97 (m, 2H), 2.88–2.82 (m, 2H), 1.71–1.55 (m, 4H); ^{13}C NMR (100 MHz) δ 140.6, 140.4, 135.6, 130.2, 129.2, 128.6, 128.6, 128.5, 127.0, 126.8, 82.6, 55.5, 48.9, 26.2. Anal. Calcd for $C_{22}H_{23}N_3$: C, 76.80; H, 6.96; N, 7.17, found: C, 76.42; H, 7.05; N, 6.99.

4.2.15. 2-Chlorophenyl-1,3-bis-((R)-1-phenyl-ethyl)-imidazoline (9a). The crude product was purified by Kugelrohr distillation (0.5 mbar, 200 °C) to afford the title compound **9a** as a clear yellow oil (81%). $[\alpha]_D^{25} = -30$ ($c=1$ in $CHCl_3$),

MS (EI), *m/e* 391 ($M^+ + H$, 15%), 279 ($M^+ - PhCl$, 100), 105 (65); IR (neat) 2970s, 1490s, 1450s, 1370s, 1030s, 760s, 700s cm^{-1} ; 1H NMR (400 MHz) δ 7.98 (d, $J=8.0$ Hz, 1H), 7.38–7.14 (m, 13H), 4.97 (s, 1H), 3.81–3.71 (m, 2H), 3.20–3.14 (m, 1H), 2.90–2.85 (m, 1H), 2.74–2.63 (m, 2H), 1.42 (d, $J=6.5$ Hz, 3H), 1.15 (d, $J=6.5$ Hz, 3H); ^{13}C NMR (100 MHz) δ 145.0, 144.4, 141.9, 134.6, 132.3, 129.2, 128.9, 128.6, 128.2, 127.9, 127.7, 127.2, 127.1, 126.8, 78.5, 62.2, 55.4, 50.0, 49.1, 44.7, 23.4, 14.4. Anal. Calcd for $C_{25}H_{27}N_2Cl$: C, 76.81; H, 6.97; N, 7.17, found: C, 76.43; H, 6.95; N, 7.12.

4.2.16. 4-Chlorophenyl-1,3-bis-((R)-1-phenyl-ethyl)-imidazoline (9b). The crude product was purified by Kugelrohr distillation (0.5 T, 200 °C) to afford the title compound **9b** as a clear yellow oil (80%). $[\alpha]_D^{25} = -70$ ($c=1$ in $CHCl_3$), MS (EI), *m/e* 391 ($M^+ + H$, 25%), 279 ($M^+ - PhCl$, 100), 105 (65); IR (neat) 2970s, 1490s, 1450s, 1090s, 700s cm^{-1} ; 1H NMR (400 MHz) δ 7.26–7.13 (m, 14H), 4.35 (s, 1H), 3.66 (q, $J=6.5$ Hz, 1H), 3.56 (q, $J=6.5$ Hz, 1H), 3.14–3.02 (m, 2H), 2.90–2.82 (m, 2H), 1.33 (d, $J=6.5$ Hz, 3H), 1.22 (d, $J=6.5$ Hz, 3H); ^{13}C NMR (100 MHz) δ 144.6, 144.3, 144.4, 133.1, 130.7, 128.5, 128.3, 128.09, 128.06, 127.99, 127.2, 127.1, 82.0, 60.3, 59.2, 48.3, 47.0, 23.7, 17.9. Anal. Calcd for $C_{25}H_{27}N_2Cl$: C, 76.81; H, 6.97; N, 7.17, found: C, 76.55; H, 7.02; N, 7.16.

4.2.17. 2-(2-Chloro-phenyl)-1,3-diphenyl-imidazolidine (11a). As a white solid (99%). Mp 128 °C (Lit.³¹ 128–129 °C). The spectral data were consistent with literature values.³¹

4.2.18. Methyl-1,3-diphenyl-imidazolidine (11b). The crude product was filtered of and recrystallised from methanol to afford the title compound **11b** as a white solid. (42%). Mp 95–96 °C (Lit.³² mp 97 °C). The spectral data were consistent with literature values.³³

4.2.19. 1,3-Dimethyl-2-phenyl-imidazolidine (13). As a clear liquid (67%). The spectral data were consistent with literature values.³⁴

4.2.20. 1,1'-(2-Chloro-phenylmethanediyl)-bis-piperidine (15). 2 equiv. piperidine were used in the reaction. The product was isolated as a yellow liquid (99%). (Lit.³⁵ 62 °C). MS (EI), *m/e* 292 (M^+ , 5%), 208 (M^+ , –piperidinyl, 95%), 125 (90), 84 (100); IR (neat) 2930s, 1470s, 1440s, 1270s, 1100s, 910s, 735s cm^{-1} ; 1H NMR (200 MHz) δ 7.44–7.12 (m, 4H), 4.39 (s, 1H), 2.84–2.28 (m, 8H), 1.56–1.34 (m, 12H); ^{13}C NMR (50 MHz) δ 134.8, 134.2, 130.0, 129.3, 127.7, 125.4, 83.1, 49.8, 26.2, 25.2.

4.2.21. (\pm)-1,3-Dibenzyl-2-(2-pyridinyl)-octahydrobenzoimidazole (17). As a white solid (95%). Mp 49–50 °C; MS (EI), *m/e* 383 (M^+ , 5%), 305 (M^+ , –pyridinyl, 50), 187 (25), 91 (100); IR (KBr) 2925s, 2800s, 1590s, 1450s, 1440s, 1145s, 700s cm^{-1} ; 1H NMR (400 MHz) δ 8.40–8.38 (m, 1H), 7.52 (td, $J=7.6, 1.9$ Hz, 1H), 7.38–7.35 (m, 1H), 7.20–7.05 (m, 11H), 4.74 (s, 1H), 3.84 (d, $J=13.8$ Hz, 1H), 3.79 (d, $J=13.7$ Hz, 1H), 3.53 (d, $J=14.4$ Hz, 1H), 3.47 (d, $J=14.4$ Hz, 1H), 2.99–2.94 (m, 1H), 2.55–2.49 (m, 1H), 1.83–1.70 (m, 2H), 1.31–1.13 (m, 2H); ^{13}C NMR (100 MHz) δ 162.0, 148.6, 141.3, 139.6,

135.8, 129.4, 128.4, 128.2, 128.1, 126.9, 126.7, 124.5, 122.5, 87.8, 69.3, 67.9, 56.9, 52.9, 30.6, 30.3, 25.0, 24.9. Anal. Calcd for $C_{26}H_{29}N_3$: C, 81.42; H, 7.62; N, 10.96, found: C, 81.22; H, 7.65; N, 10.90.

Acknowledgements

Financial support by Fonds der Chemischen Industrie, BMBF, DFG and Nieders. Vorab der Volkswagen Stiftung is gratefully acknowledged.

References and notes

- Duhamel, L. *The chemistry of amino, nitroso and nitro compounds and their derivatives*; Patai, S., Ed.; Wiley: New York, 1982; Vol. 2, pp 849–890.
- Wanzlick, H.-W.; Löchel, W. *Chem. Ber.* **1953**, *86*, 1463–1466.
- Ono, A.; Okamoto, T.; Inada, M.; Nara, H.; Matsuda, A. *Chem. Pharm. Bull.* **1994**, *42*, 2231–2237.
- Marek, I.; Alexakis, A.; Normant, J.-F. *Tetrahedron Lett.* **1991**, *32*, 5329–5332.
- Alexakis, A.; Lensen, N.; Mangeney, P. *Tetrahedron Lett.* **1991**, *32*, 1171–1174.
- For general use of amination in asymmetric synthesis see: Alexakis, A.; Mangeney, P.; Lensen, N.; Tranchier, J. P.; Gosmini, R.; Raussou, S. *Pure Appl. Chem.* **1996**, *68*, 531–534.
- Kallen, R. G.; Jencks, W. P. *J. Biol. Chem.* **1966**, *241*, 5851–5864.
- Benkovic, S. J.; Benkovic, P. H.; Comfort, D. R. *J. Am. Chem. Soc.* **1969**, *91*, 5270–5279.
- Benkovic, S. J.; Benkovic, P. H.; Chrzanowski, R. *J. Am. Chem. Soc.* **1970**, *92*, 523–528.
- Messer, W. S.; Abuh, Y. F.; Liu, Y.; Periyasamy, S.; Ngur, D. O.; Edgar, M. A. N.; El-Assadi, A. A.; Sbeih, S.; Dunbar, P. G.; Roknich, S.; Rho, T.; Fang, A.; Ojo, B.; Zhang, H.; Huzl, J. J.; Nagy, P. I. *J. Med. Chem.* **1997**, *40*, 1230–1246.
- Weinhardt, K.; Wallach, M. B.; Marx, M. *J. Med. Chem.* **1985**, *28*, 694–698.
- Liebermann, S. V. *J. Am. Chem. Soc.* **1955**, *77*, 1114–1116.
- Kerfanto, M.; Brault, A.; Venien, F.; Morvan, J. M.; LeRouzc, A. *Bull. Soc. Chim. Fr.* **1975**, 196–200.
- Sekiya, M.; Sakai, H. *Chem. Pharm. Bull.* **1969**, *17*, 32–39.
- Stewart, A. T.; Hauser, C. R. *J. Am. Chem. Soc.* **1955**, *77*, 1098–1103.
- Senkus, M. *J. Am. Chem. Soc.* **1946**, *68*, 1611–1613.
- Simion, A.; Simion, C.; Kanda, T.; Nagashima, S.; Mitoma, Y.; Yamada, T.; Mimura, K.; Tashiro, M. *J. Chem. Soc., Perkin Trans. 1* **2001**, 2071–2078.
- Hine, J.; Narducy, K. W. *J. Am. Chem. Soc.* **1973**, *95*, 3362–3368.
- Alexakis, A.; Tranchier, J.-P.; Lensen, N.; Mangeney, P. *J. Am. Chem. Soc.* **1995**, *117*, 10767–10768.
- Organic synthesis in water*; Grieco, P. A., Ed.; Blackie Academic and Professional: London, 1998.
- Li, C.-J. *Chem. Rev.* **1993**, *93*, 2023–2035.
- Niitsu, M.; Samejima, K. *Chem. Pharm. Bull.* **1986**, *34*, 1032–1038.
- Maerkl, G.; Jin, G. Y. *Tetrahedron Lett.* **1980**, *21*, 3467–3470.

24. Denmark, S. E.; Stadler, H.; Dorow, R. L.; Kim, J.-H. *J. Org. Chem.* **1991**, *56*, 5063–5079.
25. Still, W. C.; Kahn, M.; Mitra, A. *J. Org. Chem.* **1978**, *43*, 2923.
26. Wilson, W. L.; LeBelle, M. J. *J. Pharm. Sci.* **1997**, *68*, 1322–1323.
27. Chapuis, C.; Gauvreau, A.; Klaebe, A.; Lattes, A.; Perie, J. J.; Roussel, J. *J. Bull. Soc. Chim.* **1973**, 2676–2680.
28. Chapuis, C.; Gauvreau, A.; Klaebe, A.; Lattes, A.; Perie, J. J.; Roussel, J. *Tetrahedron* **1974**, *30*, 1383–1386.
29. Lob, R. *Recl. Trav. Chim. Pays-Bas.* **1936**, *55*, 859–862.
30. Kalyanam, N.; Parthasarathy, P. C.; Ananthan, L.; Manjunatha, S. G.; Likhate, M. A. *Indian J. Chem. Soc. B* **1992**, *31*, 243–247.
31. Eynde, J. J. V.; Delfosse, F.; Lor, P.; Yves, Y. V. *Tetrahedron* **1995**, *51*, 5813–5818.
32. Salerno, A.; Ceriani, V.; Perillo, I. A. *J. Heterocycl. Chem.* **1997**, *34*, 709–716.
33. Salerno, A.; Ceriani, V.; Perillo, I. A. *J. Heterocycl. Chem.* **2001**, *38*, 849–852.
34. Salerno, A.; Ceriani, C.; Perillo, I. A. *J. Heterocycl. Chem.* **1992**, *29*, 1725–1733.
35. Garner, G. V.; Mobbs, D. B.; Suschitz, H.; Millersh, J. S. *J. Chem. Soc. C* **1971**, 3693–3701.



Oxymethylcrowned chromene: photoswitchable stoichiometry of metal ion complex and ion-responsive photochromism

Saleh A. Ahmed,^{a,†} Mutsuo Tanaka,^{a,*} Hisanori Ando,^a Hitoshi Iwamoto^b and Keiichi Kimura^{b,*}

^aSpecial Division for Human Life Technology, AIST Kansai, 1-8-31, Midorigaoka, Ikeda, Osaka 563-8577, Japan

^bDepartment of Applied Chemistry, Faculty of Systems Engineering, Wakayama University, 930, Sakae-dani, Wakayama, Wakayama 640-8510, Japan

Received 20 January 2004; revised 10 February 2004; accepted 10 February 2004

Abstract—Chromene derivatives bearing oxymethyl-12-crown-4 (**1**), -15-crown-5 (**2**), -18-crown-6 (**3**) ether moieties, and non-cyclic analogue (**4**) were synthesized, and their metal ion binding properties and photochromism were examined. NMR titration with alkali metal ions revealed that **1** formed a 1:2 complex (metal ion: ligand) with Na⁺, while Li⁺ afforded a 1:1 complex of **1**. In cases of K⁺ and Rb⁺, the complexes were a mixture of 1:1 and 1:2 complexes, but the formation of 1:1 complex was observed again with Cs⁺. Under UV irradiation, however, the complex stoichiometry of **1** with all alkali metal ions was 1:1. As a comparison of NMR spectra between the Li⁺ and Na⁺ complexes of **1** indicated considerable upfield shift for the chromene moiety of the Na⁺ complex, π – π stacking of the chromene moiety seems to induce formation of the 1:2 complex. These results indicate that the chromene moiety is not only to show photochromism but also to induce aggregation to form the 1:2 complex resulted in switching of the complex stoichiometry by UV irradiation. The formation of 1:2 complex appeared only with **1** because flexibility of the crown moieties for **2** and **3** interfered the formation of 1:2 complex. Studies on photochromism in the presence of a metal ion demonstrated that the chromene derivatives bearing crown ether moieties show ion-responsive photochromism depending on the metal ion binding ability of their crown ether moieties.

© 2004 Elsevier Ltd. All rights reserved.

1. Introduction

Photochromism is a reversible photoinduced phenomenon in which a photosensitive compound is converted to another isomer exhibiting a different absorption spectrum in the visible region. For recent several decades, various photochromic compounds have been designed, and their photochromism has been examined.¹ In view of practical application, physical properties such as colorability, decoloration rate, photofatigue resistance and so on, have been widely scrutinized. On the other hand, combination of photochromic compounds with ion-responsive molecules such as crown ether has been reported to afford ion-responsive photochromic compounds. Incorporation of a crown ether moiety to azobenzene,² diarylethene,³ spiro-pyran,⁴ and spirooxadine⁵ have been reported to show their fascinating ion-responsive photochromism. In our previous work, chromene derivatives bearing monoazacrown ether⁶ and *t*-butylcalix[4]arene⁷ moieties also showed ion-responsive photochromism. In this paper, we report chromene derivatives bearing an oxymethylcrown ether moiety,

namely, crowned chromene, which show not only ion-responsive photochromism but also photoswitchable stoichiometry of metal ion complexes.

2. Results and discussion

2.1. Synthesis of chromene derivatives

Crowned chromenes **1–3** and non-cyclic analogue **4** for comparison were synthesized according to the outline as shown in Scheme 1. Bromomethylchromene was prepared by following a method in the literature.⁸ The reaction of bromomethylchromene with hydroxymethylcrown ethers or non-cyclic analogue was carried out in the presence of powdered sodium hydroxide using THF as a solvent at room temperature. Conventional treatment of the reaction mixture afforded the corresponding products with 59–83% yields after purification by gel permeation chromatography.

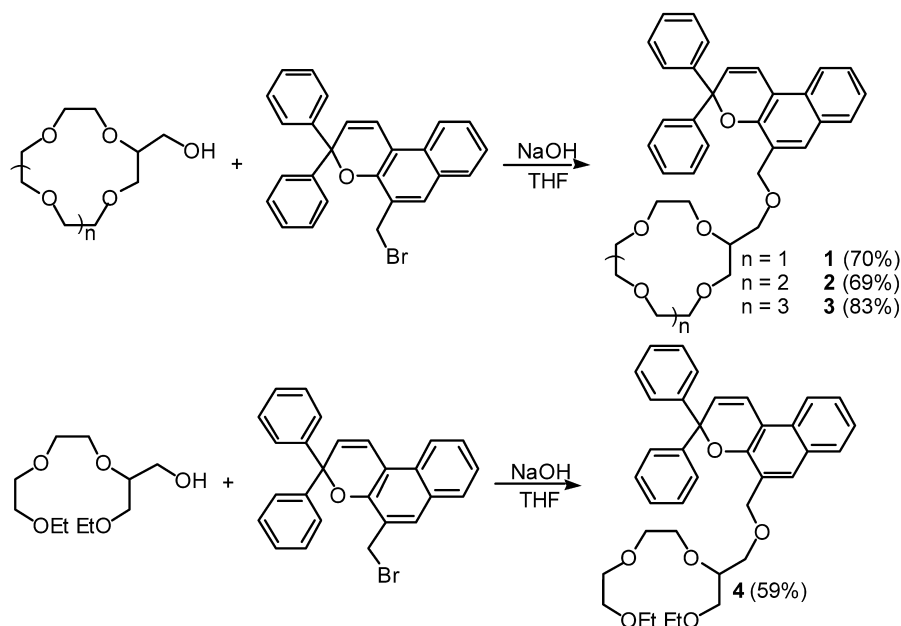
2.2. Binding properties with metal ions

The metal ion binding properties of the obtained crowned chromenes and non-cyclic analogue were examined by ¹³C NMR titration using alkali and alkaline-earth metal perchlorates in acetonitrile-*d*₃ at room temperature. In control experiments using **1** with Li⁺, NMR spectra for

Keywords: Chromene; Crown ether; Photochromism; Metal ion binding.

* Corresponding authors. Tel.: +81-72-751-9209; fax: +81-72-751-9629; e-mail address: mutsuo-tanaka@aist.go.jp

[†] JSPS Fellow. Permanent address: Department of Chemistry, Faculty of Science, Assiut University, 71516 Assiut, Egypt.



Scheme 1. Synthesis outline.

the crown ether moiety showed significant downfield shift upon addition of Li^+ , however, there was serious difficulty in assignment. For the chromene moiety, any meaningful change in chemical shift was not observed. On the other hand, the benzyl carbon adjacent to the crown ether moiety was assignable with a considerable change in chemical shift. Therefore, we chose this carbon as an indicator for NMR titration.

When the molar ratio of Li^+ /ligand was greater than 1, the chemical shift of the benzyl carbon of **1** was almost constant. This result suggests formation of a 1:1 complex. To determine the Li^+ complex stoichiometry of **1** precisely, we examined a Job plot as depicted in Figure 1. A clear maximum point was observed at 0.5 in the molar fraction of ligand to indicate a 1:1 stoichiometry of the Li^+ complex. Similarly, ^{13}C NMR titration of **1** was carried out using Na^+ . Interestingly, the chemical shift was constant when the molar ratio of Na^+ /ligand was greater than 0.5. This tendency implies that the Na^+ complex stoichiometry of **1** is

1:2 (Na^+ : ligand). Job plots (Fig. 2) showed a maximum around 0.67 in the molar fraction of ligand which confirms that the Na^+ complex stoichiometry of **1** is 1:2 (Na^+ : ligand). In cases of K^+ and Rb^+ , Job plots gave a maximum between 0.5 and 0.67. These tendencies suggest that these complexes were a mixture of 1:1 and 1:2 complexes. For Cs^+ , Job plots again gave the maximum point at 0.5 in the molar fraction, indicating that complex stoichiometry of **1** with Cs^+ was 1:1. The formation of 1:2 complex is not usual for monomeric (monocyclic) 12-crown-4 derivatives, and this phenomenon will be discussed later in detail. On the other hand, the complex stoichiometries with alkali metal ions for **2** and **3** were always 1:1. For **4**, the spectral change in chemical shift induced by addition of an alkali metal ion was too small to evaluate metal ion binding properties. It is obvious that non-cyclic analogue **4** is lack of metal ion binding ability as compared with other chromene derivatives bearing the crown ether moieties.

When alkaline-earth metal perchlorates were added to the

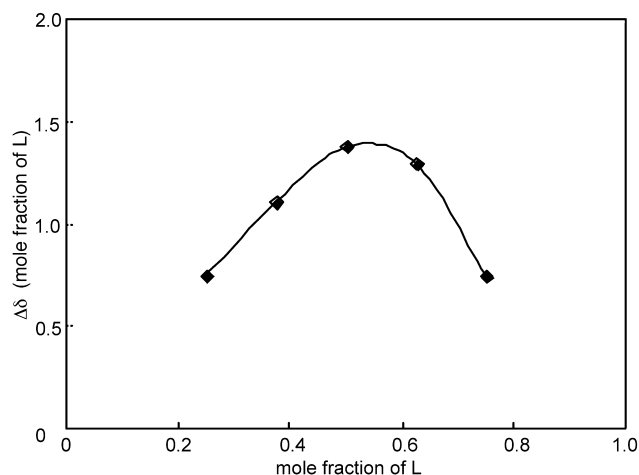


Figure 1. Job plots for Li^+ complex of **1**.

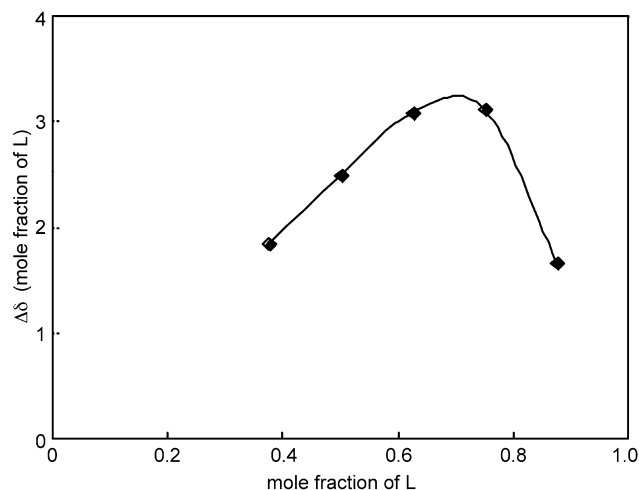


Figure 2. Job plots for Na^+ complex of **1**.

Table 1. Binding constants^a

	Li ⁺	Na ⁺	K ⁺	Rb ⁺	Cs ⁺
1	4.2	(71)	—	—	0.24
2	20	29	16	4.6	2.3
3	0.51	58	75	10	5.9
4	—	—	—	—	—

^a The units for k_{11} and k_{12} (in parenthesis) are $10^3 \text{ mol}^{-1} \text{ dm}^3$ and $10^5 \text{ mol}^{-2} \text{ dm}^6$, respectively.

solution of **1**, spectral broadening occurred with coloration of the solution to hamper the measurement. A similar tendency was observed with other chromene derivatives. As the coloration of the solution means that thermal isomerization is induced, alkaline-earth metal ions interacted with the chromene derivatives more strongly enough to induce thermal isomerization than alkali metal ions. Therefore, the binding constants with alkaline-earth metal ions could not be determined by NMR titration.

The binding constants⁹ for 1:1 complexes (k_{11}) with alkali metal ions were evaluated through the binding isotherms by non-linear least-square regression using the NMR titration data, and the values are summarized in Table 1. In the case of Na⁺ complex of **1**, the binding constant of 1:2 complex (k_{12}) was also evaluated as two molecules of **1** were regarded as one bidentate ligand to form 1:1 complex. The binding constants for **1** showed that Li⁺ was far preferable to Cs⁺. In cases of K⁺ and Rb⁺, the binding constants could not be determined because these complexes were a mixture of 1:1 and 1:2 complexes. Crowned chromene **2** showed the binding ability to Na⁺, while the complex of **3** with K⁺ appeared to be the most stable. Generally, 12-crown-4, 15-crown-5, and 18-crown-6 are known to show the binding ability to Li⁺, Na⁺, and K⁺ depending on their ring size, respectively. As the binding properties of the crowned chromenes were consistent with the binding properties of the parent crown ethers, the lariat effect of

the chromene moieties upon the binding properties seems to be negligible.

2.3. Ion-responsive photochromism

The photochromism of the chromene derivatives was evaluated in the presence of alkali and alkaline-earth metal ions. Without UV irradiation, no spectral change of **1** solution was observed in the presence of an alkali metal ion as shown in Figure 3. This indicates that there is no thermal isomerization induced by the metal ion complexation of its crown ether moiety. Upon UV irradiation, the most significant change in spectra was induced with Li⁺, reflecting that Li⁺ formed the most stable complex. In cases of alkaline-earth metal ions, Ca²⁺ induced slight thermal isomerization, and the other alkaline-earth metal ions induced significant spectral change under UV irradiation (Fig. 4). Considerable red-shift in the spectra¹⁰ was induced by metal ions as was observed in the chromene derivatives bearing monoazacrown ether⁶ and *t*-butylcalix[4]arene⁷ moieties.

In the case of solution of **2** (Fig. 5), thermal isomerization was not observed in the presence of any alkali metal ions similar to the solution of **1**. When UV light was irradiated on the solution of **2**, the most significant spectral change was induced with Na⁺. Among alkaline-earth metal ions, Ca²⁺, Sr²⁺, and Ba²⁺ induced significant spectral change for the solution of **2**, but Mg²⁺ showed no influence on photoisomerization (Fig. 6).

In Figure 7, the solution of **3** with K⁺ afforded the most spectral change upon UV irradiation, but the influence of alkali metal ions on photoisomerization was not remarkable. Contrary to alkali metal ions, all alkaline-earth metal ions induced distinguished spectral change for the solution of **3** upon UV irradiation as shown in Figure 8. Especially, the Mg²⁺ influence on photoisomerization was notable compared with the Mg²⁺ solutions of **1** and **2**. This tendency

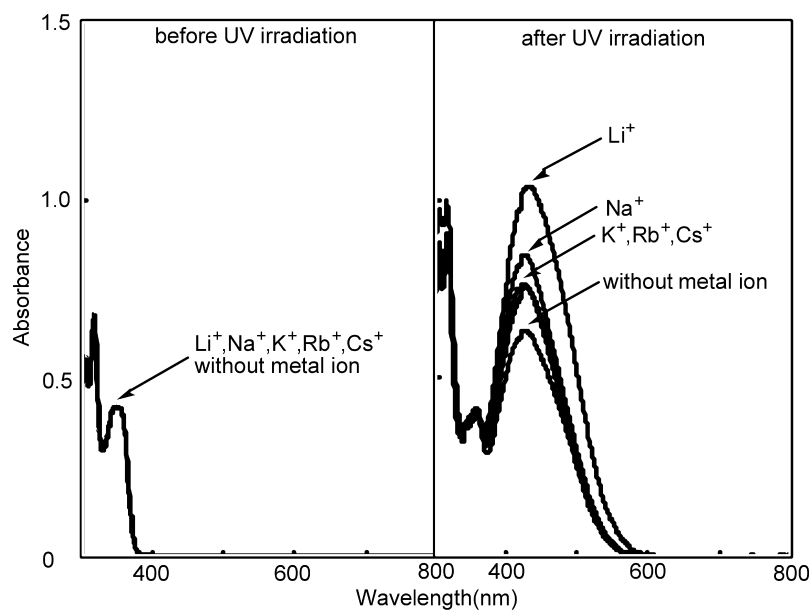


Figure 3. Absorption spectra of **1** in the presence of alkali metal ions.

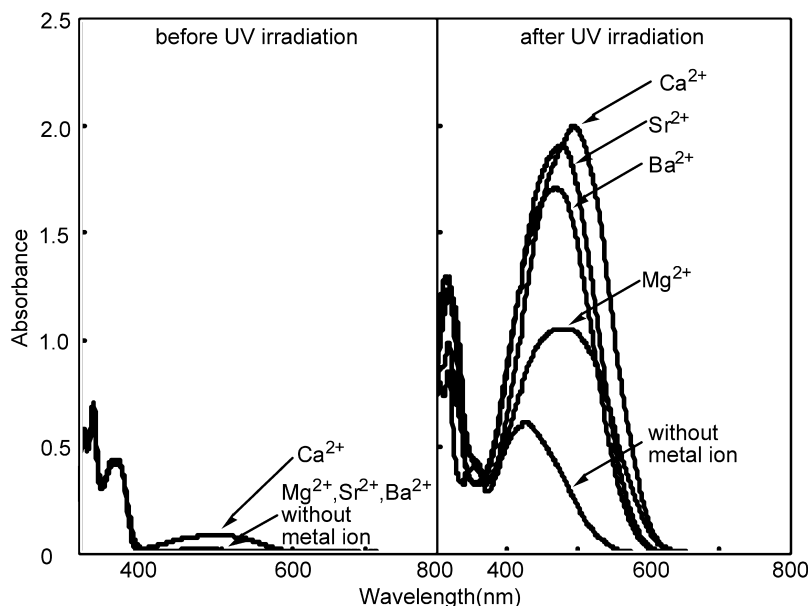


Figure 4. Absorption spectra of **1** in the presence of alkaline-earth metal ions.

might be derived from the flexibility of the 18-crown-6 moiety, which may capture two small metal ions. For non-cyclic analogue **4**, any influence of alkali metal ions on photochromism was hardly observed, but significant spectral changes were induced by alkaline-earth metal ions similar to the crowned chromenes (the data not shown).

It is reported that chromene is converted to the open (quinoidal) form by UV irradiation¹¹ in which there is a carbonyl group to interact with a metal ion (Scheme 2). In previous work,⁶ we pointed out that there are two interactions with a metal ion derived from the crown ether moiety and the carbonyl group in the open form (Scheme 3) similar to the crowned spiropyrans.¹² Among alkali metal ions, the most significant influence on photoisomerization was induced with Li⁺, Na⁺, and K⁺ for the solution of **1**, **2**, and **3**, respectively. This tendency seems to reflect the metal

ion binding ability of the crown ether moieties as 12-crown-4, 15-crown-5, and 18-crown-6 to Li⁺, Na⁺, and K⁺ depending on their ring size, respectively. However, alkaline-earth metal ions did not show such tendency depending on the ring size of the crown ether moieties. This difference might reflect that alkali metal ions interact with the crown ether moieties predominantly, while alkaline-earth metal ions tend to interact with the carbonyl group¹³ more strongly than with the crown ether moiety in the open form. This is supported by the tendency of non-cyclic analogue **4** where alkali metal ions did not show any influence on photochromism, but alkaline-earth metal ions induced significant spectral change upon UV irradiation.

In order to estimate the conversion (%) of chromene derivatives to the open form from the closed form upon UV irradiation, extinction coefficient, ϵ for the open form was

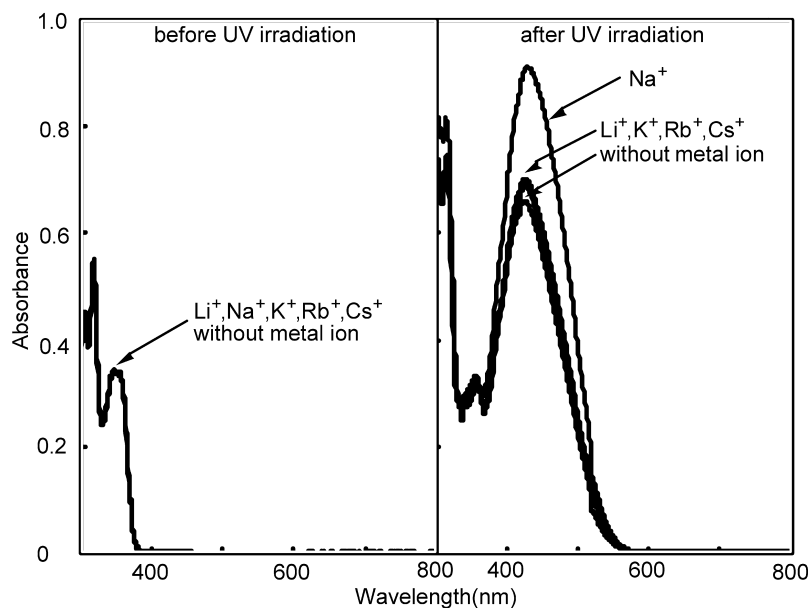


Figure 5. Absorption spectra of **2** in the presence of alkali metal ions.

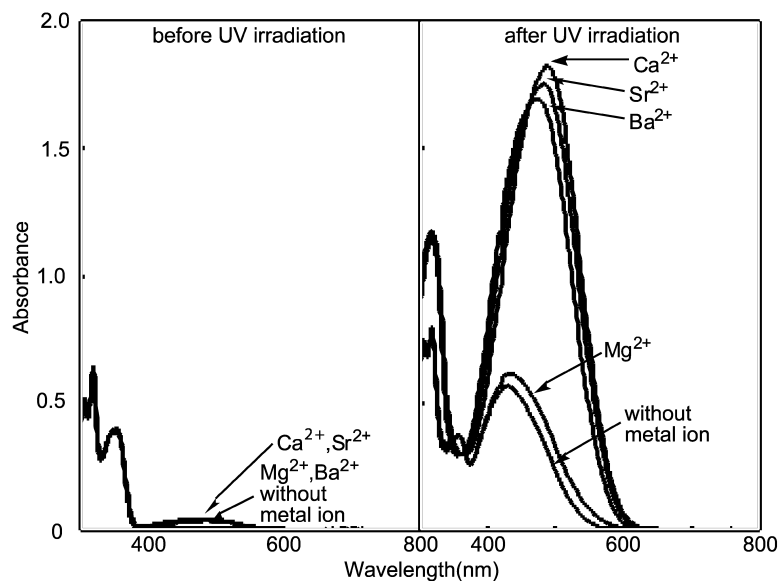


Figure 6. Absorption spectra of **2** in the presence of alkaline-earth metal ions.

evaluated. When the interaction of a metal ion with the chromene derivatives is strong enough, the conversion is regarded as 100% in the presence of excess amount of the metal ion upon UV irradiation. As Ca^{2+} showed notable interaction with all of the chromene derivatives, their absorption spectra were measured in the presence of ten-fold excess amount of Ca^{2+} to evaluate ϵ for the open form. The obtained ϵ values were 2.0, 1.8, 1.7, and $2.0 \times 10^4 \text{ mol}^{-1} \text{ dm}^3$ for **1**, **2**, **3**, and **4**, respectively. Therefore, the conversion in the absence of a metal ion was evaluated as 32, 37, 36, and 31% for **1**, **2**, **3**, and **4**, respectively. In the presence of Li^+ , **1** was converted to the open form in 69%. The conversion for **2** and **3** was 51 and 47% in the presence of Na^+ and K^+ , respectively. These tendencies reflect the influence of metal ions on the photoisomerization equilibrium. In the case of **4**, the conversion in the presence of alkali metal ions was between 31 and 35% and any meaningful influence on the conversion

ratio was not observed. Among alkaline-earth metal ions, Ca^{2+} , Sr^{2+} , and Ba^{2+} afforded high conversion with more than 85% for **1**, **2**, and **3**, and the conversion was more than 80% even for **4**. This result indicates that the influence on photoisomerization equilibrium by alkaline-earth metal ions is far greater than that by alkali metal ions.

Chromene, which is colorless in the closed form, is colored upon UV irradiation by adopting the open form (Scheme 2).¹¹ The colored open form restores to the colorless closed form thermally. If there is any specific interaction between a metal ion captured by the crown ether moiety and the carbonyl group in the open form, the open form of the crowned chromene should be stabilized, resulting in a significant delay of the decoloration process (Scheme 3). Therefore, the decoloration rate constants reflect the thermal stability of the crowned chromene complex with a metal ion under UV irradiation.

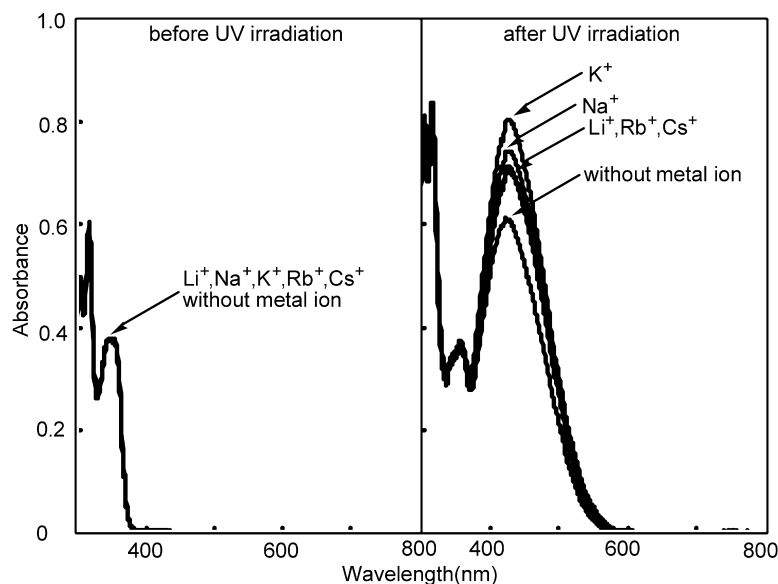


Figure 7. Absorption spectra of **3** in the presence of alkali metal ions.

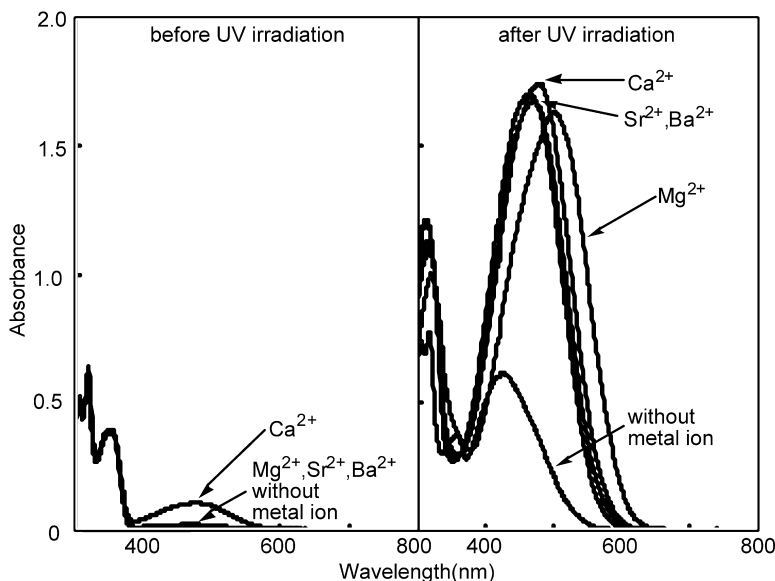
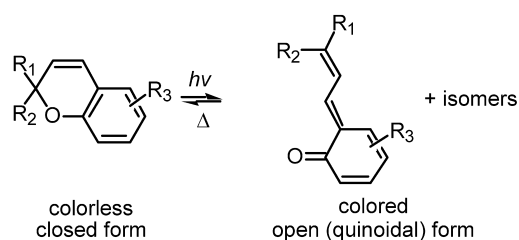
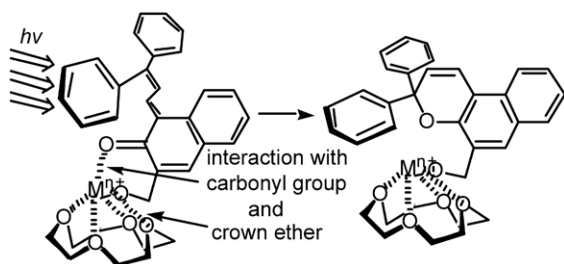


Figure 8. Absorption spectra of **3** in the presence of alkaline-earth metal ions.



Scheme 2. Photoisomerization of chromene.



Scheme 3. Photoisomerization of crowned chromene.

When the complex stoichiometry of the crowned chromene with a metal ion is 1:1, the decoloration process from the open form (O) to the closed form (C) is expressed as a first-order reaction. The decoloration rate constant (k) is defined by Eq. 1 in Scheme 4 with the elapsed time (t), initial

$$\frac{d[C]_t}{dt} = k([O]_0 - [C]_t), \quad kt = \ln \frac{[O]_0}{[O]_0 - [C]_t} \quad \text{Eq. 1}$$

$$[O]_0 = \frac{A_0 - A_\infty}{\varepsilon} \quad [C]_t = \frac{A_0 - A_t}{\varepsilon}$$

$$kt = \ln \frac{A_0 - A_\infty}{A_t - A_\infty} \quad \text{Eq. 2}$$

Scheme 4. Equations for decoloration rate constant.

concentration of O at $t=0$ ($[O]_0$), and concentration of C at a given time ($[C]_t$). $[O]_0$ and $[C]_t$ are expressed with the initial absorbance of a crowned chromene solution (A_0), final absorbance at $t=\infty$ (A_∞), absorbance at a given time (A_t), and the molar absorption coefficient of O (ε). Eq. 1 is then converted to Eq. 2 in Scheme 4. According to Eq. 2, the thermal decoloration rate constants of the crowned chromene under UV irradiation can be determined, where the smaller value means the more stable complex formation.

To determine the decoloration rate constants, time-course absorption-spectral changes of the crowned chromene acetonitrile solutions in the presence of a metal ion were followed at room temperature after turning off UV light.¹⁴ The decoloration rate constants are summarized in Table 2. Among the alkali metal ion complexes of **1**, the Li^+ complex was the most stable one, while Na^+ forms the most stable complex with **2**. However, the complexes of **3** and **4** did not show clear stabilization effect with alkali metal ions. On the other hand, alkaline-earth metal ions showed remarkable stabilization effect in all of the chromene derivatives, even in non-cyclic analogue **4**. This tendency also suggests that the interaction of the carbonyl group with alkaline-earth metal ions¹³ seems to be stronger than that with alkali metal ions, resulting in the stabilization of the complexes regardless of ring size of the crown ether moieties.

2.4. Complex stoichiometry of **1**

The metal ion binding ability of 12-crown-4 to Li^+ is well known to form 1:1 complex.¹⁵ On the other hand, bis(12-crown-4) derivatives generally show a high binding ability to Na^+ by formation of a sandwich type complex, namely, 1:2 (metal ion: crown ether ring) complex.¹⁶ In the case of polymers carrying a 12-crown-4 moiety at the side chain, their binding ability towards Na^+ is also attained through formation of a similar sandwich type complex.¹⁷ On the other hand, it has been reported that various lariat crown

Table 2. Decoloration rate constants (10^{-2} s^{-1})

	Without metal ion	Li ⁺	Na ⁺	K ⁺	Rb ⁺	Cs ⁺	Mg ²⁺	Ca ²⁺	Sr ²⁺	Ba ²⁺
1	6.1	4.4	5.7	6.2	6.2	6.2	1.6	0.029	0.10	0.28
2	6.0	6.2	4.6	5.8	5.7	5.9	2.6	0.051	0.033	0.086
3	6.7	6.5	6.3	6.0	6.1	6.2	0.25	0.021	0.063	0.060
4	5.8	5.8	5.4	5.9	5.9	5.6	2.7	0.17	0.34	0.61

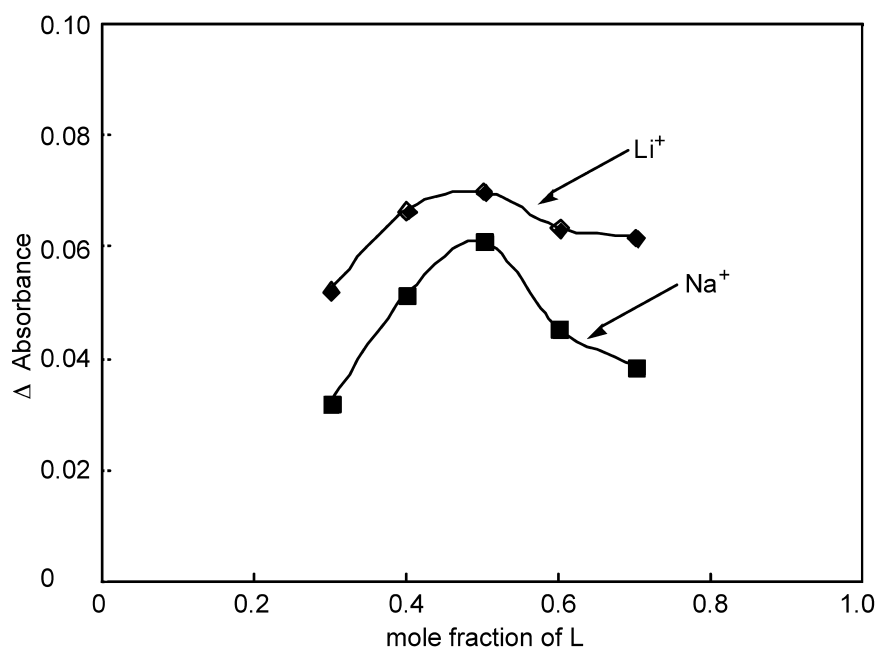
ethers form metal ion complexes in which the lariat moiety interacts with the metal ion captured by the crown ether moiety intramolecularly.¹⁸ To the best of our knowledge, however, the sandwich type complex formation of monomeric (monocyclic) 12-crown-4 derivatives seems to be possible only in the presence of a large excess of crown ether. In the case of the sandwich type Na⁺-complex formation of our crowned chromene, therefore, the chromene moiety must play an essential role to induce an intermolecular interaction resulting in the 1:2 complex formation of its 12-crown-4 moiety with Na⁺.

In order to investigate the 1:2 complex structure of **1**, ¹H NMR measurement was conducted in the presence of Li⁺ and Na⁺. The concentrations for **1** and metal ions were 2 and $4 \times 10^{-2} \text{ mol dm}^{-3}$, respectively. Li⁺ induced significant downfield shifts (<ca. 0.2 ppm) for the crown ether ring protons and slight downfield shifts (<0.02 ppm) for the chromene moiety and the benzyl protons. In the case of Na⁺, the crown ether moiety protons indicated moderate downfield shifts (<0.06 ppm), but the chromene moiety and the benzyl protons exhibited moderate upfield shifts (<0.05 ppm). As upfield shifts are induced by diamagnetic anisotropy of aromatic rings,¹⁹ π - π stacking of the chromene moieties is strongly suggested. However, further attempts to obtain information about the 1:2 complex structure by X-ray crystallography was failed.

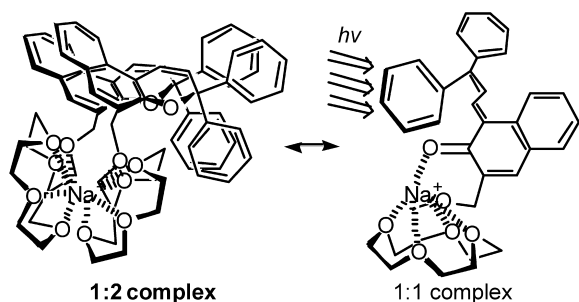
The formation of 1:2 complex was only observed in the case of **1**. With increasing metal ion radius from Li⁺ to Cs⁺, the

complex stoichiometry of **1** changed from 1:1 to 1:2, between 1:1 and 1:2, and finally, returned to 1:1. It is well known that Na⁺ is the most suitable to form 1:2 complex with 12-crown-4, but Li⁺ and Cs⁺ have significant disadvantage to form 1:2 complex with 12-crown-4, where Li⁺ and Cs⁺ are too small and large in size, respectively. This tendency implies that not only π - π stacking of the chromene moiety but also the size fitness of the metal ion to the crown ether moiety promotes the formation of 1:2 complex. Although the formation of 1:2 complex is also reported with various 15-crown-5 and 18-crown-6 derivatives in the presence of K⁺ and Cs⁺, respectively, the corresponding crowned chromenes, **2** and **3**, did not form 1:2 complex. The fact that 15-crown-5 and 18-crown-6 are more flexible than 12-crown-4 implies that flexibility of the crown ether moieties hampers π - π stacking of the chromene moieties. Probably due to rigidity of the 12-crown-4 moiety, the formation of 1:2 complex occurs only for **1** in the presence of appropriate metal ion.

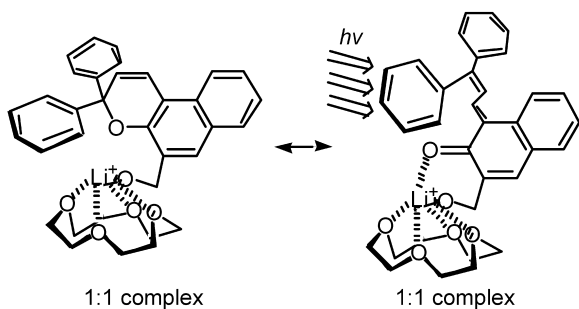
The complex stoichiometry of **1** with Li⁺ and Na⁺ under UV irradiation was examined by Job plot method using the absorption spectra data at 420 nm, where there was no absorbance derived from the closed form, as shown in Figure 9. As the chromene derivatives are converted to the open form by UV irradiation in the absence of a metal ion, the absorbance difference between the chromene solutions with and without a metal ion was applied to Job plots to evaluate the complex stoichiometry for the open form under UV irradiation. Both plots afforded the maximum points at

**Figure 9.** Job plots for Li⁺ and Na⁺ complexes of **1** under UV irradiation.

0.5, indicating that both complex stoichiometries with Li^+ and Na^+ were 1:1 under UV irradiation. Therefore, it is clear that the Na^+ complex of **1** changed its stoichiometry from 1:2 to 1:1 (Na^+ : ligand) by UV irradiation (Scheme 5). On the other hand, the Li^+ complex of **1** adopted 1:1 stoichiometry regardless of UV irradiation (Scheme 6).



Scheme 5. Photoisomerization of Na^+ complex of **1**.



Scheme 6. Photoisomerization of Li^+ complex of **1**.

3. Conclusions

In summary, the Na^+ complex of **1** showed a drastic change in the complex stoichiometry by UV irradiation. The complex stoichiometry of **1** with Na^+ was 1:2 (Na^+ : ligand) for the closed form (without UV irradiation), but it turned out to 1:1 for the open form (with UV irradiation) (Scheme 5). On the contrary, Li^+ formed 1:1 stoichiometry complexes regardless of UV irradiation (Scheme 6). This phenomenon indicates that the chromene moiety in the crowned chromenes is a unique functional group not only to show a photochromism but also to switch the complex stoichiometry of its crown ether upon UV irradiation in the presence of a metal ion. Furthermore, the chromene derivatives bearing crown ether moieties showed ion-responsive photochromism depending on the metal ion binding ability of their crown ether moieties.

4. Experimental

4.1. General

All chemicals for synthesis were of available purity and used without further purification. For spectral measurements, spectroscopic grade acetonitrile was used as a solvent, while all metal perchlorates were of the commercially highest purity.

4.2. Synthesis of chromene derivatives: general procedures

Under nitrogen atmosphere, a THF solution (20 mL) of 5-bromomethylchromene (427 mg, 1 mmol) with hydroxymethyl crown ether or non-cyclic analogue (3 mmol) was placed to a three-necked flask at room temperature. Powdered sodium hydroxide (360 mg, 9 mmol) was added, and the reaction mixture was stirred for 1 h at room temperature. Then, acetic acid (540 mg, 9 mmol) was added to the reaction mixture. The reaction mixture was poured into water and the product was extracted with chloroform. The crude product obtained by solvent evaporation was purified by gel permeation chromatography.

4.2.1. Oxymethyl-12-crown-4-chromene 1. The reaction of bromomethylchromene with hydroxymethyl-12-crown-4 by the general procedures afforded the compound in 70% yield as yellow-orange viscous oil: ^1H NMR (CDCl_3 , 400 MHz) δ 3.5–3.9 (17H, m, OCH_2), 4.81 (2H, s, PhCH_2), 6.20 (1H, d, $J=10.0$ Hz, $\text{CH}=\text{}$), 7.2–7.5 (13H, ArH, $\text{CH}=\text{}$), 7.70 (1H, d, $J=8.4$ Hz, ArH), 7.73 (1H, s, ArH), 7.93 (1H, d, $J=8.4$ Hz, ArH); IR (neat, cm^{-1}): 3019 (CH_2), 1221 (OCH_2), 752 ($\text{C}=\text{C}$); m/z 552 (M^+). Anal. Calcd for $\text{C}_{35}\text{H}_{36}\text{O}_6$: C 76.06, H 6.57, Found: C 76.15, H 6.37.

4.2.2. Oxymethyl-15-crown-5-chromene 2. The reaction of bromomethylchromene with hydroxymethyl-15-crown-5 afforded the compound in 69% yield as yellow-orange viscous oil: ^1H NMR (CDCl_3 , 400 MHz) δ 3.6–3.9 (21H, m, OCH_2), 4.82 (2H, s, PhCH_2), 6.19 (1H, d, $J=10.0$ Hz, $\text{CH}=\text{}$), 7.1–7.5 (13H, ArH, $\text{CH}=\text{}$), 7.70 (1H, d, $J=8.0$ Hz, ArH), 7.75 (1H, s, ArH), 7.91 (1H, d, $J=8.4$ Hz, ArH); IR (neat, cm^{-1}): 3019 (CH_2), 1211 (OCH_2), 769 ($\text{C}=\text{C}$); m/z 596 (M^+). Anal. Calcd for $\text{C}_{37}\text{H}_{40}\text{O}_7$: C 74.47, H 6.76, Found: C 74.28, H 6.73.

4.2.3. Oxymethyl-18-crown-6-chromene 3. The reaction of bromomethylchromene with hydroxymethyl-18-crown-6 afforded the compound in 83% yield as yellow-brown viscous oil: ^1H NMR (CDCl_3 , 400 MHz) δ 3.6–3.9 (25H, m, OCH_2), 4.82 (2H, s, PhCH_2), 6.21 (1H, d, $J=9.6$ Hz, $\text{CH}=\text{}$), 7.2–7.5 (13H, ArH, $\text{CH}=\text{}$), 7.71 (1H, d, $J=8.0$ Hz, ArH), 7.74 (1H, s, ArH), 7.94 (1H, d, $J=8.4$ Hz, ArH); IR (neat, cm^{-1}): 3019 (CH_2), 1209 (OCH_2), 727 ($\text{C}=\text{C}$); m/z 640 (M^+). Anal. Calcd for $\text{C}_{39}\text{H}_{44}\text{O}_8$: C 73.10, H 6.92, Found: C 72.93, H 6.95.

4.2.4. Non-cyclic analogue-chromene 4. The reaction of bromomethylchromene with non-cyclic analogue afforded the compound in 59% yield as yellow viscous oil: ^1H NMR (CDCl_3 , 400 MHz) δ 1.16 (3H, t, $J=7.0$ Hz, CH_3), 1.17 (3H, t, $J=6.2$ Hz, CH_3), 3.4–3.9 (17H, m, OCH_2), 4.83 (2H, s, PhCH_2), 6.20 (1H, d, $J=10.0$ Hz, $\text{CH}=\text{}$), 7.2–7.5 (13H, ArH, $\text{CH}=\text{}$), 7.71 (1H, d, $J=7.6$ Hz, ArH), 7.75 (1H, s, ArH), 7.93 (1H, d, $J=8.0$ Hz, ArH); IR (neat, cm^{-1}): 3019 (CH_2), 1221 (OCH_2), 781 ($\text{C}=\text{C}$); m/z 582 (M^+). Anal. Calcd for $\text{C}_{37}\text{H}_{42}\text{O}_6$: C 76.26, H 7.26, Found: C 76.30, H 7.24.

4.3. NMR titration

The solutions for NMR titration were prepared by solvent substitution. For the determination of binding constants

with Li⁺ and Na⁺, the concentration range of metal ions was 5–40×10⁻³ mol dm⁻³, and the concentration of the chromene derivatives were fixed on 2×10⁻² mol dm⁻³. On the other hand, the concentrations for K⁺, Rb⁺, and Cs⁺ were between 0.5–7×10⁻³ mol dm⁻³, and the concentration for the chromene derivatives were constant at 5×10⁻³ mol dm⁻³. For the Job plots, the sum of concentrations for the crowned chromenes and metal perchlorates was 4×10⁻² mol dm⁻³ for Li⁺ and Na⁺, while that was 1×10⁻² mol dm⁻³ with K⁺, Rb⁺, and Cs⁺. In order to determine the binding constants, the binding isotherms by non-linear least-square regression were applied, and the chemical shifts for the complexes were evaluated experimentally by extrapolation.

4.4. Absorption spectra measurement

Absorption spectra measurement was carried out using acetonitrile as the solvent at room temperature. The absorption spectra before UV irradiation were taken after allowing a measuring solution to stand overnight under dark condition. The absorption spectra measurements after UV irradiation were carried out after photoirradiation for 3 min, while irradiating the UV light on the measurement cell in the perpendicular direction to the measuring incident light. The UV light (525 mW/cm²), obtained by passing light of a 200-W Hg–Xe lamp through a light filter (central wavelength; 363 nm, half width; 9.5 nm, transmittance 0.53), was introduced to the cell compartment of a spectrophotometer by using a glass fiber guide and was irradiated on the quartz cell containing a solution. The concentrations for the chromene derivatives and alkali metal perchlorates were 1×10⁻⁴ and 5×10⁻⁴ mol dm⁻³, respectively. In the case of alkaline-earth metal perchlorates, the concentration was 1×10⁻⁴ mol dm⁻³. For the Job plots, the sum of concentrations for the crowned chromenes and metal perchlorates was 1×10⁻⁴ mol dm⁻³.

Acknowledgements

We are very much indebted to Japan Society for Promotion of Science (JSPS) for the financial support of this work by a Grant-in-Aid for JSPS fellows. Also, financial support by a Grant-in-Aid for Scientific Research (B) (No. 15350043) from the Ministry of Education, Culture, Sports, Science, and Technology, Japan is gratefully acknowledged.

References and notes

- Organic photochromic and thermochromic compounds*; Crano, J. C., Guglielmetti, R. J., Eds.; Kluwer Academic/Plenum: New York, 1999; Vols. 1 and 2.
- (a) Shinkai, S.; Nakaji, T.; Ogawa, T.; Shigematsu, K.; Manabe, O. *J. Am. Chem. Soc.* **1981**, *103*, 111–115. (b) Shinkai, S.; Ogawa, T.; Kusano, Y.; Manabe, O.; Kikukawa, K.; Goto, T.; Matsuda, T. *J. Am. Chem. Soc.* **1982**, *104*, 1960–1967. (c) Shinkai, S.; Minami, T.; Kusano, Y.; Manabe, O. *J. Am. Chem. Soc.* **1982**, *104*, 1967–1972. (d) Shinkai, S.; Minami, T.; Kusano, Y.; Manabe, O. *J. Am. Chem. Soc.* **1983**, *105*, 1851–1856. (e) Shinkai, S.; Miyazaki, K.; Manabe, O. *J. Chem. Soc., Perkin Trans. 1* **1987**, 449–456. (f) Shinkai, S.; Shigematsu, K.; Sato, M.; Manabe, O. *J. Chem. Soc., Perkin Trans. 1* **1982**, 2735–2739. (g) Shinkai, S.; Ishihara, M.; Ueda, K.; Manabe, O. *J. Chem. Soc., Perkin Trans. 2* **1985**, 511–518. (h) Wei, W.; Tomohiro, T.; Kodaka, M.; Okuno, H. *J. Org. Chem.* **2000**, *65*, 8979–8987.
- Takeshita, M.; Irie, M. *J. Org. Chem.* **1998**, *63*, 6643–6649.
- (a) Sasaki, H.; Ueno, A.; Anzai, J.; Osa, T. *Bull. Chem. Soc. Jpn* **1986**, *59*, 1953–1956. (b) Inouye, M.; Akamatsu, K.; Nakazumi, H. *J. Am. Chem. Soc.* **1997**, *119*, 9160–9165. (c) Inouye, M.; Noguchi, Y.; Isagawa, K. *Angew. Chem. Int. Ed. Engl.* **1994**, *33*, 1163–1166. (d) Inouye, M.; Ueno, M.; Kitao, T. *J. Org. Chem.* **1992**, *57*, 1639–1641. (e) Kimura, K.; Yamashita, T.; Yokoyama, M. *J. Phys. Chem.* **1992**, *96*, 5614–5617. (f) Kimura, K.; Yamashita, T.; Yokoyama, M. *J. Chem. Soc., Perkin Trans. 2* **1992**, 613–619. (g) Kimura, K.; Kado, S.; Sakamoto, H.; Sakai, A.; Yokoyama, M.; Tanaka, M. *J. Chem. Soc., Perkin Trans. 2* **1999**, 2538–2544. (h) Kimura, K.; Teranishi, T.; Yokoyama, M.; Yajima, S.; Miyake, S.; Sakamoto, H.; Tanaka, M. *J. Chem. Soc., Perkin Trans. 2* **1999**, 119–204.
- (a) Inouye, M.; Ueno, M.; Tsuchiya, K.; Nakayama, N.; Konishi, T.; Kitao, T. *J. Org. Chem.* **1992**, *57*, 5377–5383. (b) Fedorova, O. A.; Gromov, S. P.; Pershina, Y. V.; Sergeev, S. S.; Strokach, Y. P.; Barachevsky, V. A.; Alifimov, M. V.; Pepe, G.; Samat, A.; Guglielmetti, R. *J. Chem. Soc., Perkin Trans. 2* **2000**, 563–570. (c) Kimura, K.; Kaneshige, M.; Yamashita, T.; Yokoyama, M. *J. Org. Chem.* **1994**, *59*, 1251–1256.
- Ahmed, S. A.; Tanaka, M.; Ando, H.; Kimura, K. *Eur. J. Org. Chem.* **2003**, 2437–2442.
- Ahmed, S. A.; Tanaka, M.; Ando, H.; Kimura, K. *Tetrahedron* **2003**, *59*, 4135–4142.
- (a) Samat, A.; Lokshin, V.; Chamontin, K.; Levi, D.; Pepe, G.; Guglielmetti, R. *Tetrahedron* **2001**, *57*, 7349–7359. (b) Chamontin, K.; Lokshin, V.; Rossollin, V.; Samat, A.; Guglielmetti, R. *Tetrahedron* **1999**, *55*, 5821–5830.
- Binding constants*; Connors, K. A., Ed.; Wiley-Interscience: New York, 1987.
- (a) Reichardt, C. *Chem. Rev.* **1994**, *94*, 2319–2358. (b) Pozzo, J.; Samat, A.; Guglielmetti, R.; Dubest, R.; Aubard, J. *Helv. Chim. Acta* **1997**, *80*, 725–738. (c) Pozzo, J.; Lokshin, V.; Samat, A.; Guglielmetti, R.; Dubest, R.; Aubard, J. *J. Photochem. Photobiol. A: Chem.* **1998**, *114*, 185–191.
- (a) Berthet, J.; Delbaere, S.; Levi, D.; Samat, A.; Guglielmetti, R.; Vermeersch, G. *Photochem. Photobiol. Sci.* **2002**, *1*, 665–672. (b) It has been reported that several isomers for the open form are possible in the case of chromene. See Ref. 1 (Vol. 1, chapter 3).
- (a) Tanaka, M.; Ikeda, T.; Xu, Q.; Ando, H.; Shibutani, Y.; Nakamura, M.; Sakamoto, H.; Yajima, S.; Kimura, K. *J. Org. Chem.* **2002**, *67*, 2223–2227. (b) Tanaka, M.; Nakamura, M.; Salhin, A. M. A.; Ikeda, T.; Kamada, K.; Ando, H.; Shibutani, Y.; Kimura, K. *J. Org. Chem.* **2001**, *66*, 1533–1537. (c) Salhin, A. M. A.; Tanaka, M.; Kamada, K.; Ando, H.; Ikeda, T.; Shibutani, Y.; Yajima, S.; Nakamura, M.; Kimura, K. *Eur. J. Org. Chem.* **2002**, 655–662.
- Bühlmann, P.; Pretsch, E.; Bakker, E. *Chem. Rev.* **1998**, *98*, 1593–1687.
- Tanaka, M.; Kamada, K.; Ando, H.; Kitagaki, K.; Shibutani, Y.; Kimura, K. *J. Org. Chem.* **2000**, *65*, 4342–4347.
- (a) Pedersen, C. J.; Frensdorff, H. K. *Angew. Chem.* **1972**, *84*, 16–26. (b) Popov, A. I.; Lehn, J. M. In *Coordination*

- chemistry of macrocyclic compounds*; Nelson, G. A., Ed.; Plenum: New York, 1979. (c) Weber, E.; Vögtle, F. In *Host-guest complex chemistry: macrocycles*; Vögtle, F., Weber, E., Eds.; Springer: Berlin, 1985.
16. (a) Pedersen, C. J. *J. Am. Chem. Soc.* **1970**, *92*, 386–391. (b) Frensdorff, H. K. *J. Am. Chem. Soc.* **1971**, *93*, 600–606. (c) Bourgoin, M.; Wong, K. H.; Hui, J. Y.; Smid, J. *J. Am. Chem. Soc.* **1975**, *97*, 3462–3467. (d) Kimura, K.; Tsuchida, T.; Maeda, T.; Shono, T. *Talanta* **1980**, *27*, 801–805.
17. Allcock, H. R.; Olmeijer, D. L.; O'Connor, S. J. M. *Macromolecules* **1998**, *31*, 753–759.
18. (a) Wall, S. L. D.; Meadows, E. S.; Barbour, L. J.; Gokel, G. W. *Chem. Commun.* **1999**, 1553–1554. (b) Meadows, E. S.; Wall, S. L. D.; Barbour, L. J.; Gokel, G. W. *Chem. Commun.* **1999**, 1555–1556. (c) Meadows, E. S.; Wall, S. L. D.; Barbour, L. J.; Fronczek, F. R.; Kim, M.; Gokel, G. W. *J. Am. Chem. Soc.* **2000**, *122*, 3325–3335. (d) Meadows, E. S.; Wall, S. L. D.; Barbour, L. J.; Gokel, G. W. *J. Am. Chem. Soc.* **2001**, *123*, 3092–3107. (e) Hu, J.; Barbour, L. J.; Gokel, G. W. *J. Am. Chem. Soc.* **2001**, *123*, 9486–9487. (f) Hu, J.; Barbour, L. J.; Gokel, G. W. *Chem. Commun.* **2002**, 1808–1809. (g) Hu, J.; Barbour, L. J.; Ferdani, R.; Gokel, G. W. *Chem. Commun.* **2002**, 1810–1811.
19. (a) Inouye, M.; Hyodo, Y.; Nakazumi, H. *J. Org. Chem.* **1999**, *64*, 2704–2710. (b) Wall, S. L. D.; Meadows, E. S.; Barbour, L.; Gokel, G. W. *J. Am. Chem. Soc.* **1999**, *121*, 5613–5614. (c) Bartoli, S.; Roelens, S. *J. Am. Chem. Soc.* **1999**, *121*, 11908–11909.

An efficient phosphine-free palladium coupling for the synthesis of new 2-arylbenzo[*b*]thiophenes

Jérémie Fournier Dit Chabert, Lionel Joucla, Emilie David and Marc Lemaire*

Laboratoire de Catalyse et Synthèse Organique, Université Claude Bernard Lyon 1, UMR 5181, Bât 308 CPE, 43 Bd. Du 11 Novembre 1918, 69616 Villeurbanne Cedex, France

Received 23 October 2003; revised 3 February 2004; accepted 9 February 2004

Abstract—Straightforward and rapid access to 2-arylbenzo[*b*]thiophenes has been developed. It involved a catalytic coupling of 3-activated benzo[*b*]thiophenes with several aryl halides in the presence of a phosphine-free palladium system. In case of fragile functional groups such as aldehydes, a quaternary ammonium was used as an additive as with the other substrates, the coupling performed better and faster in the presence of a crown ether, the best one being DCH-18-C-6, with good yields and low reaction times. This method would provide a direct access to novel structures of biological interest.

© 2004 Elsevier Ltd. All rights reserved.

1. Introduction

The benzo[*b*]thiophene core was found to be present in several drug candidates, exhibiting some interesting biological properties, e.g. antipsychotic,¹ antiinflammatory,² antiallergic,³ antithrombotic-fibrinolytic⁴ and herpes virus inhibitor.⁵

A particular interest was given to 2-arylbenzo[*b*]thiophenes for the treatment of various cancers. Indeed, some derivatives were found to be potent selective estrogen receptor modulators (SERMs)⁶—the most famous of which being Raloxifene and Arzoxifene (Fig. 1)—also used as antitubulin agents.^{7,8}

The recent interest to this class of compounds lead to the investigation of new synthetic routes to substituted benzo[*b*]thiophenes. An intramolecular cyclisation from substituted thiobenzyls was generally used, according to the procedure described by Kost.⁹ However, this method, which involved two steps, one basic and the following acidic, proved to be non-regioselective and was not compatible with acid or base sensitive functional groups. Thus, other methods were developed, starting from thiobenzyl¹⁰ or thioanisole¹¹ derivatives. Recently, Flynn et al. described an efficient synthesis of 2,3-disubstituted benzo[*b*]thiophenes with tubulin binding activity.¹² However, even if the synthetic path afforded the desired products in high yields, no more than seven steps were required. Consequently,

catalytic routes were investigated for direct access to 2-arylbenzo[*b*]thiophenes. For instance, Sall¹³ and Samat¹⁴ have synthesised some of these derivatives by Suzuki coupling.¹⁵

We focused on a method allowing the direct arylation of benzo[*b*]thiophenes. On the contrary to the usual arylation methods,¹⁶ of the Stille,¹⁷ Kumada¹⁸ and Suzuki-type,¹⁵ which all involve a regioselective halogenation of the substrate and the use of an organometallic reagent prior to the coupling, the ‘Heck-type’ coupling is carried out in one single step. Indeed, Miura¹⁹ and Otha²⁰ previously managed to arylate benzo[*b*]thiophene selectively in moderate yields with palladium, triphenylphosphine and, for the first one, an over stoichiometric (i.e. 2 equiv.) amount of copper iodide.

We have recently reported the direct arylation of 3-substituted benzo[*b*]thiophenes²¹ based on the improvements of a catalytic coupling previously developed on thiophene derivatives.^{22,23}

It involved the use of a system based on Pd(OAc)₂, *n*-Bu₄NBr, an inorganic base (K₂CO₃) in a polar aprotic solvent, DMF being the most suitable.²⁴ In this paper, we will describe the extensions of this method as well as some improvements achieved in order to develop an easy parallel

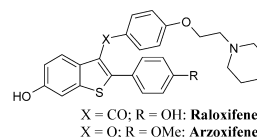


Figure 1.

Keywords: Benzo[*b*]thiophene; Heck-type aryl coupling; Palladium catalysis.

* Corresponding author. Tel.: +33-4-72-44-82-09; fax: +33-4-72-43-14-08; e-mail address: marc.lemaire@univ-lyon1.fr

synthesis of valuable new benzo[*b*]thiophene derivatives for biological studies.

2. Results and discussion

2.1. Synthesis of the starting materials

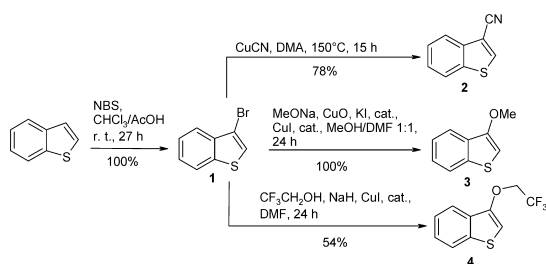
The 3-bromobenzo[*b*]thiophene **1** was quantitatively and selectively synthesised by direct bromination of benzo[*b*]thiophene with *N*-bromosuccinimide under acidic conditions, according to a procedure described by Kellogg.²⁵ Then, a nucleophilic aromatic substitution with copper cyanide²⁶ afforded benzo[*b*]thiophene-3-carbonitrile **2** in 78% yield. Similarly, according to a procedure previously described by our group,²⁷ 3-methoxybenzo[*b*]thiophene **3** and 3-(2,2,2-trifluoroethoxy)-benzo[*b*]thiophene **4** were synthesised in 100 and 54% yields, respectively (Scheme 1).

2.2. Coupling studies and improvements

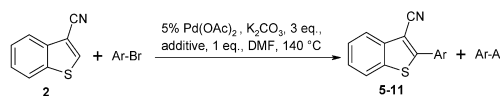
The following Heck-type coupling required an aromatic halide and a catalytic system based on palladium salt. We have previously described this coupling with a system based on the use of 5% of palladium diacetate, a stoichiometric amount of tetra-*n*-butylammonium bromide, an excess of potassium carbonate in DMF (Scheme 2).²¹

The reaction conditions have already been studied a few years ago by our group.²⁴ Among species of Pd⁽⁰⁾ and Pd^(II), Pd(OAc)₂ was found to give the best yields. Following the Jeffery conditions,²⁸ we also used a quaternary ammonium additive which enhanced the reaction rates and improved the yields, although the nature of its effect was not proved (formation of a very reactive palladium complex, better homogenisation of the reactants?). Amatore and Jutand have reported²⁹ that the quaternary ammonium would increase the salinity of the mixture. Palladium species may then be stabilised by halide ions.

It was also reported that the whole catalytic system only slightly differed from the one used for the Ullmann³⁰ catalytic coupling by the nature of the base (potassium carbonate instead of diisopropylethylamine).³¹ Therefore, various amounts of biaryl product (Ar–Ar) could be obtained. In addition, supposing that the basicity would affect the conversion and the reaction rate, the quaternary ammonium was replaced by a crown ether, that of being dicyclohexyl-18-crown-6 (DCH-18-C-6). We used four different phenyl bromides, three of them bearing a chlorine atom at different positions and one bearing a cyano group at the *ortho* position (Table 1).



Scheme 1.



Scheme 2.

In most cases, better conversions (and also better isolated yields) were observed in the case of the additive being the crown ether. The reaction was found in all cases to be more selective towards the formation of the biaryl by-products and, especially in the case of 2-bromobenzonitrile (entry 4), the reaction was much faster.

We then performed this coupling on a heteroaryl halide, the first one being 2-bromopyridine (Table 2 entries 1–5). We assumed that this substrate would relatively be non-reactive due to its tendency to easily form 2,2'-bipyridine as previously observed during the Ullmann coupling.³¹ Although little selective, the Heck-type coupling performed to afford the major desired product **9**. Reaction times were divided by 5 when using the crown ethers (entry 2 and 3) instead of the ammonium bromide (entry 1). In addition, isolated yields were improved as well as the selectivity towards the biaryl formation, DCH-18-C-6 being more efficient than 18-C-6. In order to prevent from the use of a toxic solvent, DMF could also be replaced by DMSO (entry 4 and 5).

The reaction was found to perform slightly faster with similar yields and this, even with 0.1 equiv. of DCH-18-C-6 (entry 5). However, moderate yields (i.e. 45%) were still obtained with this substrate, mainly due to the low selectivity of the reaction. In addition, the use of DMSO sometimes involved the degradation of the nitrile function into the corresponding amide therefore decreasing the efficiency of the catalytic system.

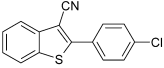
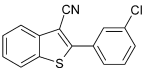
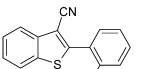
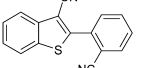
Some improvements were observed with 3-bromopyridine and 3-bromoquinoline (Table 2 entries 6–10). The replacement of the quaternary ammonium by DCH-18-C-6 dramatically enhanced the reaction rate (entries 7 and 10). However, in the case of 3-bromopyridine, DMF proved to be the best solvent giving a better reaction rate, selectivity and isolated yield (entries 7 and 8). At last, the use of DCH-18-C-6 instead of *n*-Bu₄NBr with 3-bromoquinoline (entries 9 and 10) afforded similar isolated yields but with a lower reaction time, a better selectivity and thus a straightforward purification.

The use of DCH-18-C-6 appeared to be particularly attractive with benzo[*b*]thiophene **2**, giving better yields with short reaction times. DMSO could be used as a solvent in replacement of DMF if the substrates did not degrade themselves under these conditions.

2.3. Effect of the substituent at position 3

As for a comparison between benzo[*b*]thiophenes bearing different functional groups at the position 3, we used a catalytic system which involved the use of 5% of palladium diacetate, in the presence of tetra-*n*-butylammonium bromide and an excess of potassium carbonate. Indeed, benzo[*b*]thiophene-3-carboxaldehyde (commercially

Table 1. Coupling studies on benzo[*b*]thiophene **2**. Influence of the additive

Entry	Product	Additive	Time (h)	Conversion (isolated yield) (%)	Selectivity Pdct/Ar–Ar
1		<i>n</i> -Bu ₄ NBr	1.5	98 (69)	10
		DCH-18-C-6	1.5	93 (68)	30
2		<i>n</i> -Bu ₄ NBr	2.5	99 (72)	5
		DCH-18-C-6	2	100 (76)	30
3		DCH-18-C-6	1.5	96 (73)	>50
4		<i>n</i> -Bu ₄ NBr	48	88 (44)	14
		DCH-18-C-6	2	100 (63)	>50

Typical procedure: see Section 4 procedures A and B.

available) was rapidly degrading in the presence of DCH-18-C-6, yielding non substituted benzo[*b*]thiophene by decarbonylation, hence the use of the ammonium salt. The coupling with 4-iodoanisole was then performed on 6 substituted benzo[*b*]thiophenes (Scheme 3, Table 4).

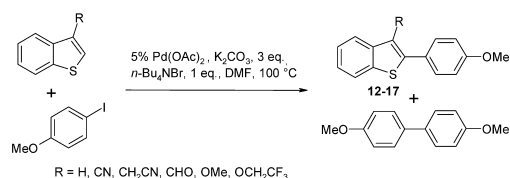
Unexpectedly, only benzo[*b*]thiophenes bearing either a mesomeric donating (OCH₃, OCH₂CF₃) or withdrawing (CHO, CN) group gave significant results in an acceptable reaction time (1–2 days). Non-substituted benzo[*b*]thiophene (entry 1) and the 3-acetonitrile one both showed a low

conversion and a poor selectivity towards the biaryl by-product (Table 3).

It was therefore reasonable to assume that an activation of the C2–C3 double bond was required and may enhance the reactivity of the benzo[*b*]thiophene in different parts of the catalytic cycle (see Section 2.6 for mechanistic considerations).

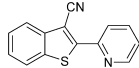
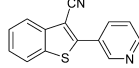
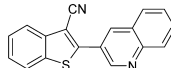
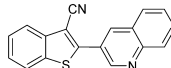
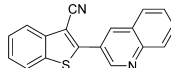
2.4. Effect of the nature of the halide

It is generally admitted for the Heck³² and the Ullmann³⁰ reactions that the reactivity of the halide was the following: I>Br>Cl>F. As in the case of compounds **5**, **6**, **7** (Table 1) only a few traces of the product, where a substitution of the chlorine occurred, were detected by GC/MS, we reckoned that aryl chlorides were not reactive enough in our conditions.

**Scheme 3.**

We therefore compared the difference of reactivity of two

Table 2. Coupling studies on benzo[*b*]thiophene **2**. Influence of the additive and the solvent

Entry	Product	Additive	Solvent	Time (h)	Conversion (isolated yield) (%)	Selectivity Pdct/Ar–Ar
1		<i>n</i> -Bu ₄ NBr	DMF	96	56 (27)	0.6
		18-C-6	DMF	20	87 (35)	2
		DCH-18-C-6	DMF	20	89 (44)	2
		DCH-18-C-6	DMSO	17	100 (47)	3
		DCH-18-C-6 ^(a)	DMSO	15	98 (46)	2
6		<i>n</i> -Bu ₄ NBr	DMF	120	98 (41)	>50
		DCH-18-C-6	DMF	3	92 (57)	>50
8		DCH-18-C-6 ^(a)	DMSO	15	96 (52)	20
9		<i>n</i> -Bu ₄ NBr	DMF	72	100 (67)	5
10		DCH-18-C-6	DMF	7	95 (67)	>50

Typical procedure: see Section 4 procedures A, B and C. (a) DCH-18-C-6=0.1 equiv.

Table 3. Effect of the substituent at position 3

Entry	R	Pdct	Time (h)	Conversion (isolated yield)	Selectivity Pdct/Ar–Ar
1	H	12	48	15	0.6
2	CN	13	20	86 (66)	3.5
3	CH ₂ CN	14	48	12	1.2
4	CHO	15	24	82 (50)	2.8
5	OCH ₃	16	28	95 (61)	3.5
6	OCH ₂ CF ₃	17	48	98 (66)	11

aryl bromides with their corresponding iodides in the presence of benzo[*b*]thiophene-3-carboxaldehyde under the conditions cited above on Scheme 3 (Table 4). Unexpectedly, aryl bromides were found to react faster and more selectively than their iodine analogues. As a consequence, isolated yields were also much better, partly due to the ease of the separation. Indeed, with aryl iodides, the palladium specie underwent a rapid oxidative addition. Then we assumed that a second oxidative addition of Ar-I occurred, preventing the benzo[*b*]thiophene to react with the Ar-Pd-X specie. Thus the major product of the reaction was the biaryl compound and not the desired 2-arylbenzo[*b*]thiophene.

Aryl bromides were therefore employed rather than their iodides analogues and also due to their better availability and cheaper cost.

2.5. Coupling studies on benzo[*b*]thiophene-3-carboxaldehyde

Benzo[*b*]thiophene-3-carboxaldehyde was thus coupled with various aryl bromides with the conditions cited above on Scheme 3. Products of arylation were formed in acceptable reaction times (3–48 h) with a good selectivity (Table 5).

It was remarkable that isolated yields were not affected by the steric hindrance of cyano and nitro groups at *ortho* position in spite of longer reaction times than their *para* substituted analogues (entries 1–3). We also noticed that the nature of the substituent on the aryl had almost no effect, the coupling being as efficient with electron-donating groups such as OMe (Table 4, entry 1) as with electron-withdrawing groups such as CN or NO₂ (Table 5 entries 1–3). However, the purification of compound **21** (entry 3) proved to be tedious hence yielding lower quantities of the desired compound. Finally, although the reaction time was longer than with other substrates, a quite good yield was obtained

with 3-bromoquinoline (entry 5) with the same observed selectivity as with benzo[*b*]thiophene-3-carbonitrile (Table 2, entry 9).

2.6. Coupling studies on electron-rich benzo[*b*]thiophenes **3** and **4**

We have already described²¹ the syntheses of some 2-arylbenzo[*b*]thiophenes derived from the 3-methoxy substituted compound **3** (see entry 1 and 2 of Table 6 as examples). The coupling reaction was carried out at 100 °C as higher temperatures did not give better results. It was performed on **3** with other aryl halides, such as 2-bromotoluene (entries 3–4) and 3-bromoquinoline (entry 5). Similarly as observed with benzo[*b*]thiophene-3-carbonitrile, the use of DCH-18-C-6 in replacement of the ammonium bromide dramatically decreased the reaction time and, in parallel, improved the yields from 42 to 75%. Good yield and selectivity were also obtained with 3-bromoquinoline when using DCH-18-C-6 (entry 5).

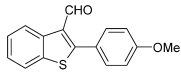
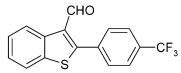
Compound **4**, 3-(2,2,2-trifluoroethoxy)benzo[*b*]thiophene also reacted rapidly with excellent selectivities and good yields (entries 6 and 7). The *ortho*-substituted bromobenzonitrile even gave the coupled compound **29** within only 45 min (entry 7). However, it was noticed for electron-rich benzo[*b*]thiophenes that the conversion often stopped before being complete (entries 2, 3, 5 and 6). Indeed, the catalytic system was apparently less stable than with electron-poor benzo[*b*]thiophenes, as traces of palladium 'black' were observed after only a few hours. Therefore, we assumed that the catalytic cycle was different depending on the nature of the benzo[*b*]thiophene.

2.7. Catalytic cycle

It is noteworthy to outline that no conversion was observed with the benzo[*b*]thiophene-2-carbonitrile (synthesised via the 2-iodobenzo[*b*]thiophene according to the method described by Gaertner³³). We reckon that a preliminary complexation of the palladium by the sulfur atom may lead the organometallic complex close to the position 2. In addition, the sulfur atom would probably stabilise a possible positive charge at position 2.

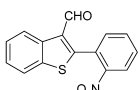
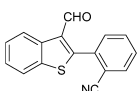
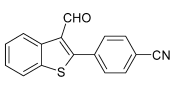
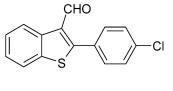
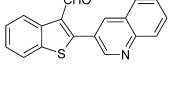
Considering the catalytic scheme generally admitted for the Heck reaction,³² a Pd⁽⁰⁾ complex undergoes an oxidative addition by the aryl halide. The complex may be formed in situ from several oxidised palladium species, the most

Table 4. Influence of the nature of the halide on the coupling

Entry	Product	Halide	Time (h)	Conversion (isolated yield) (%)	Selectivity Pdct/Ar–Ar
1		I	24	82 (50)	2.8
		Br	4	99 (64)	9
2		I	16	53 (21)	0.5
		Br	3	99 (70)	10

Typical procedure: see Section 4 procedure A.

Table 5. Coupling studies on benzo[*b*]thiophene-3-carboxaldehyde

Entry	Product	Time (h)	Conversion and (isolated yield) (%)	Selectivity Pdct/Ar–Ar
1		18	99 (56)	7
2		20	99 (54)	18
3		3	95 (41)	7
4		5	98 (58)	8
5		48	86 (52)	5

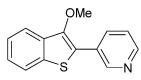
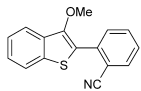
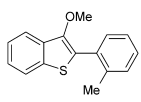
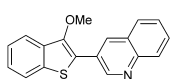
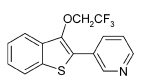
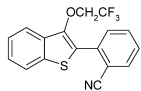
Typical procedure: see Section 4 procedure A.

occurring one being Pd(OAc)₂/PPh₃.²⁰ In our case, a phosphine free system was used. Recently, Yao et al. proposed a mechanism of the Heck reaction for a phosphine free system based on palladium diacetate and K₃PO₄.³⁴ However, this mechanism could not be generalised to our system as their cycle made no difference on the nature of the olefin and therefore could not explain the lack of reactivity observed with benzo[*b*]thiophene and benzo[*b*]thiophene-3-acetonitrile (Table 3, entries 1 and 3). In addition, as in each reaction little quantities of benzo[*b*]thiophene dimer were isolated, we assumed that the reducing agent was the substrate itself, hence the gap between the conversion and the isolated yield. Indeed, Itahara³⁵ used palladium diacetate for direct aromatic arylation, yielding biaryls and

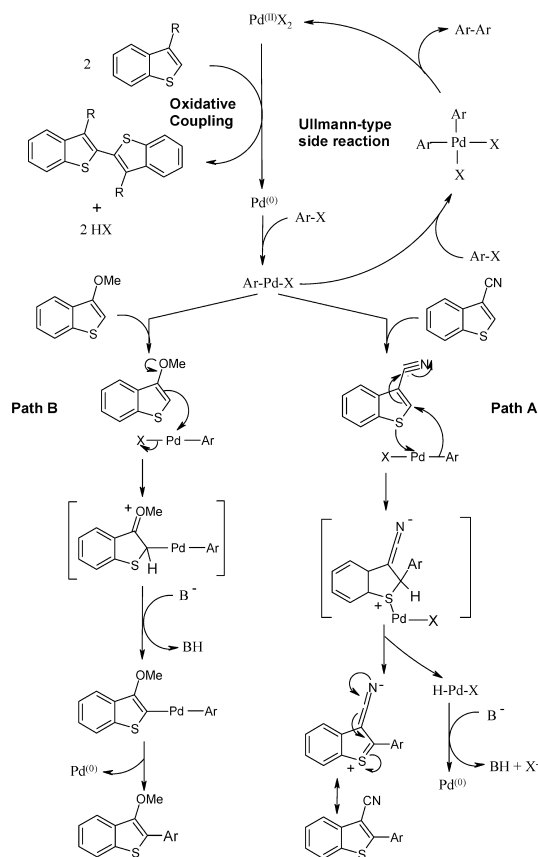
palladium zero-valent. Thus it was noticed that, for most of the substrates, the better the selectivity between the main catalytic cycle and the Ullmann side reaction, the better the isolated yield. Indeed, the Ullmann path¹⁶ generated some Pd^(II) which should then be reduced by the substrate, hence lowering the yield.

It is reasonable to assume that there were two different mechanisms depending on the nature of the R group at position 3. For instance, Sharp et al. proposed³⁶ two different paths about the arylation at positions 2 or 5 of 3-carboalkoxy furan and thiophen. Similarly, we suppose that, in the case of R being a withdrawing group, the Ar-Pd-X specie would undergo a preliminary complexation from

Table 6. Coupling studies on benzo[*b*]thiophenes **3** and **4**

Entry	Substrate	Procedure	Product	Time (h)	Conversion and (isolated yield) (%)	Selectivity Pdct/Ar–Ar
1	3	A		24	95 (66)	>50
2	3	A		25	92 (69)	25
3	3	A		26	71 (42)	>50
4	3	B		27	93 (62)	20
5	4	B		28	91 (59)	>50
6	4	B		29	99 (76)	>50

Typical procedure: see Section 4 procedures A and B.



Scheme 4.

the sulfur atom, followed by an insertion of the aryl at position 2. The resulting complex would then undergo a β -H elimination to yield the desired 2-arylbenzo[*b*]thiophene and a H-Pd-X specie which is then regenerated into Pd⁽⁰⁾ by the base (Scheme 4, path A).

In the case of R being a donating group, the mechanism is analogous to the one recently proposed by Miura.³⁷ The electron-rich benzo[*b*]thiophene would first undergo an addition on the Ar-Pd-X specie. Then the base would eliminate the proton at position 2, hence regenerating the C2–C3 double bond. Finally, a reductive elimination would yield the desired compound and regenerate the catalyst (Scheme 4, path B).

3. Conclusion

In conclusion, we have shown that Pd(OAc)₂, in combination with K₂CO₃ and DCH-18-C-6 in either DMF or DMSO can be an efficient system for direct access to 2-arylbenzo[*b*]thiophenes. The reaction performed with both electron donating and electron withdrawing substituents on aryl bromides in the absence of any supplementary stabilising ligands such as phosphines. In addition, although only benzo[*b*]thiophenes bearing an electron-withdrawing group or an electron-donating group at position 3 reacted, this system provided new interesting structures which diversity will constitute a pool of building blocks for a library of new drugs.

4. Experimental

4.1. General

The experimental details for the synthesis and the physical chemical data for compounds **6**, **13**, **24** and **25** have already been described in Ref. 21. Compound **16** has been described in Ref. 10.

Reactants and solvents have been supplied by Acros, Aldrich, Alfa Aesar, Fluka and Lancaster. TLCs were performed with Merck 60 F₂₅₄ silica gel plates. Flash chromatographies were performed with Merck Si 60 (40–63 μ m) silica. Gas chromatographies were performed with Shimadzu GC-14A models with an apolar column and a flame ionisation detector and with the following programming: 100 °C (1 min) then +10 °C/min then 300 °C (1 min). Mass spectra were performed with a GC/MS FISIONS INSTRUMENT MD 800 with the same temperature program as described above. NMR spectra were performed on either a Bruker AMX 300 (¹H: 300 MHz; ¹³C: 75 MHz) or a Bruker DPX 500, 500 MHz. Elemental analyses were made by the 'Service Central d'Analyse du CNRS' (Solaize, France). Melting points were measured on a Köfler bench.

4.1.1. 3-Bromo-benzo[*b*]thiophene 1. To a solution of benzo[*b*]thiophene (10 g; 74.5 mmol) in chloroform (75 mL) and acetic acid (75 mL), was added stepwise *N*-bromosuccinimide (16.6 g; 93.1 mmol) for 4 h at 0 °C and then allowed to stir at room temperature for 24 h. Then chloroform (30 mL) was added and the resulting mixture was successively washed with a saturated sodium thiosulfate solution (200 mL), a saturated sodium carbonate solution (200 mL) and water (150 mL). The extracted organic layer was then dried over MgSO₄, filtered and evaporated. The resulting red liquid was then filtered of a pad of silica, eluting with cyclohexane to afford **1** as a yellow oil (15.87 g, 100%); δ_{H} (300 MHz, CDCl₃) 7.43 (ddd, 1H, *J*=1.5, 7.4, 8.1 Hz), 7.45 (s, 1H), 7.49 (ddd, 1H, *J*=1.1, 7.4, 7.7 Hz), 7.85 (m, 2H) ppm; *m/z* 214 (100), 212 (90), 133 (50), 89 (70).

4.1.2. Benzo[*b*]thiophene-3-carbonitrile 2. A solution of 3-bromobenzo[*b*]thiophene **1** (15 g; 70.4 mmol), copper cyanide (7.7 g; 84 mmol) in dry dimethylacetamide (100 mL) was heated under reflux for 3 days under argon atmosphere. The mixture was diluted with ethylene diamine (35 mL) and water (70 mL) and extracted with dichloromethane (6×100 mL). The organic phase was successively washed with a 10% solution of sodium cyanide (2×100 mL), brine (100 mL) and water (100 mL), then dried over MgSO₄, filtered and evaporated. The brown crude mixture was filtered over a short pad of silica, eluting with cyclohexane, to afford **2** as a white crystalline powder (5.5 g, 78%); mp 71–72 °C; *R*_f 0.3 (silica, cyclohexane/AcOEt 90:10); δ_{H} (300 MHz, CDCl₃) 7.48 (ddd, 1H, *J*=1.1, 7.0, 7.0 Hz), 7.53 (ddd, 1H, *J*=1.1, 7.0, 7.0 Hz), 7.91 (ddd, 1H, *J*=0.7, 1.1, 7.0 Hz), 8.00 (ddd, 1H, *J*=0.7, 1.1, 7.0 Hz), 8.14 (s, 1H); δ_{C} (75 MHz, CDCl₃) 107.2 (C), 114.4 (CN), 122.6 (CH), 122.9 (CH), 126.1 (CH), 126.3 (CH), 137.3 (C), 137.6 (CH), 138.6 (C) ppm; *m/z* 159 (100), 132 (10).

4.1.3. 3-Methoxy-benzo[*b*]thiophene 3. To a solution of **1** (4.45 g; 20.9 mmol) in methanol (40 mL), was added sodium methoxyde (11.26 g; 209 mmol), copper oxide (835 mg; 10.5 mmol), KI (50 mg; 0.24 mmol), CuI (80 mg; 0.4 mmol) and DMF (50 mL) and then was refluxed for 24 h. The mixture was hydrolysed by water (40 mL), filtered and then DCM (70 mL) was added. The mixture was successively washed with a saturated solution of ammonium chloride (100 mL), a saturated sodium thiosulfate solution (2×100 mL) and water (100 mL). The extracted organic layer was then dried over MgSO₄, filtered and evaporated. The resulting red liquid was then purified by flash chromatography, eluting with cyclohexane to afford **3** as a pale yellow oil (3.48 g, 100%); *R_f* 0.5 (silica, cyclohexane/AcOEt 95:5); δ_H (300 MHz, CDCl₃) 3.96 (s, 3H, OCH₃), 6.28 (s, 1H), 7.33–7.38 (m, 2H), 7.74–7.80 (m, 2H); δ_C (75 MHz, CDCl₃) 57.6 (CH₃), 95.9 (CH), 121.3 (CH), 123.2 (CH), 124.1 (CH), 125.6 (CH), 132.5 (C), 138.2 (C), 152.3 (C) ppm; *m/z* 164 (70), 149 (100), 121 (60).

4.1.4. 3-(2,2,2-Trifluoroethoxy)benzo[*b*]thiophene 4. In a round bottomed flask containing NaH (505 mg, 21 mmol) was added stepwise, at 0 °C under argon, a solution of 2,2,2-trifluoroethanol (1.5 mL, 21 mmol) in anhydrous DMF (4 mL). After stirring for 20 min, 3-bromobenzo[*b*]thiophene **1** (3.19 g, 15 mmol) and CuI (143 mg, 0.75 mmol) were added. The resulting mixture was refluxed for 17 h and then cooled. Dichloromethane (40 mL) was added, the mixture was filtered of a short pad of celite and then successively washed with a saturated solution of ammonium chloride (30 mL) and water (30 mL). The organic layer was dried over MgSO₄, filtered and evaporated. The crude product was then purified by flash chromatography (cyclohexane) to afford **4** as a yellow oil (1.73 g, 54%); *R_f* 0.1 (silica, cyclohexane); found C 52.25, H 2.84%; C₁₀H₇F₃OS requires C 51.72, H 3.04%; δ_H (300 MHz, CDCl₃) 4.49 (q, CH₂, *J*=8.1 Hz), 6.39 (s, 1H), 7.42 (m, 2H), 7.78 (m, 1H), 7.88 (m, 1H); δ_C (75 MHz, CDCl₃) 67.7 (q, CH₂, *J*=36 Hz), 98.8 (CH), 121.4 (CH), 123.3 (CH), 124.6 (CH), 126.1 (CH), 131.8 (C), 138.1 (C), 149.5 (C); δ_F (188 MHz, CDCl₃) -74.3 (t, 3F, *J*=8.1 Hz) ppm; *m/z* 234 (10), 232 (90), 151 (20), 149 (100).

4.2. Typical procedure A

A suspension of potassium carbonate (3.75 mmol), tetra-*n*-butylammonium bromide (1.25 mmol), substituted benzo[*b*]thiophene (1.25 mmol) and aryl halide (1.25 mmol) in *N,N*-dimethylformamide (1.25 mL) was stirred under argon at the indicated temperature for 5 min. Palladium diacetate (0.0625 mmol) was then added and the resulting mixture was allowed to stir for the time indicated, adding stepwise aryl halide (0.375 by 0.375 mmol) until no change of the chemical yield (determined by G.C). After cooling to room temperature, the mixture was filtered over Celite[®], rinsed with dichloromethane (10 mL) and then successively washed with brine (10 mL), a saturated sodium thiosulfate solution (10 mL) and water (10 mL). The organic phase was dried over MgSO₄, filtered and concentrated to give a brown residue. The latter was then purified by flash column chromatography (silica, cyclohexane/AcOEt) to afford the pure desired compound.

4.3. Typical procedure B

Same as procedure A but dicyclohexyl-18-crown-6 (1.25 mmol) was used instead of tetra-*n*-butylammonium bromide.

4.4. Typical procedure C

Same as procedure A but dicyclohexyl-18-crown-6 (0.13 mmol) was used instead of tetra-*n*-butylammonium bromide and the reaction was performed in DMSO (1.25 mL) instead of DMF.

4.4.1. 2-(4'-Chlorobenzyl)-benzo[*b*]thiophene-3-carbonitrile 5. Prepared according to procedure B. Isolated yield: 68%; white solid; mp 135–136 °C; *R_f* 0.20 (silica, cyclohexane/AcOEt 95:5); found C 66.49, H 3.06, N 5.14, S 12.00, Cl 13.00%. C₁₅H₈CINS requires C 66.79, H 2.99, N 5.19, S 11.89, Cl 13.14%; δ_H (500 MHz, CDCl₃) 7.47 (ddd, 1H, *J*=1.0, 7.4, 8.2 Hz), 7.50 (d, 2H, *J*=8.7 Hz), 7.54 (ddd, 1H, *J*=1.0, 7.4, 8.1 Hz), 7.83 (d, 2H, *J*=8.7 Hz), 7.85 (d, 1H, *J*=8.2 Hz), 7.97 (d, 1H, *J*=8.1 Hz); δ_C (75 MHz, CDCl₃) 102.9 (C), 115.3 (CN), 122.8 (CH), 123.1 (CH), 126.7 (CH), 126.8 (CH), 129.8 (2CH), 130.0 (2CH), 130.3 (C), 137.1 (C), 137.8 (C), 139.5 (C), 153.8 (C) ppm; *m/z* 271 (30), 269 (100), 233 (20).

4.4.2. 2-(2'-Chlorobenzyl)-benzo[*b*]thiophene-3-carbonitrile 7. Prepared according to procedure B. Isolated yield: 73%; pale yellow solid; m.p. 133–134 °C; *R_f* 0.15 (silica, cyclohexane/AcOEt 97:3); found C 67.06, H 2.91, N 5.20%, C₁₅H₈CINS requires C 66.79, H 2.99, N 5.19%; δ_H (500 MHz, CDCl₃) 7.41 (ddd, 1H, *J*=1.0, 7.5, 7.8 Hz), 7.46 (ddd, 1H, *J*=1.9, 7.5, 8.0 Hz), 7.51 (ddd, 1H, *J*=1.0, 7.2, 7.9 Hz), 7.54–7.60 (m, 3H), 7.89 (d, 1H, *J*=7.8 Hz), 8.01 (d, 1H, *J*=8.0 Hz); δ_C (75 MHz, CDCl₃) 107.3 (C), 114.5 (C), 122.8 (CH), 123.2 (CH), 126.5 (CH), 126.8 (CH), 127.6 (CH), 130.6 (C), 130.9 (CH), 131.9 (CH), 132.5 (CH), 134.0 (C), 138.2 (C), 139.1 (C), 152.1 (C) ppm; *m/z* 271 (10), 269 (100), 233 (70), 189 (80).

4.4.3. 2-(2'-Benzonitrile)-benzo[*b*]thiophene-3-carbonitrile 8. Prepared according to procedure B. Isolated yield: 63%; pale yellow solid; mp 191–193 °C; *R_f* 0.15 (silica, cyclohexane/AcOEt 95:5); found C 73.29, H 3.09, N 10.48%, C₁₆H₈N₂S requires C 73.82, H 3.10, N 10.76%; δ_H (300 MHz, CDCl₃) 7.54 (ddd, 1H, *J*=1.3, 7.2, 7.3 Hz), 7.60 (ddd, 1H, *J*=1.3, 7.3, 7.5 Hz), 7.66 (m, 1H), 7.77 (m, 2H), 7.88 (d, 1H, *J*=8.86 Hz), 7.92 (d, 1H, *J*=7.5 Hz), 8.03 (d, 1H, *J*=7.2 Hz); δ_C (75 MHz, CDCl₃) 107.41 (C), 113.25 (C), 114.21 (CN), 117.56 (CN), 122.96 (CH), 123.52 (CH), 126.91 (CH), 127.33 (CH), 130.90 (CH), 131.69 (CH), 133.62 (CH), 134.63 (CH), 134.94 (C), 138.38 (C), 139.07 (C), 150.09 (C) ppm; *m/z* 260 (100), 233 (10).

4.4.4. 2-(2'-Pyridine)-benzo[*b*]thiophene-3-carbonitrile 9. Prepared according to procedure C. Isolated yield: 46%; pale yellow solid; mp 170–171 °C; *R_f* 0.1 (silica, cyclohexane/AcOEt 95:5); found C 70.95, H 3.04, N 11.74%, C₁₄H₈N₂S requires C 71.16, H 3.41, N 11.86%; δ_H (300 MHz, CDCl₃) 7.36 (ddd, 1H, *J*=0.9, 4.9, 7.7 Hz), 7.47 (ddd, 1H, *J*=1.3, 7.2, 7.2 Hz), 7.52 (ddd, 1H, *J*=1.3, 7.2, 7.2 Hz), 7.85 (dd, 1H, *J*=1.9, 8.1 Hz), 7.88 (dd, 1H,

$J=1.3, 7.2$ Hz), 7.97 (dd, 1H, $J=1.3, 7.2$ Hz), 8.40 (ddd, 1H, $J=0.9, 8.1, 8.1$ Hz), 8.70 (ddd, 1H, $J=0.9, 1.5, 4.7$ Hz); δ_C (75 MHz, $CDCl_3$) 102.3 (C), 115.6 (CN), 121.6 (CH), 122.9 (CH), 123.0 (CH), 125.1 (CH), 126.5 (CH), 127.1 (CH), 137.7 (C), 138.7 (C), 139.8 (C), 150.1 (CH), 150.4 (C), 155.4 (C) ppm; m/z 236 (100), 209 (10), 78 (10).

4.4.5. 2-(3'-Pyridine)-benzo[*b*]thiophene-3-carbonitrile 10. Prepared according to procedure C. Isolated yield: 52%; yellow solid; mp 150–152 °C; R_f 0.15 (silica, cyclohexane/AcOEt 95:5); found C 71.28, H 3.54, N 11.71, S 13.69%; $C_{14}H_8N_2S$ requires C 71.16, H 3.41, N 11.86, S 13.57%; δ_H (300 MHz, $CDCl_3$) 7.43 (ddd, 1H, $J=1.3, 7.3, 8.1$ Hz), 7.45 (dd, 1H, $J=4.0, 8.1$ Hz), 7.52 (ddd, 1H, $J=1.0, 7.3, 7.5$ Hz), 7.84 (d, 1H, $J=7.5$ Hz), 7.94 (dd, 1H, $J=1.0, 8.1$ Hz), 8.21 (ddd, 1H, $J=1.6, 1.6, 8.1$ Hz), 8.73 (d, 1H, $J=4.0$ Hz), 9.06 (d, 1H, $J=1.6$ Hz); δ_C (75 MHz, $CDCl_3$) 103.9 (C), 114.9 (CN), 122.9 (CH), 123.2 (CH), 124.3 (CH), 126.8 (CH), 127.1 (CH), 128.2 (C), 135.6 (CH), 138.0 (C), 139.2 (C), 149.2 (CH), 151.0 (C), 151.6 (CH) ppm; m/z 236 (100).

4.4.6. 2-(4'-Anisyl)-benzo[*b*]thiophene-3-carboxaldehyde 15. Prepared according to procedure A. Isolated yield: 64%; pale yellow solid; mp 75–76 °C; R_f 0.4 (silica, cyclohexane/AcOEt 95:5); found C 71.34, H 4.39, O 11.88, S 11.74%; $C_{16}H_{12}O_2S$ requires C 71.62, H 4.51, O 11.93, S 11.95%; δ_H (300 MHz, $CDCl_3$) 3.87 (s, 3H, OCH_3), 6.99 (d, 2H, $J=8.8$ Hz), 7.39 (ddd, 1H, $J=0.6, 7.4, 8.1$ Hz), 7.47 (m, 1H), 7.51 (d, 2H, $J=8.8$ Hz), 7.79 (d, 1H, $J=7.9$ Hz), 8.76 (dd, 1H, $J=0.7, 7.4$ Hz), 10.05 (s, 1H, CHO); δ_C (75 MHz, $CDCl_3$) 55.9 (CH_3), 114.8 (2CH), 122.0 (CH), 124.2 (C), 125.4 (CH), 126.0 (CH), 126.6 (CH), 130.0 (C), 132.3 (2CH), 137.7 (C), 138.0 (C), 161.4 (C), 161.6 (C), 187.2 (CHO) ppm; m/z 268 (100), 267 (70), 237 (30).

4.4.7. 2-(4'-Anisyl)-3-methoxybenzo[*b*]thiophene 16. Prepared according to procedure A. Isolated yield 61%; pink solid; mp 62–64 °C; R_f 0.35 (silica, cyclohexane/AcOEt 95:5); δ_H (300 MHz, $CDCl_3$) 3.75 (s, CH_3), 3.76 (s, CH_3), 6.99 (d, 2H, $J=8.9$ Hz), 7.34 (ddd, 1H, $J=1.3, 7.3, 7.3$ Hz), 7.40 (ddd, 1H, $J=1.2, 7.3, 7.3$ Hz), 7.72–7.78 (m, 2H), 7.81 (d, 2H, $J=8.9$ Hz); δ_C (75 MHz, $CDCl_3$) 55.7 (CH_3), 61.1 (CH_3), 114.6 (2CH), 121.1 (CH), 123.1 (CH), 124.7 (CH), 125.1 (CH), 125.9 (C), 127.1 (C), 129.6 (2CH), 135.3 (C), 135.7 (C), 146.8 (C), 159.7 (C) ppm; m/z 270 (70), 255 (100), 227 (80), 212 (70), 184 (60).

4.4.8. 2-(4'-Anisyl)-3-(2,2,2-trifluoroethoxy)benzo[*b*]thiophene 17. Prepared according to procedure A. Isolated yield 66%; pink crystals; mp 78–80 °C; R_f 0.10 (silica, cyclohexane); found C 60.17, H 3.96%, $C_{17}H_{13}F_3O_2S$ requires C 60.35, H 3.87%; δ_H (300 MHz, $CDCl_3$) 3.88 (s, OCH_3), 4.23 (q, CH_2 , $J=8.4$ Hz), 7.01 (d, 2H, $J=8.9$ Hz), 7.36 (ddd, 1H, $J=1.4, 7.5, 7.9$ Hz), 7.42 (ddd, 1H, $J=1.3, 7.4, 7.5$ Hz), 7.74 (d, 2H, $J=8.9$ Hz), 7.76 (m, 2H); δ_C (75 MHz, $CDCl_3$) 55.7 (CH_3), 69.4 (q, CH_2 , $J=35.0$ Hz), 114.9 (2CH), 116.3 (C), 120.8 (CH), 123.1 (CH), 124.7 (C), 125.1 (CH), 125.5 (CH), 129.9 (2CH), 134.4 (C), 135.6 (C), 143.8 (C), 160.2 (C); δ_F (282 MHz, $CDCl_3$) –74.9 (t, 3F, $J=8.4$ Hz) ppm; m/z 340 (30), 338 (60), 255 (100).

4.4.9. 2-(4'-Benzotrifluoride)-benzo[*b*]thiophene-3-carboxaldehyde 18. Prepared according to procedure A. Isolated yield: 70%; pale brown solid; mp 96–98 °C; R_f 0.6 (silica, cyclohexane/AcOEt 95:5); found C 62.64, H 2.76, F 18.81%, $C_{16}H_9F_3OS$ requires C 62.74, H 2.96, F 18.61%; δ_H (300 MHz, $CDCl_3$) 7.48 (ddd, 1H, $J=1.2, 7.4, 8.2$ Hz), 7.55 (ddd, 1H, $J=1.0, 7.4, 8.2$ Hz), 7.72 (d, 2H, $J=8.3$ Hz), 7.80 (d, 2H, $J=8.3$ Hz), 7.87 (d, 1H, $J=7.4$ Hz), 8.80 (dd, 1H, $J=1.2, 8.0$ Hz), 10.05 (s, 1H); δ_C (75 MHz, $CDCl_3$) 120.8 (CH), 122.8 (q, CF_3 , $J=272.8$ Hz), 124.4 (CH), 124.9 (q, 2CH, $J=3.7$ Hz), 125.4 (CH), 125.7 (CH), 129.9 (C), 130.0 (2CH), 131.0 (q, C, $J=32.7$ Hz), 134.3 (C), 136.0 (C), 137.2 (C), 157.0 (C), 185.0 (CHO) ppm; m/z 306 (80), 305 (100), 237 (60), 208 (50), 160 (20).

4.4.10. 2-(2'-Nitrophenyl)-benzo[*b*]thiophene-3-carboxaldehyde 19. Prepared according to procedure A. Isolated yield: 56%; yellow solid; mp 155–156 °C; R_f 0.1 (silica, cyclohexane/AcOEt 95:5); found C 63.72, H 3.20, N 5.01, O 17.12%, $C_{15}H_9NO_3S$ requires C 63.59, H 3.20, N 4.94, O 16.94%; δ_H (300 MHz, $CDCl_3$) 7.48 (ddd, 1H, $J=1.4, 7.2, 8.0$ Hz), 7.55 (ddd, 1H, $J=1.4, 7.2, 8.0$ Hz), 7.61 (dd, 1H, $J=1.5, 6.2$ Hz), 7.70 (ddd, 1H, $J=1.5, 6.2, 7.5$ Hz), 7.75 (ddd, 1H, $J=1.5, 6.7, 7.5$ Hz), 7.86 (dd, 1H, $J=1.5, 6.7$ Hz), 8.16 (dd, 1H, $J=1.4, 7.2$ Hz), 8.71 (dd, 1H, $J=1.4, 7.2$ Hz), 9.86 (s, 1H); δ_C (75 MHz, $CDCl_3$) 121.9 (CH), 125.0 (CH), 125.1 (CH), 126.4 (CH), 126.5 (C), 126.6 (CH), 131.1 (CH), 131.9 (C), 132.9 (CH), 133.7 (CH), 136.2 (C), 138.8 (C), 146.6 (C), 153.9 (C), 185.0 (CHO) ppm; m/z 283 (40), 163 (100), 119 (80), 93 (50).

4.4.11. 2-(2'-Benzonitrile)-benzo[*b*]thiophene-3-carboxaldehyde 20. Prepared according to procedure A. Isolated yield: 54%; orange crystals; mp 172–174 °C; R_f 0.1 (silica, cyclohexane/AcOEt 95:5); found C 72.97, H 3.54, N 5.50%, $C_{16}H_9NOS$ requires C 72.98, H 3.45, N 5.32%; δ_H (500 MHz, $CDCl_3$) 7.53 (ddd, 1H, $J=1.3, 7.6, 7.6$ Hz), 7.59 (ddd, 1H, $J=1.0, 7.6, 7.9$ Hz), 7.68 (ddd, 1H, $J=1.2, 7.6, 8.2$ Hz), 7.69 (d, 1H, $J=7.9$ Hz), 7.77 (ddd, 1H, $J=1.3, 7.6, 7.9$ Hz), 7.89 (dd, 1H, $J=1.3, 7.9$ Hz), 7.91 (d, 1H, $J=8.2$ Hz), 8.71 (dd, 1H, $J=1.0, 7.6$ Hz), 9.91 (s, 1H, CHO); δ_C (75 MHz, $CDCl_3$) 114.4 (C), 117.4 (C), 122.2 (CH), 125.8 (CH), 126.9 (CH), 127.0 (CH), 130.7 (CH), 132.6 (CH), 133.2 (CH), 134.0 (CH), 135.4 (C), 136.7 (C), 139.1 (C), 154.3 (C), 185.4 (CHO) ppm; m/z 262 (80), 235 (100), 190 (90).

4.4.12. 2-(4'-Benzonitrile)-benzo[*b*]thiophene-3-carboxaldehyde 21. Prepared according to procedure A. Isolated yield: 41%; pale green solid; mp 168–169 °C; R_f 0.1 (silica, cyclohexane/AcOEt 95:5); found C 72.67, H 3.45, N 5.31, O 6.43%, $C_{16}H_9NOS$ requires C 72.98, H 3.45, N 5.32, O 6.08%; δ_H (300 MHz, $CDCl_3$) 7.48 (ddd, 1H, $J=1.0, 7.3, 8.1$ Hz), 7.55 (ddd, 1H, $J=1.1, 7.4, 8.1$ Hz), 7.70 (d, 2H, $J=7.5$ Hz), 7.81 (d, 2H, $J=7.5$ Hz), 7.89 (dd, 1H, $J=1.1, 7.3$ Hz), 8.77 (dd, 1H, $J=1.0, 7.4$ Hz), 10.03 (s, 1H); δ_C (75 MHz, $CDCl_3$) 113.9 (C), 118.1 (C), 121.9 (CH), 125.5 (CH), 126.6 (C), 126.8 (C), 131.1 (C), 131.3 (2CH), 132.7 (2CH), 136.3 (C), 137.0 (C), 138.3 (C), 157.1 (C), 185.7 (CHO) ppm; m/z 263 (70), 262 (100), 235 (20), 190 (60).

4.4.13. 2-(4'-Chloro-phenyl)-benzo[*b*]thiophene-3-carboxaldehyde 22. Prepared according to procedure

A. Isolated yield: 58%; pale yellow solid; mp 96–98 °C; R_f 0.35 (silica, cyclohexane/AcOEt 97:3); found C 66.40, H 3.44, Cl 13.04%, $C_{15}H_9ClOS$ requires C 66.05, H 3.33, Cl 13.00%; δ_H (300 MHz, $CDCl_3$) 7.38–7.57 (m, 6H), 7.78 (ddd, 1H, $J=0.8, 1.4, 7.5$ Hz), 8.77 (ddd, 1H, $J=0.8, 1.3, 7.5$ Hz), 10.01 (s, 1H, CHO); δ_C (75 MHz, $CDCl_3$) 122.0 (CH), 125.6 (CH), 126.4 (CH), 126.8 (CH), 129.6 (2CH), 130.4 (C), 130.7 (C), 132.1 (2CH), 136.9 (C), 137.4 (C), 138.3 (C), 159.2 (C), 186.5 (CHO) ppm; m/z 271 (100), 243 (30), 163 (98).

4.4.14. 2-(3'-Quinoly)-benzo[b]thiophene-3-carboxaldehyde 23. Prepared according to procedure A. Isolated yield: 52%; white solid; mp 179–180 °C; R_f 0.1 (silica, cyclohexane/AcOEt 95:5); found C 74.61, H 3.84, N 4.81%, $C_{18}H_{11}NOS$ requires C 74.72, H 3.83, N 4.84%; δ_H (500 MHz, $CDCl_3$) 7.49 (ddd, 1H, $J=1.2, 7.9, 8.2$ Hz), 7.56 (ddd, 1H, $J=1.1, 8.1, 8.2$ Hz), 7.67 (ddd, 1H, $J=1.3, 7.0, 8.2$ Hz), 7.84 (ddd, 1H, $J=1.6, 7.0, 8.3$ Hz), 7.89 (d, 1H, $J=7.9$ Hz), 7.93 (d, 1H, $J=8.2$ Hz), 8.22 (d, 1H, $J=8.3$ Hz), 8.39 (d, 1H, $J=2.2$ Hz), 8.83 (d, 1H, $J=8.1$ Hz), 9.16 (d, 1H, $J=2.2$ Hz), 10.12 (s, 1H, CHO); δ_C (75 MHz, $CDCl_3$) 122.1 (CH), 125.4 (C), 125.7 (CH), 126.7 (CH), 127.0 (CH), 127.4 (C), 128.4 (CH), 128.7 (CH), 130.0 (CH), 131.5 (CH), 131.6 (C), 137.4 (C), 138.1 (CH), 138.7 (C), 148.7 (C), 150.7 (CH), 156.5 (C), 186.2 (CHO) ppm; m/z 290 (10), 289 (100), 288 (90), 260 (30).

4.4.15. 2-(2'-Toluy)-3-methoxybenzo[b]thiophene 26. Prepared according to procedure B. Isolated yield 75%; slightly yellow oil; R_f 0.6 (silica, cyclohexane/AcOEt 98:2); found C 75.27, H 5.55%, $C_{16}H_{14}OS$ requires C 75.56, H 5.55%; δ_H (500 MHz, $CDCl_3$) 2.40 (s, 3H, CH_3), 3.68 (s, 3H, OCH_3), 7.27 (ddd, 1H, $J=1.8, 7.3, 7.8$ Hz), 7.33 (m, 1H), 7.35 (ddd, 1H, $J=1.1, 7.8, 8.0$ Hz), 7.39 (ddd, 1H, $J=1.3, 7.3, 8.6$ Hz), 7.43 (ddd, 1H, $J=1.0, 7.3, 7.9$ Hz), 7.49 (dd, 1H, $J=1.1, 7.3$ Hz), 7.77 (ddd, 1H, $J=0.6, 1.0, 7.9$ Hz), 7.83 (ddd, 1H, $J=0.6, 1.3, 8.6$ Hz); δ_C (75 MHz, $CDCl_3$) 20.8 (CH_3), 61.0 (OCH_3), 121.6 (CH), 122.6 (C), 122.9 (CH), 124.5 (CH), 125.3 (CH), 126.0 (CH), 129.1 (CH), 130.6 (CH), 131.8 (CH), 132.8 (C), 134.4 (C), 137.1 (C), 138.8 (C), 147.3 (C) ppm; m/z 254 (30), 239 (30), 221 (60), 211 (40), 178 (100).

4.4.16. 2-(3'-Quinoly)-3-methoxybenzo[b]thiophene 27. Prepared according to procedure B. Isolated yield: 62%; orange-red solid; mp 70–71 °C; R_f 0.55 (silica, cyclohexane/AcOEt 95:5); found C 73.80, H 4.51, N 4.67%, $C_{18}H_{13}NOS$ requires C 74.20, H 4.50, N 4.81%; δ_H (500 MHz, $CDCl_3$) 3.94 (s, 3H, CH_3), 7.38 (dd, 1H, $J=6.9, 7.3$ Hz), 7.42 (dd, 1H, $J=6.9, 7.8$ Hz), 7.58 (dd, 1H, $J=6.9, 7.8$ Hz), 7.72 (dd, 1H, $J=6.9, 8.2$ Hz), 7.81 (d, 1H, $J=7.8$ Hz), 7.82 (d, 1H, $J=7.3$ Hz), 7.87 (d, 1H, $J=7.8$ Hz), 8.13 (d, 1H, $J=8.2$ Hz), 8.50 (d, 1H, $J=2.1$ Hz), 9.46 (d, 1H, $J=2.1$ Hz); δ_C (125 MHz, $CDCl_3$) 61.7 (CH_3), 121.7 (CH), 123.4 (CH), 123.7 (C), 125.0 (CH), 126.0 (CH), 126.9 (C), 127.6 (CH), 128.3 (C), 128.5 (CH), 129.6 (CH), 130.2 (CH), 134.2 (CH), 134.7 (C), 136.6 (C), 147.5 (C), 149.3 (C), 150.1 (CH) ppm; m/z 291 (95), 276 (100), 248 (70), 76 (70).

4.4.17. 2-(3'-Pyridyl)-3-(2,2,2-trifluoroethoxy)benzo[b]thiophene 28. Prepared according to procedure

B. Isolated yield 59%; colourless oil; R_f 0.15 (silica, cyclohexane/AcOEt: 95/5); found C 58.27, H 3.18, N 4.51%, $C_{15}H_{10}F_3NOS$ requires C 58.25, H 3.26, N 4.53%; δ_H (500 MHz, $CDCl_3$) 4.29 (q, 2H, $J=8.2$ Hz), 7.41 (m, 2H), 7.45 (ddd, 1H, $J=1.3, 7.5, 7.9$ Hz), 7.78 (dd, 1H, $J=1.5, 7.6$ Hz), 7.80 (dd, 1H, $J=1.3, 7.2$ Hz), 8.13 (ddd, 1H, $J=1.3, 1.6, 8.2$ Hz), 8.61 (dd, 1H, $J=1.3, 4.7$ Hz), 9.01 (d, 1H, $J=1.6$ Hz); δ_C (75 MHz, $CDCl_3$) 70.0 (q, CH_2 , $J=35$ Hz), 121.1 (CH), 121.6 (C), 123.4 (CH), 124.0 (C), 124.9 (C), 125.4 (CH), 126.3 (CH), 127.0 (C), CF_3 , $J=257$ Hz), 133.5 (CH), 135.4 (CH), 136.3 (C), 145.7 (C), 149.2 (CH), 149.6 (CH); δ_F (282 MHz, $CDCl_3$) –74.74 (t, 3F, $J=8.2$ Hz) ppm; m/z 309 (40), 226 (100), 198 (80).

4.4.18. 2-(2'-Benzonitrile)-3-(2,2,2-trifluoroethoxy)benzo[b]thiophene 29. Prepared according to procedure B. Isolated yield 76%; colourless oil; R_f 0.3 (silica, cyclohexane/AcOEt: 95/5); found C 61.42, H 2.97, N 4.28%, $C_{17}H_{10}F_3NOS$ requires C 61.26, H 3.02, N 4.20%; δ_H (500 MHz, $CDCl_3$) 4.24 (q, 2H, $J=8.2$ Hz), 7.44 (ddd, 1H, $J=1.6, 6.9, 7.0$ Hz), 7.47 (ddd, 1H, $J=1.5, 7.0, 7.2$ Hz), 7.53 (ddd, 1H, $J=2.5, 6.3, 7.9$ Hz), 7.67–7.71 (m, 2H), 7.80–7.85 (m, 3H); δ_C (75 MHz, $CDCl_3$) 70.3 (q, CH_2 , $J=35$ Hz), 113.7 (C), 118.2 (C), 121.6 (CH), 123.3 (CH), 125.4 (CH), 126.5 (CH), 129.4 (CH), 132.1 (CH), 132.8 (C), 133.2 (CH), 134.2 (CH), 135.6 (C), 137.3 (C), 146.7 (C), 149.9 (C); δ_F (282 MHz, $CDCl_3$) –75.10 (t, 3F, $J=8.2$ Hz) ppm; m/z 333 (60), 250 (100), 222 (70).

References and notes

- (a) Martinez, J.; Pérez, S.; Oficialdegui, A. M.; Heras, B.; Orús, L.; Villanueva, H.; Palop, J. A.; Roca, J.; Mourelle, M.; Bosch, A.; Del Castillo, J.-C.; Lasheras, B.; Tordera, R.; del Rio, J.; Monge, A. *Eur. J. Med. Chem.* **2001**, *36*, 55–61. (b) Hrib, N. J.; Jurcak, J. G.; Bregna, D. E.; Dunn, R. W.; Geyer, H. M.; Hartman, H. B.; Roehr, J. R.; Rogers, K. L.; Rush, D. K.; Szczepanik, A. M.; Szweczek, M. R.; Wilmot, C. A.; Conway, P. G. *J. Med. Chem.* **1992**, *35*, 2712–2715.
- Boschelli, D. H.; Kramer, J. B.; Khatana, S. S.; Sorenson, R. J.; Connor, D. T.; Ferin, M. A.; Wright, C. D.; Lesch, M. E.; Imre, K.; Okonkwo, G. C.; Schrier, D. J.; Conroy, M. C.; Ferguson, E.; Woelle, J.; Saxena, U. *J. Med. Chem.* **1995**, *38*, 4597–4614.
- Connor, D. T.; Cetenko, W. A.; Mullican, M. D.; Sorenson, R. J.; Weikert, R. J.; Adolphson, R. L.; Kennedy, J. A.; Thueson, D. O.; Wright, C. D.; Conroy, M. C. *J. Med. Chem.* **1992**, *35*, 958–965.
- De Nanteuil, G.; Lila-Ambroise, C.; Vallez, M.-O.; Verbeuren, T. J. *Bioorg. Med. Chem. Lett.* **2003**, *13*, 1705–1708.
- Boulware, S. L.; Bronstein, J. C.; Nordby, E. C.; Weber, P. C. *Antiviral Res.* **2001**, *51*, 111–125.
- (a) Jones, C. D.; Jevnikar, M. G.; Pike, A. J.; Peters, M. K.; Black, L. J.; Thompson, A. R.; Falcone, J. F.; Clemens, J. A. *J. Med. Chem.* **1984**, *27*, 1057–1066. (b) Palkowitz, A. D.; Glasebrook, A. L.; Thrascher, K. J.; Hauser, K. L.; Short, L. L.; Phillips, D. L.; Muehl, B. S.; Sato, M.; Shetler, P. K.; Cullinan, G. J.; Pell, T. R.; Bryant, H. U. *J. Med. Chem.* **1997**, *40*, 1407–1416.
- Pinney, K. G.; Bounds, A. D.; Dingeman, K. M.; Mocharla,

- V. P.; Pettit, G. P.; Bai, R.; Hamel, E. *Biorg. Med. Chem. Lett.* **1999**, *9*, 1081–1086.
8. Chen, Z.; Mocharla, V. P.; Farmer, J. M.; Pettit, G. R.; Hamel, E.; Pinney, K. G. *J. Org. Chem.* **2000**, *65*, 8811–8815.
9. Kost, A. N.; Budylin, V. E.; Matveeva, E. D.; Sterligov, D. O. *Zh. Org. Khim.* **1970**, *6*, 1503.
10. Sauter, F. FR 79-2897; *CAN* **1979**, *95*, 42896.
11. Mukherjee, C.; Kamila, S.; De, A. *Tetrahedron* **2003**, *59*, 4767–4774.
12. Flynn, B. L.; Verdier-Pinard, P.; Hamel, E. *Org. Lett.* **2001**, *3*, 651–654.
13. Sall, D. J.; Bailey, D. L.; Bastian, J. A.; Buben, J. A.; Chirgadze, N. Y.; Clemens-Smith, A. C.; Denney, M. L.; Fischer, M. J.; Giera, D. D.; Gifford-Moore, D. S.; Harper, R. W.; Johnson, L. M.; Klimkowski, V. J.; Kohn, T. J.; Lin, H.-S.; McCowan, J. R.; Palkowitz, A. D.; Richett, M. E.; Smith, G. F.; Snyder, D. W.; Takeuchi, K.; Toth, J. E.; Zhang, M. *J. Med. Chem.* **2000**, *43*, 649–663.
14. Heynderickx, A.; Samat, A.; Guglielmetti, R. *Synthesis* **2002**, *2*, 213–216.
15. Miyaoura, N.; Suzuki, A. *Chem. Rev.* **1995**, *95*, 2457–2483.
16. For a review, see: Hassan, J.; Sévignon, M.; Gozzi, C.; Schulz, E.; Lemaire, M. *Chem. Rev.* **2002**, *5*, 1359–1470.
17. Stille, J. K. *Angew. Chem. Int. Ed. Engng* **1986**, *25*, 508–524.
18. Kumada, M. *Pure Appl. Chem.* **1980**, *52*, 669–679.
19. Pivsa-Art, S.; Satoh, T.; Kawamura, Y.; Miura, M.; Nomura, M. *Bull. Chem. Soc. Jpn* **1998**, *71*, 467–473.
20. Ohta, A.; Akita, Y.; Ohkuwa, T.; Fukunaga, M. C. R.; Miyafuji, A.; Nakata, T.; Tani, N.; Aoyagi, Y. *Heterocycles* **1990**, *11*, 1951–1958.
21. Fournier Dit Chabert, J.; Gozzi, C.; Lemaire, M. *Tetrahedron Lett.* **2002**, *43*, 1829–1833.
22. Lavenot, L.; Gozzi, C.; Ilg, K.; Orlova, I.; Penalva, V.; Lemaire, M. *J. Organomet. Chem.* **1998**, *567*, 49–55.
23. Gozzi, C.; Lavenot, L.; Ilg, K.; Penalva, V.; Lemaire, M. *Tetrahedron Lett.* **1997**, *38*, 8867–8870.
24. Penalva, V.; Lavenot, L.; Gozzi, C.; Lemaire, M. *Appl. Catal., A: General* **1999**, *182*, 399–405.
25. Kellogg, R. M.; Schaap, A. P.; Harper, E. T.; Wynberg, H. *J. Org. Chem.* **1968**, *33*, 2902–2909.
26. Friedmann, L.; Schechter, H. *J. Org. Chem.* **1961**, *26*, 2522–2525.
27. El Kassmi, A.; Héraud, G.; Büchner, W.; Fache, F.; Lemaire, M. *J. Mol. Catal.* **1992**, *72*, 299–305.
28. Jeffery, T. *Tetrahedron* **1996**, *52*, 10113–10130.
29. Amatore, C.; Jutand, A.; Mottier, L. *Eur. J. Inorg. Chem.* **1999**, 1081–1085.
30. Ullmann, F.; Bielecki, J. *Chem. Ber.* **1901**, *34*, 2174–2184.
31. Hassan, J.; Penalva, V.; Lavenot, L.; Gozzi, C.; Lemaire, M. *Tetrahedron* **1998**, *54*, 13793–13804.
32. Heck, R. F. *Palladium reagents in organic syntheses*. Academic: New York, 1985.
33. Gaertner, R. *J. Am. Chem. Soc.* **1952**, *74*, 4950–4951.
34. Yao, Q.; Kinney, E. P.; Yang, Z. *J. Org. Chem.* **2003**, *68*, 7528–7531.
35. Itahara, T. *J. Org. Chem.* **1985**, *50*, 5272–5275.
36. Glover, B.; Harvey, K. A.; Liu, B.; Sharp, M. J.; Tymoschenko, M. F. *Org. Lett.* **2003**, *5*, 301–304.
37. For a review about the mechanism, see: Miura, M.; Nomura, M. *Topics in current chemistry*; Springer: Berlin, 2002; Vol. 219.



A study of some molecularly imprinted polymers as protic catalysts for the isomerisation of α -pinene oxide to *trans*-carveol

William B. Motherwell,* Matilda J. Bingham, Julien Pothier and Yvan Six

Department of Chemistry, Christopher Ingold Laboratories, University College London, 20 Gordon Street, WC1H 0AJ London, UK

Received 27 January 2003; revised 12 January 2004; accepted 5 February 2004

Abstract—A range of acidic Molecularly Imprinted Polymers (MIPs) were synthesised using the imprint molecule *trans*-carvyl amine as a transition state analogue for the selective isomerisation of α -pinene oxide to *trans*-carveol. The amine functionality of the imprint molecule was used to selectively position a sulfonic acid group in the MIP binding pocket utilising 4-styrene sulfonic acid as the functional monomer. Co-polymerisation with varying ratios of styrene and divinylbenzene afforded a range of MIPs which were tested for their ability to effect selective formation of *trans*-carveol from α -pinene oxide. Although successful imprinting was demonstrated in binding studies, it was shown that solvent effects were dominant in effecting selective formation of *trans*-carveol. Using DMF as solvent, up to 70% of the products from acid catalysed isomerisation of α -pinene oxide with the polystyrene MIPs were obtained via the necessary *para* menthyl tertiary carbocation, and industrially important *trans*-carveol was obtained in 45% yield.

© 2004 Elsevier Ltd. All rights reserved.

1. Introduction

The conceptually elegant polymerization technique of molecular imprinting,¹ as encapsulated in Figure 1, produces macroporous polymers which contain binding sites capable of selective molecular recognition of the original imprint molecule or template around which they were constructed. The enormous potential of this method has not gone unrecognized and, in consequence, molecularly imprinted polymers (MIPs) have been used as separation and extraction materials,² as microreactors containing reagents for selective reductions,³ as biomimetic sensors,⁴ as specific adsorbents capable of shifting the equilibrium of a thermodynamically unfavourable enzymatic reaction,⁵ and as 'protecting groups' using an external reagent.⁶ The selection of an imprint molecule which can be regarded as a transition state mimic for a given reaction then leads on to the idea that the preparation of such shape selective polymers can be used in catalyst design, as in the seminal studies of Lerner and Schultz on catalytic antibodies.⁷ Even though selective binding of a transition state mimic represents only one facet of enzyme like catalysis, several recent studies⁸ testify to the potential of MIPs as selective catalysts, and therefore stimulated our interest in using this approach for proton mediated rearrangements.

From the outset, it is important to recognise both the advantages and the limitations of the process of molecular imprinting as outlined below (Fig. 1). In the first step, monomers containing functional groups which can interact with the imprint molecule, are pre-organised around the imprint molecule **1**. A mixture of standard monomer and cross-linker is then co-polymerised around this imprint molecule/monomer complex **2** in a radical polymerisation process, to form a macroporous polymer which contains sites at which the imprint molecule is bound **3**. Finally, the imprint molecule is removed from the polymer to leave well defined, shape specific cavities **4** which are spatially and functionally compatible with the imprint molecule **1**.

The interactions between the imprint molecule **1** and the functional monomers can be electrostatic, covalent or non-covalent. In the latter case the description pre-organisation is a slight misnomer, since the combination of weak intermolecular forces involved leads rather to a dynamic associated complex **2** in constant exchange with solution. This, along with other factors, leads to the inherent heterogeneity of the molecular recognition sites produced within the polymer. This has proven to be one of the major sticking points in catalytic applications of MIPs. Despite this drawback, the manifest stability of MIPs when compared to natural enzymes or other artificial analogues, means that the realisation of catalytic MIPs remains a highly desirable goal.

With the above principles in mind, the present paper describes our initial studies towards the application of this

Keywords: Molecularly imprinted polymers; α -Pinene oxide; *trans*-Carveol.

* Corresponding author. Tel.: +44-207-679-7533; fax: +44-207-679-7524; e-mail address: w.b.motherwell@ucl.ac.uk

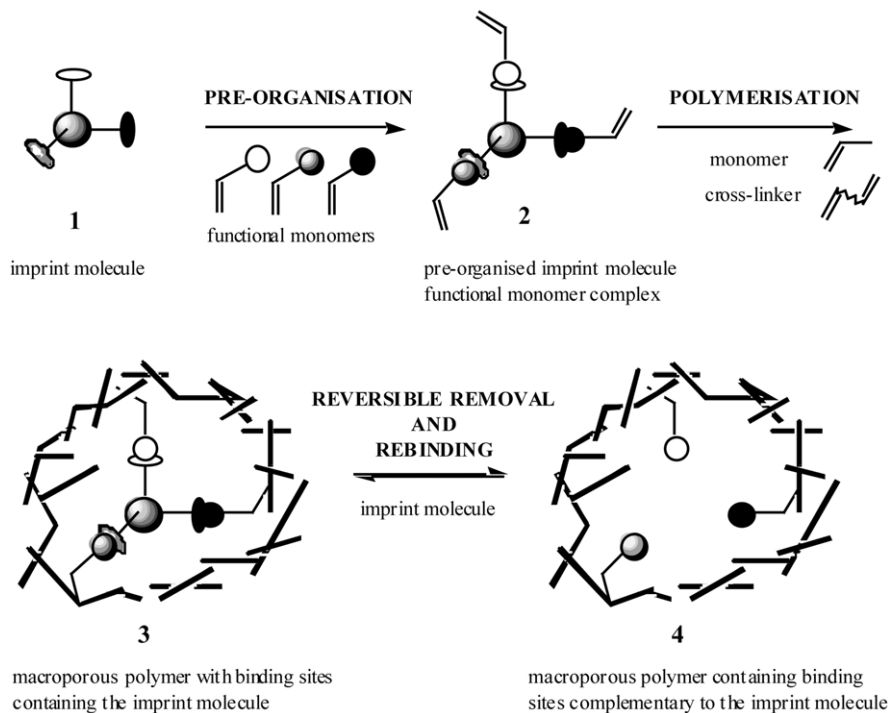
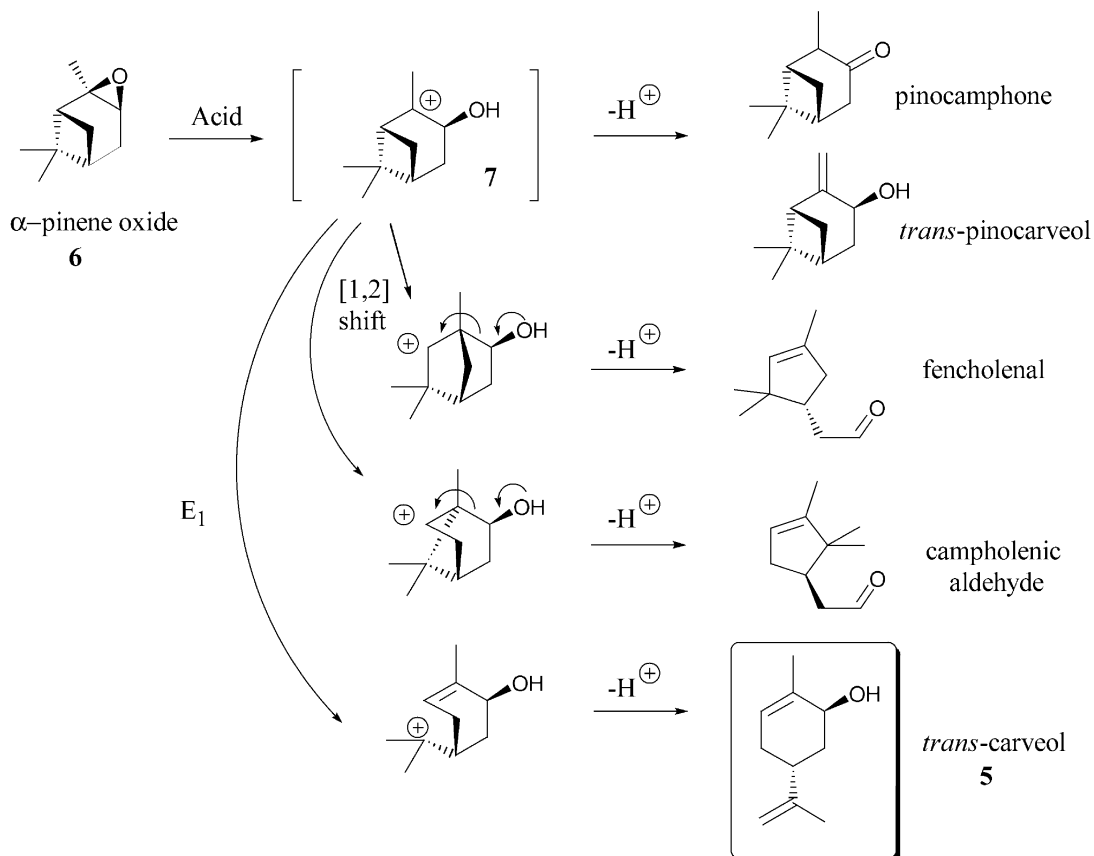


Figure 1.

technology for the selective isomerisation of α -pinene oxide to *trans*-carveol. (–)-*trans*-Carveol **5**,⁹ one of the constituents of the Valencia orange essence oil, is an important compound for the fragrance chemical industry. It is usually

commercially available as an expensive mixture of isomers. A selective and efficient solid-phase procedure to obtain it from α -pinene oxide **6** is therefore an important objective (Fig. 2).

Figure 2. Representative major products arising from the acid-catalysed opening of α -pinene oxide.

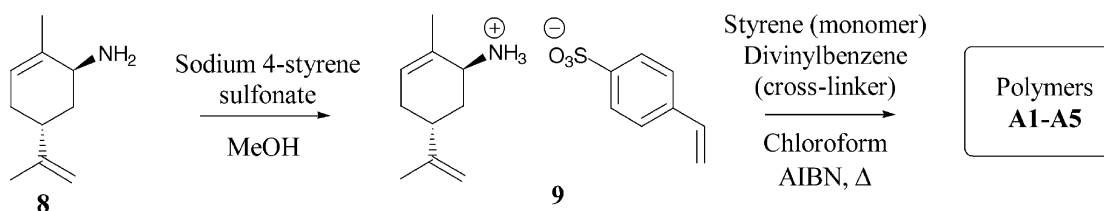


Figure 3.

The acid-catalysed opening of α -pinene oxide **6** (Fig. 2) is well documented and typical of the structural rearrangements often encountered within terpenoid chemistry. In this instance, the initially formed carbocation **7** can undergo several competing processes, including 1,2 hydride migration to give pinocamphone, proton loss to give *trans*-pinocarveol, and no less than three alkyl shifts to release the strain inherent in the four membered ring. Remarkably, both the [1,2] shift which leads to campholenic aldehyde and the 'E₁ elimination' leading to *trans*-carveol **5** both require movement of the same pair of electrons from the same σ bond. In general, Lewis acids usually display a high selectivity in favour of cyclopentenic aldehydes,¹⁰ while in the presence of Brønsted acids, various amounts of *trans*-carveol **5** and other *para*-menthenic compounds are also produced.¹¹ When solid catalysts are used, campholenic aldehyde, fencholenal, pinocamphone and *trans*-pinocarveol are usually the major products and only small amounts of **5** are observed.¹² It is worthy of note that Noyori et al. achieved a 72% yield of *trans*-carveol **5** from **6** by treatment with a mixture of trimethylsilyl trifluoromethanesulfonate and 2,6-lutidine followed by addition of DBU.¹³ Such a combination of reagents is not however, a practical proposition for industrial application.

Given these previous studies and with the goal of trying to achieve selectivity towards the formation of **5**, it therefore appeared logical to focus our attention onto the design of Brønsted acid-supported imprinted polymers.

2. Results and discussion

2.1. Preparation of imprinted polystyrenes

In the first instance we elected to conduct our preliminary studies with imprinted styrene/divinylbenzene polymers since their synthesis and use as MIPs was already well precedented in the literature.¹⁴ In the choice of the imprint molecule, we hoped to achieve two goals. The strategic location of an acidic group in the active site which could initiate the conversion of **6** to **5** was of course the primary objective. Moreover, in order to obtain selectivity, we also wished to use a molecule which would create a shape selective site capable of influencing the product ratio in favour of the product **5**. The identification of a good transition-state analogue for the transformation of α -pinene oxide **6** into **5** was far from obvious. The mechanisms are still under debate,¹⁵ but carbonium ion **7** is generally accepted to be the preliminary intermediate. Although formation of this carbocation should be the rate-determining step, the selectivity of the transformation is determined during the subsequent collapse of this reactive intermediate

7 since most of the products derive from this common species. For our work, we therefore selected the crude imprint molecule **8**¹⁶ (Fig. 3) in the hope that this molecule would both locate the acidic group in the binding site and produce a cavity in the polymer which was complementary to the desired product **5**, thus affecting the product distribution in its favour. In these early studies we were more concerned with selectivity than turnover, thus a product like binding site was considered acceptable.

Five polymers **A1-A5** of varying monomer to crosslinker ratio's were synthesised with various loadings of imprint molecule-monomer complex **9** (Fig. 3) by co-polymerising styrene and divinylbenzene with the pre-formed salt **9**¹⁷ under radical conditions. The relative quantities of the reagents are reflected in the degree of crosslinking and have important consequences on the physical and molecular recognition properties of the MIPs produced¹⁸ (vide infra). A reference polymer **R**, imprinted with 3-methyl-butylamine instead of carvylamine **8**, was also synthesised (Table 1).

Table 1.

Polymer	Imprint molecule	Cross-linker monomer ratio ^a	Loading ^b
R		6	1/35
A1	8	6	1/35
A2	8	3	1/35
A3	8	2	1/35
A4	8	2	1/15
A5	8	3	1/10

^a Crosslinker monomer ratio. The crosslinker:monomer ratio is the ratio of moles of divinylbenzene to styrene. A higher ratio indicates a higher level of crosslinking.

^b Loadings. Loadings refer to the ratio of the number of moles of salt **9** to the total number of moles of polymerisable molecules. A higher loading indicates more sites per unit volume of polymer.

The imprint molecules were removed by washing with triethylamine and the sulfonic acid functions of these polymers were then regenerated with HCl:diethyl ether followed by exhaustive washing to neutral pH. Five polymer catalysts **A1***–**A5*** were thus obtained (Fig. 4). A reference catalyst **R*** was also produced from polymer **R** using the same experimental protocol.

2.2. Catalysis studies

The acid-catalysed α -pinene oxide ring-opening reactions were carried out at room temperature in toluene using stoichiometric amounts of MIP. The selectivities in the presence of *p*-toluene sulfonic acid (*p*-TSA) and polymers **R***, **A1***–**A4*** are displayed in Table 2.

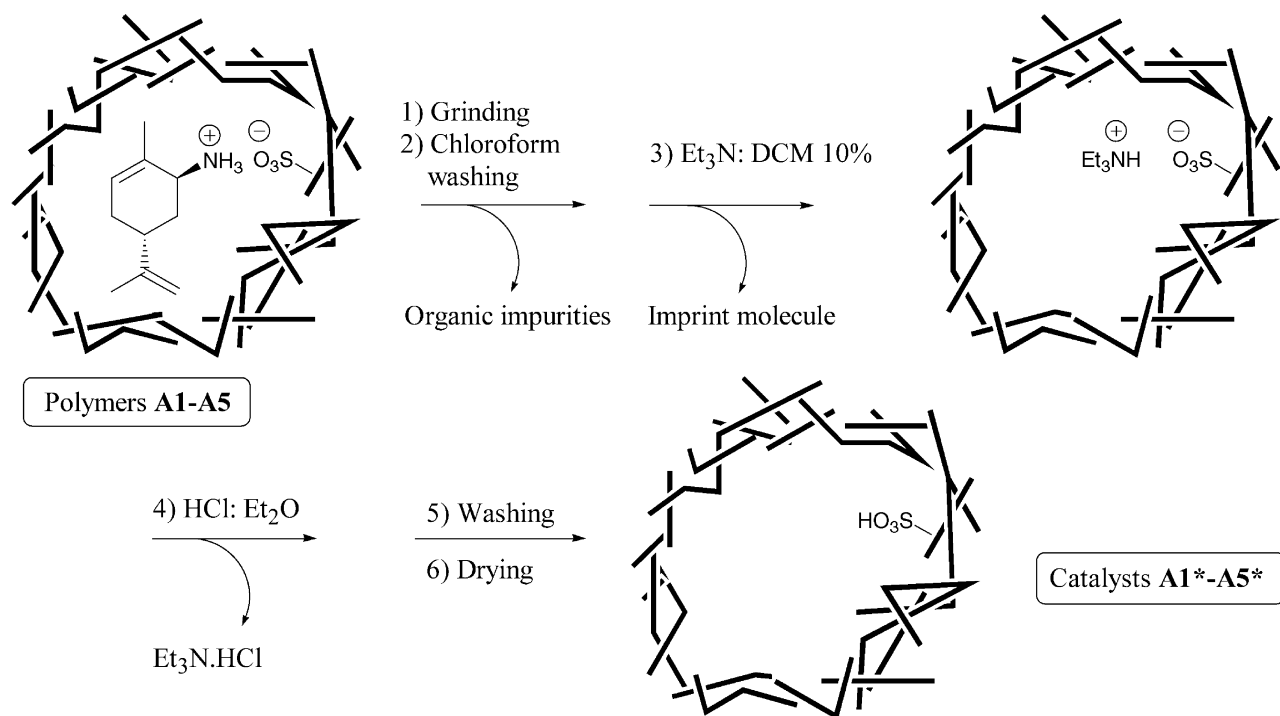


Figure 4.

In the event, it was particularly striking that all the polymer catalysts exhibited a much better selectivity for the formation of **5** than was observed in the homogeneous reaction with *para*-toluene sulfonic acid. However, the polymers **A1***–**A4*** imprinted with (–)-*trans*-carvyl amine **8** did not appear to be better than the reference polymer **R***. Indeed, all the polymers tested led to similar product distributions. This suggested that the shape of the polymer site had little effect on selectivity and the main influence seemed to be local media effects in the vicinity of the sulfonic acid group. This was interesting, since toluene had been specifically selected as the solvent since it closely resembled the hydrophobic environment expected in the polystyrene binding site. It was therefore logical to further study the influence of the nature of the solvent.

Although we had initially avoided protic solvents due to the potential complication of specific acid catalysis, we next turned to methanol as the solvent. The data obtained are presented in Table 3.

These results show that the choice of solvent can profoundly affect the selectivity of this isomerisation reaction. The compounds **5**, **15** and **16**, derived from cation **18** (Fig. 5), a secondary intermediate in the isomerisation to *trans*-carveol, are now the major products, accounting for as much as 54% of the reaction mixture. As before, all polymers displayed more or less equivalent selectivities for **5** and were significantly better than *p*-TSA.

Since these results indicated that the use of a more polar solvent was promoting the reaction pathway via the carbocation **18**, we turned our attention towards DMF, in the belief that this solvent would also favour the formation of **18** without acting as a nucleophilic trap, thereby increasing the amount of **5** produced. These expectations were verified as can be seen in Table 4.

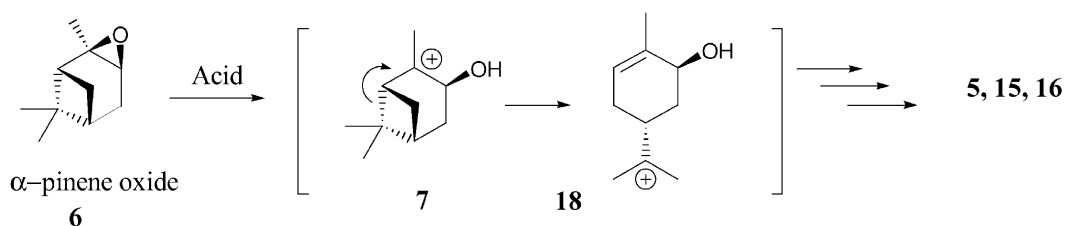
In this case no significant differences between all the catalysts, including *p*-TSA, were observed. However, in all cases, *trans*-carveol **5** became the major product. Although this result was not encouraging in terms of selective MIP

Table 2. Product distribution in the isomerisation of α -pinene oxide in toluene at room temperature. Product distributions were determined by GC analysis using authentic samples of **10**, **11**, **5**, and **12** for comparison

Catalyst	Product distribution				Total Yield
	10	11	5	12	
<i>p</i> -TSA.H ₂ O	59%	11%	5%	5%	80%
R*	60%	8%	22%	3%	93%
A1*	54%	9%	16%	13%	92%
A2*	60%	9%	20%	4%	93%
A3*	59%	10%	20%	4%	93%
A4*	62%	12%	11%	5%	90%

Table 3. Product distribution in the opening of α -pinene oxide in methanol at room temperature. Product distributions were determined by GC analysis using authentic samples of **14**, **15**, **5**, **17** and **16** for comparison

Catalyst	Product distribution					Total Yield
	14	15	5	16	17	
<i>p</i> -TSA.H ₂ O	23%	17%	6%	13%	10%	69%
R *	26%	40%	12%	2%	10%	90%
A1 *	27%	41%	11%	-	11%	90%
A2 *	32%	36%	10%	4%	11%	93%
A3 *	29%	38%	12%	3%	10%	92%
A4 *	31%	36%	12%	-	11%	90%
A5 *	27%	40%	10%	2%	11%	90%

**Figure 5.****Table 4.** Product distribution in the isomerisation of α -pinene oxide in DMF at room temperature. Product distributions were determined by GC analysis using authentic samples of **10**, **5**, and **19** for comparison

Catalyst	Product distribution			Total Yield
	10	5	19	
<i>p</i> -TSA.H ₂ O	21%	42%	24%	87%
R *	23%	42%	23%	88%
A1 *	24%	45%	25%	94%
A2 *	29%	41%	24%	94%
A3 *	39%	38%	20%	97%
A4 *	31%	41%	21%	93%
A5 *	32%	39%	21%	92%

recognition it does represent a simple method for the formation of **5** from commercially available α -pinene oxide.

Two primary explanations may be considered for the similar reactivity profiles of the polymers prepared. The first is that the imprinting process was inefficient and the second possibility is that specific acid catalysis was operating, although this would tend to predicate the same product distribution with both *p*-TSA and the polymers. In order to eliminate the first possibility we therefore studied the binding characteristics of the polymers **A1***–**A5***, in order to check the quality of their molecular imprinting. Their molecular recognition properties were assessed using a simple modification of the filtration protocol as described in the experimental section.

When polymers **A1***–**A5*** and **R*** were suspended in a solution containing the imprint molecule **8**, polymer **R*** proved to be the least efficient at reabsorbing amine **8** (Fig. 6), which is consistent with the fact that an amine other than **8** was used to imprint this reference polymer. It should be noted that in all cases, the rebinding process was very sluggish, with equilibration taking more than 15 h. Accordingly, the extraction of **8** from the polymers using DCM and then 10% *n*-PrNH₂: DCM was also slow, as illustrated in Figure 6(b).

Competitive rebinding studies were also performed on polymers **A1***, **A4*** and **R*** using equimolar mixtures of (–)-*trans*-carvyl amine **8** and α -methyl benzylamine **20** (Fig. 7) in DCM. Although selectivities were modest, after 15 h, **A1*** and **A4*** had absorbed more imprint molecule **8** than competitor **20**, while the converse was observed with reference polymer **R*** (Table 5). Given however, that the dominant interaction of **8** involves electrostatic interactions through salt formation and that ‘shape selectivity’ can only involve very modest π – π interactions between the alkene residues and the aromatic rings of the polymer, the observed selectivities for preferential binding of **8** are very encouraging.

Nevertheless, from all of the foregoing results, it can be concluded that various different binding characteristics were observed depending on the MIPs tested. Polymer **A4*** displayed the fastest and most selective recognition for the imprint molecule **4**. In contrast, the reference polymer **R*** clearly exhibited much poorer performances than all the other polymers **A1***–**A5***. This constitutes strong evidence

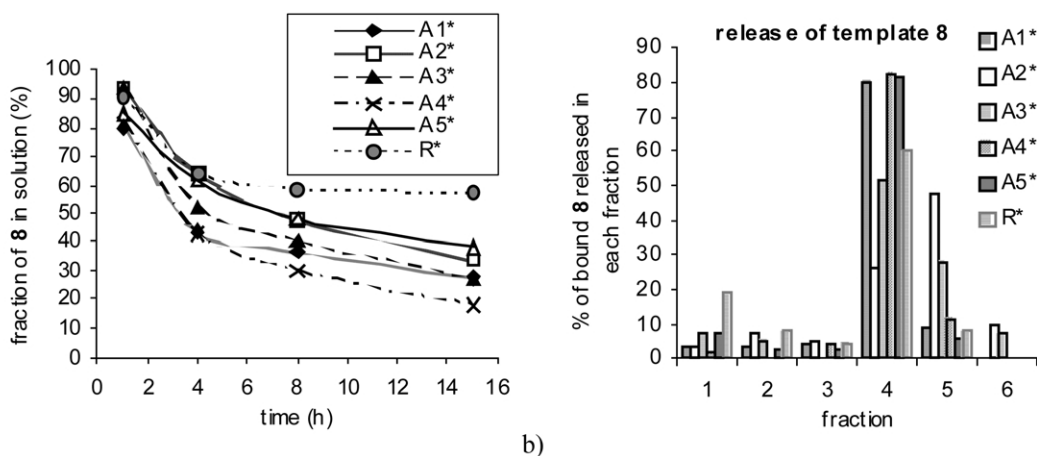


Figure 6. (a) Rebinding of **8** by polymers **A1***–**A5*** and **R*** in DCM. (b) Release of template **8** from MIPs **A1–A5** and **R**, using DCM (3 fractions) and then 10% *n*-PrNH₂:DCM (3 fractions).

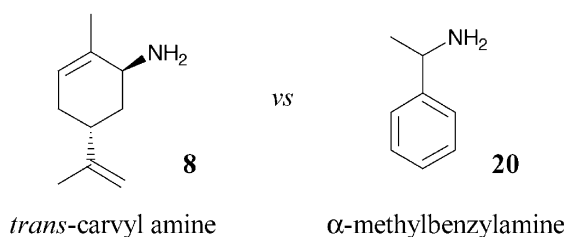


Figure 7.

Table 5. Competitive binding of equimolar amounts of **4** and **7** by polymers **A1***, **A4*** and **R*** in DCM

Polymer	A1*	A4*	R*
Molar ratio 8:20 left in solution after 15 h	47:53	44:56	53:47

that the molecular imprinting process had per se been effective.

On considering that all of the imprinted polymers tested, including the reference polymer **R***, exhibited similar behaviours towards α -pinene oxide, despite their differing binding behaviour towards imprint molecule **8** one may wonder if the reactions did indeed proceed within the imprinted sites at all. The pK_a values of the species involved (Table 6) may suggest that none of our reactions were actually catalysed by the acidic groups of the polymers, but rather by protonated methanol, protonated DMF or by the hydronium ion.

Table 6. pK_a values for the species involved¹⁹

Acid	Base	Approximate pK_a
ArSO ₃ H	ArSO ₃ ⁻	-6.5
MeOH ₂ ⁺	MeOH	-2
H ₃ O ⁺	H ₂ O	-1.74
DMF·H ⁺	DMF	-0.5

The actual catalytic entity would therefore be the same with all polymers and thus specific acid catalysis could occur outside the polymeric framework, which is consistent with the uniformity of the results obtained. It remains to be

explained why *p*-TSA gave different results in methanol and toluene when compared with the MIPs. If the reaction were truly occurring in the bulk solvent there should be no difference between the MIPs and *p*-TSA since it is unlikely that a proton transfer process is the rate determining step.

There are two possible explanations for this phenomenon. It is possible that the reactions are occurring in a heterogeneous fashion and that although no selectivity is exerted on the reaction by the differing shapes in the different MIPs, the local media effects are such as to favour formation of the desired product. It is not unusual in enzyme systems for the local environment in the active site to modify the pK_a of the functional groups involved in enzyme catalysis and hence influence the product outcome.²⁰ Indeed Kirby and Tawfik have recently highlighted the importance of these local media effects in a study of modified PEI synzymes,²¹ and have shown that local microenvironments alone 'in the absence of efficient positioning of the catalytic amine base relative to the substrate, can give rate accelerations as high as 10⁵'. The other possibility is that the reaction is occurring within the polymer, but the sites are poorly accessible, consistent with the slow kinetics observed in the binding studies, and thus diffusion of the reactant into the binding site becomes the rate limiting step. Thus the improved yield of the desired product is due rather to a more sluggish reaction resulting in less product decomposition, than to effective selective catalysis.

Notwithstanding these subtleties, it seems clear that the collapse of carbonium **7** into **18** rather than the [1,2] shift to afford campholenic aldehydes **10** (Fig. 2), is favoured when a nucleophilic trap, either reversible or irreversible is present. Indeed, much higher yields of *trans*-carveol-derived products were observed in solvents such as methanol or DMF. Future efforts directed towards exploiting this observation should hopefully provide an efficient, cheap and commercially viable one step synthesis of *trans*-carveol **5**.

In conclusion, the results described herein, have shown that it is possible to prepare a polystyrene based sulfonic acid polymer which can channel up to 70% of the products from acid catalysed isomerisation of α -pinene oxide via the

necessary *para* menthyl tertiary carbocation and produce industrially important *trans*-carveol **5** in 45% yield. However, in spite of evidence that several of the polymers used were successfully imprinted with *trans*-carvyl amine **8** as a potential transition state mimic for the desired reaction, the nature of the solvent chosen clearly played the determining role in the final outcome. The present study should therefore also serve as a caveat as to the perfidious and promiscuous behaviour of the proton which evidently did not wish to return to its sulfonate counterion in the imprinted polymers.

3. Experimental

3.1. General

All reactions were performed under an inert atmosphere. Chloroform was distilled from calcium hydride, toluene was distilled over sodium, and methanol was distilled from magnesium turnings. DMF was dried with MgSO₄(s) and distilled over Linde type 4 Å molecular sieves under reduced pressure. Styrene (inhibitor 10–15 ppm *p*-*t*butylcatechol) and 80% divinylbenzene tech. (mixture of *cis* and *trans*-isomers, inhibitor 1000 ppm *p*-*t*butylcatechol) were supplied by Aldrich and were distilled from hydroquinone at low pressure prior to use. A.I.B.N. was recrystallised from DCM and all amine reagents were distilled before use. ¹H NMR Spectra were recorded at 500 MHz on a Bruker Avance 500, at 400 MHz on a Varian VXR-400 or a Bruker AMX-400 or at 300 MHz on a Bruker AMX-300. ¹³C NMR spectra were recorded at 125.8, 100.6 MHz or 75.4 MHz on the instruments above. Infrared spectra were recorded as thin films on KBr plates or as KBr discs on a Perkin–Elmer FT-IR 1605 instrument Gas Chromatography was performed on a Hewlett–Packard 5890A machine (flame ionisation detector) with a 25 m×0.50 mm BPX5 column using hydrogen as the carrier gas.

3.1.1. Synthesis of (1*R*,5*R*)-*trans*-carvyl amine **8.** (1*R*,5*R*)-*trans*-Carvyl amine- **8**, was prepared according to literature procedure from (R)-(-)-carvone.¹⁶

Bp: 95–98 °C/0.75 mbar; [α]_D²⁵: –182.4 (CH₂Cl₂, *c*=1); ¹H NMR (CDCl₃, 400 MHz): δ _H 5.40 (1H, m), 4.68 (1H, s-), 4.67 (1H, s), 3.15 (1H, s(br)), 2.23–1.57 (5H, m), 1.72 (3H, s-), 1.69 (3H, s), 1.29 (2H, s(br)-); ¹³C NMR (CDCl₃, 100 MHz): δ _C 149.5, 136.2, 122.8, 108.7, 49.8, 37.5, 35.1, 31.0, 21.2, 20.9. IR (neat): $\tilde{\nu}_{\max}$ 3293 (w), 3217 (w), 3074 (w), 2959 (m), 2914 (s), 1648 (m), 1441 (s), 1375 (m), 1150 (w), 1046 (w), 942 (w), 883 (s), 806 (m); LRMS (FAB) *m/z*: 152 [M+H]⁺, 135, 119, 107.

3.1.2. Synthesis of 4-styrenesulfonic acid, (1*R*,5*R*)-*trans*-carvyl amine salt **9.** A solution of acetyl chloride:MeOH (1:20 v/v, 6.0 mL) was made up under nitrogen at 0 °C and added dropwise with stirring to (1*R*,5*R*)-*trans*-carvyl amine **8** (500 mg, 3.3 mmol, 1 equiv.) at 0 °C. After 20 min the solution was concentrated in vacuo to afford the amine hydrochloride. This was immediately dissolved in methanol (25 mL) and added to a solution of 4-styrenesulfonic acid, sodium salt (680 mg, 3.3 mmol, 1 equiv.) in methanol (125 mL). The solution was stirred for 4 h, then concen-

trated in vacuo to afford an off white solid. Chloroform (30 mL) was added and any remaining solid was removed by suction filtration. The filtrate was concentrated in vacuo to afford a pale yellow solid (1.05 g) containing a mixture of (1*R*,5*R*)-*trans*-carvyl amine hydrochloride **21** and 4 styrenesulfonic acid, (1*R*,5*R*)-*trans*-carvyl amine salt **9**. The ratio **9**:**21**, 1.4:1 was determined by ¹H NMR.

¹H NMR (CDCl₃, 300 MHz): δ _H 8.11 (3H, s(br)), 7.69 (2H, AA'BB', d, *J*=12.5 Hz), 7.40 (2H, AA'BB', d, *J*=12.5 Hz), 6.69 (1H, dd, *J*=17.5, 11.0 Hz), 5.72 (1H, d, *J*_{*trans*}=17.5 Hz), 5.63 (1H, m), 5.30 (1H, d, *J*_{*cis*}=11.0 Hz), 4.68 (1H, s), 4.64 (1H, s), 3.60 (1H, m(br)), 2.49 (1H, m(br)), 2.10 (2H, m), 1.79 (3H, s), 1.63 (3H, s); ¹³C NMR (CDCl₃, 100 MHz): δ _C 147.8, 143.2, 139.5, 135.9, 129.3, 128.4, 126.2, 126.0, 115.5, 109.5, 50.1, 34.3, 31.7, 30.3, 20.9; LRMS (FAB) *m/z*: 336 [M_{salt}+H]⁺; (CI negative) *m/z*: 182.8 [M_{acid}-H]⁻; (CI positive) *m/z*: 151.9 [M_{amine}+H]⁺.

3.1.3. Synthesis of 4-styrenesulfonic acid, isoamylamine salt **22.** HCl:diethyl ether (5 mL) was added dropwise to a stirred solution of isoamylamine (436 mg, 50 mmol, 1 equiv.) in diethyl ether (15 mL) to produce a white precipitate. The solvent was removed in vacuo and the residue taken up in MeOH (60 mL) and stirred at room temperature. 4-Styrenesulfonic acid, sodium salt (1.02 g, 60 mmol, 1.2 equiv.) was added and the solution stirred for 18 h. The solvent was removed in vacuo, the residue taken up in chloroform (70 mL), filtered, and concentrated in vacuo to afford a pale yellow solid (776 mg) containing a mixture of 4-styrenesulfonic acid, isoamylamine salt **22** and isoamylamine hydrochloride **23**. The ratio **22**:**23** 1.3:1 was determined by ¹H NMR.

¹H NMR (CDCl₃, 300 MHz): δ _H 7.77 (2H, AA'BB', d, *J*=12.5 Hz), 7.71 (3H, s(br)), 7.38 (2H, AA'BB', d, *J*=12.5 Hz), 6.66 (1H, dd, *J*=17.5, 11.0 Hz), 5.74 (1H, d, *J*_{*trans*}=17.5 Hz), 5.28 (1H, d, *J*_{*cis*}=11.0 Hz), 2.84 (1H, m), 1.49 (4H, m(br)), 0.75 (6H, d, *J*=3.5 Hz); ¹³C NMR (CDCl₃, 75 MHz): δ _C 143.0, 139.7, 135.7, 126.1, 115.8, 38.4, 35.9, 25.5, 22.0; LRMS (CI negative) *m/z*: 183 [M_{acid}-H]⁻; (CI positive) *m/z*: 88, [M_{amine}+H]⁺.

3.2. General procedure for the synthesis of polystyrene MIPs

Styrene, divinylbenzene, 4-styrenesulfonic acid, (1*R*,5*R*)-*trans*-carvyl amine salt **9**, and AIBN (2 mol% per polymerisable double bond) were dissolved in chloroform (1.7 v/v of polymerisable molecules) in a Schlenk flask of diameter 3.0 cm. Three freeze thaw cycles were carried out and the polymerisation mixture was placed in a preheated bath at 70 °C and heated under nitrogen with stirring (300 rpm) for 40 min. The bath was cooled to 60 °C and the polymerisation mixture was incubated for a further 23 h 20 min. The flask was cooled to room temperature and the solvent removed under vacuum. The resultant polymer monolith was ground.

3.2.1. Synthesis of polystyrene A1. Loading: 1/35, cross-linker-monomer ratio 6:1. 4-Styrenesulfonic acid, (1*R*,5*R*)-*trans*-carvyl amine salt **9**²² (200 mg, 0.43 mmol), styrene (224 mg, 246 μ L, 2.15 mmol), divinylbenzene

(1.68 g, 1.84 mL, 12.9 mmol), AIBN (92 mg, 0.6 mmol) and chloroform (3.55 mL) were polymerised according to the general procedure.

3.2.2. Synthesis of polystyrene A2. Loading: 1/35, cross-linker-monomer ratio 3:1. 4-Styrenesulfonic acid, (1*R*,5*R*)-*trans*-carvyl amine salt **9**²² (200 mg, 0.43 mmol), styrene (329 mg, 430 μ L, 1.3 mmol), divinylbenzene (1.47 g, 1.61 mL, 3.8 mmol), AIBN (86.5 mg, 0.53 mmol) and chloroform (3.47 mL) were polymerised according to the general procedure.

3.2.3. Synthesis of polystyrene A3. Loading: 1/35, cross-linker-monomer ratio 2:1. 4-Styrenesulfonic acid, (1*R*,5*R*)-*trans*-carvyl amine salt **9**²² (200 mg, 0.43 mmol), styrene (523 mg, 575 μ L, 5.0 mmol), divinylbenzene (1.31 g, 1.43 mL, 10.0 mmol), AIBN (82 mg, 0.5 mmol) and chloroform (3.41 mL) were polymerised according to the general procedure.

3.2.4. Synthesis of polystyrene A4. Loading: 1/15, cross-linker-monomer ratio 2:1. 4-Styrenesulfonic acid, (1*R*,5*R*)-*trans*-carvyl amine salt **9**²² (200 mg, 0.43 mmol), styrene (224 mg, 246 μ L, 2.15 mmol), divinylbenzene (560 mg, 612 μ L, 4.3 mmol), AIBN (35 mg, 0.22 mmol) and chloroform (1.46 mL) were polymerised according to the general procedure.

3.2.5. Synthesis of polystyrene A5. Loading: 1/10, cross-linker-monomer ratio 3:1. 4-Styrenesulfonic acid, (1*R*,5*R*)-*trans*-carvyl amine salt **9**²² (184 mg, 0.43 mmol), styrene (115 mg, 126 μ L, 1.1 mmol), divinylbenzene (417 mg, 456 μ L, 3.2 mmol), AIBN (24.6 mg, 0.15 mmol) and chloroform (1.0 mL) were polymerised according to the general procedure.

3.2.6. Synthesis of the reference polystyrene R. Styrene (224 mg, 246 μ L, 2.1 mmol), divinylbenzene (1.68 g, 1.84 mL, 12.9 mmol), 4-styrenesulfonic acid, isoamylamine salt **22** (158 mg, 0.43 mmol) and AIBN (92 mg, 0.6 mmol, 2 mol% per polymerisable double bond) were dissolved in chloroform (3.55 mL, 1.7 v/v of polymerisable molecules) in a Schlenk flask of diameter 3.0 cm. Three freeze thaw cycles were carried out and the polymerisation mixture was placed in a preheated bath at 70 °C and heated under nitrogen with stirring (300 rpm) for 40 min. The bath was cooled to 60 °C and the polymerisation mixture was incubated for a further 23 h 20 min. The flask was cooled to room temperature and the solvent removed under vacuum. The resultant polymer monolith was ground.

3.3. Procedure for the washing and generation of acid sites in the crude polystyrenes A1*–A5* and R*

The ground crude polymer was placed in a sintered glass funnel and washed with chloroform (5 \times 10 mL). The solvent was removed in vacuo and the residue analysed by ¹H NMR, which identified AIBN decomposition products and trace amounts of unreacted reagents as determined by comparison with reference spectra. The polymer was washed with 10% Et₃N:DCM (5 \times 10 mL) to remove the bound (1*R*,5*R*)-*trans*-carvyl amine **8**, as determined by ¹H NMR analysis of the filtrate, then DCM (10 mL). The polymer was stirred in

HCl:diethyl ether (20 mL) for 3 h at 0 °C, filtered, then washed with diethyl ether (2 \times 20 mL), DCM (2 \times 20 mL), water (2 \times 20 mL), methanol (2 \times 20 mL or until pH 7), and DCM (5 \times 10 mL). The polymer was then dried in vacuo to give the active polymer A1*–A5* and R*.

Polymer A1* 1/35 6:1. Elemental analysis: found C 88.16, H 7.85, N 0.18, S 0.70.

Polymer A2* 1/35 3:1. Elemental analysis: found C 86.92, H 7.74, N 0.32, S 0.85

Polymer A3* 1/35 2:1. Elemental analysis: found C 88.02, H 8.01, N 0.27, S 0.82.

Polymer A4* 1/15 2:1. Elemental analysis: found C 86.04, H 7.76, N 0.24, S 0.93.

Polymer A5* 1/10 3:1. Elemental analysis: found C 85.04, H 7.72, N 0.38, S 0.92.

Polymer R* 1/35 6:1. Elemental analysis: found C 88.25, H 7.82, N 0.24, S 0.75.

3.4. General method for binding studies

The dried polymer A1*–A5* was placed in a sealed soxhlet extraction thimble and suspended in a beaker containing a known quantity of DCM (60 mL). The solution was stirred for 20 min at 0 °C, the level of the solvent was marked and the soxhlet thimble was removed (slowly, allowing residual non-absorbed solvent to drip from the soxhlet back into the beaker). The amount of solvent absorbed by the polymer was measured using the difference between the volume of DCM remaining and the original volume of DCM (60 mL). (1*R*,5*R*)-*trans*-Carvyl amine **8** (65 mg, 0.43 mmol, 1 equiv.) was then added to the beaker, the extraction thimble was suspended as previously and DCM was added up to the mark[†] (vide supra). The solution was stirred and, at specific intervals, the thimble was raised, the remaining solvent removed in vacuo, and the quantity of (1*R*,5*R*)-*trans*-carvyl amine **8** remaining in solution was determined. After each measurement the (1*R*,5*R*)-*trans*-carvyl amine **8** was redissolved in DCM to the previously marked level.

3.5. General method for determining the percentage of imprint molecule: (1*R*,5*R*)-*trans*-carvyl amine **8** bound in the polymer

In the binding studies carried out according to the general method above there is always a certain quantity of (1*R*,5*R*)-*trans*-carvyl amine **8** present in the polymer due to non-specific binding (i.e., the solvent absorbed by the polymer will naturally contain a certain amount of (1*R*,5*R*)-*trans*-carvyl amine **8**). The approximation we have made is that

[†] An important distinction between adding DCM (60 mL) and adding the solvent up to the mark is necessary here. The polymers absorb significant quantities of solvent which they retain for a considerable time. If one adds another (60 mL) of solvent then there will be more solvent present due to preabsorbed DCM in the polymer. In order to avoid lengthy drying procedures in between steps the marked level is used. This is the level at which the total of the DCM absorbed in the polymer and in the rest of the beaker is equal to 60 mL.

the percentage of (1*R*,5*R*)-*trans*-carvyl amine **8** bound due to 'non-specific binding' is equal to the percentage of DCM absorbed by the polymer. To avoid overestimating the level of binding, the calculation of the amount of template bound in the polymer at each point in the binding study includes a correction factor to account for this phenomenon (Eq. 1).

$$\mathbf{8} \text{ bound/mg} : M = y - x(alb) \quad (1)$$

percentage of **8** remaining in solution

$$= M(\text{mg})/\text{original weight}(65.0 \text{ mg}) \quad (2)$$

Where y =original weight of **8** (65.0 mg, 0.43 mmol, 1 equiv.), x =weight of **8** in remaining in solution, (alb) =correction factor: original volume of DCM (60 mL)/(original volume of DCM (60 mL)–volume of DCM absorbed by polymer).

3.6. Binding studies on MIPs A1*–A5*, and R*

Binding studies were carried out on the polymers A1*–A5*, and R* according to the general method. The amount of solvent absorbed by each MIP was determined according to this general method, and the corrected percentage (Eq. 2) of (1*R*,5*R*)-*trans*-carvyl amine **8** remaining in solution was determined after 1, 4, 8, and 15 h for each of the MIPs

MIP	Volume of solvent absorbed (mL)	% of 8 bound					15 h mmol of 8 bound
		0 h	1 h	4 h	8 h	15 h	
A1*	12.0	0	20	56	63	72	71%
A1* (repeat) ^a	12.0	0	34	50	62	70	0.31
A2*	14.0	0	7	36	52	66	0.28
A3*	13.0	0	6	48	60	73	0.31
A4*	8.0	0	19	57	70	82	0.35
A5*	7.5	0	15	39	52	62	0.27
R*	14.0	0	10	36	42	43	0.13

The percentage of **8** bound after 15 h was taken to be the amount of **8** required for saturation of the all the available sulfonic acid sites in the MIP, and was used to calculate the number of mmol of active sites in each polymer. These values were used to calculate the number of equivalents used in the subsequent catalytic studies.

3.7. General method for the debinding studies of polystyrene–divinylbenzene MIPs A1*–A5*, and R*

The apparatus used was the same as for the binding studies. The beaker was filled up to the mark with DCM (vide supra). The solution was stirred at 0 °C for 1 h before the Soxhlet was removed, the remaining solvent reduced in vacuo and the residue analysed by ¹H NMR. This was carried out three times. The beaker was then filled with 10% *n*-PrNH₂:DCM (60 mL), stirred at 0 °C for 2 h, then reduced in vacuo and the residue analysed by ¹H NMR. This was carried out three times. The amount of (1*R*,5*R*)-*trans*-carvyl amine **8** in each fraction was calculated from the weight and the molar ratio of **8**: *n*-PrNH₃(CO₃)₂: *n*-PrNH₂ as observed

by ¹H NMR. In each case the mass balance of (1*R*,5*R*)-*trans*-carvyl amine **8** over the entire binding-debinding experiment was in the region of 90%.

In each case the ratios were determined by comparing the integration of the following peaks.

¹H NMR (CDCl₃, 300 MHz): δ_H (1*R*,5*R*)-*trans*-carvyl amine **8** 5.40 (1H, m, =CHR) and/or 4.67 (2H, 2s, =CH₂); *n*-PrNH₃(CO₃)₂ 0.79 (3H, t, $J=7.5$ Hz, CH₃); *n*-PrNH₂ 0.68, (3H, t, $J=7.5$ Hz, CH₃)

MIP	Amount of 8 removed in each washing (mg)					
	DCM	DCM	DCM	<i>n</i> -PrNH ₂ DCM	<i>n</i> -PrNH ₂ DCM	<i>n</i> -PrNH ₂ DCM
A1*	1.9	1.9	2.2	41.2	4.5	0
A2*	1.2	2.4	1.6	8.4	15.3	3.1
A3*	3.0	2.1	0.0	20.4	11.2	3.0
A4*	0.7	0.1	1.9	38.8	5.5	0.0
A5*	3.1	1.0	0.9	34.2	2.5	0
R*	7.6	3.1	1.8	24.0	3.3	0

3.8. General method for competitive binding studies

The apparatus used was the same as for the binding studies. The amount of solvent absorbed by the polymer was determined as previously. (1*R*,5*R*)-*trans*-carvyl amine **8** (1 equiv. of the calculated number of binding sites in the polymer, vide supra) and α-methyl benzylamine **20** (1 equiv.) were added to the beaker and the 1:1 ratio was confirmed by ¹H NMR. DCM (60 mL) was added up to the mark (vide supra) and the solution was stirred at 0 °C for 15 h. The solution was then concentrated in vacuo and the ratio **8**:**20** of the amines not bound by the polymer was determined by ¹H NMR.

In each case the ratio's were determined by comparing the integration of the following peaks.

¹H NMR (CDCl₃, 300 MHz): δ_H α-methyl benzylamine **20**, 4.27 (1H, q, $J=6.5$ Hz, CH₃CHN); (1*R*,5*R*)-*trans*-carvyl amine **8**, 5.40 (1H, m, =CHR) and/or 4.67 (2H, 2s, =CH₂)

Competitive binding of equimolar amounts of **8** and **20** by polymers A1*, A4* and R* in DCM

Polymer	A1*	A4*	R*
Molar ratio 8 : 20 left in solution after 15 h	47:53	44:56	53:47

3.9. General method for polymer regeneration

Polymers were regenerated after the binding studies. The apparatus used was the same as for the binding studies. The polymer was washed with DCM (2×60 mL/1 h/0 °C) to remove any excess *n*-PrNH₂ and then stirred with HCl:diethyl ether (60 mL/1 h/0 °C) to regenerate the acid sites. The polymer was washed with ether (3×60 mL), methanol (n ×60 mL until pH neutral) and DCM (2×60 mL).

3.10. General procedure for the reaction of α -pinene oxide **6** with polystyrenedivinylbenzene MIPs in toluene

α -Pinene oxide **6** was added to a stirred suspension of the polystyrene–divinylbenzene MIP (1 equiv.) in toluene (0.015 M to **6**) at room temperature. An example of the reaction scale is α -pinene oxide **6** (22.9 mg, 24 μ L, 0.15 mmol, 1 equiv.), **A1*** (913 mg, 0.15 mmol, 1 equiv.), and toluene (10.0 mL). The reaction was stirred for 1 h and analysed by GC comparison with authentic samples. The polymer was then filtered off, washed with DCM (3 \times 10 mL) and the filtrate concentrated in vacuo and analysed by ^1H and ^{13}C NMR.

3.11. General procedure for the reaction of α -pinene oxide **6** with polystyrene–divinylbenzene MIPs in methanol

α -Pinene oxide **6** was added to a stirred suspension of the polystyrene–divinylbenzene MIP (1 equiv.) in methanol (0.015 M to **6**) at room temperature. An example of the reaction scale is α -pinene oxide **6** (22.9 mg, 24 μ L, 0.15 mmol, 1 equiv.), **A1*** (913 mg, 0.15 mmol, 1 equiv.), and methanol (10.0 mL). The reaction was stirred for 1 h and analysed by GC comparison with authentic samples. The polymer was then filtered off, washed with DCM (3 \times 10 mL) and the filtrate concentrated in vacuo and analysed by ^1H and ^{13}C NMR.

3.12. General procedure for the reaction of α -pinene oxide **6** with polystyrene–divinylbenzene MIP's in DMF

α -Pinene oxide **6** was added to a stirred suspension of the polystyrene–divinylbenzene MIP (1 equiv.) in DMF (0.015 M to **6**) at room temperature. An example of the reaction scale is α -pinene oxide **6** (22.9 mg, 24 μ L, 0.15 mmol, 1 equiv.), **A1*** (913 mg, 0.15 mmol, 1 equiv.), and DMF (10.0 mL). The reaction was stirred until consumption of all the starting material was observed by GC comparison with authentic samples (3–7.5 h). The polymer was then filtered off, and washed with DCM (3 \times 10 mL). The organic layer was washed with distilled water (5 \times 10 mL), dried over MgSO_4 (s), concentrated in vacuo and analysed by ^1H and ^{13}C NMR.

3.13. Solution reactions of *p*-TSA monohydrate with α -pinene oxide **6**

α -Pinene oxide **6** (24 μ L, 0.15 mmol, 1 equiv.) was added to a stirred solution of *p*-toluenesulfonic acid (28.5 mg, 0.15 mmol, 1 equiv.) in toluene (10.0 mL) and the reaction stirred at room temperature for 1 h and analysed by GC comparison with authentic samples.

3.13.1. 2-Methyl-5-(1-methylethenyl)-2-cyclohexen-1-ol, or *trans*-carveol **5.**²³ R_f 0.3 (SiO₂, 20% EtOAc:petrol 40–60 °C); ^1H NMR (CDCl₃, 400 MHz): δ_{H} 5.59 (1H, dm, $J=5.5$ Hz), 4.11 (1H, s), 4.09 (1H, s), 4.02 (1H, s(br)), 2.32 (1H, m), 2.14 (1H, dm, $J=13.5$ Hz), 2.03–1.55 (4H, m), 1.80 (3H, s), 1.75 (3H, s); ^{13}C NMR (CDCl₃, 100 MHz): δ_{C} 149, 134.3, 125.4, 109.0, 68.6, 36.7, 35.2, 31.0, 20.9. IR (neat): $\tilde{\nu}_{\text{max}}$ 3333 (s, OH), 3082 (w), 2966 (s), 2916 (s), 1645 (m, C=C), 1438 (s), 1375 (m), 1264 (m), 1156 (m), 1164

(m), 1054 (s), 1032 (s), 962 (s), 944 (m), 887 (s); LRMS (EIMS) m/z : 152 [M^+], 109, 84, 69, 54, 38.

3.13.2. (2,2,4-Trimethyl-cyclopent-3-enyl)-acetaldehyde, or campholenic aldehyde **10.**²⁴ R_f 0.7 (SiO₂, 20% EtOAc:petrol 40–60 °C). ^1H NMR (CDCl₃, 400 MHz): δ_{H} 9.80 (1H, t, $J=2.5$ Hz), 5.29 (1H, m), 2.55–2.25 (4H, m), 1.89 (1H, m), 1.61 (3H, d(br), $J=2.5$ Hz), 1.00 (3H, s), 0.79 (3H, s); ^{13}C NMR (CDCl₃, 100 MHz): δ_{C} 201.8, 147.8, 121.5, 46.8, 45.0, 44.3, 35.4, 25.5, 19.9, 12.5. IR (neat): $\tilde{\nu}_{\text{max}}$ 3038 (w), 2957 (s), 2716 (w, CHO), 1726 (s, C=O), 1463 (m), 1437 (w), 1384 (w), 1362 (m), 1016 (w), 794 (m); LRMS (EIMS) m/z : 152 [M^+], 108, 93, 82, 67, 57.

3.13.3. 4,4,7-Trimethyl-6-oxa-bicyclo[3.2.1]oct-3-ene **11.**²⁵ R_f 0.7 (SiO₂, 20% EtOAc:petrol 40–60 °C); ^1H NMR (CDCl₃, 500 MHz): δ_{H} 5.16 (1H, m), 3.95 (1H, d, $J=5.0$ Hz), 2.22–2.19 (2H, m), 2.18 (1H, dd, $J=10.5$, 5.0 Hz), 2.10 (1H, m), 1.80 (1H, d, $J=10.5$ Hz), 1.67 (3H, m), 1.28 (3H, s), 1.16 (3H, s); ^{13}C NMR (CDCl₃, 75 MHz): δ_{C} 139.5, 120.2, 82.7, 76.6, 41.8, 34.5, 30.4, 30.3, 25.4, 21.4. IR (neat): $\tilde{\nu}_{\text{max}}$ 2968 (s), 2874 (m), 2840 (m), 1441 (m), 1358 (m), 1297 (w), 1209 (m), 1114 (m), 1033 (m), 1006 (s); LRMS (CI) m/z : 153 [$\text{M}+\text{H}$]⁺, 135, 107, 93.

3.13.4. 6,6-Dimethyl-2-methylene-bicyclo[3.1.1]heptan-3-ol, or *trans*-pinocarveol **12.**²⁶ R_f 0.3 (SiO₂, 20% EtOAc:petrol 40–60 °C); ^1H NMR (CDCl₃, 400 MHz): δ_{H} 4.97 (1H, s), 4.80 (1H, s), 4.40 (1H, d, $J=7.5$ Hz), 2.49 (1H, t, $J=5.5$ Hz), 2.36 (1H, m), 2.22 (1H, d, $J=14.5$, 7.5 Hz), 1.97 (1H, m), 1.82 (1H, dd, $J=14.5$, 4.0 Hz), 1.69 (1H, d, $J=10$ Hz), 1.25 (3H, s), 0.62 (3H, s); ^{13}C NMR (CDCl₃, 75 MHz): δ_{C} 156.3, 111.8, 67.2, 51.0, 40.8, 40.2, 34.9, 28.6, 26.3, 21.5. IR (neat): $\tilde{\nu}_{\text{max}}$ 3383 (s, b, OH), 3071 (w), 2974 (s), 2921 (s), 2869 (s), 1646 (m, C=C), 1452 (m), 1384 (s), 1387 (m), 1340 (w), 1296 (m), 1145 (m), 1106 (w), 1086 (w), 1022 (m), 1002 (m), 895 (m); LRMS (CI) m/z : 153 [$\text{M}+\text{H}$]⁺, 135, 107, 93, 79.

3.13.5. (2,2,3-Trimethyl-cyclopent-3-enyl)-acetaldehyde dimethyl acetal, or campholenic aldehyde dimethyl acetal **14.**²⁷ R_f 0.5 (SiO₂, 20% EtOAc:petrol 40–60 °C); mp (petrol 30–40 °C/EtOAc): 76–78 °C; ^1H NMR (CDCl₃, 400 MHz): δ_{H} : 5.23 (1H, m), 4.43 (1H, dd, $J=7.5$, 4.0 Hz), 3.34 (3H, s), 3.31 (3H, s), 2.31 (1H, m), 1.90–1.76 (3H, m), 1.61 (3H, d, $J=1.5$ Hz), 1.54 (1H, m), 0.99 (3H, s), 0.76 (3H, s). ^{13}C NMR (CDCl₃, 100 MHz) δ_{C} /ppm: 148.5, 121.7, 104.0, 53.0, 52.0, 46.8, 45.9, 35.5, 32.8, 25.6, 19.7, 12.7. IR (neat): $\tilde{\nu}_{\text{max}}$ 3036 (w), 2953 (s), 2830 (m), 1464 (m), 1382 (m), 1361 (m), 1193 (w), 1138 (m), 1124 (s), 1059 (s), 1016 (m), 965 (m), 937 (w), 795 (m); LRMS (FABS) m/z : 198 [M]⁺, 133.

3.13.6. 5-(1-Methoxy-1-methyl-ethyl)-2-methyl-cyclohex-2-enol, or Sobrerol-monomethyl ether **15.**²⁸ R_f 0.1 (SiO₂, 20% EtOAc:petrol 40–60 °C); ^1H NMR (CDCl₃, 400 MHz): δ_{H} 5.57 (1H, dm, $J=5.0$ Hz), 4.01 (1H, m), 3.19 (3H, s), 2.04–1.89 (3H, m), 1.78 (3H, s), 1.74 (1H, s(br)), 1.38 (1H, td, $J=13.0$, 4.0 Hz), 1.1 (6H, s); ^{13}C NMR (CDCl₃, 100 MHz) δ_{C} 134.3, 125.4, 76.2, 68.5, 48.7, 35.3, 32.7, 27.0, 22.4, 22.1, 20.9. IR (neat): $\tilde{\nu}_{\text{max}}$ 3394 (s, b, OH), 2970 (s), 2919 (s), 1456 (m), 1380 (m), 1364 (m), 1252 (w), 1158 (m), 1140 (m), 1075 (s), 1035 (m), 961 (w), 805 (w).

3.13.7. trans-2-Methyl-5-(1-methoxy,1-methylethyl)-2-cyclohexenmethyl ether, or Sobrerol dimethyl ether 16.²⁹ R_f 0.4 (SiO₂, 20% EtOAc:petrol 40–60 °C); ¹H NMR (CDCl₃, 400 MHz): δ_H 5.59 (1H, m), 3.50 (1H, m), 3.40 (3H, s), 3.19 (3H, s), 2.11 (1H, dd, $J=15.5, 2.0$ Hz), 1.98 (2H, m), 1.76 (3H, d, $J=1.5$ Hz), 1.761.69 (2H, m), 1.12 (3H, s), 1.11 (3H, s); ¹³C NMR (CDCl₃, 100 MHz): δ_C 133.2, 125.8, 79.7, 76.1, 57.1, 48.6, 34.7, 27.2, 26.8, 22.7, 22.5, 21.0. IR (neat): $\tilde{\nu}_{max}$ 2972 (s), 2921 (s), 2834 (s), 1455 (m), 1381 (m), 1384 (m), 1333 (w), 1250 (m), 1189 (m), 1157 (m), 1140 (m), 1078 (s), 914 (m), 807 (w).

3.13.8. 1,7,7-Trimethyl-6-exo-methoxy bicyclo[2.2.1]-heptan-2-endo-ol 17. R_f 0.3 (SiO₂, 20% EtOAc:petrol 40–60 °C); ¹H NMR (CDCl₃, 500 MHz): δ_H 4.79 (1H, d, $J=10.5$ Hz, OH), 4.02 (1H, m), 3.79 (1H, dt, $J=9.5, 3.0$ Hz), 3.32 (3H, s), 2.38 (1H, m), 2.27 (1H, m), 1.73 (1H, t, $J=5.0$ Hz), 1.32 (1H, dd, $J=13.0, 3.5$ Hz), 1.20 (1H, dd, $J=13.5, 4.0$ Hz), 1.03 (3H, s), 0.80 (3H, s), 0.81 (3H, s); ¹³C NMR (CDCl₃, 75 MHz): δ_C 89.9, 79.0, 58.2, 50.1, 48.8, 43.2, 39.8, 36.0, 20.0, 19.7, 12.1. IR (neat): $\tilde{\nu}_{max}$ 3483 (s, OH), 2986 (m), 2952 (s), 2877 (m), 1450 (m), 1369 (m), 1298 (w), 1190 (m), 1230 (s), 1190 (m), 1130 (s), 1086 (s), 1062 (m), 1004 (w), 970 (w), 899 (w).

3.13.9. 5-Isopropylidene-2-methyl-cyclohex-2-enol 19. R_f 0.4 (SiO₂, 20% EtOAc:petrol 40–60 °C); ¹H NMR (CDCl₃, 500 MHz): δ_H 5.47 (1H, m), 3.97 (1H, m), 2.85 (1H, d(br), $J=20$ Hz), 2.65 (1H, dd, $J=13.5, 4.0$ Hz), 2.31 (1H, dm, 24 Hz), 1.77 (3H, m), 1.71 (3H, s), 1.66 (3H, s), 1.44 (1H, s(br)); ¹³C NMR (CDCl₃, 100 MHz): δ_C 135.9, 125.8, 124.3, 123.1, 70.4, 35.9, 29.8, 20.4, 20.2, 19.9. IR (neat): $\tilde{\nu}_{max}$ 3257 (s, OH), 3160 (m), 2966 (m), 2935 (m), 2884 (m), 1607 (w), 1436 (w), 1366 (w), 1320 (w), 1058 (w), 1014 (s), 912 (w), 803 (w); LRMS (FABS) m/z : 152 [M]⁺, 149, 133, 107.

Acknowledgements

We wish to thank Professor John H. Ridd for useful discussions. We are grateful to Quest International and the Leverhulme Trust for funding.

References and notes

- For recent reviews on molecular imprinting see (a) Wulff, G. *Chem. Rev.* **2002**, *1*, 27. (b) Whitcombe, M. J.; Alexander, C.; Vulfson, E. N. *Synlett* **2000**, 911–923. (c) Cormack, P. A. G.; Mosbach, K. *React. Funct. Polym.* **1999**, *41*, 115–124. (d) Wulff, G. *Angew. Chem., Int. Ed.* **1995**, *34*, 1812–1832.
- (a) Haupt, K. *Analyst* **2001**, *126*, 747–756. (b) Andersson, L. I. *J. Chromatogr. B* **2000**, *745*, 3–13, and references therein.
- Byström, S. E.; Börje, A.; Akermark, B. *J. Am. Chem. Soc.* **1993**, *115*, 2081–2083.
- Haupt, K.; Mosbach, K. *Chem. Rev.* **2000**, *100*, 2495–2504.
- Ye, L.; Ramström, O.; Mansson, M.-O.; Mosbach, K. *J. Mol. Recog.* **1998**, *11*, 75–78.
- Alexander, C.; Smith, C. R.; Whitcombe, M. J.; Vulfson, E. N. *J. Am. Chem. Soc.* **1999**, *121*, 6640–6651.
- (a) Tramontano, A.; Janda, K. D.; Lerner, R. A. *Science* **1986**, *234*, 1566–1570. (b) Pollack, S. J.; Jacobs, J. W.; Schultz, P. G. *Science* **1986**, *234*, 1570–1573.
- See Ref. 1a.
- Dictionary of organic compounds*; 5th ed. Buckingham, J., Ed.; Chapman and Hall: London, 1982; p I-01178.
- Vialemarine, M.; Campagnole, M.; Bourgeois, M.-J.; Montaudon, E. *C. R. Acad. Sci. Paris, t.2, Série IIc* **1999**, 449–454, and references therein.
- (a) Royals, E. E.; Leffingwell, J. C. *J. Org. Chem.* **1964**, *29*, 2098–2099. (b) Hartshorn, M. P.; Kirk, D. N.; Wallis, A. F. A. *J. Chem. Soc.* **1964**, 549. (c) King, L. C.; Farber, H. *J. Org. Chem.* **1961**, *26*, 326–329.
- (a) Arata, K.; Tanabe, K. *Chem. Lett.* **1979**, 1017–1018. (b) Joshi, V. S.; Dev, S. *Tetrahedron* **1977**, *33*, 2955–2957.
- Murata, S.; Suzuki, M.; Noyori, R. *Bull. Chem. Soc. Jpn* **1982**, *55*, 247–254.
- (a) Sherrington, D. C. *Chem. Commun.* **1998**, 2275–2286. (b) See also Ref. 1d.
- Car, G.; Dosanjh, G.; Millar, A. P.; Whittaker, D. *J. Chem. Soc., Perkin Trans. 2* **1994**, 1419–1422.
- trans*-Carvyl amine **8** was prepared according to literature procedure; (a) Sen, S. E.; Roach, S. L. *Synthesis* **1995**, 756–758. starting from *cis*-carveol obtained by LAH reduction of (*R*)-carvone (b) Ireland, R. E.; Maienfisch, P. *J. Org. Chem.* **1988**, *53*, 640–651.
- For another example of an imprint molecule-polymer linkage realised by an ammonium sulfonate salt: Dunkin, I. R.; Lenfield, J.; Sherrington, D. C. *Polymer* **1993**, *34*, 77–84.
- Andersson, H. S.; Karlsson, J. G.; Piletsky, S. A.; Koch-Schmidt, A.-C.; Mosbach, K.; Nicholls, I. A. *J. Chromatogr., A* **1999**, *848*, 39–49.
- March, J. *Advanced organic chemistry: reactions, mechanisms and structure*; 4th ed. Wiley: New York, 1985; pp 250–251 and references therein.
- Harris, T. K.; Turner, G. J. *IUBMB Life* **2002**, *53*, 85–98.
- Hollfelder, F.; Kirby, A. J.; Tawfik, D. S. *J. Org. Chem.* **2001**, *66*, 5866–5874.
- The number of moles of salt **9:21** was calculated using the molar ratio of the 4-styrenesulfonic acid, (*1R,5R*)-*trans*-carvyl amine salt **9:21** to (*1R,5R*)-*trans*-carvyl amine hydrochloride **9**, as determined by ¹H NMR. This method was used throughout.
- Lajunen, M. K.; Maunula, T.; Koskinen, A. M. P. *Tetrahedron* **2000**, *56*, 8167–8171.
- Farges, G.; Kergomard, A. *Bull. Soc. Chim. Fr.* **1975**, 315–318.
- Ravindranath, B.; Srinivas, P. *Tetrahedron* **1983**, *39*, 3991–3994.
- (a) Kaminska, J.; Schwegler, M. A.; Hoefnagel, A. J.; Van Bekkum, H. *Recl. Trav. Chim. Pays Bas* **1992**, *111*, 432–437. (b) Warpehoski, M. A.; Chabaud, B.; Sharpless, K. B. *J. Org. Chem.* **1982**, *47*, 2897–2900.
- Meinwald, J.; Chapman, R. A. *J. Am. Chem. Soc.* **1968**, *90*, 3218–3226.
- Selva, A.; Ferrario, F.; Ventura, P. *Org. Mass Spectrom.* **1988**, *23*, 677–679.
- Gora, J.; Smigielski, K.; Kula, J. *Synthesis* **1989**, 759–761.

Theoretical study of photoinduced ring-isomerization in the 1,2,4-oxadiazole series

Silvestre Buscemi,^a Maurizio D'Auria,^{b,*} Andrea Pace,^a Ivana Pibiri^a and Nicolò Vivona^a

^aDipartimento di Chimica Organica 'E. Paternò', Università di Palermo, Viale delle Scienze, Parco d'Orleans II, 90128 Palermo, Italy

^bDipartimento di Chimica, Università della Basilicata, Via N. Sauro 85, 85100 Potenza, Italy

Received 21 November 2003; revised 15 January 2004; accepted 5 February 2004

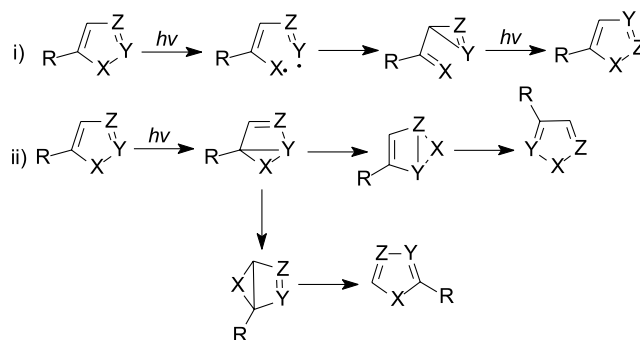
Abstract—A theoretical study of photoinduced ring-isomerization of 3-amino-5-methyl- and 3-amino-5-phenyl-1,2,4-oxadiazoles is reported. The results well agree with the reported experimental data: in particular, they explain the ring-photoisomerization into the corresponding 2-amino-1,3,4-oxadiazoles through a ring contraction-ring expansion route; moreover, the occurrence of competing pathways involving both the ring contraction and the internal cyclization–isomerization mechanism during irradiation of the 5-alkyl substituted substrates in the presence of a base has been also substantiated.

© 2004 Elsevier Ltd. All rights reserved.

1. Introduction

Photoinduced ring rearrangements of five-membered heterocycles represent a wide class of reactions that received a lot of attention both for the development of synthetic procedure and the description of their mechanisms.^{1–3} Among these, two generally observed pathways are represented by (i) the ring contraction-ring expansion mechanism, which explains the interchange of two adjacent ring atoms and involves a three-membered ring intermediate, and (ii) the internal cyclization–isomerization route (also named 'electrocyclic ring closure-heteroatom migration' route), which involves an initial bicyclic isomer (the Dewar isomer) through the formation of a bond between positions 2 and 5 of the starting ring, followed by a sigmatropic shift to form the rearranged ring (Scheme 1). A general scheme which is a combination of the two pathways above has also been proposed; furthermore, a 'zwitterion-tricyclic' route in sulfur containing heterocycles, and a 'fragmentation–addition' route have been also recognized.²

For a given heterocycle, competing pathways involving both ring contraction and internal cyclization have been documented, and they have been shown to depend on the structure of the starting ring and on the photoreaction medium.^{4,5} In some cases, e.g. in the isothiazole series the occurrence of the above competing pathways was also



Scheme 1. The photoisomerization of five-membered heterocycles.

affected by the presence of a base such as triethylamine (TEA) in the irradiation medium.⁵

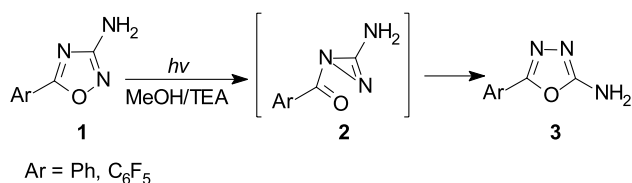
A theoretical approach has been used to rationalize many of these photochemical isomerizations. In this respect, we recently proposed a unified description by using semi-empirical calculations,^{6–9} in some case also confirmed by ab initio studies.^{10–13} By this description, a singlet excited state of a heterocyclic molecule will decay into the corresponding triplet state or into the corresponding Dewar isomer, depending on energetic factors. The Dewar isomer will develop into the internal cyclization–isomerization route; in turn, the triplet state will develop through cleavage of the weakest bond of the ring (generally, the X–C_α bond, where X is a heteroatom of the ring) giving open-chain products or ring contraction products, and then the corresponding ring expansion isomer.

In the frame-work of our general project on the

Keywords: Photochemistry; Photoisomerization; Ab initio calculations; Heterocycles; 1,2,4-Oxadiazole.

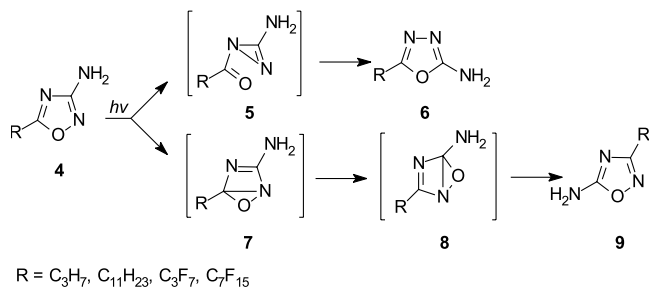
* Corresponding author. Tel.: +39-0971-202-240; fax: +39-0971-202-223; e-mail address: dauria@pzuniv.unibas.it

photoreactivity of O–N bond containing azoles, we previously described¹⁴ the occurrence of ring photorearrangement of 1,2,4-oxadiazoles into 1,3,4-oxadiazoles which was found to be restricted to oxadiazoles containing an XH group at C(3) of the ring in one hand, and favored by the presence of a base in the irradiation medium, in the other.¹⁵ On this basis, tautomeric or acid–base equilibria in the starting oxadiazole or in the intermediates are supposed to be involved during the transformation, which was framed in the ring contraction–ring expansion pattern. Experimental observations on 3-amino-5-phenyl-1,2,4-oxadiazole showed that the yield of photorearranged 2-amino-1,3,4-oxadiazole was enhanced when irradiation was carried out in the presence of a base (Scheme 2).¹⁵



Scheme 2. Photoisomerization of 5-aryl-3-amino-1,2,4-oxadiazoles.s.

By contrast, during the irradiations of some 3-amino-5-alkyl-1,2,4-oxadiazoles, the occurrence of two competing photorearrangements has been recently revealed (see Scheme 3):¹⁶ in methanol, the ring contraction–ring expansion was the only process involved, whereas, in the presence of triethylamine (TEA) as a base, both ring contraction–ring expansion and internal cyclization–isomerization routes were observed (the latter reported for the first time in the oxadiazole series leads to a ring-degenerate photoisomerization).



Scheme 3. Photoisomerization of 5-alkyl-3-amino-1,2,4-oxadiazoles.

Irradiations performed on the corresponding fluorinated analogues showed the same trend of photoreactivity: 3-amino-5-perfluoroalkyl- and 3-amino-5-pentafluorophenyl-1,2,4-oxadiazoles behaved differently towards the ring-phototransformation process.¹⁷

To gain some information on the substituent effect and to test the validity of the above-described hypothesis for more complex heterocycles, we have now performed a computational survey on the 3-amino-5-methyl-1,2,4-oxadiazole (model compound for 5-alkyl derivatives) and on 3-amino-5-phenyl-1,2,4-oxadiazole (model compound for 5-aryl derivatives) considering all the possible species that could be involved in the very first steps of the photoreaction. Taking into account previous results using this theoretical approach, we investigated the ground and the lowest triplet

state of the substrate, the triplet biradicals that result from the homolytic cleavage of O(1)–N(5) and O(1)–C(5) bonds (the former being the species supposed to occur in the isomerization process leading to the formation of diazine intermediates and therefore of the 1,3,4-oxadiazoles).[†] Moreover, the Dewar isomers of 3-amino-5-methyl-(phenyl)-1,2,4-oxadiazoles (precursors of the ring-degenerate isomers) in their singlet state have been also considered. To simulate irradiations in the presence of TEA, all the above mentioned species have been also treated in their deprotonated forms.

2. Results and discussion

2.1. General methodology

We performed ab initio calculations using 6-31G** basis set on Gaussian 98, using UHF method.¹⁸ The calculations were usually done using Møller–Plesset perturbations (MP2). The Polak–Ribiere algorithm with gradient calculations was adopted for geometry optimizations. The open-shell states were treated at the same level of accuracy as the closed state states. We verified that the obtained structures

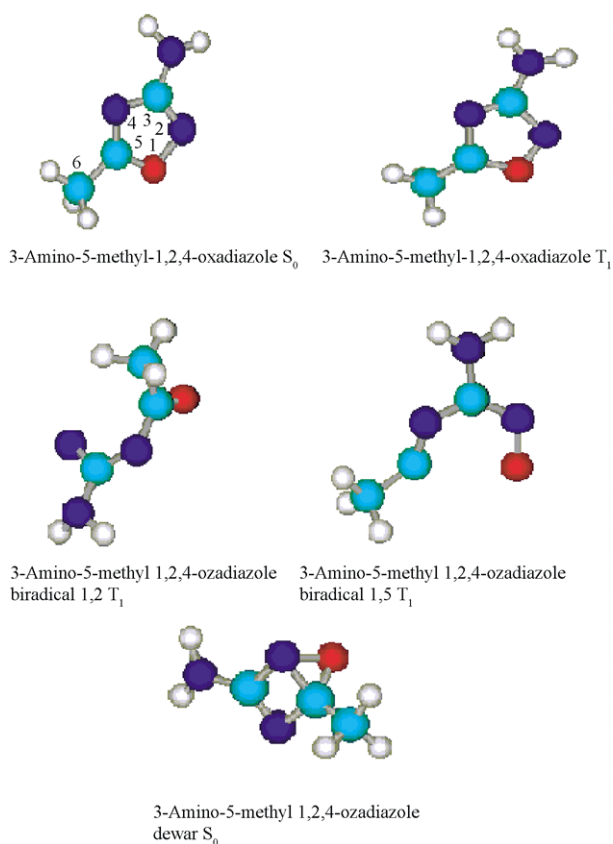


Figure 1. Structures of possible intermediates in the photochemical isomerization of 3-amino-5-methyl-1,2,4-oxadiazole.

[†] The O(1)–N(2) bond cleavage has been recognized in several phototransformation of O–N bond containing heterocycles such as 1,2,4-oxadiazoles or isoxazoles, however, we choose to include 1,5-biradical [from O(1)–C(5) bond cleavage] in our calculations for a complete comparison of potential species involved.

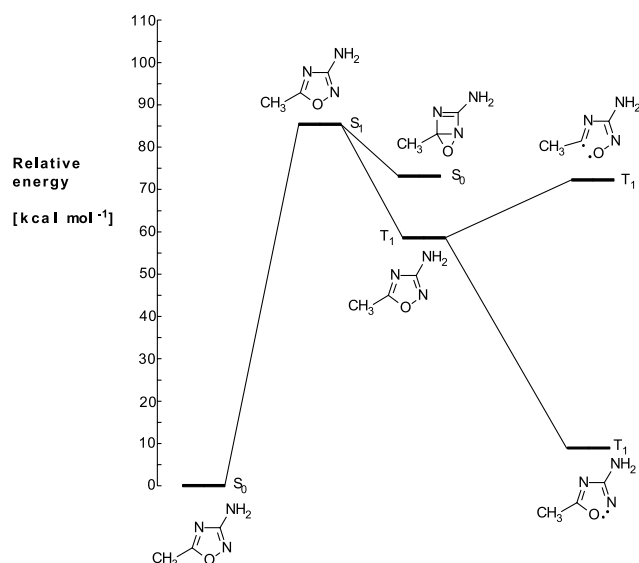


Figure 2. Relative energies of the species involved in the photoisomerization of 3-amino-5-methyl-1,2,4-oxadiazole.

were minima on the potential energy surfaces calculating the frequencies of the optimized structures.

2.2. 3-Amino-5-methyl-1,2,4-oxadiazole

Structures referring to the 3-amino-5-methyl-1,2,4-oxadiazole are illustrated in Figure 1; the relative energy profile referring to these structures is reported in Figure 2; energy values and geometrical data (bond distances and angles) are reported in Tables 1 and 2. In the ground state the substrate shows bond lengths in agreement with the aromatic character of the molecule: N_2-C_3 and N_4-C_5

resemble double bonds, C_5-O_1 as well as O_1-N_2 shows an intermediate length between a single and a double bond, C_3-N_4 resembles a single bond. In the triplet state N_2-C_3 , N_4-C_5 , and C_5-O_1 appear to be single bonds while C_3-N_5 has the length of a double bond. The triplet state of 3-amino-5-methyl-1,2,4-oxadiazole showed a π, π^* character with the LSOMO at -6.32 eV and the HSOMO at -3.86 eV. The 1,2 biradical is a π, π^* triplet with the LSOMO at -6.68 eV and the HSOMO at -6.50 eV. Furthermore, the 1,5 biradical is a π, π^* triplet with the LSOMO at -5.24 eV and the HSOMO at -4.71 eV. It is clear from the energy diagram (Fig. 2) that the formation of the triplet species is significantly favored over the formation of the Dewar isomer; furthermore the formation of the 1,2-biradical is strongly favored with respect to the formation of the 1,5-biradical, and this drives the reaction towards the formation of the 1,3,4-oxadiazole product.

2.3. Deprotonated 3-amino-5-methyl-1,2,4-oxadiazole

The same kind of calculations were performed on the conjugated bases of the species described above. In the presence of a base, in fact, we could observe the formation of the corresponding conjugated bases of all the possible intermediates in the photochemical reaction. However it is not possible to exclude that the base is involved in the acid–base equilibria of one of the intermediates or of the excited states of the substrate rather than on the deprotonation of the substrate in its ground state. The structural properties of this compound are collected in Figure 3 and in Tables 1 and 2.

It is noteworthy that the structure of the triplet state strictly resembles that of the ground state. The triplet state of the conjugated base of 3-amino-5-methyl-1,2,4-oxadiazole showed a π, π^* character with the LSOMO at -5.82 eV

Table 1. Structural properties and energies of possible intermediates and their corresponding conjugated bases (c.b.) in the photochemical isomerization of 1,2,4-oxadiazole derivatives

Compound ^a	Electr. state	Structural element						Relative energy (kcal mol ⁻¹)
		O_1-N_2 (Å)	N_2-C_3 (Å)	C_3-N_4 (Å)	N_4-C_5 (Å)	C_5-O_1 (Å)	N_2-C_5 (Å)	
3-Amino-5-methyl-1,2,4-oxadiazole	S ₀	1.394	1.286	1.369	1.281	1.305		0
3-Amino-5-methyl-1,2,4-oxadiazole	S ₁							86
3-Amino-5-methyl-1,2,4-oxadiazole	T ₁	1.336	1.438	1.260	1.398	1.431		58
3-Amino-5-methyl-1,2,4-oxadiazole 1,2-biradical	T ₁	–	1.352	1.305	1.410	1.186		9
3-Amino-5-methyl-1,2,4-oxadiazole 1,5-biradical	T ₁	1.287	1.309	1.388	1.244	–		71
3-Amino-5-methyl-1,2,4-oxadiazole dewar	T ₁	1.472	1.456	1.273	1.458	1.361	1.438	73
3-Amino-5-methyl-1,2,4-oxadiazole c.b.	S ₀	1.352	1.404	1.334	1.357	1.441		0
3-Amino-5-methyl-1,2,4-oxadiazole c.b.	S ₁							57
3-Amino-5-methyl-1,2,4-oxadiazole c.b.	T ₁	1.352	1.406	1.334	1.357	1.442		64
3-Amino-5-methyl-1,2,4-oxadiazole c.b. 1,2-biradical	T ₁	–	1.355	1.364	1.323	1.229		33
3-Amino-5-methyl-1,2,4-oxadiazole c.b. 1,5-biradical	T ₁	1.278	1.373	1.419	1.229	–		79
3-Amino-5-methyl-1,2,4-oxadiazole c.b. dewar	S ₀	1.480	1.496	1.343	1.415	1.390	1.423	44
3-Amino-5-phenyl-1,2,4-oxadiazole	S ₀	1.428	1.338	1.422	1.336	1.365		0
3-Amino-5-phenyl-1,2,4-oxadiazole	T ₁	1.341	1.471	1.355	1.386	1.433		32
3-Amino-5-phenyl-1,2,4-oxadiazole 1,2-biradical	T ₁	–	1.339	1.361	1.438	1.216		12
3-Amino-5-phenyl-1,2,4-oxadiazole 1,5-biradical	T ₁	1.182	1.445	1.386	1.278	–		41
3-Amino-5-phenyl-1,2,4-oxadiazole dewar	S ₀	1.628	1.484	1.331	1.538	1.379	1.545	61
3-Amino-5-phenyl-1,2,4-oxadiazole c.b.	S ₀	1.428	1.338	1.422	1.336	1.365		0
3-Amino-5-phenyl-1,2,4-oxadiazole c.b.	S ₁							98
3-Amino-5-phenyl-1,2,4-oxadiazole c.b.	T ₁	2.008	1.360	1.413	1.370	1.260		56
3-Amino-5-phenyl-1,2,4-oxadiazole c.b. 1,2-biradical	T ₁	–	1.367	1.387	1.408	1.226		7
3-Amino-5-phenyl-1,2,4-oxadiazole c.b. 1,5-biradical	T ₁	1.234	1.404	1.434	1.212	–		70
3-Amino-5-phenyl-1,2,4-oxadiazole c.b. dewar	S ₀	1.621	1.516	1.398	1.492	1.401	1.520	57

^a c.b.=conjugated base.

Table 2. Other structural properties of possible intermediates and their corresponding conjugated bases (c.b.) in the photochemical isomerization of 1,2,4-oxadiazole derivatives

Compound ^a	Angle (°)									
	1–2–3	2–3–4	3–4–5	4–5–1	5–1–2	2–5–4	3–2–5	5–2–1	1–5–2	2–5–6
3-Amino-5-methyl-1,2,4-oxadiazole S ₀	102.45	114.9	101.67	113.85	107.13					
3-Amino-5-methyl-1,2,4-oxadiazole T ₁	102.78	115.52	105.33	107.56	108.78					
3-Amino-5-methyl-1,2,4-oxadiazole 1,2-diradical	71.65	121.72	121.31	121.6	58.94					
3-Amino-5-methyl-1,2,4-oxadiazole 1,5-diradical	114.52	128.44	122.24	78.57	88.40					
3-Amino-5-methyl-1,2,4-oxadiazole dewar	99.04	101.57	84.98	109.99	60.87	93.94	79.45	55.74	63.39	127.33
3-Amino-5-methyl-1,2,4-oxadiazole c.b. S ₀	104.05	113.58	105.54	108.28	108.05					
3-Amino-5-methyl-1,2,4-oxadiazole c.b. T ₁	104.08	113.49	105.61	108.26	108.06					
3-Amino-5-methyl-1,2,4-oxadiazole c.b. 1,2-biradical	80.03	127.31	118.76	129.86	84.05					
3-Amino-5-methyl-1,2,4-oxadiazole c.b. 1,5-biradical	115.53	120.45	122.21	79.00	89.86					
3-Amino-5-methyl-1,2,4-oxadiazole c.b. dewar	100.42	96.9	85.80	112.92	59.34	97.08	80.07	57.19	63.47	126.18
3-Amino-5-phenyl-1,2,4-oxadiazole S ₀	107.28	108.74	106.89	110.47	106.61					
3-Amino-5-phenyl-1,2,4-oxadiazole T ₁	107.50	108.32	107.50	109.36	107.33					
3-Amino-5-phenyl-1,2,4-oxadiazole 1,2-biradical	66.72	123.17	125.57	115.61	56.03					
3-Amino-5-phenyl-1,2,4-oxadiazole 1,5-biradical	122.70	128.96	126.97	77.42	83.78					
3-Amino-5-phenyl-1,2,4-oxadiazole dewar	101.98	95.82	92.27	107.28	61.16	85.64	86.18	51.54	67.42	130.09
3-Amino-5-phenyl-1,2,4-oxadiazole c.b. S ₀	107.28	108.74	106.89	110.47	106.61					
3-Amino-5-phenyl-1,2,4-oxadiazole c.b. T ₁	93.22	117.55	111.50	117.96	99.77					
3-Amino-5-phenyl-1,2,4-oxadiazole c.b. 1,2-biradical	69.67	118.02	124.58	120.14	47.31					
3-Amino-5-phenyl-1,2,4-oxadiazole c.b. 1,5-biradical	121.51	123.40	139.01	50.95	76.63					
3-Amino-5-phenyl-1,2,4-oxadiazole c.b. dewar	103.27	92.83	91.68	110.64	59.88	89.09	86.22	52.86	67.26	128.74

^a c.b.=conjugated base.

and the HSOMO at -1.67 eV. The 1,2 biradical is a n,π^* triplet with the LSOMO at -5.35 eV and the HSOMO at -1.62 eV. Furthermore, the 1,5 biradical is a n,π^* triplet with the LSOMO at -3.59 eV and the HSOMO at -3.12 eV. The relative energies for the five above-mentioned structures are shown in Figure 4 and Table 1. It is evident that the excitation of the oxadiazole anion to its singlet state is favored compared to the excitation of the

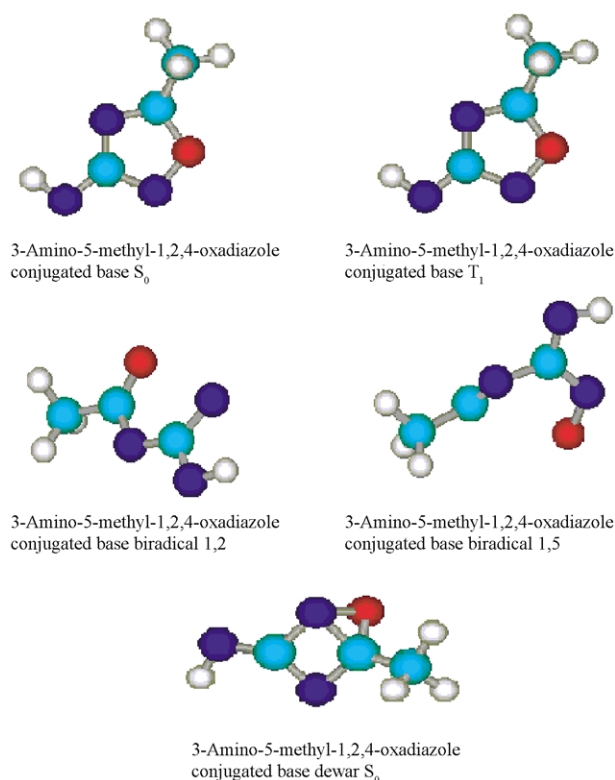


Figure 3. Structures of possible intermediates in the photochemical isomerization of the conjugated base of 3-amino-5-methyl-1,2,4-oxadiazole.

neutral form. The more interesting data, however, come from the possible evolution pattern of the first formed S₁ excited state. In fact, the intersystem crossing S₁→T₁ has a small barrier (~ 7 kcal/mol) and the formation of the 1,3,4-oxadiazole through the more stable 1,2-biradical is slowed down. On the other hand, the formation of the Dewar isomer is favored over the intersystem crossing (i.s.c.) to the T₁ state and, as confirmed by experimental results, the ring-degenerate isomerization through the internal cyclization–isomerization route starts competing with the ring contraction–ring expansion pathway.

2.4. 3-Amino-5-phenyl-1,2,4-oxadiazole

To justify the absence of the above competing pathways in the reactivity of 5-aryl derivatives, similar calculations have

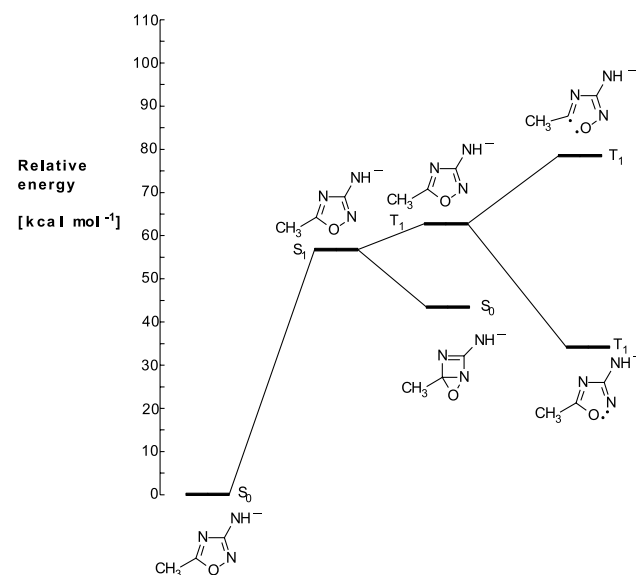


Figure 4. Relative energies of the species involved in the photoisomerization of the conjugated base of 3-amino-5-methyl-1,2,4-oxadiazole.

been considered for the 3-amino-5-phenyl-1,2,4-oxadiazole. At the ground state, this compound already showed some different properties with respect to the corresponding 5-methyl derivative, its structure presenting a highly dienic character (see Fig. 5 and Tables 1 and 2). In fact the N_2-C_3 and N_4-C_5 distances are intermediate between a single and a double C–N bond, the C_3-N_4 and C_5-O_1 bonds show typical distances for single bonds. In the triplet state the structure is clearly deformed with some inverted distances: in fact, the N_2-C_3 distance is similar to that of a single C–N bond while C_3-N_4 showed an intermediate distance between single and double C–N bond. Both S_0 and T_1 states of 3-amino-5-phenyl-1,2,4-oxadiazole are planar.

The triplet state of 3-amino-5-phenyl-1,2,4-oxadiazole showed a π,π^* character with the LSOMO at -6.47 eV and the HSOMO at -3.72 eV. The 1,2 biradical is a π,π^* triplet with the LSOMO at -6.57 eV and the HSOMO at -6.39 eV. On the contrary, the 1,5 biradical is a π,σ^* triplet with the LSOMO at -4.70 eV and the HSOMO at -4.31 eV. The relative energies for the five above-mentioned structures are shown in Figure 6 and Table 1. Interestingly, the data are in strong agreement with the experimental results: the singlet state (whose energy of 92 kcal/mol was obtained from the fluorescence spectrum)

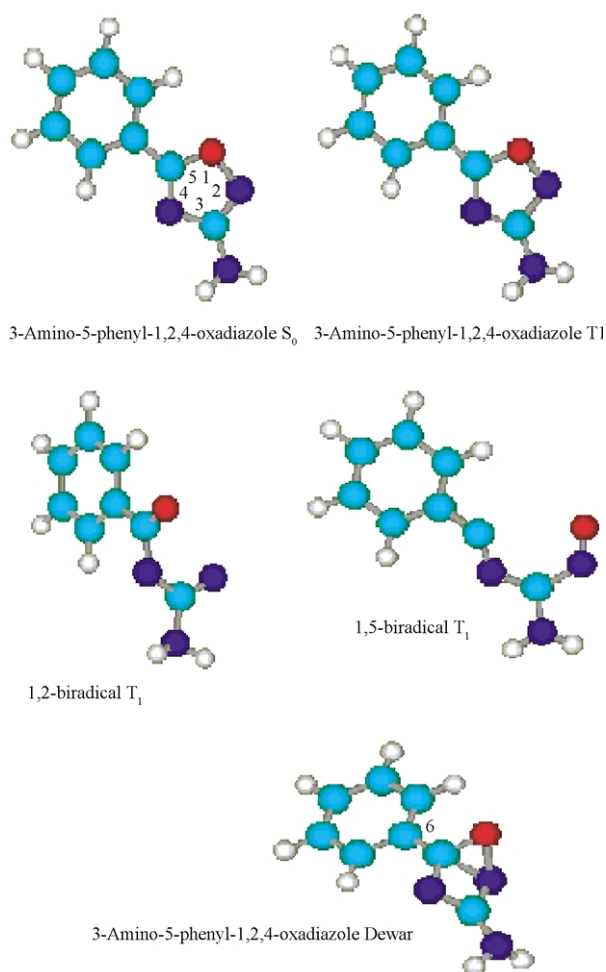


Figure 5. Structures of possible intermediates in the photochemical isomerization of 3-amino-5-phenyl-1,2,4-oxadiazole.

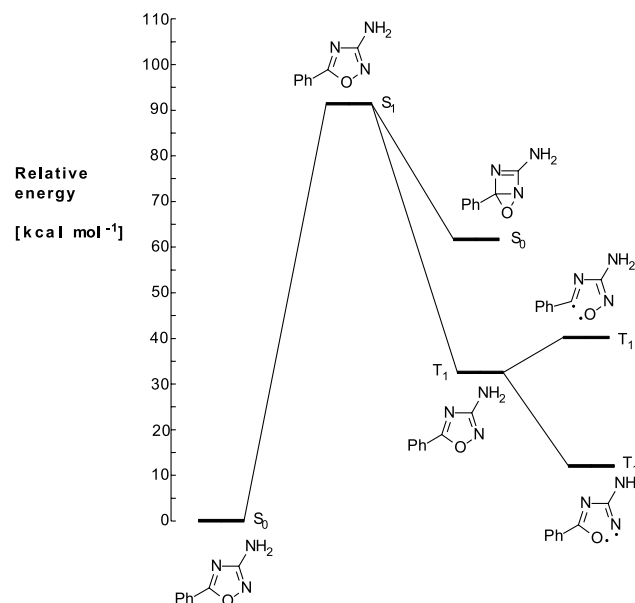


Figure 6. Relative energies of the species involved in the photoisomerization of 3-amino-5-phenyl-1,2,4-oxadiazole.

could evolve to give both the Dewar isomer and the corresponding triplet state; however, the formation of the triplet state is strongly favored and the ring-degenerate isomerization from the Dewar species is not observed.

2.5. Deprotonated 3-amino-5-phenyl-1,2,4-oxadiazole

The structural properties of the conjugated bases of all the possible intermediates in the irradiation of 3-amino-5-phenyl-1,2,4-oxadiazole are collected in Figure 7 and in Tables 1 and 2. We can see that the triplet state is deformed with the O_1-N_2 bond almost broken (and this will play a significant role driving the reaction towards the formation of the 1,2-biradical) and the C_5-O_1 bond similar to a double C–O bond. The triplet state of the conjugated base of 3-amino-5-phenyl-1,2,4-oxadiazole showed π,σ^* character with the LSOMO at -1.00 eV and the HSOMO at -0.11 eV. The 1,2 biradical is a π,π^* triplet with the LSOMO at -1.54 eV and the HSOMO at -0.50 eV. Furthermore, the 1,5 biradical is a π,π^* triplet with the LSOMO at -0.38 eV and the HSOMO at 0.69 eV. The relative energies for the five above-mentioned structures are shown in Figure 8 and Table 1. These data also agree with the experimental findings: the Dewar isomer and the triplet state of the anion have almost the same energy, however, the geometry of the triplet state (see above) and the significant stability of the triplet 1,2-biradical, will drive the reaction towards the formation of the 1,3,4-oxadiazole as the only product.

3. Conclusion

Although the reactions have all been carried out in methanol, which as a protic solvent will favor acid–base equilibria and could stabilize the intermediates involved, calculations performed on the model compounds in the gas phase are in agreement with the experimental results previously reported. For the 5-phenyl derivative, the

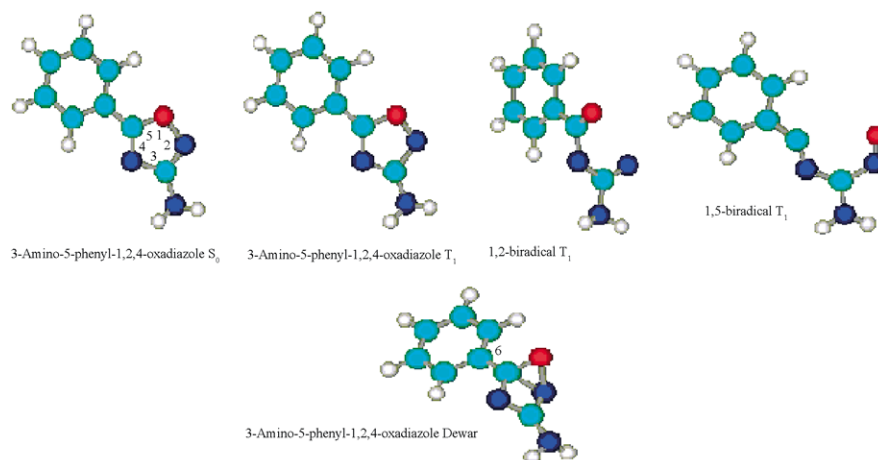


Figure 7. Structures of possible intermediates in the photochemical isomerization of the conjugated base of 3-amino-5-phenyl-1,2,4-oxadiazole.

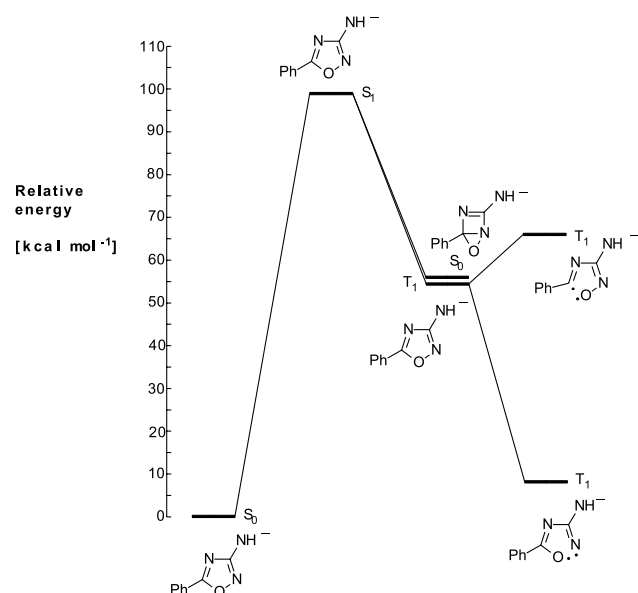


Figure 8. Relative energies of the species involved in the photoisomerization of the conjugated base of 3-amino-5-phenyl-1,2,4-oxadiazole.

computational study clearly explained the absence of the internal cyclization–isomerization route due to a more favored route through the formation of the 1,2-biradical leading to the diazirine intermediate and therefore to the 1,3,4-oxadiazole as the only product. This appears valid both for neutral and anionic forms. For the 5-methyl series, the computational model on the neutral form still showed that the ring contraction–ring expansion route is the favoured one. In the presence of a base, instead, we witness an inversion in the relative stability of the Dewar isomer and the first triplet state intermediate; the formation of the more stable 1,2-biradical still drives the reaction mainly towards the formation of the 1,3,4-oxadiazole ring, but the formation of the 1,2,4-oxadiazole regioisomer is now present as the result of a more competitive process.

As a comment on the role of the base, the authors believe that the involvement of the base in the deprotonation of the excited state cannot be excluded: besides the process described, a deprotonation of the oxadiazole excited state

can lead to the formation of the deprotonated anion that can evolve into the final products.

References and notes

1. Lablache-Combiere, A. In *Photochemistry of heterocyclic compounds*; Buchardt, O., Ed.; Wiley: New York, 1976.
2. Padwa, A. *Rearrangements in ground and excited states*; De Mayo, P., Ed.; Academic Press: New York, 1980; Vol. 3, p 501.
3. Lablache-Combiere, A. In *CRC handbook of organic photochemistry and photobiology*; Horspool, W., Ed.; CRC: Boca Raton, FL, 1995; p 1063.
4. See, e.g. (a) Baltrop, J. A.; Day, A. C.; Mack, A. G.; Shahrissa, A.; Wakamatsu, S. *J. Chem. Soc., Chem. Commun.* **1981**, 604–606. (b) Pavlik, J. W.; Kurzweil, E. M. *J. Org. Chem.* **1991**, 56, 6313–6320. (c) Maeda, M.; Kojima, M. *J. Chem. Soc., Perkin Trans. 1* **1977**, 239–247. (d) Tanaka, H.; Matsushita, T.; Nishimoto, K. *J. Am. Chem. Soc.* **1983**, 105, 1753–1760.
5. Pavlik, J. W.; Tongcharoensirikul, P. *J. Org. Chem.* **2000**, 65, 3626–3632.
6. D'Auria, M. *Internet J. Sci.* **1997**, 4, 15–26.
7. D'Auria, M. *Heterocycles* **1999**, 50, 1115–1135.
8. D'Auria, M. *Targets in heterocyclic systems, chemistry and properties*; Attanasi, O. A., Spinelli, D., Eds.; Italian Society of Chemistry: Rome, 1999; Vol. 2, p 233.
9. D'Auria, M. *Adv. Heterocycl. Chem.* **2001**, 79, 41–88.
10. D'Auria, M. *J. Org. Chem.* **2000**, 65, 2494–2498.
11. D'Auria, M. *J. Photochem. Photobiol., A: Chem.* **2002**, 149, 31–37.
12. D'Auria, M. *Tetrahedron* **2002**, 58, 8037–8042.
13. D'Auria, M.; Racioppi, R. *Lett. Org. Chem.* **2004**, 149, 12–19.
14. (a) Buscemi, S.; Cicero, M. G.; Vivona, N.; Caronna, T. *J. Chem. Soc., Perkin Trans. 1* **1988**, 1313–1315. (b) Buscemi, S.; Cicero, M. G.; Vivona, N.; Caronna, T. *J. Heterocycl. Chem.* **1988**, 25, 931–935.
15. Buscemi, S.; Pace, A.; Vivona, N.; Caronna, T. *J. Heterocycl. Chem.* **2001**, 38, 777–780. For excellent work on TEA-assisted ring-phototransposition in the isothiazole series, see also: Pavlik, J. W.; Tongcharoensirikul, P.; French, K. M. *J. Org. Chem.* **1998**, 63, 5592–5603.

16. Buscemi, S.; Pace, A.; Pibiri, I.; Vivona, N. *J. Org. Chem.* **2002**, *67*, 6253–6255.
17. Buscemi, S.; Pace, A.; Pibiri, I.; Vivona, N.; Caronna, T. *J. Fluorine Chem.* in press.
18. Frisch, M. J.; Trucks, G. W.; Schlegel, H. B.; Scuseria, G. E.; Robb, M. A.; Cheeseman, J. R.; Zakrzewski, V. G.; Montgomery, J. A., Jr.; Stratmann, R. E.; Burant, J. C.; Dapprich, S.; Millam, J. M.; Daniels, A. D.; Kudin, K. N.; Strain, M. C.; Farkas, O.; Tomasi, J.; Barone, V.; Cossi, M.; Cammi, R.; Mennucci, B.; Pomelli, C.; Adamo, C.; Clifford, S.; Ochterski, J.; Petersson, G. A.; Ayala, P. Y.; Cui, Q.; Morokuma, K.; Malick, D. K.; Rabuck, A. D.; Raghavachari, K.; Foresman, J. B.; Ciolsowski, J.; Ortiz, J. V.; Stefanov, B. B.; Liu, G.; Liashenko, A.; Piskorz, P.; Komaromi, I.; Gomperts, R.; Martin, R. L.; Fox, D. J.; Keith, T.; Al-Laham, M. A.; Peng, C. Y.; Nanayakkara, A.; Gonzales, C.; Challacombe, M.; Gill, P. M. W.; Johnson, B.; Chen, W.; Wong, M. W.; Andres, J. L.; Gonzales, C.; Head-Gordon, M.; Replogle, E. S.; Pople, J. A. *Gaussian 98*, Revision A.1; Gaussian, Inc.: Pittsburgh, PA, 1998.



Self-assembly of β -turn forming synthetic tripeptides into supramolecular β -sheets and amyloid-like fibrils in the solid state

Samir Kumar Maji,^a Debasish Haldar,^a Michael G. B. Drew,^b Arijit Banerjee,^a
Apurba Kumar Das^a and Arindam Banerjee^{a,*}

^aDepartment of Biological Chemistry, Indian Association for the Cultivation of Science, Jadavpur, Kolkata 700 032, India

^bDepartment of Chemistry, The University of Reading, Whiteknights, Reading RG6 6AD, UK

Received 19 November 2003; revised 12 January 2004; accepted 5 February 2004

Abstract—We have described here the self-assembling properties of the synthetic tripeptides Boc-Ala(1)-Aib(2)-Val(3)-OMe **1**, Boc-Ala(1)-Aib(2)-Ile(3)-OMe **2** and Boc-Ala(1)-Gly(2)-Val(3)-OMe **3** (Aib= α -amino isobutyric acid, β -Ala= β -alanine) which have distorted β -turn conformations in their respective crystals. These turn-forming tripeptides self-assemble to form supramolecular β -sheet structures through intermolecular hydrogen bonding and other noncovalent interactions. The scanning electron micrographs of these peptides revealed that these compounds form amyloid-like fibrils, the causative factor for many neurodegenerative diseases including Alzheimer's disease, Huntington's disease and Prion-related encephalopathies.

© 2004 Elsevier Ltd. All rights reserved.

1. Introduction

Oligopeptides with appropriate conformations can self-assemble to form many regular structures such as sheets, ribbons, rods and tubes which have numerous applications in biological and material sciences.^{1,2} For example, Ghadiri and his coworkers have established that self-assembling cyclic peptides form hollow nanotubes, which can act as artificial ion channels and biosensors.³ Zhang and his colleagues have shown that a self-assembling peptide scaffold can serve as a substrate for neurite outgrowth and synapse formation and this type of biologically compatible scaffold is also important for tissue repair and tissue engineering.⁴ Self-assembling peptides sometimes form gels when they encapsulate solvent molecules under suitable conditions.⁵ Very recently, Artzner and his co-workers have demonstrated that self-assembly of a synthetic therapeutic octapeptide, Lanreotide, leads to the formation of supramolecular β -sheets which upon further self-assembly ultimately form monodisperse nanotubes in water with diameters that are tunable by suitable modifications in the molecular structure.⁶ Higher order molecular self-assembly of a peptide into a β -sheet structure is not only important for designing biomaterials, but also useful in studying pathogenesis of certain age-related disease causing fibrils where self-assembly of mis-folded proteins or protein fragments leads to the formation of the aggregated mass that

is known as amyloid fibrils.⁷ The supramolecular β -sheet stabilization and consequent insoluble amyloid plaque formation are associated with several neurodegenerative diseases including Alzheimer's disease⁸ and Prion-protein diseases.⁹ Sequences and three dimensional structures of disease-causing amyloid proteins and/or protein fragments are enormously varied. However, they self-assemble into supramolecular β -sheets and consequently form protease resistant amyloid fibrils and exhibit similar physicochemical properties (viz.: congophilicity, binds to thioflavin T).¹⁰ The therapeutic challenge in all forms of these fatal neurodegenerative diseases is to prevent amyloid fibril formation, a goal that requires a detailed understanding of the pathway(s) of β -sheet aggregation as well as fibrillation. Recently, many research groups also have used self-assembling, β -sheet forming peptides as amyloid fibril inhibitors.¹¹

Previously, we have demonstrated that short peptides with extended backbone conformations can self-assemble to form supramolecular β -sheet structures in crystals and amyloid-like fibrils in the solid state.¹² As A β -peptides (Amyloid β -peptide) contain many short loops and turn conformations in their backbones,¹³ self-assembly of turn-forming peptides is important for model studies. Recently, Kirschner and his co-workers measured the powder diffraction patterns of a solubilized and dried A β 31-35 sample and demonstrated that this peptide adopts an intramolecular hydrogen bonded reverse-turn conformation which is important for amyloid fibril formation and its cytotoxicity.¹⁴ However, the crystal structures of model peptides which form an intermolecularly hydrogen-bonded

Keywords: Amyloid-like fibril; β -Turn; Supramolecular β -sheet; Self-assembling peptides.

* Corresponding author. Tel.: +91-33-2473-4971; fax: +91-33-2473-2805; e-mail address: bcab@mahendra.iacs.res.in

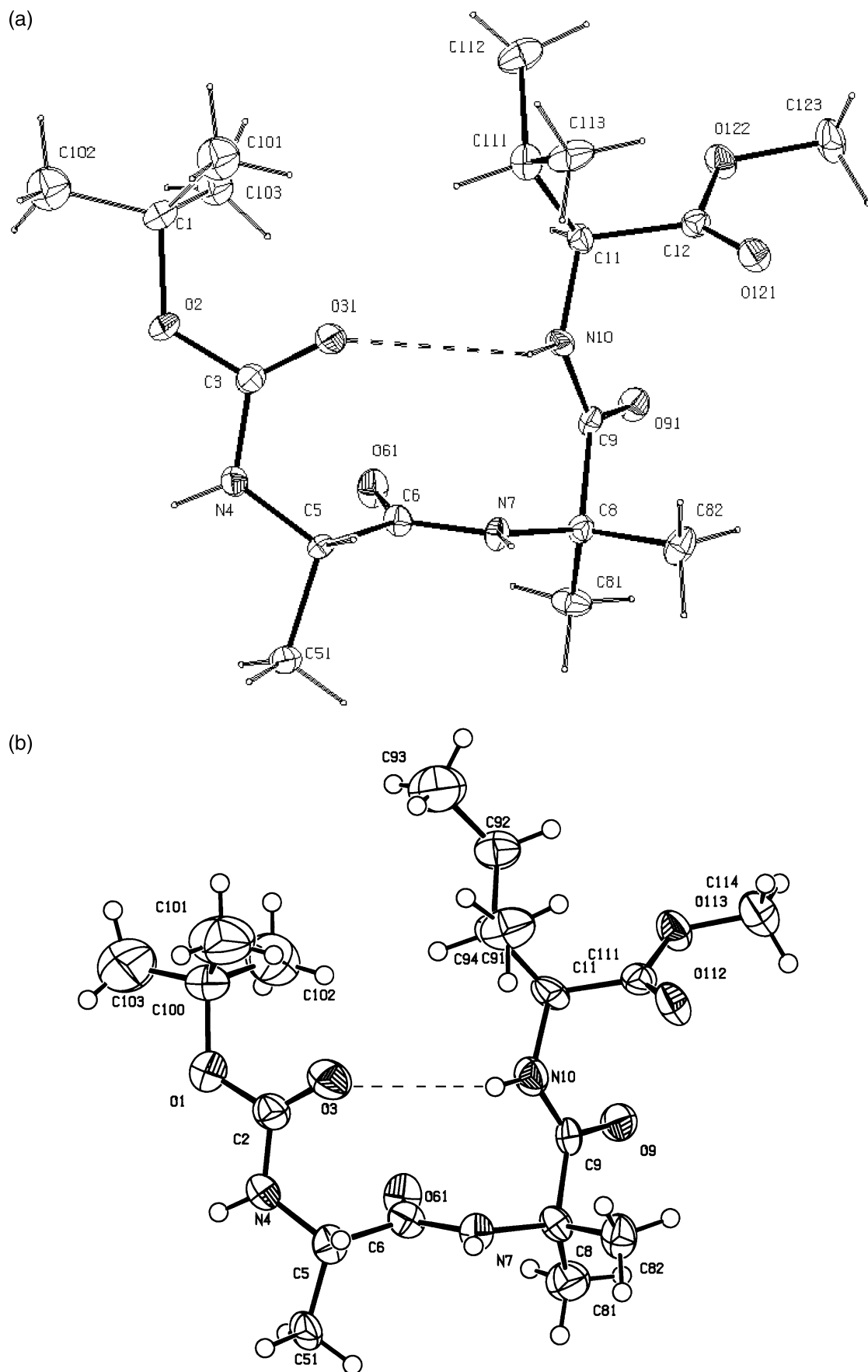


Figure 1 (legend opposite)

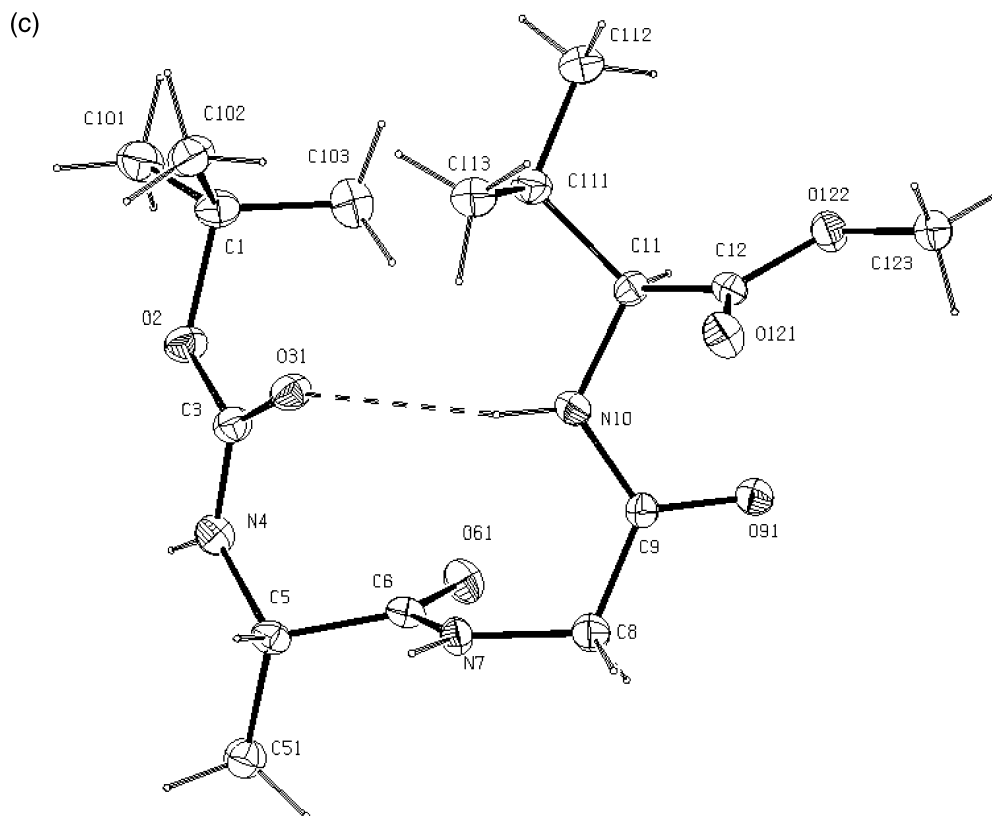


Figure 1. (a) The structure of peptide **1** showing the atomic numbering scheme. Ellipsoids at 20% probability. The weak intramolecular hydrogen bond is shown as a dotted line. (b) Molecular conformation of peptide **2** showing the atomic numbering scheme. The weak intramolecular hydrogen bond is shown as a dotted line. Ellipsoids at 30% probability. (c) ORTEP diagram with atomic numbering scheme of the peptide **3**. Thermal ellipsoids are shown at 30% probability level. The weak intramolecular hydrogen bond is shown as a dotted line.

supramolecular β -sheet from a turn-forming semi-cyclic peptide backbone are still rarely obtained. In our very recent communication, we have demonstrated that a β -turn forming peptide can form supramolecular β -sheet structure through self-aggregation and can exhibit amyloid-like fibrillar morphology in the solid state.¹⁵ Continuing our research in this field, we report here the results of our studies on three synthetic terminally blocked tripeptides, Boc-Ala(1)-Aib(2)-Val(3)-OMe **1**, Boc-Ala(1)-Aib(2)-Ile(3)-OMe **2** and Boc-Ala(1)-Gly(2)-Val(3)-OMe **3** which all adopt reverse turn conformations and self-assemble to form supramolecular β -sheets in crystals and amyloid-like fibrils in the solid state.

2. Results and discussion

Peptides **1** and **2** contain the centrally located confor-

Table 1. Selected backbone torsion angles ($^{\circ}$) of peptides **1**, **2** and **3**

Torsional angles	Peptide 1	Peptide 2	Peptide 3
ω_0	169.6(7)	170.8(4)	173.9(6)
ϕ_1	-58.1(9)	-54.6(6)	-55.6(9)
ψ_1	146.7(6)	147.1(4)	139.6(6)
ω_1	170.6(6)	171.4(5)	171.0(6)
ϕ_2	60.1(9)	60.0(6)	72.7(8)
ψ_2	30.8(9)	30.0(5)	19.1(10)
ω_2	170.8(6)	170.6(4)	175.9(6)
ϕ_3	-63.8(8)	-60.8(5)	-56.7(8)
ψ_3	143.7(7)	142.2(4)	137.9(8)

mationally constrained Aib (α -aminoisobutyric acid) residue together with hydrophobic Val (valine) and Ile (isoleucine) residues at the C terminus and both adopt a turn structure. In tripeptide **3**, the centrally positioned Aib has been substituted by the structurally very flexible Gly (glycine) residue with the aim of investigating whether or not peptide **3** forms the folded turn conformation. These peptides were studied using X-ray crystallography, NMR, scanning electron microscopy and optical microscopy.

Table 2. Intra and intermolecular hydrogen bonding parameters of peptides **1**, **2** and **3**

D-H...A	H...A (\AA)	D...A (\AA)	D-H...A ($^{\circ}$)
Peptide 1			
N10-H10...O31	2.89	3.61	142
N4-H4...O121 ^a	2.33	3.10	150
N7-H7...O91 ^b	2.14	3.00	172
Peptide 2			
N10-H10...O3	2.77	3.48	141
N4-H4...O112 ^c	2.37	3.12	145
N7-H7...O9 ^d	2.16	3.02	172
Peptide 3			
N10-H10...O31	2.56	3.29	143
N4-H4...O91 ^e	2.29	3.03	145
N7-H7...O91 ^f	2.10	2.93	160

^a Symmetry equivalent $x+0.5, y+0.5, z$.

^b Symmetry equivalent $x, 1+y, z$.

^c Symmetry equivalent $0.5+x, 0.5+y, z$.

^d Symmetry equivalent $x, 1+y, z$.

^e Symmetry equivalent $1-x, y-0.5, 2-z$.

^f Symmetry equivalent $x-1, y, z$.

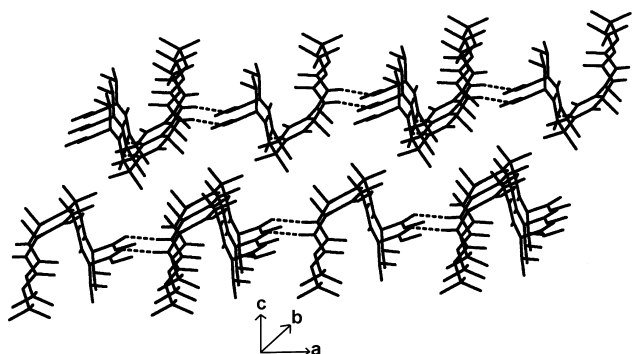


Figure 2. Packing of β -turn conformations of peptide **1** along the crystallographic b axis forming semi-cylindrical ribbon structure and further self-assembly along the crystallographic a and b axes to form a two dimensional monolayer β -sheet structure. Hierarchical self-assembly of individual β -sheets along the c direction results in the formation of a highly ordered cross β -sheet structure.

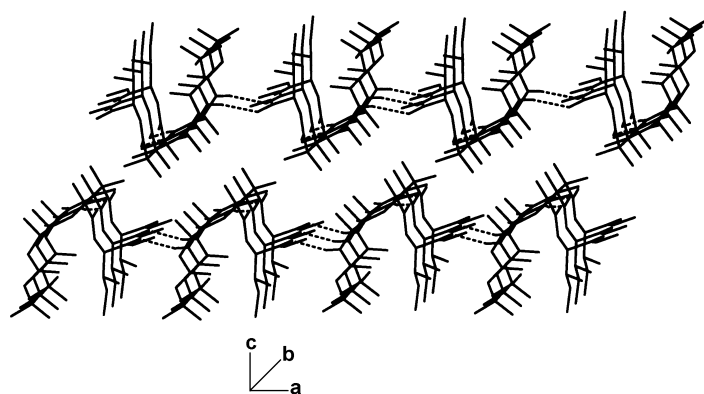


Figure 3. Two dimensional monolayer β -sheet structure obtained by the packing of individual β -turn conformations of peptide **2** along the crystallographic a and b axes which on further self-assembly gives supramolecular cross β -sheet structure along the c direction.

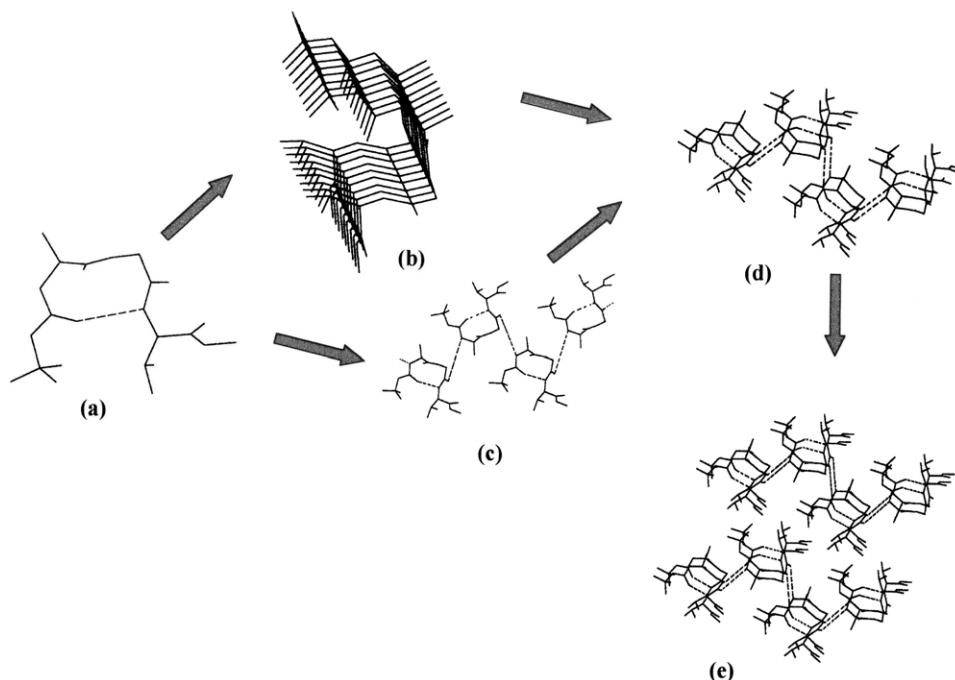


Figure 4. Self-assembly of peptide **3** in the β -turn conformation to form supramolecular β -sheet structure in crystal. (a) the β -turn building block, (b) packing of β -turn conformations along the crystallographic a axis forming semi-cylindrical ribbon structure, (c) and (d) the spacing of β -turn conformation along crystallographic b axis through intermolecular hydrogen bonds to form corrugated sheet like structures, (e) packing of individual β -sheets along the crystallographic c axis by van der Waals interactions forming highly ordered β -sheet structure in crystal.

2.1. X-ray crystallography

The molecular conformations of tripeptides Boc-Ala(1)-Aib(2)-Val(3)-OMe **1**, Boc-Ala(1)-Aib(2)-Ile(3)-OMe **2** and Boc-Ala(1)-Gly(2)-Val(3)-OMe **3** are shown in Figure 1(a)–(c), respectively. Figure 1 reveals that peptides **1**, **2** and **3** adopt folded conformations corresponding to the distorted β -turn structure. Backbone torsion angles for these peptides **1**, **2** and $\mathbf{3}$ are listed in Table 1. For peptides **1** and **3** there exists a very weak 4 \rightarrow 1 hydrogen bond between Boc-CO and Val (3) NH (N10 \cdots O31, 3.61 and 3.29 Å for **1** and **3**, respectively) and for peptide **2** the weak hydrogen bond is between Boc-CO and Ile(3) NH (N10 \cdots O3, 3.48 Å). These hydrogen bonds are illustrated in Figure 1(a)–(c) and dimensions are detailed in Table 2. In peptide **1** there are two intermolecular hydrogen bonds (N7–H7 \cdots O91 and N4–H4 \cdots O121) that are responsible for connecting individual peptide molecules to form and stabilize the

Table 3. Crystal and data collection parameters of peptides **1**, **2** and **3**

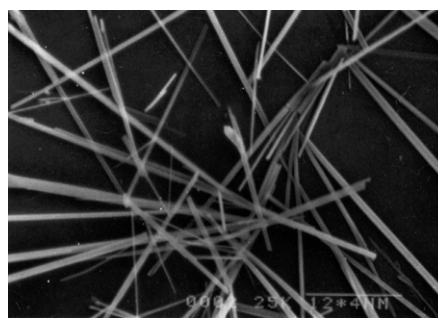
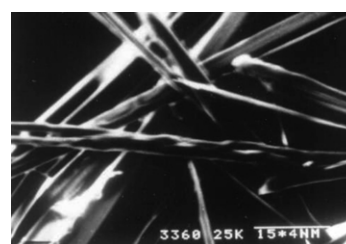
	Peptide 1	Peptide 2	Peptide 3
Empirical formula	C ₁₈ H ₃₃ N ₃ O ₆	C ₁₉ H ₃₅ N ₃ O ₆	C ₁₆ H ₂₉ N ₃ O ₆
Crystallizing solvent	Dimethylsulphoxide	Methanol–water	Ethyl acetate
Crystal system	Monoclinic	Monoclinic	Monoclinic
Space group	C2	C2	P2 ₁
<i>a</i> (Å)	19.349(25)	19.345(22)	6.112(12)
<i>b</i> (Å)	6.094(10)	6.068(8)	12.515(14)
<i>c</i> (Å)	19.438(25)	20.323(21)	13.357(14)
α (°)	(90)	(90)	(90)
β (°)	101.34(1)	101.27(1)	102.89(1)
γ (°)	(90)	(90)	(90)
<i>U</i> (Å ³)	2248	2339	997
<i>Z</i>	4	4	2
Mol. wt.	387.5	401.5	359.4
Density (calcd, Mg/mm ³)	1.145	1.140	1.197
Unique data	3758	4115	3152
Observed reflns. (<i>I</i> >2 σ (<i>I</i>))	2347	2132	1246
<i>R</i>	0.1059	0.0736	0.0858
<i>wR2</i>	0.2440	0.1776	0.2554

supramolecular monolayer sheet assembly along the crystallographic *b* and *a* axes, respectively. These β -sheets are regularly stacked via van der Waals interactions as shown by the projection of the unit cells in the *c* direction to form the complex quaternary sheet structure (Fig. 2). The hydrogen bonding parameters of peptide **1** are listed in Table 2. In peptide **2**, the β -turn building blocks are aggregated via two unique intermolecular hydrogen bonds N7–H7···O9 and N4–H4···O112 (Table 2) along the *b* and *a* axes respectively to form two-dimensional sheet-like structures which on further self-assembly form a supramolecular β -sheet structure via van der Waals interactions in the *c* direction (Fig. 3). Figure 4 schematically illustrates the stepwise β -sheet formation for peptide **3**. Each turn-like conformation (Fig. 4(a)) self-assembles via an intermolecular hydrogen bond (N7–H7···O91) to form a semi-cylindrical ribbon structure along the short crystallographic *a* axis (Fig. 4(b)). These ribbons are connected along the screw axis parallel to *b* via intermolecular hydrogen bonds N4–H4···O91 to form two-dimensional corrugated sheet-like structures (Fig. 4(c)) which are regularly stacked via van der Waals interactions as shown by the projection of the unit cells in the *c* direction to form a supramolecular β -sheet structure (Fig. 4(e)). Hydrogen bonding data for peptide **3** are also listed in Table 2. Crystal data for these three peptides are detailed in Table 3.

**Figure 5.** SEM image of peptide **1** showing a bunch of rod-like fibrils in the solid state.

2.2. Morphology of peptides

The scanning electron microscope (SEM) was used for the morphological studies of these peptides. The SEM image of peptide **1** obtained from dried fibrous materials (which were grown slowly from methanol–water mixture) clearly shows that the aggregate in the solid state is a bundle of long filaments (Fig. 5). The SEM images (Figs. 6 and 7) of the dried fibrous materials (which were grown slowly from a methanol–water mixture) of peptides **2** and **3** exhibit that the aggregates in the solid state have amyloid-like fibrillar morphology.¹⁶ Moreover, the time-dependent optical microscopic studies of peptide **1** in chloroform solution clearly indicates that these fibrils were grown from

**Figure 6.** Typical SEM image of peptide **2** in the solid state.**Figure 7.** SEM image of peptide **3** exhibits filamentous fibrillar morphology in solid state.

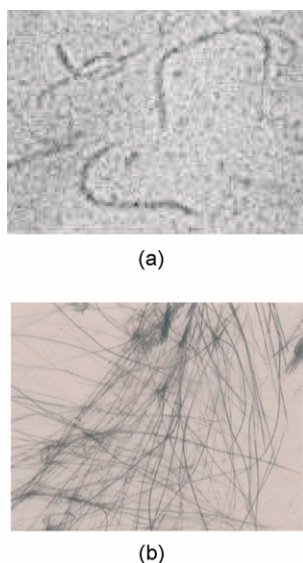


Figure 8. (a) Optical microscopic image of peptide **1** showing intermediate protofibril formation in CHCl_3 solution. (b) Optical microscopic image of peptide **1** showing full-length fibril formation in CHCl_3 solution.

relatively smaller protofibrils (Fig. 8(a)), which ultimately form higher order mature fibrils (Fig. 8(b)), a characteristic feature of amyloid fibril formation.^{7b,d,17} These fibrils obtained from peptides **1**, **2** and **3** were stained with a physiological dye, Congo red, and exhibit distinct green-gold birefringence under polarized light (Fig. 9). These results are consistent with Congo red binding to an amyloid β -sheet fibrillar structure.¹⁰

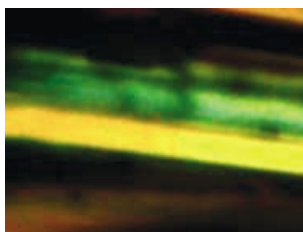


Figure 9. Congo red stained peptide **3** fibrils observed through crossed polarizers showing green-gold birefringence a characteristic feature of amyloid fibrils.

3. Conclusion

In spite of having different sequences and compositions, all three reported peptides adopt a distorted β -turn conformation in their crystal structures. Moreover, these turn-forming peptides self-associate to form supramolecular β -sheet structures via non-covalent interactions including intermolecular hydrogen bonds, in which all the hydrogen bonds are formed between the peptide linkages. These turn-forming peptides also form amyloid-like fibrils upon further self-aggregation, as is evident from the characteristic Congo red binding studies and observing the typical birefringence of these fibrils under a cross polarizer. So, these peptides represent a good model system for self-assembling β -sheets from turn-forming model synthetic peptides. These results have also established that the unconventional folded, β -turn-like structure (apart from the conventional extended backbone conformations) is a competent subunit for

supramolecular β -sheets and amyloid-like fibrils in short model peptides.

4. Experimental

4.1. Peptide synthesis

The tripeptides were synthesized by conventional solution phase methods using racemization-free fragment condensation strategy.¹⁸ The Boc group was used for N-terminal protection and the C terminus was protected as a methyl ester. Couplings were mediated by dicyclohexylcarbodiimide-1-hydroxybenzotriazole (DCC/HOBt). All intermediates have been characterized by ^1H NMR (300 MHz) and thin layer chromatography (TLC) on silica gel and used without further purification. The final products were purified by column chromatography using silica (100–200-mesh size) gel as stationary phase and ethyl acetate as eluent. Purified final compounds have been fully characterized by 300 MHz ^1H NMR spectroscopy.

4.1.1. Boc-Ala-OH (4). A solution of Ala (3.56 g, 40 mmol) in a mixture of dioxan (80 mL), water (40 mL) and 1 M NaOH (40 mL) was stirred and cooled in an ice-water bath. Di-*tert*-butylpyrocarbonate (9.6 g, 44 mmol) was added and stirring was continued at room temperature for 6 h. Then the solution was concentrated in vacuum to about 40–60 mL, cooled in an ice water bath, covered with a layer of ethylacetate (about 50 mL) and acidified with a dilute solution of KHSO_4 to pH 2–3 (congo red). The aqueous phase was extracted with ethyl acetate and this operation was done repeatedly. The ethyl acetate extracts were pooled, washed with water and dried over anhydrous Na_2SO_4 and evaporated in vacuum. Pure material was obtained as white solid.

Yield=7.308 g (36 mmol, 90%). Mp 85 °C. Anal. Calcd for $\text{C}_8\text{H}_{15}\text{NO}_4$ (189): C, 50.79; H, 7.94; N, 7.40. Found: C, 50.62; H, 7.77; N, 7.52.

4.1.2. Boc-Ala(1)-Aib(2)-OMe (5). A sample of Boc-Ala-OH (4.54 g, 24 mmol) was dissolved in dichloromethane (DCM) (40 mL) in an ice-water bath. H-Aib-OMe was isolated from the corresponding methyl ester hydrochloride (3.36 g, 48 mmol) by neutralization and subsequent extraction with ethyl acetate and the ethyl acetate extract was concentrated to 20 mL. This was added to the reaction mixture, followed immediately by di-cyclohexylcarbodiimide (DCC) (4.94 g, 24 mmol). The reaction mixture was allowed to come to room temperature and stirred for 24 h. DCM was evaporated, and the residue was taken up in ethyl acetate (30 mL), and dicyclohexylurea (DCU) was filtered off. The organic layer was washed with 2 M HCl (3×30 mL), brine, 1 M sodium carbonate (3×30 mL) and brine (2×30 mL) and dried over anhydrous sodium sulfate, and evaporated in vacuum to yield **5** as waxy solid.

Yield=5.48 g (19 mmol, 79.17 %). ^1H NMR (CDCl_3 , 300 MHz, δ ppm): 6.77 [Aib(2)NH, 1H, s]; 5.06 [Ala(1)NH, 1H, d]; 4.16 [C^αH s of Ala(1), 1H, t]; 3.73 [$-\text{OCH}_3$, 3H, s]; 1.54 [C^βH_3 s of Aib, 6H, s]; 1.45 [Boc- CH_3 s, 9H, s]; 1.35 [C^βH s of Ala(1), 3H, m]. Anal. Calcd for $\text{C}_{13}\text{H}_{24}\text{N}_2\text{O}_5$

(288): C, 54.16; N, 9.72; H, 8.33. Found: C, 54.4; N, 9.8; H, 8.5.

4.1.3. Boc-Ala(1)-Aib(2)-OH (6). To a sample of **5** (4.6 g, 16 mmol), MeOH (40 mL) and 2 M NaOH (24 mL) were added and the progress of saponification was monitored by thin layer chromatography (TLC). The reaction mixture was stirred. After 10 h, methanol was removed under vacuum, the residue was taken up in 30 mL of water, washed with diethyl ether (2×20 mL). Then the pH of the aqueous layer was adjusted to **2** using 1 M HCl and it was extracted with ethyl acetate (3×20 mL). The extracts were pooled, dried over anhydrous sodium sulfate, and evaporated in vacuum to yield 2.72 g of **6** as white solid.

Yield=2.72 g (13.6 mmol, 85%). Mp 176 °C. ¹H NMR ((CD₃)₂SO, 300 MHz, δ in ppm): 11.8 [–COOH, 1H, br.]; 7.8 [Aib(2) NH, 1H, s]; 6.73 [Ala(1) NH, 1H, d]; 3.94 [C^αHs of Ala(1), 1H, m]; 1.41 [C^βH₃ s of Aib(2), 6H, s]; 1.36 [Boc-CH₃ s, 9H, s]; 1.14 [C^βH₃ s of Ala(1), 3H, m]. Anal. Calcd for C₁₂H₂₂N₂O₅ (274): C, 52.55; N, 10.21; H, 8.029. Found: C, 52.6; N, 10.16; H, 8.2.

4.1.4. Boc-Ala(1)-Aib(1)-Val(3)-OMe 1. A sample of Boc-Ala-Aib-OH (0.82 g, 3 mmol) in DMF (8 mL) was cooled in an ice-water bath and H-Val-OMe was isolated from the corresponding methyl ester hydrochloride (1.0 g, 6 mmol) by neutralization, subsequent extraction with ethyl acetate and concentration (5 mL) and it was added to the reaction mixture, followed immediately by DCC (0.62 g, 3 mmol) and HOBt (0.4 g, 3 mmol). The reaction mixture was stirred for 3 days. The residue was taken in ethyl acetate (20 mL) and the DCU was filtered off. The organic layer was washed with 2 M HCl (3×20 mL), brine, 1 M sodium carbonate (3×20 mL), brine (2×20 mL), dried over anhydrous sodium sulfate and evaporated in vacuum to yield 0.77 g (2 mmol, 66.66 %) of white solid. Purification was done by silica gel column (100–200 mesh) using ethyl acetate as eluent. Colourless single crystals were grown from dimethylsulphoxide by slow evaporation.

Yield=0.77 g (2 mmol, 66.66 %). Mp 184 °C. ¹H NMR (CDCl₃, 300 MHz, δ ppm): 7.06 [Val (3) NH, 1H, d, *J*=4.58 Hz]; 6.71 [Aib(2) NH, 1H, s]; 4.96 [Ala(1) NH, 1H, d, *J*=4.98 Hz]; 4.50 [C^αH of Ala(1), 1H, m]; 4.09 [C^αH of Val(3), 1H, m]; 3.74 [–OCH₃, 3H, s]; 2.16–2.20 [C^βH of Val(3), 1H, m]; 1.54 [C^βHs of Aib, 6H, s]; 1.45 [Boc-CH₃, 9H, s]; 1.35, 1.36 [C^βHs of Ala(1), 3H, d, *J*=4.23 Hz]; 0.89–0.94 [C^γHs of Val (3), 6H, m]. Anal. Calcd for C₁₈H₃₃N₃O₆ (387): C, 55.81; H, 8.53; N, 10.85. Found: C, 55.75; H, 8.37; N, 11.92. Mass spectral data M+Na⁺=410, *M*_{calcd}=387.

4.1.5. Boc-Ala(1)-Aib(2)-Ile(3)-OMe (2). Boc-Ala-Aib-OH (1.37 g, 5 mmol) in DMF (15 mL) was cooled in an ice-water bath and H-Ile-OMe was isolated from the corresponding methyl ester hydrochloride (1.82 g, 10 mmol) by neutralization and subsequent extraction with ethyl acetate and the ethyl acetate extract was concentrated to 8 mL. It was then added to the reaction mixture, followed immediately by DCC (1.03 g, 5 mmol) and HOBt (0.68 g, 5 mmol). The reaction mixture was stirred for 3 days. The residue was taken up in ethyl acetate 20 mL and the DCU

was filtered off. The organic layer was washed with 2 M HCl (3×40 mL), brine, 1 M sodium carbonate (3×40 mL), brine (2×40 mL), dried over anhydrous sodium sulfate and evaporated in vacuum to yield 1.6 g (4 mmol) of white solid. Purification was done by silica gel column (100–200 mesh) using ethyl acetate as eluent.

Yield=1.6 g, 80%. Mp 178 °C. ¹H NMR (CDCl₃, 300 MHz, δ ppm): 7.08 [Ile(3) NH, 1H, d, *J*=8.16 Hz]; 6.68 [Aib(2) NH 1H, s]; 4.96 [Ala(1) NH, 1H, d, *J*=7.5 Hz]; 4.51–4.55 [C^αH of Ala(1), 1H, m]; 4.09–4.11 [C^αH of Ile(3), 1H, m]; 3.72 [–OCH₃, 3H, s]; 1.89–1.94 [C^βHs of Ile(3), 1H, m]; 1.61 [C^βH₃ s of Aib(2), 6H, s]; 1.45 [Boc-CH₃ s, 9H, s]; 1.34–1.39 [C^βHs of Ala(1), 3H, d, *J*=8.82 Hz]; 1.25 [C^γs of Ile(3), 3H, d]; 0.89–0.96 [C^γs & C^δHs of Ile(3), 5H, m]. Anal. Calcd for C₁₉H₃₅N₃O₆ (401): C, 56.85; N, 10.47; H, 8.72. Found: C, 56.71; N, 10.35; H, 8.8. Mass spectral data M+Na⁺ +H⁺=425, *M*_{calcd}=401.

4.1.6. Boc-Ala(1)-Gly(2)-OBz (7). A sample of Boc-Ala-OH (3.78 g, 20 mmol) was dissolved in a mixture of dichloromethane-*N,N*-dimethylformamide (DCM/DMF) (30 mL) in an ice-water bath. H-Gly-OCH₂Ph was isolated from of the corresponding benzyl ester *p*-toluene sulphonate (13.48 g, 40 mmol) by neutralization, subsequent extraction with ethyl acetate and concentration (10 mL) and this was added to the reaction mixture, followed immediately by di-cyclohexylcarbodiimide (DCC) (4.12 g, 20 mmol) and 1-hydroxybenzotriazole (HOBt) (2.7 g, 20 mmol). The reaction mixture was allowed to come to room temperature and stirred for 24 h. DCM was evaporated, the residue was taken in ethyl acetate (40 mL), and dicyclohexylurea (DCU) was filtered off. The organic layer was washed with 2 M HCl (3×40 mL), brine, 1 M sodium carbonate (3×40 mL) and brine (2×40 mL) and dried over anhydrous sodium sulfate, and evaporated in vacuum to yield of the dipeptide **7** as white solid.

Yield=5.712 g (17 mmol, 85%). Mp 73 °C. ¹H NMR (CDCl₃, 300 MHz, δ ppm): 7.35 [Ph, 5H, m]; 6.73 [Gly(2) NH, 1H, t]; 5.18 [–benzyl CH₂, 2H, s]; 5.01–5.03 [Ala(1) NH, 1H, d]; 4.22 [C^αH of Ala(1), 1H, t]; 4.04–4.09 [C^αHs of Gly(2), 2H, t]; 1.44 [Boc-CH₃, 9H, s]; 1.35–1.37 [C^βHs of Ala(1), 3H, d]. Anal. Calcd for C₁₇H₂₄N₂O₅ (336): C, 60.71; H, 7.14; N, 8.33. Found: C, 60.67; H, 6.98; N, 8.36.

4.1.7. Boc-Ala(1)-Gly(2)-OH (8). To Boc-Ala(1)-Gly(2)-OBz **7** (4.37 g, 13 mmol), MeOH (40 mL) and 2 M NaOH (15 mL) were added and the progress of saponification was monitored by thin layer chromatography (TLC). The reaction mixture was stirred. After 10 h methanol was removed under vacuum, the residue was taken in 20 mL of water, washed with diethyl ether (2×20 mL). Then the pH of the aqueous layer was adjusted to **2** using 1 M HCl and it was extracted with ethyl acetate (3×20 mL). The extracts were pooled, dried over anhydrous sodium sulfate, and evaporated in vacuum to yield 2.70 g of **8** as white solid.

Yield=2.70 g (11 mmol, 84.61%). Mp 88 °C. ¹H NMR (70% (CD₃)₂SO+30% CDCl₃, 300 MHz, δ in ppm): 12.4 [–COOH, 1H, br]; 7.93 [Gly(2) NH, 1H, t]; 6.67 [Ala(1)

NH, 1H, d]; 4.06 [C^αH of Ala(1), 1H, t]; 3.76–3.80 [C^αHs Gly(2), 2H, m]; 1.40 [Boc-CH₃, 9H, s]; 1.22–1.24 [C^βHs of Ala(1), 3H, m]. Anal. Calcd for C₁₀H₁₈N₂O₅ (246): C, 48.78; H, 7.31; N, 11.38. Found: C, 48.66; H, 7.29; N, 11.42.

4.1.8. Boc-Ala(1)-Gly(2)-Val(3)-OMe (3). A sample of Boc-Ala-Gly-OH (1.23 g, 5 mmol) in DMF (10 mL) was cooled in an ice-water bath and H-Val-OMe was isolated from the corresponding methyl ester hydrochloride (1.67 g, 10 mmol) by neutralization, subsequent extraction with ethyl acetate and concentration (7 mL) and it was added to the reaction mixture, followed immediately by of DCC (1.03 g, 5 mmol) and HOBt (0.67 g, 5 mmol). The reaction mixture was stirred for 3 days. The residue was taken in ethyl acetate (40 mL) and the DCU was filtered off. The organic layer was washed with 2 M HCl (3×40 mL), brine, 1 M sodium carbonate (3×40 mL), brine (2×40 mL), dried over anhydrous sodium sulfate and evaporated in vacuum to yield 1.32 g of white solid. Purification was done by silica gel column (100–200 mesh) using ethyl acetate as eluent. Colourless single crystals were grown from ethyl acetate by slow evaporation.

Yield=1.32 g (3.7 mmol, 74%). Mp 97 °C. ¹H NMR (CDCl₃, 300 MHz, δ ppm): 6.90 [Gly(2) NH, 1H, t]; 6.68 [Val (3) NH, 1H, d, *J*=8.4 Hz]; 5.02 [Ala(1) NH, 1H, d, *J*=6.6 Hz]; 4.52 [C^αH of Ala(1), 1H, m]; 4.23 [C^αH of Val(3), 1H, m]; 3.95–4.0 [C^αHs of Gly(2), 2H, m]; 3.73 [–OCH₃, 3H, s]; 2.16–2.22 [C^βH of Val(3), 1H, m]; 1.44 [Boc-CH₃, 9H, s]; 1.37–1.40 [C^βHs of Ala(1), 3H, d, *J*=7.2 Hz]; 0.89–0.95 [C^γHs of Val(3), 6H, m]. Mass spectral data *M*+Na⁺=382, *M*_{calcd}=359. Anal. Calcd for C₁₆H₂₉N₃O₆ (359): C, 53.48; H, 8.07; N, 11.70. Found: C, 53.46; H, 8.02; N, 11.77.

4.2. Single crystal X-ray diffraction study

For tripeptides **1**, **2** and **3** intensity data were collected with Mo K_α radiation using the MAR research Image Plate System. For all peptides the crystals were positioned at 70 mm from the Image Plate. Selected details of the structure solutions and refinements are given in Table 3. 100 frames were measured at 2° intervals with a counting time of 2–5 min for various peptides. Data analyses were carried out with the XDS program.¹⁹ The structures were solved using direct methods with the Shelx86²⁰ program. For peptide **1**, the *tert*-butyl group was disordered, with each methyl group taking up two different sites each refined with 50% occupancy. Apart from the disordered atoms in peptide **1**, all non-hydrogen atoms of all peptides were refined with anisotropic thermal parameters. The hydrogen atoms were included in geometric positions and given thermal parameters equivalent to 1.2 times those of the atom to which they were attached. The structures were refined on F² using Shelxl.²¹ Crystallographic data for the three structures have been deposited at the Cambridge Crystallographic Data Center (CCDC 222157, 222158 and 173625).

4.3. NMR experiments

All NMR studies were carried out on a Brüker DPX 300 MHz spectrometer at 300 K. Peptide concentrations were in the range 1–10 mM in CDCl₃ and (CD₃)₂SO.

4.4. Mass spectrometry

Mass spectra of final compounds (tripeptides **1**, **2** and **3**) were recorded on a HEWLETT PACKARD Series 1100MSD mass spectrometer by positive mode electrospray ionization.

4.5. Morphological study

The Morphology of the tripeptides was investigated using an optical microscope and scanning electron microscope (SEM). For the SEM study, fibrous materials (slowly grown from methanol–water mixtures) were dried and gold coated. Then the micrographs were taken in a SEM apparatus (Hitachi S-415A). For the optical microscopic study of the peptide **1** in CHCl₃, Olympus CH 30 imaging microscope equipped with Image Pro Plus ver 4.0 software was used.

4.6. Congo red binding study

An alkaline saturated Congo red solution was prepared. The peptide fibrils were stained with alkaline Congo red solution (80% methanol/20% glass distilled water containing 10 μL of 1% NaOH) for 2 min then the excess stain (Congo red) was removed by rinsing the stained fibril with 80% methanol/20% glass distilled water solution for several times. The stained fibrils were dried in vacuum at room temperature for 24 h, then visualized at 100× or 500× magnification and birefringence was observed between crossed polarizers.

Acknowledgements

We thank EPSRC and the University of Reading, UK for funds for the Image Plate System. We also acknowledge Department of Science and Technology, New Delhi, India for the grant No. SR/S5/OC-29/2003.

References and notes

- (a) Krejchi, M. T.; Atkins, E. D. T.; Waddon, A. J.; Fournier, M. J.; Mason, T. L.; Tirrell, D. A. *Science* **1994**, *265*, 1427–1432. (b) Aggeli, A.; Boden, N.; Cheng, Y.; Findlay, J. B. C.; Knowles, P. F.; Kovatchev, P.; Turnbull, P. J. H. *Biochemistry* **1996**, *35*, 16213–16221. (c) Otzen, D. E.; Kristensen, O.; Oliveberg, M. *Proc. Natl Acad. Sci. USA* **2000**, *97*, 9907–9912.
- (a) Whetstones, G. M.; Mathias, J. P.; Seto, C. T. *Science* **1991**, *254*, 1312–1319. (b) Lehn, J. M. *Science* **1993**, *260*, 1762–1763. (c) Bong, D. T.; Clark, T. D.; Granja, J. R.; Ghadiri, M. R. *Angew. Chem., Int. Ed.* **2001**, *40*, 988–1011.
- (a) Granja, J. R.; Ghadiri, M. R. *J. Am. Chem. Soc.* **1994**, *116*, 10785–10786. (b) Ghadiri, M. R.; Granja, J. R.; Milligran, R. A.; McRee, D. E.; Khazanovich, N. *Nature* **1993**, *366*, 324–327. (c) Ghadiri, M. R.; Granja, J. R.; Buehler, L. K. *Nature* **1994**, *369*, 301–304. (d) Hartgerink, J. D.; Clark, T. D.; Ghadiri, M. R. *Chem. Eur. J.* **1998**, *4*, 1367–1372. (e) Hartgerink, J. D.; Granja, J. R.; Milligran, R. A.; Ghadiri, M. R. *J. Am. Chem. Soc.* **1996**, *118*, 43–50.

4. Holmes, T. C.; Lacalle, S. D.; Su, X.; Liu, G.; Rich, A.; Zhang, S. *Proc. Natl Acad. Sci. USA* **2000**, *97*, 6728–6733.
5. (a) Aggeli, A.; Bell, M.; Boden, N.; Keen, J. N.; Knowles, P. F.; Mcleish, T. C. B.; Pitkeathly, M.; Radford, S. E. *Nature* **1997**, *386*, 259–262. (b) Maji, S. K.; Malik, S.; Drew, M. G. B.; Nandi, A. K.; Banerjee, A. *Tetrahedron Lett.* **2003**, *44*, 4103–4107.
6. Valéry, C.; Paternostre, M.; Robert, B.; Gulik-Krzywicki, T.; Narayanan, T.; Dedieu, J.; Keller, G.; Torres, M.; Cherif-Cheikh, R.; Calvo, P.; Artzner, F. *Proc. Natl Acad. Sci. USA* **2003**, *100*, 10258–10262.
7. (a) Koo, E. H.; Lansbury, Jr., P. T.; Kelly, J. W. *Proc. Natl Acad. Sci. USA* **1999**, *96*, 9989–9990. (b) Walsh, D. M.; Hartley, D. M.; Kusumoto, Y.; Fezoui, Y.; Condrón, M. M.; Lomakin, A.; Benedek, G. B.; Selkoe, D. J.; Teplow, D. B. *J. Bio. Chem.* **1999**, *274*, 25945–25952. (c) Goldfarb, L. G.; Brown, P.; Haltia, M.; Ghiso, J.; Frangione, B.; Gajdusek, D. C. *Proc. Natl Acad. Sci. USA* **1993**, *90*, 4451–4454. (d) Walsh, D.; Lomakin, M. A.; Benedek, G. B.; Condrón, M. M.; Teplow, D. B. *J. Bio. Chem.* **1997**, *272*, 22364–22372.
8. (a) Taubes, G. *Science* **1996**, *271*, 1493–1495. (b) Lansbury, Jr. P. T. *Acc. Chem. Res.* **1996**, *29*, 317–321. (c) Roses, A. D. *Curr. Opin. Neurobio.* **1996**, *644*, 650. (d) Baumeister, R.; Eimer, S. *Angew. Chem., Int. Ed.* **1998**, *37*, 2978–2982.
9. (a) Prusiner, S. B. *Proc. Natl Acad. Sci. USA* **1998**, *95*, 13363–13383. (b) Baldwin, M. A.; Cohen, F. E.; Prusiner, S. B. *J. Bio. Chem.* **1995**, *270*, 19197–19200. (c) Ng, S. B. L.; Doig, A. *J. Chem. Soc. Rev.* **1997**, *26*, 425–432.
10. (a) Kim, Y. S.; Randolph, T. W.; Manning, M. C.; Stevens, F. J.; Carpenter, J. F. *J. Bio. Chem.* **2003**, *278*, 10842–10850. (b) Taylor, D. L.; Allen, R. D.; Benditt, E. P. *J. Histochem. Cytochem.* **1974**, *22*, 1105–1112. (c) Lim, A.; Makhov, A. M.; Bond, J.; Inouye, H.; Connors, L. H.; Griffith, J. D.; Erickson, W. B.; Kirschner, D. A.; Costello, C. E. *J. Struct. Bio.* **2000**, *130*, 363–370. (d) Azriel, R.; Gazit, E. *J. Bio. Chem.* **2001**, *226*, 34156–34161.
11. Mason, J. M.; Kokkoni, N.; Stott, K.; Doig, A. *J. Curr. Opin. Struct. Bio.* **2003**, *13*, 1–7.
12. (a) Maji, S. K.; Drew, M. G. B.; Banerjee, A. *Chem. Commun.* **2001**, 1946–1947. (b) Banerjee, A.; Maji, S. K.; Drew, M. G. B.; Haldar, D.; Banerjee, A. *Tetrahedron Lett.* **2003**, *44*, 6741–6744. (c) Maji, S. K.; Haldar, D.; Banerjee, A.; Banerjee, A. *Tetrahedron* **2002**, *58*, 8695–8702. (d) Maji, S. K.; Haldar, D.; Velmurugan, D.; Rajakannan, V.; Banerjee, A. *Let. Pept. Sci.* **2002**, *8*, 61–67.
13. Kirschner, D. A.; Inouye, H.; Bond, J. P.; Deverin, S. P.; Teeter, M. T.; El-Agnaf, O. M. A.; Henry, C.; Costello, C. E.; Lim, A. *Polym. Prepr.* **2002**, *43*, 187–188.
14. Bond, J. P.; Deverin, S. P.; Inouye, H.; El-Agnaf, O. M. A.; Teeter, M. M.; Kirschner, D. A. *J. Struct. Bio.* **2003**, *41*, 156–170.
15. Banerjee, A.; Maji, S. K.; Drew, M. G. B.; Haldar, D.; Banerjee, A. *Tetrahedron Lett.* **2003**, *44*, 335–339.
16. (a) Sipe, J. D.; Cohen, A. S. *J. Struct. Bio.* **2000**, *130*, 88–98. (b) Goldsbury, C. S.; Wirtz, S.; Müller, S. A.; Sunderji, S.; Wicki, P.; Aebi, U.; Frey, P. *J. Struct. Bio.* **2000**, *130*, 217–231.
17. Nilsberth, C.; Westlind-Danielsson, A.; Eckman, C. B.; Condrón, M. M.; Axelman, K.; Forsell, C.; Stenh, C.; Luthman, J.; Teplow, D. B.; Younkin, S. G.; Näslund, J.; Lannfelt, L. *Nat. Neurosci.* **2001**, *4*, 887–893.
18. Bodanszky, M.; Bodanszky, A. *The practice of peptide synthesis*. Springer: New York, 1984; pp 1–282.
19. Kabsch, W. *J. Appl. Cryst.* **1988**, *21*, 916.
20. Sheldrick, G. M. *Acta. Crystallogr. Sect. A: Fundam. Crystallogr.* **1990**, *46*, 467.
21. Sheldrick, G. M. *Program for Crystal Structure Refinement*; University of Göttingen: Germany, 1993.

CeCl₃·H₂O/NaI-Promoted stereoselective synthesis of 2,4-disubstituted chiral tetrahydroquinolines

Jhillu S. Yadav,* B. V. S. Reddy, M. Srinivas and B. Padmavani

Division of Organic Chemistry, Indian Institute of Chemical Technology, Hyderabad 500 007, India

Received 31 October 2003; revised 12 January 2004; accepted 5 February 2004

Abstract—D-Glycals readily undergo cyclization with aryl amines in the presence of CeCl₃·7H₂O–NaI under mild and neutral conditions to afford a novel sugar derived tetrahydroquinoline derivatives in good yields with high stereoselectivity. The stereochemistry of the products was assigned by using various NMR studies.

© 2004 Elsevier Ltd. All rights reserved.

1. Introduction

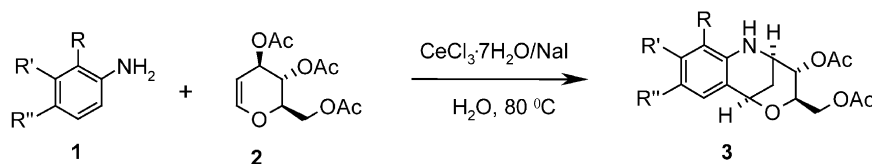
The tetrahydroquinoline moiety is a core structure in many biologically important natural products¹ such as flindersine, oricine, and veprisine. Derivatives of these alkaloids possess a wide range of biological activities such as psychotropic, antiallergic, and anti-inflammatory behavior² and are used as a potential pharmaceuticals.³ Recently, great attention has been focussed on the use of water as a green solvent in organic synthesis. In addition to its abundance, and for economical and safety reasons, water has naturally become a substitute and an alternative environmentally benign solvent in organic synthesis.⁴ The use of aqueous medium as solvent also reduces the harmful effects of organic solvents on the environment. Lanthanide salts are unique Lewis acids that are currently of great research interest.⁵ In particular, cerium reagents are relatively non-toxic, readily available at low cost and are fairly stable to air or moisture. Owing to its unique properties, CeCl₃ has been extensively used for a variety of organic transformations.^{6,7}

2. Results and discussions

In continuation of our interest in the synthesis of *C*- and *O*-

glycosides,⁸ we herein report a novel approach for the synthesis of sugar derived chiral tetrahydroquinolines from D-glucal and aryl amines. Thus, treatment of 3,4,6-tri-*O*-acetyl-D-glucal **2** with aniline in the presence of an equimolar ratio of CeCl₃·7H₂O and NaI in water afforded sugar fused tetrahydroquinoline **3a** in 82% yield (Scheme 1). The reaction proceeded efficiently in water at 80 °C and the product was obtained with high stereoselectivity. The product **3a** was characterized by various NMR experiments like double quantum filtered correlation spectroscopy (DQFCOSY), nuclear Overhauser effect spectroscopy (NOESY), heteronuclear single quantum correlation spectroscopy (HSQC) and ³J_{CH} optimized HMBC experiments. The edited HSQC spectrum showed the presence of two methylene groups in addition to eight methine and two methyl groups. The location of methylene at the bridge head of bicyclononene like structure was confirmed by the presence of small couplings between these protons and the bridge protons H₁ and H₃ *J*_{H–2H}=3.7 Hz, *J*_{H–2H}=1.8 Hz, *J*_{2H–3H}=2.4 Hz, and *J*_{2H–3H}=4.6 Hz. Fusion of the bicyclononene and the aromatic ring at C₁₁–NH was confirmed by NOE between H₁–H₁₂ (Fig. 1a).

Further support for the structure came from HMBC peaks between H₁–C₁₂, H₁–C₁₁, H₁–C₁₆ and H₁₂–C₁. The two



Scheme 1.

Keywords: D-Glucal; Cerium reagents; Glycal cyclization; Tetrahydroquinolines.

* Corresponding author. Tel.: +91-40-27193434; fax: +91-40-27160512; e-mail address: yadav@iict.ap.nic.in

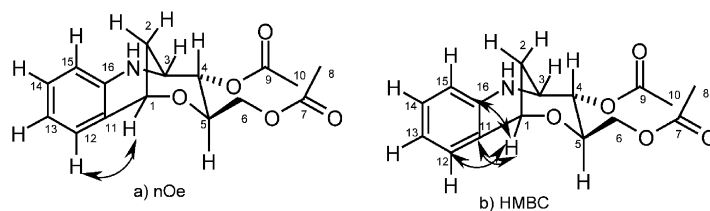


Figure 1. Important NOE's and chemical structure of **3a**.

six-membered rings of the bicyclononene moiety have two different conformations. The oxygen containing ring takes a chair form, whereas the other ring with nitrogen and fused to the aromatic ring exists in the half chair form. HMBC peaks between H_2-C_{11} and H_2-C_4 are consistent with the structure. Large coupling constant value of $J_{H_4-H_5}=10.4$ Hz and a NOESY cross-peak between H_2-H_4 further support the chair form for the ring containing these protons. Ring current effect due to the aromatic ring causes a high field chemical shifts of H_2 ($\delta=1.96$ ppm) and H_5 ($\delta=3.58$ ppm).

Encouraged by the results obtained with aniline, we turned our attention to various aryl amines and glycols. Interestingly, a variety of aryl amines including mono-, and di-substituted anilines reacted smoothly with glucal triacetate under similar conditions to afford the corresponding benzo-fused heterobicycles in good yields. However, 3,4,6-tri-*O*-methyl-D-glucal or 3,4,6-tri-*O*-benzyl-D-glucal did not react with aryl amines under identical reaction conditions (entry **o**, Table 1). The reaction was successful

only with glucal triacetate. Furthermore, the reaction did not proceed with 2,6-disubstituted anilines such as 2,6-dichloroaniline and 2,6-dimethylaniline under the reaction conditions (entry **n**, Table 1). These results clearly indicated that one of the *ortho* positions of aniline should be free from substitution for the success of the reaction. The probable mechanism seems to be addition of aniline to the α,β -unsaturated aldehyde, which is formed in situ from D-glucal and water. Thus, the initially formed 1,4-adduct may undergo an intramolecular cyclization resulting in the formation of fused tetrahydroquinolines (Scheme 2). This method is clean and highly stereoselective, affording sugar fused tetrahydroquinolines in a one-pot operation. The efficacy of various metal halides such as $CeCl_3 \cdot 7H_2O$, YCl_3 , $YbCl_3$, $BiCl_3$, and $ZrCl_4$ was studied in water. Among these catalysts, $CeCl_3 \cdot 7H_2O$ was found to be the most effective reagent in terms of conversion and reaction rates. It is important to mention that simple cyclic enol ethers such as 3,4-dihydro-2*H*-pyran and 2,3-dihydrofuran gave the corresponding *cis*-fused pyrano- and furano-tetrahydroquinolines, respectively, under similar reaction conditions.⁹

Table 1. $CeCl_3 \cdot 7H_2O$ /NaI-promoted synthesis of fused chiral tetrahydroquinolines

Entry	Aryl amine	D-Glucal	Product ^a	Reaction time (h)	Yield (%) ^b
1a	$R=R^1=R^2=H$		3a	7.0	82
1b	$R=R^1=H; R^2=Cl$		3b	8.0	80
1c	$R=R^1=H; R^2=Me$		3c	7.5	85
1d	$R=R^1=H; R^2=F$		3d	9.0	75
1e	$R=R^1=H; R^2=Br$		3e	8.5	72
1f	$R=R^2=H; R^1=Me$		3f	7.5	83 ^c

Table 1 (continued)

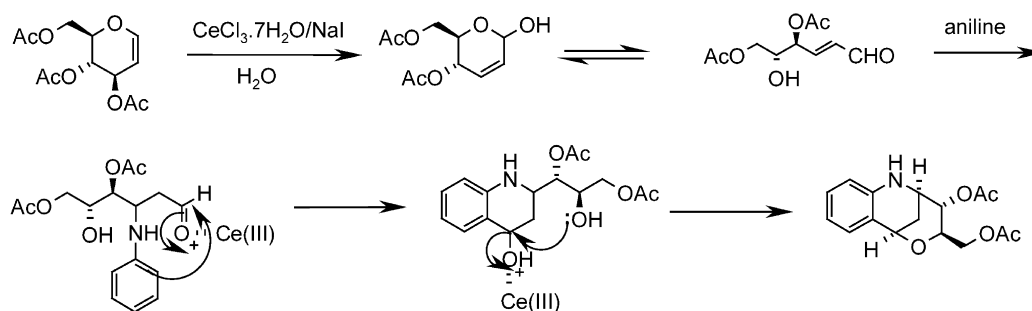
Entry	Aryl amine	D-Glucal	Product ^a	Reaction time (h)	Yield (%) ^b
1g	R=R ¹ =H; R ² =OMe		3g	8.0	70
1h	R=R ² =H; R ¹ =Cl		3h	9.0	80 ^c
1i	R=Cl; R ¹ =Me; R ² =H;		3i	8.5	79
1j	R=Cl; R ¹ =R ² =H		3j	7.5	82
1k	R=Me; R ¹ =R ² =H		3k	8.0	86
1l	R=Br; R ¹ =H; R ² =nMe		3l	9.5	65
1m	α -Naphthalamine		3m	8.5	70
1n	2,6-Dichloroaniline		No reaction	8.0	—
1o	Aniline		No reaction	9.0	—

R¹=Me or Bn^a Products were characterized by ¹H NMR, ¹³C NMR, IR and mass spectroscopy.^b Yield refers to pure products after chromatography.^c 5–10% other regioisomer was obtained.

Water appears to give the best results as solvent. Finally, we have examined the possibility of CeCl₃·7H₂O functioning catalytically or at least, in less than stoichiometric amounts. But best results were obtained with an equimolar ratio of CeCl₃·7H₂O and NaI. However, in the absence of NaI the reaction was very slow by CeCl₃ alone in refluxing water and took a longer reaction time (15–36 h) to achieve complete conversion. This clearly indicates that the addition of 1 equiv. of NaI is crucial in this transformation. It is well-

known in literature that sodium iodide activates the CeCl₃ to accelerate the reaction.⁶ Although, the reactions proceeded with hydrochloric acid, low conversions (14–25%) were obtained even after long reaction times (15–24 h). The scope and generality of this process is illustrated with respect to various aryl amines and D-glucal (Table 1).

In summary, we describe a novel protocol for the synthesis of sugar derived chiral tetrahydroquinolines from D-glucal



Scheme 2.

and aryl amines using the inexpensive and readily available $\text{CeCl}_3 \cdot 7\text{H}_2\text{O}/\text{NaI}$ reagent system under mild and neutral conditions. The use of water as solvent makes this method quite simple and a more convenient and environmentally benign process to prepare sugar based heterobicycles in a single-step operation.

3. Experimental

3.1. General

Melting points were recorded on Buchi R-535 apparatus and are uncorrected. IR spectra were recorded on a Perkin–Elmer FT-IR 240-c spectrophotometer using KBr optics. ^1H NMR and ^{13}C spectra were recorded on Gemini-200 and Varian Unity-500 spectrometer in CDCl_3 using TMS as internal standard. Mass spectra were recorded on a Finnigan MAT 1020 mass spectrometer operating at 70 eV. The optical rotations were measured on a Jasco Dip 360 Digital polarimeter.

3.2. General procedure

A mixture of 3,4,6-tri-*O*-acetyl-D-glucal (2 mmol), aniline (3 mmol), $\text{CeCl}_3 \cdot 7\text{H}_2\text{O}$ (2 mmol) and NaI (2 mmol) in water (10 mL) was stirred at 80 °C temperature for the specified time as required to complete the reaction (Table 1). After complete conversion, as indicated by TLC, the reaction mixture was extracted with ethyl acetate (2×10 mL). The combined organic layers were dried over anhydrous Na_2SO_4 , concentrated in vacuo and purified by column chromatography on silica gel (Merck, 100–200 mesh, ethyl acetate–hexane, 1:9) to afford the pure tetrahydroquinoline derivative. Spectral data for products.

3.2.1. Compound 3a. Colourless liquid, $[\alpha]_{\text{D}}^{27}=95.5$ ($c=1.0$, CHCl_3), IR (KBr): ν_{max} : 3427, 2935, 2857, 1730, 1607, 1461, 1365, 1257, 1098, 835 cm^{-1} . ^1H NMR (500 MHz, CDCl_3): δ 7.16 (dt, $J=1.5$, 7.9 Hz, 1H, H13), 7.13 (dd, $J=1.5$, 7.9 Hz, 1H, H15), 6.69 (dt, $J=1.5$, 7.9 Hz, 1H, H14), 6.61 (dd, $J=1.5$, 7.9 Hz, 1H, H12), 4.84 (dd, $J=3.1$, 10.4 Hz, 1H, H4), 4.81 (dd, $J=1.8$, 3.7 Hz, 1H, H1), 4.44 (brs, 1H, NH), 4.19 (dd, $J=4.2$, 12.0 Hz, 1H, H6), 3.99 (dd, $J=2.2$, 12.0 Hz, 1H, H6'), 3.84 (ddd, $J=2.4$, 3.1, 4.6 Hz, 1H, H3), 3.58 (ddd, $J=2.1$, 4.2, 10.4 Hz, 1H, H5), 2.29 (ddd, $J=2.4$, 3.7, 13.2 Hz, 1H, H2), 2.10 (s, 3H, CH_3 -10), 2.06 (s, 3H, CH_3 -8), 1.96 (ddd, $J=1.8$, 4.6, 13.2 Hz, 1H, H2). ^{13}C NMR (proton decoupled, 75 MHz, CDCl_3): δ 170.8, 169.8, 145.0, 130.5, 129.9, 118.8, 117.2, 112.9, 71.8, 68.5, 67.4, 63.0, 46.6, 27.9, 21.0, 20.7. FAB Mass: 305 M^+ , 259, 191, 144, 130, 119, 91, 69, 57. HRMS calcd for $\text{C}_{16}\text{H}_{19}\text{NO}_5$: 305.1263. Found: 305.1281.

3.2.2. Compound 3b. Pale yellow liquid, $[\alpha]_{\text{D}}^{27}=93.5$ ($c=2.0$, CHCl_3), IR (KBr): ν_{max} : 3409, 2928, 1728, 1607, 1495, 1372, 1242, 1045, 870 cm^{-1} . ^1H NMR (500 MHz, CDCl_3): δ 7.05–7.20 (m, 2H), 6.50–6.57 (m, 1H), 4.75 (dd, $J=3.2$, 10.5 Hz, 1H), 4.65 (dd, $J=1.8$, 3.8 Hz, 1H), 4.32 (brs, 1H, NH), 4.25 (dd, $J=4.2$, 12.0 Hz, 1H), 4.0 (dd, $J=2.1$, 12.0 Hz, 1H), 3.78 (ddd, $J=2.5$, 3.2, 4.5 Hz, 1H), 3.60 (ddd, $J=2.1$, 4.2, 10.3 Hz, 1H), 2.23 (ddd, $J=2.5$, 3.8, 13.0 Hz, 1H), 2.10 (s, 3H), 2.05 (s, 3H), 1.90 (ddd, $J=1.8$,

4.5, 13.0 Hz, 1H). ^{13}C NMR (proton decoupled, 75 MHz, CDCl_3): δ 170.8, 169.8, 143.5, 129.7, 121.4, 119.9, 115.0, 114.1, 71.5, 68.0, 67.4, 62.9, 46.4, 27.5, 20.9, 20.7. FAB Mass: 340 M^+ , 325, 309, 295, 281, 267, 251, 221, 207, 191, 164, 147, 133, 117, 91, 77. HRMS calcd for $\text{C}_{16}\text{H}_{18}\text{ClNO}_5$: 339.08735. Found: 339.08313.

3.2.3. Compound 3c. Viscous liquid, $[\alpha]_{\text{D}}^{27}=57.4$ ($c=0.7$, CHCl_3), IR (KBr): ν_{max} : 3409, 2926, 1729, 1622, 1510, 1440, 1248, 1045, 815, 758 cm^{-1} . ^1H NMR (500 MHz, CDCl_3): δ 6.98–6.90 (m, 2H), 6.50 (d, $J=8.0$ Hz, 1H), 4.80 (dd, $J=3.2$, 10.5 Hz, 1H), 4.77 (dd, $J=1.7$, 3.8 Hz, 1H), 4.40 (brs, 1H, NH), 4.20 (dd, $J=4.2$, 12.0 Hz, 1H), 3.85 (dd, $J=2.1$, 12.0 Hz, 1H), 3.78 (ddd, $J=2.4$, 3.2, 4.5 Hz 1H), 3.50 (ddd, $J=2.1$, 4.2, 10.5 Hz, 1H), 2.30 (ddd, $J=2.4$, 3.7, 13.0 Hz, 1H), 2.25 (s, 3H), 2.10 (s, 3H), 2.05 (s, 3H), 1.95 (ddd, $J=1.7$, 4.5, 13.0 Hz, 1H). ^{13}C NMR (proton decoupled, 75 MHz, CDCl_3): δ 170.6, 170.1, 145.0, 129.6, 127.3, 118.6, 117.4, 112.7, 71.8, 67.4, 65.2, 62.9, 46.6, 29.6, 21.6, 20.8, 20.6. FAB Mass: 319 M^+ , 281, 207, 158, 144, 105, 91, 73, 57. HRMS calcd for $\text{C}_{17}\text{H}_{21}\text{NO}_5$: 319.1419. Found: 319.1437.

3.2.4. Compound 3d. Oily liquid, $[\alpha]_{\text{D}}^{27}=67.1$ ($c=0.75$, CHCl_3), IR (KBr): ν_{max} : 3356, 2961, 1733, 1505, 1260, 1040, 809 cm^{-1} . ^1H NMR (500 MHz, CDCl_3): δ 6.78–6.90 (m, 2H), 6.45–6.50 (m, 1H), 4.80 (dd, $J=3.1$, 10.5 Hz, 1H), 4.70 (dd, $J=1.8$, 3.8 Hz, 1H), 4.30 (brs, 1H, NH), 4.20 (dd, $J=4.2$, 12.0 Hz, 1H), 3.90 (dd, $J=2.1$, 12.0 Hz, 1H), 3.80 (ddd, $J=2.5$, 3.1, 4.5 Hz, 1H), 3.50 (ddd, $J=2.1$, 4.2, 10.3 Hz, 1H), 2.25 (ddd, $J=2.5$, 3.8, 13.1 Hz, 1H), 2.10 (s, 3H), 2.0 (s, 3H), 1.95 (ddd, $J=1.8$, 4.5, 13.1 Hz, 1H). ^{13}C NMR (proton decoupled, 75 MHz, CDCl_3): δ 170.3, 169.4, 156.9, 141.1, 119.6, 117.2, 116.9, 113.9, 71.7, 68.1, 67.7, 62.9, 46.7, 27.9, 21.0, 20.8. FAB Mass: 323 M^+ 267, 221, 191, 147, 133, 73. HRMS calcd for $\text{C}_{16}\text{H}_{18}\text{FNO}_5$: 323.1169. Found: 323.1127.

3.2.5. Compound 3e. Brown liquid, $[\alpha]_{\text{D}}^{27}=169.2$ ($c=1.5$, CHCl_3), IR (KBr): ν_{max} : 3410, 3019, 2955, 1738, 1603, 1490, 1371, 1246, 1046, 813, 757 cm^{-1} . ^1H NMR (500 MHz, CDCl_3): δ 7.10–7.20 (m, 2H), 6.50 (d, $J=8.1$ Hz, 1H), 4.80 (dd, $J=3.2$, 10.5 Hz, 1H), 4.70 (dd, $J=1.8$, 3.8 Hz, 1H), 4.40 (brs, 1H, NH), 4.25 (dd, $J=4.2$, 12.0 Hz, 1H), 4.10 (dd, $J=2.1$, 12.0 Hz, 1H), 3.90 (ddd, $J=2.5$, 3.2, 4.5 Hz, 1H), 3.80 (ddd, $J=2.1$, 4.2, 10.3 Hz, 1H), 2.30 (ddd, $J=2.5$, 3.8, 13.0 Hz, 1H), 2.10 (s, 3H), 2.04 (s, 3H), 1.90 (ddd, $J=1.8$, 4.5, 13.0 Hz, 1H). ^{13}C NMR (proton decoupled, 75 MHz, CDCl_3): δ 170.8, 169.8, 143.9, 132.8, 132.6, 129.1, 120.6, 114.6, 71.5, 68.0, 67.5, 62.9, 46.5, 27.5, 20.9, 20.7. FAB Mass: 383 M^+ , 368, 340, 327, 289, 265, 239, 224, 219, 191, 165. HRMS calcd for $\text{C}_{16}\text{H}_{18}\text{BrNO}_5$: 383.0368. Found: 383.0393.

3.2.6. Compound 3f. Viscous liquid, $[\alpha]_{\text{D}}^{27}=67.5$ ($c=1.4$, CHCl_3), IR (KBr): ν_{max} : 3413, 2972, 2854, 1741, 1620, 1583, 1492, 1439, 1371, 1329, 1241, 1171, 1047, 815 cm^{-1} . ^1H NMR (200 MHz, CDCl_3): δ 6.90 (d, $J=8.0$ Hz, 1H), 6.50 (d, $J=8.0$ Hz, 1H), 6.40–6.35 (s, 1H), 4.85 (dd, $J=3.1$, 10.3 Hz, 1H), 4.75 (dd, $J=1.7$, 3.8 Hz, 1H), 4.40 (brs, 1H, NH), 4.20 (dd, $J=4.2$, 12.0 Hz, 1H), 3.90 (dd, $J=2.1$, 12.0 Hz, 1H), 3.80 (ddd, $J=2.4$, 3.1, 4.5 Hz 1H), 3.55 (ddd, $J=2.1$, 4.2, 10.3 Hz, 1H), 2.30 (ddd, $J=2.4$, 3.7, 13.0 Hz,

1H), 2.25 (s, 3H), 2.10 (s, 3H), 2.05 (s, 3H), 1.90 (ddd, $J=1.7, 4.5, 13.0$ Hz, 1H). ^{13}C NMR (proton decoupled, 50 MHz, CDCl_3): δ 170.3, 169.9, 145.0, 132.5, 127.3, 118.7, 117.5, 112.8, 71.8, 67.4, 65.2, 62.9, 46.6, 29.6, 21.6, 20.7, 20.6. FAB Mass: 319 M^+ , 282, 170, 144, 91, 43. HRMS calcd for $\text{C}_{17}\text{H}_{21}\text{NO}_5$: 319.1419. Found: 319.1458.

3.2.7. Compound 3g. Oily liquid, $[\alpha]_{\text{D}}^{25}=21.5$ ($c=0.7$, CHCl_3), ^1H NMR (500 MHz, CDCl_3): δ 6.58–6.65 (m, 2H), 6.40 (d, $J=7.9$ Hz, 1H), 4.70 (dd, $J=3.0, 10.3$ Hz, 1H, H4), 4.63 (dd, $J=1.7, 3.8$ Hz, 1H), 4.15 (dd, $J=4.2, 12.0$ Hz, 1H), 3.90 (dd, $J=2.1, 12.0$ Hz, 1H), 3.75 (ddd, $J=2.4, 3.0, 4.5$ Hz, 1H), 3.65 (s, 3H), 3.45 (ddd, $J=2.1, 4.2, 10.3$ Hz, 1H), 2.20 (ddd, $J=2.4, 3.8, 13.2$ Hz, 1H), 2.05 (s, 3H), 2.0 (s, 3H), 1.90 (ddd, $J=1.7, 4.5, 13.2$ Hz, 1H). ^{13}C NMR (proton decoupled, 75 MHz, CDCl_3): δ 170.9, 169.8, 151.8, 129.7, 123.5, 119.6, 117.0, 114.9, 71.8, 68.7, 67.2, 63.1, 55.8, 46.7, 28.1, 21.0, 20.7. IR (KBr): ν_{max} : 3325, 3015, 1739, 1505, 1462, 1221, 1041, 759 cm^{-1} . FAB Mass: 335 M^+ , 281, 267, 249, 221, 207, 191, 177, 160, 147, 133, 117, 105, 91, 73, 65, 55. HRMS calcd for $\text{C}_{17}\text{H}_{21}\text{NO}_6$: 335.13688. Found: 335.13259.

3.2.8. Compound 3h. Light yellow liquid, $[\alpha]_{\text{D}}^{27}=64.5$ ($c=2.8$, CHCl_3), IR (KBr): ν_{max} : 3390, 2926, 2854, 1731, 1599, 1485, 1428, 1371, 1242, 1128, 1047, 846, 760 cm^{-1} . ^1H NMR (500 MHz, CDCl_3): δ 7.15–6.95 (m, 1H), 6.60–6.58 (m, 1H), 6.45–6.40 (m, 1H), 4.73 (dd, $J=3.2, 10.5$ Hz, 1H), 4.60 (dd, $J=1.8, 3.8$ Hz, 1H), 4.30 (brs, 1H, NH), 4.23 (dd, $J=4.2, 12.0$ Hz, 1H), 4.05 (dd, $J=2.1, 12.0$ Hz, 1H), 3.79 (ddd, $J=2.5, 3.2, 4.5$ Hz, 1H), 3.60 (ddd, $J=2.1, 4.2, 10.3$ Hz, 1H), 2.25 (ddd, $J=2.5, 3.8, 13.0$ Hz, 1H), 2.10 (s, 3H), 2.05 (s, 3H), 1.95 (ddd, $J=1.8, 4.5, 13.0$ Hz, 1H). ^{13}C NMR (proton decoupled, 75 MHz, CDCl_3): δ 170.5, 169.6, 143.2, 130.4, 121.3, 119.9, 115.2, 114.0, 71.4, 68.0, 67.5, 62.7, 46.3, 27.4, 20.8, 20.6. FAB Mass: 339 M^+ , 333, 292, 220, 281, 194, 166, 153, 128, 97, 84, 44. HRMS calcd for $\text{C}_{16}\text{H}_{18}\text{ClNO}_5$: 339.08735. Found: 339.08419.

3.2.9. Compound 3i. Brown solid, mp 49–51 °C, $[\alpha]_{\text{D}}^{27}=28.0$ ($c=1.6$, CHCl_3), IR (KBr): ν_{max} : 3417, 2927, 1739, 1622, 1594, 1468, 1370, 1239, 1064, 814, 769 cm^{-1} . ^1H NMR (500 MHz, CDCl_3): δ 7.05–6.90 (m, 1H), 6.60–6.675 (m, 1H), 4.89 (dd, $J=3.2, 10.5$ Hz, 1H), 4.76 (dd, $J=1.8, 3.7$ Hz, 1H), 4.35 (brs, 1H, NH), 4.20 (dd, $J=4.2, 12.0$ Hz, 1H), 3.95 (dd, $J=2.2, 12.0$ Hz, 1H), 3.85 (ddd, $J=2.4, 3.2, 4.6$ Hz, 1H), 3.50 (ddd, $J=2.1, 4.2, 10.5$ Hz, 1H), 2.25 (ddd, $J=2.4, 3.7, 13.2$ Hz, 1H), 2.15 (s, 3H), 2.10 (s, 3H), 2.05 (s, 3H), 1.93 (ddd, $J=1.8, 4.6, 13.2$ Hz, 1H, H2). ^{13}C NMR (proton decoupled, 75 MHz, CDCl_3): δ 170.3, 169.5, 134.6, 133.4, 130.2, 127.3, 120.1, 107.4, 71.5, 68.7, 67.6, 63.0, 46.8, 27.9, 21.2, 20.7, 20.3. FAB Mass: 353 M^+ , 336, 178, 83, 57, 43. HRMS calcd for $\text{C}_{17}\text{H}_{20}\text{ClNO}_5$: 353.1030. Found: 353.1073.

3.2.10. Compound 3j. Light yellow solid, mp 119–120 °C, $[\alpha]_{\text{D}}^{27}=52.2$ ($c=2.0$, CHCl_3), IR (KBr): ν_{max} : 3412, 2970, 2927, 1727, 1607, 1499, 1256, 1044, 842, 740 cm^{-1} . ^1H NMR (500 MHz, CDCl_3): δ 7.25 (d, $J=8.0$ Hz, 1H), 7.05 (d, $J=7.9$ Hz, 1H), 6.60 (t, $J=7.9$ Hz, 1H), 4.90 (dd, $J=3.2, 10.5$ Hz, 1H), 4.80 (dd, $J=1.8, 3.8$ Hz, 1H), 4.25 (dd, $J=4.0, 12.0$ Hz, 1H, H6), 3.98 (dd, $J=2.0, 12.0$ Hz, 1H), 3.90 (ddd, $J=2.3, 3.2, 4.7$ Hz, 1H), 3.58 (ddd, $J=2.0, 4.0, 10.5$ Hz,

1H), 2.30 (ddd, $J=2.3, 3.8, 13.2$ Hz, 1H), 2.10 (s, 3H), 2.06 (s, 3H), 1.90 (ddd, $J=1.8, 4.7, 13.2$ Hz, 1H). ^{13}C NMR (proton decoupled, 75 MHz, CDCl_3): δ 170.8, 169.9, 141.0, 129.7, 128.9, 120.2, 117.0, 112.7, 71.3, 68.2, 67.5, 62.9, 46.6, 27.6, 21.0, 20.7. FAB Mass: 340 M^+ , 329, 325, 309, 295, 281, 267, 251, 221, 207, 191, 164, 147, 133, 117, 91, 77. HRMS calcd for $\text{C}_{16}\text{H}_{18}\text{ClNO}_5$: 339.08735. Found: 339.08908.

3.2.11. Compound 3k. Viscous liquid, $[\alpha]_{\text{D}}^{27}=83.7$ ($c=0.8$, CHCl_3), IR (KBr): ν_{max} : 3422, 2931, 2858, 1734, 1604, 1472, 1367, 1254, 1093, 837 cm^{-1} . ^1H NMR (500 MHz, CDCl_3): δ 6.98–6.95 (m, 2H), 6.60 (t, $J=7.9$ Hz, 1H), 4.82 (dd, $J=3.2, 10.5$ Hz, 1H), 4.78 (dd, $J=1.7, 3.8$ Hz, 1H), 4.22 (dd, $J=4.2, 12.0$ Hz, 1H), 4.20 (brs, 1H, NH), 3.95 (dd, $J=2.1, 12.0$ Hz, 1H), 3.90 (ddd, $J=2.4, 3.2, 4.5$ Hz, 1H), 3.55 (ddd, $J=2.1, 4.2, 10.5$ Hz, 1H), 2.30 (ddd, $J=2.4, 3.7, 13.0$ Hz, 1H), 2.15 (s, 3H), 2.10 (s, 3H), 2.05 (s, 3H), 1.95 (ddd, $J=1.7, 4.5, 13.0$ Hz, 1H). ^{13}C NMR (proton decoupled, 75 MHz, CDCl_3): δ 170.9, 169.9, 143.0, 130.8, 128.4, 120.1, 118.4, 116.8, 71.7, 68.8, 67.3, 63.1, 46.9, 29.6, 27.9, 21.0, 20.8. FAB Mass: 319 M^+ , 281, 207, 158, 144, 105, 91, 73, 57. HRMS calcd for $\text{C}_{17}\text{H}_{21}\text{NO}_5$: 319.1419. Found: 319.1451.

3.2.12. Compound 3l. Yellow solid, mp 165 °C, $[\alpha]_{\text{D}}^{27}=51.2$ ($c=1.35$, CHCl_3), IR (KBr): ν_{max} : 3416, 2965, 2362, 1728, 1618, 1505, 1432, 1373, 1232, 1043, 861 cm^{-1} . ^1H NMR (500 MHz, CDCl_3): δ 7.20 (s, 1H), 6.90 (s, 1H), 4.85 (dd, $J=3.1, 10.4$ Hz, 1H), 4.78 (dd, $J=1.8, 3.7$ Hz, 1H), 4.25 (brs, 1H, NH), 4.20 (dd, $J=4.2, 12.0$ Hz, 1H), 3.90 (dd, $J=2.2, 12.0$ Hz, 1H), 3.85 (ddd, $J=2.4, 3.1, 4.6$ Hz, 1H), 3.50 (ddd, $J=2.1, 4.2, 10.4$ Hz, 1H), 2.25 (ddd, $J=2.4, 3.7, 13.2$ Hz, 1H), 2.15 (s, 3H), 2.10 (s, 3H), 2.05 (s, 3H), 1.95 (ddd, $J=1.8, 4.6, 13.2$ Hz, 1H, H2). ^{13}C NMR (proton decoupled, 75 MHz, CDCl_3): δ 170.5, 169.6, 139.7, 133.4, 130.3, 127.1, 120.2, 107.3, 71.3, 68.5, 67.5, 62.8, 46.9, 27.9, 21.0, 20.8, 20.1. FAB Mass: 397 M^+ , 385, 355, 341, 327, 311, 295, 281, 267, 221, 207, 191, 147, 133, 77. HRMS calcd for $\text{C}_{17}\text{H}_{20}\text{BrNO}_5$: 397.05148. Found: 397.05205.

3.2.13. Compound 3m. Viscous oil, $[\alpha]_{\text{D}}^{27}=85.6$ ($c=0.5$, CHCl_3), IR (KBr): ν_{max} : 3400, 2956, 2859, 1730, 1605, 1467, 1254, 1093, 838 cm^{-1} . ^1H NMR (500 MHz, CDCl_3): δ 7.80–7.70 (m, 3H), 7.38–7.45 (m, 2H), 7.10–7.18 (m, 1H), 4.90 (dd, $J=3.0, 10.5$ Hz, 1H), 4.82 (dd, $J=1.7, 3.8$ Hz, 1H), 4.40 (brs, 1H, NH), 4.05 (dd, $J=4.2, 12.0$ Hz, 1H), 3.90 (dd, $J=2.0, 12.0$ Hz, 1H), 3.84 (ddd, $J=2.3, 3.0, 4.6$ Hz, 1H), 3.50 (ddd, $J=2.0, 4.2, 10.5$ Hz, 1H), 2.30 (ddd, $J=2.3, 3.8, 13.2$ Hz, 1H), 2.10 (s, 3H), 2.04 (s, 3H), 1.96 (ddd, $J=1.7, 4.6, 13.2$ Hz, 1H). ^{13}C NMR (proton decoupled, 75 MHz, CDCl_3): δ 170.9, 169.7, 143.5, 130.7, 129.6, 124.5, 123.2, 122.8, 122.0, 121.1, 120.3, 119.5, 71.9, 68.4, 67.1, 63.5, 46.7, 28.0, 20.9, 20.5. FAB Mass: 355 M^+ , 341, 325, 281, 265, 251, 221, 207, 191, 177, 147, 133, 117, 105, 91, 73, 65, 55. HRMS calcd for $\text{C}_{20}\text{H}_{21}\text{NO}_5$: 355.1419. Found: 355.1458.

Acknowledgements

B.V.S. thanks CSIR New Delhi for the award of fellowship.

References and notes

1. (a) Ramesh, M.; Mohan, P. A.; Shanmugam, P. *Tetrahedron* **1984**, *40*, 4041–4049. (b) Jurd, L.; Wong, R. V. *Aust. J. Chem.* **1981**, *34*, 1625–1632. (c) Coppola, G. M. *J. Heterocycl. Chem.* **1983**, *20*, 1217–1221.
2. (a) Yamada, N.; Kadowaki, S.; Takahashi, K.; Umezu, K. *Biochem. Pharmacol.* **1992**, *44*, 1211. (b) Faber, K.; Stueckler, H.; Kappe, T. *J. Heterocycl. Chem.* **1984**, *21*, 1177–1178. (c) Johnson, J. V.; Rauckman, S.; Baccanari, P. D.; Roth, B. *J. Med. Chem.* **1989**, *32*, 1942–1949.
3. Mohamed, E. A. *Chem. Pap.* **1994**, *48*, 261. *Chem. Abstr.* **1995**, *123*, 9315x.
4. (a) Grieco, P. A. *Organic synthesis in water*; Blackie Academic: London, 1998. (b) Li, C. J.; Chan, T. H. *Organic reactions in aqueous media*; Wiley: New York, 1997; p 159.
5. Imamoto, T. *Lanthanides in organic synthesis*; Academic: New York, 1994.
6. (a) Cappa, A.; Marcantoni, E.; Torregiani, E.; Bartoli, G.; Bellucci, M. C.; Bosco, M.; Sambri, L. *J. Org. Chem.* **1999**, *64*, 5696. (b) Marcantoni, E.; Nobili, F.; Bartoli, G.; Bosco, M.; Sambri, L.; Torregiani, E. *J. Org. Chem.* **1997**, *62*, 4183. (c) Di-Dea, M.; Marcantoni, E.; Torregiani, E.; Bartoli, G.; Bellucci, M. C.; Bosco, M.; Sambri, L. *J. Org. Chem.* **2000**, *65*, 2830.
7. (a) Yadav, J. S.; Reddy, B. V. S.; Reddy, K. S. *Synlett* **2002**, 468. (b) Yadav, J. S.; Reddy, B. V. S.; Reddy, M. S.; Sabitha, G. *Synlett* **2001**, 1134. (c) Yadav, J. S.; Reddy, B. V. S. *Synlett* **2000**, 1275.
8. (a) Yadav, J. S.; Reddy, B. V. S. *Synthesis* **2002**, 511. (b) Yadav, J. S.; Reddy, B. V. S.; Raju, A. K.; Rao, C. V. *Tetrahedron Lett.* **2002**, *43*, 5437. (c) Yadav, J. S.; Reddy, B. V. S.; Reddy, K. B.; Satyanarayan, M. *Tetrahedron Lett.* **2002**, *43*, 7009. (d) Yadav, J. S.; Reddy, B. V. S.; Rao, K. V.; Saritha Raj, K.; Prasad, A. R.; Kiran Kumar, S.; Kunwar, A. C.; Jayaprakash, P.; Jagannadh, B. *Angew. Chem., Int. Ed.* **2003**, *42*, 5198–5201.
9. Yadav, J. S.; Reddy, B. V. S.; Patil, K. S.; Reddy, P. S. R. *Tetrahedron Lett.* **2002**, *43*, 3853.



Synthesis of terminal disaccharide unit of *Klebsiella pneumoniae* ssp. R20

Mukund K. Gurjar* and Arindam Talukdar

National Chemical Laboratory, Pune 411 008, India

Received 7 October 2003; revised 13 January 2004; accepted 5 February 2004

Abstract—Synthesis of the terminal disaccharide unit of a novel α -(1 \rightarrow 2) linked heptoglycan of *K. pneumoniae* ssp. strain R20 from methyl α -D-mannopyranoside has been presented. Central to the strategy is the application of Sharpless asymmetric dihydroxylation to introduce a new center at C-6 position of mannopyranoside. The coupling of two heptoglycans (**12** and **13**) was accomplished by a Lewis acid catalyst. © 2004 Elsevier Ltd. All rights reserved.

1. Introduction

Klebsiella pneumoniae is an important gram-negative pathogenic bacterium associated with nosocomial infections.¹ *K. pneumoniae* is most commonly the cause of pneumonia, or hospital-acquired urinary tract or burn wound infections. *Klebsiella* species seems to have resistant plasmids (R-plasmids), which imparts resistance to antibiotics such as ampicillin and carbenicillin.² The capsular polysaccharides and lipopolysaccharides (LPS) are thought to participate in many physiological process and play a key role in the pathogenesis and manifestation of infection.³ The O-polysaccharide and core oligosaccharide moieties of LPS is immunogenic, which can give antibodies having specific serological properties and that can also be of diagnostic importance. Antibodies can be directed against the conserved region of LPS, which might provide an useful approach to chemotherapy for infections from *K. pneumoniae*.⁴ Such applications require a detailed knowledge of the molecular structure of the targeted LPS molecules the enormous structural variations. Structural investigation of LPS core region began only recently. In a preliminary investigation⁵ of LPS from the rough mutant *K. pneumoniae* ssp. *pneumoniae* R20,⁶ a major fraction of the carbohydrate backbone was isolated and its structure was established. The structure (Fig. 1) is unique with regard to the presence of a novel heptoglycan of α -(1 \rightarrow 2) linkage and does not contain phosphate substituent in the core region. As a part of our on going studies to synthesize various carbohydrate units present in the LPS of *K. pneumoniae*, herein, we report the synthesis of the terminal disaccharide

unit of the heptoglycan of α -(1 \rightarrow 2) linkage present in *K. pneumoniae* ssp. *pneumoniae* strain R20.

2. Results and discussion

The literature procedure to introduce a new centre at C-6 involved the reaction of α -D-manno-hexodialdo-1,5-pyranoside and the Grignard complex of benzyloxymethylchloride⁷ or isopropoxydimethylsilyl-methyl chloride followed by oxidative cleavage of the carbon–silicon bond.⁸ We envisaged a new protocol to achieve the objective by employing the Sharpless asymmetric dihydroxylation⁹ of the 6-methylene sugar derivative with an appropriate ligand.

The synthesis started from methyl α -D-mannopyranoside (**1**) (Scheme 1), which was converted into the dibenzyl derivative **2** by following the reported procedure.¹⁰ The primary hydroxyl group of **2** was first protected as its TBS ether on treatment with TBS-Cl and imidazole in DMF and subsequently the free OH group at C-2 was blocked with MPM-Br in the presence of NaH in THF to afford **4**. Removal of TBS group with *n*-Bu₄NF in THF gave **5**. Successive oxidation by Swern oxidation reaction¹¹ and Wittig reaction with PPh₃CH₃I and NaNH₂ in anhydrous ether gave olefin **6**.¹²

The Sharpless asymmetric dihydroxylation of **6** (Scheme 2) with (DHQD)₂PYR ligand, K₃Fe(CN)₆, K₂CO₃ and catalytic OsO₄ in *tert*-BuOH–H₂O (1:1 v/v) afforded an inseparable (9:1, chiral HPLC) mixture of diastereomers **7**. However the corresponding acetonide derivatives (**8a** and **8b**) prepared by treating **7** with DMP and PPTS, were conveniently separated by silica gel chromatography. The stereochemistry at C-6 of **8b** was confirmed converting it into

Keywords: *K. pneumoniae*; manno-Heptopyranose; Sharpless asymmetric dihydroxylation; Glycosidation.

* Corresponding author. Tel.: +91-20-25882456; fax: +91-20-25882456; e-mail address: gurjar@dalton.ncl.res.in

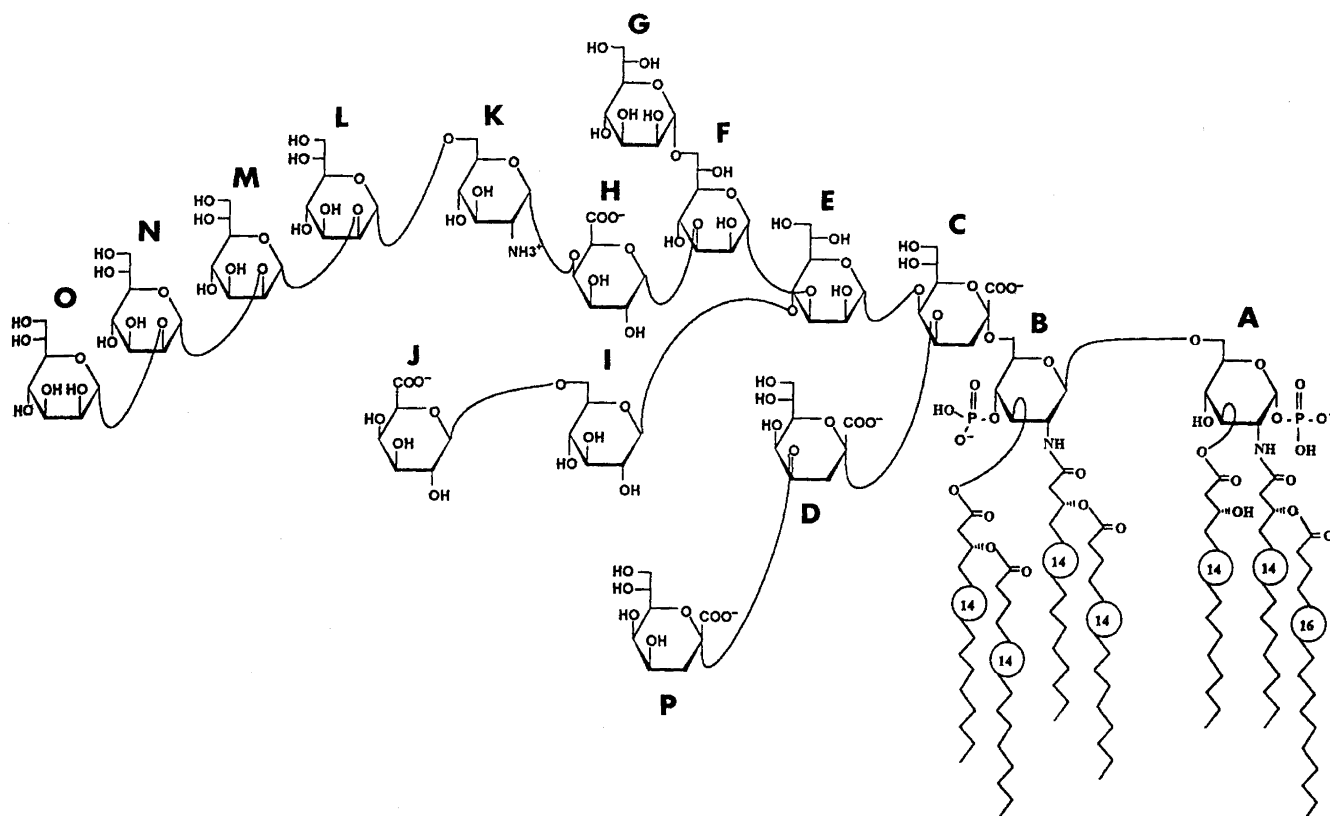


Figure 1. Structure of *K. pneumoniae* lipopolysaccharide.

the known compounds: **9** $\{[\alpha]_D^{20} = +22.4$ (*c* 0.98, CHCl_3); lit.¹³ $[\alpha]_D^{20} = +23$ (*c* 1, CHCl_3) and **10** $\{[\alpha]_D^{20} = +27.3$ (*c* 0.85, CHCl_3), lit.¹³ $[\alpha]_D^{20} = +27$ (*c* 1, CHCl_3)}. These studies indirectly ensured the stereochemical assignment of compound **8a** as indicated.

The diol **7a** on treatment with BnBr and NaH in THF provided the benzylated product **11** (Scheme 2). The MPM group at C-2 was then deprotected with DDQ¹⁴ to furnish **12** with a free OH group suitable for glycosylation reaction.

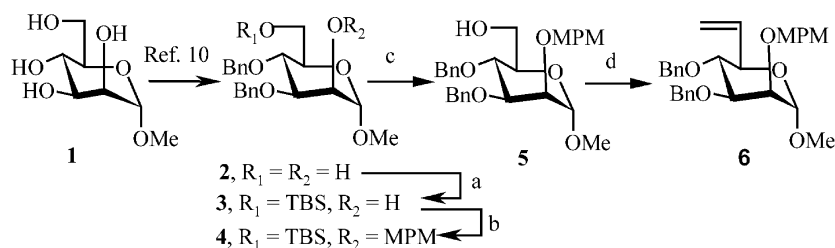
Subsequently, compound **12** was converted into glycosyl donor **13** under acetylation condition¹⁵ at 0 °C. The ¹H NMR spectrum of **13** showed two characteristic singlets at 2.05 and 2.11 ppm.

The final coupling between **12** and **13** was conducted¹⁶ (Scheme 3) in presence of catalytic $\text{BF}_3 \cdot \text{OEt}_2$ and 4 Å molecular sieves in dry CH_2Cl_2 to provide the disaccharide

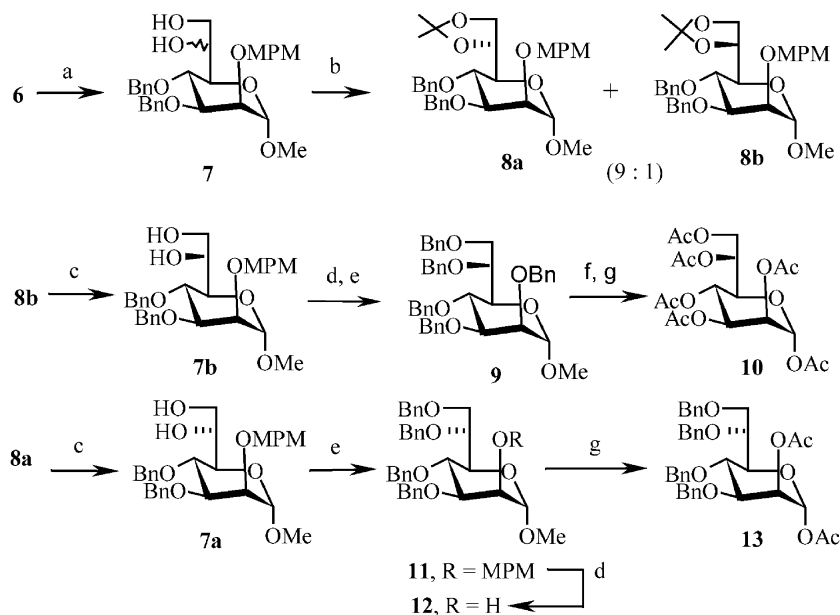
14. The ¹H NMR spectrum of **14** showed resonance due to the methyl of C(2)-OAc and anomeric methoxyl as two singlets respectively at 2.09 and 3.29 ppm. A doublet at 5.22 ppm was assigned to H-2 proton. In the ¹³C NMR spectrum, two anomeric carbon signals were visible at 99.5 and 99.8 ppm, confirming α -configuration at both the anomeric carbons.

Compound **14** on deacetylation (Scheme 3) under Zemplen conditions¹⁷ provided **15**, which in principle can behave as a building block to synthesize higher homologous saccharide. Hydrogenolysis¹⁸ of **15** using 10% $\text{Pd}(\text{OH})_2\text{-C}$ in MeOH gave the required disaccharide **16**. In the ¹H NMR spectrum of **16**, signals due to two anomeric protons were observed at 4.77 and 4.90 ppm as doublet ($J = 1.7$ Hz). The characteristic coupling constants observed in ¹H NMR along with the ¹³C NMR signals for the anomeric carbons, revealed α -configuration at C-1 as well as C-1'.

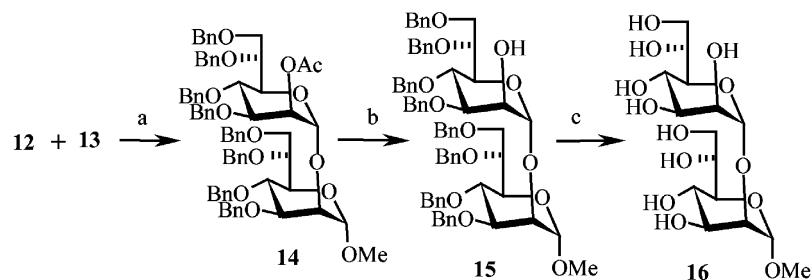
In conclusion, an efficient linear synthesis of terminal



Scheme 1. Reagents and conditions: (a) Imidazole, TBDMS-Cl, DMF, 0 °C to rt, 1 h, 82%; (b) NaH , MPM-Br, THF, 4 h, 73%; (c) $n\text{-Bu}_4\text{NF}$, THF, 1 h, 74%; (d) (i) $(\text{COCl})_2$, DMSO, Et_3N , -78 °C; (ii) $\text{PPh}_3\text{CH}_3\text{I}$, NaNH_2 , Et_2O , -40 °C, 30 min, 32%.



Scheme 2. Reagents and conditions: (a) $(\text{DHQ})_2\text{Pyr}$, $\text{K}_3\text{Fe}(\text{CN})_6$, K_2CO_3 , cat. OsO_4 , *tert*-BuOH–H₂O (1:1 v/v), 0 °C, 6 h; (b) DMP, PPTS, 4 h; (c) PPTS, MeOH, 6 h, 65%; (d) DDQ, CH₂Cl₂–H₂O (9:1), 3 h, 70%; (e) NaH, BnBr, DMF, 30 min, 57%; (f) H₂, Pd/C, MeOH, 30 h (g) AcOH–Ac₂O–H₂SO₄ (5:2:0.3), 60%.



Scheme 3. Reagents and conditions: (a) $\text{BF}_3 \cdot \text{OEt}_2$, 4 Å mol sieves, CH₂Cl₂, 0 °C to rt, 12 h, 26%; (b) MeONa, MeOH, 10 min, 72%; (c) H₂, Pd(OH)₂–C, MeOH, 40 h, 52%.

disaccharide unit of the hepto-glycan of α (1→2) linkage has been accomplished from methyl α -D-mannopyranoside.

3. Experimental

3.1. General

Chemicals used in this study were purchased from Aldrich, Fluka or Lancaster and used as received. Moisture-sensitive reactions were performed in an inert atmosphere of either N₂ or Ar using dry solvents. The elemental analysis was recorded on Elementar-Vario-EL (Heraeus Company Ltd. Germany). IR spectra were obtained on a Perkin–Elmer FT-IR spectrometer. The NMR spectra were obtained on a Bruker 200 Fourier transform spectrometer. Optical rotations were measured with a JASCO DIP 370 digital polarimeter. Reactions were monitored by Thin Layer chromatography (TLC) carried out on 0.25 mm E-Merck silica gel plates (60F-254) with UV, I₂ and anisaldehyde in ethanol as development reagents.

3.1.1. Methyl 3,4-di-*O*-benzyl-6-*O*-(*tert*-butyldimethylsilyl)-D-mannopyranoside (3).

A solution of **2** (15.0 g, 40.1 mmol), imidazole (8.2 g, 120 mmol) and TBS-Cl (6.0 g, 40.0 mmol) in CH₂Cl₂ (120 mL) was stirred for 1 h, concentrated and purified on silica gel using EtOAc–light petroleum (1:9) to afford **3** (16.0 g, 82%) as a colourless syrup; $[\alpha]_{\text{D}}^{20} = +33.9$ (*c* 0.49, CHCl₃); ¹H NMR (200 MHz, CDCl₃) data: δ 0.2 (s, 6H), 0.80 (s, 9H), 2.27 (br s, 1H), 3.33 (s, 3H), 3.71 (m, 6H), 4.66 (m, 5H), 7.29 (m, 10H); ¹³C NMR (50 MHz, CDCl₃): δ –5.5, 17.7, 23.5, 54.3, 62.0, 70.4, 71.3, 72.3, 74.6, 74.9, 99.1, 127.5, 127.6, 128.2, 128.4, 137.9. Anal. calcd for C₂₇H₄₀O₆Si: C, 66.36; H, 8.25. Found: C, 66.69; H, 8.26.

3.1.2. Methyl 3,4-di-*O*-benzyl-6-*O*-(*tert*-butyldimethylsilyl)-2-*O*-(*p*-methoxybenzyl)- α -D-mannopyranoside (4).

A solution of **3** (11.0 g, 22.5 mmol) and NaH (1.8 g, 45.0 mmol, 60% dispersion in oil) in THF (75 mL) was stirred for 30 min and then MPM-Br (5.0 g, 24.9 mmol) was added. After 4 h, the reaction was quenched with ice and concentrated. The residue was partitioned between EtOAc–water, dried (Na₂SO₄), concentrated and purified on silica gel using EtOAc–light petroleum (0.5:9.5) to give **4** (10.0 g, 73%) as a colourless syrup; $[\alpha]_{\text{D}}^{20} = +30.2$ (*c* 0.9, CHCl₃); ¹H NMR (200 MHz, CDCl₃) data: δ 0.2 (s, 6H), 0.82 (s, 9H), 3.20 (s, 3H), 3.41 (m, 1H), 3.96 (s, 3H), 3.74 (m, 5H), 4.51

(m, 6H), 4.82 (d, 1H, $J=10.8$ Hz), 6.76 (d, 2H, $J=8.8$ Hz), 7.21 (m, 12H); ^{13}C NMR (50 MHz, CDCl_3): δ -5.4, 18.1, 25.7, 54.1, 54.6, 62.6, 71.8, 71.9, 72.9, 74.4, 74.7, 76.7, 80.0, 98.6, 113.4, 127.2, 127.3, 127.6, 128.0, 129.0, 130.4, 138.5, 138.7. Anal. calcd for $\text{C}_{35}\text{H}_{48}\text{O}_7\text{Si}$: C, 69.04; H, 7.95. Found: C, 68.91; H, 7.66.

3.1.3. Methyl 3,4-di-*O*-benzyl-2-*O*-(*p*-methoxybenzyl)- α -D-mannopyranoside (5). A solution of **4** (10.0 g, 16.4 mmol) and *n*-Bu₄NF (33.0 mL, 33.0 mmol, 1 M) was stirred for 1 h and concentrated. The residue was partitioned between EtOAc–water, dried (Na_2SO_4), concentrated and purified on silica gel using EtOAc and light petroleum ether (1:4) to give **5** (6.0 g, 74%) as colourless oil; $[\alpha]_{\text{D}}^{25} = +28.6$ (*c* 0.7, CHCl_3); IR (cm^{-1}): 3359, 3032, 2868, 1602, 1211, 1155; ^1H NMR (200 MHz, CDCl_3) data: δ 2.05 (brs, 1H), 3.21 (s, 3H), 3.55 (m, 1H), 3.77 (s, 3H), 3.81 (m, 5H), 4.57 (m, 7H), 6.76 (d, 2H, $J=8.7$ Hz), 7.23 (m, 12H); ^{13}C NMR (50 MHz, CDCl_3): δ 54.7, 55.1, 62.4, 72.2, 72.6, 74.4, 74.9, 75.1, 80.2, 99.5, 113.8, 127.5, 128.0, 128.3, 129.4, 130.3, 138.6. Anal. calcd for $\text{C}_{29}\text{H}_{34}\text{O}_7$: C, 70.43; H, 6.93. Found: C, 70.59; H, 7.11.

3.1.4. Methyl 3,4-di-*O*-benzyl-6-eno-2-*O*-(*p*-methoxybenzyl)- α -D-mannoheptopyranoside (6). A solution of DMSO (2.8 mL, 32.4 mmol) and oxalyl chloride (1.4 mL, 16.2 mmol) in CH_2Cl_2 (50 mL) at -78°C was stirred for 30 min and then **5** (4.0 g, 8.1 mmol) was added. After 45 min, Et_3N (6.8 mL, 48.6 mmol) was added and the reaction slowly brought to RT. The CH_2Cl_2 layer was washed with water, dried (Na_2SO_4) and concentrated to obtain the aldehyde (3.4 g), which was dissolved in dry ether (30 mL), cooled to -40°C and $\text{Ph}_3\text{P}=\text{CH}_2$ {generated from $\text{PPh}_3\text{CH}_3\text{I}$ (11.2 g, 27.6 mmol) and sodamide (1.0 g, 25.6 mmol)} was added. After 30 min, reaction mixture was concentrated and the residue purified on silica gel using EtOAc–light petroleum (0.07:0.93) to give **6** (1.3 g, 32%) as a colourless syrup; $[\alpha]_{\text{D}}^{25} = +24.4$ (*c* 1, CHCl_3); IR (cm^{-1}): 3025, 2890, 1638, 1604, 1205, 1137; ^1H NMR (200 MHz, CDCl_3) data: δ 3.29 (s, 3H), 3.71 (m, 3H), 3.78 (s, 3H), 3.91 (t, 1H, $J=6.9$ Hz), 4.64 (m, 7H), 5.25 (d, 1H, $J=8.8$ Hz), 5.43 (d, 1H, $J=14.4$ Hz), 5.96 (m, 1H), 6.80 (d, 2H, $J=8.4$ Hz), 7.28 (m, 12H); ^{13}C NMR (50 MHz, CDCl_3): δ 54.7, 55.2, 72.5, 72.5, 72.9, 74.7, 75.1, 79.0, 80.1, 99.4, 113.9, 117.7, 127.6, 128.0, 128.3, 128.4, 129.5, 130.6, 135.8. Anal. calcd for $\text{C}_{30}\text{H}_{34}\text{O}_6$: C, 73.45; H, 6.98. Found: C, 73.68; H, 6.92.

3.1.5. Methyl 3,4-di-*O*-benzyl-6,7-*O*-isopropylidene-2-*O*-(*p*-methoxybenzyl)-D-glycero- α -D-mannopyranoside (8a) and methyl 3,4-di-*O*-benzyl-6,7-*O*-isopropylidene-2-*O*-(*p*-methoxybenzyl)-L-glycero- α -D-mannopyranoside (8b). A solution of K_2CO_3 (1.1 g, 8.0 mmol), $\text{K}_3\text{Fe}(\text{CN})_6$ (2.6 g, 8.0 mmol), OsO_4 (27 mg, 0.1 mmol) and (DHQ)₂ PYR (23 mg, 0.026 mmol) in *t*-BuOH– H_2O (16.0 mL, 1:1) was added to **6** (1.3 g, 2.65 mmol). After 6 h at 0°C , the reaction was quenched with solid sodium sulphite and extracted with EtOAc, dried (Na_2SO_4) and concentrated to give **7a/7b** (1.0 g), which was treated with DMP (5 mL) and PPTS (0.53 g) for 4 h. The reaction mixture was neutralized with Et_3N , concentrated and chromatograph on silica gel using EtOAc–light petroleum (1:9) to give **8a** (0.71 g, 47%); $[\alpha]_{\text{D}}^{25} = +30.8$ (*c* 0.8, CHCl_3); ^1H NMR (200 MHz,

CDCl_3) data: δ 1.20 and 1.30 (2s, 6H), 3.18 (s, 3H), 3.56 (m, 5H), 3.65 (s, 3H), 3.85 (t, 1H, $J=7.9$ Hz), 4.18 (m, 1H), 4.47 (m, 6H), 4.83 (d, 1H, $J=11.0$ Hz), 6.67 (d, 2H, $J=8.7$ Hz), 7.17 (m, 12H); ^{13}C NMR (50 MHz, CDCl_3): δ 27.2, 54.9, 55.6, 65.1, 69.5, 72.3, 72.6, 73.0, 74.5, 74.8, 75.2, 80.2, 99.7, 127.6, 127.7, 127.8, 128.0, 128.4, 128.6, 129.8, 138.5. Anal. calcd for $\text{C}_{33}\text{H}_{40}\text{O}_8$: C, 70.19; H, 7.14. Found: C, 69.92; H, 7.18. Further elution gave **8b** (0.078 g, 5.2%) as a colourless oil; $[\alpha]_{\text{D}}^{25} = +19.4$ (*c* 1.05, CHCl_3); ^1H NMR (200 MHz, CDCl_3) data: δ 1.38 and 1.44 (2s, 6H), 3.32 (s, 3H), 3.80 (s, 3H), 3.83 (m, 3H), 4.01 (m, 3H), 4.41 (dd, 1H, $J=2.3, 6.1$ Hz), 4.62 (m, 6H), 4.98 (d, 1H, $J=8.3$ Hz), 6.83 (d, 2H, $J=7.2$ Hz), 7.29 (m, 12H). Anal. Calcd for $\text{C}_{33}\text{H}_{40}\text{O}_8$: C, 70.19; H, 7.14. Found: C, 70.04; H, 7.26.

3.1.6. Methyl 2,3,4,6,7-penta-*O*-benzyl-L-glycero- α -D-mannoheptopyranoside (9). A solution of **8b** (1.0 g, 1.8 mmol) and DDQ (0.47 g, 2.1 mmol) in CH_2Cl_2 : H_2O (9:1, 7 mL) was stirred for 3 h, concentrated and purified on silica gel using EtOAc–light petroleum (1:4). The resulting product (0.5 g) and NaH (0.2 g, 4.9 mmol, 60% dispersion in oil) in dry DMF (5 mL) were stirred for 30 min followed by addition of BnBr (0.45 mL, 3.7 mmol). After 12 h, the reaction was worked up as usual to afford a residue which was purified on silica gel using EtOAc–light petroleum (1:10) to give **9** (0.68 g, 57%) as a colourless syrup; $[\alpha]_{\text{D}}^{25} = +22.4$ (*c* 0.98, CHCl_3); IR (cm^{-1}): 3012, 2866, 1611, 1219, 1131; ^1H NMR (200 MHz, CDCl_3) δ 3.26 (s, 3H), 3.81 (m, 7H), 4.55 (m, 11H), 7.25 (m, 25H); ^{13}C NMR (50 MHz, CDCl_3): δ 54.7, 70.9, 72.1, 72.4, 72.6, 73.2, 74.8, 75.0, 75.2, 78.5, 80.5, 98.8, 127.2, 127.3, 127.5, 127.6, 128.2, 138.5, 138.6. Anal. calcd for $\text{C}_{43}\text{H}_{46}\text{O}_7$: C, 76.53; H, 6.87. Found: C, 76.30; H, 6.78.

3.1.7. Methyl 3,4,6,7-tetra-*O*-benzyl-2-*O*-(*p*-methoxybenzyl)-D-glycero- α -D-mannoheptopyranoside (11). A solution of **8a** (0.68 g, 1.2 mmol) and PPTS (0.33 g, 1.3 mmol) in MeOH (10 mL) was stirred for 6 h, neutralized by Et_3N and concentrated. The resulting compound **7a** (0.5 g, 1.0 mmol) was dissolved in dry THF (7 mL) and NaH (0.15 g, 3.8 mmol, 60% dispersion in oil) was added. After 30 min, BnBr (0.3 mL, 2.4 mmol) was introduced, stirred for another 12 h and worked up as usual to afford a residue which was purified on silica gel using EtOAc–light petroleum (1:10) to give **11** (0.55 g, 65%) as a colourless syrup; $[\alpha]_{\text{D}}^{25} = +29.2$ (*c* 1.07, CHCl_3); IR (cm^{-1}): 3022, 2875, 1612, 1216, 1140; ^1H NMR (200 MHz, CDCl_3): δ 3.31 (s, 3H), 3.70 (m, 5H), 3.77 (m, 3H), 3.96 (s, 2H), 4.65 (m, 11H), 6.76 (d, 2H, $J=7.3$ Hz), 7.26 (m, 22H); ^{13}C NMR (50 MHz, CDCl_3) data: δ 54.6, 55.1, 63.2, 72.0, 72.3, 73.2, 74.7, 74.9, 75.0, 80.5, 99.7, 113.6, 127.4, 127.5, 127.9, 128.3, 129.5, 138.7, 138.9. Anal. calcd for $\text{C}_{44}\text{H}_{48}\text{O}_8$: C, 74.98; H, 6.86. Found: C, 74.69; H, 7.08.

3.1.8. Methyl 3,4,6,7-tetra-*O*-benzyl-D-glycero- α -D-mannoheptopyranoside (12). A solution of **11** (1.3 g, 1.8 mmol) and DDQ (0.46 g, 2.0 mmol) in CH_2Cl_2 – H_2O (9:1) was stirred for 3 h, concentrated and the residue purified on silica gel using EtOAc–light petroleum (1:4) to give **12** (0.76 g, 70%) as a colourless oil; $[\alpha]_{\text{D}}^{25} = +17.3$ (*c* 0.9, CHCl_3); IR (cm^{-1}): 3376, 3035, 2892, 1615, 1210, 1190; ^1H NMR (200 MHz, CDCl_3) data: δ 3.35 (s, 3H), 3.85 (m, 7H), 4.65 (m, 9H), 7.31 (m, 20H); ^{13}C NMR (50 MHz,

CDCl₃): δ 54.8, 68.2, 70.8, 72.0, 72.6, 73.3, 74.4, 78.3, 80.8, 100.2, 127.5, 127.6, 127.7, 127.9, 128.3, 128.5, 138.0, 138.6. Anal. calcd for C₃₆H₄₀O₇: C, 73.95; H, 6.89. Found: C, 73.81; H, 6.93.

3.1.9. 1,2-Di-O-acetyl-3,4,6,7-tetra-O-benzyl-D-glycero- α -D-mannoheptopyranoside (13). A mixture of acetic acid, acetic anhydride and sulfuric acid (3.0 mL; 25:5:1.5) and **12** (0.3 g, 0.5 mmol) was stirred for 1 h at 0 °C. The reaction was neutralized with NaHCO₃ solution, extracted with EtOAc, dried (Na₂SO₄), evaporated and purified on silica gel using EtOAc–light petroleum (1:9) to give **13** (0.2 g, 60%) as a colourless oil; $[\alpha]_D^{25} = +22.5$ (c 0.9, CHCl₃); IR (cm⁻¹): 3015, 2912, 1710, 1611, 1145; ¹H NMR (200 MHz, CDCl₃): δ 2.05, 2.11 (2s, 6H), 3.94 (m, 4H), 4.24 (m, 2H), 4.64 (m, 8H), 5.28 (br.d, 1H, $J = 5.6$ Hz), 6.05 (d, 1H, $J = 2.0$ Hz), 7.32 (m, 20H); ¹³C NMR (50 MHz, CDCl₃): δ 20.4, 64.3, 71.8, 72.1, 72.3, 73.6, 74.4, 74.8, 79.1, 91.5, 127.1, 127.3, 127.5, 127.7, 127.9, 128.1, 128.7, 137.7, 137.8, 138.0, 138.2, 168.2, 169.8. Anal. calcd for C₃₉H₄₂O₉: C, 71.54; H, 6.46. Found: C, 71.41; H, 6.25.

3.1.10. Methyl 2-O-acetyl-3,4,6,7-tetra-O-benzyl-D-glycero- α -D-mannoheptopyranosyl-(1 \rightarrow 2)-3,4,6,7-tetra-O-benzyl-D-glycero- α -D-mannoheptopyranoside (14). To a mixture of **12** (0.14 g, 0.2 mmol), **13** (0.2 g, 0.3 mmol) and activated 4 Å molecular sieves (0.1 g) in dry CH₂Cl₂ (3 mL), BF₃·OEt₂ (0.05 mL) was added. After 12 h, the reaction was neutralized with Et₃N, filtered, concentrated and purified on silica gel using EtOAc–light petroleum (1:10) to give the disaccharide **14** (0.07 g, 26%) as a colourless syrup; $[\alpha]_D^{25} = +28.9$ (c 1, CHCl₃); IR (cm⁻¹): 3041, 2882, 1725, 1600, 1208, 1180; ¹H NMR (200 MHz, CDCl₃) data: δ 2.09 (s, 3H), 3.29 (s, 3H); 3.76 (m, 13H), 4.59 (m, 18H), 5.22 (brd, 1H, $J = 5.4$ Hz), 7.21 (m, 40H); ¹³C NMR (50 MHz, CDCl₃): δ 21.0, 54.7, 68.8, 72.0, 72.3, 72.4, 75.2, 75.3, 78.5, 78.6, 79.5, 99.5, 99.8, 127.5, 127.7, 128.0, 128.4, 135.1, 135.6, 138.5, 169.8. Anal. calcd for C₇₃H₇₈O₁₄: C, 74.34; H, 6.66. Found: C, 74.51; H, 6.92.

3.1.11. Methyl 3,4,6,7-tetra-O-benzyl-D-glycero- α -D-mannoheptopyranosyl-(1 \rightarrow 2)-3,4,6,7-tetra-O-benzyl-D-glycero- α -D-mannoheptopyranoside (15). A solution of **14** (0.06 g, 0.05 mmol) and MeONa (3 mg) in MeOH (2 mL) was stirred for 10 min, quenched by adding solid CO₂ and concentrated. The residue purified on silica gel using EtOAc–light petroleum (1:9) to give **15** (0.042 g, 72%) as a colourless syrup; $[\alpha]_D^{25} = +32.7$ (c 1.12, CHCl₃); IR (cm⁻¹): 3390, 3027, 2870, 1613, 1217, 1163; ¹H NMR (200 MHz, CDCl₃) data: δ 3.41 (s, 3H), 3.86 (m, 14H), 4.72 (m, 18H), 7.26 (m, 40H); ¹³C NMR (50 MHz, CDCl₃): δ 54.6, 65.5, 68.8, 72.6, 73.0, 73.5, 75.4, 78.1, 78.4, 79.8, 98.7, 98.9, 127.4, 127.7, 127.8, 128.0, 128.2, 128.4, 135.2, 135.8, 138.0. Anal. calcd for C₇₁H₇₆O₁₃: C, 74.98; H, 6.73. Found: C, 75.18; H, 6.99.

3.1.12. Methyl D-glycero- α -D-mannoheptopyranosyl-

(1 \rightarrow 2)-D-glycero- α -D-mannoheptopyranoside (16). A suspension of 10% Pd(OH)₂-C (10 mg) and **15** (0.035 g, 0.03 mmol) in MeOH (5 mL) was hydrogenolyzed at rt for 40 h. Filtration of the catalyst followed by concentration gave **16** (0.007 g, 52%) as a colourless oil; $[\alpha]_D^{25} = +65$ (c 0.8, H₂O); IR (cm⁻¹): 3390, 2871, 1209, 1161; ¹H NMR (200 MHz, D₂O) data: δ 3.41 (s, 3H), 3.79 (m, 14H), 4.77 (d, 1H, $J = 1.7$ Hz), 4.90 (d, 1H, $J = 1.7$ Hz); ¹³C NMR (50 MHz, D₂O): δ 54.3, 62.1, 62.2, 67.6, 67.8, 69.9, 70.1, 71.0, 72.2, 72.4, 74.2, 74.2, 101.9, 102.4. Anal. Calcd for C₁₅H₂₈O₁₃: C, 43.27; H, 6.78. Found: C, 43.41; H, 6.93.

References and notes

1. Cryz, Jr. S. J. *Vaccine* **1987**, *5*, 261–265.
2. Kim, B. N.; Woo, J. H.; Kim, M. N.; Ryu, J.; Kim, Y. S. *J. Hosp. Infect.* **2002**, *52*, 99–106.
3. Rietschel, E. T.; Brade, L.; Lindner, B.; Zahringer, U. *Bacterial endotoxic lipopolysaccharides*; Morrison, D. C., Ryan, J. L., Eds.; CRC: Boca Raton, 1992; Vol. I, p 3.
4. Libon, C.; Haeuw, J. F.; Crouzet, F.; Mugnier, C.; Bonnefoy, J. Y.; Beck, A.; Corvaia, N. *Vaccine* **2002**, *20*, 2174–2180.
5. Susskind, M.; Muller-Loennies, S.; Nimmich, W.; Brade, H.; Holst, O. *Carbohydr. Res.* **1995**, *269*, C1–C7.
6. Susskind, M.; Brade, L.; Brade, H.; Holst, O. *J. Biol. Chem.* **1998**, *273*, 7006–7017.
7. (a) Bernlind, C.; Bennett, S.; Oscarson, S. *Tetrahedron: Asymmetry* **2000**, *11*, 481–492. (b) Bernlind, C.; Oscarson, S. *J. Org. Chem.* **1998**, *63*, 7780–7788.
8. Boons, G. J. P. H.; Van der Marcel, G. A.; Van Boom, J. H. *Tetrahedron Lett.* **1989**, *30*, 229–232.
9. Hartmuth, C. K.; Van Nieuwenhze, M. S.; Sharpless, B. K. *Chem. Rev.* **1994**, *94*, 2483–2547.
10. (a) Bhattacharjee, S. S.; Gorin, P. A. J. *Can. J. Chem.* **1969**, *47*, 1195–1206. (b) Bhattacharjee, S. S.; Gorin, P. A. J. *Can. J. Chem.* **1969**, *47*, 1207–1215.
11. (a) Swern, D. *Synthesis* **1981**, 165–185. (b) Tidwell, T. T. *Org. React.* **1990**, *39*, 297.
12. Sudha, A. V. R. L.; Nagarajan, M. *Chem. Commun.* **1998**, 925–926.
13. Garegg, P. J.; Oscarson, S.; Szonyi, M. *Carbohydr. Res.* **1990**, *205*, 125–132, and references cited therein.
14. Oikawa, Y.; Yoshioka, T.; Yonemitsu, O. *Tetrahedron Lett.* **1982**, *23*, 885–888.
15. (a) Kaczmarek, J.; Kaczynski, Z.; Trumpakaj, Z.; Szafranek, J.; Bogalecka, M.; Lonnberg, H. *Carbohydr. Res.* **2000**, *325*, 16–29. (b) Katano, K.; Millar, A.; Pozsgay, V.; Primeau, J. L.; Hecht, S. M. *J. Org. Chem.* **1986**, *51*, 2927–2932.
16. Toshima, K.; Kuniaki Tatsuta, K. *Chem. Rev.* **1993**, *93*, 1503–1531.
17. McAuliffe, J. C.; Hindsgaul, O. *J. Org. Chem.* **1997**, *62*, 1234–1239.
18. Heathcock, C. H.; Ratcliffe, R. *J. Am. Chem. Soc.* **1971**, *93*, 1746–1756.

Total syntheses of (–)-vallesamidine and related *Aspidosperma* and *Hunteria* type indole alkaloids from the common intermediate

Hideo Tanino, Kazuhisa Fukuishi, Mina Ushiyama and Kunisuke Okada*

Faculty of Pharmacy, Meijo University, Tenpaku, Nagoya 468-8503, Japan

Received 22 December 2003; accepted 2 February 2004

Dedicated to Professor A. Ian Scott on the occasion of his 75th birthday

Abstract—A new synthetic method of (–)-vallesamidine, including a unique 2,2,3-trialkylindoline skeleton, was developed by reductive radical cyclization reaction from the 2,3-dialkylindole derivative, which has been known to be an intermediate for the synthesis of aspidospermidine.

© 2004 Elsevier Ltd. All rights reserved.

1. Introduction

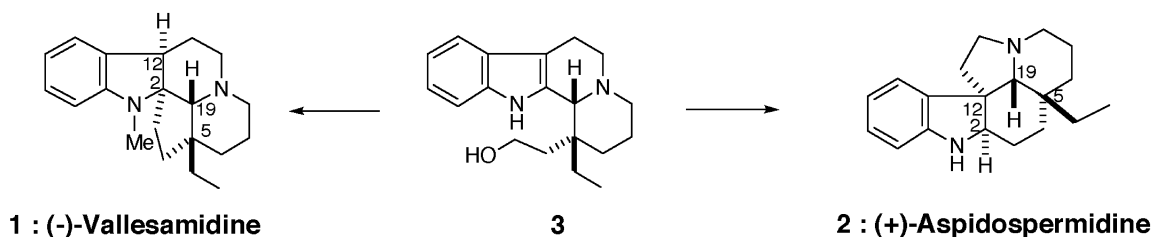
Vallesamidine **1** is one of 28 alkaloids isolated from *Vallesia dichotoma* Ruiz and Pav in 1965 and its structure and absolute configuration were determined by Djerassi in 1968.¹ The defined structure shows a unique and abnormal indole alkaloid including a 2,2,3-trialkylindoline skeleton, which differs from (+)-aspidospermidine **2**, a typical indole alkaloid, having 2,3,3-trialkylindoline chromophore (Scheme 1). The stereochemistry of vallesamidine at C-5 and C-19 is identical to that of aspidospermidine, suggesting that these two alkaloids are possibly biosynthesized from the same intermediate. A great amount of research has been reported on the synthesis of 2,3,3-trialkylated indoline alkaloids such as *Aspidosperma* and *Strychnos* families,² but little research has been carried out on 2,2,3-trialkylated indoline alkaloids such as vallesamidine.³

In 1990, Heathcock reported the first total synthesis of (±)-vallesamidine via newly developed methodology, wherein the indolenine skeleton is formed in the late stage of its synthesis.⁴ In his paper, it is noted that alkylation at C-2 of a

2,3-disubstituted indole **3** is not generally useful, because of the propensity of the resulting cation to rearrange to the more stable 2,3,3-trialkylindolenium ion. In fact, Harley-Mason,⁵ Fuji⁶ and Schultz⁷ have succeeded in the synthesis of the aspidosperidine skeleton from **3**, being used as a key intermediate, in the cyclization which includes the interesting rearrangement as shown in Scheme 2.

On the other hand, Levy's elegant transformation of the pentacyclic vallesamidine skeleton from tabersonine was achieved by treatment with Zn powder in acetic acid.⁸ It has been proposed that 2,2,3-trialkylindoline intermediate **6** is included in the equilibrium reaction mixture, in addition to 2,3,3-trialkylindoline **4** and quebrachamine chromophore **5** (Scheme 3). In this way, enantiomeric (+)-vallesamidine was obtained in 24% yield.

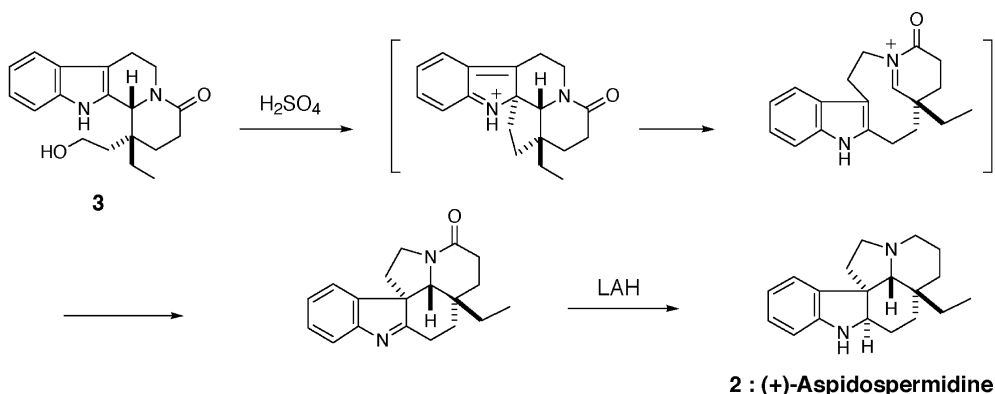
Because of the above discussion, we have been interested in investigating a new synthetic approach to vallesamidine wherein the reductive radical cyclization of the known 2,3-dialkylindole derivative **3a** provides the 2,2,3-trialkylindoline skeleton. Although many novel ring systems and



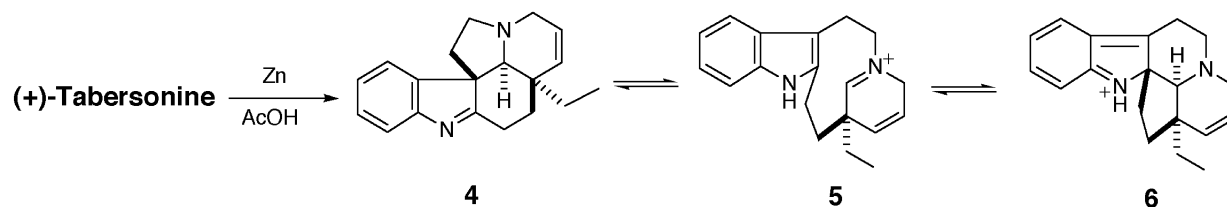
Scheme 1.

Keywords: Radical reaction; Cyclization; Indole; Asymmetric synthesis.

* Corresponding author. Tel.: +81-52-832-1781x250; fax: +81-52-834-8780; e-mail address: kokada@ccmfs.meijo-u.ac.jp



Scheme 2.



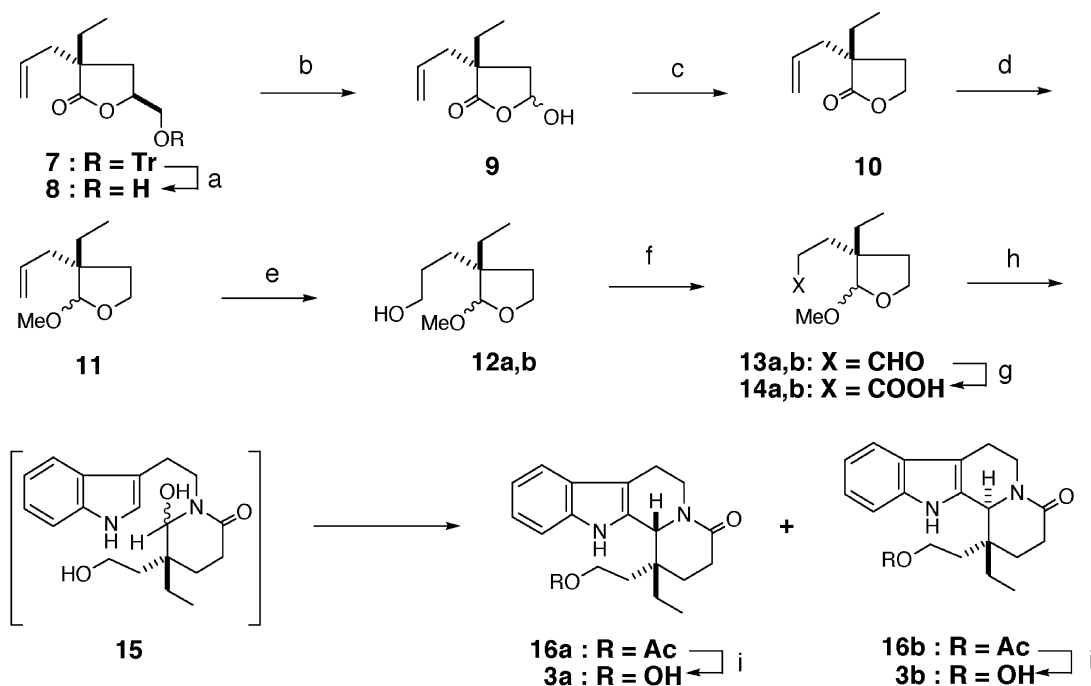
Scheme 3.

natural products have been synthesized by radical reactions, a small amount of research has been devoted to the synthesis of indoline alkaloids.⁹ In this article, we first describe a successful total synthesis of (–)-vallesamidine **1** from **3a**, prepared by the following line (Scheme 4),¹⁰ and second the additional transformation of **3a** into (+)-aspidospermidine **2** and (+)-dihydroeburnamenine **24a** from the common intermediate **3a**.

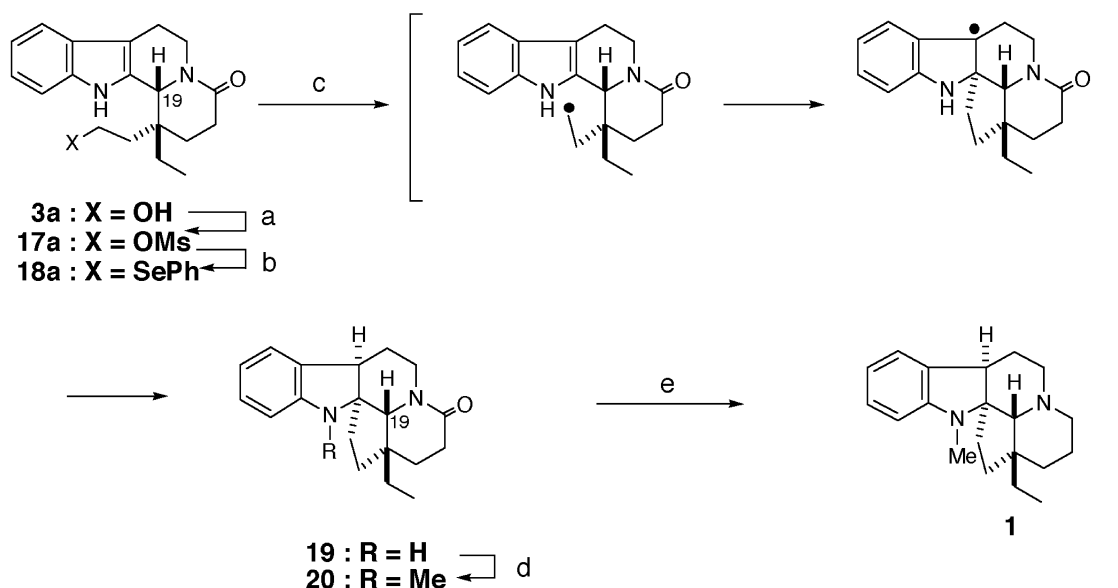
2. Results and discussion

2.1. Synthesis of (–)-vallesamidine

The synthesis of the chiral key intermediate **3a** was started from **7**, which was obtained from the double alkylation of (*S*)- γ -trityloxymethyl- γ -butyrolactone by using the method reported by Koga.¹¹ Detritylation of **7** afforded an alcohol **8**



Scheme 4. Reagents and conditions: (a) 80% AcOH, 80 °C, 1 h; (i) 4 M aq. NaOH, dioxane, 100 °C, 1 h; (ii) CO₂; (iii) aq. NaIO₄, rt, 3 h; (iv) 1 M HCl; (c) (i) NaBH₄, MeOH, rt, 1 h; (ii) 4 M HCl–MeOH, 70 °C, 1 h; (d) (i) DiBAL–H, Et₂O, –78 °C, 1 h; (ii) CH(OMe)₃, *p*-TsOH, MeOH, 80 °C, 40 min; (e) (i) 9-BBN, THF, rt, overnight; (ii) 30% H₂O₂, 3 M aq. NaOH, THF, rt, 1 h; (f) SO₃-Py, DMSO, TEA, CH₂Cl₂, rt, 0.5 h; (g) NaClO₂, *t*-BuOH, aq. NaH₂PO₄, Me₂C=CHMe, rt, 1 h; (h) tryptamine, AcOH, 125 °C, 6 days; (i) 20% aq. NaOH, MeOH, rt, 1 h.



Scheme 5. Reagents and conditions: (a) MsCl, pyridine, 0 °C, 2 h; (b) (PhSe)₂, NaBH₄, EtOH, 0 °C→rt, 3 h; (c) *n*-Bu₃SnH, AIBN, toluene, 100 °C, 0.5 h; (d) 35% HCHO, NaBH₃CN, CH₃CN, then AcOH, rt, 1 h; (e) LAH, THF, 70 °C, 0.5 h.

in 98% yield, which was hydrolyzed with 4 M aqueous NaOH in dioxane followed by neutralization with CO₂. The resulting mixture was oxidized with sodium periodate to give hemiacetal **9** in 95% yield. Reduction of **9** with sodium borohydride in methanol gave γ -lactones **10** (92%). The lactone was then converted to methylacetal **11** by reduction with diisobutylaluminum hydride at -78 °C, followed by treatment with trimethyl orthoformate and *p*-toluenesulfonic acid in methanol, in 84% yield in two steps. Transformation of the double bond in **11** into primary alcohols **12a,b** was performed by following successive reactions of hydroboration with 9-BBN in THF and oxidation with hydrogenperoxide in alkali in 87% yield. The alcohols **12a,b** were further oxidized to carboxylic acids **14a,b** (95% yield)¹² via **13a,b** in the usual way.

The next condensation reaction was performed by heating the mixture of carboxylic acids **14a,b** with tryptamine in AcOH at refluxing temperature. In this reaction mixture, the intermediate **15** was always detected on a silica gel TLC. The structure of **15** was proposed by spectral data and further confirmed by its chemical transformation into the same products **16a,b**. After 6 days, the intermediate **15** completely disappeared and then, the reaction mixture was separated by using a silica gel column chromatography to give a tetracyclic indole lactam derivatives **16a** (43%) and **16b** (44%)⁶ as acetates. Exposure of **16a** to 20% aqueous NaOH in MeOH solution afforded the desired alcohol **3a**, corresponding to the natural form, and **16b** gave another stereoisomer **3b** under the same conditions. The stereochemistry of each product was characterized by comparison with ¹H NMR spectra of the authentic samples.⁶ The structure of **3a** was further confirmed by the conversion into the known compound (+)-aspidospermidine **2** under the usual acidic conditions followed by LAH reduction.⁶ The next approach from **3a** to **1** is outlined in Scheme 5.

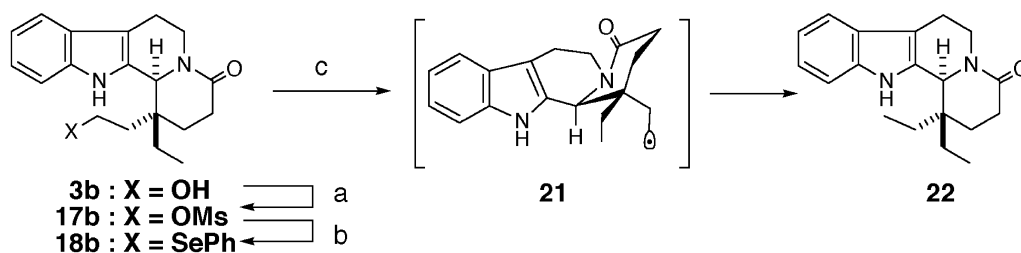
The primary hydroxy group in the side chain of **3a** was

converted into mesylate by using MsCl–DMAP in pyridine at 0 °C in 92% yield. The resulting mesylate **17a** was treated with diphenydiselenide and NaBH₄ in EtOH at room temperature, giving the desired selenide **18a** in 68% yield together with N-alkylated product (4% yield, *Hunteria* type chromophore). Treatment of the selenide **18a** with a mixture of tributyltin hydride (*n*-Bu₃SnH) and 2,2'-azobisisobutyronitrile (AIBN) in toluene at 100 °C under argon for 30 min gave a single product in 91% yield, the structure of which was assumed to be pentacyclic compound **19** based on the following physical data; in ¹H NMR (δ): the signal at 4.77 ppm (1H, s; C19-proton) of **18a** moved to 3.28 ppm (1H, s); in ¹³C NMR (δ): two sp² carbon signals at 126–136 ppm, corresponding to α and β -carbon in the indole ring of **18a**, disappeared and in place of these signals, two new signals were observed at 44.6 ppm (-CH-) and 76.3 ppm (quaternary carbon). N-Methylation of **19** with the mixture of HCHO–NaBH₃CN–AcOH in acetonitrile gave **20** in 87% yield.

Finally, reduction of the lactam **20** by using LAH in THF under refluxing temperature for 30 min was achieved to provide (-)-vallesamidine **1** in 82% yield. The structure of the synthetic material was confirmed by comparison with the physical data reported by Heathcock.^{4b}

2.2. Radical reduction of the epimer **18b**

Another stereoisomer **3b** was also converted into phenylselenide **18b** through mesylate **17b** as shown in Scheme 6. Exposure of the isomer **18b** with *n*-Bu₃SnH and AIBN in toluene at 100 °C for 1 h under an argon atmosphere gave a single product **22** in 70% yield. None of the cyclized product was detected on silica gel TLC. The ¹H NMR spectrum of **22** indicated the presence of two methyl groups. This observation may reflect a reduction of the radical intermediate generated from the 2'-phenylselenylethyl side chain in **18b**, because the location of the radical is separated from indole ring as depicted in **21**.



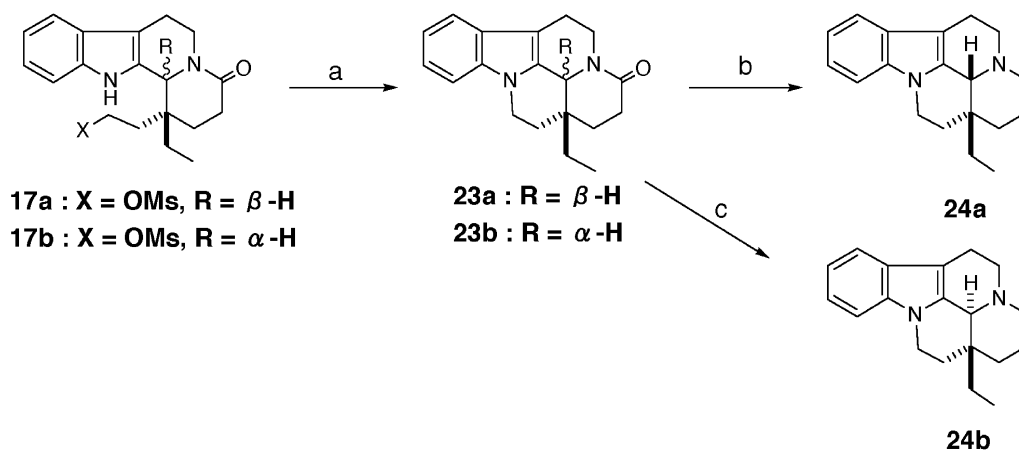
Scheme 6. Reagents and conditions: (a) MsCl, DMAP, pyridine, 0 °C, 2 h; (b) (PhSe)₂, NaBH₄, EtOH, 0 °C, 0.5 h→rt, 3 h; (c) *n*-Bu₃SnH, AIBN, toluene, 100 °C, 1 h.

2.3. Syntheses of (+)-dihydroburnamenine **24a** and (–)-epidihydroburnamenine **24b**

It is interesting to note that the mesylate **17b** was readily converted into N-alkylated pentacyclic product **23b** by treatment with NaOH in THF at room temperature in 88% yield, although ring closure of **18b** was not observed under radical reaction conditions as described above. The other stereoisomer of the mesylate **17a** was also converted into a cyclization product **23a** in 94% yield with alkali. (+)-Dihydroburnamenine **24a** was obtained from **23a** on reduction with LiAlH₄ in THF under refluxing temperature in 91% yield. Reduction of another isomer **23b** was not succeeded under the same conditions because of decomposition. However, when **23b** was treated with an excess amount of NaBH₄–TFA in dioxane, the desired (–)-epidihydroburnamenine **24b** was obtained in 87% yield (Scheme 7). The structures of **24a**⁶ and **24b**^{3,6,13} were characterized by comparison with the physical data reported in the literature, respectively.

3. Conclusions

We have developed a new strategy for preparation of the 2,2,3-trialkylindoline skeletons via reductive radical cyclization reaction, and demonstrated five steps for the synthesis of vallesamidine **1** from the intermediate **3a**, which has been known to be a common substrate for the synthesis of *Aspidosperma* and *Hunteria* type indole alkaloids. It is noteworthy that vallesamidine **1** and the co-occurring aspidosperma-type indole alkaloids have been shown to have the same absolute configuration at carbon 2,



Scheme 7. Reagents and conditions: (a) NaOH, THF, rt, 20 min; (b) LAH, TAF, 70 °C, 0.5 h; (c) NaBH₄, TFA, dioxane, 100 °C, 45 min.

5, 12, 19, which may suggest one route for biosynthesis of these alkaloids is carried out from the common intermediate **3a**.

4. Experimental

4.1. General information

All melting points were uncorrected. ¹H NMR spectra (600 MHz) and ¹³C NMR spectra (150 MHz) were recorded on a JEOL JNM-A 600 spectrometer. ¹³C NMR assignments were carried out using DEPT experiments. IR spectra were recorded on a JASCO IR-810 spectrometer. UV spectrum was recorded on a JASCO UVIDEK-6100 spectrometer. MS spectra were recorded on a JEOL-MS700. Optical rotations were measured on a JASCO DIP-370 polarimeter. Separation of the products by flash column chromatography was carried out on silica gel (Fuji Silysia Chem. Co., BW-300). Separation of the products by TLC was carried out on silica gel (MERCK 1.05744).

4.1.1. (2R)-2,3-Dideoxy-2-ethyl-2-(2-propenyl)-D-glyceropentanoic acid γ-lactone (8). A solution of **7** (1.96 g, 4.60 mmol) in 80% AcOH (15.5 mL) was stirred at 80 °C for 1 h. After the mixture was concentrated under reduced pressure, the residue was diluted with AcOEt. The organic phase was washed with saturated aqueous NaHCO₃ and brine, dried over anhydrous Na₂SO₄ and concentrated. The residual oil was purified by flash column chromatography on silica gel with hexane–AcOEt (1:1) as eluant to give **8** (827 mg, 98%) as a colorless oil; [α]_D²⁰ +22.3° (c 1.7, CHCl₃); IR (neat) 3450, 1760, 1645, 1195, 930 cm⁻¹; ¹H

NMR (CDCl₃): δ 0.93 (3H, t, $J=7.3$ Hz), 1.58–1.73 (2H, m), 2.03 (1H, dd, $J=13.2, 7.8$ Hz), 2.09 (1H, dd, $J=13.2, 9.3$ Hz), 2.30 (1H, dd, $J=13.7, 7.8$ Hz), 2.37 (1H, dd, $J=13.7, 7.3$ Hz), 3.59 (1H, dd, $J=12.7, 4.9$ Hz), 3.88 (1H, dd, $J=12.7, 2.9$ Hz), 4.44–4.54 (1H, m), 5.13–5.22 (2H, m), 5.71–5.86 (1H, m); ¹³C NMR (CDCl₃; DEPT) δ 8.6 (CH₃), 29.2 (CH₂), 31.6 (CH₂), 41.5 (CH₂), 48.6 (C), 63.9 (CH₂), 77.7 (CH), 119.5 (CH₂), 132.6 (CH), 180.8 (C); MS (EI): 184 (M⁺); HRMS (EI), calcd for C₁₀H₁₆O₃: 184.1099; found: 184.1122.

4.1.2. (3R)-3-Ethyldihydro-5-hydroxy-3-(2-propenyl)-2(3H)-furanone (9). To a solution of **8** (827 mg, 4.49 mmol) in dioxane (113 mL) was added 4 M aqueous NaOH (45 mL) and the mixture was heated at 100 °C for 1 h. After cooling, the reaction mixture was neutralized with dry ice. To the milky suspension was added a solution of NaIO₄ (2.42 g, 11.3 mmol) in H₂O (20 mL) and the suspension was stirred at room temperature for 3 h. After quenched with 1 M HCl–H₂O (180 mL), the reaction mixture was extracted with CH₂Cl₂ (3×100 mL). The combined extracts were washed with saturated aqueous NaHCO₃, brine, and dried over anhydrous Na₂SO₄ and concentrated. The residual oil was purified by flash column chromatography on silica gel with hexane–AcOEt (2:1) as eluant to afford diastereoisomers **9** (727 mg, 95%) as colorless oil. The ratio of the diastereoisomeric mixture could not be determined because of broad signals observed in the ¹H NMR spectrum; IR (neat) 3400, 1750, 1645, 1195, 930 cm⁻¹; ¹H NMR (CDCl₃): δ 0.94 (3H, br s), 68 (2H, br s), 2.07 (1H, br s), 2.35 (2H, br s), 4.98 (1H, br s), 5.10–5.20 (2H, br m), 5.73 (1H, br s), 5.83 (1H, br s); ¹³C NMR (CDCl₃; DEPT) δ 8.7 (CH₃), 29.8 (CH₂), 38.4 (CH₂), 41.0 (CH₂), 48.4 (C), 96.9 (CH), 119.7 (CH₂), 132.8 (CH), 180.6 (C); MS (EI): 170 (M⁺); HRMS (EI), calcd for C₉H₁₄O₃: 170.0943; found: 170.0932.

4.1.3. (3R)-3-Ethyldihydro-3-(2-propenyl)-2(3H)-furanone (10). Sodium borohydride (156 mg, 4.12 mmol) was added to a solution of **9** (350 mg, 2.06 mmol) in MeOH (7.7 mL). After stirring at room temperature for 1 h, the reaction mixture was acidified with 4 M HCl–MeOH (0.94 mL) and heated at 70 °C for 1 h. After the reaction mixture was allowed to cool to room temperature, the resulting mixture was diluted with CH₂Cl₂ and the solution was washed with saturated aqueous NaHCO₃, brine, and dried over anhydrous Na₂SO₄ and concentrated. The residual oil was purified by flash column chromatography on silica gel with hexane–AcOEt (4:1) as eluant to afford **10** (293 mg, 92%) as a colorless oil; $[\alpha]_D^{20} -23.3^\circ$ (*c* 1.6, CHCl₃); IR (neat) 2980, 1770, 1375, 1190, 1030 cm⁻¹; ¹H NMR (CDCl₃): δ 0.96 (3H, t, $J=7.3$ Hz), 1.65 (2H, qd, $J=7.3, 1.5$ Hz), 2.10 (1H, dq, $J=14.6, 7.3$ Hz), 2.19 (1H, dq, $J=14.6, 7.3$ Hz), 2.30 (1H, ddt, $J=13.7, 8.3, 1.0$ Hz), 2.17 (1H, ddt, $J=13.7, 6.8, 1.5$ Hz), 4.22 (2H, t, $J=7.3$ Hz), 5.12–5.19 (2H, m), 5.68–5.82 (1H, m); ¹³C NMR (CDCl₃; DEPT) δ 8.7 (CH₃), 29.2 (CH₂), 30.8 (CH₂), 40.4 (CH₂), 46.5 (C), 65.3 (CH₂), 119.3 (CH₂), 132.9 (CH), 180.8 (C); MS (EI): 154 (M⁺); HRMS (EI), calcd for C₉H₁₄O₂: 154.0994; found: 154.0985.

4.1.4. (3R)-3-Ethyltetrahydro-2-methoxy-3-(2-propenyl)furan (11). A solution of 0.95 M diisobutylaluminum

hydride in hexane (0.95 mol/L, 6.0 mL, 5.70 mmol) was added dropwise to a stirred solution of **10** (385 mg, 2.50 mmol) in anhydrous ether (19.0 mL) at –78 °C under nitrogen. The mixture was stirred at the same temperature for 1 h. After the reaction mixture was allowed to warm to room temperature, MeOH (12 mL), methyl orthoformate (1.0 mL, 9.14 mmol) and *p*-toluenesulfonic acid (1.59 g, 8.36 mmol) were added to the mixture, and the resulting solution was heated at refluxing temperature for 40 min. After cooling, the mixture was diluted with AcOEt and the organic solution was washed with saturated aqueous NaHCO₃, brine, and dried over anhydrous Na₂SO₄ and then concentrated. The residual oil was purified by flash column chromatography on silica gel with hexane–AcOEt (10:1) as eluant to afford **11** (355 mg, 84%) as an inseparable mixture of diastereoisomers (17:14). IR (neat) 1645, 1455, 1105, 1030, 915 cm⁻¹; ¹H NMR (CDCl₃): δ 0.87 and 0.88 (3H, t, $J=7.3$ Hz), 1.25–1.59 (2H, m), 1.66–1.81 (2H, m), 2.03–2.34 (2H, m), 3.33 and 3.34 (3H, s), 3.84–3.92 (1H, m), 3.93–3.98 (1H, m), 4.47 and 4.48 (1H, s), 5.00–5.10 (2H, m), 5.72–5.83 (1H, m); ¹³C NMR (CDCl₃; DEPT) δ 8.2 and 9.2 (CH₃), 24.5 and 26.8 (CH₂), 33.7 and 33.8 (CH₂), 36.0 and 37.9 (CH₂), 49.5 and 50.0 (C), 54.6 and 54.7 (CH₃), 65.9 and 65.9 (CH₂), 108.6 and 108.8 (CH), 116.7 and 117.7 (CH₂), 134.4 and 135.8 (CH); MS (EI): 170 (M⁺); HRMS (EI), calcd for C₁₀H₁₈O₂: 170.1307; found: 170.1332.

4.1.5. (3R)-3-Ethyltetrahydro-2-methoxy-3-furanpropanol (12a,b). To a solution of **11** (976 mg, 5.73 mmol) in absolute THF (23 mL) was added a solution of 0.5 M 9-borabicyclo[3,3,1]nonane (9-BBN; 36.7 mL, 18.4 mmol) in hexane dropwise for a period of 15 min under nitrogen atmosphere and the mixture was stirred at room temperature overnight. The mixture was allowed to cool to 0 °C. To the cold solution was added H₂O (20 mL), 3 M aqueous NaOH (31.2 mL, 93.6 mmol), and 30% H₂O₂ (8.33 mL, 81.5 mmol) and the mixture was warmed again to room temperature. After stirring for 1 h, the mixture was extracted with ether (twice). The combined organic extracts were washed with H₂O and brine, and dried over anhydrous Na₂SO₄ and concentrated to give an oil that was purified by flash column chromatography on silica gel with hexane–AcOEt (1:1) as eluant to afford **12a,b** (567 mg, 87% as collected yield) as a mixture of diastereoisomers (17:14) and recovered **11** (377 mg, 39%). The sample for physical analysis was separated by repeated TLC on silica gel with hexane–AcOEt (2:3). **12a**: $[\alpha]_D^{20} +79.9^\circ$ (*c* 1.6, CHCl₃); IR (neat) 3400, 1460, 1100, 1055, 920 cm⁻¹; ¹H NMR (CDCl₃): δ 0.86 (3H, t, $J=7.3$ Hz), 1.34 (1H, dq, $J=14.7, 7.3$ Hz), 1.43 (1H, dq, $J=14.7, 7.3$ Hz), 1.48–1.53 (4H, m), 1.67–1.77 (2H, m), 3.33 (3H, s), 3.58–3.70 (2H, m), 3.87 (1H, q, $J=8.4$ Hz), 3.93 (1H, td, $J=8.4, 4.3$ Hz), 4.47 (1H, s); ¹³C NMR (CDCl₃; DEPT) δ 8.2 (CH₃), 26.2 (CH₂), 26.9 (CH₂), 28.1 (CH₂), 34.1 (CH₂), 49.4 (C), 54.5 (CH₃), 63.4 (CH₂), 65.8 (CH₂), 108.9 (CH); MS (EI): 187 (M⁺–1); HRMS (EI), calcd for C₁₀H₁₉O₃ (M⁺–1): 187.1334; found: 187.1342. **12b**: $[\alpha]_D^{20} -83.7^\circ$ (*c* 0.99, CHCl₃); IR (neat) 3400, 1460, 1100, 1055, 920 cm⁻¹; ¹H NMR (CDCl₃) δ 0.85 (3H, t, $J=7.3$ Hz), 1.31–1.39 (1H, m), 1.40–1.46 (1H, m), 1.46–1.60 (4H, m), 1.67–1.78 (2H, m), 3.33 (3H, s), 3.64 (2H, t, $J=6.6$ Hz), 3.88 (1H, q, $J=8.4$ Hz), 3.94 (1H, td, $J=8.4, 4.0$ Hz), 4.47 (1H, s); ¹³C NMR (CDCl₃; DEPT): δ

9.2 (CH₃), 24.2 (CH₂), 27.3 (CH₂), 29.6 (CH₂), 34.4 (CH₂), 49.5 (C), 54.7 (CH₃), 63.5 (CH₂), 65.8 (CH₂), 109.0 (CH); MS (EI): 187 (M⁺–1); HRMS (EI), calcd for C₁₀H₁₉O₃ (M⁺–1): 187.1334; found: 187.1353.

4.1.6. (3R)-3-Ethyltetrahydro-2-methoxy-3-furanpropanal (13a,b). Sulfur trioxide pyridine complex (1.90 g, 11.9 mmol) was added to a solution of **12a,b** (274 mg, 1.46 mmol), methyl sulfoxide (14.0 mL, 197 mmol) and triethylamine (5.5 mL, 39.5 mmol) in CH₂Cl₂ (5.5 mL) and the mixture was stirred at room temperature for 0.5 h under nitrogen atmosphere. The resulting mixture was diluted with AcOEt and washed with H₂O, saturated aqueous NH₄Cl, saturated aqueous NaHCO₃, and brine and dried over anhydrous Na₂SO₄. Concentration of the solvent under reduced pressure provided crude aldehyde **13a,b** which was used for next reaction without any purification; **13a** (prepared from **12a**): [α]_D²⁰ +89.6° (c 1.4, CHCl₃); IR (neat) 1730, 1460, 1100, 1055, 920 cm⁻¹; ¹H NMR (CDCl₃): δ 0.86 (3H, t, J=7.3 Hz), 1.34 (1H, dq, J=14.7, 7.3 Hz), 1.42 (1H, dq, J=14.7, 7.3 Hz), 1.68–1.78 (2H, m), 1.79–1.89 (2H, m), 2.30–2.44 (2H, m), 3.30 (3H, s), 3.88 (1H, q, J=8.1 Hz), 3.94 (1H, td, J=8.1, 5.1 Hz), 9.74 (1H, t, J=2.2 Hz); ¹³C NMR (CDCl₃; DEPT) δ 8.2 (CH₃), 23.7 (CH₂), 26.4 (CH₂), 33.8 (CH₂), 39.8 (CH₂), 49.1 (C), 54.5 (CH₃), 65.8 (CH₂), 108.7 (CH), 202.7 (CH); MS (EI): 186 (M⁺); HRMS (EI), calcd for C₁₀H₁₈O₃: 186.1256; found: 186.1237. **13b** (prepared from **12b**): [α]_D²⁰ –91.4° (c 1.5, CHCl₃); IR (neat) 1730, 1460, 1380, 1100, 1060, 1030 cm⁻¹; ¹H NMR (CDCl₃): δ 0.85 (3H, t, J=7.3 Hz), 1.48 (1H, dq, J=14.7, 7.3 Hz), 1.56 (1H, dq, J=14.7, 7.3 Hz), 1.62–1.72 (3H, m), 1.73–1.82 (1H, m), 2.35–2.45 (2H, m), 3.31 (3H, s), 3.89 (1H, q, J=8.1 Hz), 3.95 (1H, td, J=8.1, 4.0 Hz), 9.80 (1H, t, J=1.5 Hz); ¹³C NMR (CDCl₃; DEPT) δ 9.1 (CH₃), 24.3 (CH₂), 25.5 (CH₂), 34.2 (CH₂), 39.1 (CH₂), 49.2 (C), 54.7 (CH₃), 65.7 (CH₂), 108.6 (CH), 202.0 (CH); MS (EI): 186 (M⁺); HRMS (EI), calcd for C₁₀H₁₈O₃: 186.1256; found: 186.1243.

4.1.7. (3R)-3-Ethyltetrahydro-2-methoxy-3-furanpropanoic acid (14a,b). To a solution of aldehydes **13a,b** in *tert*-butylalcohol (11.8 mL) was added 2-methyl-2-butene (0.68 mL, 6.42 mmol), sodium dihydrogenphosphate dihydrate (228 mg, 1.46 mmol) and H₂O (3.0 mL) and sodium chlorite (544 mg, 6.02 mmol) portionwise over 1 h under vigorous stirring. After cooling to 0 °C, the mixture was acidified with 1 M HCl, and then extracted with CH₂Cl₂ (three times). The combined extracts were dried over anhydrous Na₂SO₄ and concentrated to give an oil which was purified by flash column chromatography on silica gel with hexane–AcOEt (1:1) as eluant to afford **14a,b** (280 mg, 95%) as a mixture of diastereomers (17:14). **14a** (prepared from **13a**): [α]_D²⁰ +77.8° (c 1.3, CHCl₃); IR (neat) 1710, 1460, 1100, 1050, 975 cm⁻¹; ¹H NMR (CDCl₃): δ 0.87 (3H, t, J=7.3 Hz), 1.33 (1H, dq, J=14.7, 7.3 Hz), 1.42 (1H, dq, J=14.7, 7.3 Hz), 1.69–1.80 (2H, m), 1.80–1.90 (2H, m), 2.26–2.37 (2H, m), 3.32 (3H, s), 3.88 (1H, q, J=8.1 Hz), 3.95 (1H, td, J=8.1, 5.1 Hz), 4.46 (1H, s); ¹³C NMR (CDCl₃; DEPT) δ 8.2 (CH₃), 26.3 (CH₂), 26.4 (CH₂), 29.9 (CH₂), 33.8 (CH₂), 49.1 (C), 54.6 (CH₃), 65.8 (CH₂), 108.7 (CH), 180.0 (C); MS (EI): 201 (M⁺–1); HRMS (EI), calcd for C₁₀H₁₇O₄ (M⁺–1): 201.1127; found: 201.1119. **14b** (prepared from **13b**): mp 41–42 °C; [α]_D²⁰ –83.2° (c

1.2, CHCl₃); IR (KBr) 1710, 1450, 1190, 1100, 1025 cm⁻¹; ¹H NMR (CDCl₃): δ 0.86 (3H, t, J=7.3 Hz), 1.47 (1H, dq, J=14.7, 7.3 Hz), 1.56 (1H, dq, J=14.7, 7.3 Hz), 1.65–1.81 (4H, m), 2.27–2.37 (2H, m), 3.33 (3H, s), 3.90 (1H, q, J=8.1 Hz), 3.95 (1H, td, J=8.1, 4.4 Hz), 4.48 (1H, s); ¹³C NMR (CDCl₃; DEPT) δ 9.1 (CH₃), 24.2 (CH₂), 28.3 (CH₂), 29.2 (CH₂), 34.1 (CH₂), 49.3 (C), 54.8 (CH₃), 65.7 (CH₂), 108.5 (CH), 179.7 (C); MS (EI): 201 (M⁺–1). Anal. calcd for C₁₀H₁₈O₄: C, 59.39; H, 8.97. Found: C, 58.99; H, 8.99.

4.1.8. (1R,12bR)-1-Ethyl-2,3,6,7,12,12b-hexahydro-1-(2-acetoxyethyl)-indolo[2,3-a]quinolizin-4 (1H)-one (16a) and (1R,12bS)-1-ethyl-2,3,6,7,12,12b-hexahydro-1-(2-acetoxyethyl)-indolo[2,3-a]quinolizin-4(1H)-one (16b). A mixture of **14a,b** (205 mg, 1.01 mmol) and tryptamine (211 mg, 1.32 mmol) in AcOH (3.0 mL) was heated at 125 °C for 6 days. After the solvent was removed under reduced pressure, the resulting residue was purified by flash column chromatography on silica gel with CH₂Cl₂–MeOH (20:1) as eluant to afford **16a** (154 mg, 43%) and **16b** (158 mg, 44%) as a crystalline solid. Additional product **15** was isolated as an intermediate in this reaction; **16a** (recrystallization from AcOEt–hexane): mp 79–81 °C; [α]_D²⁰ +77.8° (c 1.3, CHCl₃); IR (KBr) 1740, 1620, 1240, 1135, 745 cm⁻¹; ¹H NMR (DMSO-d₆): δ 1.08 (3H, t, J=7.3 Hz), 1.16 (1H, ddd, J=14.7, 9.9, 5.9 Hz), 1.51 (1H, ddd, J=14.7, 9.9, 5.9 Hz), 1.52–1.59 (1H, m), 1.78 (1H, dq, J=14.7, 7.3 Hz), 1.87 (3H, s), 1.89–1.96 (1H, m), 1.99 (1H, dq, J=14.7, 7.3 Hz), 2.31–2.44 (2H, m), 2.54–2.61 (1H, m), 2.65 (1H, td, J=11.7, 2.2 Hz), 2.72 (1H, br d, J=14.3 Hz), 3.79 (1H, td, J=10.6, 5.9 Hz), 3.95 (1H, td, J=10.6, 5.9 Hz), 4.88 (1H, s), 4.88–4.91 (1H, m), 6.99 (1H, td, J=7.7, 1.0 Hz), 7.07 (1H, td, J=7.7, 1.0 Hz), 7.42 (1H, dd, J=7.7, 1.0 Hz), 7.45 (1H, dd, J=7.7, 1.0 Hz), 10.31 (1H, br s); ¹³C NMR (CDCl₃; DEPT) δ 8.2 (CH₃), 20.9 (CH₃), 21.1 (CH₂), 27.5 (CH₂), 28.9 (CH₂), 30.3 (CH₂), 30.5 (CH₂), 38.8 (C), 41.2 (CH₂), 60.3 (CH₂), 60.7 (CH), 111.1 (CH), 113.5 (C), 118.3 (CH), 119.9 (CH), 122.4 (CH), 126.4 (C), 130.4 (C), 136.3 (C), 169.8 (C), 171.1 (C); MS (EI): 354 (M⁺). Anal. calcd for C₂₁H₂₆N₂O₃: C, 71.16; H, 7.39; N, 7.90. Found: C, 70.74; H, 7.51; N, 7.86. **16b** (recrystallization from AcOEt–hexane): mp 75–77 °C; [α]_D²⁰ –84.0° (c 1.3, CHCl₃); IR (KBr) 1720, 1630, 1235, 1035, 740 cm⁻¹; ¹H NMR (DMSO-d₆): δ 0.64 (3H, t, J=7.3 Hz), 0.89 (1H, dq, J=14.7, 7.3 Hz), 1.28 (1H, dq, J=14.7, 7.3 Hz), 1.60 (1H, ddd, J=13.6, 6.2, 4.4 Hz), 1.90–2.02 (2H, m), 2.06 (3H, s), 2.18 (1H, ddd, J=15.0, 8.8, 6.6 Hz), 2.26 (1H, ddd, J=17.6, 11.0, 6.2 Hz), 2.38 (1H, ddd, J=17.6, 6.2, 4.4 Hz), 2.53–2.60 (1H, m), 2.65 (1H, td, J=11.7, 3.0 Hz), 2.68–2.74 (1H, m), 4.29 (1H, ddd, J=11.0, 8.8, 6.6 Hz), 4.39 (1H, ddd, J=11.0, 8.8, 5.9 Hz), 4.88 (1H, dd, J=11.7, 3.0 Hz), 4.94 (1H, s), 6.99 (1H, td, J=7.3, 1.0 Hz), 7.07 (1H, td, J=7.3, 1.0 Hz), 7.41 (1H, dd, J=7.3, 1.0 Hz), 7.42 (1H, dd, J=7.3, 1.0 Hz), 10.32 (1H, br s); ¹³C NMR (CDCl₃; DEPT) δ 6.9 (CH₃), 21.2 (2 carbons: CH₃ and CH₂), 23.8 (CH₂), 27.2 (CH₂), 28.9 (CH₂), 34.9 (CH₂), 38.9 (C), 40.8 (CH₂), 60.5 (CH), 61.4 (CH₂), 111.4 (CH), 112.9 (C), 117.9 (CH), 119.4 (CH), 122.0 (CH), 126.2 (C), 129.8 (C), 136.7 (C), 169.7 (C), 172.8 (C); MS (EI): 354 (M⁺). Anal. calcd for C₂₁H₂₆N₂O₃: C, 71.16; H, 7.39; N, 7.90. Found: C, 71.09; H, 7.48; N, 7.89.

Compound **15**. [α]_D²⁰ +27.4° (c 1.2, CHCl₃); IR (neat) 3300,

1635, 1460, 1040, 740 cm^{-1} ; ^1H NMR (DMSO-d_6): δ 0.75 (3H, t, $J=7.3$ Hz), 1.23 (1H, dq $J=14.7$, 7.3 Hz), 1.30 (1H, dq, $J=14.7$, 7.3 Hz), 1.50 (1H, ddd, $J=13.6$, 9.9, 5.5 Hz), 1.67 (1H, dt, $J=13.6$, 5.5 Hz), 1.73 (1H, ddd, $J=12.8$, 8.4, 6.6 Hz), 1.83 (1H, ddd, $J=12.8$, 8.1, 5.9 Hz), 2.21 (1H, dt, $J=17.2$, 5.5 Hz), 2.33 (1H, ddd, $J=17.2$, 9.9, 5.5 Hz), 2.85 (1H, ddd, $J=13.9$, 9.2, 4.8 Hz), 2.95 (1H, ddd, $J=13.9$, 9.5, 7.0 Hz), 3.40 (1H, ddd, $J=13.2$, 9.2, 7.0 Hz), 3.65 (1H, ddd, $J=13.2$, 9.5, 4.8 Hz), 3.69 (1H, td, $J=8.4$, 5.9 Hz), 3.79 (1H, q, $J=8.4$ Hz), 4.50 (1H, s), 6.98 (1H, t, $J=7.3$ Hz), 7.06 (1H, t, $J=7.3$ Hz), 7.13 (1H, d, $J=2.2$ Hz), 7.33 (1H, d, $J=7.3$ Hz), 7.57 (1H, d, $J=7.3$ Hz), 10.80 (1H, br s); ^{13}C NMR (DMSO-d_6 ; DEPT) δ 8.4 (CH_3), 23.5 (CH_2), 26.4 (CH_2), 28.2 (CH_2), 29.7 (CH_2), 34.1 (CH_2), 42.9 (C), 46.1 (CH_2), 64.1 (CH_2), 94.7 (CH), 111.3 (CH), 111.5 (C), 118.1 (CH), 118.2 (CH), 120.8 (CH), 122.6 (CH), 127.2 (C), 136.2 (C), 169.7 (C); MS (EI): 312 ($\text{M}^+ - \text{H}_2\text{O}$); HRMS (EI), calcd for $\text{C}_{19}\text{H}_{24}\text{N}_2\text{O}_2$ ($\text{M}^+ - \text{H}_2\text{O}$): 312.1838; found: 312.1837.

4.1.9. (1R,12bR)-1-Ethyl-2,3,6,7,12,12b-hexahydro-1-(2-hydroxyethyl)-indolo[2,3-a]quinolizin-4(1H)-one (3a) and (1R,12bS)-1-ethyl-2,3,6,7,12,12b-hexahydro-1-(2-hydroxyethyl)-indolo[2,3-a]quinolizin-4(1H)-one (3b). To a solution of **16a** (72.2 mg, 0.204 mmol) in MeOH (2.0 mL) was added 20% aqueous NaOH solution (80 μL , 0.40 mmol). After stirring at room temperature for 1 h, the reaction mixture was neutralized with AcOH. The resulting mixture was diluted with AcOEt and washed with saturated aqueous NaHCO_3 and brine, dried over anhydrous Na_2SO_4 , and concentrated. The resulted crystalline solid was washed with AcOEt and collected by filtration to give **3a** (45.9 mg, 72%); **3a** (recrystallization from CH_2Cl_2 -MeOH): mp 264–268 $^\circ\text{C}$ decomp.; $[\alpha]_{\text{D}}^{20} +188.1^\circ$ (c 0.15, CH_3OH); IR (KBr) 3300, 1610, 1415, 1155, 745 cm^{-1} ; ^1H NMR (DMSO-d_6): δ 1.01–1.07 (1H, m), 1.06 (3H, t, $J=7.3$ Hz), 1.39 (1H, ddd, $J=13.9$, 10.3, 5.9 Hz), 1.54 (1H, dt, $J=13.2$, 5.1 Hz), 1.76 (1H, dq, $J=14.7$, 7.3 Hz), 1.87 (1H, ddd, $J=13.2$, 10.3, 7.3 Hz), 1.96 (1H, dq, $J=14.7$, 7.3 Hz), 2.32–2.40 (2H, m), 2.52–2.60 (1H, m), 2.60–2.68 (1H, m), 2.68–2.74 (1H, m), 3.22 (1H, td, $J=10.3$, 5.9 Hz), 3.30 (1H, td, $J=10.3$, 5.5 Hz), 4.83 (1H, s), 4.87–4.93 (1H, m), 6.98 (1H, t, $J=7.3$ Hz), 7.06 (1H, t, $J=7.3$ Hz), 7.41 (1H, d, $J=7.3$ Hz), 7.45 (1H, d, $J=7.3$ Hz), 10.30 (1H, br s); ^{13}C NMR (DMSO-d_6 ; DEPT) δ 8.3 (CH_3), 20.8 (CH_2), 27.2 (CH_2), 28.8 (CH_2), 29.4 (CH_2), 35.0 (CH_2), 38.2 (C), 40.0 (CH_2), 56.3 (CH_2), 60.0 (CH), 110.9 (C), 111.6 (CH), 117.3 (CH), 118.5 (CH), 120.9 (CH), 125.8 (C), 131.6 (C), 136.5 (C), 169.0 (C); MS (EI): 312 (M^+). Anal. calcd for $\text{C}_{19}\text{H}_{24}\text{N}_2\text{O}_2$: C, 73.05; H, 7.74; N, 8.97. Found: C, 72.73; H, 7.84; N, 8.93.

The preparation of **3b** was carried out under the same procedure described above in 85% yield; **3b** (recrystallization from CH_2Cl_2 -MeOH): mp 123–127 $^\circ\text{C}$; $[\alpha]_{\text{D}}^{20} -141.2^\circ$ (c 0.24, CH_3OH); IR (KBr) 3380, 1615, 1440, 1305, 745 cm^{-1} ; ^1H NMR (DMSO-d_6): δ 0.74 (3H, t, $J=7.3$ Hz), 1.21 (1H, dq, $J=14.7$, 7.3 Hz), 1.29 (1H, dq, $J=14.7$, 7.3 Hz), 1.52 (1H, ddd, $J=13.2$, 6.6, 3.7 Hz), 1.79 (1H, dt, $J=15.4$, 5.9 Hz), 1.94–2.02 (1H, m), 2.05 (1H, ddd, $J=15.4$, 8.1, 5.9 Hz), 2.24 (1H, ddd, $J=17.6$, 11.0, 6.6 Hz), 2.38 (1H, ddd, $J=17.6$, 6.6, 3.7 Hz), 2.51–2.59 (1H, m), 2.62 (1H, td, $J=11.7$, 2.2 Hz), 2.70 (1H, dt,

$J=13.9$, 2.2 Hz), 3.71–3.80 (1H, br m), 3.82–3.90 (1H, br m), 4.87–4.93 (1H, m), 5.03 (1H, br s, OH), 5.06 (1H, s), 6.98 (1H, t, $J=7.3$ Hz), 7.06 (1H, t, $J=7.3$ Hz), 7.41 (1H, d, $J=7.3$ Hz), 7.43 (1H, d, $J=7.3$ Hz), 10.29 (1H, br s); ^{13}C NMR (DMSO-d_6 ; DEPT) δ 7.0 (CH_3), 20.8 (CH_2), 24.4 (CH_2), 26.8 (CH_2), 28.8 (CH_2), 38.2 (CH_2), 38.4 (C), 40.1 (CH_2), 56.6 (CH_2), 60.2 (CH), 110.9 (C), 111.5 (CH), 117.3 (CH), 118.5 (CH), 120.9 (CH), 125.9 (C), 132.0 (C), 136.0 (C), 169.0 (C); MS (EI): 312 (M^+). Anal. calcd for $\text{C}_{19}\text{H}_{24}\text{N}_2\text{O}_2$: C, 73.05; H, 7.74; N, 8.97. Found: C, 72.81; H, 7.90; N, 8.80.

4.1.10. (1R,12bR)-1-Ethyl-2,3,6,7,12,12b-hexahydro-1-[2-[(methanesulfonyl)oxy]ethyl]indolo[2,3-a]quinolizin-4(1H)-one (17a) and (1R,12bS)-1-ethyl-2,3,6,7,12,12b-hexahydro-1-[2-[(methanesulfonyl)oxy]ethyl]indolo[2,3-a]quinolizin-4(1H)-one (17b). Methanesulfonyl chloride (40.7 mg, 0.355 mmol) was added dropwise to a solution of **3a** (11.1 mg, 0.0355 mmol) and 4-(dimethylamino)pyridine (14.7 mg, 0.120 mmol) in pyridine (1.3 mL) at 0 $^\circ\text{C}$ under N_2 atmosphere. After stirring at 0 $^\circ\text{C}$ for 2 h, the reaction mixture was diluted with AcOEt. The solution was washed with saturated aqueous NaHCO_3 and brine, dried over anhydrous Na_2SO_4 , and concentrated. The residue was purified by preparative TLC on silica gel with CH_2Cl_2 -MeOH (25:1) to afford **17a** (12.7 mg, 92%) as a colorless oil; $[\alpha]_{\text{D}}^{20} +110.0^\circ$ (c 0.69, CHCl_3); IR (neat) 1630, 1355, 1175, 955, 745 cm^{-1} ; ^1H NMR (CDCl_3): δ 1.22 (3H, t, $J=7.3$ Hz), 1.53 (1H, dq, $J=14.7$, 7.3 Hz), 1.69 (1H, ddd, $J=13.9$, 6.6, 2.9 Hz), 1.82–1.98 (2H, m), 1.99–2.07 (1H, m), 2.52 (1H, ddd, $J=14.9$, 11.7, 6.6 Hz), 2.60 (1H, ddd, $J=18.3$, 6.6, 2.9 Hz), 2.71–2.82 (3H, m), 2.81 (3H, s), 3.94–4.02 (1H, m), 4.06–4.15 (1H, m), 4.82 (1H, s), 5.13–5.19 (1H, m), 7.14 (1H, t, $J=7.3$ Hz), 7.22 (1H, t, $J=7.3$ Hz), 7.38 (1H, d, $J=7.3$ Hz), 7.52 (1H, d, $J=7.3$ Hz), 7.98 (1H, br s); ^{13}C NMR (CDCl_3 ; DEPT) δ 8.3 (CH_3), 21.1 (CH_2), 28.0 (CH_2), 29.0 (CH_2), 30.4 (CH_2), 31.1 (CH_2), 37.2 (CH_3), 39.3 (C), 40.8 (CH_2), 60.3 (CH), 65.7 (CH_2), 111.1 (CH), 113.7 (C), 118.3 (CH), 120.1 (CH), 122.7 (CH), 126.3 (C), 130.1 (C), 136.2 (C), 169.7 (C); MS (EI): 294 ($\text{M}^+ - \text{MsOH}$); HRMS (EI), calcd for $\text{C}_{19}\text{H}_{22}\text{N}_2\text{O}$ ($\text{M}^+ - \text{MsOH}$): 294.1732; found: 294.1744.

The preparation of **17b** was carried out under the same procedure described above in 90% yield; **17b** (colorless oil): $[\alpha]_{\text{D}}^{20} -77.8^\circ$ (c 1.0, CHCl_3); IR (neat) 3400, 1625, 1355, 1180, 955 cm^{-1} ; ^1H NMR (CDCl_3): δ 0.75 (3H, t, $J=7.3$ Hz), 0.99 (1H, dq $J=14.7$, 7.3 Hz), 1.52 (1H, dq, $J=14.7$, 7.3 Hz), 1.73 (1H, ddd, $J=13.9$, 6.6, 3.7 Hz), 1.90 (1H, td, $J=13.9$, 6.6 Hz), 2.20 (1H, ddd, $J=14.7$, 8.8, 5.8 Hz), 2.42 (1H, dt, $J=15.4$, 8.1 Hz), 2.49 (1H, ddd, $J=17.6$, 11.7, 6.6 Hz), 2.55 (1H, ddd, $J=17.6$, 6.6, 3.7 Hz), 2.69–2.83 (2H, m), 3.11 (3H, s), 4.50–4.59 (1H, m), 4.70 (1H, dt, $J=15.4$, 8.1 Hz), 4.91 (1H, s), 5.12–5.17 (1H, m), 7.12 (1H, t, $J=7.3$ Hz), 7.19 (1H, t, $J=7.3$ Hz), 7.39 (1H, d, $J=7.3$ Hz), 7.51 (1H, d, $J=7.3$ Hz), 8.72 (1H, br s); ^{13}C NMR (CDCl_3 ; DEPT) δ 7.0 (CH_3), 21.1 (CH), 24.0 (CH_2), 27.2 (CH_2), 28.8 (CH_2), 36.4 (CH_2), 38.2 (CH_3), 39.3 (C), 40.9 (CH_2), 60.7 (CH), 66.3 (CH_2), 111.3 (CH), 113.7 (C), 118.1 (CH), 119.8 (CH), 122.3 (CH), 126.3 (C), 129.8 (C), 136.6 (C), 169.6 (C); MS (EI): 294 ($\text{M}^+ - \text{MsOH}$); HRMS (EI), calcd for $\text{C}_{19}\text{H}_{22}\text{N}_2\text{O}$ ($\text{M}^+ - \text{MsOH}$): 294.1732; found: 294.1776.

4.1.11. (1R,12bR)-1-Ethyl-2,3,6,7,12,12b-hexahydro-1-[2-[(phenylseleno)ethyl]-indolo[2,3-a]quinolizin-4(1H)-one (18a) and (1R,12bS)-1-ethyl-2,3,6,7,12,12b-hexahydro-1-[2-[(phenylseleno)ethyl]-indolo[2,3-a]quinolizin-4(1H)-one (18b). Sodium borohydride (11 mg, 0.29 mmol) was added to a solution of **17a** (29.3 mg, 0.065 mmol) and diphenyl diselenide (47.9 mg, 0.153 mmol) in EtOH (2.5 mL) at 0 °C and the mixture was stirred at 0 °C for 30 min and then allowed to warm to room temperature. Sodium borohydride (20 mg, 0.53 mmol) was frequently added to the reaction mixture during 3 h. The mixture was allowed to cool to 0 °C, neutralized with AcOH, and then diluted with AcOEt. The organic phase was washed with saturated aqueous NaHCO₃ and brine, and dried over anhydrous Na₂SO₄ and concentrated. The residue was purified by preparative TLC on silica gel with AcOEt–hexane (3:1) to afford **18a** (23.0 mg, 68%) and **23a** (0.8 mg, 4%) as a colorless oil; **18a** (recrystallized from MeOH): mp 180–181 °C; $[\alpha]_D^{20} +151.9^\circ$ (*c* 0.40, CHCl₃); IR (CDCl₃) 1630, 1440, 1420, 1305 cm⁻¹; ¹H NMR (CDCl₃): δ 1.15 (3H, t, *J*=7.3 Hz), 1.50 (1H, dt, *J*=13.9, 4.4 Hz), 1.62 (1H, ddd, *J*=13.9, 6.6, 3.7 Hz), 1.74 (1H, dt, *J*=13.9, 4.4 Hz), 1.81 (1H, dq, *J*=14.7, 7.3 Hz), 1.85–1.94 (2H, m), 2.37 (1H, ddd, *J*=18.3, 11.6, 6.6 Hz), 2.46–2.55 (2H, m), 2.61–2.76 (4H, m), 4.77 (1H, s), 5.05–5.13 (1H, m), 7.08–7.19 (4H, m), 7.22 (1H, t, *J*=7.3 Hz), 7.24–7.30 (2H, m), 7.33 (1H, d, *J*=7.3 Hz), 7.52 (1H, d, *J*=7.3 Hz), 7.78 (1H, br s); ¹³C NMR (150 MHz, CDCl₃; DEPT) δ 8.2 (CH₃), 21.0 (CH₂), 21.9 (CH₂), 27.8 (CH₂), 28.9 (CH₂), 30.0 (CH₂), 33.1 (CH₂), 40.5 (C), 40.9 (CH₂), 60.4 (CH), 111.0 (CH), 113.5 (C), 118.3 (CH), 120.0 (CH), 122.4 (CH), 126.4 (C), 127.2 (CH), 129.0 (CH), 129.5 (C), 130.5 (C), 133.3 (C), 136.1 (C), 169.8 (C); MS (EI): 452 (M⁺). Anal. calcd for C₂₅H₂₈N₂OSe: C, 66.51; H, 6.25; N, 6.21. Found: C, 66.28; H, 6.31; N, 6.21.

The preparation of **18b** was carried out under the same procedure described above in 88% yield and **23b** at 5.6% yield as a by-product; **18b** (a colorless oil): $[\alpha]_D^{20} -20.8^\circ$ (*c* 0.64, CHCl₃); IR (neat) 3320, 1620, 1440, 1310, 740 cm⁻¹; ¹H NMR (CDCl₃): δ 0.69 (3H, t, *J*=7.3 Hz), 0.89 (1H, dq, *J*=14.7, 7.3 Hz), 1.40 (1H, dq, *J*=14.7, 7.3 Hz), 1.67 (1H, ddd, *J*=13.9, 6.6, 3.7 Hz), 1.92 (1H, td, *J*=13.9, 6.6 Hz), 2.04 (1H, ddd, *J*=14.7, 12.5, 5.1 Hz), 2.23 (1H, ddd, *J*=14.7, 12.5, 5.1 Hz), 2.44 (1H, ddd, *J*=18.3, 11.7, 6.6 Hz), 2.52 (1H, ddd, *J*=18.3, 6.6, 3.7 Hz), 2.65–2.77 (3H, m), 3.05 (1H, dt, *J*=12.5, 5.1 Hz), 3.12 (1H, td, *J*=12.5, 5.1 Hz), 4.85 (1H, s), 5.12 (1H, dt, *J*=11.7, 2.9 Hz), 7.07–7.12 (2H, m), 7.16 (1H, t, *J*=7.3 Hz), 7.33 (1H, br s), 7.40 (2H, t, *J*=7.3 Hz), 7.43 (1H, d, *J*=7.3 Hz), 7.47 (1H, d, *J*=7.3 Hz), 7.67 (2H, d, *J*=7.3 Hz); ¹³C NMR (CDCl₃; DEPT) δ 7.0 (CH₃), 21.1 (CH₂), 22.1 (CH₂), 24.1 (CH₂), 26.9 (CH₂), 28.9 (CH₂), 38.4 (CH₂), 40.5 (C), 40.9 (CH₂), 60.1 (CH), 111.0 (CH), 113.5 (C), 118.1 (CH), 119.8 (CH), 122.2 (CH), 126.2 (C), 128.2 (CH), 129.0 (C), 129.7 (CH), 130.4 (C), 134.1 (CH), 136.0 (C), 169.8 (C); MS (EI): 452 (M⁺); HRMS (EI), calcd for C₂₅H₂₈N₂OSe: 452.1386; found: 452.1378.

4.1.12. (6aR,11aS,13aS,13bR)-13a-Ethyl-1,2,5,6,6a,11,12,13,13a,13b-decahydro-3H-cyclopenta[*ij*]-indolo[2,3-*a*]quinolizin-3-one (19). To a solution of **18a** (7.5 mg, 0.017 mmol) and 2,2'-azobisisobutyronitrile (0.67 mg,

0.0041 mmol) in toluene (0.75 mL) was added tributyltin hydride (19.4 mg, 0.067 mmol), and the mixture was stirred at 100 °C for 0.5 h under argon atmosphere. After the solvent was removed under reduced pressure, the residual crude material was purified by preparative TLC on silica gel with CH₂Cl₂–MeOH (25:1) to afford **19** (4.5 mg, 91%) as a colorless needles (re-crystallization from benzene); mp 194–195 °C; $[\alpha]_D^{20} +26.6^\circ$ (*c* 0.23, CHCl₃); IR (neat) 3340, 1635, 1465, 1270, 750 cm⁻¹; UV (MeOH, log ε) 245.8 (3.57), 296.4 (3.18) nm; ¹H NMR (CDCl₃): δ 0.96 (3H, t, *J*=7.3 Hz), 1.63–1.96 (9H, m), 1.96–2.03 (1H, m), 2.27 (1H, ddd, *J*=17.2, 10.6, 5.1 Hz), 2.38 (1H, dt, *J*=17.2, 4.8 Hz), 2.75 (1H, ddd, *J*=12.8, 8.1, 4.8 Hz), 3.15 (1H, t, *J*=5.9 Hz), 3.28 (1H, s), 4.34 (1H, dt, *J*=12.8, 6.6 Hz), 6.63 (1H, d, *J*=7.3 Hz), 6.78 (1H, t, *J*=7.3 Hz), 7.06 (1H, t, *J*=7.3 Hz), 7.17 (1H, d, *J*=7.3 Hz); ¹³C NMR (CDCl₃; DEPT) δ 9.1 (CH₃), 24.6 (CH₂), 28.8 (CH₂), 29.1 (CH₂), 35.2 (CH₂), 36.2 (CH₂), 36.5 (CH₂), 40.1 (CH₂), 43.6 (C), 44.6 (CH), 69.7 (CH), 76.3 (C), 109.7 (CH), 119.4 (CH), 123.5 (CH), 127.9 (CH), 130.8 (C), 149.1 (C), 171.0 (C); MS (EI): 296 (M⁺); HRMS (EI), calcd for C₁₉H₂₄N₂O: 296.1889; found: 296.1867.

4.1.13. (6aR,11aS,13aS,13bR)-13a-Ethyl-1,2,5,6,6a,11,12,13,13a,13b-decahydro-11-methyl-3H-cyclopenta[*ij*]-indolo[2,3-*a*]quinolizin-3-one (20). To a solution of **19** (4.4 mg, 0.015 mmol) and 35% formaldehyde (24 μL, 0.30 mmol) in acetonitrile (0.66 mL) was added sodium cyanoborohydride (2.8 mg, 0.045 mmol) and the mixture was stirred at room temperature. After 10 min, acetic acid (30 μL, 0.50 mmol) was added to the reaction mixture, which was further stirred at room temperature for 1 h. The mixture was diluted with AcOEt and washed with saturated aqueous NaHCO₃ and brine, dried over anhydrous Na₂SO₄ and concentrated. The residue was purified by preparative TLC on silica gel with CH₂Cl₂–MeOH (20:1) to afford **20** (4.0 mg, 87%) as a colorless oil; $[\alpha]_D^{20} -37.5^\circ$ (*c* 0.40, CHCl₃); IR (neat) 2880, 1645, 1480, 1210, 755 cm⁻¹; ¹H NMR (CDCl₃): δ 0.93 (3H, t, *J*=7.3 Hz), 1.58–1.68 (2H, m), 1.69–1.86 (6H, m), 1.96–2.06 (2H, m), 2.28–2.40 (2H, m), 2.56 (1H, ddd, *J*=13.2, 11.0, 5.1 Hz), 2.80 (3H, s), 3.06 (1H, t, *J*=6.6 Hz), 3.40 (1H, s), 4.46 (1H, ddd, *J*=13.2, 6.6, 3.7 Hz), 6.55 (1H, d, *J*=7.3 Hz), 6.77 (1H, t, *J*=7.3 Hz), 7.03 (1H, d, *J*=7.3 Hz), 7.12 (1H, t, *J*=7.3 Hz); ¹³C NMR (CDCl₃; DEPT) δ 8.9 (CH₃), 26.2 (CH₂), 27.6 (CH₂), 28.4 (CH₂), 31.4 (CH₂), 32.5 (CH₂), 32.8 (CH₃), 34.5 (CH₂), 39.7 (CH₂), 44.3 (C), 44.4 (CH), 70.3 (CH), 78.5 (C), 110.2 (CH), 119.4 (CH), 122.8 (CH), 127.7 (CH), 134.8 (C), 152.0 (C), 170.4 (C); MS (EI): 310 (M⁺); HRMS (EI), calcd for C₂₀H₂₆N₂O: 310.2045; found: 310.2046.

4.1.14. (–)-Vallesamidine (1). To a solution of **20** (6.9 mg, 0.022 mmol) in anhydrous THF (1.5 mL) was added lithium aluminum hydride (6.0 mg, 0.16 mmol), and the mixture was heated with stirring at 70 °C for 0.5 h under an argon atmosphere. After cooling to 0 °C, two drops of water were added to the reaction mixture, which was then diluted with AcOEt, and filtered through a hyflo super-cel. Evaporation of the solvent afforded an oil. The crude material was purified by preparative TLC on silica gel with CH₂Cl₂–MeOH (10:1) to afford (–)-vallesamidine (**1**) (5.4 mg, 82%) as a colorless oil; $[\alpha]_D^{20} -76.6^\circ$ (*c* 0.25, CHCl₃); IR (neat) 2750, 1610, 1485, 1115, 735 cm⁻¹; UV (MeOH, log ε)

258.6 (3.69), 302.4 (3.18) nm; ^1H NMR (CDCl_3): δ 0.90 (3H, t, $J=7.3$ Hz), 1.35–2.15 (12H, m), 2.25–2.50 (3H, m), 2.78 (3H, s), 2.70–3.00 (3H, br m), 6.44 (1H, br d, $J=7.3$ Hz), 6.67 (1H, br t, $J=7.3$ Hz), 7.03 (1H, d, $J=7.3$ Hz), 7.07 (1H, t, $J=7.3$ Hz); ^{13}C NMR (CDCl_3 ; DEPT) δ 9.1 (CH_3), 18.1 (CH_2), 26.4 (CH_2), 27.3 (CH_2), 30.1 (CH_2), 31.0 (CH_3), 31.2 (CH_2), 35.4 (CH_2), 44.0 (CH), 44.4 (C), 49.6 (CH_2), 50.1 (CH_2), 72.6 (CH), 78.6 (C), 107.6 (CH), 117.7 (C), 122.9 (CH), 127.3 (CH), 134.6 (C), 151.3 (C); MS (EI): 296 (M^+); HRMS (EI), calcd for $\text{C}_{20}\text{H}_{28}\text{N}_2$: 296.2252; found: 296.2216.

4.1.15. (12bS)-1,1-Diethyl-2,3,6,7,12,12b-hexahydro-indolo[2,3-*a*]quinolizin-4(1H)-one (22). Tributyltin hydride (20.4 mg, 0.070 mmol) was added to a solution of **18b** (8.9 mg, 0.020 mmol) and 2,2'-azobisisobutyronitrile (1.8 mg, 0.011 mmol) in toluene (0.9 mL), and the mixture was stirred at 100 °C for 1 h under an argon atmosphere. After the solvent was removed under reduced pressure, obtained the residue was purified by preparative TLC on silica gel with CH_2Cl_2 –MeOH (25:1) to afford **22** (4.1 mg, 70%) as a colorless needles (recrystallization from CH_2Cl_2 –MeOH); mp 293–294 °C; $[\alpha]_{\text{D}}^{20}$ -91.8° (c 0.41, CHCl_3); IR (neat) 3270, 1620, 14440, 1310, 750 cm^{-1} ; ^1H NMR (CDCl_3): δ 0.74 (3H, t, $J=7.3$ Hz), 0.99 (1H, dq, $J=14.7$, 7.3 Hz), 1.20 (1H, t, $J=7.3$ Hz), 1.48 (1H, dq, $J=14.7$, 7.3 Hz), 1.62 (1H, ddd, $J=11.7$, 6.6, 2.9 Hz), 1.81 (1H, dq, $J=14.7$, 7.3 Hz), 1.86–1.96 (2H, m), 2.46 (1H, ddd, $J=17.6$, 11.7, 6.6 Hz), 2.53 (1H, ddd, $J=17.6$, 6.6, 2.9 Hz), 2.53 (1H, ddd, $J=17.6$, 6.6, 2.9 Hz), 2.70–2.80 (3H, m), 4.85 (1H, s), 5.17 (1H, ddd, $J=10.3$, 3.7, 1.5 Hz), 7.13 (1H, t, $J=8.1$ Hz), 7.19 (1H, t, $J=8.1$ Hz), 7.35 (1H, d, $J=8.1$ Hz), 7.51 (1H, d, $J=8.1$ Hz), 7.80 (1H, br s); ^{13}C NMR (CDCl_3 ; DEPT) δ 7.1 (CH_3), 8.2 (CH_3), 21.1 (CH_2), 24.3 (CH_2), 26.5 (CH_2), 28.9 (CH_2), 29.9 (CH_2), 39.1 (C), 40.9 (CH_2), 60.4 (CH), 110.8 (CH), 113.2 (C), 118.2 (CH), 119.8 (CH), 122.2 (CH), 126.4 (C), 131.2 (C), 136.0 (C), 170.0 (C); MS (EI): 296 (M^+); HRMS (EI), calcd for $\text{C}_{19}\text{H}_{24}\text{N}_2\text{O}$: 296.1889; found: 296.1903.

4.1.16. (3R,16R)-14,15-Dihydroeburnamenin-19-one (23a). A powder of NaOH (2 mg, 0.05 mmol) was added to a solution of **17a** (12.4 mg, 0.0318 mmol) in THF (1.0 mL) and the mixture was stirred at room temperature for 20 min. The reaction mixture was diluted with AcOEt and then washed with saturated aqueous NaHCO_3 and brine, dried over anhydrous Na_2SO_4 , and concentrated. The residue was purified by preparative TLC on silica gel with CH_2Cl_2 –MeOH (25:1) to afford **23a** (8.8 mg, 94%) as a colorless oil; $[\alpha]_{\text{D}}^{20}$ $+81.9^\circ$ (c 0.45, CHCl_3); IR (neat) 2930, 1650, 1460, 1010, 750 cm^{-1} ; ^1H NMR (CDCl_3): δ 1.01 (3H, t, $J=7.3$ Hz), 1.45–1.60 (3H, m), 2.03–2.11 (2H, m), 2.11–2.18 (1H, m), 2.26 (1H, ddd, $J=17.6$, 5.1, 1.5 Hz), 2.45 (1H, ddd, $J=17.6$, 13.2, 5.9 Hz), 2.70 (1H, dd, $J=15.4$, 5.1 Hz), 3.03 (1H, td, $J=12.5$, 5.1 Hz), 3.07–3.15 (1H, m), 3.69 (1H, td, $J=11.7$, 5.2 Hz), 4.23 (1H, ddd, $J=11.7$, 5.9, 1.5 Hz), 4.36 (1H, s), 4.96 (1H, dd, $J=12.5$, 5.9 Hz), 7.13 (1H, t, $J=7.3$ Hz), 7.20 (1H, t, $J=7.3$ Hz), 7.29 (1H, d, $J=7.3$ Hz), 7.47 (1H, d, $J=7.3$ Hz); ^{13}C NMR (CDCl_3 ; DEPT) δ 7.3 (CH_3), 20.8 (CH_2), 22.3 (CH_2), 28.7 (CH_2), 28.9 (CH_2), 31.0 (CH_2), 33.4 (C), 38.6 (CH_2), 43.3 (CH_2), 60.7 (CH), 107.7 (C), 109.6 (CH), 118.4 (CH), 120.0 (CH), 121.4 (CH), 128.2 (C), 133.8 (C), 136.8 (C), 169.5 (C); MS (EI): 294 (M^+);

HRMS (EI), calcd for $\text{C}_{19}\text{H}_{22}\text{N}_2\text{O}$: 194.1732; found: 194.1746.

4.1.17. 14,15-Dihydroeburnamenine (24a). Lithium aluminum hydride (11.1 mg, 0.298 mmol) was added to a solution of **23a** (9.3 mg, 0.032 mmol) in anhydrous THF (4.5 mL) and the mixture was stirred at 70 °C for 0.5 h under argon atmosphere. After cooling, two drops of water were added to the reaction mixture, which was then diluted with AcOEt. The mixture was filtered through hyflo super-cel and the filtrate was dried over anhydrous Na_2SO_4 and then concentrated. The residue was purified by preparative TLC on silica gel with CH_2Cl_2 –MeOH (10:1) to afford **24a** (8.1 mg, 91%) as a colorless oil; $[\alpha]_{\text{D}}^{20}$ $+17.3^\circ$ (c 0.23, CH_3OH); IR (neat) 2940, 1460, 1355, 1100, 740 cm^{-1} ; ^1H NMR (CDCl_3): δ 0.93 (3H, t, $J=7.3$ Hz), 1.09 (1H, dt, $J=13.9$, 4.4 Hz), 1.31 (1H, dt, $J=13.9$, 1.5 Hz), 1.38 (1H, dt, $J=13.9$, 1.5 Hz), 1.56 (1H, dq, $J=14.7$, 7.3 Hz), 1.73–1.83 (1H, m), 1.90–2.02 (2H, m), 2.15 (1H, dq, $J=14.7$, 7.3 Hz), 2.47 (1H, td, $J=11.7$, 2.9 Hz), 2.55–2.65 (2H, m), 2.95–3.05 (1H, m), 3.24–3.37 (2H, m), 3.78 (1H, td, $J=11.7$, 5.9 Hz), 3.93 (1H, s), 4.16 (1H, ddd, $J=11.7$, 5.9, 1.5 Hz), 7.11 (1H, t, $J=7.3$ Hz), 7.17 (1H, t, $J=7.3$ Hz), 7.29 (1H, d, $J=7.3$ Hz), 7.49 (1H, d, $J=7.3$ Hz); ^{13}C NMR (CDCl_3 ; DEPT) δ 7.5 (CH_3), 17.0 (CH_2), 20.6 (CH_2), 23.8 (CH_2), 28.9 (CH_2), 31.9 (CH_2), 34.1 (C), 38.4 (CH_2), 44.5 (CH_2), 51.2 (CH_2), 59.2 (CH), 104.3 (C), 109.2 (CH), 118.1 (CH), 119.3 (CH), 120.6 (CH), 127.9 (C), 136.3 (C); MS (EI): 280 (M^+); HRMS (EI), calcd for $\text{C}_{19}\text{H}_{24}\text{N}_2$: 280.1939; found: 280.1919.

4.1.18. (3R,16S)-14,15-Dihydroeburnamenin-19-one (23b). The synthesis of **23b** was carried out under the same procedure described above in 88% yield; **23b** (colorless oil); $[\alpha]_{\text{D}}^{20}$ -132.6° (c 0.49, CHCl_3); IR (neat) 2930, 1650, 1460, 1310, 740 cm^{-1} ; ^1H NMR (CDCl_3): δ 0.62 (1H, dq, $J=14.7$, 7.3 Hz), 0.79 (3H, t, $J=7.3$ Hz), 1.35 (1H, dq, $J=14.7$, 7.3 Hz), 1.63 (1H, td, $J=13.2$, 7.3 Hz), 1.87 (1H, td, $J=13.9$, 7.3 Hz), 2.01 (1H, ddd, $J=13.2$, 7.3, 0.7 Hz), 2.21 (1H, dd, $J=13.9$, 5.9 Hz), 2.47–2.61 (2H, m), 2.70–2.88 (2H, m), 3.07 (1H, ddd, $J=13.2$, 10.3, 5.1 Hz), 3.79 (1H, td, $J=11.7$, 5.9 Hz), 4.22 (1H, dd, $J=11.7$, 6.6 Hz), 4.44 (1H, s), 4.90 (1H, ddd, $J=13.2$, 5.1, 2.2 Hz), 7.14 (1H, t, $J=7.3$ Hz), 7.21 (1H, t, $J=7.3$ Hz), 7.29 (1H, d, $J=7.3$ Hz), 7.50 (1H, d, $J=7.3$ Hz); ^{13}C NMR (CDCl_3 ; DEPT) δ 7.1 (CH_3), 16.9 (CH_2), 20.2 (CH₂), 28.7 (CH_2), 29.3 (CH_2), 30.4 (CH_2), 35.7 (C), 38.9 (CH_2), 39.8 (CH_2), 60.0 (CH), 106.5 (C), 109.7 (CH), 118.5 (CH), 119.9 (CH), 121.4 (CH), 127.7 (C), 132.1 (C), 138.3 (C), 169.7 (C); MS (EI): 294 (M^+); HRMS (EI), calcd for $\text{C}_{19}\text{H}_{22}\text{N}_2\text{O}$: 294.1732; found: 294.1703.

4.1.19. (3S)-14,15-Dihydroeburnamenine (24b). Sodium borohydride (9.0 mg, 0.24 mmol) was added to a solution of **23b** (7.0 mg, 0.024 mmol) and TFA (19.0 μL , 0.25 mmol) in absolute dioxane (1.2 mL), and the mixture was stirred at 100 °C for 45 min under nitrogen atmosphere. Concentration of the solvent under reduced pressure to give a residual oil which was purified by preparative TLC on silica gel with CH_2Cl_2 –MeOH (20:1) to afford **24b** (5.8 mg, 87%) as a colorless oil; $[\alpha]_{\text{D}}^{20}$ -54.4° (c 0.55, CH_3OH); IR (neat) 2940, 1635, 1470, 1135, 740 cm^{-1} ; ^1H NMR (CDCl_3): δ 0.76 (3H, t, $J=7.3$ Hz), 0.74–0.84 (1H, m), 1.12 (1H, td,

$J=13.2$, 4.4 Hz), 1.60 (1H, br d, $J=13.6$ Hz), 1.68–1.82 (2H, m), 1.88 (1H, br dt, $J=12.8$, 2.2 Hz), 1.91–2.02 (1H, m), 2.06 (1H, dd, $J=13.9$, 5.1 Hz), 2.24 (1H, td, $J=12.8$, 2.2 Hz), 2.47 (1H, td, $J=12.1$, 4.4 Hz), 2.71 (1H, dt, $J=15.4$, 2.6 Hz), 2.90–2.99 (1H, m), 2.95 (1H, s), 3.02–3.12 (2H, m), 3.77 (1H, td, $J=12.1$, 5.5 Hz), 4.11 (1H, dd, $J=11.7$, 6.6 Hz), 7.09 (1H, t, $J=7.3$ Hz), 7.14 (1H, t, $J=7.3$ Hz), 7.25 (1H, d, $J=7.3$ Hz), 7.46 (1H, d, $J=7.3$ Hz); ^{13}C NMR (CDCl_3 ; DEPT) δ 7.3 (CH_3), 18.5 (CH_2), 21.4 (CH_2), 21.6 (CH_2), 31.4 (CH_2), 32.0 (CH_2), 35.2 (C), 39.3 (CH_2), 53.5 (CH_2), 56.1 (CH_2), 68.0 (CH), 105.2 (C), 109.1 (CH), 118.1 (CH), 119.2 (CH), 120.3 (CH), 127.9 (C), 134.0 (C), 137.3 (C); MS (EI): 280 (M^+); HRMS (EI), calcd for $\text{C}_{19}\text{H}_{24}\text{N}_2$: 280.1939; found: 280.1910.

References and notes

- (a) Walser, A.; Djerassi, C. *Helv. Chim. Acta* **1965**, *48*, 391–404. (b) Brown, S. H.; Djerassi, C.; Simpson, P. G. *J. Am. Chem. Soc.* **1968**, *90*, 2445–2446.
- (a) Cordell, G. A. *The alkaloids*; Manske, R. H. F., Rodrigo, R., Eds.; Academic: New York, 1979; Vol. XVII, pp 199–384. (b) Smith, G. F. *The alkaloids*; Manske, R. H. F., Ed.; Academic: New York, 1960; Vol. VIII, pp 591–671.
- Padwa, A.; Haring, S. R.; Semones, M. A. *J. Org. Chem.* **1998**, *63*, 44–54.
- (a) Dickman, D. A.; Heathcock, C. H. *J. Am. Chem. Soc.* **1989**, *111*, 1528–1530. (b) Heathcock, C. H.; Norman, M. H.; Dickman, D. A. *J. Org. Chem.* **1990**, *55*, 798–811.
- Harley-Mason, J.; Kaplan, M. *J. Chem. Soc., Chem. Commun.* **1967**, 915–916.
- (a) Fuji, K.; Node, M.; Nagasawa, H.; Naniwa, Y.; Terada, S. *J. Am. Chem. Soc.* **1986**, *108*, 3855–3856. (b) Node, M.; Nagasawa, H.; Fuji, K. *J. Org. Chem.* **1990**, *55*, 517–521.
- Schultz, A. G.; Pettus, L. *J. Org. Chem.* **1997**, *62*, 6855–6861.
- Levy, J.; Mauperin, P.; Maindreville, M. D.; Le Men, J. *Tetrahedron Lett.* **1971**, 1003–1006.
- (a) Zhang, W. *Tetrahedron* **2001**, *57*, 7237–7262, and references cited therein. (b) Ziegler, F. E.; Belema, M. *J. Org. Chem.* **1994**, *59*, 7962–7967.
- Tanino, H.; Fukuishi, K.; Ushiyama, M.; Okada, K. *Tetrahedron Lett.* **2002**, *43*, 2385–2388.
- Tomioka, K.; Cho, Y. S.; Sato, F.; Koga, K. *Chem. Lett.* **1981**, 1621–1624.
- In Ref. 6, it is noted that optical purity of (3*S*,2*E*)-3-ethyltetrahydro-3-(2-nitroethenyl)-2*H*-Pyran-2-one, a starting material for the synthesis of indole alkaloids, is 82% ee. Our starting material **7** utilized for the synthesis of vallesamidine is ~100% optically pure.
- Coffen, D. L.; Katonak, D. A.; Wong, F. *J. Am. Chem. Soc.* **1974**, *96*, 3966–3973.

Hexaazatriisothianaphthenes: new electron-transport mesogens?

Matthias Lehmann,^a Vincent Lemaire,^b Jérôme Cornil,^{b,c} Jean-Luc Brédas,^{b,c} Simon Goddard,^d Ilaria Grizzi^d and Yves Geerts^{a,*}

^aLaboratoire de Chimie des Polymères CP206/1, Université Libre de Bruxelles, Boulevard du Triomphe, 1050 Bruxelles, Belgium

^bLaboratory for Chemistry of Novel Materials, Center for Research in Molecular Electronics and Photonics, University of Mons-Hainaut, Place du Parc 20, B-7000 Mons, Belgium

^cSchool of Chemistry and Biochemistry, Georgia Institute of Technology, Atlanta, GA 30332-0400, USA

^dCDT Limited, Greenwich House, Madingley Rise, Madingley Road, Cambridge CB3 0HJ, England, UK

Received 18 February 2003; revised 19 January 2004; accepted 27 January 2004

Abstract—Hexaazatriisothianaphthenes substituted with six alkylsulfanyl chains (propyl and dodecylsulfanyl) have been synthesised and their thermotropic, photophysical and oxidation–reduction properties characterised. Their synthesis has been motivated by the results of quantum-chemical calculations that point to efficient transport properties for these new electron-deficient mesogens since electron transport is predicted to be only slightly affected by rotational degrees of freedom in the discotic mesophase.

© 2004 Elsevier Ltd. All rights reserved.

1. Introduction

Discotic aromatic compounds emerge as attractive materials to promote efficient transport properties in organic-based devices such as light-emitting diodes, photovoltaic cells, or field effect transistors. Columnar liquid crystals combine the advantages of ease of preparation of oriented thin films, high order in the columns upon self-assembly, and self-healing capacity. Since such functional materials are used as one-dimensional semiconductors, both the orientation of the columnar structures at interfaces and the intracolumnar order of the aromatic cores play an important role in defining the device performance.¹ While a large number of p-type semiconducting columnar mesogens is known, few n-type materials have been reported to date.² Hexaazatriphenylenes (HAT), incorporating six nitrogen heteroatoms within a triphenylene core, are known to be electron-deficient and should thus facilitate electron injection. Columnar liquid crystals of derivatives based on a hexaazatriphenylene core have been obtained by supplying the electron-deficient core with three to six lateral chains.³ In contrast, the electron-rich thiophene unit yields p-type semiconductivity in polythiophenes. Enhanced electron transport has been observed recently in conjugated polymers containing both thiophene and electron deficient units;⁴ the substitution of sexithienyl with perfluorated carbon chains has also provided n-type semiconducting

materials.⁵ Our interest in electron-deficient columnar mesogens^{3a} has led us to combine the HAT and thiophene building blocks to generate compound **1** (Fig. 1) as potential electron transport material. We have introduced peripheral alkylsulfanyl chains to increase solubility, stabilise the radical anions,⁶ and induce supramolecular columnar liquid crystalline order. The preparation of **1** has also been triggered by the results of quantum-chemical calculations indicating that the electron transport properties are expected to be improved in hexaazatriisothianaphthene compounds

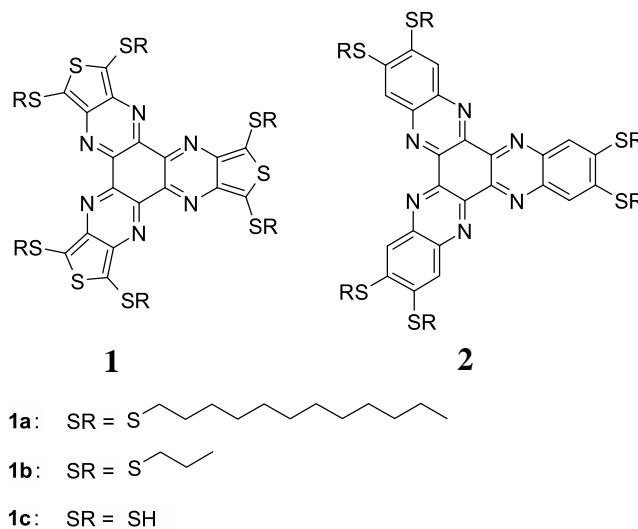
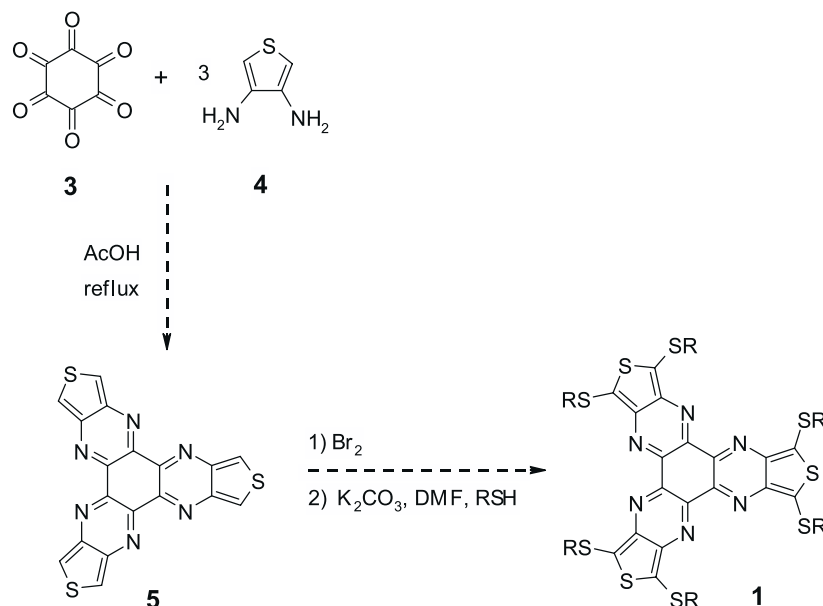


Figure 1. Chemical structure of hexaazatriisothianaphthenes **1** not forming LC phases and of hexaazatriisothianaphthalenes **2** forming LC phases for R=C_nH_{2n+1} (n=6, 8, 10, 12).^{3a}

Keywords: Discotic mesogens; n-Type semiconductor; Electron mobility; Electronic splitting.

* Corresponding author. Tel.: +32-2-650-5390; fax: +32-2-650-5410; e-mail address: ygeerts@ulb.ac.be



Scheme 1. Unsuccessful divergent synthesis of alkylsulfanyl-substituted **1**.

compared to triphenylene derivatives, as described below. The convergent synthesis of the new electron-deficient potential mesogen **1** containing linear lateral alkylsulfanyl chains is reported here and its thermotropic, photophysical and electrochemical properties are characterised.

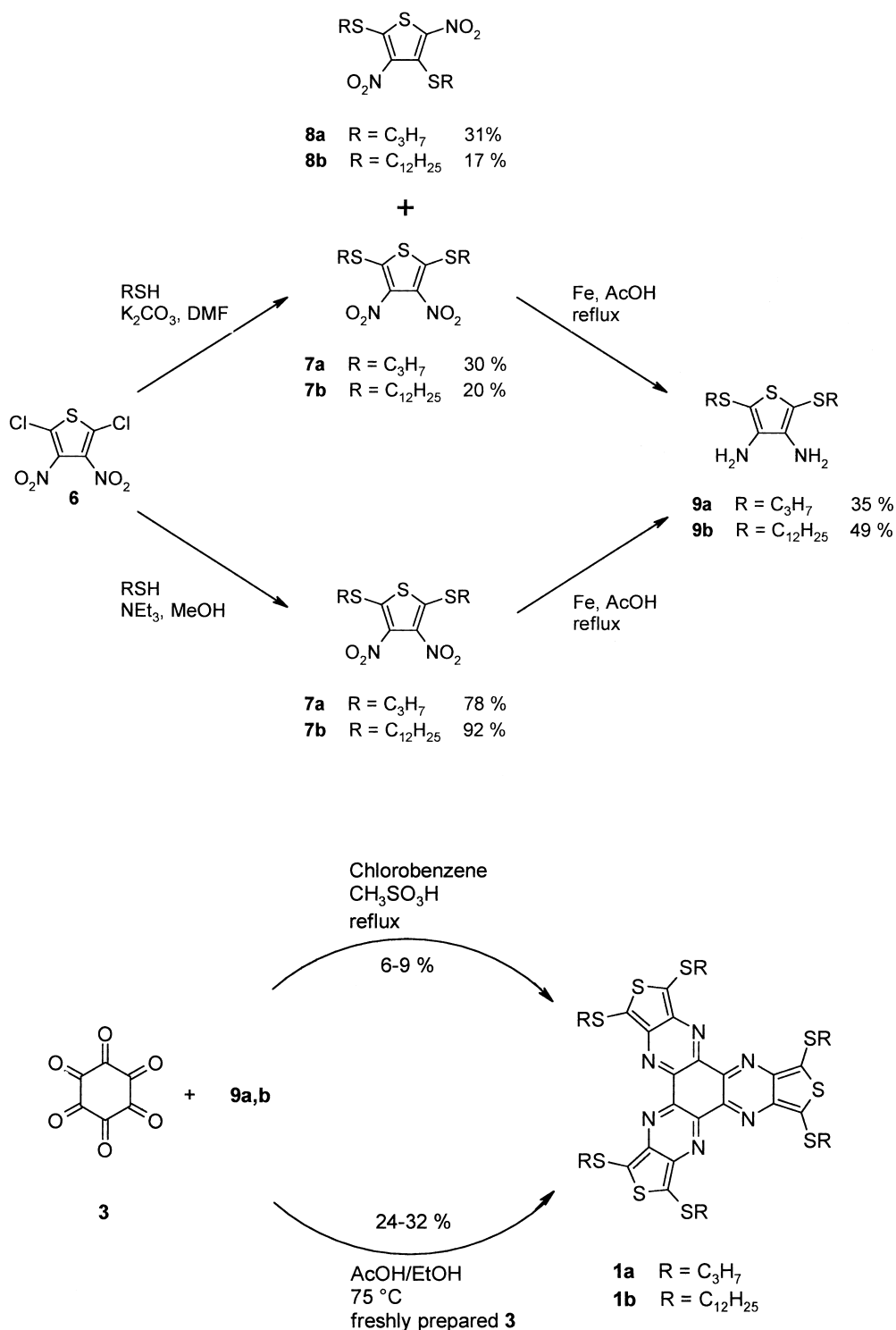
2. Results and discussion

2.1. Synthesis

Hexaazatriisothianaphthene is a molecule with a threefold symmetry built on the hexaazatriphenylene core. This class of compounds can be prepared by a threefold condensation of either 1,2-diketones with hexaaminobenzene⁷ or of 1,2-diamines with hexaketocyclohexane.⁸ Since hexaketocyclohexane **3** is commercially available and the preparation of diaminothiophenes is well established, we have chosen the latter route to reach our synthetic goal. A first attempt to obtain the parent hexaazatriisothianaphthene **5** by the condensation of 3,4-diaminothiophene **4** with hexaketone **3** is shown in **Scheme 1**. A subsequent hexabromination and nucleophilic substitution with mercaptoalkanes should give the alkylsulfanyl-substituted molecules. This approach offers as an advantage that the thermotropic properties can be easily tuned in the final reaction step by introduction of different lateral, flexible groups, as recently achieved for hexaalkylsulfanyltriphenylenes⁹ and hexaalkylsulfanylhexaazatriisothianaphthyls.^{3a} After the threefold condensation, a black insoluble powder was obtained, from which the hexaazatriisothianaphthene **5** could not be isolated. In order to improve the solubility of the final product, a convergent strategy has been adopted (**Scheme 2**). By nucleophilic substitution of the chlorine atoms of thiophene **6** in *N,N*-dimethylformamide, the symmetric 2,5-dialkylsulfanyl-3,4-dinitrothiophenes **7a,b** were obtained in much lower yields than those previously reported for similar compounds.¹⁰ In addition, non-*C*₂

symmetric isomers **8a,b** with a nitro group shifted to the vicinal position were isolated; this side product was not described by Erker,¹⁰ although it forms even at reaction temperatures as low as 10 °C.^{†11} The modification of the reaction conditions, using methanol as a protic solvent and triethylamine as a base yielded the symmetrical thiophenes **7a,b** almost quantitatively.¹² The reduction of **7a,b** with Fe/AcOH afforded the dialkylsulfanyldiaminothiophenes **9a,b** in 35 and 49% yields, respectively. The target compounds **1a,b** were obtained by the subsequent threefold condensation of **9a,b** with hexaketocyclohexane **3**. It is known that 3-aminothiophene can undergo a transamination reaction in the presence of catalytic amounts of acid.¹³ In order to avoid this side reaction, which can lead to undesirable oligomers, the condensation has been carried out only with molecular sieves 4 Å; no transformation was observed unless a small amount of methylsulfonic acid was added. Under these conditions, the yield of **1a,b** ranges from 6 to 9%. Reaction conditions could be optimised using freshly prepared hexaketocyclohexane octahydrate^{8b} **3** and a mixture of acetic acid and ethanol as reaction medium, which resulted in up to 31% isolated pure product. The purity and symmetry of the discotic product is demonstrated by NMR, FT-IR spectroscopy and elemental analysis. ¹H NMR spectra of **1a,b** show only protons of the lateral chains

[†] Analytical data confirm the composition of the product **8a,b**. ¹H NMR spectra present signals corresponding to two distinguishable α -CH₂ groups. ¹³C NMR shows four different signals for the carbon atoms of the thiophene ring, while EI mass spectra exhibit the same molecular mass peak as in the symmetrical product **7a,b**. Since FT-IR spectra are similar for **7a,b** and **8a,b**, no rearrangement from a nitro to a nitrite group (at 1610–1680 cm⁻¹) takes place. Thus, we find an unusual process where the nucleophilic substitution is accompanied by a shift of a nitro group. The reaction process and mechanism have not been further investigated. With the conditions given in Ref. 10 (DMF, RSH, K₂CO₃, 0 °C) the non-symmetric products **8a,b** were always isolated. The reaction at lower temperature is very slow, but even at -10 °C the side product was formed. Cine substitutions on 3,4-dinitro-substituted thiophenes, where the leaving groups are at a neighbouring position of the incoming nucleophile, were observed previously, see Ref. 11.



Scheme 2. Convergent synthesis of alkylsulfanyl-substituted hexaazatriisothianaphthenes **1**.

and the FT-IR data confirm the absence of amino groups. Interestingly, the IR spectra show a signal at 1734 cm^{-1} , which cannot be attributed to the absorption of a keto group according to mass analysis and ^{13}C NMR spectra. Thus, this signal is probably a combination or overtone of vibrations of the polycyclic aromatic system. The threefold symmetry of the product is verified by the ^{13}C NMR data where only three signals are found for the aromatic core, as expected (Table 1).

2.2. Theoretical support

Charge transport in discotic liquid crystals is generally considered to operate via a hopping mechanism whereby charges move from disc to disc down the one-dimensional stacks. The hopping rate, and hence the charge mobility, strongly depends on the intermolecular transfer integrals that describe the strength of the electronic coupling between adjacent neighbours. The transfer integrals can be

Table 1. ^{13}C NMR data obtained in CDCl_3 for the C_3 -symmetric molecules **1a,b**

Compound	Aromatic carbons ^a	Aliphatic carbons
1a	131.4 (C_{ia})	13.3 (CH_3)
	142.8, 143.7 (C_{ta})	23.0 (CH_2)
		40.1 (SCH_2)
1b	131.3 (C_{ia})	14.1 (CH_3)
	142.7, 143.6 (C_{ta})	22.7, 28.7, 29.2–29.7, 31.9 (CH_2)
		37.9 (SCH_2)

^a C_{ia} quaternary carbons of the inner aromatic ring, C_{ta} quaternary carbons of the thiophene unit; peaks were assigned by increment estimation of chemical shifts.

calculated to a good approximation for holes [electrons] as half the splitting of the HOMO [LUMO] levels in a dimer formed by two neutral molecules;¹⁴ they are highly sensitive to the relative positions of the interacting units, in particular to ring rotations and displacements within the stacks, that are expected in mesophases.¹⁵ In the case of the triphenylene molecules, we have shown that the transfer integrals become vanishingly small for specific rotational angles, a feature that is strongly detrimental to the transport properties. This motivated us to characterise, prior to chemical synthesis, the charge transport properties in hexaazatriisothianaphthene. We have thus calculated at the semiempirical Intermediate Neglect of Differential Overlap (INDO) level¹⁶ the electronic splittings in dimers

made of two hexaazatriisothianaphthene cores substituted by six sulfanyl groups, **1c** (Fig. 1) and have compared the results to those previously obtained for triphenylene derivatives. The geometry of the hexaazatriisothianaphthene core has been optimised at the Density Functional Theory (DFT) level using the B3LYP functionals and a 6-31G** basis set.

As expected, the HOMO and LUMO splittings calculated in cofacial dimers (where the two molecules are exactly superimposed on top of one another) decrease with the intermolecular distance. The splittings are found to be rather high, 0.6 and 0.4 eV for the HOMO and LUMO levels, respectively, for an intracolumnar separation of 0.35 nm. The HOMO splitting of molecule **1** is smaller than the corresponding value calculated for the triphenylene derivatives (~ 0.8 eV);¹⁵ in contrast, the LUMO splittings are similar, in the order of 0.4 eV, in the two compounds. In all cases, the electronic splittings decrease when going away from a cofacial conformation by laterally displacing one molecule with respect to the other.

We report in Figure 2 the evolution of the HOMO and LUMO splittings in a dimer built with two hexaazatriisothianaphthene cores substituted by six sulfanyl groups **1c** when rotating one disc with respect to the other around the stacking axis, together with the corresponding evolution obtained for the triphenylene molecule. While the HOMO

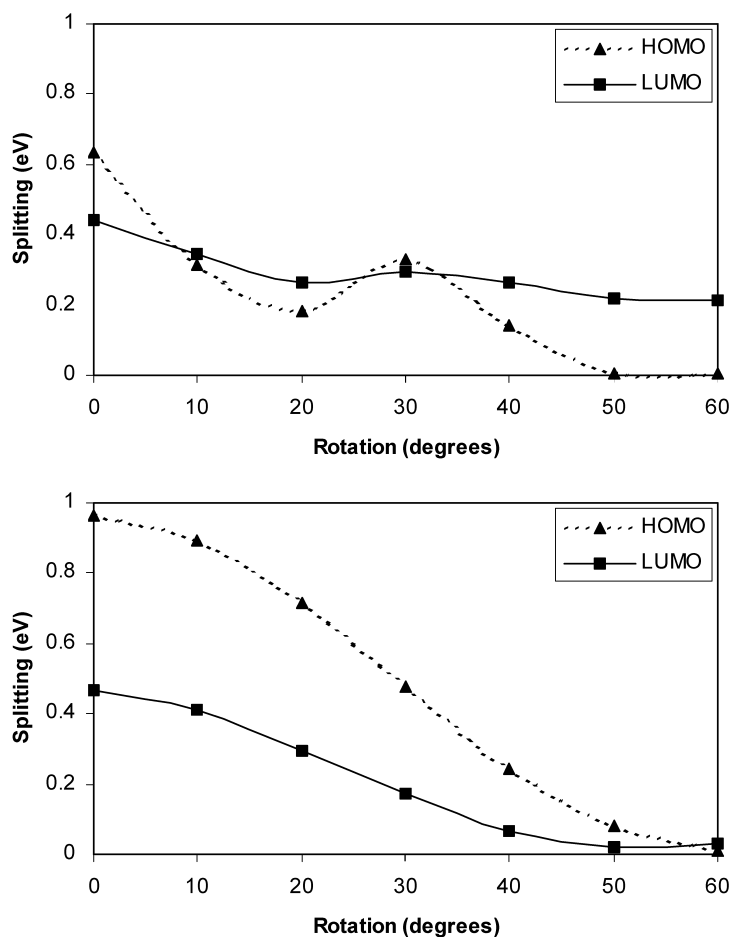


Figure 2. INDO-calculated angular dependence of the HOMO and LUMO splittings in a dimer made of: (top) two hexaazatriisothianaphthene cores substituted by six sulfanyl groups; and (bottom) two triphenylene molecules. The intermolecular distance is fixed here at 0.35 nm.

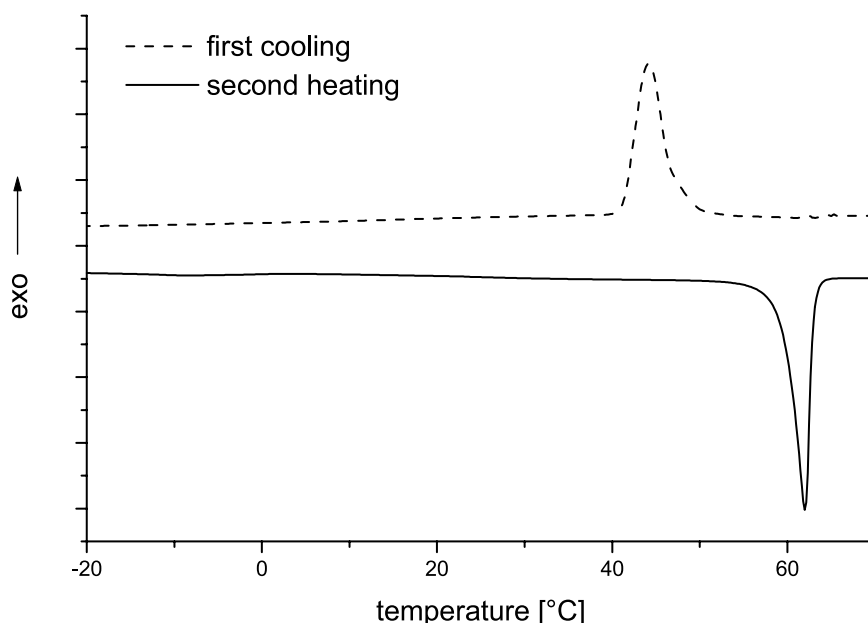


Figure 3. DSC curves (first cooling and second heating) of hexaazatriisothianaphthene **1b** (heating rate 10°/min).

splitting exhibits clear maxima and minima, the LUMO splitting is almost constant between 0 to 60 °, in contrast to the results obtained for the triphenylene derivatives. That the calculated LUMO splittings are large and insensitive to rotational degrees of freedom thus makes molecule **1** a potentially very attractive electron-transport mesogen.

2.3. Thermotropic and photophysical properties

The thermotropic properties were investigated by means of polarised optical microscopy (POM) and differential scanning calorimetry (DSC). The hexaalkylsulfanylhexaazatriisothianaphthenes **1a,b** do not show liquid crystalline behavior despite the fact that similar systems, such as hexaalkylsulfanylhexaazatrinaphthalene **2** (Fig. 1), possess a rich mesomorphism.^{3a} Compound **1a** is crystalline under POM and shows a melting transition in the second heating cycle of DSC (onset at 147 °C, $\Delta H = 33.8$ kJ/mol). After the first heating cycle where crystals melt at 69 °C, compound **1b** is a rather waxy material. However, this material also shows in the second heating trace a transition at 59 °C (onset) with a large enthalpy of 87.9 kJ/mol (Fig. 3). Subsequent heating and cooling cycles show a hysteresis of 12 °C. POM studies reveal a typical crystal growth upon cooling from the isotropic phase. The non-mesogenic behavior is surprising; it could be related to Coulomb repulsion effects linked to the charge distribution found on the aromatic cores (a Mulliken population analysis performed from the DFT calculations yields atomic charges of $-0.54|e|$ on the nitrogen atoms, see Fig. 4), which could dominate over the stabilizing forces induced by van der Waals interactions.

The photophysical properties of **1a** and **1b** were investigated by UV–Vis and emission spectroscopy. The absorption spectrum of **1b** in CHCl_3 is displayed in Figure 5; as expected, the same spectrum is obtained for compound **1a** since the size of the alkyl side chains does not impact the optical properties. The absorption spectrum is characterised

by two maxima at 290 nm (with a molar extinction coefficient $\epsilon = 4.6 \pm 0.1 \times 10^4$ l/mol cm) and at 373 nm (with $\epsilon = 6.0 \pm 0.1 \times 10^4$ l/mol cm). In addition, we observe a shoulder around 400 nm which appears as a vibronic satellite of the lowest intense absorption band as well as a tail extending down to 770 nm, which corresponds to a small optical bandgap of 1.6 eV (Fig. 5, insert). A thin solid film of **1** shows essentially the same absorption features as in the dilute solution. However, when the absorption is measured at room temperature in the crystalline phase, a strong bathochromic shift of 23 nm is observed (Fig. 5), which points to a strong interaction between chromophores in the crystal. In contrast, such a shift is not present in the spectra recorded in the isotropic liquid. Since it has been suggested from X-ray data that aromatic mesogens maintain columnar aggregates in the isotropic phase,¹⁷ the similarity of the spectra in dilute solution and in the isotropic liquid in

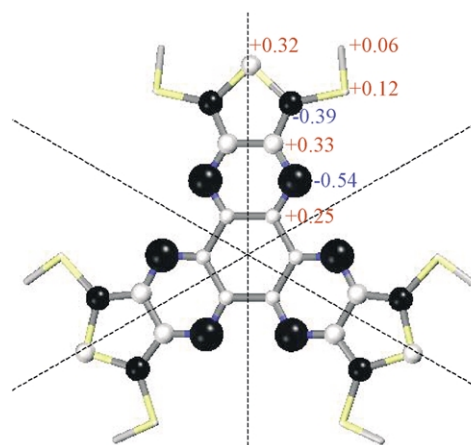


Figure 4. Charge distribution in the hexaazatriisothianaphthene molecule substituted by six sulfanyl groups **1c**, as calculated at the DFT level from Mulliken population analysis. The size of the spheres is proportional to the net charge on each atom; black [white] spheres relate to negative [positive] charges. The charge on the nitrogen atoms is calculated to be $-0.54|e|$.

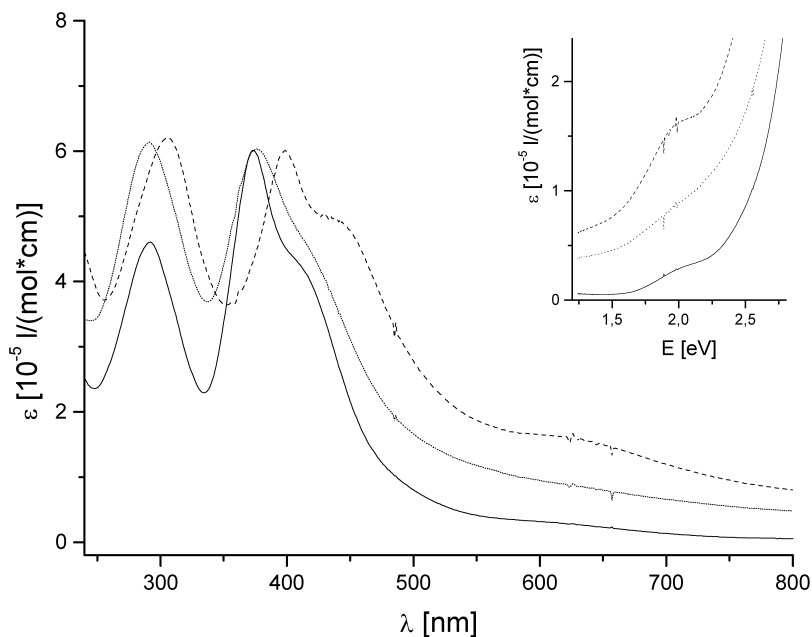


Figure 5. UV–Vis absorption spectra of hexaazatriisothianaphthene **1b** in CHCl_3 (solid line) and normalised spectra in a neat thin film heated to the isotropic liquid (dotted line) and cooled to the crystalline phase (dashed line). The insert shows the absorption edge of the same spectra versus the energy in eV.

vicinity of the melting transition for molecule **1** points to a weak interaction of mesogens and thus to a small tendency towards aggregation. The emission of compounds **1a,b** is so weak that reliable fluorescence spectra could not be recorded.

2.4. Oxidation–reduction properties

Cyclic voltammetry traces were recorded for thin films of **1a**, casted on the working electrode from a toluene solution, versus the standard calomel electrode (SCE). The first half wave potential for reduction amounts to -0.89 V and the one for oxidation to 0.28 V. From the onset of these reduction and oxidation waves, the LUMO and HOMO energies can be estimated to -3.9 and -4.8 eV, respectively,¹⁸ in reference to ferrocene. The energy of the LUMO level is relatively low compared to other electron deficient aromatic disks, such as tributoxycarbonylhexaazatrinaphthylenes^{3b} (-3.4 eV), perylenediimide¹⁹ (-3.3 eV) and even tris-8-hydroxyquinoline aluminium²⁰ (-2.9 eV), a commonly used electron-transport material in light emitting diodes.²¹ Consequently, hexaalkylsulfanyl-triisothianaphthene **1** exhibits an inherent electron deficient nature and is therefore a potential n-type semiconductor.

3. Conclusions

In view of their promising electron transport properties suggested by quantum-chemical calculations, the electron-deficient and potentially mesogenic hexaazatriisothianaphthene cores substituted by propylsulfanyl and dodecylsulfanyl chains have been prepared in a convergent synthesis by condensation of diamines with hexaketocyclohexane. Cyclic voltammetry on thin films demonstrates the electron-deficient nature of the new material, with a surprisingly low energy for the LUMO level estimated at -3.9 eV. Despite the fact that the closely related hexa-

azatrinaphthalene discs substituted by six alkylsulfanyl chains form columnar LC phases, POM and DSC studies do not establish the existence of liquid crystalline phases for the new compounds; this has probably to be attributed to strong Coulombic repulsion among the conjugated cores. Lateral substituents other than alkylsulfanyl chains should be found to promote supramolecular columnar organisation.

4. Experimental

Solvents and reagents were purchased from Aldrich and used as received. Column chromatographies were performed on silica gel (Merck silica gel 60, mesh size 0.2–0.5 mm). ^1H NMR spectra were recorded on a Bruker Avance 300 with solvent signal as internal standard. Mass spectra were recorded on a VG Micromass 7070F instrument (electron impact, 70 eV) and a VG instruments ZAB 2-SE-FPD using FD. Elemental analysis was carried out at the micro analytical laboratory of the University of Mainz (Germany). UV/Vis absorption measurements were carried out with a HP 8453 spectrophotometer. The thermal behaviour of the materials synthesised was investigated by polarizing optical microscopy (JENA microscope equipped with a Mettler FP 52 hot stage) and differential scanning calorimetry (Mettler Toledo DSC) with heating and cooling scans performed at 10 °C min^{-1} . The cyclic voltammograms reported here were recorded with a computer controlled EG&G potentiostat/galvanostat at a constant scan rate of 1000 mV/s. A three electrode configuration undivided cell was used. The working electrode was glassy carbon (3 mm diameter), with a Pt wire auxiliary electrode and a non-aqueous reference electrode containing 0.01 M AgNO_3 , 0.1 M tetrabutylammoniumperchlorate (TBAP) in acetonitrile, and silver wire. The electrolyte was 0.1 M TBAP in acetonitrile. The oxidation voltage sweeping range was from -1.0 to 1.3 V. The polymer film is casted directly on the working electrode from a toluene solution (3 mg/ml).

Bubbling Argon through the electrolyte for 20 min prior to the experiment purges the solution of dissolved oxygen. The measurements were carried out under a positive pressure of Argon. HOMO and LUMO levels were measured at the onset of, respectively, the first oxidation and reduction events of the second cycle. The potentials were referenced to the ferrocene half wave potential ($-E_{\text{HOMO/LUMO}} = E_{\text{oxidation/reduction}} - E_{\text{ferrocene}} + 4.8 \text{ eV}$).

4.1. General procedures

In a first attempt, dinitro and diamino derivatives **7**, **8** and **9** have been prepared following the procedure reported in the literature.¹⁰ However, since the nucleophilic substitution of **6** afforded a mixture of products, which were difficult to purify, the synthesis had to be modified. In the following the original and modified procedures are described, which were used for the synthesis of **7** and **9**. Moreover, a general optimised synthesis for the final step of the reaction scheme, the condensation of **9** with hexaketocyclohexane, is given.

*General procedure (1). Nucleophilic substitution of 2,5-dichloro-3,4-dinitrothiophene **6**.*

*Method 1.*¹⁰ Alkylthiol (11.0 mmol) was added to a suspension of K_2CO_3 (1.5 g) in dry DMF (10 ml) under nitrogen and stirred at ambient temperature for 20 min. The mixture was cooled with an ice bath and a solution of thiophene **6** (4.1 mmol) in DMF (4 ml) was added dropwise. The reaction was controlled by thin layer chromatography. After 2 h, no further reaction could be observed. The mixture was poured on 100 g ice and the precipitate was collected and recrystallised from acetone. The crude product consisted of two different compounds, which were purified by column chromatography. In contrast to previous work,¹⁰ a non-symmetrical product **8a,b** could be isolated in the same amount as symmetrical product **7a,b**.

*Method 2.*¹² To solution of thiophene **6** (12 mmol) and alkylthiol (27 mmol) in methanol (50 ml) at 5 °C, triethylamine (3 ml) was added. The ice bath was removed after 10 min and the mixture was stirred additional 2 h at room temperature.

*General procedure (2). Reduction of 2,5-dialkylsulfanyl-3,4-dinitrothiophene **7**.*

Thiophene **7** (0.8 mmol) was dissolved in acetic acid/water (4.4 ml, 10:1) and heated to 75 °C. 624 mg (11 mmol) iron powder were added in two portions, the mixture was refluxed for 1 h, poured on water and extracted with CH_2Cl_2 . After drying the organic phase with Na_2SO_4 and evaporation of the solvent, the product was isolated by column chromatography.

General procedure (3). Condensation with hexaketocyclohexane octahydrate (optimised procedure).

Freshly prepared hexaketocyclohexane $\times 8\text{H}_2\text{O}$ (180 mg, 0.58 mmol) and 3,4-diamino-2,5-dialkylsulfanylthiophene (1.9 mmol) in ethanol/glacial acid (1:1, 40 ml) were stirred over night at room temperature under argon atmosphere. The reaction mixture was then poured on water (80 ml) and

extracted with CH_2Cl_2 (2 \times 50 ml). The combined organic phases were washed with a saturated solution of NaHCO_3 and water and dried over NaSO_4 . Evaporation yielded a crude black product, which was purified as described below.

4.1.1. 2,5-Dipropylsulfanyl-3,4-dinitrothiophene (**7a**) and 2,4-dipropylsulfanyl-3,5-dinitrothiophene (**8a**).

Method 1. The general procedure (1) (method 1) led to a yellow precipitate, which was purified by chromatography on silica (toluene/hexane/ethyl acetate). Compound **7a** (0.98 g) was isolated as a yellow solid, mp 92 °C, yield 30%. As a side product, non-symmetrical compound **8a** (1.02 g) was obtained in 31% yield, mp 73 °C; this was not reported in previous investigations.¹⁰

Method 2. The general procedure (1) (method 2), using 1-propanethiol, afforded a suspension of a yellow precipitate. Water (100 ml) was added to the reaction mixture and the precipitate was collected, washed with 20 ml cold methanol and dried to yield 3.10 g (78%) of a yellow solid **7a**.

Compound 7a. ^1H NMR (CDCl_3 , 300 MHz) 1.08 (t, 6H, CH_3), 1.78 (m, 4H, CH_2), 2.99 (t, 4H, SCH_2). ^{13}C NMR (CDCl_3 , 75 MHz) 13.2 (CH_3), 22.2 (CH_2), 38.5 (SCH_2), 138.5, 141.4 ($\text{C}_{\text{Thiophene}}$). FT-IR $\nu(\text{cm}^{-1}) = 2964, 2933, 2869, 1508, 1461, 1367, 1321, 1304$. Mass (EI) m/z (rel. intensity) = 322 (100), 126 (19), 112 (34), 101 (35), 84 (72).

Compound 8a. ^1H NMR (CDCl_3 , 300 MHz) 0.98, 1.13 (2t, 6H, CH_3), 1.59, 1.89 (2dt, 4H, CH_2), 2.97, 3.07 (2t, 4H, SCH_2). ^{13}C NMR (CDCl_3 , 75 MHz) 13.2, 13.4 (CH_3), 21.3, 22.7 (CH_2), 37.1, 38.3 (SCH_2), 136.8 (C-SR), 141.1 (C-NO_2), 141.4 (C-NO_2), 154.3 (C-SR). FT-IR $\nu(\text{cm}^{-1}) = 2979, 2968, 2954, 2931, 2871, 1516, 1494, 1450, 1383, 1308, 1242$. Mass (EI) m/z (rel. intensity) = 322 (28), 170 (43), 112 (60), 101 (100).

4.1.2. 2,5-Didodecylsulfanyl-3,4-dinitrothiophene (**7b**) and 2,4-didodecylsulfanyl-3,5-dinitrothiophene (**8b**).

Method 1. Following the general procedure (1) (method 1), a yellow precipitate was obtained, which was purified by column chromatography on silica (hexane/ethyl acetate). Compound **7b** (0.47 g) was isolated as a yellow solid, mp 77–79 °C, yield 20%. As a side product, non-symmetrical compound **8b** (0.40 g) was obtained in 17% yield, mp 60–63 °C; this was not reported in previous investigations.¹⁰

Method 2. The general procedure (1) (method 2) using 1-dodecanethiol afforded a yellow precipitate, which was collected by filtration and washed with methanol. Compound **7b** was obtained as a yellow solid (6.50 g, 92%).

Compound 7b. ^1H NMR (CDCl_3 , 300 MHz) 0.92 (t, 6H, CH_3), 1.20–1.85 (m, 40H, CH_2), 3.03 (t, 4H, SCH_2). ^{13}C NMR (CDCl_3 , 75 MHz) 14.1 (CH_3), 22.7, 28.6, 28.7, 29.0, 29.3, 29.5, 29.6, 29.7, 31.9 (CH_2), 36.6 (SCH_2), 141.4, 138.5 ($\text{C}_{\text{Thiophene}}$). FT-IR $\nu(\text{cm}^{-1}) = 2952, 2818, 2850, 1512, 1467, 1427, 1371, 1327, 1304$. Mass (EI) m/z (rel. intensity) = 574 (100), 544 (12), 402 (10), 389 (9), 201 (9).

Compound 8b. ^1H NMR (CDCl_3 , 300 MHz) 0.88 (t, 6H, CH_3), 1.10–2.00 (m, 40H, CH_2), 2.99, 3.08 (2t, 4H, SCH_2).

^{13}C NMR (CDCl_3 , 75 MHz) 14.1 (CH_3), 22.7, 27.7, 28.6, 28.8, 28.96, 29.0, 29.3, 29.5, 29.6, 31.9 (CH_2), 35.3, 36.4 (SCH_2), 137.0 (C-SR), 141.1 (C-NO_2), 141.3 (C-NO_2), 154.5 (C-SR). FT-IR $\nu(\text{cm}^{-1}) = 2952, 2920, 2848, 1520, 1489, 1468, 1440, 1373, 1338, 1304, 1282, 1244$. Mass (EI) m/z (rel. intensity) = 574 (4), 557 (12), 544 (10), 528 (11), 57 (100).

4.1.3. 3,4-Diamino-2,5-dipropylsulfanyl-thiophene (9a).

After reduction, following the general procedure (2), **9a** was obtained by column chromatography (silica/hexane/ethyl acetate/ NEt_3) as a light brownish solid, yield 1.19 g (47%). The product was not stable in air and consequently used directly for the next reaction. ^1H NMR (CDCl_3 , 300 MHz) 0.96 (t, 6H, CH_3), 1.61 (m, 4H, CH_2), 2.61 (t, 4H, SCH_2), 3.76 (broad, 4H, NH_2). ^{13}C NMR (CDCl_3 , 75 MHz) 13.2 (CH_3), 23.0 (CH_2), 40.0 (SCH_2), 108.1, 140.4 ($\text{C}_{\text{Thiophene}}$).

4.1.4. 3,4-Diamino-2,5-didodecylsulfanyl-thiophene (9b).

After reduction, following the general procedure (2), **9b** was obtained by column chromatography (silica/hexane/ethyl acetate) as a light brownish waxy solid, yield 0.2 g (49%). The product was not stable in air and consequently used directly for the next reaction. ^1H NMR (CDCl_3 , 300 MHz) 0.88 (t, 6H, CH_3), 1.20–1.40, 1.58 (m, 40H, CH_2), 2.62 (t, 4H, SCH_2), 3.75 (broad, 4H, NH_2). ^{13}C NMR (CDCl_3 , 75 MHz) 14.1 (CH_3), 22.7, 28.6, 29.2, 29.3, 29.5, 29.6, 29.7, 31.9 (CH_2), 38.0 (SCH_2), 108.2, 140.3 ($\text{C}_{\text{Thiophene}}$).

4.1.5. 1,3,8,10,15,17-Hexapropylsulfanyl-4,7,11,14,18,20-hexaazatriisothianaphthene (1a).

300 mg (1.14 mmol) **9a**, 60 mg (0.19 mmol) hexaketocyclohexane \times $8\text{H}_2\text{O}$ (Aldrich) (**3**) were dissolved in 10 ml chlorobenzene and 60 mg molecular sieves (4 Å) were added. The mixture was refluxed for 2 days. Since no reaction was observed by TLC control, one drop of methanesulfonic acid was added. After 2 h at reflux, the solvent was evaporated under vacuum and the product was purified by column chromatography (silica 60, hexane/ethyl acetate = 5:1). Compound **1a** (15 mg) was isolated as a dark yellow solid, yield 6%.

Optimised procedure. 550 mg of a crude product obtained by the general procedure was purified by column chromatography (silica 60, hexane/ethyl acetate/triethylamine = 80:4:1). The almost pure product (170 mg) was recrystallised from ethanol/methylene chloride by slow evaporation (approx. 2–3 days) of the solvent at room temperature. Filtration afforded 156 mg (32%) of black needle-like crystals, mp 147 °C (onset DSC). ^1H NMR (CDCl_3 , 300 MHz) 1.29 (t, 18H, CH_3), 1.82 (m, 12H, CH_2), 3.03 (t, 12H, SCH_2). ^{13}C NMR (CDCl_3 , 75 MHz) 13.3 (CH_3), 23.0 (CH_2), 40.1 (SCH_2), 131.4, 142.8, 143.7 ($\text{C}_{\text{aromatic}}$). FT-IR $\nu(\text{cm}^{-1}) = 2957, 2924, 2851, 1734, 1459, 1379, 1288, 1125$. Mass (EI) m/z (rel. intensity) = 848 (M^+ , 12), 182 (52), 150 (100), 108 (73). Elemental analysis calcd for $\text{C}_{36}\text{H}_{42}\text{N}_6\text{S}_9$ (%): C 51.03, H 5.00, N 9.92; found: C 51.33, H 5.16, N 9.67.

4.1.6. 1,3,8,10,15,17-Hexadodecylsulfanyl-4,7,11,14,18,20-hexaazatriisothianaphthene (1b). 200 mg (0.39 mmol) **9b**, 20 mg (0.065 mmol) hexaketocyclohexane \times $8\text{H}_2\text{O}$ (Aldrich) (**3**) were dissolved in 10 ml chlorobenzene and one drop of methanesulfonic acid was added. The mixture

was refluxed for 2 h. Then the solvent was evaporated under vacuum and the product was purified by column chromatography (silica 60, hexane/ethyl acetate). Compound **1b** (9 mg) was isolated as a dark yellow solid, yield 9%.

Optimised procedure. The crude product, obtained by the general procedure (3), was purified by column chromatography (silica 60, hexane/ethyl acetate/triethylamine = 80:2:1). The purest fractions (136 mg) were again chromatographed to yield 95 mg of a dark yellow solid. The material was crystallised from ethanol/methylene chloride by slow evaporation of methylene chloride at 40 °C and reduced pressure (800–500 mbar). Filtration afforded 72 mg (24%) of brown to black solid powder, mp 69 °C (Onset DSC). ^1H NMR (CDCl_3 , 300 MHz) 0.89 (t, 18H, CH_3), 1.20–1.40, 1.55, 1.80 (m, 120H, CH_2), 3.36 (t, 12H, SCH_2). ^{13}C NMR (CDCl_3 , 75 MHz) 14.1 (CH_3), 22.7, 28.7, 29.2, 29.3, 29.5, 29.6, 29.7, 31.9 (CH_2), 37.9 (SCH_2), 131.3, 142.7, 143.6 ($\text{C}_{\text{aromatic}}$). FT-IR $\nu(\text{cm}^{-1}) = 2962, 2926, 2853, 1734, 1467, 1380, 1262, 1125, 1097, 1073, 1024, 803$. Mass (FD) m/z (rel. intensity) = 1605 (17), 1618 (100). Elemental analysis calcd for $\text{C}_{90}\text{H}_{150}\text{N}_6\text{S}_9$ (%): C 67.36, H 9.42, N 5.24; found: C 67.39, H 9.45, N 5.16.

Acknowledgements

This work was financially supported by the Belgian National Fund for Scientific Research (FNRS FRFC-n° 2.4597.01, crédit aux chercheurs n° 1.5.074.00), Université Libre de Bruxelles, Banque Nationale de Belgique, and Communauté Française de Belgique (ARC n° 00/05-257). The work in Mons is partly supported by the Belgian Federal Government 'Service des Affaires Scientifiques, Techniques et Culturelle (SSTC)' in the framework of the 'Pôle d'Attraction Interuniversitaire en Chimie Supramoléculaire et Catalyse Supramoléculaire (PAI 5/3)' and FNRS-FRFC. The work in Atlanta is partly supported by the US National Science Foundation and the Office of Naval Research. V. L. acknowledges a grant from the 'Fonds pour la Formation à la Recherche dans l'Industrie et dans l'Agriculture' (FRIA); JC is an FNRS Research Associate. We are grateful to the group of Prof. H. Meier (University of Mainz) for carrying out the elemental analysis and to Dr. Clare Foden (CDT Cambridge) for fruitful discussions.

References and notes

- (a) van de Craats, A. M.; Warman, J. M.; de Haas, M. P.; Simmerer, J.; Haarer, D.; Schuhmacher, P. *Adv. Mater.* **1996**, *8*, 823. (b) van de Craats, A. M.; Warman, J. M.; Fechtenkötter, A.; Brand, J. D.; Harbison, M. H.; Müllen, K. *Adv. Mater.* **1999**, *11*, 1469–1472. (c) Cornil, J.; Beljonne, D.; Calbert, J.-P.; Brédas, J.-L. *Adv. Mater.* **2001**, *13*, 1053–1067.
- Eichhorn, H. *J. Phorphyrins Phthalocyanines* **2000**, *4*, 88.
- (a) Kestemont, G.; de Halleux, V.; Lehmann, M.; Ivanov, D. A.; Watson, M.; Geerts, Y. H. *Chem. Commun.* **2001**, 2074–2075. (b) Bock, H.; Babeau, A.; Seguy, I.; Jolinat, P.; Destruel, P. *ChemPhysChem* **2002**, *6*, 532–535. (c) Pieterse, K.; van Hal, A.; Kleppinger, R.; Vekemans, J. A. J. M.; Janssen, R. A. J.; Meijer, E. W. *Chem. Mater.* **2001**, *13*,

- 2675–2679. (d) Pieterse, K.; Vekemans, J. A. J. M.; Meijer, E. W. *Polym. Prepr.* **1999**, *40*, 404–405.
4. (a) Cui, Y.; Zhang, X.; Jenekhe, S. A. *Macromolecules* **1999**, *32*, 3824–3826. (b) Meng, H.; Huang, W. *J. Org. Chem.* **2000**, *65*, 3894–3901.
5. (a) Facchetti, A.; Deng, Y.; Wang, A.; Koide, Y.; Sirringhaus, H.; Marks, T. J.; Friend, R. H. *Angew. Chem. Int. Ed.* **2000**, *39*, 4547–4551. (b) Marks, T. J.; Facchetti, A.; Sirringhaus, H.; Friend, R. H. PCT Int. Appl. WO 0209201, 2002.
6. Tucker, J. H. R.; Gingras, M.; Brand, H.; Lehn, J.-M. *J. Chem. Soc. Perkin Trans. 2* **1997**, 1303–1307.
7. (a) Kohne, B.; Praefke, K. *Liebigs Ann. Chem.* **1985**, 522–528. (b) Rogers, D. Z. *J. Org. Chem.* **1986**, *51*, 3904–3905. (c) Boden, N.; Bushby, R. J.; Headdock, G.; Lozman, O. R.; Wood, A. *Liq. Cryst.* **2001**, *28*, 139–144.
8. (a) Rademacher, J. T.; Kanakarajan, K.; Czarnik, A. W. *Synthesis* **1994**, 378–380. (b) Kanakarajan, K.; Czarnik, A. W. *J. Org. Chem.* **1986**, *51*, 5241–5243. (c) Skujins, S.; Webb, G. A. *Tetrahedron* **1969**, *25*, 3935–3945.
9. Kohne, B.; Poules, W.; Praefke, K. *Chem.-Ztg.* **1984**, *108*, 113.
10. Erker, T. *Monatsh. Chem.* **1998**, *129*, 679–687.
11. (a) Petrillo, G.; Novi, M.; Garbarino, G.; Dell'Erba, C.; Mugnoli, A. *J. Chem. Soc., Perkin Trans. 2* **1985**, 1291–1296. (b) Novi, M.; Guanti, G.; Sancassan, F.; Dell'Erba, C. *J. Chem. Soc., Perkin Trans. 1* **1978**, 1140–1144.
12. Spinelli, D.; Consiglio, G.; Dell'Erba, C.; Novi, M. In *The chemistry of heterocyclic compounds. Thiophene and its derivatives*; Gronowitz, S., Ed.; Wiley: New York, 1991; p 295.
13. Outurquin, F.; Lerouge, P.; Paulmier, C. *Bull. Soc. Chim. Fr.* **1986**, 267–275.
14. Brédas, J.-L.; Calbert, J.-P.; da Silva Filho, D. A.; Cornil, J. *Proc. Natl. Acad. Sci. U. S. A.* **2002**, *99*, 5804–5809.
15. Cornil, J.; Lemaire, V.; Calbert, J.-P.; Brédas, J.-L. *Adv. Mater.* **2002**, *14*, 726–729.
16. Zerner, M. C.; Loew, G. H.; Kirchner, R. F.; Mueller-Westerhoff, U. *J. Am. Chem. Soc.* **1980**, *102*, 589–599.
17. (a) Kleppinger, R.; Lillya, C. P.; Yang, C. *J. Am. Chem. Soc.* **1997**, *119*, 4097. (b) Lee, W. K.; Heiney, P. A.; Mccauley, J. P., Jr.; Smith, A. B., III. *Mol. Cryst. Liq. Cryst.* **1991**, *198*, 273.
18. Janitz, S.; Bradeley, D. D. C.; Grell, M.; Giebeler, C.; Inbasekaran, M.; Woo, E. P. *Appl. Phys. Lett.* **1998**, *73*, 2453.
19. Schmidt-Mende, L.; Fechtenkötter, A.; Müllen, K.; Moons, E.; Friend, R. H.; MacKenzie, D. *Science* **2001**, *293*, 1119–1122.
20. Tian, W.; Huang, J.; Wu, F.; Sun, C.; Liu, X.; Ma, Y.; Liu, S.; Shen, J. *Chin. Phys. Lett.* **1996**, *13*, 790.
21. Tang, C. W.; Van Slyke, S. A. *Appl. Phys. Lett.* **1987**, *51*, 913.



The influence of electronegativity on triangular three-centre two-electron bonds: the relative stability of carbonium ions, π -complex chemistry and the $-2h\beta$ effect

Christopher A. Ramsden*

Lennard-Jones Laboratories, School of Chemistry and Physics, Keele University, Keele, Staffordshire ST5 5BG, UK

Received 23 October 2003; revised 6 January 2004; accepted 29 January 2004

Abstract—Using the HMO approximation, bond energy equations for triangular three-centre, two-electron [3c-2e] bonded species AB_2^+ (π -complexes) and the isomeric systems ($AB-B^+$, $BB-A^+$, $BA-B^+$ and $A^++B=B$) are described. The electronegativity difference ($\Delta\chi$) between the atoms or groups A and B is assumed to be related to the difference (h) in their Coulomb integrals and the variation of relative energies with electronegativity difference is explored. The bond energy curve for π -complexes is displaced relative to those of the two-centre, two-electron [2c-2e] bonded species and this displacement accounts for the significant influence of electronegativity difference on reactions proceeding via [3c-2e] bonded intermediates or transition states. The origin of the displacement of the bond energy versus electronegativity difference curve for the π -complexes is identified as a $-2h\beta_{BB}$ term in the bond energy equation. In contrast to [2c-2e] bonds, this term makes the influence of electronegativity difference on triangular [3c-2e] bonds directional, that is, the bond energies of AB_2^+ and BA_2^+ are different in contrast to those of AB and BA. A more electronegative atom A destabilises the [3c-2e] bond by removing electron density from the bonding interaction BB (β_{BB}) whereas a less electronegative atom A will strengthen the bond by increasing the electron density between the atoms B. Reactions involving [3c-2e] AB_2^+ bonds are classified as homo- or heteroprocesses and the influence of electronegativity difference on these discrete transformations is discussed in terms of the contribution of h , h^2 and $-2h\beta$ functions to differences in bond energy. The analysis is extended to π -complexes with back-donation and the equivalence of the description of onium ions using either two [2c-2e] bonds or two [3c-2e] bonds is demonstrated. Extension of the analysis to 2-norbornyl cations suggests that, due to the shape of the bond energy versus electronegativity difference curve, this cation exists within a window of stability between the alternative isomers. 1,2-Disubstituted norbornyl cations are used as a model of π -complexes and the influence of substituent effects on relative stability is explored using the AM1 method. After allowance for resonance and hyperconjugation effects, the results are found to be consistent with the general conclusions of the simple HMO model.

© 2004 Elsevier Ltd. All rights reserved.

1. Introduction

Accurate calculations of molecular structure and properties are now readily accessible and can be applied to a wide range of chemical problems.¹ These calculations are structure specific and it is not always easy to make generalisations from the accurate data that they produce. In contrast, simple and approximate semi-quantitative models can produce general analytical expressions for molecular properties but these are lacking in accuracy and reliability. Nevertheless, used with care they can usefully bridge the gap between qualitative theories and specific calculations by (i) providing a semi-quantitative general model of the effects of structure variation on properties and by (ii) directing attention to areas worthy of detailed investigation by accurate structure-specific techniques. Both

approaches, particularly when used together, can make a useful contribution to an understanding of structure and reactivity² and can focus experimental studies on new areas worthy of investigation.

We have recently described³ a semi-quantitative model of triangular three-centre, two-electron [3c-2e] bonds of the type AB_2^+ based on the HMO approximation.^{4,5} This model suggests that the bond energies of these [3c-2e] bonds (AB_2^+ defined relative to $A^++B^++B^+$), like those of two-centre, two-electron [2c-2e] bonds (AB defined relative to A^++B^+), are related to the electronegativity difference ($\Delta\chi$) between the atoms or groups A and B. However, for the [3c-2e] bonds the influence of electronegativity on bond energy is a function of both $(\Delta\chi)^2$ and $\Delta\chi$ and, in contrast to bonds AB, the influence of $\Delta\chi$ is directional, that is, the bond energies of AB_2^+ and BA_2^+ are different whereas those of AB and BA are the same. This directional relationship may at least in part be responsible for the observation that reactions occurring via triangular three-centre bonds (π -complexes) appear to be significantly affected by electronegativity

Keywords: Norbornyl cations; Electronegativity; Three-centre bonds; π -Complex; Carbonium ions; Bond energies.

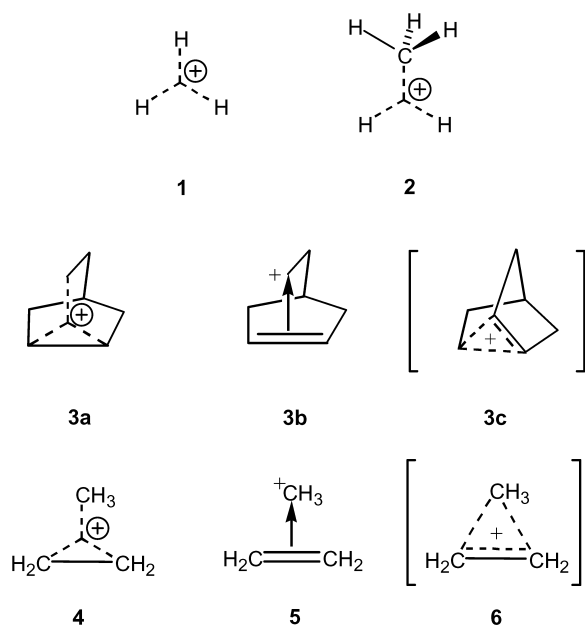
* Tel.: +44-1782-583045; fax: +44-1782-712378;

e-mail address: c.a.ramsden@chem.keele.ac.uk

difference. We have described this additional influence of electronegativity difference as the $-2h\beta$ effect because it is this term in the general bond energy equation that gives rise to the directional effect. Details of the derivation of this model have been described elsewhere,³ where it was discussed primarily using experimental data for reactions involving σ bonds. In this paper we explore the application of this model to three-centre bonds formed from π bonds (π -complexes) and extend the application to include a semi-quantitative model of 'back-donation'. We then explore conclusions and predictions of this model using more accurate structure-specific MO calculations.

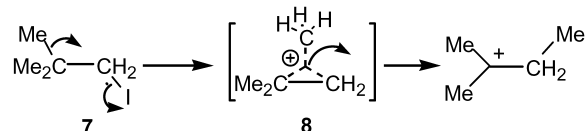
2. Background

Many organic reactions involving electrophiles proceed via species (intermediates or transition states) that involve triangular $[3c-2e]$ bonding.^{6–10} These species are often, but not always, cations. In the gas phase, cations containing a $[3c-2e]$ bond are often more stable than isomeric systems in which the electron pair is associated with a $[2c-2e]$ bond. The simplest examples are the triatomic hydrogen molecular ion H_3^+ , which has an equilateral triangle structure **1**,^{11,12} and the methonium ion CH_5^+ **2**.^{13–16} In solution, solvation usually favours two-centre bonding and only rarely are $[3c-2e]$ bonded species, such as the 2-norbornyl cation **3**, stable enough to be observed experimentally.^{17–19} Nevertheless, their involvement in chemical reactions of both σ and π bonds is now well established.⁶



Dewar in 1945, was the first to recognise that alkenes could form dative bonds with electrophiles.^{20–23} He described these products as π -complexes, recognised their relationship to aromatic species, and represented them using a dative bond arrow between double bond and electrophile, for example, **5**. Using this representation of $[3c-2e]$ bonds the 2-norbornyl cation is represented by structure **3b**. Many electrophilic addition reactions of alkenes and 1,2-rearrangements of carbenium ions are interpreted in terms of π -complex formation. A well-known example is the

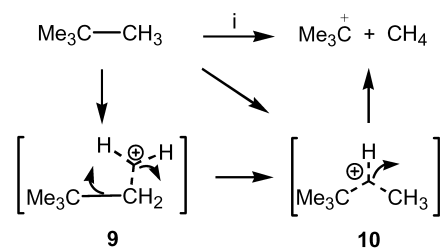
Wagner–Meerwein rearrangement, exemplified by the rearrangement of neopentyl iodide **7** via the π -complex **8**, as shown in Scheme 1.^{24,25} Whether the π -complex is an intermediate or transition state in these rearrangements and whether it is preceded by carbenium ion formation (e.g., $Me_3C-CH_2^+$) appears to depend on the individual structure and reaction conditions.²⁶ The π -complex concept was extended by Dewar to incorporate back-donation by an electron pair on the electrophile (a reverse dative bond).^{27,28}



Scheme 1.

Based on AIM and ELF studies of the 2-norbornyl cation,^{29–31} it has been proposed that the alternative representation of $[3c-2e]$ bonds by structures of the type **3c** and **6** is misleading and should be avoided. A study of the calculated electron density in the 2-norbornyl cation **3** indicated that there is no 'bond path' connecting the bridging carbon and each of its neighbours. Structures of the type **4** or **5**, implying tetracoordinate carbon, appear to be a more realistic representation of the bonding. Here, and throughout, we represent π -complexes (e.g., **8**) using the branched dashed line convention advocated by Olah^{6,32} to represent the three-centre bonding. This provides a consistent representation for both π and σ bonds, facilitates the writing of mechanisms using curly arrows and is consistent with the electron density studies described above.^{29–31} Additional reasons for favouring the representation **4** in preference to the dative representation **5**, based on the implications of dative bond arrows, are given in Section 3.1.4.

Sigma bonds are weaker donors than π -bonds and only react with electrophiles under much more severe conditions. It was not until the 1960s that Olah^{32–35} and others,^{36,37} using superacids and other new methodology, were able to demonstrate the σ -basicity of C–H and C–C single bonds with a range of electrophiles to give products via triangular $[3c-2e]$ bond formation. Thus, the protolysis of neopentane in $HF-SbF_5$ gives predominantly C–C cleavage with methane formation (Scheme 2).³⁸ This reaction occurs via the $[3c-2e]$ bonded cation **10**, which is analogous to a π -complex and could be represented using a dative bond (cf. **4**). Formation of the species **10** may be preceded by C–H bond protonation to give the cation **9** which then undergoes a bond–bond rearrangement (**9**→**10**).^{39–41} The universal role of $[3c-2e]$ bonding in the reactions of σ - and π -bonds (σ and π donors) with electrophiles has been



Scheme 2. Reagents: (i) $HF-SbF_5$.

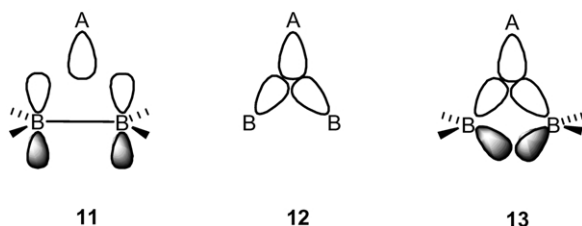
emphasised by Olah.³² Dewar²² has emphasised that [3c-2e] bonded species/ π -complexes are associated with strong chemical bonds and are distinct from more weakly bonded van der Waals complexes.

The bonding of π -complexes, carbonium ions and other [3c-2e] bonded systems has been described by qualitative MO models and by increasingly sophisticated computer-aided MO calculations on specific systems. The HMO model that we have recently described³ extends the qualitative analysis to a semi-quantitative description of [3c-2e] bonding in terms of generalised analytical expressions for relative bond energies. This permits some cautious generalisations on the influence of the electronegativity of the participating atoms on the relative strength of three-centre bonds and their ease of reaction. This model, therefore, bridges the gap between qualitative general pictures and sophisticated structure specific calculations and allows some conclusions that are not readily forthcoming from the other approaches, and which may be useful as a general reactivity guide to practicing chemists. We are aware of the limitations of the HMO method^{4,5,42} but we emphasise that the objective of this study is to identify general trends and their origins and not to calculate accurate energies. We now explore in more detail the application of this model to structures and reactions involving ‘ π -complexes’ and extend the application to include ‘back-donation.’

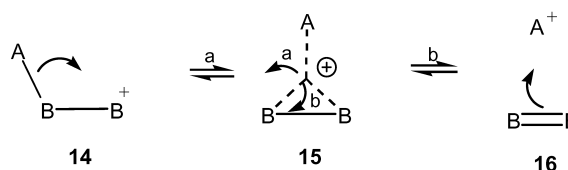
3. Results and discussion

3.1. π -Complex formation: a semi-quantitative model

3.1.1. Bond energies. A π -complex can be considered to be formed by overlap of the p_z orbitals of a π bond B=B with a hybrid orbital on atom A (**11**). Here the BB overlap is different to the AB overlap and any interaction with the BB σ bond is neglected. The orbital topology is similar to but different from that envisaged for formation of a three-centre bond by a σ bond (i.e., **12**). A closer relationship between these types of three-centre, two-electron bond is achieved if the double bond forming the π -complex is considered to be formed by overlap of sp hybrid orbitals. The three-centre bond is then formed by overlap with two of these hybrids as shown in structure **13**. This approach has the advantage that participation of the BB σ bond is not neglected.



The purpose of the semi-quantitative model described here is to focus attention on generic features that merit further investigation by accurate structure specific calculations. Considering the approximations used, we do not believe that the extra refinement of the four-electron model **13** is either justified or provides additional insight (see later). Only the



Scheme 3.

two-electron model **11** will be employed in the following discussion.

Consider the formation of the π -complex **15** from the classical precursors **14** and **16** (Scheme 3). In the HMO model, details of which we have described elsewhere,³ the orbital energies (E_{14} , E_{15} and E_{16}) of the localised orbitals accommodating the electron pair involved in the change of bonding are given by Eqs. 1–3.

$$E_{14} = \alpha_B + 1/2h + 1/2[h^2 + 4\beta'_{AB}{}^2]^{1/2} \quad (1)$$

$$E_{15} = \alpha_B + 1/2(h + \beta_{BB}) + 1/2[h^2 - 2h\beta_{BB} + \beta_{BB}^2 + 8\beta_{AB}^2]^{1/2} \quad (2)$$

$$E_{16} = \alpha_B + \beta_{BB} \quad (3)$$

In Eqs. 1–3, the parameter h is the difference between the Coulomb integrals of atoms A and B (i.e., $h = \alpha_A - \alpha_B$) and can be taken as a measure of the electronegativity difference ($\Delta\chi$) between the atoms A and B (i.e., $h \propto \Delta\chi$).⁴ The resonance integrals in the π -complex are defined as β_{AB} and β_{BB} , and β'_{AB} is the resonance integral of the σ -bond in the ion **14**. As previously, based on second-moment scaling,⁴³ we assume that the resonance integral of the σ bond AB (β'_{AB}) is related to the corresponding integral in the π -complex (β_{AB}) by $\beta'_{AB} = \sqrt{2}\beta_{AB}$. Although the choice of $\beta_{AB} = \sqrt{2}\beta_{AB}$ may appear arbitrary it is not unreasonable (the two-centre bond is shorter) and it is easily shown that the choice does not affect the general conclusions (see later).

The bond energies (BE) of the species **14**, **15** and **16** relative to the energy of the dissociated system $A^+ + B^- + B^+$ (i.e., $2\alpha_B + h$) are therefore given by Eqs. 4–6. Note that the choice of the reference point does not matter since we are only interested in the relative energies of the species **14**, **15** and **16** and these are independent of the reference frame chosen. This is illustrated by comparing Figure 1(c) and (d) (see below).

$$BE_{14} = -[h^2 + 8\beta_{AB}^2]^{1/2} \quad (4)$$

$$BE_{15} = -\beta_{BB} - [h^2 - 2h\beta_{BB} + \beta_{BB}^2 + 8\beta_{AB}^2]^{1/2} \quad (5)$$

$$BE_{16} = h - 2\beta_{BB} \quad (6)$$

Eq. 4 is in agreement with Pauling's empirical relationship for two-centre bond energies:^{44–47} bond energy (BE_{14}) is at a minimum when $h=0$ (i.e., $\Delta\chi=0$) and increases as electronegativity difference increases. Note that it does not matter if h is positive or negative since h^2 is always positive. In the region $h=0$ the hyperbola (Eq. 4) is relatively flat ($\partial BE_{14}/\partial h=0$ when $h=0$). For small values of h the variation of bond energy will be small, in agreement with calculated values of intrinsic bond energies.^{48,49}

The bond energy equation for the three-centre bond **15**

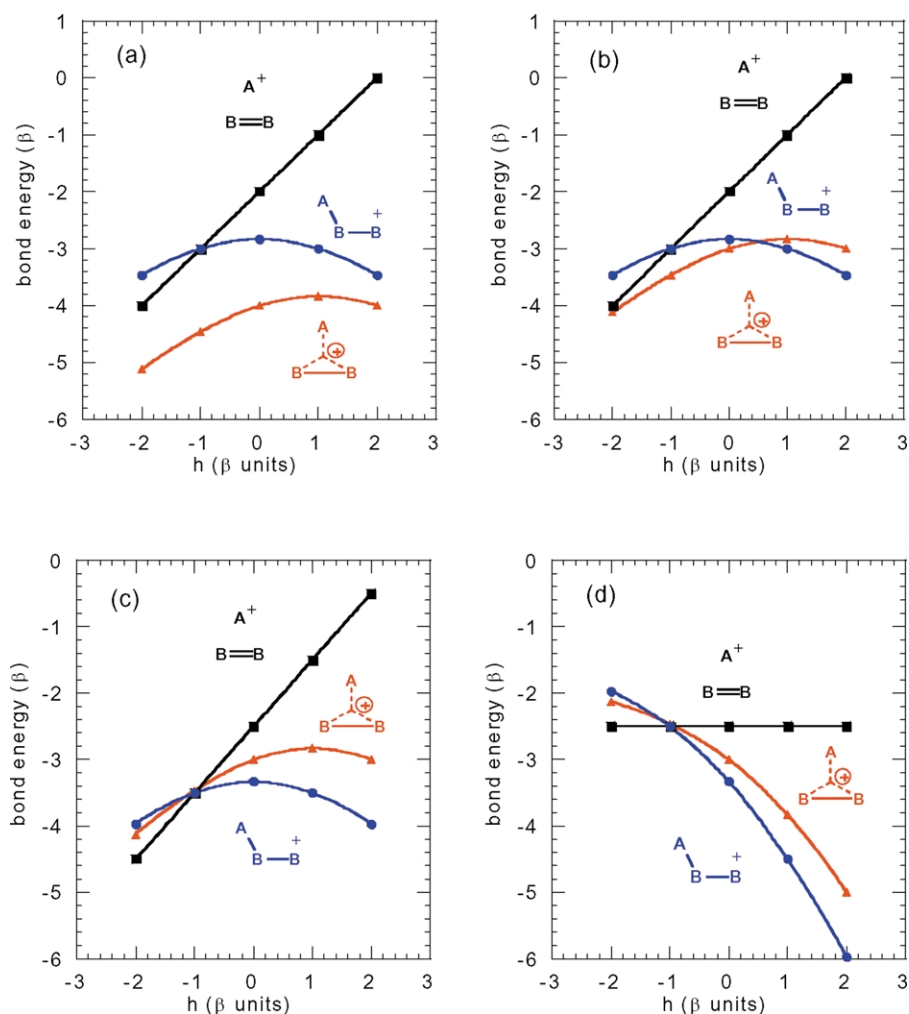


Figure 1. Calculated relative energies of species **14**, **15** and **16** with variation of h : (a) relative bond energies using Eqs. 4–6; (b) relative energies with allowance for nuclear repulsion; (c) relative energies with allowance for nuclear repulsion and solvation; (d) relative energies defined with respect to $A^+ + 2B^-$ instead of $A^+ + B^- + B^+$.

(Eq. 5) shows interesting similarities to and differences from the expression for the two-centre bond **14** (Eq. 4). Both curves are hyperbolas but the $[3c-2e]$ bond curve is displaced along the h -axis by β_{BB} . Both bond energy expressions contain h^2 and $8\beta_{AB}^2$ terms, which seems reasonable. Although each A–B bonding interaction in the three-centre bond will be weaker, there are two interactions instead of one, which compensates. For the three-centre bond (Eq. 5) there are three additional terms each involving β_{BB} . The first two terms essentially reflect the new bonding interaction (B–B) that takes place as the bond forms and accounts for the greater stability of the $[3c-2e]$ bond in the gas phase (Fig. 1(a)). These β_{BB} terms can be considered to describe the favourable cyclic conjugation relative to a linear $[3c-2e]$ bond ($B \cdot \cdot A \cdot \cdot B$).

Figure 1(a) shows a plot of the bond energies given by Eqs. 4–6 against h , assuming that $\beta_{AB} = \beta_{BB}$. If the bond energy expression for the π -complex **15** was limited to these two additional terms in β_{BB} then it also would be a symmetrical hyperbola with minimum energy when $h=0$. If this were the case, then variation of the electronegativity difference between atoms A and B would have little influence on the difference in bond energy between **14** and **15**. However,

there is an additional term ($-2h\beta_{BB}$) that considerably modifies the form of the hyperbola. This term in effect displaces the hyperbola along the h axis and increases or decreases the bond energy depending upon whether h is positive or negative. When h is positive there is a negative contribution to BE_{15} and vice versa. The minimum bond energy occurs when $h = \beta_{BB}$ and when $h=0$ the gradient ($\partial BE_{15}/\partial h$) is 0.33. The bond energy difference between the isomeric systems **14** and **15** will therefore vary significantly with electronegativity difference (h), especially in the region $h=0$. In other words, in contrast to $[2c-2e]$ bonds, there is a directional influence of electronegativity difference on the bond energy of $[3c-2e]$ bonds. We have described this influence of electronegativity difference as the $-2h\beta$ effect because it is this term that accounts for it in the HMO model and this emphasises the contribution of both h and β_{BB} . This influence of electronegativity difference (h) on the bond energy of isomers **14** and **15** is not the result of dative bond formation (e.g., **4**), which would involve a full h term in the bond energy difference. The contribution of h to dative bonds is discussed in Section 3.1.3.

The bond energy expression for the dissociated system **16** is

much simpler and in this model is represented by a linear relationship (Eq. 6) (Fig. 1).

Before allowing for the effects of nuclear repulsion and solvation it is informative to consider the relative values of the energies given by Eqs. 4–6. If we assume that the energies of all the other electrons remain unchanged, Eqs. 4–6 give the relative electronic energies of the isomeric cations **14–16**. A plot of Eqs. 4–6 is given in Figure 1(a). This shows that the bond energy for the π -complex is greatest over a wide range of h values. However, some allowance for the differences in nuclear repulsion (ΔE_{nuc}) and for solvation (ΔE_{solv}) needs to be made in order to model relative energies. Here it is necessary to take a semi-empirical approach and use values that lead to a model consistent with experimental observations. We have assumed that ΔE_{nuc} and ΔE_{solv} are independent of h . The nuclear repulsion energy will be greatest for the cyclic cation **15** and we can allow for this by decreasing the relative bond energy of species **15** by $+\Delta E_{\text{nuc}}$. Using a value of $+\Delta E_{\text{nuc}}=1.0\beta_{\text{AB}}$ gives the gas phase energy profile shown in Figure 1(b). With this allowance for nuclear repulsion the gas phase π -complexes **15** are expected to be more stable than the isomers **14** and **16** over a wide range of h values and this is in agreement with experiment and theory. A large part of the extra stability of the gas phase π -complexes **15** relative to the isomers **14** is attributable to the BB interactions in the bond energy expression (Eq. 5).

Most reactions of interest occur in the solution phase, in which the relative stabilities of the classical and non-classical ions are reversed. The $[2c-2e]$ bonded systems **14** and **16** are more stable and the $[3c-2e]$ bonded systems **15** correspond to intermediates or transition states. This reversal of stability can be partially attributed to greater solvation of the classical cations **14** and **16** with localised positive charge than that of the non-classical cations **15** with greater delocalisation of charge. This extra solvation of classical ions can be modelled by lowering the bond energies of the cations **14** and **16** by ΔE_{solv} . Again it is necessary to be pragmatic in selecting a value for ΔE_{solv} . It is known that for simple organic reactions (in the region $h=0$) the π -complex is an intermediate/transition state in the degenerate rearrangement of the cations **14** and the activation energy is quite small.^{36,50–52} This, therefore, places the hyperbola of the non-classical species **15** only just above the hyperbola of the classical ion **14**. We have therefore used a value of $\Delta E_{\text{solv}}=-0.5\beta_{\text{AB}}$. Using this allowance for nuclear repulsion and solvation, the relative bond energies (RBE) of the species **14–16** are modelled by Eqs. 7–9. The resulting plot of relative energies in solution is shown in Figure 1(c) where it is assumed that $\beta_{\text{AB}}=\beta_{\text{BB}}$.

$$\text{RBE}_{14} = -[h^2 + 8\beta_{\text{AB}}^2]^{1/2} - 0.5\beta_{\text{AB}}(\Delta E_{\text{solv}}) \quad (7)$$

$$\begin{aligned} \text{RBE}_{15} = & -\beta_{\text{BB}} - [h^2 - 2h\beta_{\text{BB}} + \beta_{\text{BB}}^2 + 8\beta_{\text{AB}}^2]^{1/2} \\ & + 1.0\beta_{\text{AB}}(\Delta E_{\text{nuc}}) \end{aligned} \quad (8)$$

$$\text{RBE}_{16} = h - 2\beta_{\text{BB}} - 0.5\beta_{\text{AB}}(\Delta E_{\text{solv}}) \quad (9)$$

At this stage some comments on the assumptions and estimations used in this model are appropriate. The allowance for nuclear repulsion and solvation is purely

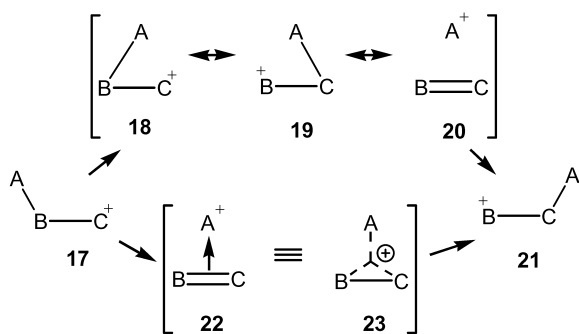
empirical and the values are chosen to give a model consistent with the observation that simple π -complexes are not detectable in solution but are accessible during reactions. The separation of the parameters ΔE_{solv} and ΔE_{nuc} is artificial and is done only to acknowledge their contributions. There is some evidence that the difference in solvation energies in aqueous solution is smaller than we have suggested.⁵³ An alternative approach would be to arbitrarily choose parameters to allow for these and other effects that only move the curves on the y-axis and thereby place the bond energy relationships in the same juxtaposition. We also recognise that we have assumed that $\beta_{\text{AB}}=\beta_{\text{BB}}$ without justification and that the relationship $\beta'_{\text{AB}}=\sqrt{2}\beta_{\text{AB}}$ is imprecise. However, variation of the relative β values makes little difference to the general features of Figure 1. For example, different values for β simply move the hyperbola for the classical ion **14** up or down the y-axis and the effect is therefore incorporated into the semi-empirical parameters (ΔE_{solv} and ΔE_{nuc}) discussed above. We regard the main value of the model summarised by Figure 1 as providing an approximate evaluation of the relative energies of the species **14–16** as electronegativity difference varies. This provides insight into the nature of the bonding that is not forthcoming from either qualitative models or highly accurate calculated properties of a limited number of structures. It is important to reiterate here that the parameters ΔE_{solv} and ΔE_{nuc} and the β values only move the relative positions of the bond energy graphs in Figure 1 up or down the y-axis. They do not move the curves along the x-axis and this leads to important conclusions. It is relevant to point out here that the use of the four-electron model **13** also only moves the relative positions of the bond energy graphs on the y-axis and does not alter the conclusions, which is why we have used the simpler two-electron model **11**.

Figure 1(d) shows the energies of species **14–16** calculated relative to $A^+ + 2B^-$ and demonstrates that their relative energies are independent of the reference frame chosen (cf. Fig. 1(c) and (d)).

3.1.2. π -Complex structure and stability. Eqs. 7–9 describe a semi-quantitative model for the relative bond energies of the species **14**, **15** and **16** in solution. This model suggests certain features that are worthy of further exploration and which may give further insight into the nature of triangular three-centre bonding. First, because of the $-2h\beta$ effect, there is a crossover of the relative energies of the classical **14** and non-classical ion **15**. However, as the non-classical species (π -complex) becomes more favoured so does the dissociated product **16**. This suggests that simple π -complexes **15** (without back-donation) are never more stable in solution than the isomers **14** and **16**. It is interesting to question how close they come to being the most stable structure in solution or even whether there is always a small window of stability. The special case of the 2-norbornyl cation is discussed in Section 3.3.

A second point that becomes clear from the bond energy expression for π -complexes **15** (Eq. 5) is that the B–B interaction (β_{BB}) makes an important contribution to their stability and that part of this contribution is dependant on electronegativity difference. For molecular rearrangements

the contribution of the B–B interaction in terms of qualitative resonance theory was recognised by Wheland.⁵⁴ He pointed out that in the general rearrangement **17**→**21** (Scheme 4) the intermediate species is a resonance hybrid of the structures **18**, **19** and **20**. Interestingly, Wheland emphasised the contribution of the structures **18** and **19** but made little comment on structure **20**, other than to say that it may ‘also have a significant weight’, and its contribution to rearrangement mechanisms was largely ignored in subsequent discussion. Here it is worth noting that the π -complex approach of Dewar (i.e., **22**) clearly emphasises the contribution of hybrid **20** but neither of these qualitative analyses focus attention on the combined influence of $\Delta\chi$ and β (i.e., $-2h\beta$). Later, the relative importance of the resonance hybrids **18**–**20** as electronegativity varies was briefly discussed in qualitative terms by Berson and Suzuki⁵⁵ and using qualitative arguments Dewar showed that classical ions, for example, **17**, can be expected to be favoured as the electronegativity of the apical group A increases.²⁸ Based on the semi-quantitative model described by Eqs. 7–9, the important quantitative contribution of the resonance hybrid **20** in determining relative stability of the intermediate species **23** with respect to the reactant **17** and product **21** can be appreciated. In particular the important β_{BB} terms in Eq. 5 describe the contribution of the hybrid **20**. This contribution is enhanced or reduced depending upon the relative electronegativity of the atoms and the absolute value of the resonance integral (β_{BB} or β_{BC}). This is the $-2h\beta$ effect: rearrangement will be easier when $-h$ and β are maximised. On their own, the hybrids **18** and **19**



Scheme 4.

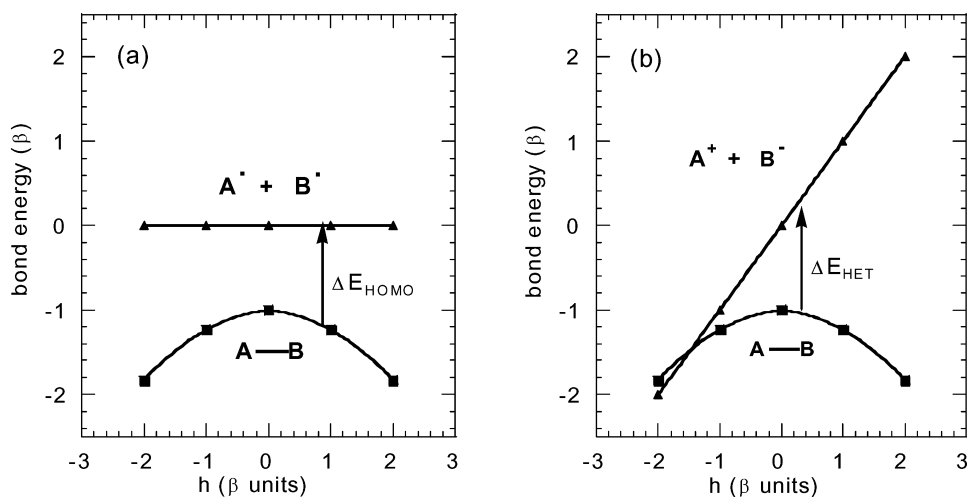
have little energetic influence relative to the precursor **17** (cf. Eqs. 4 and 5). The HMO model permits the general qualitative analysis of three-centre bonding based upon qualitative resonance⁵⁵ and MO^{20–22,27,28} theories to be developed into a general semi-quantitative analysis and this is explored further in Section 3.1.3

3.1.3. The influence of electronegativity on heterolytic and homolytic cleavage of two-centre bonds (A–B). To analyse the influence of electronegativity on reactions involving [3c-2e] bonds, it is useful to recognise a distinction between heterolytic and homolytic transformations. This is also relevant to deciding whether [3c-2e] bonds are appropriately represented as dative bonds (e.g., **5**) or by alternative representations (e.g., **4**), and this point is discussed further in Section 3.1.4.3. To emphasise similarities to and differences from two-centre bonds, we briefly discuss the influence of electronegativity on two-electron dative bonds ($B^- \rightarrow A^+$) before further discussing three-centre bonds.

All covalent bonds can in principle be regarded as dative bonds: a simple C–C bond can be envisaged as $C^- \rightarrow C^+$. Consider the general case of a dative bond between a Lewis acid A^+ and a Lewis base B^- [$B^- + A^+ \rightleftharpoons B^- \rightarrow A^+ \leftrightarrow B-A$]. The energies of the precursor lone pair and [2c-2e] bond, relative to $A^+ + B^-$ using the HMO model described above, are h and $-[h^2 + 4\beta_{AB}^2]^{1/2}$, respectively. In other words, the bond energy of the dative bond $B^- \rightarrow A^+$ relative to $B^- + A^+$ is given by the expression:

$$\{-h - [h^2 + 4\beta_{AB}^2]^{1/2}\}$$

It is made up of two components: these are the energy involved in transferring one electron from donor to acceptor ($-h$) and the bond energy of the covalent bond between A^+ and B^- ($-[h^2 + 4\beta_{AB}^2]^{1/2}$). Depending upon the direction of the reaction, the term $-h$ is characteristic of dative bond formation or heterolytic cleavage and makes an important contribution to the energetics of chemical transformations. After allowing for nuclear repulsion ($+1.0\beta_{AB}$), plots of bond energy versus electronegativity difference (h) for the species $B^- + A^+$, $B^- \rightarrow A^+ \leftrightarrow B-A$ and $B^+ + A^-$ are shown in Figure 2.

Figure 2. The calculated influence of h on the energy of (a) homolytic and (b) heterolytic cleavage of a two-centre, two-electron bond A–B.

Here, and elsewhere, it is important to recognise the difference between the theoretical bond energy and the experimental bond dissociation energy, which will involve a number of other factors. The HMO model describes important but incomplete contributions to the bond dissociation energy and should only be used to discuss trends rather than actual energies. Within this model, when $h \approx 0$ the energy of $B^- + A^+$ and $B^\cdot + A^\cdot$ are the same because, among other things, no allowance is made for electron–electron repulsion which is less in the diradical. In reality when $h = 0$ the diradical will be more stable than the ion-pair (e.g., $C^\cdot + C^\cdot$ vs $C^+ + C^-$) and homolytic cleavage (ΔE_{HOMO}) of the bond is optimal (Fig. 2(a)). However, when one of the atoms becomes more electronegative ($h < 0$) heterolytic cleavage rapidly becomes the energetically favoured mode of reaction (ΔE_{HET}) (Fig. 2(b)). The greater the electronegativity (or more correctly the greater the Coulomb integral) of the donor atom B relative to the acceptor A, the easier heterolytic cleavage (ΔE_{HET}) becomes and this is directly related to the $-h$ term in the bond energy expression. A crossover of the energies occurs when $-h$ reaches a certain value and ionisation predominates. Increasing the electronegativity (Coulomb integral) of an atom facilitates heterolytic cleavage (e.g., $-\text{OH} \rightarrow -\text{OH}^\cdot$ and $-\text{F} \rightarrow -\text{FSbF}_5$).^{56,57}

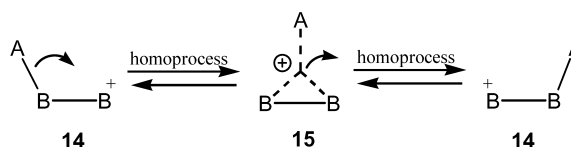
Although we have described bonds as dative (i.e., $B^- \rightarrow A^+$) in the preceding discussion, the concept of dative bonds is unnecessary, although sometimes convenient, and all dative bonds can be represented as conventional covalent bonds (e.g., $\text{Me}_3\text{N}^+ - \text{BF}_3^-$ instead of $\text{Me}_3\text{N} \rightarrow \text{BF}_3$).⁵⁸ For heterolytic cleavage the bond energy of covalent bonds is related to electronegativity difference (h) by a simple $-h$ term plus an h^2 function and the ease of heterolytic cleavage is highly dependant upon h . As h becomes increasingly more negative the bond rapidly weakens (Fig. 2(b)). For homolytic cleavage there is no $-h$ term in the energy of cleavage (only an h^2 function) and as a result homolytic cleavage is not enhanced as the electronegativity difference (h) increases (Fig. 2(a)). Although not necessarily expressed in terms of a simple HMO model, these features of [2c-2e] covalent bonds are well known. Figure 2(a) is in good qualitative agreement²³ with Pauling's empirical relationship between [2c-2e] homolytic bond energies and electronegativity.^{44–47} In applying the HMO approximation to [3c-2e] bonds it is reassuring that a similar application to [2c-2e] bonds gives a semi-quantitative model that is consistent with general experimental observations.

We have briefly discussed two-centre bonding here so that similarities and differences in three-centre bonding can be emphasised. In three-centre bonding, in addition to energy differences for bond formation and cleavage being related to $-h$ (heterolytic cleavage) and an h^2 function (heterolytic and homolytic cleavage), a dependence on a $-2h\beta$ function, not encountered with [2c-2e] bonding, influences the energy of some [3c-2e] bond transformations. Just as for two-centre bonds, it is important to distinguish between the types of transformation involved in the reactions of triangular [3c-2e] bonded species AB_2 .

3.1.4. Homoprocesses and heteroprocesses of [3c-2e] bonds (AB_2). We refer to the formation and breaking of a

[3c-2e] bond AB_2 as a *heteroprocess* if the pair of electrons moves from an association with only nuclei B to an association with both A and B, or vice versa. We refer to the formation and breaking of a [3c-2e] bond AB_2 as a *homoprocess* if the pair of electrons retains an association with both nuclei A and B during the transformation. These processes correspond to heterolytic and homolytic mechanisms in two-centre bonds A–B but we use different terms to avoid confusion.

3.1.4.1. Degenerate rearrangements. Consider the generalised degenerate 1,2-shift occurring via a transition state that is assumed to resemble the [3c-2e] bonded species **15** as shown in Scheme 5. Both steps in this transformation involve homoprocesses and as a result there is not a large influence of electronegativity difference on the activation energy (i.e., no $-h$ term). However, because of the involvement of the three-centre bonding, there is a contribution of both h^2 and $-2h\beta$ functions to the energy difference. This results in asymmetry of the hyperbolas describing the relative bond energies of reactant and transition state. The relative energies of the species **14** and **15** are given by Eqs. 7 and 8 and a plot of these energies (assuming $\beta_{\text{AB}} = \beta_{\text{BB}}$) is shown in Figure 3(a). Inspection of Figure 3(a) reveals that the activation energy of the rearrangement can be expected to increase as the electron-withdrawing power (electronegativity) of the migrating group A increases relative to B (i.e., h increasing). Degenerate 1,2-hydride and alkyl shifts are usually very fast and a number of factors including steric and conformational effects will also determine the rate of reaction. However, the influence of electronegativity difference summarised in Figure 3(a) is consistent with the general view that the inherent migratory aptitude of groups is $\text{H} > \text{alkyl}$ and $\text{Me}_3\text{C} > \text{H}_3\text{C}$.^{59,60}



Scheme 5.

Migratory aptitude of alkyl substituents is often discussed in terms of hyperconjugation and the stabilisation of developing positive charge on atom A. This deserves some comment. In the positively charged [3c-2e] bonded species **15** the Coulomb integral (electronegativity) of alkyl groups A will vary. Hyperconjugation and the electronegativity/electron-withdrawing power of a charged alkyl group are intimately related. The electronegativity (Coulomb integral) of a methyl cation (Me radical IP 9.8 eV) is greater than that of a *t*-butyl cation (tBu radical IP 7.2 eV) and this can be rationalised in terms of hyperconjugation. The group orbitals of the methyl substituents in the tertiary cation interact with the empty orbital and reduce the Coulomb integral: an electron is held more weakly than by a methyl cation. During the change **14**→**15** the positive charge will increase on atom A and it can be interpreted that more electropositive groups will be better able to stabilise this charge. We suggest that an alternative interpretation of the influence of migrating group A on energy, which is highlighted by the HMO model, is the extent to which an atom or group A draws the pair of electrons away from the

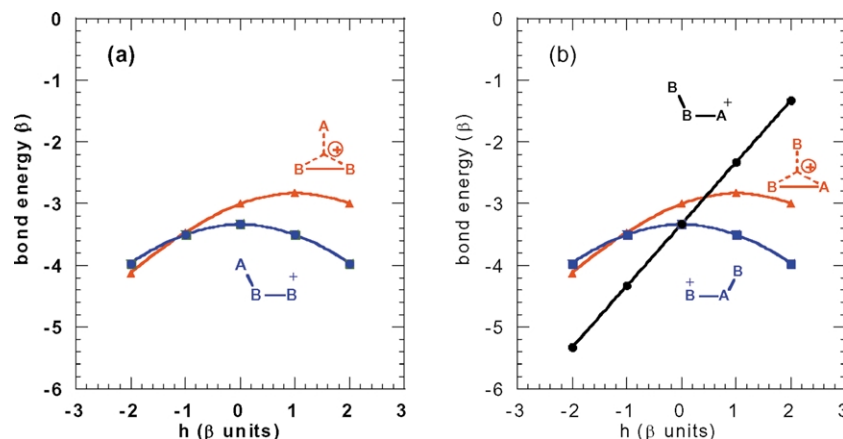


Figure 3. The calculated influence of h on the relative energies of products formed from a three-centre, two-electron bond AB_2^+ by (a) a homoprocess and (b) a heteroprocess.

bonding interaction BB (β_{BB}), or the reverse, and this effect is a function of both h and β_{BB} . This is the interaction that modifies the bond energy (Eq. 5) and this substituent effect on bond energy will also modify the distribution of the electron pair. The influence of $-2h\beta_{BB}$ on energy is therefore reflected in the distribution of positive charge,⁶¹ and also in the bond lengths BB and AB (see Section 3.3.2 and references cited therein). A migrating *t*-Bu group will allow the retention of more bonding between BB in the transition state **15** than the more electronegative Me group and this accounts for a variation in activation energy as h varies (Fig. 3(a)). If this is the case, then it is important not to focus only on substituent effects (e.g., hyperconjugation) on the migrating group A. Substituent effects on the atoms B will also influence the relative energies. The difference in the properties of A and B (e.g., h) should be emphasised rather than effects at a single centre. On the basis of Figure 3(a), 1,2-hydride and 1,2-alkyl shifts between secondary carbons can be expected to be faster than those between tertiary carbons.⁶²

For a discussion of electronegativity difference of functional groups, group electronegativities are available but these have been derived for application to $[2c-2e]$ bonds in neutral species.^{63,64} In fact the electronegativities of carbon atoms in alkyl groups vary little in these bonds and this is reflected in fairly constant bond energies in CC bonds.^{48,49} This is not the case for charged species in which the electron-withdrawing power of alkyl groups will vary much more with structure. Strictly, different values of h should be used for species **14** and **15** but neglect of this does not change the conclusions.

On the basis of the above discussion, more electropositive substituents such as $SiMe_3$ should have a very high migratory aptitude. There is evidence to support this conclusion,^{65,66} which is also related to the well known β -effect in silicon-substituted carbocations.^{67,68} However, because the electropositive silyl substituent has a weaker hold on the pair of bonding electrons (thereby increasing the bonding interaction BB) elimination is also thermodynamically favoured (i.e., **15**→**16**; $A=SiR_3$) (Fig. 1(c), h negative) and products related to this alternative mode of cleavage are often formed. In accord with the general

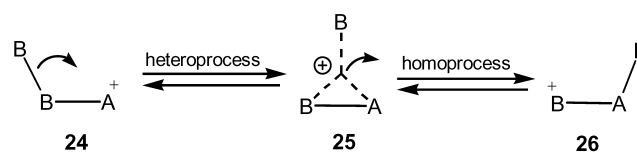
features of Figure 1(c), by using the more electronegative $SiCl_3$ substituent both elimination and the β -effect (and presumably the migratory aptitude) are diminished.^{69,70} For the same reasons the migratory aptitude of fluoroalkyl substituents (e.g., CF_3) can be expected to be very low.

It is also important to emphasise that the above analysis only concerns the energy of the electron pair involved in the $[3c-2e]$ bond. Changes in the energies of other electrons may be relevant. For example, the cation B^+ (**14**) may be stabilised by resonance interactions (including hyperconjugation) and similar interactions with empty anti-bonding orbitals may stabilise cation **15**. These are important additional effects and should not be overlooked. They are well understood and are best taken into account on an individual basis (see also Section 3.3.2). Hyperconjugation effects must be separated into those that influence the energy of the bond electron pair and those that influence the energy of other electrons in the molecule (e.g., by stabilising B^+).

3.1.4.2. Non-degenerate rearrangements. Consider the non-degenerate 1,2-shifts shown in Scheme 6. The first step, which is $[3c-2e]$ bond formation, is now a heteroprocess and, just as for two-centre bonds (Figure 2), the energy difference involves a $-h$ term. Assuming $\beta_{AB}=\beta_{BB}$, within the HMO model the bond energies for the species **25** and **26** are the same as for the isomers **15** and **14** respectively and are given by Eqs. 7 and 8. The relative bond energy for species **24** is given by Eq. 10 (cf. Eq. 9). Figure 3(b) shows a plot of the relative energies.

$$RBE_{24} = h - 2\sqrt{2}\beta_{BB} - 0.5\beta_{AB}(\Delta E_{\text{solv}}) \quad (10)$$

It can be seen from Figure 3(b) that as the atom or group A becomes increasingly more electronegative relative to B the energy difference rapidly increases and there is a strong driving force for rearrangement (**24**→**26**). Even small electronegativity differences will have a big influence on

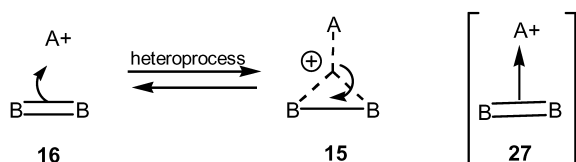


Scheme 6.

relative energies in the region $h \sim 0$. Figure 3(b) suggests that over a narrow range of positive h values the π -complex **25** will be a transition state with the activation energy rapidly decreasing as h increases. Above a certain h value the π -complex is no longer a transition state but simply a point on the energy surface describing the collapse of the cation **24** to the isomer **26**. It is well known that 1,2-shifts rapidly take place towards an electronegative electron-deficient centre such as O or N. The particularly strong driving force and influence of h arises because these rearrangements are heteroprocesses. Resonance stabilisation of the cations by substituents will also contribute to the observed relative stabilities.

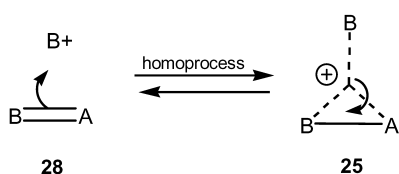
It is worth noting that Figure 3(b) may also provide some insight into concerted reactions such as the Baeyer–Villiger rearrangement⁷¹ in which the transition state is polarised and approximates to three-centre bonding. The relationship is similar to that of cyclopropanone to the cyclopropenyl cation. In the Baeyer–Villiger rearrangement the electronegative CH_3 substituent (B) has a low migratory aptitude and in practice never migrates whereas more electropositive R_3C groups migrate well. It also follows that as A becomes more electronegative, for example if the polarity of the reaction increases, selectivity in the migrating groups can be expected to decrease.

3.1.4.3. Addition–elimination. The addition of electrophiles (e.g., A^+ or B^+) to double bonds to form π -complexes AB_2^+ can also be classified as hetero- or homoprocesses. The relative bond energies for the addition **16**→**15** are given in Figure 1(c). As A^+ becomes more electronegative the reaction becomes increasingly exothermic due to the direct dependence on electronegativity difference (h) (Scheme 7).



Scheme 7.

For this heteroprocess (**16**→**15**) the dative π -complex representation **27** is excellent in many ways and is consistent with a $-h$ term in the bond energy difference. However, formation of the same species **15** by the homoprocess **14**→**15** (Scheme 5) does not involve a $-h$ term and structure **27** is not a meaningful representation of **15** when formed from the precursor **14**. As for two-centre bonds, the dative bond representation (e.g., **27**) is more a characteristic of the mode of formation (a heteroprocess) rather than of the structure. To use structure **27** correctly it is necessary to know the history of the molecule (or its fate).⁵⁸



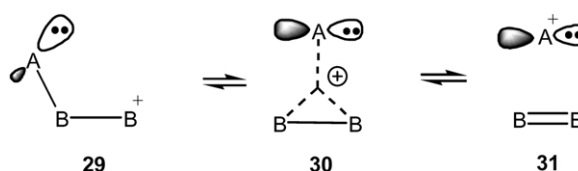
Scheme 8.

It is desirable to have a unique structural representation of $[3c-2e]$ bonds that has no reaction implications, in the same way that all $[2c-2e]$ σ bonds can be represented uniquely without the use of the dative notation. For this reason, together with the reasons discussed in Section 2, we prefer the universal use of the dotted line notation **15**.

Addition of an electrophile B^+ to an $\text{A}=\text{B}$ bond is a homoprocess (**28**→**25**) (Scheme 8) and the exothermicity of subsequent reactions will be determined by the structure of the alternative products **24** or **26** (Scheme 6). The structure of the thermodynamically more stable product (**24** or **26**) (Fig. 3(b)) is in accord with Markovnikoff's rule.

3.2. π -Complex formation with back-donation

3.2.1. Bond energies and the equivalence of three- and two-centre bonding.



Scheme 9.

Consider the formation of the π -complex **30** (Scheme 9) in which the atom or group A has a lone pair of electrons that can be used for back-donation to the anti-bonding orbital on BB. The bonding MO formed by this interaction is summarised by structure **32** and arises from the interaction of the atomic orbitals shown in structure **33**. Within the HMO approximation, the secular determinant for the system is:

$$\begin{vmatrix} \alpha_B + h - E & \beta''_{AB} & -\beta''_{AB} \\ \beta''_{AB} & \alpha_B - E & \beta_{BB} \\ -\beta''_{AB} & \beta_{BB} & \alpha_B - E \end{vmatrix} = 0$$

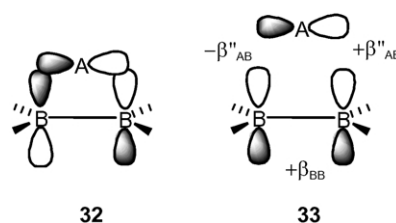
This is the same as the secular determinant for the $[3c-2e]$ bond interaction **11**, discussed in Section 3.1, except that one of the resonance integrals is negative. Solving this determinant gives the energy of the three-centre MO **32** in the form of Eq. 11.³

$$E_{32} = \alpha_B + 1/2(h - \beta_{BB}) + 1/2[h^2 + 2h\beta_{BB} + \beta_{BB}^2 + 8\beta_{AB}''^2]^{1/2} \quad (11)$$

The bond energy (BE_{32}) of the bond **32** relative to an isolated lone pair A: ($2\alpha_B + 2h$) is therefore given by Eq. 12.

$$\text{BE}_{32} = h + \beta_{BB} - [h^2 + 2h\beta_{BB} + \beta_{BB}^2 + 8\beta_{AB}''^2]^{1/2} \quad (12)$$

Note particularly that apart from the h term, which is discussed below, this differs from the bond energy



expression for the simple [3c-2e] bond **15** (BE₁₅) (Eq. 5) only in that the signs of the β_{BB} and $2h\beta_{\text{BB}}$ terms have been reversed. Here we have a $+2h\beta$ effect, which occurs because the interaction is with the anti-bonding orbital of the BB double bond.

Using our common reference points ($A^+ + A + B + B^+ = 4\alpha_{\text{B}} + 3h$), we are now able to write expressions for the bond energies of all four-electrons in the species **29–31** and these are given by Eqs. 13–15.

$$\text{BE}_{29} = -[h^2 + 8\beta_{\text{AB}}^2]^{1/2} \quad (13)$$

$$\text{BE}_{30} = h - [h^2 - 2h\beta_{\text{BB}} + \beta_{\text{BB}}^2 + 8\beta_{\text{AB}}^2]^{1/2} - [h^2 + 2h\beta_{\text{BB}} + \beta_{\text{BB}}^2 + 8\beta_{\text{AB}}^2]^{1/2} \quad (14)$$

$$\text{BE}_{31} = h - 2\beta_{\text{BB}} \quad (15)$$

Eqs. 14 and 15 both contain an h term. Before discussing the significance of these terms, first consider the bond energy expression for the three-centre bond with back donation **30** (BE₃₀). The two square root terms in Eq. 14 only differ in the sign of the $2h\beta_{\text{BB}}$ component and the values of the resonance integrals β_{AB} and β'_{AB} . For the purposes of analysis, let us first assume that $\beta_{\text{AB}} = \beta'_{\text{AB}}$. It can then be shown that because $[h\beta_{\text{BB}}]^2 \ll [h^2 + \beta_{\text{BB}}^2 + 8\beta_{\text{AB}}^2]^2$ the two $2h\beta$ terms effectively cancel each other out, that is,

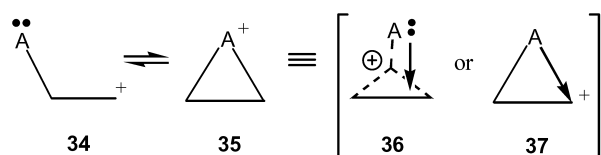
$$\begin{aligned} & -[h^2 - 2h\beta_{\text{BB}} + \beta_{\text{BB}}^2 + 8\beta_{\text{AB}}^2]^{1/2} - [h^2 + 2h\beta_{\text{BB}} \\ & + \beta_{\text{BB}}^2 + 8\beta_{\text{AB}}^2]^{1/2} \\ & \approx -2[h^2 + \beta_{\text{BB}}^2 + 8\beta_{\text{AB}}^2]^{1/2} \\ & = -2[h^2 + \beta_{\text{BB}}^2 + 4\beta'_{\text{AB}}^2]^{1/2} \quad (16) \end{aligned}$$

Eq. 16 is effectively the bond energy expression for two σ bonds (cf. Eqs. 4 and 13)—strengthened by some BB interaction (β_{BB}). In other words, with the assumption that $\beta_{\text{AB}} = \beta'_{\text{AB}}$, the bond energy (BE₃₀) of the [3c-2e] bond with back donation **30** (i.e., two three-centre bonds) is equivalent to that of two two-centre σ bonds plus an h term, that is,

$$\text{BE}_{30} \approx h - 2[h^2 + \beta_{\text{BB}}^2 + 4\beta'_{\text{AB}}^2]^{1/2} \quad (17)$$

The h terms in Eqs. 14, 15 and 17 arise because the back-donation of the lone pair A: is a heteroprocess, that is, the lone pair is forming a dative bond with the anti-bonding orbital. This therefore, introduces a strong dependence on electronegativity difference (h) for the transformation **29**→**30**.

The HMO model described by Eqs. 13–17 is therefore, entirely consistent with the representation of bromonium ions and related species (**35**; A=Br, Cl, OH, SR) by two covalent C–A bonds. When formed from the precursors **34** one of these bonds can be regarded as a dative bond (e.g.,



Scheme 10.

37) and is a heteroprocess. The species **35** can be regarded as being bonded by two three-centre bonds (**36**; Eq. 14) or by a pair of two-centre bonds (**35** or **37**; Eq. 17). The two descriptions are equivalent but the representation **35** is preferred (Scheme 10).

In practice the resonance integrals β_{AB} and β'_{AB} in Eq. 14 will not be equal in magnitude. The integral β'_{AB} can be expected to be smaller. Also the Coulomb integral for the lone pair electrons on atom A (α'_A) will be slightly smaller than α_A . If we assume that $\beta'_{\text{AB}} = 0.5\beta_{\text{AB}}$ and $h' = \alpha'_A - \alpha_B$ then the new bond energy expression for the cation **30** (BE'₃₀) is given by Eq. 18.

$$\begin{aligned} \text{BE}'_{30} = h' - [h^2 - 2h\beta_{\text{BB}} + \beta_{\text{BB}}^2 + 8\beta_{\text{AB}}^2]^{1/2} - [(h')^2 \\ + 2h'\beta_{\text{BB}} + \beta_{\text{BB}}^2 + 2\beta_{\text{AB}}^2]^{1/2} \quad (18) \end{aligned}$$

If $h-h'$ is small but significant it can be shown that the opposing $-2h\beta_{\text{BB}}$ and terms $+2h'\beta_{\text{BB}}$ in Eq. 18 still effectively cancel each other out. Eq. 19 is a reasonable approximation and like Eq. 17 describes bonding equivalent to one σ bond and one weaker σ bond.

$$\begin{aligned} \text{BE}'_{30} \approx h' - [h^2 + \beta_{\text{BB}}^2 + 8\beta_{\text{AB}}^2]^{1/2} \\ - [(h')^2 + \beta_{\text{BB}}^2 + 2\beta'_{\text{AB}}^2]^{1/2} \\ = h' - [h^2 + \beta_{\text{BB}}^2 + 4\beta'_{\text{AB}}^2]^{1/2} \\ - [(h')^2 + \beta_{\text{BB}}^2 + \beta'_{\text{AB}}^2]^{1/2} \quad (19) \end{aligned}$$

3.2.2. The influence of electronegativity on onium ion stability. If we make the same assumptions about inter-nuclear repulsion ($\Delta E_{\text{nuc}} = 1.0\beta_{\text{AB}}$) and solvation ($\Delta E_{\text{solv}} = -0.5\beta_{\text{AB}}$) as made in Section 3.1 but now include the contribution of back donation to the bond energy of ion **30** in the form of Eq. 18, the relative bond energies of the species **29–31** are as shown in Figure 4(a). For the purposes of the plot we have assumed that $h'=h$ and, as previously, $\beta_{\text{AB}} = \beta_{\text{BB}}$. Note in particular how the stability of the cyclic ion **30** has been increased relative to the acyclic species **29** and **31**. Figure 4(b) compares the bond energies of the onium ion **30** and the π -complex without back-donation **15**. In accord with experimental observation, the π -complex with back-donation is now stable for a wide range of h values and this stability extends to species where A is more electronegative than B ($h > 0$) (e.g., A=Br, B=CR₂).

Note that as h increases and back donation becomes increasingly difficult, due to the electronegativity of A, the bond energy of the onium ion **35** tends towards that of the simple [3c-2e] bond **15** (Fig. 4(b)). This can be appreciated from the form of Eq. 18. As h' increases the $2\beta_{\text{AB}}^2$ term rapidly becomes small compared to $[(h')^2 + 2h'\beta_{\text{BB}} + \beta_{\text{BB}}^2]$. Eq. 19 then approximates to the form of Eq. 20, which is the bond energy expression for the bond **15** (Eq. 5).

$$\begin{aligned} \text{BE}'_{30} = h' - [h^2 - 2h\beta_{\text{BB}} + \beta_{\text{BB}}^2 + 8\beta_{\text{AB}}^2]^{1/2} \\ - [(h' + \beta_{\text{BB}})^2 + 2\beta_{\text{AB}}^2]^{1/2} \end{aligned}$$

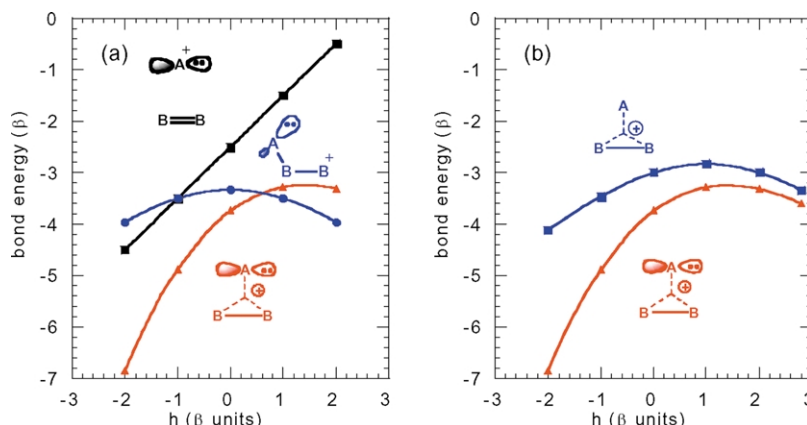


Figure 4. (a) Calculated energies of four-electron species **29**, **30** and **31** with variation of h ; (b) comparison of relative energies of three-centre, two-electron bonds AB_2^+ with and without back donation.

$$\text{If } 2\beta_{AB}^2 \ll (h' + \beta_{BB})^2$$

$$BE'_{30} \approx h' - [h^2 - 2h\beta_{BB} + \beta_{BB}^2 + 8\beta_{AB}^2]^{1/2} - [(h' + \beta_{BB})^2]^{1/2} \quad (20)$$

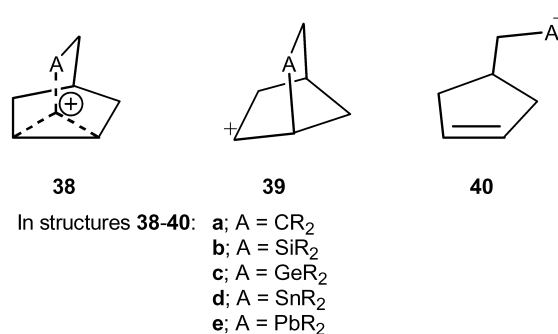
$$\therefore BE'_{30} \approx -\beta_{BB} - [h^2 - 2h\beta_{BB} + \beta_{BB}^2 + 8\beta_{AB}^2]^{1/2} = BE_{15}$$

The bond energy expressions discussed above are therefore consistent with the following general conclusions. When formed by rearrangement from an acyclic cation the resulting π -complex can be regarded as being bonded by a σ bond and a weaker σ dative bond as summarised by structure **37**. As the atom or group A becomes more electropositive the dative bond strengthens and as A becomes more electronegative it weakens and tends towards a simple $[3c-2e]$ bond without back-donation. Eqs. 13–19 therefore, provide a simple quantitative analysis of π -complexes involving back-donation. Back-donation in π -complexes has been discussed extensively by Dewar using both qualitative analysis^{7,28} and MNDO calculations⁷² and the semi-quantitative model discussed above is consistent with these studies. Detailed MNDO calculations on a number of specific structures were consistent with the earlier postulate that there is a ‘continuous transition, with changing electronegativity of the apical group, from species best represented as π -complexes to ones best represented as classical microcycles’,⁷² (i.e., Fig. 4(b)). The position between the two extremes (**15** and **35**) will be reflected in the molecular geometry and CC stretching frequency of specific species. These aspects have been discussed extensively elsewhere.^{72,73} In practice the acyclic ion **34** may well become more stable than the onium ion **35** before it effectively becomes a simple π -complex **15** (Fig. 4(a)).

3.3. 2-Norbornyl cations

3.3.1. A semi-quantitative model of the influence of electronegativity. There is of course one particularly well-known example of a stable π -complex, namely the 2-norbornyl cation **38a** (R=H). This ion owes its relative stability to the relief of some ring strain in going from the classical structure **39a** to the non-classical structure **38a**.⁷⁴ This strain energy can be modelled by increasing the energy of the species **14** relative to **15** and **16**. For the purposes of modelling this effect we have used a value of 0.4β for the

extra energy and a plot of the corresponding energies is shown in Figure 5(b). It can be seen that a modest increase in the relative energy of the classical cation results in a window in which the non-classical ion **15** is now more stable than either of the alternatives (**14** and **16**). Presumably the 2-norbornyl cation exists within this window. How large is this window and how much can the 2-norbornyl cation be modified without loss of the non-classical structure? Are there 2-norbornyl cation derivatives or analogues that are relatively more stable than the parent structure? These are interesting questions that are intimately associated with the influence of electronegativity on three-centre, two-electron bonds.



On the basis of the model summarised in Figure 5(b), making the apical atom or group A of a norbornyl system **38** more electropositive can be expected to increase the stability of the non-classical ion **38** relative to the classical ion **39**. The relative ring strain will of course differ depending upon the nature of the atom A. Synthetic studies have demonstrated the stability of the norbornyl cation analogues **38b–e** and NMR studies have fully characterised these species.^{75–77} Associated quantum mechanical calculations show that as the electronegativity of the elements Si→Pb decreases, then the intramolecular stabilisation of the norbornyl cations **38** relative to the ring-opened isomeric cations **40** also decreases, in agreement with the general trend summarised in Figure 5(b). This trend arises primarily because the transformation $38 \rightleftharpoons 40$ is a heteroprocess (Section 3.1.4) but the relative stability of the norbornyl structure **38** is also favourably influenced by the C1–C2 interaction (β) and the $-2h\beta$ effect. Furthermore, the calculated C1–C2 bond lengths increase along the series **38**

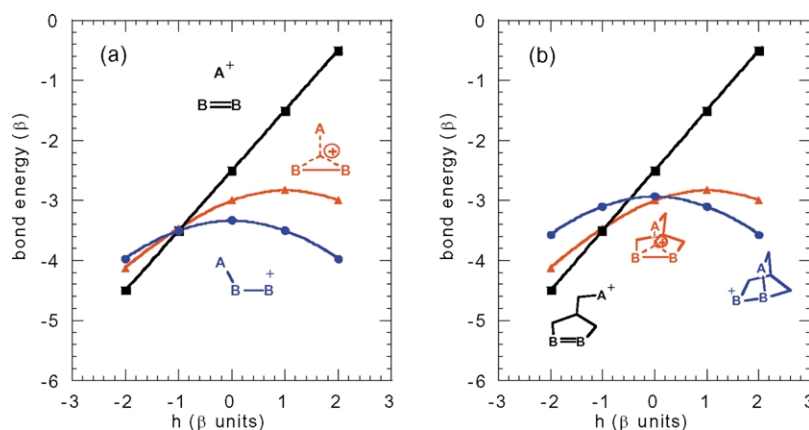


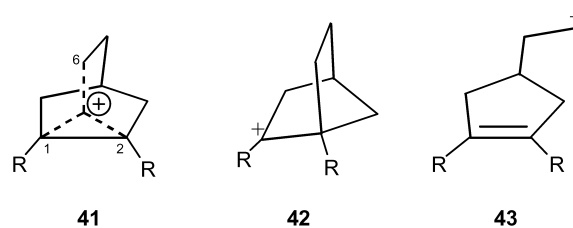
Figure 5. A comparison of (a) the relative energies of species **14**, **15** and **16** and (b) the relative energies of the 2-norbornyl cation and related species with allowance for ring strain in the classical cation.

Si→Pb consistent with increasing electron-transfer to the C–C bonding interaction as h decreases. These recent preparative and advanced quantum mechanical studies are therefore in satisfactory agreement with the semi-quantitative model summarised in Figure 5(b) but it must be appreciated that in the series **38a–e** other factors neglected in the HMO model will also contribute to the relative stabilities.

The HMO model has been pushed to its limits and further investigations must rely on more accurate MO calculations. In the next Section 3.3.2 we use the 2-norbornyl cation **38a** (R=H) as a model system to probe the influence of 1,2-substituents on π -complex stability.

3.3.2. An AM1 study of substituent effects on the 2-norbornyl cation. The 2-norbornyl cation **41** is an excellent model for investigating the influence of substituent effects on the three participating atoms of a $[3c-2e]$ bond. In this study the variation of electronic effects of substituents is used as a probe of the influence of ‘electronegativity’ variation. We appreciate that other effects, such as hyperconjugation and resonance interactions, will influence bonding and relative stability and this must be taken into account. We have chosen the AM1 method⁷⁸ for this quantitative study of the semi-quantitative model discussed in Section 3.1. For this investigation the AM1 method has advantages and disadvantages. An important advantage is that much less computer time is required than for more sophisticated ab initio calculations thus enabling a large number of substituted cations to be investigated (75 for this study). It does not seem unreasonable to explore the more accessible model first. A disadvantage is that the AM1 method calculates the classical cation **42** (R=H) to be more stable than the non-classical ion **41** (R=H) and therefore does not give an accurate description of the absolute energies. However, we have taken this inherent systematic error into account by correcting the calculated heats of formation of the 2-norbornyl cations **41** ($\Delta H_f[\mathbf{41}]$) by $-22.7 \text{ kcal mol}^{-1}$ ($\Delta H_f^c[\mathbf{41}]$), which gives an energy difference for the unsubstituted non-classical and classical cations **41** and **42** (R=H) of $-13.6 \text{ kcal mol}^{-1}$ corresponding to accurate ab initio calculations.⁷⁹ Since we are specifically interested in the influence of substituents on

relative energies rather than absolute energies, we do not regard a systematic error in the calculated absolute energies as a problem.



In the AM1 method, because of the overestimation of the energy of the classical cation, both cations **41** and **42** correspond to energy minima making it straightforward to calculate heats of formation for both species. This is an advantage over ab initio methods in which the classical ion **42** is not necessarily an energy minimum and can be difficult to locate.⁷⁹ With these limitations in mind and emphasising that our main interest is the influence of substituents on the relative energies, we have carried out AM1 calculation on 25 symmetrical 1,2-disubstituted-2-norbornyl cations **41** together with the corresponding classical cations **42** and primary cations **43**. These cations correspond to the general species **14**, **15** and **16** (Section 3.1) and the calculated heats of formation are given in Tables 1 and 2.

Table 1 shows the AM1 calculated heats of formation for the cations **41** ($\Delta H_f[\mathbf{41}]$ and $\Delta H_f^c[\mathbf{41}]$) and **42** ($\Delta H_f[\mathbf{42}]$) with all geometrical variables minimised. The substituents R were chosen to give a wide range of electronic effects. Table 1 also gives the difference in the calculated heats of formation ($\Delta\Delta H_f^c[\mathbf{41-42}] = \Delta H_f^c[\mathbf{41}] - \Delta H_f[\mathbf{42}]$). Inspection of Table 1 shows that in general, and as expected based on Figure 5(b), the stability of the non-classical ion **41** increases relative to the classical ion **42** as the electron-withdrawing power of the substituents R increases.

To provide a quantitative basis for evaluating any relationship between relative stability and substituent effect, the correlation of $\Delta\Delta H_f^c[\mathbf{41-42}]$ for the 25 pairs of cations in Table 1 (entries 1–25) with σ_p^+ was investigated by linear regression. The most appropriate electronic parameter for

Table 1. AM1 calculated heats of formation of 2-norbornyl cations **41** and classical isomers **42**

Entry	Substituent	$\Delta H_f[41]$	$\Delta H_f^c[41]$	$\Delta H_f[42]$	$\Delta\Delta H_f^c[41-42]$	σ^+	\mathfrak{J}	\mathfrak{R}^+
1	H	212.0	189.3	202.9	-13.6	0.0	0.0	0.0
2	CONH ₂	142.1	119.4	134.9	-15.5	0.36	0.24	0.12
3	CN	292.8	270.1	286.1	-16.0	0.66	0.51	0.15
4	CCl ₃	196.9	174.2	190.9	-16.7	0.33	0.31	0.02
5	NO ₂	254.5	231.8	253.3	-21.5	0.79	0.67	0.12
6	CF ₃	-73.3	-96.0	-74.1	-21.9	0.61	0.38	0.23
7	SOMe	155.6	132.9	157.6	-24.7	0.49	0.52	-0.03
8	SO ₂ Me	108.0	85.3	112.9	-27.6	0.72	0.54	0.18
9	CH ₂ CN	268.2	245.5	258.6	-13.1	0.16	0.21	-0.05
10	Cl	202.6	179.9	190.2	-10.3	0.11	0.41	-0.30
11	C≡CH	316.4	293.7	303.3	-9.6	0.18	0.19	-0.01
12	CH ₃	191.1	168.4	177.8	-9.4	-0.31	-0.04	-0.27
13	F	128.2	105.5	112.8	-7.3	-0.08	0.43	-0.51
14	SMe	197.5	174.8	171.9	2.9	-0.54	0.20	-0.74
15	OMe	124.4	101.7	98.8	2.9	-0.78	0.26	-1.04
16	NHCOMe	117.2	94.5	85.1	9.4	-0.60	0.28	-0.88
17	CH ₂ OMe	109.1	86.4	100.1	-13.7	-0.05	0.01	-0.06
18	CO ₂ Me	58.7	36.0	54.7	-18.7	0.49	0.33	0.16
19	Br	228.0	205.3	219.3	-14.0	0.15	0.44	-0.29
20	Ph	257.4	234.7	233.7	1.0	-0.18	0.08	-0.26
21	Et	177.9	155.2	164.3	-9.1	-0.30	-0.05	-0.25
22	OPh	204.1	181.4	179.3	2.1	-0.50	0.34	-0.84
23	I	252.4	229.7	245.4	-15.7	0.13	0.04	0.09
24	cycloPr	246.1	223.4	231.1	-7.7	-0.41	-0.03	-0.38
25	PhCH ₂	241.7	219.0	229.3	-10.3	-0.20	-0.08	-0.12

quantifying the electronic effect of each substituent is probably σ_p^+ .⁸⁰ Although this parameter is derived for p-substituted aromatic systems it should be more relevant to the cations **41** and **42** than the simple Hammett constant σ_p . Values for σ_p^+ are given in Table 1. The relationship shown in Eq. 21 was obtained. Inspection of Eq. 21 reveals that there is a significant correlation and that σ_p^+ accounts for 80% of the variation in energy difference.

Table 2. AM1 calculated heats of formation of 2-norbornyl cations **41** and primary cations **43**

Entry	Substituent	$\Delta H_f^c[41]$	$\Delta H_f[43]$	$\Delta\Delta H_f^c[41-43]$
1	H	189.3	221.3	-32.0
2	CONH ₂	119.4	146.7	-27.3
3	CN	270.1	294.0	-23.9
4	CCl ₃	174.2	197.4	-23.2
5	NO ₂	231.8	251.2	-19.4
6	CF ₃	-96.0	-75.7	-20.3
7	SOMe	132.9	157.7	-24.8
8	SO ₂ Me	85.3	110.9	-25.6
9	CH ₂ CN	245.5	272.6	-27.1
10	Cl	179.9	209.9	-30.0
11	C≡CH	293.7	329.0	-35.3
12	CH ₃	168.4	203.9	-35.5
13	F	105.5	136.5	-31.0
14	SMe	174.8	214.6	-39.8
15	OMe	101.7	146.3	-44.6
16	NHCOMe	94.5	131.6	-37.1
17	CH ₂ OMe	86.4	126.0	-39.6
18	CO ₂ Me	36.0	63.5	-27.5
19	Br	205.3	232.5	-27.2
20	Ph	234.7	271.5	-36.8
21	Et	155.2	192.2	-37.0
22	OPh	181.4	226.8	-45.4
23	I	229.7	255.4	-25.7
24	cycloPr	223.4	263.0	-39.6
25	PhCH ₂	219.0	256.4	-37.4

$$\Delta\Delta H_f^c[41-42] = -10.205 - 18.681\sigma_p^+ \quad (21)$$

$$n = 25, \quad r^2 = 0.802, \quad s = 4.187$$

$$\Delta\Delta H_f^c[41-42] = -12.572 - 10.704\mathfrak{J} - 21.434\mathfrak{R}^+ \quad (22)$$

$$n = 25, \quad r^2 = 0.838, \quad s = 3.865$$

The correlation between the calculated energy difference between the isomeric cations **41** and **42** and the parameter σ_p^+ is rather good. Since the energy term is a difference between two calculated values and since σ_p^+ is a general parameter it would be unreasonable to expect to obtain a better correlation using this data. Although values for individual pairs of cations should be treated with caution a general and significant trend is clear. The influence of substituents on the energy difference is entirely in accord with the simple model summarised in Figure 5. In particular the relative stability of the non-classical cation increases as the electron-withdrawing power (σ_p^+) of the substituent increases, that is, as the electronegativity of the carbon atoms increases. Based on Eq. 21, the crossover point of the relative energies of the carbonium ion **41** and the classical carbocation **42** can be expected to occur when $\sigma_p^+ \approx -0.5$. From accurate calculations^{81,82} and X-ray crystallography,^{83,84} we know that the 1,2-dimethyl-2-norbornyl cation (Table 1, entry 12) is more stable than the classical ion **42** (R=Me) ($\sigma_p^+ = -0.31$) and the crossover is therefore in the range $0 > \sigma_p^+ \geq -0.5$.

However, it is clear that for some substituents, in addition to an electronegativity effect, there is also a resonance/hyperconjugation effect on the relative stability of the cations **41** and **42**. To explore the relative importance of these effects we next investigated the relationship using the Swain and Lupton polar (\mathfrak{J}) and resonance (\mathfrak{R}^+) constants which

separate these discrete effects ($\sigma_p^+ = \mathfrak{J} + \mathfrak{R}^+$).⁸⁰ For the set of substituents used (Table 1) there was no correlation between \mathfrak{J} and \mathfrak{R}^+ ($r=0.187$). Using multiple regression the significant relationship shown in Eq. 22 was obtained.

We interpret Eq. 22 to mean that there are two significant electronic effects that determine the relative stability of the 1,2-substituted cations **41** and **42**. A positive inductive effect (\mathfrak{J} positive) increases the relative stability of the non-classical ion **41**. This is entirely consistent with the semi-quantitative model described in Section 3.1 and summarised in Figure 5. These substituents (\mathfrak{J} positive) effectively increase the Coulomb integrals (electronegativity) of the carbon atoms at positions 1 and 2. In addition there is a large resonance effect, which includes hyperconjugation. Substituents with negative resonance effects (\mathfrak{R}^+ negative) stabilise the classical ion **42** relative to the non-classical ion **41**. To increase the relative stability of the non-classical 2-norbornyl cation an electron-withdrawing substituent in which both \mathfrak{J} and \mathfrak{R}^+ are positive is desirable (e.g., CF_3). Of course, introducing electron-withdrawing groups will also make it increasingly difficult to generate cations (**41** or **42**) and may favour alternative modes of reaction, such as deprotonation to nortricyclane derivatives. These and other limitations need to be considered.

We next investigated the energies of the non-classical cations **41** relative to the primary cations **43**. For the parent carbocations **42** and **43** ($\text{R}=\text{H}$) the AM1 calculated energy difference is $18.4 \text{ kcal mol}^{-1}$. This does not seem to be an unreasonable value. We would not expect the energy difference between a primary and secondary carbocation to be less than this. In addition to hyperconjugation, a σ -bond is replaced by a weaker π -bond but there is also significant relief of ring strain. If we accept that the energy difference between cations **42** and **43** ($\text{R}=\text{H}$) is at least $18.4 \text{ kcal mol}^{-1}$, then it is appropriate that to compare the energies of the primary cations **43** with the carbonium ions **41** we should use the corrected heats of formation ($\Delta H_f^c[\mathbf{41}]$). The calculated heats of formation $\Delta H_f^c[\mathbf{41}]$ and $\Delta H_f^c[\mathbf{43}]$ and their difference $\Delta\Delta H_f^c[\mathbf{41-43}]$ are given in Table 2. For the parent systems **41** and **43** ($\text{R}=\text{H}$) (Table 2, entry 1) the energy difference $\Delta\Delta H_f^c[\mathbf{41-43}]$ is $-32.0 \text{ kcal mol}^{-1}$. This is in good agreement with the results of more accurate calculations which give the energy difference in the range -24 to $-32 \text{ kcal mol}^{-1}$ depending upon the level of theory.³¹

Again a correlation of the calculated energy difference with σ_p^+ was investigated for all 25 pairs of cations and the relationship shown in Eq. 23 was obtained. This relationship is also significant and suggests a clear trend. As the electron-withdrawing power increases and the carbon atoms become more electronegative the stability of the open chain primary cation increases relative to the non-classical cation. However, the energy difference is so great that it is unlikely that the electron-withdrawing power of substituents would be sufficient to reverse the stabilities of species **41** and **43**. In this sense the simple model represented by Figure 5(b) exaggerates the stability of the primary cation **43** and, on the basis of AM1 calculations, for the 2-norbornyl system the primary cation bond energy is higher. Eq. 23 suggests that the crossover point for the relative energies of the cations **41**

and **43** is $\sigma_p^+ \approx 2$, which is far in excess of any substituent we could realistically encounter.

Using the Swain and Lupton constants the significant relationship shown in Eq. 24 was obtained. Again, there is both a field and resonance effect but note that the signs of the coefficients are opposite to those in Eq. 22 and the contribution of the resonance effect is smaller. We interpret this as a negative resonance effect stabilising the non-classical cation **41** more than the primary cation **43**. In addition a positive field effect increases the bond energy of the carbocation **43** relative to the carbonium ion **41** by increasing the effective electronegativity of the carbon atoms as predicted by the Hückel model (Fig. 5).

$$\Delta\Delta H_f^c[\mathbf{41-43}] = -32.470 + 15.167\sigma_p^+ \quad (23)$$

$$n = 25, \quad r^2 = 0.822, \quad s = 3.176$$

$$\Delta\Delta H_f^c[\mathbf{41-43}] = -33.653 + 17.875\mathfrak{J} + 13.883\mathfrak{R}^+ \quad (24)$$

$$n = 25, \quad r^2 = 0.849, \quad s = 2.997$$

On the basis of these results we conclude that the simple Hückel model described in Section 3.1 combined with resonance/hyperconjugation effects is in good agreement with the AM1 calculated relative stabilities. For the cations **41-43** both the Hückel and AM1 models provide a consistent picture. Electron-donating substituents R ($\sigma_p^+ < 0$, that is, h positive plus hyperconjugation) increasingly favour the classical ion **42** and electron-withdrawing substituents R ($\sigma_p^+ > 0$, that is, h negative) increasingly favour the primary cation **43**. The non-classical ion **41** occupies a position between these two extremes (cf. Fig. 5) but in practise reversing the stability of cations **41** and **43** by substituent effects at positions 1 and 2 is highly unlikely. It should be possible to make relatively more stable 2-norbornyl cations by introducing moderately electron-withdrawing groups at position 1 and 2. Moderately strong and acid stable electron-withdrawing groups such as CF_3 should significantly increase the stability of the carbonium ion **41** relative to the classical structure **42** and more detailed theoretical and experimental investigations of derivatives such as **41** ($\text{R}=\text{CF}_3$) may be of some interest.

Clearly, placing electron-withdrawing substituents on a molecule makes it more difficult to generate a cation and, although the relative stability of the cation **41** may increase, the absolute stability and ease of formation will decrease. An alternative strategy for formation of more stable 2-norbornyl cation derivatives is to increase the electronegativity difference (h) by placing electron-donating substituents on the carbon atom at position 6. However, the choice of suitable substituents is not obvious. Several studies of the solvolysis rates of 6,6-dimethyl-2-norbornyl derivatives have been reported but kinetic data is not a reliable guide to the relative thermodynamic stability of products.^{85–87}

Table 3 shows the AM1 calculated C–C bond lengths ($r_{1,2}$ and $\check{r}_{1,6}$) that make up the [3c-2e] bond in the norbornyl cations **41**. The absolute values are poor compared to reliably accurate ab initio calculations but the change of bond length with substituent is of some interest here. The

Table 3. AM1 calculated interatomic distances for 2-norbornyl cations **41**

Entry	Substituent	$r_{1,2}$	$\check{r}_{1,6}$
1	H	1.392	2.240
2	CONH ₂	1.380	2.356
3	CN	1.390	2.354
4	CCl ₃	1.388	2.402
5	NO ₂	1.372	2.504
6	CF ₃	1.367	2.446
7	SOMe	1.383	2.388
8	SO ₂ Me	1.361	2.613
9	CH ₂ CN	1.392	2.311
10	Cl	1.400	2.315
11	C≡CH	1.410	2.269
12	CH ₃	1.404	2.244
13	F	1.418	2.288
14	SMe	1.420	2.295
15	OMe	1.425	2.209
16	NHCOMe	1.448	2.235
17	CH ₂ OMe	1.387	2.309
18	CO ₂ Me	1.377	2.373
19	Br	1.393	2.354
20	Ph	1.414	2.230
21	Et	1.406	2.239
22	OPh	1.425	2.205
23	I	1.383	2.360
24	cycloPr	1.411	2.233
25	PhCH ₂	1.402	2.253

bond length $\check{r}_{1,6}$ was taken as the average of $r_{1,6}$ and $r_{2,6}$ where there were small deviations from symmetry. As the electron-withdrawing power of the 1,2-substituents increases the bond length $r_{1,2}$ becomes shorter and the bond lengths $r_{1,6}$ and $r_{2,6}$ increase. The relationship between the bond lengths and electronic parameters are summarised by Eqs. 25–28. Eqs. 26 and 28 suggest that bond length is influenced by both field and resonance effects.

$$r_{1,2} = 1.40 - 0.041\sigma_p^+ \quad (25)$$

$$n = 25, \quad r^2 = 0.770, \quad s = 0.010$$

$$r_{1,2} = 1.394 - 0.021\check{\mathfrak{J}} - 0.049\mathfrak{R}^+ \quad (26)$$

$$n = 25, \quad r^2 = 0.835, \quad s = 0.009$$

$$\check{r}_{1,6} = 2.312 + 0.188\sigma_p^+ \quad (27)$$

$$n = 25, \quad r^2 = 0.715, \quad s = 0.054$$

$$\check{r}_{1,6} = 2.279 + 0.273\check{\mathfrak{J}} + 0.148\mathfrak{R}^+ \quad (28)$$

$$n = 25, \quad r^2 = 0.755, \quad s = 0.003$$

Eqs. 25–28 are statistically significant but we do not wish to over-interpret their meaning. Increasing the ‘electronegativity’ of the carbon atoms at positions 1 and 2 (i.e., positive $\check{\mathfrak{J}}$) can be expected to attract the electron pair to these atoms and away from the carbon atom at position 6. This will increase the electron density in the bonding region between C1 and C2 and this is consistent with bond shortening. This interpretation is also consistent with the extra contribution to bond energy that we have referred to as the $-2h\beta$ effect. Both the extra bond energy and the C1–C2 bond length ($r_{1,2}$) are a function of the difference in electronegativity h (related to the $\check{\mathfrak{J}}$ parameter) and the C1–C2 resonance integral β . This polarisation inevitably results in lengthening of the C6–C1 and C6–C2 bond lengths ($\check{r}_{1,6}$). The

inverse variation of the interatomic distances $r_{1,2}$ and $\check{r}_{1,6}$ with electronegativity difference is also seen in the calculated interatomic distances of protonated alkanes^{40, 88–91} and related species^{92–94} and appears to be a characteristic feature of [3c-2e] bonds.

Overall, the results of the AM1 calculations on the relative energies and structures of 75 cations are consistent with the semi-quantitative Hückel model described in Section 3.1.

4. Conclusions

We have described an HMO model of [3c-2e] bonds and their formation and cleavage by homo- and heteroprocesses. This simple model is consistent with general experimental observations and the results of more accurate calculations on specific structures. In particular the model rationalises general trends in the influence of electronegativity difference and substituent effects on reactions occurring via [3c-2e] bonded intermediates or transition states and provides further insight into the major bonding interactions in these systems.

Important features of this model are the distinct profiles of the bond energy versus electronegativity difference curves (BE vs h) of the interconverting isomeric species (**14–16**). Key contributions to bond energy difference are a $-h$ term for heteroprocesses and a function of $-2h\beta$ for homo-process. Although an empirical approach is used to estimate the crossing points of the bond energy curves, the semi-quantitative conclusions concerning energy differences are not dependant upon a precise knowledge of the crossing points. The effect of substituents on transformations involving [3c-2e] bonds is often interpreted in terms of the ability of an atom and its substituents to stabilise positive charge. The model described here suggests that the relative energies are best understood by an analysis of the influence of electronegativity (electron-withdrawing power) on the bond energies of the isomeric species. Examination of the HMO bond energy equations suggest that significant variation in the relative bond energies is the result of differing dependence on electronegativity difference terms (h , h^2 and $-2h\beta$). It is the contributions of these functions of electronegativity difference that primarily determine the variation in relative energies. In contrast to [2c-2e] bonded species, the bond energy of a [3c-2e] bond AB₂ is influenced by a function of $-2h\beta$ that accounts for the extent that the atom A draws electron density away from the bonding interaction BB. In order to focus attention on this term we have described it as the $-2h\beta$ effect. This effect also influences the charge distribution and bond lengths.

In spite of the simplifications inherent in the HMO model, used with caution it continues to give valuable insight into chemical bonding. Although many terms are neglected, those that are retained are major ones that will dominate energy expressions. Many of the most useful theoretical concepts in organic chemistry rely on severe approximations but used within their limitations this does not detract from their usefulness in teaching and practice. We believe that the simple bond energy/electronegativity difference diagrams, exemplified by Figures 1–5, provide

a useful basis for understanding substituent effects in structures or reactions in which intermediates or transition states can be approximated to $[3c-2e]$ bonded species. Ultimately the tests of the usefulness of any model are: (i) does it rationalise existing facts; (ii) does it provide new insights into structure, reactions or properties and (iii) does it direct attention to new areas worthy of further investigation. It is hoped that the simple HMO model described in this paper will fulfil some of these criteria by drawing attention to general trends in the chemistry of triangular three-centre, two-electron bonds and thus contribute to a wider appreciation of the importance of this type of bonding interaction in organic chemistry.

References and notes

1. *Encyclopedia of computational chemistry*; Schleyer, P. v. R., Schaefer, H. F., III, Handy, N. C., Eds.; Wiley: New York, 1998.
2. Munzarová, M. L.; Hoffmann, R. *J. Am. Chem. Soc.* **2002**, *124*, 4787–4795.
3. Ramsden, C. A. *J. Phys. Chem. A* **2002**, *106*, 2777–2780.
4. Coulson, C. A.; O'Leary, B.; Mallion, R. B. *Hückel theory for organic chemists*; Academic: London, 1978.
5. Heilbronner, E.; Bock, H. *The HMO model and its application*; Verlag Chemie: GmbH, Weinheim, 1976.
6. Olah, G. A.; Prakash, G. K. S.; Williams, R. E.; Field, L. D.; Wade, K. *Hypercarbon chemistry*; Wiley: New York, 1987.
7. DeKock, R. L.; Bosma, W. B. *J. Chem. Ed.* **1988**, *65*, 194–197.
8. McMurry, J. E.; Lectka, T. *Acc. Chem. Res.* **1992**, *25*, 47–53.
9. *Stable carbocation chemistry*; Prakash, G. K. S., Schleyer, P. v. R., Eds.; Wiley: New York, 1997.
10. Mota, C. J. A. *Quim. Nova* **2000**, *23*, 338–345.
11. Gaillard, M. J.; Gemmell, D. S.; Goldring, G.; Levine, I.; Pietsch, W. J.; Poizat, J. C.; Ratkowski, A. J.; Remillieux, J.; Vager, Z.; Zabransky, B. *J. Phys. Rev.* **1978**, *A17*, 1797–1803.
12. Oka, T. *Phys. Rev. Lett.* **1980**, *45*, 531–534.
13. Schleyer, P. v. R.; Carneiro, J. W. de M. *J. Comp. Chem.* **1992**, *13*, 997–1003.
14. Schreiner, P. R.; Kim, S.-J.; Schaefer, H. F.; Schleyer, P. v. R. *J. Chem. Phys.* **1993**, *99*, 3716–3720.
15. Marx, D.; Parrinello, M. *Nature* **1995**, *375*, 216–218.
16. White, E. T.; Tang, J.; Oka, T. *Science* **1999**, *284*, 135–137.
17. Schleyer, P. v. R.; Fort, R. C., Jr.; Watts, W. E.; Comisarow, M. B.; Olah, G. A. *J. Am. Chem. Soc.* **1964**, *86*, 4195–4197.
18. Saunders, M.; Schleyer, P. v. R.; Olah, G. A. *J. Am. Chem. Soc.* **1964**, *86*, 5680–5681.
19. Olah, G. A.; Prakash, G. K. S.; Saunders, M. *Acc. Chem. Res.* **1983**, *16*, 440–448.
20. Dewar, M. J. S. *Nature* **1945**, *156*, 784.
21. Dewar, M. J. S. *The electronic theory of organic chemistry*; Clarendon: Oxford, 1949.
22. Dewar, M. J. S.; Marchand, A. P. *Ann. Rev. Phys. Chem.* **1965**, *16*, 321–346.
23. Dewar, M. J. S. *The molecular orbital theory of organic chemistry*; McGraw-Hill: New York, 1969.
24. Whitmore, F. C.; Wittle, E. L.; Popkin, A. H. *J. Am. Chem. Soc.* **1939**, *61*, 1586–1590.
25. Nordlander, J. E.; Jindal, S. P.; Schleyer, P. v. R.; Fort, R. C., Jr.; Harper, J. J.; Nicholas, R. D. *J. Am. Chem. Soc.* **1966**, *88*, 4475–4484.
26. Ammal, S. C.; Yamataka, H.; Aida, M.; Dupuis, M. *Science* **2003**, *299*, 1555–1557.
27. Dewar, M. J. S. *Bull. Soc. Chim. Fr.* **1951**, C71–C79.
28. Dewar, M. J. S.; Dougherty, R. C. *The PMO theory of organic chemistry*; Plenum: New York, 1975; pp 298–310.
29. Werstiuk, N. H.; Muchall, H. M. *J. Mol. Struct.* **1999**, *463*, 225–229.
30. Werstiuk, N. H.; Muchall, H. M. *J. Phys. Chem. A* **2000**, *104*, 2054–2060.
31. Werstiuk, N. H.; Muchall, H. M.; Noury, S. *J. Phys. Chem. A* **2000**, *104*, 11601–11605.
32. Olah, G. A. *Angew. Chem., Int. Ed.* **1973**, *12*, 173–254.
33. Olah, G. A. *Angew. Chem., Int. Ed.* **1995**, *34*, 1393–1405.
34. Olah, G. A.; Prakash, G. K. S.; Sommer, J. *Superacids*; Wiley: New York, 1985.
35. Olah, G. A. *J. Org. Chem.* **2001**, *66*, 5943–5957.
36. Brouwer, D. M.; Hogeveen, H. *Progress in physical organic chemistry*; Streitwieser, A., Taft, R. W., Eds.; Wiley: New York, 1972; Vol. 9, pp 179–240.
37. Sommer, J.; Bukala, J. *Acc. Chem. Res.* **1993**, *26*, 370–376.
38. Olah, G. A.; Halpern, Y.; Shen, J.; Mo, Y. K. *J. Am. Chem. Soc.* **1971**, *93*, 1251–1256.
39. Olah, G. A. *J. Am. Chem. Soc.* **1972**, *94*, 808–820.
40. Esteves, P. M.; Mota, C. J. A.; Ramírez-Solís, A.; Hernández-Lamonedá, R. *J. Am. Chem. Soc.* **1998**, *120*, 3213–3219.
41. Esteves, P. M.; Ramírez-Solís, A.; Mota, C. J. A. *J. Phys. Chem. B* **2001**, *105*, 4331–4336.
42. Coulson, C. A.; Dewar, M. J. S. *Discuss. Faraday Soc.* **1947**, *2*, 54–62.
43. Lee, S. *Acc. Chem. Res.* **1991**, *24*, 249–254.
44. Pauling, L. *The nature of the chemical bond*, 3rd ed.; Cornell University Press: New York, 1960; pp 91–95.
45. Murphy, L. R.; Meek, T. L.; Allred, A. L.; Allen, L. C. *J. Phys. Chem. A* **2000**, *104*, 5867–5871.
46. Smith, D. W. *J. Phys. Chem. A* **2002**, *106*, 5951–5952.
47. Matsunaga, N.; Rogers, D. W.; Zavitsas, A. A. *J. Org. Chem.* **2003**, *68*, 3158–3172.
48. Exner, K.; Schleyer, P. v. R. *J. Phys. Chem. A* **2001**, *105*, 3407–3416.
49. Grimme, S. *J. Am. Chem. Soc.* **1996**, *118*, 1529–1534.
50. Saunders, M.; Hagen, E. L. *J. Am. Chem. Soc.* **1968**, *90*, 2436–2437.
51. Saunders, M.; Kates, M. R. *J. Am. Chem. Soc.* **1978**, *100*, 7082–7083.
52. Saunders, M. In *Stereodynamics of molecular systems*; Sarma, J., Ed.; Pergamon: Oxford, 1979.
53. Schreiner, P. R.; Severance, D. L.; Jorgensen, W. L.; Schleyer, P. v. R.; Schaefer, H. F. *J. Am. Chem. Soc.* **1995**, *117*, 2663–2664.
54. Wheland, G. W. *Resonance in organic chemistry*; Wiley: New York, 1955; pp 523–524.
55. Berson, J. A.; Suzuki, S. *J. Am. Chem. Soc.* **1959**, *81*, 4088–4094.
56. Olah, G. A.; Tolgyesi, W. S.; Kuhn, S. J.; Moffatt, M. E.; Bastien, I. J.; Baker, E. B. *J. Am. Chem. Soc.* **1963**, *85*, 1328–1334.
57. Olah, G. A.; Baker, E. B.; Evans, J. C.; Tolgyesi, W. S.; McIntyre, J. S.; Bastien, I. J. *J. Am. Chem. Soc.* **1964**, *86*, 1360–1373.
58. Clayden, J.; Greeves, N.; Warren, S.; Wothers, P. *Organic chemistry*; Oxford University Press: Oxford, 2001; p 116.

59. Stiles, M.; Mayer, R. P. *J. Am. Chem. Soc.* **1959**, *81*, 1497–1501.
60. Bethell, D. *Comprehensive organic chemistry*; Stoddart, J. F., Ed.; Pergamon: Oxford, 1979; Vol. 1, p 435, Chapter 2.7.
61. Esteves, P. M.; Alberto, G. G. P.; Ramírez-Solís, A.; Mota, C. J. A. *J. Am. Chem. Soc.* **1999**, *121*, 7345–7348.
62. Olah, G. A.; Olah, J. A. *Carbonium ions*; Olah, G. A., Schleyer, P. v. R., Eds.; Wiley: New York, 1970; Vol. II, p 773.
63. Mullay, J. *J. Am. Chem. Soc.* **1984**, *106*, 5842–5847.
64. Mullay, J. *J. Am. Chem. Soc.* **1985**, *107*, 7271–7275.
65. Cook, M. A.; Eaborn, C.; Walton, D. R. M. *J. Organomet. Chem.* **1970**, *24*, 301–306.
66. Jarvie, A. W. P.; Holt, A.; Thompson, J. *J. Chem. Soc. (B)* **1970**, 746–748.
67. Lambert, J. B. *Tetrahedron* **1990**, *46*, 2677–2689.
68. Siehl, H.-U.; Müller, T. *The chemistry of organic silicon compounds*; Rappoport, Z., Apeloig, Y., Eds.; Wiley: Chichester, UK, 1998; Vol. 2, p 595.
69. Brook, M. A.; Neuy, A. *J. Org. Chem.* **1990**, *55*, 3609–3616.
70. Brook, M. A.; Henry, C.; Jueschke, R.; Modi, P. *Synlett* **1993**, 97–104.
71. Krow, G. R. *Comprehensive organic synthesis*; Ley, S. V., Ed.; Pergamon: Oxford, UK, 1991; Vol. 7, p 671.
72. Dewar, M. J. S.; Ford, G. P. *J. Am. Chem. Soc.* **1979**, *101*, 783–791.
73. Allen, F. H. *Tetrahedron* **1982**, *38*, 2843–2853.
74. Sargent, G. D. *Carbonium ions*; Olah, G. A., Schleyer, P. v. R., Eds.; Wiley: New York, 1972; Vol. III, p 1132.
75. Steinberger, H.-U.; Müller, T.; Auner, N.; Maerker, C.; Schleyer, P. v. R. *Angew. Chem., Int. Ed.* **1997**, *36*, 626–628.
76. Maerker, C.; Schleyer, P. v. R. *The chemistry of organic silicon compounds*; Rappoport, Z., Apeloig, Y., Eds.; Wiley: Chichester, UK, 1998; Vol. 2, p 513.
77. Müller, T.; Bauch, C.; Ostermeier, M.; Bolte, M.; Auner, N. *J. Am. Chem. Soc.* **2003**, *125*, 2158–2168.
78. Dewar, M. J. S.; Zoebisch, E. G.; Healy, E. F.; Stewart, J. J. P. *J. Am. Chem. Soc.* **1985**, *107*, 3902–3909.
79. Schleyer, P. v. R.; Sieber, S. *Angew. Chem., Int. Ed.* **1993**, *32*, 1606–1608.
80. Hansch, C.; Leo, A. *Substituent constants for correlation analysis in chemistry and biology*; Wiley: New York, 1979.
81. Schleyer, P. v. R.; Maerker, C. *Pure Appl. Chem.* **1995**, *67*, 755–760.
82. Muchall, H. M.; Werstiuk, N. H. *J. Phys. Chem. A* **1999**, *103*, 6599–6602.
83. Laube, T. *Angew. Chem., Int. Ed.* **1987**, *26*, 560–562.
84. Laube, T. *Helv. Chim. Acta* **1994**, *77*, 943–956.
85. Schleyer, P. v. R.; Donaldson, M. M.; Watts, W. E. *J. Am. Chem. Soc.* **1965**, *87*, 375–376.
86. Altmann-Schaffner, E.; Grob, C. A. *Helv. Chim. Acta* **1987**, *70*, 43–48.
87. Kirmse, W.; Mrotzeck, U.; Siegfried, R. *Chem. Ber.* **1991**, *124*, 241–245.
88. Mota, C. J. A.; Esteves, P. M.; Ramírez-Solís, A.; Hernández-Lamonedá, R. *J. Am. Chem. Soc.* **1997**, *119*, 5193–5199.
89. Okulik, N. B.; Sosa, L. G.; Esteves, P. M.; Mota, C. J. A.; Jubert, A. H.; Peruchena, N. M. *J. Phys. Chem. A* **2002**, *106*, 1584–1595.
90. Esteves, P. M.; Alberto, G. G. P.; Ramírez-Solís, A.; Mota, C. J. A. *J. Phys. Chem. A* **2000**, *104*, 6233–6240.
91. Seitz, C.; East, A. L. L. *J. Phys. Chem. A* **2002**, *106*, 11653–11662.
92. Olah, G. A.; Prakash, G. K. S.; Rasul, G. *J. Org. Chem.* **2001**, *66*, 2907–2910.
93. Olah, G. A.; Prakash, G. K. S.; Rasul, G. *J. Org. Chem.* **2002**, *67*, 8547–8551.
94. Sauers, R. R. *Tetrahedron Lett.* **2001**, *42*, 6625–6628.

A novel separation technique of diastereomeric esters of pyridylethanols by extraction: formal total synthesis of PNU-142721, HIV-1 reverse transcriptase inhibitor

Masato Matsugi,^a Kinuyo Itoh,^a Masatomo Nojima,^a Yuri Hagimoto^b and Yasuyuki Kita^{b,*}

^aDepartment of Materials Chemistry and Frontier Research Center, Graduate School of Engineering, Osaka University, 2-1, Yamada-oka, Suita, Osaka 565-0871, Japan

^bGraduate School of Pharmaceutical Sciences, Osaka University, 1-6, Yamada-oka, Suita, Osaka 565-0871, Japan

Received 22 July 2003; revised 23 January 2004; accepted 23 January 2004

Abstract—The separation of diastereomeric esters derived from (\pm)-pyridylethanols and 3 β -acetoxyetiolic acid were achieved by an extraction technique using diethyl ether and aqueous hydrochloric acid. A formal total synthesis of PNU-142721 was effectively carried out to prepare the chiral, non-racemic synthon 1-furo[2,3-*c*]pyridin-5-yl-ethanol (**1**) by means of this technique. The structure optimized using MOPAC calculations on each diastereomer suggested the presence of intramolecular CH/ π interaction in only the (*S*)-isomer of the diastereomers.

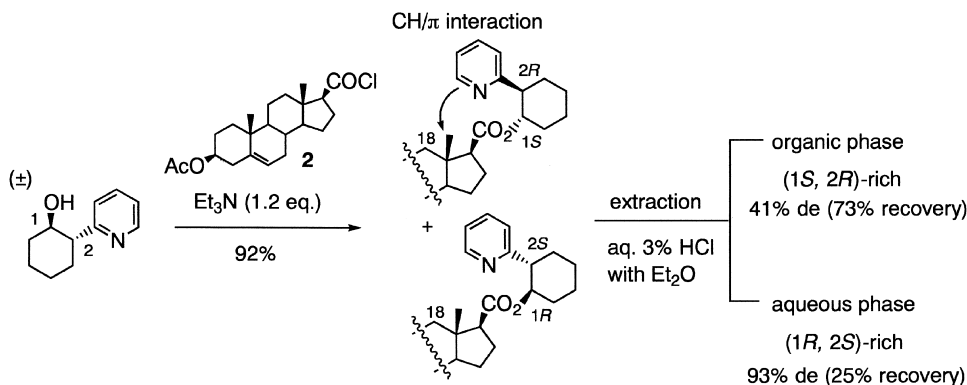
© 2004 Elsevier Ltd. All rights reserved.

1. Introduction

We recently disclosed that a diastereomeric mixture derived from (\pm)-*trans*-2-pyridylcyclohexanols and 3 β -acetoxyetiolic acid¹ could be separated by a simple extraction procedure using achiral organic media and aqueous acid (Scheme 1).² This phenomenon could be assumed by the difference in the pK_a values caused by an intramolecular CH/ π interaction³ in only one of the two diastereomers. This interaction possibly reduces the electron density on the nitrogen atom of the pyridine ring due to the charge transfer

character to CH(σ^*) from HOMO of the π moiety,⁴ or the possibility of the difference in the steric bulkiness around the nitrogen atom in the diastereomers.

Incidentally, (–)-6-chloro-2-[(1-furo[2,3-*c*]pyridin-5-yl-ethyl)thio]-4-pyrimidinamine (PNU-142721) has been announced as an HIV-1 specific, non-nucleoside reverse transcriptase inhibitor⁵ and evaluated for its inhibitory activity to the various reverse transcriptases and a panel of mutant RT enzymes etcetera (Fig. 1).⁶ The reported synthetic routes for the optically pure PNU-142721 involves



Scheme 1. Diastereomer separation by extraction.

Keywords: Chiral resolution; CH/ π interaction; Diastereomers; Extraction; PNU-142721.

* Corresponding author. Tel.: +81-668-798225; fax: +81-668-798229; e-mail address: kita@phs.osaka-u.ac.jp

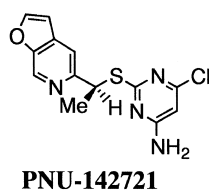


Figure 1.

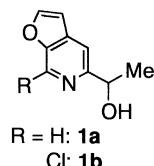
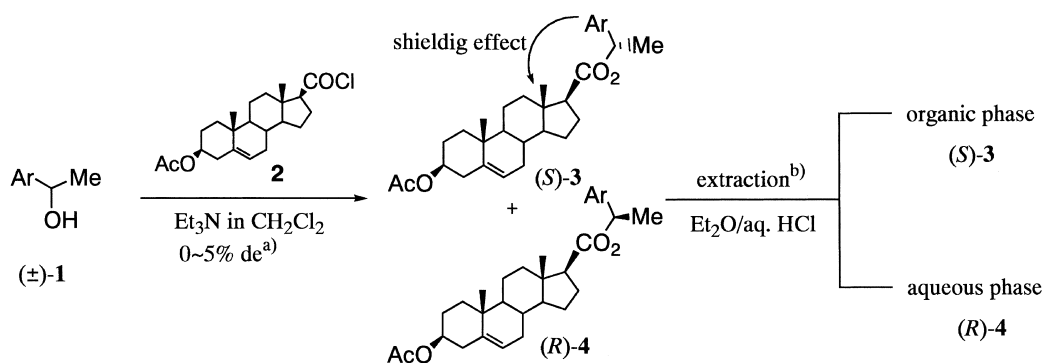


Figure 2.



^{a)} The kinetic resolution was observed in acylation process.

^{b)} Diastereomeric mixture (**3a** and **4a**) / Et₂O / aq. HCl = 300 mg / 20 ml / 50 ml

Scheme 2. The separation of diastereomers derived from pyridylethanols.

an optical resolution of (±)-1-furo[2,3-*c*]pyridin-5-yl-ethanol (**1a**)⁵ or (±)-(7-chlorofuro[2,3-*c*]pyridin-5-yl)-ethanol (**1b**)⁷ using enzymatic acylation⁸ or asymmetric reduction of the corresponding acetylpyridone⁹ as a key step to introduce the chirality to the molecule (Fig. 2). Although these synthetic routes are excellent, the kinetic resolution of (±)-**1a** has somewhat disadvantages such as the use of the expensive acyl-reagent and a long reaction time (9 days).⁵ We wish to report here that the concise preparation of both enantiomerically pure (*S*)-**1a** and (*R*)-**1a** using the convenient optical resolution technique of (±)-**1a** via a simple extraction of the corresponding diastereomeric derivatives.

2. Results and discussion

First, we examined whether the separation technique of the diastereomeric isomers can be applied to the diastereomers derived from simple (±)-pyridylethanols (**1c–1g**)¹⁰ and 3β-acetoxyetiolic acid or not (Scheme 2). We used diethyl ether as the organic phase since other solvents previously tested did not work.²

Using the acidic extraction, the diastereomers could be separated with moderate distribution if there is no electron-withdrawing group on the pyridine ring (Table 1, entries 3–13). Thus, we found that this separation technique could be applicable not only to the reported cyclic-type *trans*-(±)-

2-(2-pyridyl)cyclohexanols¹ but also to the acyclic-type pyridylethanols such as **1c–1g**. However, the separation was low when 1-(4-pyridyl)ethanol (**1e**) was used as the (±)-substrate (Table 1, entries 9 and 10). We assume that this is due to the acid catalyzed racemization of (*R*)-**4e** via a cross-conjugated intermediate during the extraction (Fig. 3).

The absolute configuration of the diastereomer which mainly existed in the organic phase, was the (*S*)-isomer.¹¹ The shielding effect of the C18–CH₃ on steroid ring was observed by ¹H NMR. These spectra corresponded to the free form of **3** and not its HCl salt. The chemical shifts of protons on C18–CH₃ in **3** [δ (ppm) in CDCl₃] were **3c**: 0.59; **3d**: 0.51; **3e**: 0.56; **3f**: 0.60; **3g**: 0.60; respectively. On the other hand, the chemical shifts of protons in **4** on C18–CH₃ were δ 0.73 in all cases.¹² These results strongly suggest that our target diastereomers derived from

Table 1. Separation of the diastereomers (**3** and **4**) by extraction

Entry	Ar	aq. HCl (%)	Organic phase		Aqueous phase	
			(<i>S</i>)- 3 (%)	de (%)	(<i>R</i>)- 4 (%)	de (%)
1	2-Pyridyl: 1c	3.0	99	3	0	—
2		5.0	97	2	1	43
3		6.0	80	15	17	70
4		7.0	63	34	33	67
5	3-Pyridyl: 1d	2.0	48	47	42	72
6		3.0	40	73	56	58
7		5.0	18	75	79	20
8	4-Pyridyl: 1e	1.0	72	19	18	45
9		2.0	39	27	54	3
10		3.0	15	39	75	2
11	2-(6-Methylpyridyl): 1f	5.0	60	54	30	71
12		6.0	63	48	30	85
13		7.0	38	61	58	31
14	2-(6-Bromopyridyl): 1g	7.0	97	6	0	—
15		15.0	95	2	0	—
16		30.0	99	3	0	—
17	2-Furo[2,3- <i>c</i>]pyridyl: 1a	3.0	77	34	18	87
18		5.0	39	91	57	49
19		7.0	37	95	54	53

The de were determined by ¹H NMR (270 MHz).

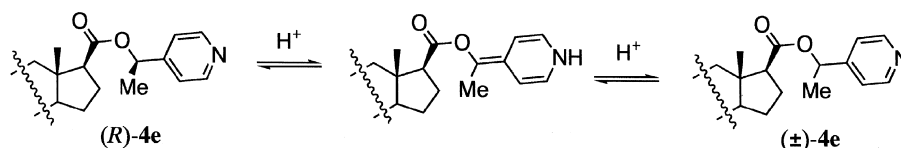


Figure 3.

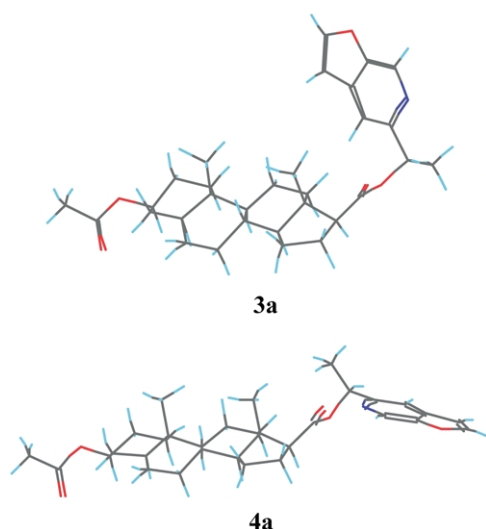


Figure 4.

(±)-furo[2,3-*c*]pyridin-5-yl-ethanol, which has no electron-withdrawing group on the pyridine ring, could also be separated in a similar manner. In fact, we separated the corresponding diastereomers with higher efficiency than we expected (Table 1, entries 17–19).

The ideal concentration of aq. HCl was ca. 5.0–7.0 wt% for separation of **1a** (Table 1, entries 18 and 19). The structure optimized with MOPAC¹³ of **3a** suggested the presence of an intramolecular CH/π interaction (Fig. 4). The shortest distance between the C18–CH₃ and the π moiety was

2.82 Å which is shorter than the sum of the each van der Waals radius.¹⁴ We assume that this interaction may be fixing the conformation to the *ap* plane¹⁵ of the chiral esters, thus suggesting that it maybe superior to the steric effect between the C18–CH₃ and the π system. In particular, the spread π plane of furo[2,3-*c*]pyridinyl ring acts as a factor of stabilizing the interaction.

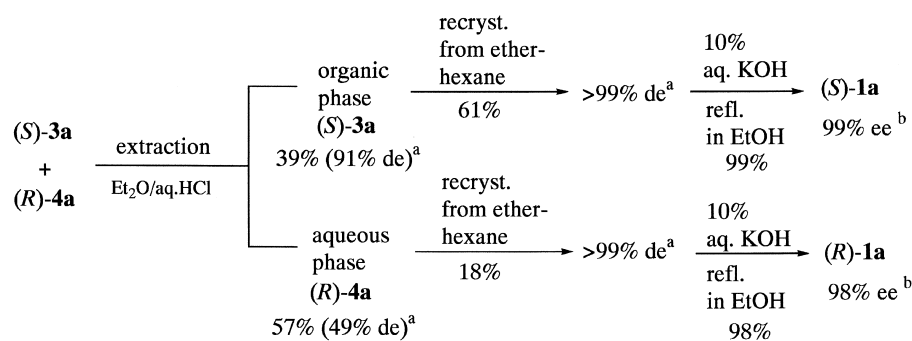
As shown in Table 2, the ¹H NMR spectrum of **3a** and **4a** in diethyl ether-D₁₀ showed an enhanced shielding effect on the C18–CH₃ than when using CDCl₃, hence the presumed major conformation of **3a** in diethyl ether appears to be close to MO calculation as in Figure 4.

After the extraction, the diastereomeric excess of both (*S*)-**3a** and (*R*)-**4a** can be further enhanced by recrystallization from diethyl ether/*n*-hexane to >99% de (Scheme 3). Cleavage of the 3β-acetoxyetiolic acid with aqueous potassium hydroxide, then provides both of **1a** for use in the synthesis of optically pure PNU-142721.

The synthesis of PNU-142721, however, was attempted without recrystallization at the diastereomer-resolution stage on the basis of information that it could be obtained optically pure by recrystallization at the end of the synthesis.⁵ The route is shown in Scheme 4. In this case, the distribution of the crude diastereomers was somewhat different from the former case. This maybe due to the change of the acidity of aq. HCl by the presence of an excess of acyl reagent 3β-acetoxyetiolic acid, which remained in the reaction mixtures. The (*S*)-furo[2,3-*c*]pyridin-5-yl-ethanol (70% ee) obtained from the organic phase after

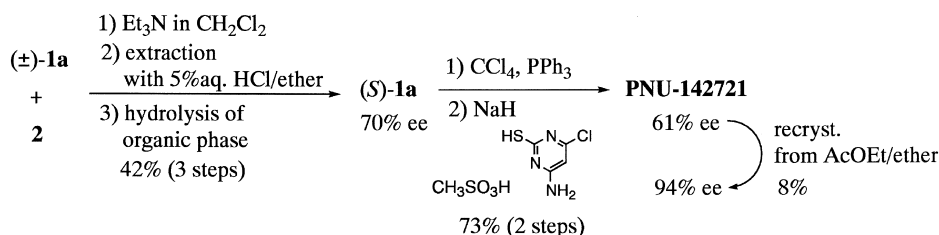
Table 2. Chemical shift values of C18–CH₃ in ¹H NMR at room temperature

Solvent	Chemical shift of protons on C18–CH ₃ in 3a [δ (ppm)]	Chemical shift of protons on C18–CH ₃ in 4a [δ (ppm)]	Difference of chemical shift between 3a and 4a [δ (ppm)]
CDCl ₃	0.54	0.73	0.19
(C ₂ D ₅) ₂ O	0.53	0.76	0.23



^a) The de was determined by ¹H NMR; ^b) The ee was determined by HPLC (CHIRAL CEL OD[®]).

Scheme 3. Optical resolution of (±)-**1a** by extraction.



Scheme 4. An alternative route for PNU-142721.

alkaline hydrolysis was converted to PNU-142721 (61% ee) according to the reported method.⁵ A single recrystallizing of the crude product from ethyl acetate/ether gave PNU-142721 with 94% ee (Scheme 4). This synthetic route has the benefit that there is no troublesome purifications such as recrystallization or column chromatography throughout the derivation from (±)-**1a** to the crude PNU-142721.

To conclude, we have shown a novel optical resolution technique of (±)-pyridylethanols by a simple extraction method using an achiral-organic solvent and acidic solution. Some features of this optical resolution technique by extraction are summarized as follows. (1) The absolute configurations of the resolved pyridylethanols can be easily determined because of the fact that the (*S*)-isomer showing the shielding effect of the C18–CH₃ of the π system exists in the organic phase upon extraction. (2) The diastereomeric purity of pyridylethanol derivatives following the acidic extraction can be further enriched by a single recrystallization. (3) It does not require a long reaction time to obtain the chiral alcohols. (4) The target compound PNU-142721 can be prepared with only one recrystallization of the final product.

We believe that this technique will play an important role in a large-scale synthesis of similar optically active pyridylethanols.

3. Experimental

3.1. General information

Melting points are taken with a micro hot-stage apparatus (Yanagimoto) and are uncorrected. Infrared (IR) absorption spectra were recorded with a SHIMADZU FTIR-8400 spectrometer as a KBr or a NaCl pellet. ¹H NMR spectra were measured on a JEOL JNM-EX270 or a JEOL JNM-AL300 spectrometers with SiMe₄ as the internal standard in CDCl₃. Mass spectra (MS) were determined on a JEOL JMS-AMII50, a JEOL JMS-700 or a JEOL JMS-600H mass spectrometer. Chiral HPLC analyses were performed with a JASCO Gulliver series PU-986, MD-910 and CO-1560 or 2060 using a Daicel chiral column (Daicel Chiralcel OD, OD-H or OJ). Specific rotations were measured by JASCO P-1020 polarimeter. Kanto Chemical Silica Gel 60 N (spherical, neutral) and Fuji Silysia Chemical silica gel BW-300 were used for flash column chromatography, respectively. (±)-1-(2-Furo[2,3-*c*]pyridyl)ethanol (**1a**),⁵ (±)-1-pyridylethanols (**1c–g**),¹⁰ 3 β -acetoxy-5-eticnic acid chloride (**2**)¹ and 4-amino-6-chloro-2-thiopyrimidine

mesylate salt⁵ were essentially prepared by the reported method.

3.1.1. (±)-1-(2-Furo[2,3-*c*]pyridyl)ethanol (1a**).**⁵ Yellow oil; ¹H NMR (270 MHz, CDCl₃): δ_{H} 1.48 (3H, d, $J=6.5$ Hz, CH₃), 4.06 (1H, br, OH), 4.93 (1H, q, $J=6.5$ Hz, CH), 6.73 (1H, d, $J=1.9$ Hz, furan-*H*), 7.46 (1H, s, pyridine-*H*), 7.70 (1H, d, $J=1.9$ Hz, furan-*H*), 8.72 (1H, s, pyridine-*H*); IR (NaCl): $\nu_{\text{max}}/\text{cm}^{-1}$ 3360 (OH).

3.1.2. (±)-1-(2-Pyridyl)ethanol (1c**).**^{10a–c} Yellow oil; ¹H NMR (300 MHz, CDCl₃): δ_{H} 1.51 (3H, d, $J=6.6$ Hz, CH₃), 4.24 (1H, br, OH), 4.90 (1H, q, $J=6.6$ Hz, CH), 7.20 (1H, ddd, $J=7.5, 5.0, 0.6$ Hz, pyridine-*H*), 7.28 (1H, ddd, $J=7.9, 0.6, 0.2$ Hz, pyridine-*H*), 7.69 (1H, td, $J=7.7, 1.8$ Hz, pyridine-*H*), 8.54 (1H, dd, $J=5.0, 1.8$ Hz, pyridine-*H*); IR (KBr): $\nu_{\text{max}}/\text{cm}^{-1}$ 3250 (OH).

3.1.3. (±)-1-(3-Pyridyl)ethanol (1d**).**^{10a,b} Yellow oil; ¹H NMR (300 MHz, CDCl₃): δ_{H} 1.54 (3H, d, $J=6.2$ Hz, CH₃), 2.21 (1H, br, OH), 4.97 (1H, q, $J=6.2$ Hz, CH), 7.29 (1H, dd, $J=7.8, 4.7$ Hz, pyridine-*H*), 7.74 (1H, d, $J=7.8$ Hz, pyridine-*H*), 8.51 (1H, dd, $J=4.7, 1.3$ Hz, pyridine-*H*), 8.59 (1H, d, $J=1.7$ Hz, pyridine-*H*); IR (KBr): $\nu_{\text{max}}/\text{cm}^{-1}$ 3202 (OH); MS (EI⁺): m/z (%) 123 (M⁺, 17), 108 (100).

3.1.4. (±)-1-(4-Pyridyl)ethanol (1e**).**^{10a} Colourless oil; ¹H NMR (270 MHz, CDCl₃): δ_{H} 1.48 (3H, d, $J=6.5$ Hz, CH₃), 3.01 (1H, br, OH), 4.88 (1H, q, $J=6.5$ Hz, CH), 7.29 (2H, d, $J=4.6$ Hz, pyridine-*H*), 8.41 (2H, d, $J=4.6$ Hz, pyridine-*H*); HRMS (EI⁺) calcd for C₇H₉NO (M⁺): 123.0684, found: 123.0694.

3.1.5. (±)-1-[2-(6-Methylpyridyl)]ethanol (1f**).**^{10d} Yellow oil; ¹H NMR (270 MHz, CDCl₃): δ_{H} 1.48 (3H, d, $J=6.2$ Hz, CH₃), 2.55 (3H, s, pyridine-6'-CH₃), 4.65 (1H, br, OH), 4.86 (1H, q, $J=6.2$ Hz, CH), 7.03 (1H, d, $J=2.2$ Hz, pyridine-*H*), 7.07 (1H, d, $J=2.2$ Hz, pyridine-*H*), 7.56 (1H, t, $J=7.6$ Hz, pyridine-*H*); IR (NaCl): $\nu_{\text{max}}/\text{cm}^{-1}$ 3376 (OH).

3.1.6. (±)-1-[2-(6-Bromopyridyl)]ethanol (1g**).**^{10d} Colourless oil; ¹H NMR (270 MHz, CDCl₃): δ_{H} 1.50 (3H, d, $J=6.5$ Hz, CH₃), 3.45 (1H, br, OH), 4.88 (1H, q, $J=5.5$ Hz, CH), 7.33 (1H, d, $J=7.4$ Hz, pyridine-*H*), 7.38 (1H, d, $J=7.4$ Hz, pyridine-*H*), 7.55 (1H, t, $J=7.7$ Hz, pyridine-*H*); IR (NaCl): $\nu_{\text{max}}/\text{cm}^{-1}$ 3391 (OH).

3.1.7. 3 β -Acetoxyeticnic acid chloride (2**).** Colourless solid; mp 193–195 °C (dec.); ¹H NMR (270 MHz, CDCl₃): δ_{H} 0.82 (3H, s, 18 β -CH₃), 0.83–2.59 (19H, m, steroid ring), 1.06 (3H, s, 19 β -CH₃), 1.98 (3H, s, 3 β -OCOCH₃), 2.88 (1H, m, 17 α -*H*), 4.81 (1H, m, 3 α -*H*), 5.43 (1H, m, 6-olefin-*H*); IR (KBr): $\nu_{\text{max}}/\text{cm}^{-1}$ 1784 (C=O).

3.1.8. 4-Amino-6-chloro-2-thiopyrimidine mesylate salt.^{5,6b} Colourless crystal; mp 166.0–167.0 °C (Et₂O); ¹H NMR (270 MHz, CDCl₃): δ_H 2.40 (3H, s, CH₃SO₃H), 3.55 (1H, br, 2-SH), 4.89 (2H, br, 4-NH₂), 6.23 (1H, s, 5-H), 1H of methanesulfonic acid was not observed; HRMS (EI⁺) calcd for C₄H₄N₃SO₃Cl (M⁺): 160.9814, found: 160.9813.

3.1.9. Typical procedure for esterification of 1a, c–g. To a stirred solution of 3β-acetoxyetienic acid (2.56 g, 7.1 mmol) in C₆H₆ (20 ml) under nitrogen atmosphere was added oxalyl chloride (3.60 ml, 40.8 mmol) and the solution was stirred for 2 h at room temperature. The acid chloride **2** was obtained as a white crystal after removal C₆H₆ in vacuo. To a solution of **2** in CH₂Cl₂ (10 ml) under nitrogen atmosphere and shielded from light, were added Et₃N (1.00 ml, 7.2 mmol) and **1a** (1.00 g, 6.1 mmol) in CH₂Cl₂ (10 ml) at 0 °C. After stirring for 4 h at room temperature, the reaction mixture was filtered. The filtrate was washed with saturated NaHCO₃ aq. and water, dried over Na₂CO₃, and concentrated in vacuo. The residue was purified by column chromatography on silica gel (eluent: hexane/AcOEt=3:1) to give **3a** and **4a** (2.41 g, 78%) as a diastereomeric mixture.

3.1.10. 3β-Acetoxy-10,13-dimethyl-2,3,4,7,8,9,10,11,12,13,14,15,16,17-tetradecahydro-1H-cyclopenta[a]-phenanthrene-17-carboxylic acid 1-(2-furo[2,3-c]pyridyl)ethyl ester (3a and 4a). Colourless solid; mp 126.5–127.0 °C; IR (KBr): ν_{max}/cm⁻¹ 1727 (C=O); HRMS (EI⁺) calcd for C₃₁H₃₉NO₅ (M⁺): 505.2828, found: 505.2827.

Compound (S)-3a. Mp 127.0–127.5 °C (Et₂O); ¹H NMR (270 MHz, CDCl₃): δ_H 0.47 (3H, s, 18β-CH₃), 0.91 (3H, s, 19β-CH₃), 1.05–2.39 (20H, m, steroid ring), 1.57 (3H, d, J=6.5 Hz, 17β-CO₂CHCH₃), 2.02 (3H, s, 3β-OCOCH₃), 4.53 (1H, m, 3α-H), 5.30 (1H, m, 6-olefine-H), 5.98 (1H, m, 17β-CO₂CHCH₃), 6.73 (1H, d, J=7.6 Hz, furan-H), 7.55 (1H, s, pyridine-H), 7.69 (1H, d, J=7.6 Hz, furan-H), 8.77 (1H, s, pyridine-H).

Compound (R)-4b. ¹H NMR (270 MHz, CDCl₃): δ_H 0.70 (3H, s, 18β-CH₃), 0.96 (3H, s, 19β-CH₃), 1.05–2.39 (20H, m, steroid ring), 1.58 (3H, d, J=6.5 Hz, 17β-CO₂CHCH₃), 2.02 (3H, s, 3β-OCOCH₃), 4.53 (1H, m, 3α-H), 5.30 (1H, m, 6-olefine-H), 5.98 (1H, m, 17β-CO₂CHCH₃), 6.73 (1H, d, J=7.6 Hz, furan-H), 7.55 (1H, s, pyridine-H), 7.69 (1H, d, J=7.6 Hz, furan-H), 8.77 (1H, s, pyridine-H).

3.1.11. 3β-Acetoxy-10,13-dimethyl-2,3,4,7,8,9,10,11,12,13,14,15,16,17-tetradecahydro-1H-cyclopenta[a]-phenanthrene-17-carboxylic acid 1-(2-pyridyl)ethyl ester (3c and 4c).^{2b} Colourless solid; mp 44.5–51.0 °C; IR (KBr): ν_{max}/cm⁻¹ 1732 (C=O); MS (EI⁺) *m/z* (%): 465 (M⁺, 1), 405 (100); HRMS (EI⁺) calcd for C₂₉H₃₉NO₄ (M⁺): 465.2879, found: 465.2885.

Compound (1S)-3c. ¹H NMR (300 MHz, CDCl₃): δ_H 0.59 (3H, s, 18β-CH₃), 1.00 (3H, s, 19β-CH₃), 1.18–2.33 (19H, m, steroid ring), 1.60 (3H, d, J=6.5 Hz, 17β-CO₂CHCH₃), 2.03 (3H, s, 3β-OCOCH₃), 2.43 (1H, dd, J=17.8, 9.0 Hz, 17α-H), 4.60 (1H, m, 3α-H), 5.37 (1H, m, 6-olefin-H), 5.93 (1H, q, J=6.5 Hz, 17β-CO₂CHCH₃), 7.19 (1H, ddd, J=7.5,

4.9, 1.2 Hz, pyridine-H), 7.38 (1H, dd, J=7.9, 1.2 Hz, pyridine-H), 7.68 (1H, td, J=7.7, 1.7 Hz, pyridine-H), 8.58 (1H, ddd, J=4.9, 1.7, 0.9 Hz, pyridine-H).

Compound (1R)-4c. ¹H NMR (300 MHz, CDCl₃): δ_H 0.73 (3H, s, 18β-CH₃), 1.03 (3H, s, 19β-CH₃), 1.18–2.33 (19H, m, steroid ring), 1.60 (3H, d, J=6.7 Hz, 17β-CO₂CHCH₃), 2.03 (3H, s, 3β-OCOCH₃), 2.43 (1H, dd, J=17.8, 9.0 Hz, 17α-H), 4.60 (1H, m, 3α-H), 5.38 (1H, d, J=4.2 Hz, 6-olefine-H), 5.95 (1H, q, J=6.7 Hz, 17β-CO₂CHCH₃), 7.19 (1H, ddd, J=7.5, 4.9, 1.3 Hz, pyridine-H), 7.36 (1H, d, J=7.9 Hz, pyridine-H), 7.67 (1H, td, J=7.7, 1.7 Hz, pyridine-H), 8.57 (1H, ddd, J=4.9, 1.7, 0.9 Hz, pyridine-H).

3.1.12. 3β-Acetoxy-10,13-dimethyl-2,3,4,7,8,9,10,11,12,13,14,15,16,17-tetradecahydro-1H-cyclopenta[a]-phenanthrene-17-carboxylic acid 1-(3-pyridyl)ethyl ester (3d and 4d). Colorless amorphous; IR (KBr): ν_{max}/cm⁻¹ 1732 (C=O); MS (FAB⁺) *m/z* (%): 466 (MH⁺), 106 (100); HRMS (FAB⁺) calcd for C₂₉H₄₀NO₄ (MH⁺): 466.2958, found: 466.2943.

Compound (S)-3d. ¹H NMR (300 MHz, CDCl₃): δ_H 0.51 (3H, s, 18β-CH₃), 0.96–2.19 (18H, m, steroid ring), 0.98 (3H, s, 19β-CH₃), 1.57 (3H, d, J=6.8 Hz, 17β-CO₂CHCH₃), 2.03 (3H, s, 3β-OCOCH₃), 2.32–2.41 (3H, m, 17α-H and steroid ring), 4.61 (1H, m, 3α-H), 5.36 (1H, d, J=5.1 Hz, 6-olefine-H), 5.91 (1H, q, J=6.8 Hz, 17β-CO₂CHCH₃), 7.27 (1H, m, pyridine-H), 7.69 (1H, ddd, J=8.1, 2.1, 1.6 Hz, pyridine-H), 8.54 (1H, dd, J=4.8, 1.6 Hz, pyridine-H), 8.66 (1H, d, J=2.1 Hz, pyridine-H).

Compound (R)-4d. ¹H NMR (300 MHz, CDCl₃): δ_H 0.71 (3H, s, 18β-CH₃), 0.96–2.19 (18H, m, steroid ring), 1.03 (3H, s, 19β-CH₃), 1.57 (3H, d, J=6.7 Hz, 17β-CO₂CHCH₃), 2.04 (3H, s, 3β-OCOCH₃), 2.32–2.41 (3H, m, 17α-H and steroid ring), 4.61 (1H, m, 3α-H), 5.38 (1H, d, J=5.0 Hz, 6-olefine-H), 5.94 (1H, q, J=6.7 Hz, 17β-CO₂CHCH₃), 7.27 (1H, m, pyridine-H), 7.67 (1H, ddd, J=7.9, 2.0, 1.7 Hz, pyridine-H), 8.54 (1H, dd, J=4.7, 1.7 Hz, pyridine-H), 8.63 (1H, d, J=2.0 Hz, pyridine-H).

3.1.13. 3β-Acetoxy-10,13-dimethyl-2,3,4,7,8,9,10,11,12,13,14,15,16,17-tetradecahydro-1H-cyclopenta[a]-phenanthrene-17-carboxylic acid 1-(4-pyridyl)ethyl ester (3e and 4e). Colorless amorphous; IR (KBr): ν_{max}/cm⁻¹ 1732 (C=O); HRMS (CI⁺) calcd for C₂₉H₃₉NO₄: 465.2879, found: 465.2876.

Compound (S)-3e. ¹H NMR (270 MHz, CDCl₃): δ_H 0.56 (3H, s, 18β-CH₃), 1.10–2.44 (20H, m, steroid ring), 1.00 (3H, s, 19β-CH₃), 1.57 (3H, d, J=6.5 Hz, 17β-CO₂CHCH₃), 2.03 (3H, s, 3β-OCOCH₃), 4.62 (1H, m, 3α-H), 5.37 (1H, d, J=5.0 Hz, 6-olefine-H), 5.84 (1H, m, 17β-CO₂CHCH₃), 7.26 (2H, m, pyridine-H), 8.58 (2H, m, pyridine-H).

Compound (R)-4e. ¹H NMR (270 MHz, CDCl₃): δ_H 0.72 (3H, s, 18β-CH₃), 1.10–2.44 (20H, m, steroid ring), 1.03 (3H, s, 19β-CH₃), 1.54 (3H, d, J=6.5 Hz, 17β-CO₂CHCH₃), 2.04 (3H, s, 3β-OCOCH₃), 4.62 (1H, m, 3α-H), 5.37 (1H, d, J=5.0 Hz, 6-olefine-H), 5.84 (1H, m, 17β-CO₂CHCH₃), 7.26 (2H, m, pyridine-H), 8.58 (2H, m, pyridine-H).

3.1.14. 3 β -Acetoxy-10,13-dimethyl-2,3,4,7,8,9,10,11,12,13,14,15,16,17-tetradecahydro-1H-cyclopenta[*a*]-phenanthrene-17-carboxylic acid 1-[2-(6-methylpyridyl)]ethyl ester (3f** and **4f**).** Colourless solid; mp 57.0–58.0 °C; IR (KBr): $\nu_{\max}/\text{cm}^{-1}$ 1732 (C=O); HRMS (CI⁺) calcd for C₂₉H₃₉NO₄ (M⁺): 479.3036, found: 479.3036.

Compound (S)-3f. ¹H NMR (270 MHz, CDCl₃): δ_{H} 0.60 (3H, s, 18 β -CH₃), 0.96 (3H, s, 19 β -CH₃), 1.10–2.48 (20H, m, steroid ring), 1.56 (3H, d, *J*=6.5 Hz, 17 β -CO₂CHCH₃), 2.04 (3H, s, 3 β -OCOCH₃), 2.54 (3H, s, pyridine-6'-CH₃), 4.61 (1H, m, 3 α -H), 5.37 (1H, m, 6-olefine-H), 5.90 (1H, m, 17 β -CO₂CHCH₃), 7.04 (1H, d, *J*=7.8 Hz, pyridine-H), 7.17 (1H, d, *J*=7.8 Hz, pyridine-H), 7.57 (1H, t, *J*=7.8 Hz, pyridine-H).

Compound (R)-4f. ¹H NMR (270 MHz, CDCl₃): δ_{H} 0.73 (3H, s, 18 β -CH₃), 1.00 (3H, s, 19 β -CH₃), 1.10–2.48 (20H, m, steroid ring), 1.58 (3H, d, *J*=6.5 Hz, 17 β -CO₂CHCH₃), 2.05 (3H, s, 3 β -OCOCH₃), 2.54 (3H, s, pyridine-6'-CH₃), 4.61 (1H, m, 3 α -H), 5.37 (1H, m, 6-olefine-H), 5.90 (1H, m, 17 β -CO₂CHCH₃), 7.04 (1H, d, *J*=7.8 Hz, pyridine-H), 7.17 (1H, d, *J*=7.8 Hz, pyridine-H), 7.57 (1H, t, *J*=7.8 Hz, pyridine-H).

3.1.15. 3 β -Acetoxy-10,13-dimethyl-2,3,4,7,8,9,10,11,12,13,14,15,16,17-tetradecahydro-1H-cyclopenta[*a*]-phenanthrene-17-carboxylic acid 1-[2-(6-bromopyridyl)]ethyl ester (3g** and **4g**).** Colourless solid; mp 56.0–57.0 °C; IR (KBr): $\nu_{\max}/\text{cm}^{-1}$ 1732 (C=O); HRMS (CI⁺) calcd for C₂₉H₃₈BrNO₄ (M⁺): 543.1984, found: 543.1987.

Compound (S)-3g. ¹H NMR (270 MHz, CDCl₃): δ_{H} 0.60 (3H, s, 18 β -CH₃), 1.02 (3H, s, 19 β -CH₃), 1.06–2.46 (20H, m, steroid ring), 1.58 (3H, d, *J*=6.5 Hz, 17 β -CO₂CHCH₃), 2.04 (3H, s, 3 β -OCOCH₃), 4.61 (1H, m, 3 α -H), 5.38 (1H, m, 6-olefine-H), 5.88 (1H, m, 17 β -CO₂CHCH₃), 7.32 (1H, d, *J*=7.6 Hz, pyridine-H), 7.39 (1H, d, *J*=7.6 Hz, pyridine-H), 7.57 (1H, m, pyridine-H).

Compound (R)-4g. ¹H NMR (270 MHz, CDCl₃): δ_{H} 0.73 (3H, s, 18 β -CH₃), 1.04 (3H, s, 19 β -CH₃), 1.06–2.46 (20H, m, steroid ring), 1.60 (3H, d, *J*=6.5 Hz, 17 β -CO₂CHCH₃), 2.04 (3H, s, 3 β -OCOCH₃), 4.61 (1H, m, 3 α -H), 5.38 (1H, m, 6-olefine-H), 5.88 (1H, m, 17 β -CO₂CHCH₃), 7.32 (1H, d, *J*=7.6 Hz, pyridine-H), 7.39 (1H, d, *J*=7.6 Hz, pyridine-H), 7.57 (1H, m, pyridine-H).

3.2. Typical procedure for extraction

To a solution of **3a** and **4a** (300 mg, 1:1 of diastereomeric mixture) in Et₂O (50 ml) was added aq. 5.0 wt% HCl (20 ml, diluted 36% HCl with dist. H₂O). After vigorous shaking, the ethereal solution was separated from the aqueous layer, dried over Na₂CO₃ and filtered. The filtrate was concentrated in vacuo to give **3a** in 39% yield with 91% de. The aqueous layer was made alkaline with NaHCO₃ (pH 8) to precipitate a white solid. The precipitation was collected by suction filtration and dried to give **4a** in 57% yield with 49% de.

3.3. General procedure for alkaline hydrolysis of **3a** or **4a**

3a (>99% de, 135 mg, 0.27 mmol), which was obtained from the ethereal layer of extraction described above and purified by recrystallization from ether, was dissolved in EtOH (25 ml). To this alcohol solution was added 10% KOH aq. (21 ml). After refluxing for 4 h, the reaction mixture was diluted with dist. H₂O (22 ml). The alkaline aqueous mixture was extracted with four portions of Et₂O. The ethereal layer was washed with saturated NaHCO₃ aq. and brine, dried over Na₂CO₃, filtered and concentrated to give (*S*)-1-[2-furo[2,3-*c*]pyridyl]ethanol [(*S*)-**1a**, 43 mg, 99%, 99% ee; Chiral HPLC analysis [Daicel Chiralcel OD; 0.5 ml/min; hexane/^{*i*}PrOH=95:5; 25 °C, ^{*t*}R: 32.4 min]].

3.3.1. (*S*)-1-(2-Furo[2,3-*c*]pyridyl)ethanol [(*S*)-1a**].⁵** Yellow oil; [α]_D²⁵ –29.2 (*c* 0.94, CHCl₃); 99% ee [chiral HPLC analysis (Daicel Chiralcel OD, hexane/^{*i*}PrOH=95:5, flow rate: 0.5 ml/min, 25 °C, ^{*t*}R: 32.4 min)].

3.3.2. (*R*)-1-(2-Furo[2,3-*c*]pyridyl)ethanol [(*R*)-1a**].⁵** Yellow oil; [α]_D²⁵ +20.1 (*c* 0.86, CHCl₃); 98% ee [chiral HPLC analysis (Daicel Chiralcel OD, hexane/^{*i*}PrOH=99:1, flow rate: 0.5 ml/min, 25 °C, ^{*t*}R: 49.3 min)].

3.4. Optical resolution of (±)-**1a** by extraction technique and synthesis of PNU-142721

The diastereomeric mixture of **3a** and **4a** (3.21 g) was separated by the extraction technique described above [Et₂O: 568 ml, aq. 5.0 wt% HCl: 247 ml (diluted 36% HCl with dist. H₂O)] and 80% de of **3a** (1.49 g) was obtained from the ethereal layer. The steroid moiety of **3a** was removed by the alkaline hydrolysis (EtOH: 278 ml, 10% KOH aq.: 223 ml) to form (*S*)-**1a** (0.43 g, 39% for 3 steps, 70% ee).

To a solution of (*S*)-**1a** (70% ee, 0.41 g, 2.5 mmol) in CHCl₃ (1.60 ml) under nitrogen atmosphere was added the solution of triphenylphosphine (1.34 g, 5.0 mmol) in carbon tetrachloride (4.8 ml) and the resulting mixture was stirred for 26 h. Hexane (1.6 ml) was added and the reaction mixture was continued to stir for 1 h. The generated precipitate was removed by succession filtration and the filtrate was concentrated. The residue was purified by column chromatography on silica gel (eluent: hexane/AcOEt=4:1) to give (+)-(*R*)-5-(1-chloroethyl)furo[2,3-*c*]pyridine [0.19 g, 42% from (*S*)-**1a**] as a colourless oil.

To a suspension of sodium hydride (90 mg, 3.8 mmol), which was washed with hexane, in DMF (3 ml) was added 4-amino-6-chloro-2-mercaptopyrimidine mesylate salt (280 mg, 1.1 mmol) at 0 °C under nitrogen atmosphere. The DMF solution was then stirred at room temperature for 1 h. To this solution was added a solution of (+)-(*R*)-5-(1-chloroethyl)furo[2,3-*c*]pyridine (190 mg, 1.1 mmol) in DMF (5 ml). After stirred for 5 days, the resulting mixture was diluted with AcOEt (25 ml), washed with 50% NaCl aq., dried over K₂CO₃/MgSO₄ and concentrated. The residue was purified by column chromatography on silica gel (eluent: hexane/AcOEt=1:1) to give (*S*)-6-chloro-2-[[1-(furo[2,3-*c*]pyridin-5-yl)ethyl]thio]-4-pyrimidinamine

(PNU-142721) [240 mg, 73% from (+)-(R)-5-(1-chloroethyl)furo[2,3-*c*]pyridine, 61% ee] as a white crystal. This crystal was purified by recrystallization from AcOEt/Et₂O to give optically pure PNU-142721 (18 mg, 8% from low optical purity of PNU-142721, 94% ee).

3.4.1. (R)-5-(1-Chloroethyl)furo[2,3-*c*]pyridine.⁵ Colourless oil; ¹H NMR (270 MHz, CDCl₃): δ_H 1.94 (3H, d, *J*=6.8 Hz, CH₃), 5.30 (1H, q, *J*=6.8 Hz, CH), 6.80 (1H, s, pyridyl-*H*), 7.72 (d, *J*=1.9 Hz, furan-*H*), 7.76 (1H, d, *J*=1.9 Hz, furan-*H*), 8.83 (1H, s, pyridyl-*H*).

3.4.2. (S)-6-Chloro-2-[[1-(furo[2,3-*c*]pyridin-5-yl)ethyl]thio]-4-pyrimidinamine (PNU-142721).⁵ Colourless crystal; 146.0–147.0 °C (AcOEt/Et₂O); ¹H NMR (270 MHz, DMSO-*d*₆): δ_H 1.72 (3H, d, *J*=6.8 Hz, CH₃), 5.12 (1H, q, *J*=6.8 Hz, CH), 6.16 (1H, s, pyridyl-*H*), 7.04 (1H, d, *J*=2.2 Hz, furan-*H*), 7.34 (2H, br, NH₂), 7.81 (1H, s, pyrimidyl-*H*), 8.23 (1H, d, *J*=2.2 Hz, furan-*H*), 8.91 (1H, s, pyridyl-*H*); IR (KBr): ν_{max}/cm⁻¹ 3308 and 3152 (NH); [α]_D²⁶ -280.6 (*c* 0.34, CHCl₃); 94% ee [chiral HPLC analysis (Daicel Chiralcel OD, hexane/PrOH=75:25, flow rate: 0.5 ml/min, 25 °C, 'R: 33.6 min)].

Acknowledgements

We thank Dr. Yoji Oderaotoshi, Graduate School of Engineering, Osaka University, for the MO calculations of the structures **3a** and **4a**.

References and notes

- (a) Staunton, J.; Eisenbraun, E. *J. Org. Synth.* **1962**, *42*, 4. (b) Djerassi, C.; Hart, P. A.; Warawa, E. J. *J. Am. Chem. Soc.* **1964**, *86*, 78.
- (a) Matsugi, M.; Nojima, M.; Hagimoto, Y.; Kita, Y. *Tetrahedron Lett.* **2001**, *42*, 8039. (b) Matsugi, M.; Itoh, K.; Nojima, M.; Hagimoto, Y.; Kita, Y. *Chem. Eur. J.* **2002**, *8*, 5551.
- For reviews of CH/π interactions, see: (a) Oki, M. *Acc. Chem. Res.* **1990**, *23*, 351. (b) Etter, M. C. *J. Phys. Chem.* **1991**, *95*, 4601. (c) Zaworotko, M. J. *Chem. Soc. Rev.* **1994**, *23*, 283. (d) Nishio, M.; Umezawa, Y.; Hirota, M.; Takeuchi, Y. *Tetrahedron* **1995**, *51*, 8665. (e) Nishio, M.; Umezawa, Y.; Hirota, M. *The CH/π interaction*; Wiley: New York, 1998.
- (a) Takagi, T.; Tanaka, A.; Matsuo, S.; Maezaki, H.; Tani, M.; Fujiwara, H.; Sasaki, Y. *J. Chem. Soc., Perkin Trans. 2* **1987**, 1015. (b) Suezawa, H.; Hashimoto, T.; Tsuchinaga, K.; Yoshida, T.; Yuzuri, T.; Sakakibara, K.; Hirota, M.; Nishio, M. *J. Chem. Soc., Perkin Trans. 2* **2000**, 1243.
- Wishka, D. G.; Graber, D. R.; Seest, E. P.; Dolak, L. A.; Han, F.; Watt, W.; Morris, J. *J. Org. Chem.* **1998**, *63*, 7851.
- (a) Lindberg, J.; Sigurosson, S.; Lowgren, S.; Andersson, H. O.; Sahlberg, C.; Noreen, R.; Fridborg, K.; Zhang, H.; Unge, T. *Eur. J. Biochem.* **2002**, *269*, 1670. (b) Wishka, D. G.; Graber, D. R.; Kopta, L. A.; Olmsted, R. A.; Friis, J. M.; Hosley, J. D.; Adams, W. J.; Seest, E. P.; Castle, T. M.; Dolak, L. A.; Keiser, B. J.; Yagi, Y.; Jeganathan, A.; Schlachter, S. T.; Murphy, M. J.; Cleek, G. J.; Nugent, R. A.; Poppe, S. M.; Swaney, S. M.; Han, F.; Watt, W.; White, W. L.; Poel, T. J.; Thomas, R. C.; Voorman, R. L.; Stefanski, K. J.; Stehle, R. G.; Tarpley, W. G.; Morris, J. *J. Med. Chem.* **1998**, *41*, 1357.
- Uenishi, J.; Takagi, T.; Ueno, T.; Hiraoka, T.; Yonemitsu, O.; Tsukube, H. *Synlett* **1999**, 41.
- For reviews of the enzyme-catalyzed acyl transfer, see: (a) Faber, K.; Riva, S. *Synthesis* **1992**, 895. (b) Carrea, G.; Riva, S. *Angew. Chem., Int. Ed. Engl.* **2000**, *39*, 2226.
- Okano, K.; Muraya, K.; Ikariya, T. *Tetrahedron Lett.* **2000**, *41*, 9277.
- These pyridylethanolols were essentially prepared by according to the reported method: (a) Bellezza, F.; Cipiciani, A.; Cruciani, G.; Fringuelli, F. *J. Chem. Soc., Perkin Trans. 1* **2000**, 4439. (b) Trecourt, F.; Breton, G.; Bonnet, V.; Mongin, F.; Marsais, F.; Queguiner, G. *Tetrahedron* **2000**, *56*, 1349. (c) Bullitt, O. H., Jr.; Maynard, J. T. *J. Am. Chem. Soc.* **1954**, *76*, 1370. (d) Uenishi, J.; Hiraoka, T.; Hata, S.; Nizhiwaki, K.; Yonemitsu, O.; Nakamura, K. *J. Org. Chem.* **1998**, *63*, 2481.
- The absolute configuration of the (S)-**1c**, which showed remarkable shielding effect in the etenic acid ester, and existed in an organic phase upon extraction, was determined by the comparison of the sense of [α]_D of the corresponding **1c** after the removal of the steroid moiety: Seemayer, R.; Schneider, M. P. *Tetrahedron: Asymmetry* **1992**, *3*, 827.
- Matsugi, M.; Itoh, K.; Nojima, M.; Hagimoto, Y.; Kita, Y. *Tetrahedron Lett.* **2001**, *42*, 6903.
- The structure of **3a** and **4a** was calculated using MOPAC program (PM3) in the CACHE system; Tektronix CACHE system, CACHE Scientific Inc, 1993.
- Bondi, A. *J. Phys. Chem.* **1964**, *68*, 441.
- Prediction of the absolute configuration of α-chiral carboxylic acids from the observation of the difference in ¹H NMR spectra between the δ values (Δδ^{RS}) of their esters with chiral non-racemic arylalcohols is reported; Ferreiro, M. J.; Latypov, S. K.; Quinñoá, E.; Riguera, R. *J. Org. Chem.* **2000**, *65*, 2658.